Neonatal EEG: Atlas and Interpretation

Akihisa Okumura
Hiroyuki Kidokoro
Editors

Springer

Neonatal EEG: Atlas and Interpretation

Akihisa Okumura • Hiroyuki Kidokoro
Editors

Neonatal EEG: Atlas and Interpretation

Springer

Editors
Akihisa Okumura
Department of Pediatrics
Aichi Medical University
Nagakute, Aichi, Japan

Hiroyuki Kidokoro
Department of Pediatrics
Nagoya University Graduate School
of Medicine
Nagoya, Aichi, Japan

ISBN 978-981-96-0725-9 ISBN 978-981-96-0726-6 (eBook)
https://doi.org/10.1007/978-981-96-0726-6

The original submitted manuscript has been translated into English. The translation was done using artificial intelligence. A subsequent revision was performed by the author(s) to further refine the work and to ensure that the translation is appropriate concerning content and scientific correctness. It may, however, read stylistically different from a conventional translation.

This Springer imprint is published by the registered company Springer Nature Singapore Pte Ltd.
The registered company address is: 152 Beach Road, #21-01/04 Gateway East, Singapore 189721, Singapore

Foreword

In neonatal medicine, it is crucial to obtain information about whether a neonate's brain is normal or injured, the degree of injury if any, when and how the injury occurred, and the potential neurological sequelae. This information is important for the treatment and prevention of brain injuries during the neonatal period and for understanding the pathogenesis of such injuries. Neuroimaging techniques such as CT, MRI, and ultrasound can provide this information; however, while they offer superior spatial resolution, they are limited in temporal resolution. In contrast, EEG offers excellent temporal resolution and is an extremely useful method for noninvasive, bedside examination of moment-to-moment changes in brain function. Recently, with the spread of compact digital electroencephalographs and the introduction of aEEG, the usefulness of EEG has been increasing. It is now possible not only to diagnose and prognosticate perinatal brain injuries, diagnose neonatal seizures, and determine the level of brain maturation but also to detect brain dysfunction in real-time through continuous monitoring, which may lead to timely intervention.

This book is composed of several sections, including a general overview, normal EEG, abnormal EEG, neonatal seizures, aEEG, neonatal EEG in practice and its applications. In the "Overview" section, it is emphasized that although interpreting the neonatal EEG presents various difficulties, it is an extremely useful examination method that is worth the effort to overcome these challenges. The characteristics of the neonatal EEG and the relationship between sleep states and EEG patterns are then explained. Newborn sleep is broadly divided into active sleep and quiet sleep, and methods are described for interpreting sleep cycles and the corresponding EEG patterns by coding them. Although it may seem difficult to understand at first glance, once you master the method, it will be useful for understanding the "normal EEG." While polygraph recordings are necessary to accurately determine sleep states, they are not always essential in clinical practice. Even though the relationship between sleep states and EEG patterns is significant, it is not an exact 1:1 correspondence. However, it is sufficient for evaluation to record all EEG patterns with an understanding of their cyclical appearance. In the "Normal EEG" section, the development of EEG is explained in an easy-to-understand manner using codes for each EEG pattern. It is important to note, as mentioned in the "Overview" section, that there are two types of high voltage slow wave patterns, each with different codes. The neurophysiological basis

of these patterns is further explained in the column. In the “Abnormal EEG” section, a wide variety of abnormal EEGs are shown, and the arrows in the figures clearly explain what we should pay attention to in particular. The “Neonatal Seizures” section introduces the new classification recently proposed, with examples of actual EEGs recorded during seizures. In the “aEEG” section, the principles and display methods of aEEG, aEEG of normal term infants and preterm infants are explained clearly. Acute-stage abnormalities and neonatal seizures are illustrated with numerous cases. In addition, this book includes PDF files of actual EEGs and “challenge questions” available on the accompanying website, making this a comprehensive and thorough textbook for neonatal EEG interpretation.

I recommend this book to all neonatologists and pediatric neurologists aiming for intact survival of high-risk newborns.

This is the English translation of the Foreword from the Japanese edition.

Department of Pediatrics
Nagoya University Graduate School of Medicine
Nagoya, Aichi, Japan
April 2019

Kazuyoshi Watanabe

Preface for the English Edition

Time flies.

I will be 60 years old next month. In Japan, the age of 60 is called *kanreki*, a custom to celebrate longevity. It may be some kind of fate that I am preparing this textbook at such a time.

I started learning about neonatal EEG 32 years ago, at the age of 28, 4 years after graduating from medical school. I was posted to Anjo Kosei Hospital, where Dr. Fumio Hayakawa taught me how to read neonatal EEG. I don't think I was ever a good student, but I found the insights into perinatal brain disorders that could be gained from neonatal EEG to be very interesting. At the time, periventricular leukomalacia (PVL) in preterm infants was a topic in neonatology. When EEG was recorded early after birth in preterm infants who later developed PVL, the EEG was always abnormal. The only straightforward explanation is that PVL had occurred before birth. However, no such insight existed anywhere in Japan or abroad at the time. The insights provided by neonatal EEG are valuable, but only a few are still aware of them. As described in the main text, the greatest advantage of neonatal EEG is its ability to assess brain function in real time. We hope that this advantage will be more widely applied in both clinical practice and research.

The impetus for publishing the first Japanese edition of this text was the attempt to develop guidelines for neonatal seizure, a project undertaken by a research group funded by the Ministry of Health, Labour and Welfare in Japan. I happened to have moved to Tokyo just before the work was to begin and was only a research collaborator. However, I was very surprised to find that none of the members tasked with drafting the guidelines was familiar with neonatal EEG. As you know, ictal EEG is essential for the diagnosis of neonatal seizures, but no one knew such a crucial fact. Coincidentally, around that time, amplitude-integrated EEG was being introduced in Japan, and the transition to digital EEG was underway. I realized that I had no choice but to take this opportunity to publish a textbook on neonatal EEG. Despite some minor obstacles, the first Japanese edition was successfully published in 2008.

In my opinion, our EEG interpretation methods are more sophisticated than those used abroad. There is no interpretation method around the world that clearly demonstrates a 2-week difference in the brain maturation of newborns. The idea of focusing on the time from the onset of brain insult, i.e., acute and recovery phase abnormalities, is also quite unique. However, it can

be said that our interpretation method still remains only local. The true value of our method will only be determined once it is globally evaluated in various ways. The publication of this English edition will bring our interpretation method to the attention of clinicians and researchers abroad. How will our methods be evaluated? I am half-excited and half-anxious. We would like to invite international readers to feel free to read this textbook and offer their opinions and criticisms.

Once again, it is quite surprising that our interpretation method was established by just two great pioneers, Professor Emeritus Kazuyoshi Watanabe and Dr. Fumio Hayakawa. As mentioned in the afterword to the first edition, the prototype of this textbook was almost complete as early as 1992. This fact is truly an incredible achievement. It is difficult to put into words how helpful their work has been in deepening our understanding of perinatal brain injury. It is nothing short of miraculous that so much great wisdom was produced in a single hospital in a rural area of Japan. I would like to express our deepest gratitude to Professor Emeritus Kazuyoshi Watanabe and Dr. Fumio Hayakawa.

The publication of this English edition would not have been possible without the significant contribution of Dr. Hiroyuki Kidokoro. Dr. Kidokoro deserves great credit for his significant contribution. As I mentioned above, I am getting old. Now I am too old to develop our knowledge of neonatal EEG. Nowadays, advanced research is being conducted on brain function in newborns. I believe that the information in this book can serve as basic knowledge to support such advanced research. From now on, I look forward to the activities of the younger generation, including Dr. Kidokoro.

I wish the young people good luck.

Finally, I would like to thank my wife and son for their support. I am very sorry that I have been so busy with work that I have not had time to take care of my family. I am very grateful that my wife supported me without reproach. I would also like to thank my wife for raising our son successfully. My son is now an adult and starting his own life. I wish him all the best for the future.

Nagakute, Aichi, Japan Akihisa Okumura
August, 2024

Preface for the English Edition

Neonatal neurology has undergone remarkable advancements over the past three decades. The application of MRI to neonates has revolutionized our ability to evaluate brain injuries from the earliest stages of life, providing detailed insights into both structural and functional alterations in the newborn brain. In parallel, therapeutic hypothermia has become the standard treatment for neonatal hypoxic-ischemic encephalopathy, offering neuroprotection for affected neonates. Furthermore, the widespread adoption of whole-exome and whole-genome sequencing has enabled the early diagnosis of genetic disorders. With the implementation of mass screening for spinal muscular atrophy, gene therapy can now be initiated in the neonatal period, offering new hope for affected infants.

The history of neonatal EEG, however, stretches much further back. Long before I began my career as a physician, pioneering doctors and researchers in the 1970s—most notably Dr. Watanabe K—conducted extensive studies on neonatal EEG. They meticulously examined the EEG patterns associated with brain injury and maturation in both term and preterm infants and explored the relationship between EEG findings and sleep states. By the early 2000s, the foundation of neonatal EEG has already been firmly established.

In the last 30 years, advancements in neonatal EEG have been made as well. Advances have moved beyond visual interpretation toward the integration of sophisticated mathematical analysis, greatly enhancing the precision of EEG assessments. Additionally, amplitude-integrated EEG has become widely used worldwide, allowing neonatologists to monitor brain activity and detect seizures at the bedside. More recently, the integration of artificial intelligence into EEG analysis promises to bring even greater advancements to clinical practice.

It is important to recognize that these cutting-edge techniques are built upon the foundational knowledge of basic neonatal EEG interpretation. This book, *The Neonatal EEG: Atlas and Interpretation*, is based on the second edition of the Japanese-language book, *The Neonatal EEG for Everyone*, which was originally written for healthcare professionals in Japan. Its aim is to make neonatal EEG interpretation accessible to all practitioners working in NICUs. Unlike traditional academic texts, this book is designed to guide readers through the interpretation of normal preterm and term EEGs at 2-week intervals, helping them to recognize both acute- and chronic-stage abnormalities.

For this English edition, several updates have been made. Notably, Chap. 17, which focuses on neonatal seizures, has been comprehensively revised, and Chap. 10 now includes twice as many artifact examples—16 in total—to provide greater clarity on this challenging topic. We have prioritized simplifying complex concepts, emphasizing the use of real EEG samples to support comprehension. While references have been deliberately kept to a minimum, we have maximized practical content to enhance clarity and applicability.

We hope that this textbook will serve as a valuable resource for practitioners worldwide who wish to learn about neonatal EEG, empowering them to deepen their understanding of neonatal EEG and apply this knowledge in clinical practice.

Nagoya, Aichi, Japan Hiroyuki Kidokoro

Preface

On the Publication of *The Neonatal EEG for Everyone*, second edition.

More than 10 years have passed since the first edition of *The Neonatal EEG for Everyone* had been published by Shindan To Chiryo Sha Inc. in 2008. In May 2019, His Majesty the Emperor abdicated the throne and the era has changed from the Heisei era to Reiwa era. It seems to be a good time to renew the contents of *The Neonatal EEG for Everyone*.

At the time of its publication, *The Neonatal EEG for Everyone* was probably the only text on interpretation of neonatal EEG in the world. Even now, with the advent of the Reiwa era, as far as I know, there seems to be no global textbook that can compare with *The Neonatal EEG for Everyone*. The publication of *The Neonatal EEG for Everyone* was around the time when amplitude-integrated EEG became widespread and its usefulness was recognized in Europe and the United States. It can be said that Western countries first realized at that time that diagnosing neonatal seizures without EEG during seizures was impossible. However, such a fact had been already quite common to us. Since then, there has been growing recognition of the importance of neonatal EEG in Europe and the United States, but I believe that there were few interpreters of neonatal EEGs, in the West at a comparable level to ours.

The pace of medical progress increases year by year, and findings that we thought were up to date until recently lose their freshness quickly. iPS cells became known to the world around the time of the publication of *The Neonatal EEG for Everyone*, and now clinical applications of iPS cells have already begun. iPS cells have been used in various research and are no longer a novel technique. Does this mean that is the skill of interpreting neonatal EEG outdated and useless? At least, I feel that the viewpoints provided by neonatal EEG are still important for the advance of neonatal medicine.

This book, *The Neonatal EEG for Everyone*, second edition, is a revision of the former publication *The Neonatal EEG for Everyone* after almost 10 years. By its nature, the fundamental content of this book has not changed. However, the contents of the previous edition have been brushed up and descriptions of neonatal seizures and amplitude-integrated EEG have been

added. This book has been crafted to enable readers to interpret neonatal EEGs comprehensively. I encourage you to use this book as your guide when interpreting neonatal EEGs.

This is English translation of the Japanese edition.

Nagakute, Aichi, Japan Akihisa Okumura
May 2019

Postscript

In the fall of my second year after graduating from medical school, I witnessed senior pediatricians enthusiastically discussing the findings of neonatal EEGs in the pediatric department office. I was eager to join the discussion and begged to learn, but I was not allowed to do so, as I had just started my pediatric residency. A year later, I finally began receiving the neonatal EEG instruction that I had longed for. The text at that time was a handwritten document authored by Dr. Fumio Hayakawa, which later formed the basis of the first edition of *The Neonatal EEG for Everyone*, second edition. During this time, Dr. Toru Kato provided me with thorough feedback, using a red pen to critique my reading reports. My interest in neonatal EEGs continued to grow, and in my third year after graduation, I visited many hospitals to read and study neonatal EEGs. I would go to the NICU at the university late at night, carry the electroencephalograph myself, attach the electrodes, and sit in front of the incubator for an hour before midnight.

Some people question the ambiguity of neonatal EEG interpretation. However, just as anyone can tell the difference between a Vincent Van Gogh and a Marc Chagall painting (even if it is difficult to explain in words), I believe that the disorganized pattern in periventricular leukomalacia (PVL) can be detected. If this leads to early diagnosis and treatment of PVL, I am eager to detect it. Experience is indispensable, as it is said that "EEG interpretation stands alone only after reading a thousand cases." However, language is essential for efficient communication and common understanding among many people. *Neonatal EEG for Everyone* is a unique textbook that conceptualizes and verbalizes the somewhat pictorial features of neonatal EEG interpretation in a way that is easy to understand and familiar to beginners.

When I was asked to edit a new edition of the book, I was honestly delighted. But what was even more gratifying was seeing that the authors had created new and exceptional manuscripts and selected better EEG samples. It is a mixed feeling of surprise, admiration, and gratitude that comes with age. I would also like to thank Mr. Kawaguchi and Mrs. Baba of Shindan To Chiryo Sha Inc. for their suggestions, advice, and pacing. Finally, I want to express my deepest gratitude to Dr. Kazuyoshi Watanabe for reviewing and advising on the final manuscript. His knowledge and experience in neonatal EEGs are far beyond my own. For nearly 20 years, I have been blessed with the opportunity to continuously receive new knowledge about neonatal EEGs

from Dr. Watanabe, Dr. Okumura, and many other professors, without ever losing interest. I hope I can do the same for the readers of this book.

In front of the painting “All Children become great Watanabrains” in the Pediatric Neurology Lab at Nagoya University.

This is English translation of the Japanese edition.

Nagoya, Aichi, Japan Hiroyuki Kidokoro
May 2019

About This Book

Features

- The book is written in an easy-to-understand manner, using minimal technical terms, making it suitable for beginners who have never read adult or pediatric EEG recordings.
- The EEG samples are displayed as large as possible to approximate the actual EEG.
- The exceptional columns written by Drs. Kazuyoshi Watanabe and Fumio Hayakawa are a must-read.
- This book includes many samples of neonatal EEG results and challenge questions as electronic supplementary materials. These resources allow readers to engage with neonatal EEGs as if they are encountering actual EEGs. The "Challenge Questions" section is useful for learning how to interpret EEG results.

List of Basic Terms

- **Slow wave**
  A wave with a frequency of <4 Hz, mostly synonymous with delta wave.
- **Theta wave**
  A wave with a frequency between 4 and 8 Hz.
- **Alpha wave**
  A wave with a frequency between 8 and 13 Hz.
- **Fast wave**
  A wave with a frequency of ≥13 Hz, mostly synonymous with beta wave.
- **Transients**
  Transients refer to EEG components that appear sporadically. This term, typically used to describe elements of physiological background activity, generally is not applied to pathological components.
- **Sharp wave and Spike**
  In general, sharp EEG components with a frequency of <12 Hz are called "sharp waves," whereas sharp EEG components with a frequency of ≥12 Hz are called "spikes"; however, this distinction is not always strict. In assessments of neonatal EEG, both sharp waves and spikes are not

necessarily pathological; they are often physiological, similar to the transients mentioned above.

- **Postmenstrual weeks**
  The postmenstrual weeks are calculated by adding the number of weeks in gestation to the number of weeks after birth, assuming that the expected date of birth is 40 weeks and 0 days (equivalent to 40 weeks and 0 days postmenstrual age). Strictly speaking, the postconceptional weeks differ from the postmenstrual weeks by approximately 2 weeks.

Placement of EEG Electrodes

The following abbreviations are used: Fp, frontal pole; C, central; T, temporal; and O, occipital region. Odd numbers indicate the left hemisphere, even numbers indicate the right hemisphere, and z indicates the midline. Therefore, for example, C3 represents the electrode in the left central region. For more details, please refer to "Chap. 21: How to Record Neonatal EEGs."

How to Identify the Location of the Appearance of EEG Components?

An EEG depicts a negative shift of electric potential in the upward direction because changes in neuronal excitability are related to depolarization, which causes a negative shift in extracellular electric potential. As will be described later, neonatal EEG is interpreted primarily via bipolar derivation. For example, as shown in Fig. 1a, negative waves from C3 are depicted with their

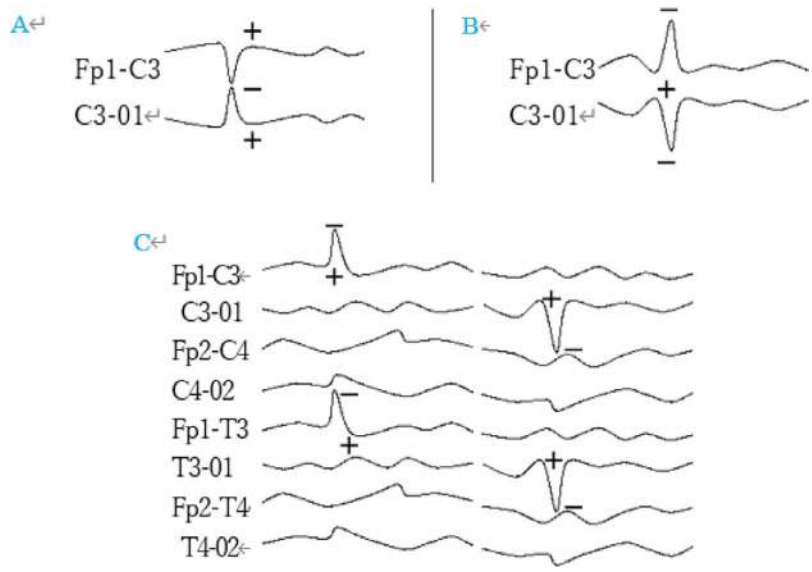

Fig. 1 Direction of EEG potentials. (**a**) Negative waves from C3. The peaks face each other. (**b**) Positive waves from C3. The peaks are symmetrically oriented in opposite directions. (**c**) Negative waves from Fp1 point upward, whereas negative waves from O1 point downward

peaks facing each other. Conversely, positive waves from C3 exhibit peaks that are symmetrically oriented in opposite directions, as shown in Fig. 1b. As shown in Fig. 1c, a negative wave from Fp1 points upward, whereas a negative wave from O1 points downward.

Contents

Contributors

Tatsuya Fukasawa Department of Pediatrics, Anjo Kosei Hospital, Anjo, Japan

Fumio Hayakawa Department of Pediatrics, Okazaki City Hospital, Okazaki, Japan

Toru Kato Department of Pediatrics, Okazaki City Hospital, Okazaki, Japan

Hiroyuki Kidokoro Department of Pediatrics, Nagoya University Graduate School of Medicine, Nagoya, Aichi, Japan

Tetsuo Kubota Department of Pediatrics, Anjo Kosei Hospital, Anjo, Japan

Koichi Maruyama Department of Pediatric Neurology, Aichi Developmental Disability Center Central Hospital, Kasugai, Japan

Akihisa Okumura Department of Pediatrics, Aichi Medical University, Nagakute, Aichi, Japan

Anna Shiraki Department of Pediatrics, Nagoya University Graduate School of Medicine, Nagoya, Aichi, Japan

Yuichiro Sugiyama Department of Pediatrics, Japanese Red Cross Aichi Medical Center Nagoya Daiichi Hospital, Nagoya, Japan

Takeshi Suzuki Department of Pediatrics, Okazaki City Hospital, Okazaki, Japan

Kazuyoshi Watanabe Department of Pediatrics, Nagoya University Graduate School of Medicine, Nagoya, Aichi, Japan

Hiroyuki Yamamoto Department of Pediatrics, Nagoya University Graduate School of Medicine, Nagoya, Aichi, Japan

List of Figures

Part I

Overview

1 Why Is It Important to Record Neonatal EEGs?

Akihisa Okumura and Fumio Hayakawa

Neonates admitted to the neonatal intensive care unit (NICU) may exhibit involvement of the central nervous system (CNS) due to various diseases and conditions. Term infants with asphyxia and preterm infants often experience hypoxic-ischemic encephalopathy and other complications, which can seriously impact their future health. However, assessing the CNS condition can be challenging for physicians and nurses who manage newborns. These difficulties mainly arise because brain function is physiologically immature during the neonatal period, and the CNS is not functioning adequately compared to older children and adults, who often exhibit brain damage through neurological symptoms and signs, such as paralysis. This phenomenon indirectly reflects the robust nerve conduction pathways from the cerebrum to the peripheral nerves.

However, even if newborns have brain damage that may leave them bedridden in the future, they are able to vigorously move their limbs during the neonatal period. In patients with periventricular leukomalacia (PVL)—a typical type of hypoxic-ischemic brain injury observed in preterm infants—it is difficult to detect CNS abnormalities on the basis of spontaneous movement or neurological examination before NICU discharge, even when PVL is sufficiently severe that the neonate will be unable to maintain a sitting position in the future. After NICU discharge, infants with PVL gradually develop truncal hypotonia and limb spasticity; neurological sequelae become apparent. These manifestations occur because limb movements are controlled by lower centers, including the brainstem, during the neonatal period, whereas voluntary movements originating from the cerebrum are limited. When the functions of lower centers are maintained, infants can move their limbs without difficulty during the neonatal period, even if the cerebrum has lost its function. Therefore, signs and symptoms may not be apparent during the neonatal period, even if the CNS is severely affected.

In neonates, the CNS is a "black box." Some readers might believe that neuroimaging techniques, such as ultrasound, computed tomography, and magnetic resonance imaging, are sufficient for evaluating brain lesions. Indeed, imaging plays a key role in the evaluation of the CNS in neonates. However, there is generally a time lag between the occurrence of an injury and the appearance of corresponding imaging abnormalities in the perinatal brain. Although magnetic resonance imaging, especially diffusion-weighted imaging, is useful for early detection of brain lesions, patients often require respiratory

A. Okumura (✉)
Department of Pediatrics, Aichi Medical University, Nagakute, Aichi, Japan
e-mail: okumura.akihisa.479@mail.aichi-med-u.ac.jp

F. Hayakawa
Department of Pediatrics, Okazaki City Hospital, Okazaki, Japan

A. Okumura, H. Kidokoro (eds.), *Neonatal EEG: Atlas and Interpretation*,
https://doi.org/10.1007/978-981-96-0726-6_1

support or their vital signs can become unstable during the acute period, making timely imaging examinations difficult. Therefore, it is important to consider the limitations of real-time assessments of pathological conditions based on current neuroimaging technology.

In contrast, electroencephalogram (EEG) assessment represents a sensitive and excellent method for real-time examination of cerebral function in neonates. Background EEG activities reflect the culmination of cerebral development from the fetal period. In the event of an acute brain injury, the background EEG results are affected according to the extent and nature of the injury. Some readers may consider EEG recording to be complicated because of the time and effort involved in attaching multiple electrodes and operating the EEG recorder. However, EEG recording is noninvasive and can be performed in a safe manner, even for assessments of infants with unstable conditions. Additionally, EEG recorders have become digitalized and compact, facilitating recording with minimal obstruction in crowded NICUs. Moreover, once clinicians become proficient in interpreting EEGs, they can estimate patient outcomes during real-time recording. In some instances, the developmental outcome of an infant can be immediately predicted during a 10-min EEG assessment on the first day of life. This prediction is feasible for preterm infants who will never be able to walk; infants with neonatal encephalopathy, which might not be caused by hypoxic-ischemia alone; and infants with intrauterine growth retardation, which could have various causes and developmental outcomes. The scientific value of the information obtained from EEGs is particularly high, and this method is essential for individuals concerned about neurological outcomes among newborn infants.

1 Why Has Neonatal EEG Not Been Widely Used Thus Far?

The absence of standard methods for interpreting EEG results is a key factor in the lack of widespread neonatal EEG use. To address this undesirable situation, this textbook aims to provide a suitable introduction for individuals with an interest in neonatal EEG.

Patient outcomes are the greatest concern for families of newborns admitted to the NICU. Currently, no method is superior to EEG assessment in terms of accurately predicting developmental outcomes. EEG findings can provide objective and comprehensive information about abnormalities in brain function, including malformations in brain development. Therefore, EEG evaluations can be reliable and accurate for the purpose of estimating brain damage severity and type, as well as infant outcomes, regardless of the underlying cause of decreased brain function and the general condition at the time of EEG recording. Improvements in neonatal care and the achievement of intact survival require evaluating the CNS of the infant, accurately identifying events leading to decreased brain function, and clarifying their causes to ensure prevention. For these purposes, neonatal EEG recordings constitute an excellent source of useful information. However, there are barriers to recording and interpreting neonatal EEG information in the NICU, including various electronic devices in the NICU that can cause EEG artifacts and the fragile appearance of newborn infants, which may cause hesitation among technicians. The value of the information obtained from neonatal EEG findings merits the dissemination of such information. The establishment of neonatal EEG as a standard practice in the NICU requires improvements in the quality of interpretation.

At first glance, neonatal EEG may appear difficult to understand. However, in our experience, neonatal EEG interpretation is relatively uncomplicated. This textbook explains neonatal EEG from various perspectives.

We hope that the contents of this textbook will help to improve the interpretation of neonatal EEGs and that EEG assessments will become a standard practice in NICUs, leading to the intact survival of all neonates admitted to NICUs.

Characteristics of Neonatal EEGs

2

Akihisa Okumura and Fumio Hayakawa

The acquisition of sufficient information from neonatal EEG requires an understanding of its characteristics, as outlined below.

1 All Sleep Stages Can be Evaluated

During the neonatal period, the sleep–wake cycle is 2–3 h, which is much shorter than the 24-h cycle in older children and adults (Fig. 2.1). During this cycle, the awake period is short, and sleep constitutes the majority of the time. Because limited information can be obtained from neonatal EEGs during the awake period, EEGs collected during sleep are useful. Therefore, we will discuss EEG findings during sleep.

In older children and adults, routine EEG recordings (approximately 1–2 h) typically cover only stages I (very light sleep) and II (light sleep) of the sleep cycle. To obtain EEGs that include stage III of the sleep cycle and the rapid eye movement (REM) stage, long-term EEG recordings are required. In neonates, EEGs representing all sleep stages can be recorded within a similar interval. In neonates, active sleep (AS, corresponding to REM sleep in adults) appears during the onset of sleep, followed by quiet sleep (QS, corresponding to stages I–IV in adults) as sleep persists. Each of these sleep stages lasts approximately 20 min, and all sleep stages can be evaluated with a 1–2-h recording (Fig. 2.2). When interpreting neonatal EEG results, it is essential to distinguish AS and QS based on EEG patterns.

A. Okumura (✉)
Department of Pediatrics, Aichi Medical University, Nagakute, Aichi, Japan
e-mail: okumura.akihisa.479@mail.aichi-med-u.ac.jp

F. Hayakawa
Department of Pediatrics, Okazaki City Hospital, Okazaki, Japan

A. Okumura, H. Kidokoro (eds.), *Neonatal EEG: Atlas and Interpretation*,
https://doi.org/10.1007/978-981-96-0726-6_2

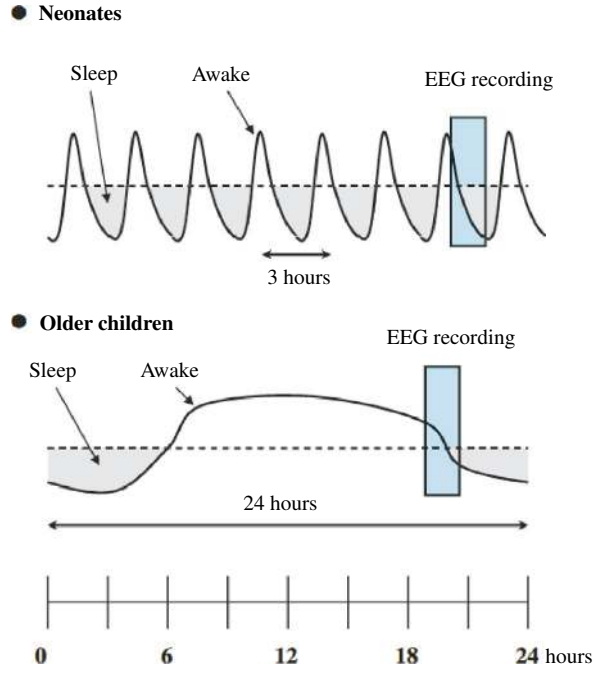

Fig. 2.1 Sleep-wake cycle and EEG recording

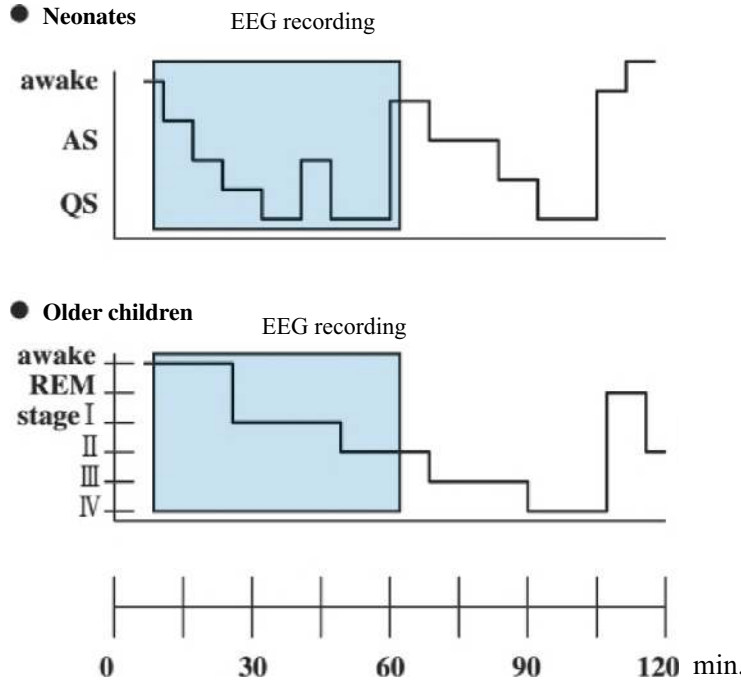

Fig. 2.2 Neonatal sleep stages and EEG recording. *AS* active sleep, *QS* quiet sleep, *REM* rapid eye movement

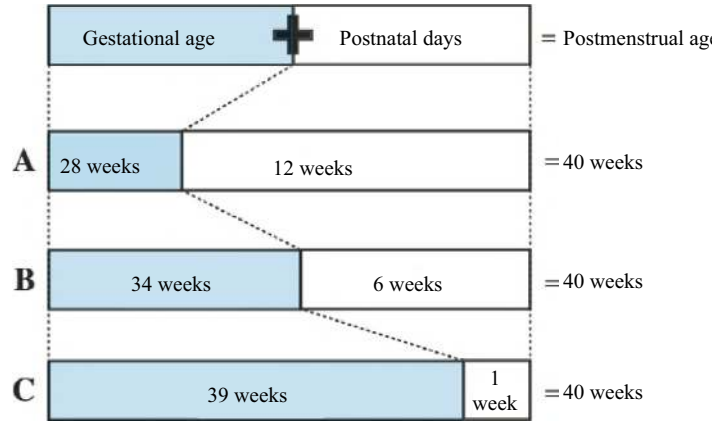

Fig. 2.3 EEG maturation and postmenstrual age

2 Sleep EEG Activity Reflects Brain Maturation

The CNS of a fetus or preterm infant undergoes remarkable maturation during the period from 22 weeks postmenstrual age (PMA), near the limit of viability, to 40 weeks PMA, which is the expected date of birth. During this period, the rate of brain maturation is assumed to be similar between intrauterine and extrauterine environments. In this textbook, the term "postmenstrual age (PMA)" is used to represent the sum of "gestational age + postnatal days." PMA is calculated based on the expected date of birth, which corresponds to 40 weeks and 0 days of PMA. Because the expected date of birth is calculated from the last menstrual period, there usually is a discrepancy between PMA and biological age as defined from the time of conception. When EEGs of preterm infants are repeatedly recorded, the findings rapidly change with increasing PMA (Fig. 2.3). EEG findings are presumed to reflect brain maturation at the time of EEG recording. We can distinguish 2–4-week differences in the characteristics of EEG physiological activities in each sleep stage. When assessing neonatal EEGs, it is important to understand the physiological EEG pattern for each PMA and to interpret EEG findings from the combined perspective of sleep stage and PMA.

3 Acute Insult and Recovery Time Can be Evaluated within a Short Timeframe

Acute brain injuries, such as hypoxic-ischemic encephalopathy, often occur in neonates. EEG activities show alterations reflecting the suppression of brain function during acute brain injuries, which recover after the insult has been alleviated, indicating the restoration of brain function. EEG abnormalities may recover over months to years in older children with acute brain injuries, whereas EEGs in neonates show suppression and recovery week by week (Fig. 2.4).

When interpreting neonatal EEGs, it is important to determine the time elapsed from injury onset. EEG findings must be interpreted according to the stage (acute, recovery, or chronic) after injury onset.

Column: When I Began Neonatal EEG Research

I began neonatal EEG research around 1967. At that time, I frequently encountered neonatal seizures, had many opportunities to record EEGs, and became aware of the importance of understanding normal EEG findings for accurate interpretation.

During the 1960s, as knowledge about the sleep–wake cycle accumulated, it became apparent that neonatal EEG findings also varied with the sleep–wake cycle; thus, simple acquisition of EEGs during wakefulness and sleep was insufficient. Consequently, my colleagues and I conducted polygraphic EEG recordings for approximately 3 h, personally attaching electrodes and observing the conditions of newborn infants. We found that the behaviors and various physiological parameters of newborns, including EEG findings, fluctuated according to their sleep–wake cycle. This type of experience cannot be gained solely through the interpretation of EEGs recorded by technicians; I recommend that individuals interpreting neonatal EEGs directly observe the newborn for at least one sleep cycle. Even when reading an EEG recorded by a technician, the direct observation experience will provide a better understanding of the conditions under which the recording was made.

My colleagues and I have conducted polygraphic recordings of newborns at various gestational ages every 2 weeks since birth. We have been amazed by the rapid brain development during the second half of the fetal period, evident in the obvious development of EEGs with each recording. Standard EEG recordings after infancy are made only until sleep stage II or early stage III are reached; in newborns, recordings should include quiet sleep (QS, which is susceptible to abnormalities) and active sleep (AS, which is necessary to determine maturity). However, reaching the QS stage often requires several tens of minutes.

In EEG laboratories, the examination time typically is scheduled in advance. However, for efficient neonatal EEG assessment, it is preferable to align the recording session with the newborn's schedule; attach electrodes, feed the baby, and begin recording as the baby falls asleep. Around the time when alternating current eliminators were introduced in EEG recorders, EEG-like waveforms were occasionally recorded even when the scalp was not sufficiently cleaned before electrodes were applied. Eventually, I found that EEGs had not been recorded in an appropriate manner; this phenomenon is sometimes called "wet cloth EEG," where such waveforms can be recorded even when electrodes are placed in a bucket of water. To prevent this issue, the scalp should be wiped thoroughly and electrode paste should be applied properly.

(Kazuyoshi Watanabe)

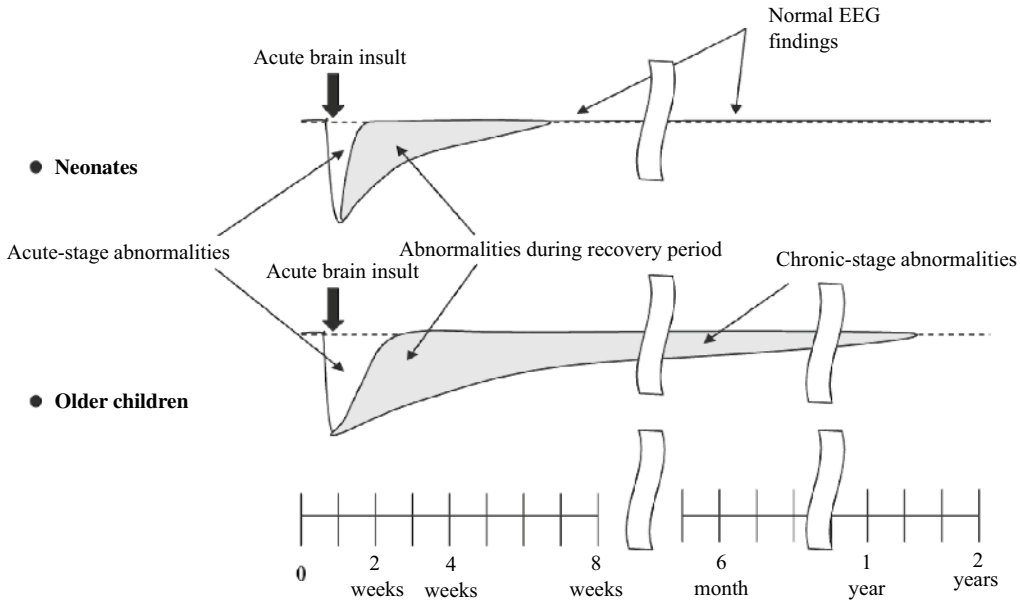

Fig. 2.4 Changes of EEG findings following acute brain insult

Sleep Stages and EEG Patterns

3

Akihisa Okumura and Fumio Hayakawa

1 Sleep Stages and EEG in Term Infants

The EEG pattern of a term infant, equivalent to the expected date of birth, is a key clinical assessment. When an infant has been fed and falls asleep, active sleep (AS) appears first. When AS is recorded using a polygraph, irregular heart rate and respiration, low chin electromyogram (EMG) activity, and rapid eye movement (REM) are observed. This sleep stage corresponds to REM sleep in adults (Table 3.1). During the AS stage after falling asleep, a mixed (M) pattern is mainly observed in which high-voltage slow waves intermittently appear and physiological transients are prominent. Subsequently, polygraphic parameters gradually indicate that body movements decrease, heart rate and respiration become regular, chin EMG activities gradually increase, and startle-like body movements are sometimes observed.

As sleep persists, body movements other than startle disappear, heart rate and respiration become regular, chin EMG activities increase, and REM disappears. This stage, known as quiet sleep (QS), corresponds to non-REM sleep in adults (Table 3.1). During QS, the EEG frequently exhibits high-voltage slow waves, hindering the identification of the baseline. As QS persists, the EEG shows an increase in high-voltage slow waves from the M pattern, and the high-voltage slow waves finally appear almost continuously. The high-voltage slow (HVS) pattern is an EEG pattern in which the baseline is difficult to identify due to the continuous appearance of high-voltage slow waves; this pattern is thought to reflect highly organized brain function in term infants.

At ≥48 weeks postmenstrual age (PMA), EEGs under physiological conditions show the HVS pattern regardless of sleep stage. Additionally, an EEG pattern known as tracé alternant (TA) appears at 40 weeks PMA; this pattern can be used to identify the neonatal period. The TA pattern is characterized by the alternating appearance of high-voltage parts such as HVS and low-voltage parts such as the low-voltage irregular (LVI) pattern, with intervals of several seconds. In preterm infants at ≤36 weeks PMA, the low-voltage parts are almost flat; they are called tracé discontinu (TD) to distinguish them from the TA pattern.

In the first sleep cycle, a neonate typically does not awaken after the TA pattern and again enters AS. During AS after QS, the voltage of background EEG activities is generally low, and irregular low-voltage activities appear with subtle

A. Okumura (✉)
Department of Pediatrics, Aichi Medical University, Nagakute, Aichi, Japan
e-mail: okumura.akihisa.479@mail.aichi-med-u.ac.jp

F. Hayakawa
Department of Pediatrics, Okazaki City Hospital, Okazaki, Japan

A. Okumura, H. Kidokoro (eds.), *Neonatal EEG: Atlas and Interpretation*,
https://doi.org/10.1007/978-981-96-0726-6_3

Table 3.1 Sleep stages and parameters

	Active sleep: AS	Quiet sleep: QS
Heart rate respiration	Irregular	Regular
REM	Observed	Not observed
Chin electromyogram	Decreased	Increased
Body movement	Observed	Startle only
	Equivalent to REM sleep In children and adults	Equivalent to non-REM sleep In children and adults

REM rapid eye movement

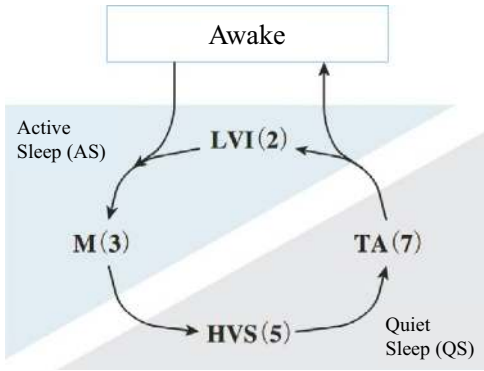

Fig. 3.1 Typical relationship between sleep stages and EEG patterns in term infants

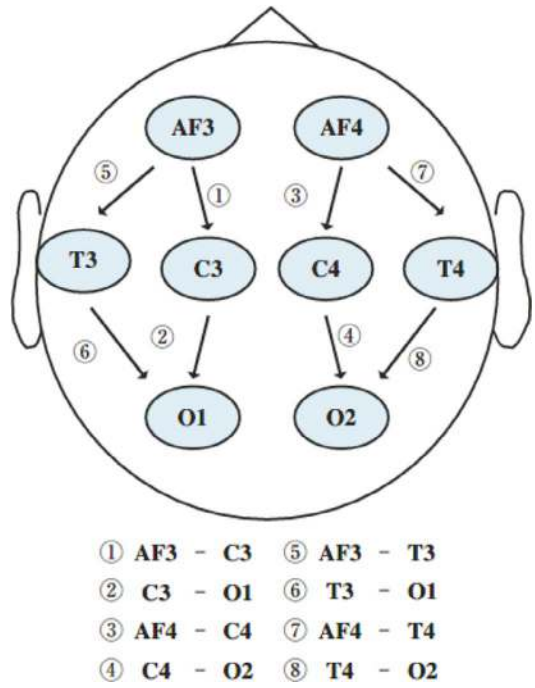

Fig. 3.2 Standard neonatal EEG montage. In the international 10-20 system, AF3 is located midway between Fp1 and F3; AF4 is located midway between Fp2 and F4. Alternatively, AF3 can be placed at Fp1, and AF4 can be placed at Fp2

baseline fluctuations. This EEG pattern is known as the LVI pattern. The neonate then enters the second sleep cycle; it often awakens after the appearance of M → HVS → TA patterns.

As described above, after infants fall asleep, they first enter AS, and the M pattern is predominant at this stage. As sleep persists, infants enter QS, and the EEG pattern changes from HVS to TA. After 10–15 min of the TA pattern, infants enter AS again, and the LVI pattern becomes predominant (Fig. 3.1). The presence of this sleep–wake cycle is the essence of physiological brain function in neonates. Neonatal EEGs are suitable for noninvasive and objective observation of brain function during the neonatal period.

It is preferable to record EEGs without altering the EEG montage because it is difficult to observe changes in EEG activities when the montage is altered during a recording. The recommended montage in which longitudinal bipolar inductions are arranged is shown in Fig. 3.2. The attachment of many electrodes to the small head of a neonate will interfere with achieving sufficient distance between electrodes, which may result hinder appropriate interpretation. Similarly, the reference derivation may be unsuitable for interpretation when stable reference electrodes are not present. The optimal montage for acquisition of clinically sufficient EEG recordings is depicted in Fig. 3.2.

2 EEG Patterns and Codes

As mentioned above, term infants exhibit four EEG patterns according to sleep stage. The EEG pattern of each sleep stage changes every 2–4 weeks during the preterm period. Therefore, during the period from 24 through 44 weeks PMA, differences in normal (physiological) EEG patterns over 2–4-week intervals can be recognized for each sleep stage. In this textbook, we use the EEG code system proposed by Parmelee et al. to display these patterns in a comprehensible manner.

The neonatal EEG code developed by Parmelee et al. is a three-digit integer code (e.g., 283 or 407) (Parmelee Jr et al. 1968). The first two digits indicate the number of postmenstrual weeks, using only even numbers, whereas the last digit indicates the EEG pattern corresponding to the sleep stage: 2, LVI pattern; 3, M pattern; 5, HVS pattern; and 7, TA/TD pattern. In the 40-week EEG pattern, 402 (40-week LVI) and 403 (40-week M) are observed during AS; 405 (40-week HVS) and 407 (40-week TA) are observed during QS (Fig. 3.3).

This EEG code system proposed by Parmelee et al. is helpful but may be confusing because brain maturation causes discrepancies between sleep stages and EEG patterns. The HVS pattern during QS (pattern 5) is only observed in term infants (≥ 38 weeks) but appears during AS in preterm infants. Because pattern 3 is used for AS, HVS in preterm infants is represented using the digit "3." Therefore, codes 245–365 do not exist, although codes 385–445 are used. Instead, the HVS pattern for AS in preterm infants is represented as 243–363. It is important to ensure that the HVS pattern in a term infant is represented using the digit "5"; the digit "3" should be used to indicate the "M" pattern. Although it may be complex, this EEG code system emphasizes the identification of sleep stages over the similarity of EEG patterns (Fig. 3.4).

The sleep cycle in a term infant can be described as 403 → 405 → 407 → 402 → 403 → 405 → 407 → 402 (Fig. 3.5). In contrast, the sleep cycle in a preterm infant (e.g., 28 weeks PMA) can be described as 282 → 283 → 287 → 282 → 283 → 287 → 282 (Fig. 3.6). A more immature brain is more likely to exhibit immature sleep stages that do not meet criteria for AS or QS; these stages are referred to as indeterminate sleep (IS). For example, REM is observed in IS despite regular respiration and heart rate. The EEG patterns observed during AS, IS, and QS are shown according to PMA in Fig. 3.7. Although there are some instances of variation and overlap between sleep stages and PMA, the EEG patterns observed in the largest portion of a recording usually correspond to PMA.

The interpretation of normal EEG requires an understanding of the characteristics of EEG patterns that correspond to each EEG code and the ability to match those patterns with recorded EEGs. Without knowledge of the normal (i.e., physiological) pattern, it is

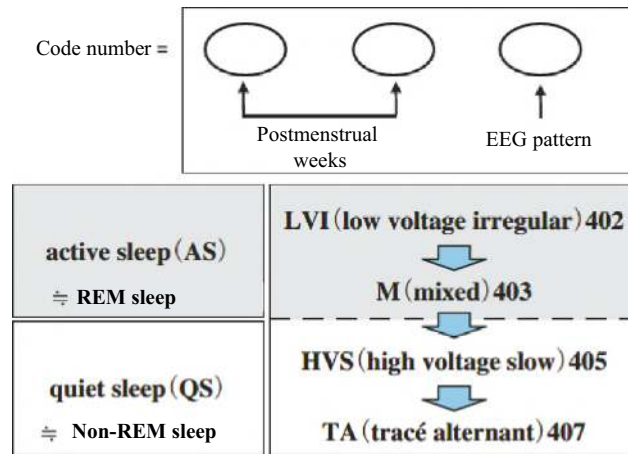

Fig. 3.3 Nomenclature of EEG codes and sleep stages. *REM* rapid eye movement

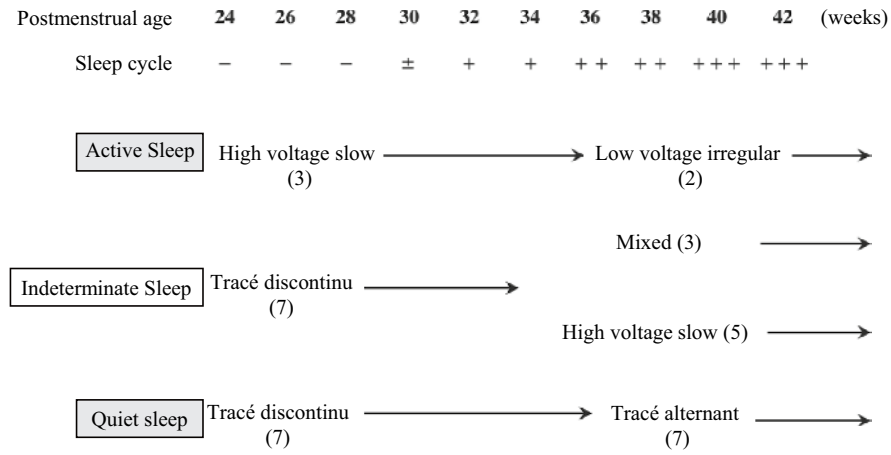

Fig. 3.4 EEG patterns in each postmenstrual age and sleep stage

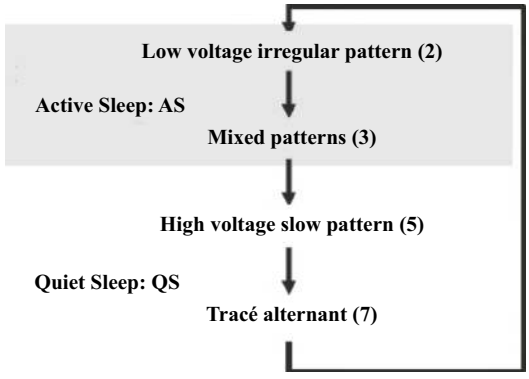

Fig. 3.5 Sleep stages and EEG patterns in term infants. Numbers in parentheses indicate codes of EEG patterns. In term infants at ≥38 weeks PMA, high-voltage slow wave patterns appear during QS and are given the code number (5)

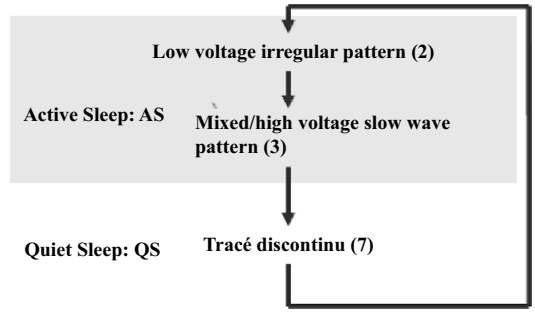

Fig. 3.6 Sleep stages and EEG patterns in preterm infants. Numbers in parentheses indicate codes of EEG patterns. In preterm infants at <38 weeks PMA, high-voltage slow wave patterns appear during AS and are given the code number (3)

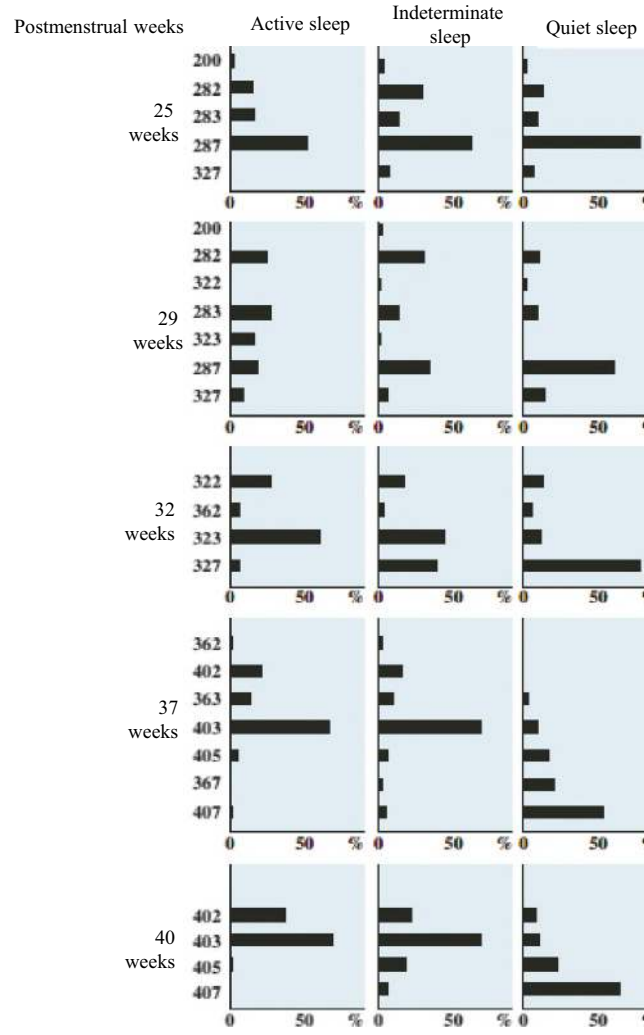

Fig. 3.7 Percentages of EEG codes at each postmenstrual age. Judged every 20 s. Code 200 is a pattern that is almost flat and contains no characteristic waves

impossible to identify an abnormal pattern. Even if the EEG pattern appears similar to a physiological pattern, it must be considered abnormal if it deviates from the physiological pattern for the corresponding PMA. Therefore, it is important to be familiar with the physiological EEG patterns appropriate for a particular PMA.

Column: Observation of Newborns
(Kazuyoshi Watanabe)
Observing newborns while recording their EEGs with a polygraph reveals that physiological phenomena other than EEG findings also change periodically. Moreover, we can see that these are changing developmentally. When I first started the polygraph EEG for neonates, I was impressed.

In general, parameters such as respiration, electrocardiogram, eye movement, and electromyogram are monitored along with EEG. In preterm infants, at 24–26 weeks PMA, these parameters do not show clear periodicity, and correlations among physiological parameters are weak. With increasing PMA, their consistency increases, and the correlations between each parameter and the EEG become stronger.

During active sleep (AS), respiration is irregular. Greater variability in respiratory rate in each 10-s window is correlated with a greater degree of immaturity. Variability in respiratory rate gradually lessens with increasing PMA; it becomes similar to the variability during quiet sleep (QS) at around 40 weeks PMA. However, the variability of one-breath intervals is larger during AS than during QS.

Heart rate is irregular during AS and regular during QS. However, in newborns at <30 weeks PMA, the heart rate is very regular, exhibits little fluctuation, and does not change according to sleep stage; it rarely changes even during body movements. It seems that heart rate is not controlled by the upper centers.

Body movements are the most readily observable indicators. A more immature infant exhibits more frequent, poorly organized, large, impulsive body movements. We have used surface electromyogram to objectively assess body movements (Hakamada et al. 1981). Characteristic body movements during AS are asynchronous whole-body movements, (i.e., generalized movements [GM]), short-lasting movements restricted to a part of the body (i.e., localized phasic movements [LPM]), movements restricted to a part of the body, lasting for >0.5 s (i.e., localized tonic movement [LTM]), and rhythmic clonic movements (i.e., clonic movements [CM]). QS is characterized by brief synchronous limb movements (i.e., generalized phasic movements [GPM]) and startle-like movements (St). GM, LPM, and GPM decrease between 30 and 40 weeks PMA. However, LPM do not decrease until after 40 weeks PMA; they subsequently decrease. Before 32 weeks PMA, the correlations between body movements and sleep stage are poor; GM even occur during QS, and GPM often occur during AS. With increasing PMA, the correlations improve, reaching good correlations at 40 weeks PMA. Because GPM are increased and LPM are decreased in newborns with hydranencephaly, it is likely that GPM arise from a subcortical origin, whereas LPM are related to the cerebral cortex.

Column: Sleep Cycle Development
(Kazunori Watanabe)
In the neonatal period, the ratio of rapid eye movement (REM) sleep to total sleep time is approximately 50%. This decreases with age, reaching ~20% in adulthood and ~ 15% in older adults. Based on this, younger children are generally presumed to exhibit more REM sleep, but the relationship is not straightforward. Sleep stages are typically determined by indices such as EEG pattern, REM, body movement, respiration, and chin electromyogram. Clinically, the three parameters of eye movement, body movement, and respiration are often used to

(continued)

determine sleep stage. However, in more immature infants, the correlation between these parameters is weaker; indeterminate sleep (IS) is more dominant in younger infants, comprising approximately 70% of sleep in infants at 30 weeks postmenstrual age (PMA). In contrast, active sleep (AS) and quite sleep (QS) each comprise ~15%. Thereafter, AS increases until 35–36 weeks PMA, then decreases, reaching approximately 50% at 40 weeks PMA. QS increases after 36 weeks PMA and is ~35% at 40 weeks PMA. The amount of IS steadily decreases to 15% by 40 weeks PMA. Regarding sleep continuity, no clear sleep cycles are observed at 30 weeks PMA or younger, whereas relatively clear cycles of AS and QS appear around 32 weeks PMA. Despite this, IS continues to occur between these sleep stages, making the sleep state unstable. Biphasic cycles of AS and QS become relatively stable after 36 weeks PMA; stable sleep cycles are established at 40 weeks PMA.

In neonates, AS first appears when falling asleep from wakefulness, which is known as sleep-onset REM. In term infants, EEGs typically show a mixed pattern. Then, transition through IS into QS occurs. EEGs show a high-voltage slow wave pattern, followed by a tracé alternant. Ater tracé alternant, EEGs subsequently exhibit a low-voltage irregular pattern in AS; this pattern corresponds to true REM sleep in older children and adults.

Traditionally, the sleep cycle in newborn infants was expected to be 40–50 min because sleep-onset REM was considered. However, if the sleep cycle is defined as the time from the end of tracé alternant/tracé discontinu and the next end of them, it remains constant from 32 to 43 weeks PMA at approximately 90 min (87.2 ± 21.5), nearly identical to REM–non-REM cycles in adults. It is fascinating that biological rest–activity cycles are intrinsic and consistent from the onset of rhythm generation.

References

Hakamada S, Watanabe K, Hara K, Miyazaki. Development of the motor behavior during sleep in newborn infants. Brain and Development. 1981;3(4):345–50.

Parmelee AH Jr, Schulte FJ, Akiyama Y, Wenner WH, Schultz MA, Stern E. Maturation of EEG activity during sleep in premature infants. Electroencephalogr Clin Neurophysiol. 1968;24(4):319–29.

Part II

Normal EEG in Neonates

Column Changes in EEG Patterns with Sleep Cycles
(Kazunori Watanabe)
We used a modified version of the EEG pattern code developed by Parmelee et al. The first two digits indicate the approximate number of corrected weeks, and the last digit indicates the EEG pattern. The low-amplitude irregular patterns including rhythmic theta waves, mixed patterns, high-amplitude slow wave patterns, and trace alternant seen in mature neonates correspond to 402, 403, 405, and 407, respectively. 361 and 401 have lower amplitudes than 362 and 402, do not have rhythmic theta waves, and are seen during arousal and body movements.

In preterm infants, 282,322,362 and 283,323,363 are continuous EEGs, with "3" indicating more high-amplitude slow waves than "2." 287, 327,367 are discontinuous EEG. At less than corrected 30 weeks, there is essentially no difference in EEG patterns between active, irregular, and quiet sleep, while QS has a tendency for having more "7." After corrected 32 weeks, "2" and "3" are found in AS, "7" is mostly found in QS, and both "3" and "7" are found in irregular sleep. The corrected 40 weeks show that 402 and 403 correspond to AS, 405 and 407 relate to QS, but 402 and 403 are also present in a few cases, and certain cases of unsteady sleep show all patterns, but primarily pattern number 403. If the so-called smoothing period is extended while determining the timing of sleep in this scenario, the association becomes more obvious.

At corrected 40 weeks, 403 is predominant in the AS before QS, and 402 is predominant in the AS immediately after QS. Although not as clear at corrected 32 and 36 weeks, 322 and 362 are predominant in the first half of AS, while 323 and 363 are predominant in the latter half of AS before QS. In contrast, 405 is more frequent in the first half of QS, whereas 407 is more frequent in the second half, around corrected 40 weeks. When the sleep cycle is stabilized after corrected 36 weeks,

(continued)

the length of QS is roughly 20 min. For therapeutic reasons, a total of 40 min of AS, with 10 min before and 10 min after the QS, is sufficient. After the commencement of sleep, the EEG pattern is 403-405-407-402-403-405-407.

Why are there "2," "3," "5," and "7" but not "4" and "6" as well? The numbers 523, 525, 526, 528, 529 and 743, 744, 745, 746, 748, 749 were actually utilized by Parmelee et al. They then preserved "4," "6," "8," and "9" for the patterns that appeared following the neonatal period. Later, as we will see in this book, our group added other patterns like 26, 30, 34, 38, 42, and 44.

EEG Patterns in Newborns

4

Akihisa Okumura and Fumio Hayakawa

A neonatal EEG provides useful clinical information. Accurate interpretation of neonatal EEGs requires familiarity with the complicated physiological EEG patterns.

In this textbook, we will present examples of EEGs and explain them to enhance the reader's understanding of normal EEG patterns in neonates at each PMA. Throughout this textbook, unless otherwise stated, the calibration is 100 μV on the vertical axis and 1 s on the horizontal axis.

1 Sleep Stages and EEG Patterns

In clinical practice, neonatal EEGs are usually recorded during sleep. When interpreting a neonatal EEG, it is important to recognize two sleep stages: active sleep (AS) and quiet sleep (QS), as shown in Table 4.1. AS in neonates corresponds to rapid eye movement (REM) sleep in older children and adults, whereas QS corresponds to non-REM sleep. Sleep stages that do not meet the criteria for AS and QS are known as indeterminate sleep (IS). The proportion of IS decreases as PMA increases. For diagnostic purposes, an EEG must be recorded during both AS and QS. The acquisition of QS on an EEG during spontaneous sleep is particularly important. The general principle of neonatal EEG is evident in the EEG pattern at 40 weeks PMA (Fig. 4.1). Sleep often begins with pattern 403, whereas pattern 402 is often observed after 407 during QS. During AS, the baseline can be traced in patterns 402 and 403. A semirhythmic low-amplitude waveform alone is observed in 402; it is classified as 403 when accompanied by high-voltage slow waves. The pattern in which high-voltage slow waves increase and remain continuously evident is 405; this pattern indicates that the infant is entering QS. Pattern 405 demonstrates continuous EEG activity across all channels, and the baseline cannot be traced. As QS deepens, rapid jerky body movements (i.e., startles) occur with an increase in the chin electromyogram, indicating a transition from 405 to 407.

A. Okumura (✉)
Department of Pediatrics, Aichi Medical University, Nagakute, Aichi, Japan
e-mail: okumura.akihisa.479@mail.aichi-med-u.ac.jp

F. Hayakawa
Department of Pediatrics, Okazaki City Hospital, Okazaki, Japan

A. Okumura, H. Kidokoro (eds.), *Neonatal EEG: Atlas and Interpretation*,
https://doi.org/10.1007/978-981-96-0726-6_4

Table 4.1 Sleep stages and EEG patterns

	Active sleep (AS)	Quiet sleep (QS)
Respiration	Irregular	Regular
Rapid eye movement	Present	Absent
Body motion	Frequent	Startle only
EEG	Continuous	Discontinuous
Term period	Low-voltage irregular pattern "2" Mixed pattern "3"	High-voltage slow wave pattern "5" Tracé alternant "7"
Preterm period	Low-voltage irregular pattern "2" Mixed/high-voltage slow wave pattern "3"	Discontinuous pattern "7"

Numbers in quotes are codes for indicated EEG patterns

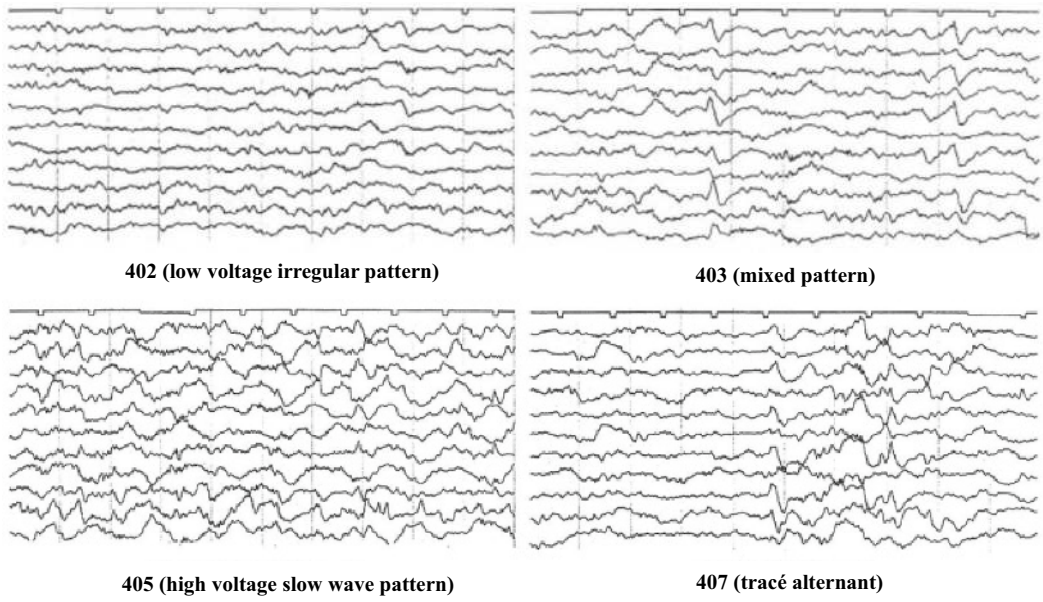

Fig. 4.1 Normal EEG findings at 40 weeks. A fundamental aspect of neonatal EEGs is the patterns observed at 40 weeks PMA. Sleep often begins with pattern 403; pattern 402 is frequently observed after pattern 407. In AS, the baseline can be traced in patterns 402 and 403. Pattern 402 consists of semirhythmic low-voltage waves alone; in pattern 403, high-voltage slow waves and sharp waves are intermittently superimposed on the semirhythmic low-voltage waves. In QS, pattern 405 is characterized by gradually increasing high-voltage slow waves, and it is impossible to trace the baseline because of continuous slow waves. Notably, the EEG shows continuous activity across all channels. As QS persists, startles occur (characterized by rapid jerking movements of the body); the increasing voltage of the chin electromyogram indicates a transition from pattern 405 to pattern 407

2 Changes in EEG Patterns Reflecting Brain Maturation

Brain functions rapidly mature in younger children; the rate of maturation slows with increasing age. This trend is also present regarding changes in the background EEG activities that reflect brain maturation. Although age-related differences in background EEG activities generally are not evident in adults, they can be distinguished at intervals of approximately 3 years in school-age children, 1 year in young children, and 3 months in infants (Fig. 4.2). The interval of discernible EEG changes according to age is presumed to reflect the rate of brain maturation. During the neonatal period, brain development occurs more rapidly than in infancy, such that changes in background EEG activities are discernible at 2-

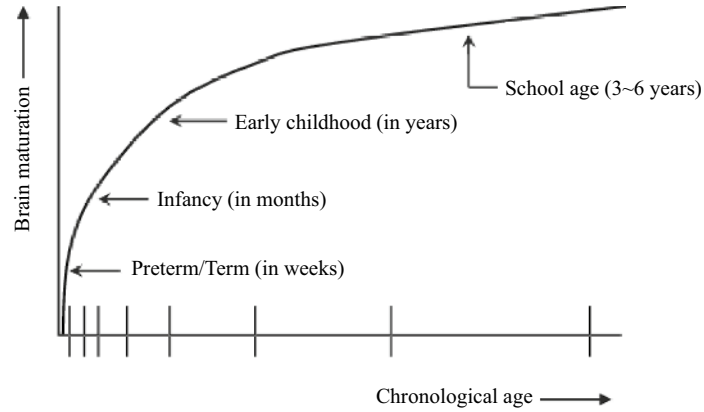

Fig. 4.2 Differences in the rate of brain maturation with age

to 4-week intervals. The rate of brain maturation is considered to be similar, regardless of whether a preterm infant is in utero or in the extrauterine environment. Assessment of EEG maturation is based on PMA, calculated as the gestational age plus the number of postnatal days.

The principles of EEG maturation up to 40 weeks PMA include increasing continuity as PMA increases, a decrease in slow wave size as PMA increases, and the presence of PMA-specific physiological transients. Accordingly, the maturation of EEG activities is based on two main principles: increased continuity of EEG activity and a decrease in the sizes of slow waves that represent major components of background EEG activities. Furthermore, the presence of PMA-specific physiological transients can help to determine EEG maturation. These principles will be explained in the following sections.

2.1 Principle of EEG Maturation 1: Continuity Increases with Maturation

A characteristic finding on neonatal EEGs is the presence of an alternating pattern during QS consisting of tracé alternant (TA) and tracé discontinu (TD). In extremely preterm infants, TD constitutes a large proportion of the EEG; the proportions of low-voltage irregular (LVI) and high-voltage slow (HVS) patterns increase with increasing PMA (Fig. 4.3). By 40 weeks PMA, the proportion of TA decreases to 20–30% (Fig. 4.4). These changes are suspected to reflect maturation of the central nervous system from 24 to 40 weeks PMA, and the proportion of continuous patterns in an EEG recording is useful for assessing brain maturation. Figure 4.5 illustrates a compressed EEG during AS. Conversely, the proportion of continuous patterns decreases when brain functions are suppressed. The continuity of an abnormal EEG may differ from the corresponding PMA-specific pattern.

Another indicator of increasing continuity with brain maturation is the interburst interval (IBI) in TA and TD. TA and TD consist of high- and low-voltage parts. The high-voltage part, also known as "burst," lasts for several seconds regardless of PMA. However, the IBI, which represents the duration of the low-voltage part between the high-voltage parts (i.e., bursts), can last 30–60 s in extremely preterm infants; it shortens to <10 s by 40 weeks PMA (Fig. 4.6). An IBI assessment is useful for estimating brain maturation (Fig. 4.7). Figure 4.8 shows a compressed EEG. An IBI lasts for >40 s at 28 weeks PMA, but it shortens to <10 s by 40 weeks PMA. The IBI duration increases when brain function is suppressed. It is important to consider that IBI-based estimations of brain maturation may be difficult in abnormal EEGs.

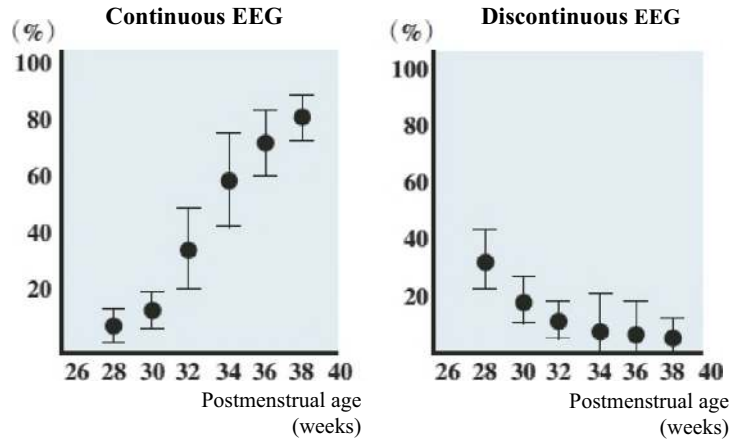

Fig. 4.3 Increase in the continuous pattern with brain maturation. Increased continuity of EEG activity is initially observed as an increase in the proportion of continuous patterns. The proportion of continuous patterns increases with increasing PMA, whereas discontinuous patterns gradually decrease with increasing PMA and are not observed after 40 weeks PMA

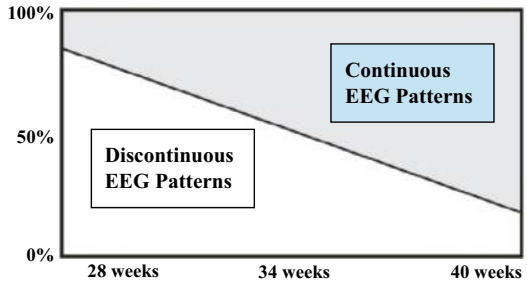

Fig. 4.4 Principle of EEG maturation 1: increased continuity. In neonatal EEGs, the proportion of continuous EEG patterns increases with brain maturation

2.2 Principle of EEG Maturation 2: A Less Mature Brain Produces Larger and More Monotonous Slow Waves

A neonatal EEG is characterized by the abundance of slow waves. During QS, the slow waves in the HVS pattern and high-voltage parts of the TA exhibit slower frequency, higher voltage, and more monotonous features compared with those aspects in older infants. These differences are more pronounced in preterm infants (Fig. 4.9). At 40 weeks PMA, the slow waves are polymorphous; their voltage is 100 μV and their frequencies are 2.5–3 Hz. Before 36 weeks PMA, slow waves are monotonous; their voltage and frequency are around 200 μV and 1 Hz at 32 weeks PMA, whereas they are approximately 300 μV and < 1 Hz at 28 weeks PMA. This change may reflect the development of cerebral projections; many cortical neurons initially respond to immature cerebral projections with monotonous signals, and smaller numbers of cortical neurons respond to well-differentiated complex cortical projections. Delta waves are monotonous and exhibit slow frequency with minimal mutual interference up to 36 weeks PMA. However, delta waves become polymorphous and mutual interference increases both temporally and spatially during the term period.

Note that the voltages and frequencies of delta waves are not constant, even in an EEG at a specific PMA. It is common to observe delta waves of various voltages and frequencies within a single EEG (Fig. 4.10). When interpreting an actual neonatal EEG, the voltages and frequencies of delta waves that are most predominant in an EEG should be considered. Empirically, the mean voltages and frequencies of slow waves are generally consistent at a particular PMA. It is important to understand PMA-specific voltages and frequencies when assessing EEG maturation.

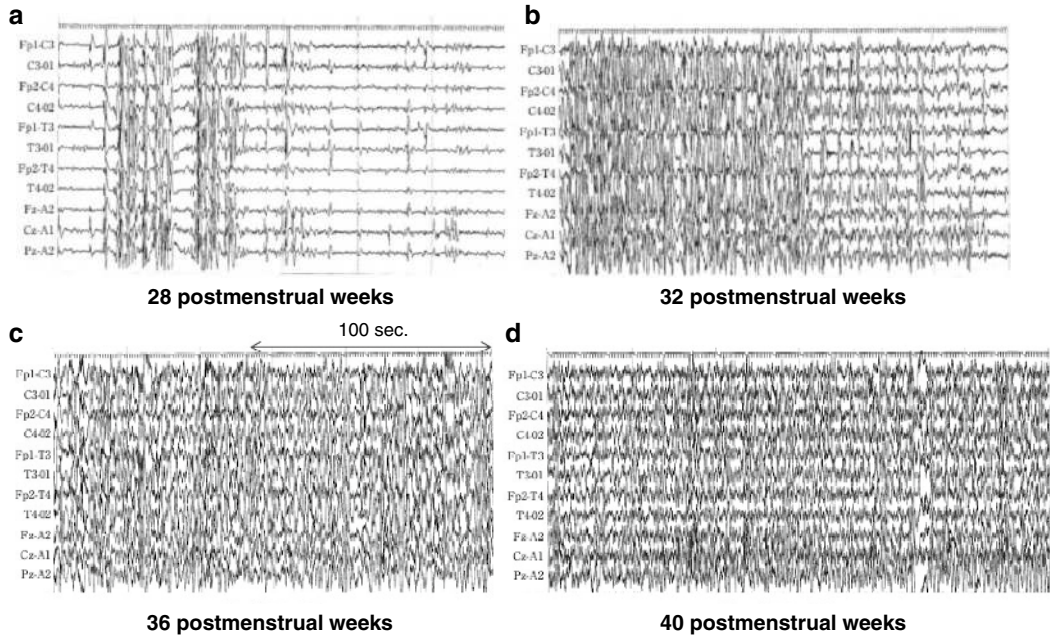

Fig. 4.5 Increased continuous pattern in compressed EEG. (**a**) At 28 weeks PMA, continuous patterns are observed during only a small proportion of active sleep (AS). (**b**) At 32 weeks PMA, continuous patterns are observed in more than half of AS, with higher-voltage activities. (**c**) Continuity increases at 36 weeks PMA in AS. (**d**) Voltage decreases at 40 weeks PMA in AS. The maturation process can be assessed to some extent simply by examining the compressed EEG

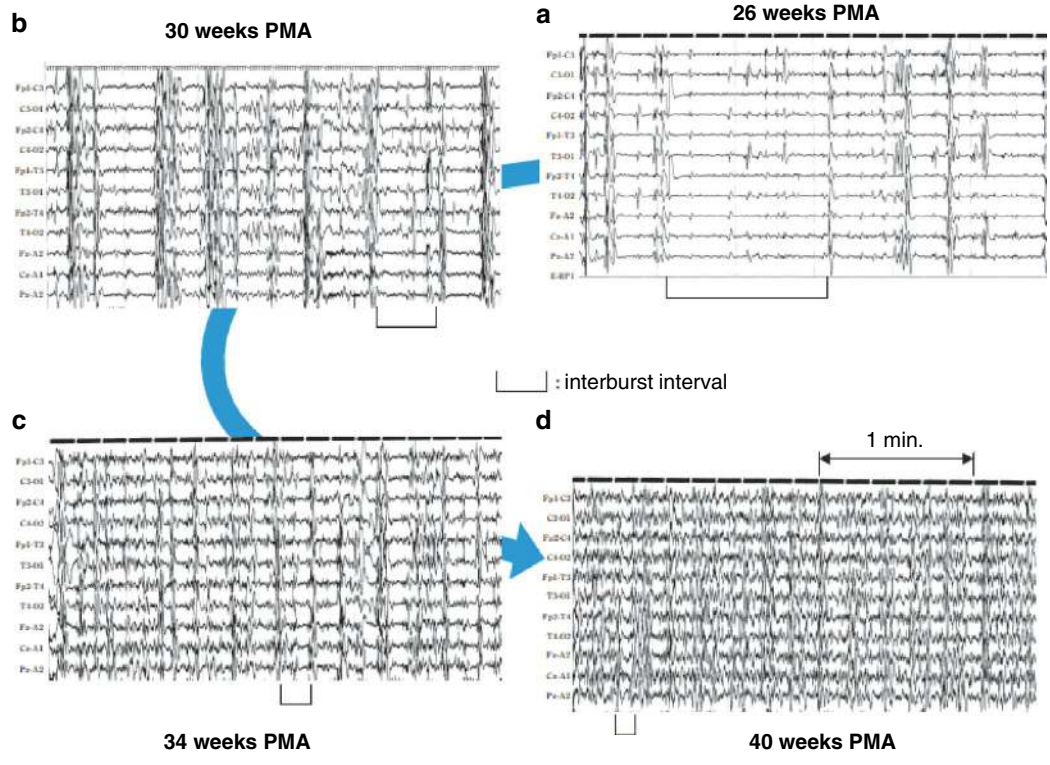

Fig. 4.6 Principles of EEG maturation 1: shortening the interburst interval. In neonatal EEGs, the interburst interval shortens with brain maturation. (**a**) 26 weeks PMA. (**b**) 30 weeks PMA. (**c**) 34 weeks PMA. (**d**) 40 weeks PMA

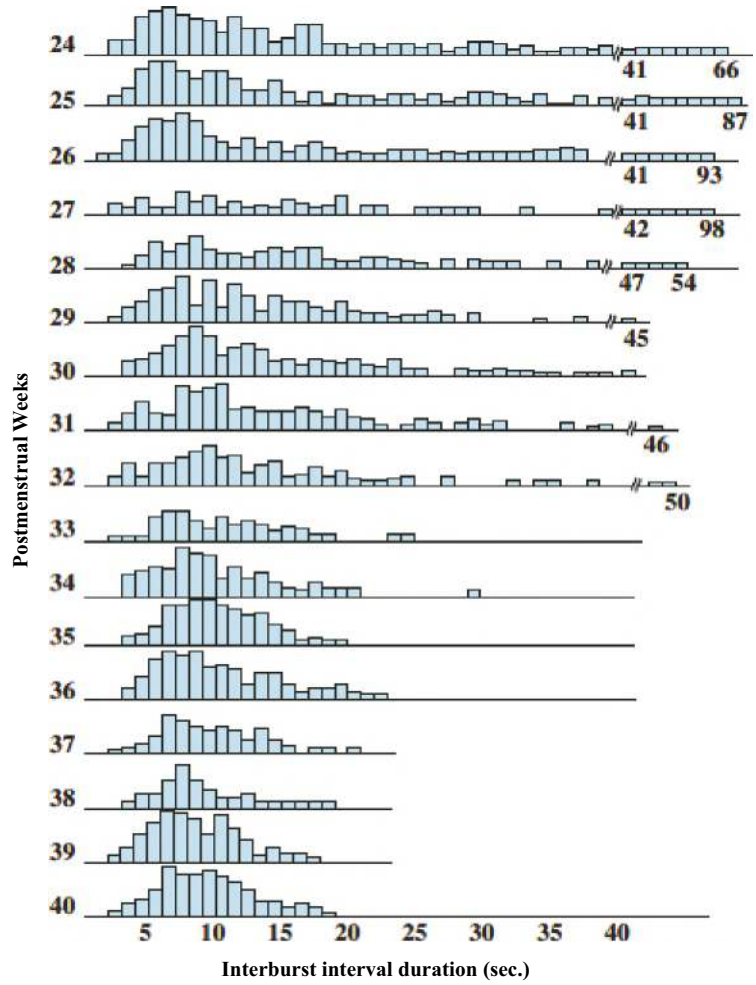

Fig. 4.7 Postmenstrual age and interburst interval

2.3 Principle of EEG Maturation 3: Characteristic Transients Appear According to PMA

In neonatal EEGs, physiological transients are observed according to PMA; for example, physiological spiky components resemble the vertex sharp waves and sleep spindles in EEGs of older children and adults. Because transients have characteristic locations and morphologies, it is possible to estimate brain maturation by focusing on these transients. When the features of physiological transients are understood, such features can be used to estimate the PMA, even when slow wave continuity and size are reduced by pathological conditions. Some transients can be misidentified as the paroxysmal discharges observed in older children with epilepsy. It is important to avoid misinterpreting physiological transients as pathological discharges.

Physiological transients in neonates are outlined below, with some examples. Table 4.2 summarizes developmental changes in physiological transients that are observed in neonatal EEGs.

2.3.1 Physiological Transients in Preterm Infants

Typical transients during the preterm period include frontal sharp bursts, occipital sharp bursts, high-amplitude theta, rhythmic temporal theta, and brush/delta brush (Fig. 4.11). In extremely preterm infants up to 26 weeks PMA, the most characteristic transients are frontal and occipital sharp bursts. In such infants, high-

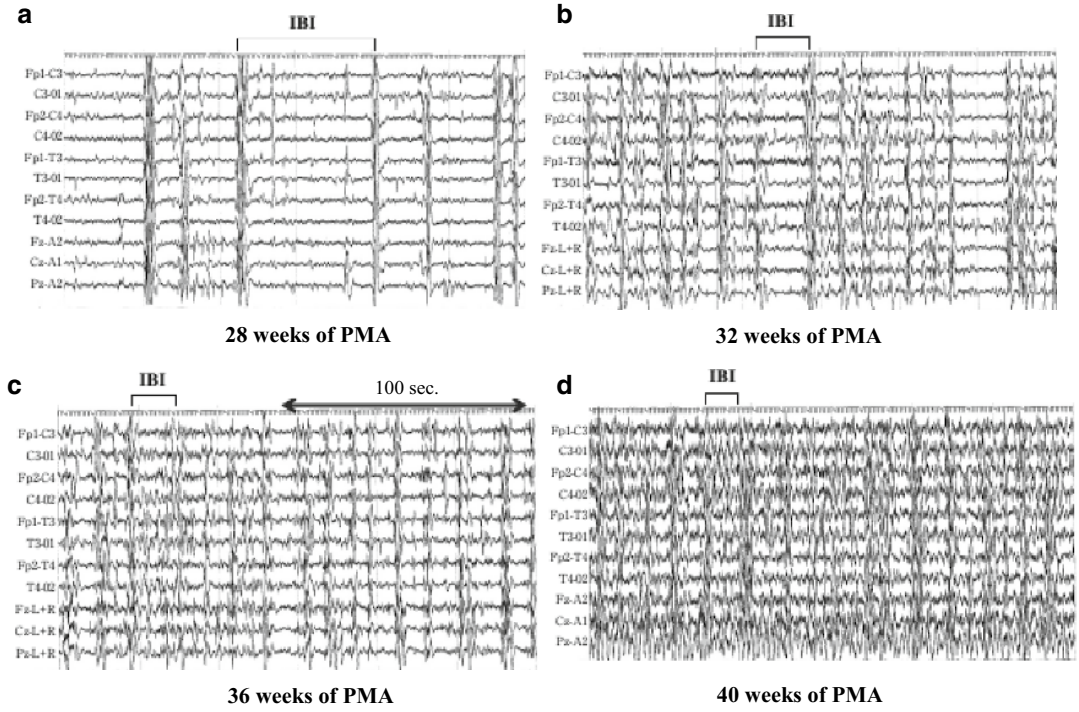

Fig. 4.8 Shortening of the interburst interval in a compressed EEG. (**a**) At 28 weeks PMA, most interburst intervals (IBIs) are longer than 20 s, and they sometimes last 40–60 s (**b**) At 32 weeks PMA, IBIs are around 10 s and can reach 15–20 s. (**c**) At 36 weeks PMA, the mean IBI is 7–10 s, and no IBI exceeds 20 s. (**d**) At 40 weeks PMA, the mean IBI is a few seconds, and no IBI exceeds 10 s. The maturation process can be partially assessed by examining alternating or discontinuous patterns in a compressed EEG. In acute-stage abnormalities, reduced continuity is the most common finding, making it difficult to determine if an IBI is physiological or pathological without knowing the PMA-specific IBI durations

amplitude theta waves and brushes are rare. Frontal and occipital sharp bursts are typical transients observed in this extremely premature period.

Two weeks later (28 weeks PMA), the characteristics of the transients change, such that high-amplitude theta and brushes become predominant. Additionally, the numbers of brushes gradually increase after this PMA.

By 30 weeks PMA, transients from temporal regions evolve from sharp waves into rhythmic theta waves with a round shape, known as rhythmic temporal theta.

The brush, a well-known characteristic transient in preterm infants, most frequently appears at 32–34 weeks PMA. A brush is often superimposed on the ascending slopes of the delta waves. In this context, it is regarded as a delta brush. Delta brushes have been described under many terms, including beta-delta complexes, spindle-delta bursts, spindle-like fast waves, or ripples of prematurity. Watanabe et al. reported that the brushing frequency in AS rapidly decreases after 32 weeks PMA, but this decrease is less pronounced in QS prior to 36 weeks PMA (Fig. 4.12) (Watanabe 1972).

Despite substantial differences among infants, the approximate PMA-specific frequencies of brushes can be used to determine PMA. However, the physiological localization and synchrony of brushes have not been elucidated.

2.3.2 Physiological Transients in Term Infants

Physiological transients observed in term infants include frontal sharp transients (also known as encoches frontales), bi-frontal slow burst (also known as anterior dysrhythmia), Fz/Cz theta/

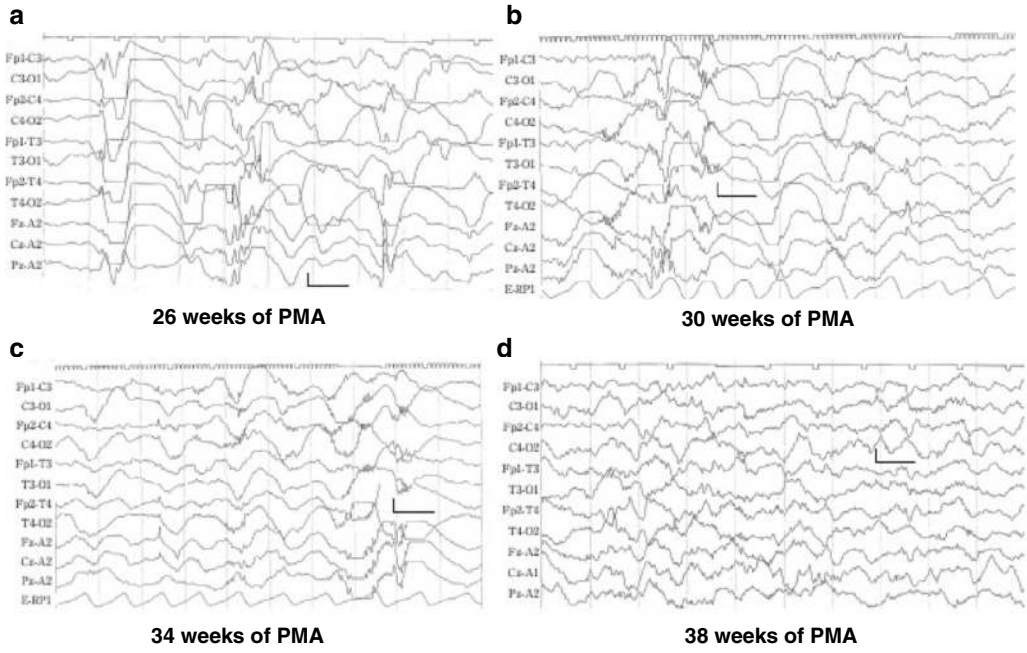

Fig. 4.9 Changes in slow waves according to PMA. (**a**) Until 26 weeks PMA, the voltage of slow wave often exceeds 300 μV and the frequency is usually <1 Hz. (**b**) At 30 weeks PMA, the voltage of slow wave is 200–300 μV and the frequency is around 1 Hz. (**c**) Until 34 weeks PMA, monotonous slow waves with a voltage of 200 μV and a frequency of 1.5–2 Hz are predominant. (**d**) At 38 weeks PMA, polymorphous slow waves with voltages of 100–150 μV and frequencies of 2–2.5 Hz are observed. EEG maturation can be approximated based on the shapes and sizes of the slow waves. It can also be determined by evaluating continuity and age-specific transients

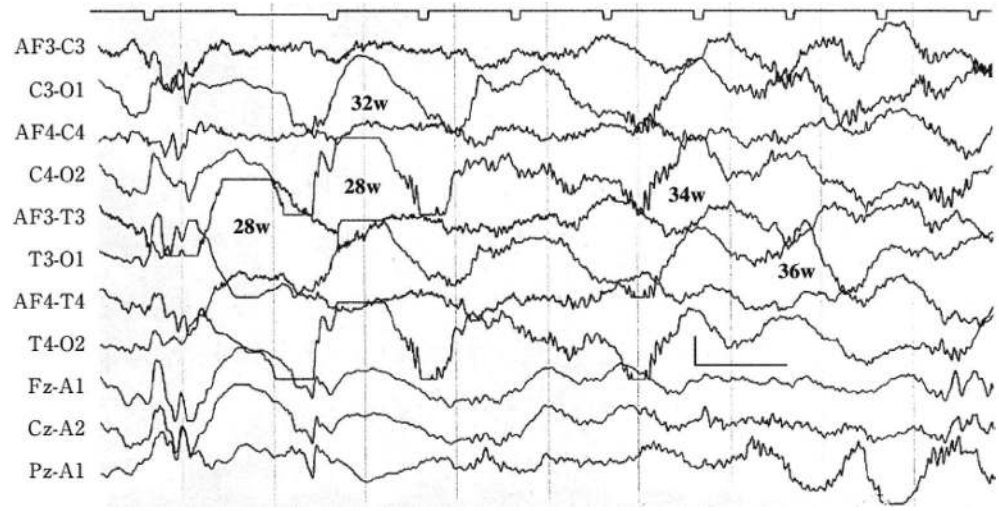

Fig. 4.10 Mixtures of slow waves at various PMAs. Slow waves of specific sizes are not always observed in EEGs at a particular PMA. In most cases, slow waves of various voltages and frequencies appear within a single EEG. It is important to note the sizes of frequent/predominant slow waves. Empirically, slow waves of intermediate size correspond to the PMA

Table 4.2 Summary of maturational changes in neonatal EEGs

PMA (weeks)	Slow waves	IBI in TA/TD (s)	Brush occurrence	PMA-specific transients
≤ 26	< 1 Hz, 300–400 μV	20–80	Not observed	Frontal sharp bursts, occipital sharp bursts
27–28	Around 1 Hz, around 300 μV	20–60	Rare	High-amplitude theta
29–30	1–1.5 Hz, 200–300 μV	10–30	Infrequent	Rhythmic temporal theta
31–32	Around 1.5 Hz, around 200 μV	10–20	Frequent	Few transients
33–34	1.5–2 Hz, 150–200 μV	10–15	Frequent	Temporal sharp transients sometimes appear
35–36	Around 2 Hz, around 150 μV	5–15	Somewhat frequent	Temporal sharp transients
37–38	≥ 2 Hz, Around 100 μV	5–10	Infrequent	Frontal sharp transients, bi-frontal slow bursts
39–40	≥ 2 Hz, Around 100 μV	3–8	Rare	Frontal sharp transients, bi-frontal slow bursts
41–42	≥ 2 Hz, Around 100 μV	2–3	Not observed	Few transients

TA tracé alternant, *TD* tracé discontinu, *IBI* interburst interval

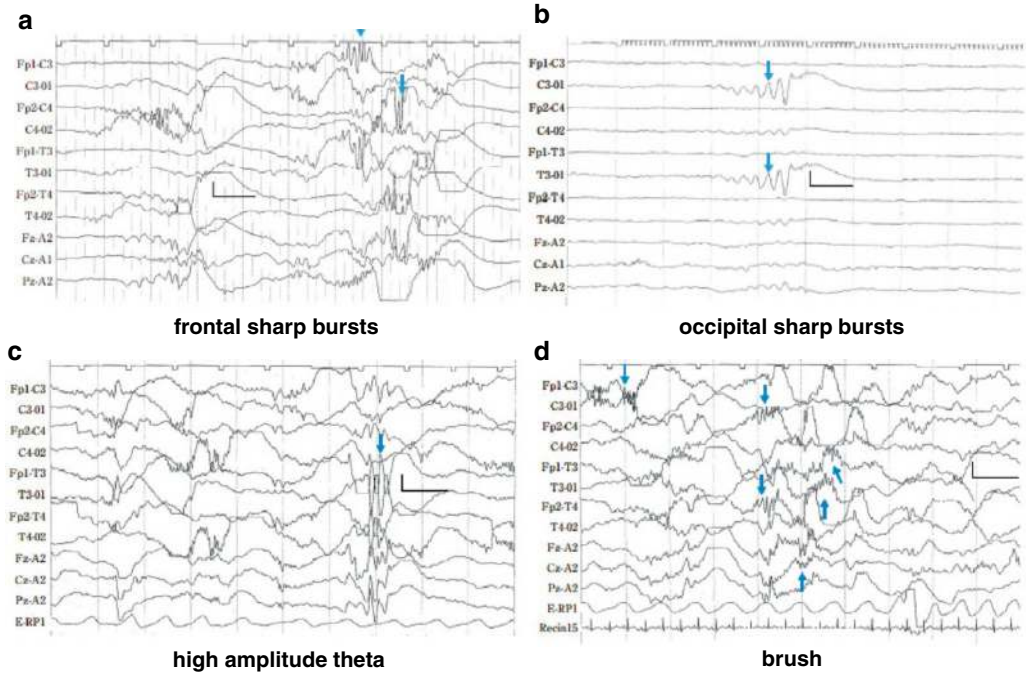

Fig. 4.11 Typical transients during the preterm period. By 26 weeks PMA, frontal (**a**) and occipital (**b**) sharp bursts are characteristic, whereas transients from temporal regions are rare. Two weeks later, high-amplitude theta (**c**) becomes predominant; brushes (**d**) are most frequent at 32–34 weeks PMA

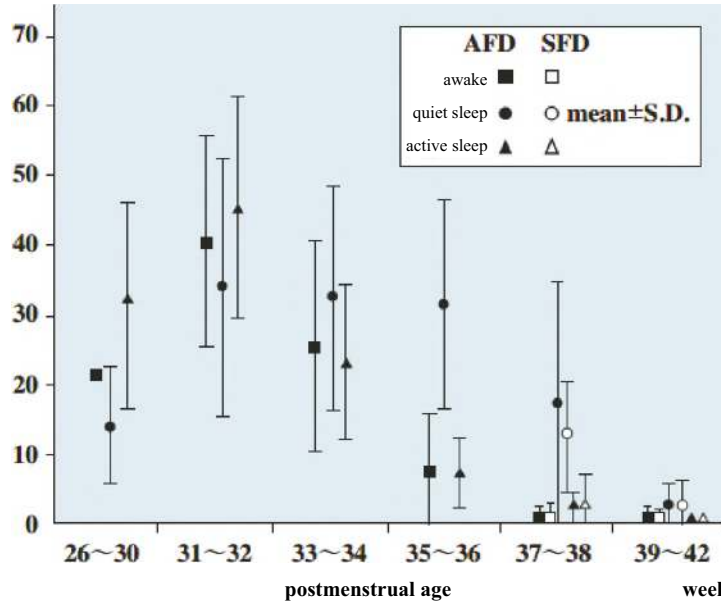

Fig. 4.12 Incidence of brush according to postmenstrual age. Brushes, a typical transient during the preterm period, are most frequent at 32–34 weeks PMA. Until 36 weeks PMA, their frequency rapidly declines in AS but slowly decreases in QS. Despite differences among individual infants, knowing the approximate incidence of brushes by PMA is helpful in estimating PMA. *AFD* appropriate for date, *SFD* small for date

alpha bursts, Fz/Cz rhythmic alpha, and temporal sharp transients.

The frequencies of frontal sharp transients, bifrontal slow bursts, and their composite waveforms are shown in Fig. 4.13. None of these transients appear before 34 weeks PMA, but they frequently appear at 36–40 weeks PMA. However, these transients may be absent in 20–30% of normal-term infants and an EEG should not be considered abnormal solely on the basis of their absence.

2.3.3 Comparison of Transients Between Term and Preterm Infants

Transients from Frontal Regions

When interpreting a neonatal EEG, the focus should be on the frontal regions at two different time points: the extremely preterm (22–26 weeks PMA) and term (36–42 weeks PMA) periods. As shown in Fig. 4.14, frontal sharp bursts in the extremely preterm period are sharp, whereas frontal sharp transients in the term period represent biphasic waves; there is a clear morphological difference. It is not difficult to distinguish between these patterns; frontal sharp bursts are characterized by large slow wave background activities, and frontal sharp transients exhibit polymorphic background activities. The maturation of EEG activities can be assessed by focusing on slow waves and characteristic transients in background EEG activities.

Transients from Temporal Regions

Transients from temporal regions are infrequent up to 26 weeks PMA; the frequency of these transients rapidly increases at 28 weeks PMA. The high amplitude and sharp activities often observed at 28 weeks PMA are known as "high-amplitude theta"; these activities are a characteristic waveform in extremely preterm infants. By 30 weeks PMA, the transients become rhythmic theta waves, known as "rhythmic temporal theta." At 32–34 weeks PMA, transients from temporal regions become less frequent. Around 36 weeks PMA, irregular sharp transients become more frequent, mainly during QS. At 36–40 weeks PMA, a single biphasic temporal sharp transient appears, as shown in Fig. 4.15.

Frontal sharp bursts are most frequent at 25–26 weeks PMA. They become less frequent by 28 weeks PMA and are rarely observed at ≥30 weeks PMA. These bursts are sharp, high-voltage, and usually clustered (indicated by blue arrows). Notably, this waveform is physiological and normal for 22–26 weeks PMA (Fig. 4.16).

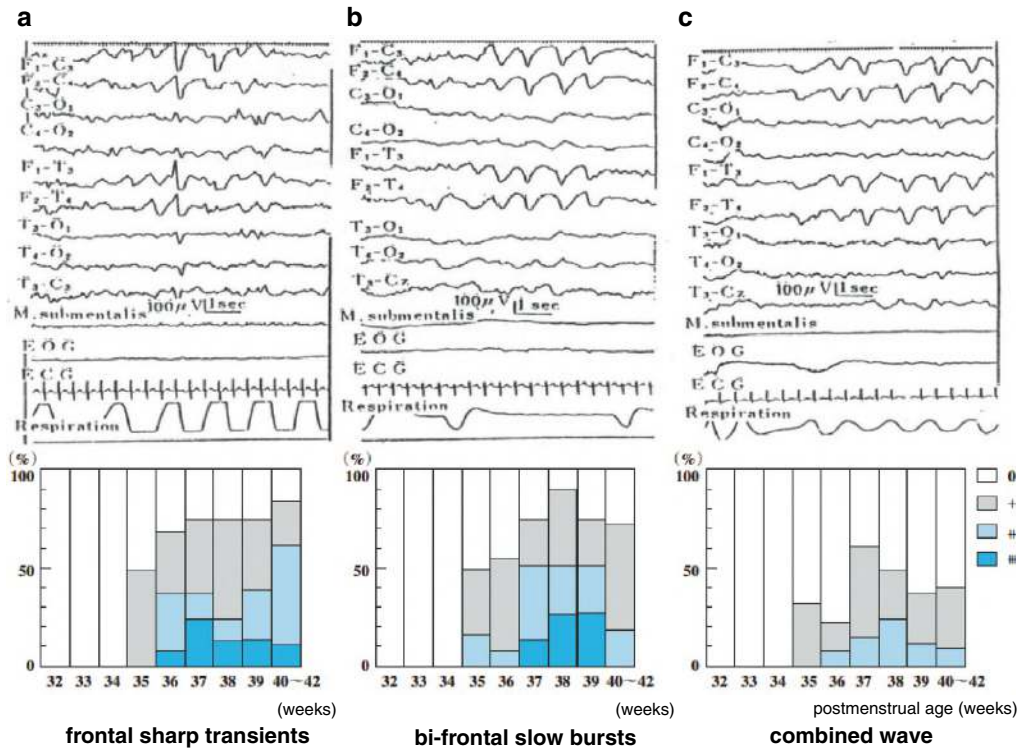

Fig. 4.13 Incidences of frontal sharp transients (**a**), bi-frontal slow bursts (**b**), and their composite waves (**c**). These transients do not appear until 34 weeks PMA; they become increasingly frequent between 36 and 40 weeks PMA. However, these transients are absent in 20–30% of healthy-term infants. An EEG should not be considered abnormal solely on the basis of the absence of these transients

Occipital sharp bursts appear during 22–26 weeks PMA (blue arrows). They appear most frequently at 25–26 weeks PMA and decrease at 28–30 weeks PMA. Frontal and occipital sharp bursts often become prominent at 25–26 weeks PMA. During this period, fast wave components are rare in background EEG activities. These waveforms suggest that the EEG was recorded at a very immature stage of brain development (Fig. 4.17).

These unique transients are specific to 28 weeks PMA (blue arrow). At this stage, a group of sharp waves with extremely high amplitude often appears at the beginning of the slow wave. These transients may sometimes be evident at 26–30 weeks PMA. However, the frequent appearance of high-amplitude theta is a strong indicator of 28 weeks PMA (Fig. 4.18).

At 30 weeks PMA, temporal transients exhibit lower voltage (100–200 μV) and tend to form a rhythmic cluster of a few bursts, each lasting approximately 1 s (blue arrow). These transients are highly age-specific and usually become rare by 32 weeks PMA. The presence of rhythmic temporal theta transients indicates that the infant is around 30 weeks PMA (Fig. 4.19).

Transients observed in extremely preterm infants at 22–26 weeks PMA include both frontal and occipital sharp bursts. Brushes are spindle-like fast waves evident throughout the preterm period, including 22–26 weeks PMA. After 28 weeks PMA, rhythmic temporal theta transients become more prominent, and the occurrence of brush increases. However, until 26 weeks PMA, the characteristic feature is a combination of high-voltage and low-frequency slow waves (> 300–400 μV, < 1 Hz), along with frontal and occipital sharp bursts (Fig. 4.20).

Brushes are the most well-known features in EEGs of preterm infants (blue arrows). These

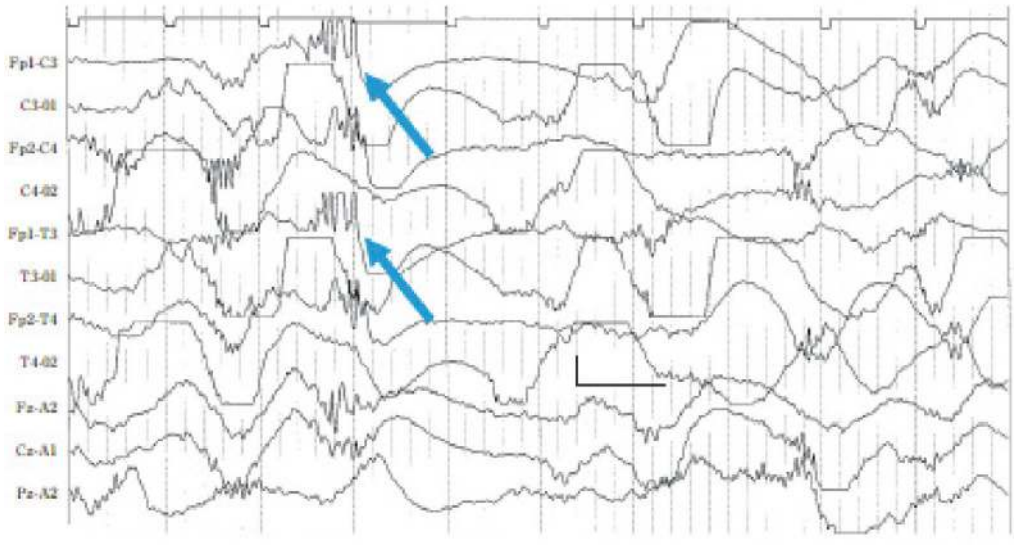

frontal sharp bursts at 26 weeks PMA

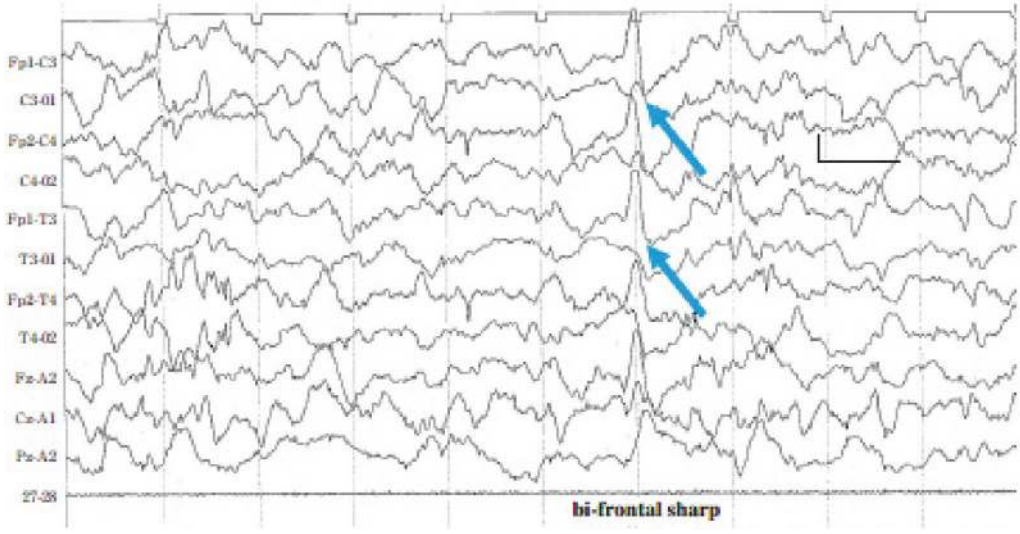

frontal sharp transients at 40 weeks PMA

Fig. 4.14 Transients from frontal regions: immature and mature. Physiological transients from frontal regions are frequently observed in the extremely preterm and term periods. In contrast, during 30–34 weeks PMA, transients from frontal regions are rarely observed. The waveforms of transients clearly differ between "frontal sharp bursts" at 26 weeks PMA and "frontal sharp transients" at term

features are often superimposed on the ascending slope of delta waves. In this context, they are regarded as delta brushes. Brushes are less frequent at 24–26 weeks PMA but increase beginning at 28 weeks PMA; they become most frequent at 32–34 weeks PMA. At 36–38 weeks PMA, they appear only during quiet sleep and are rarely observed after 40 weeks PMA (Fig. 4.21).

Frontal sharp transients are highly characteristic of term infants. Biphasic sharp waves (blue arrows) appear in frontal regions either bilaterally or unilaterally. At 38–40 weeks PMA, the presence of these waves indicates the transition from a low-voltage irregular pattern to a mixed pattern. Such waves often appear during quiet sleep and sometimes during the high-voltage part of the

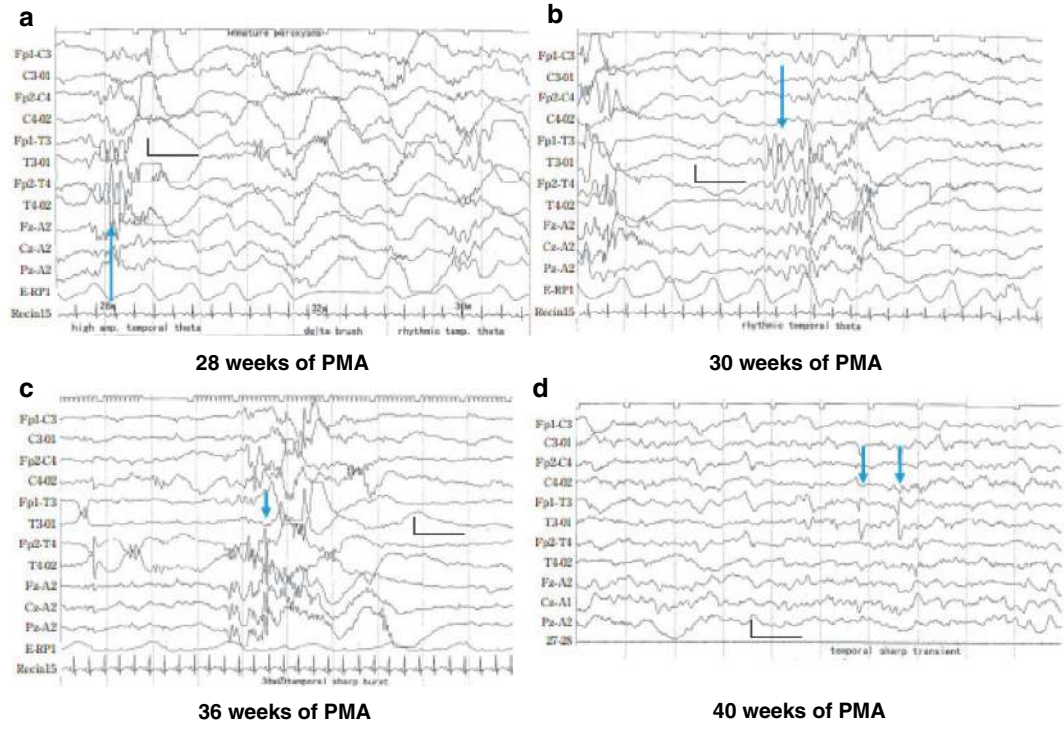

Fig. 4.15 EEG maturation and temporal transients (**a**, 28 weeks of PMA; **b**, 30 weeks of PMA; **c**, 36 weeks of PMA; and **d**, 40 weeks of PMA). Many characteristic transients from temporal regions are observed as the brain matures from the preterm period to the term period. Because the morphological features of temporal transients are closely related to PMA, they are useful indicators for determining EEG maturation. It is important to understand the morphologies of these transients in relation to PMA

tracé alternant pattern. The presence of these waves is indicative of a term infant (Fig. 4.22).

Bi-frontal slow burst is one of the transients, representative of the term period. Serial bowl-shaped slow waves of 1.5–2 Hz appear for 2–3 s in the bilateral frontal regions (blue arrows). At 38–40 weeks PMA, the presence of this transient indicates the transition from a low-voltage irregular pattern to a mixed pattern. Additionally, Fz rhythmic alpha, indicated by the black line, is sometimes present, suggesting that frontal sharp transients and bi-frontal slow bursts reflect brain maturation corresponding to the near-term and term periods (Fig. 4.23).

Fz/Cz theta/alpha bursts (blue arrows) are sharp-wave bursts emerging from the frontal or central midline. These characteristic transients rarely spread to Fp1, Fp2, C3, or C4; they almost exclusively appear on the midline. They are often observed during QS and are much less frequent than frontal sharp transients or bi-frontal slow bursts. Fz/Cz theta/alpha bursts should not be misinterpreted as ictal discharges (Fig. 4.24).

Fz/Cz rhythmic alpha (black lines) is a low-amplitude rhythmic activity that appears in the midline of the frontal and central regions after 36 weeks PMA. This waveform is an 8 Hz alpha without exception lasting for 1–3 s. Although it is usually observed during QS, it is less frequent than Fz/Cz theta/alpha bursts (see, Fig. 4.24). Even at 40 weeks PMA, it is present in fewer than 10% of infants. This type of wave may selectively appear in the low-voltage part of the tracé alternant, and it is important to avoid misinterpreting such a wave as an ictal discharge (Fig. 4.25).

At 32–34 weeks PMA, a few sharp/theta components are observed, whereas slow waves and brushes are abundant. At 36 weeks PMA, a notable change is evident, particularly in the tracé alternant (TA) patterns in QS. The appearance of background EEG activity implies poor organization due to sharp-wave transients and brushes.

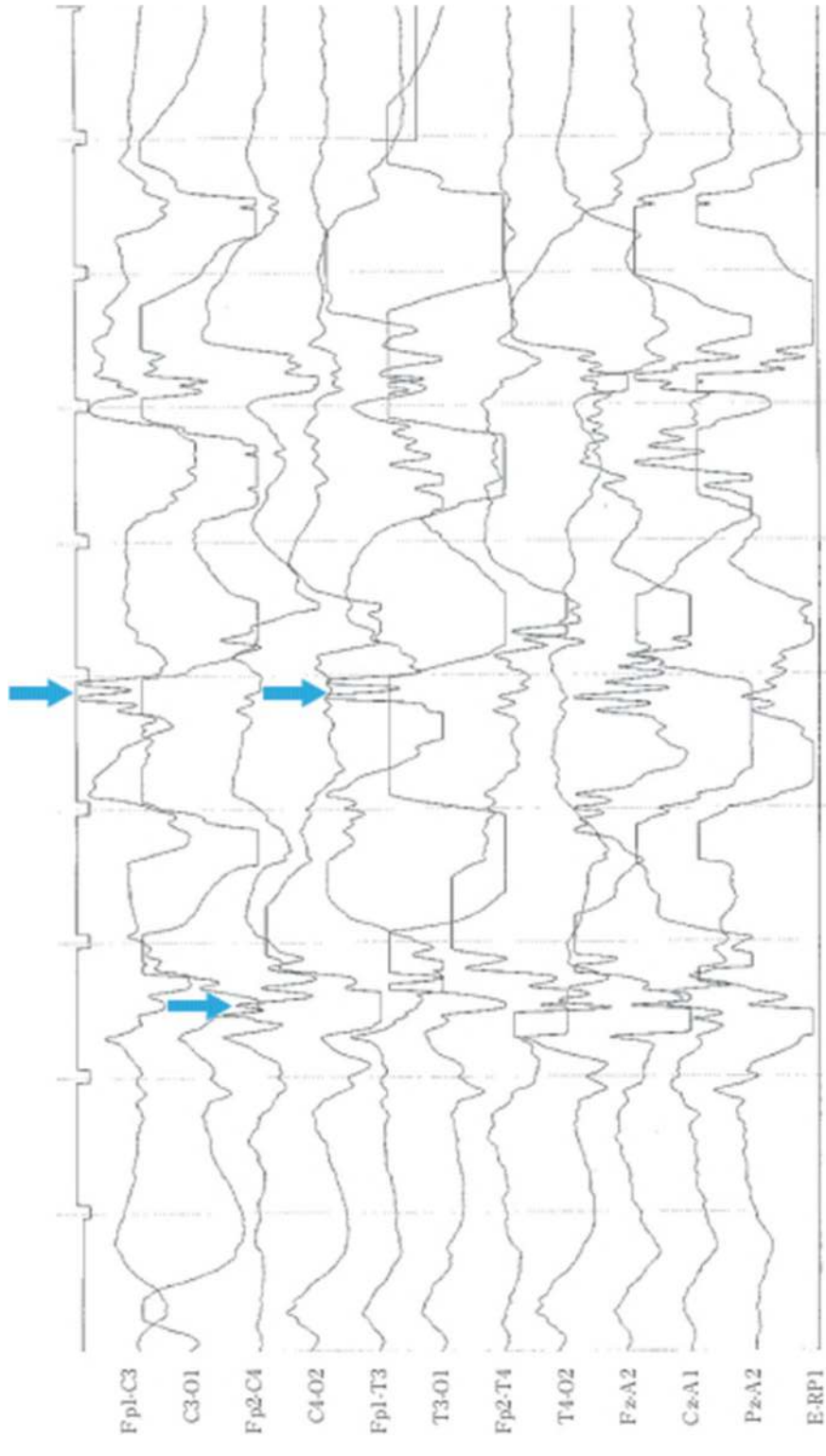

Fig. 4.16 Frontal sharp bursts (22–26 weeks PMA)

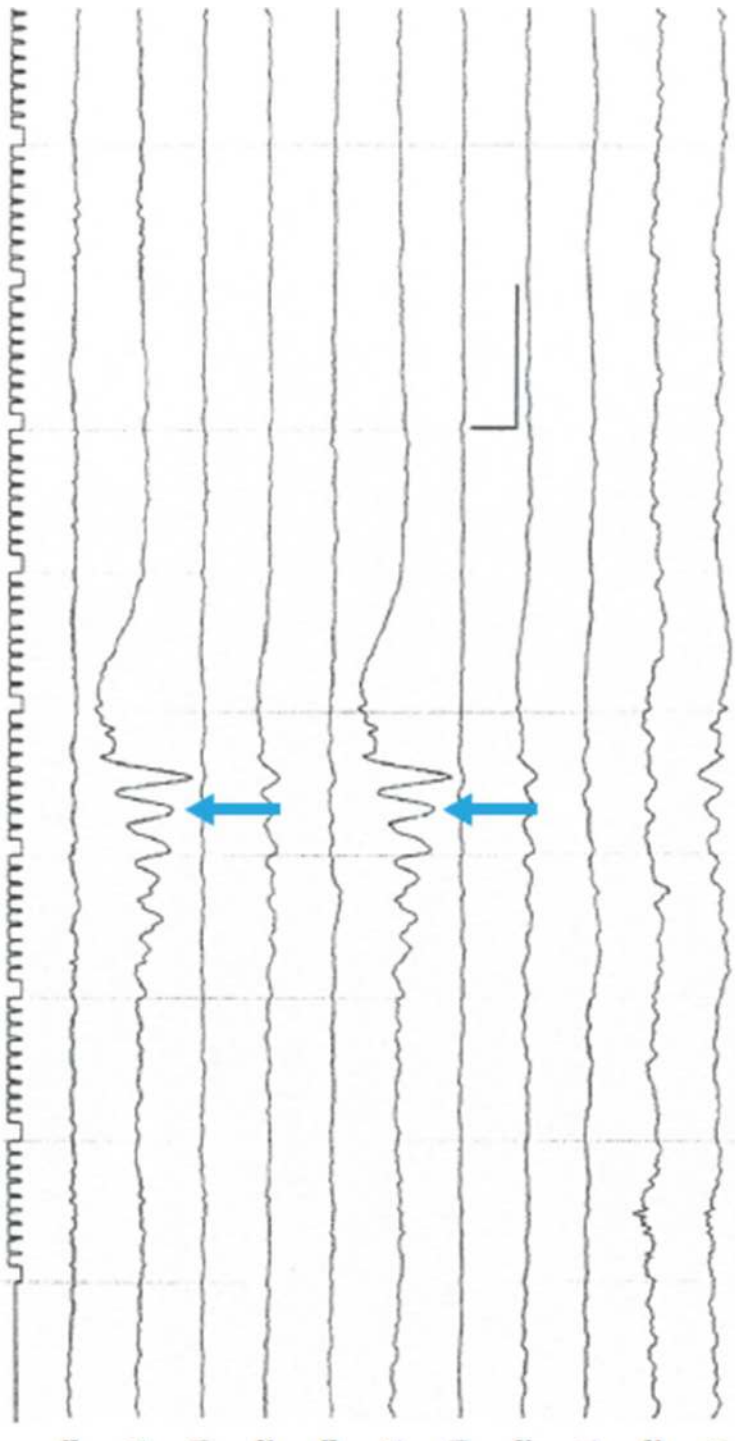

Fig. 4.17 Occipital sharp bursts: physiological transients during the preterm period (22–26 weeks PMA)

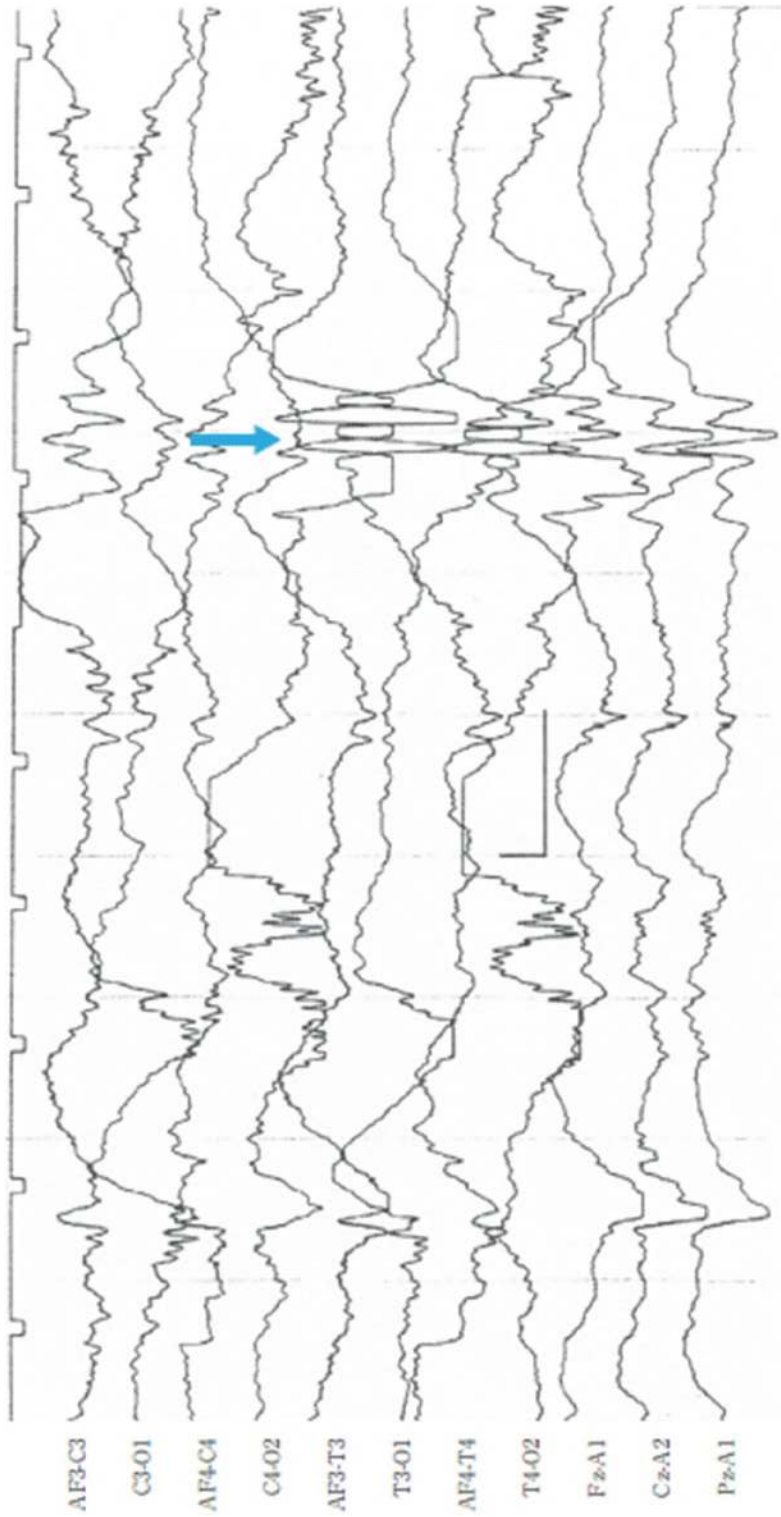

Fig. 4.18 High-amplitude theta (28 weeks PMA)

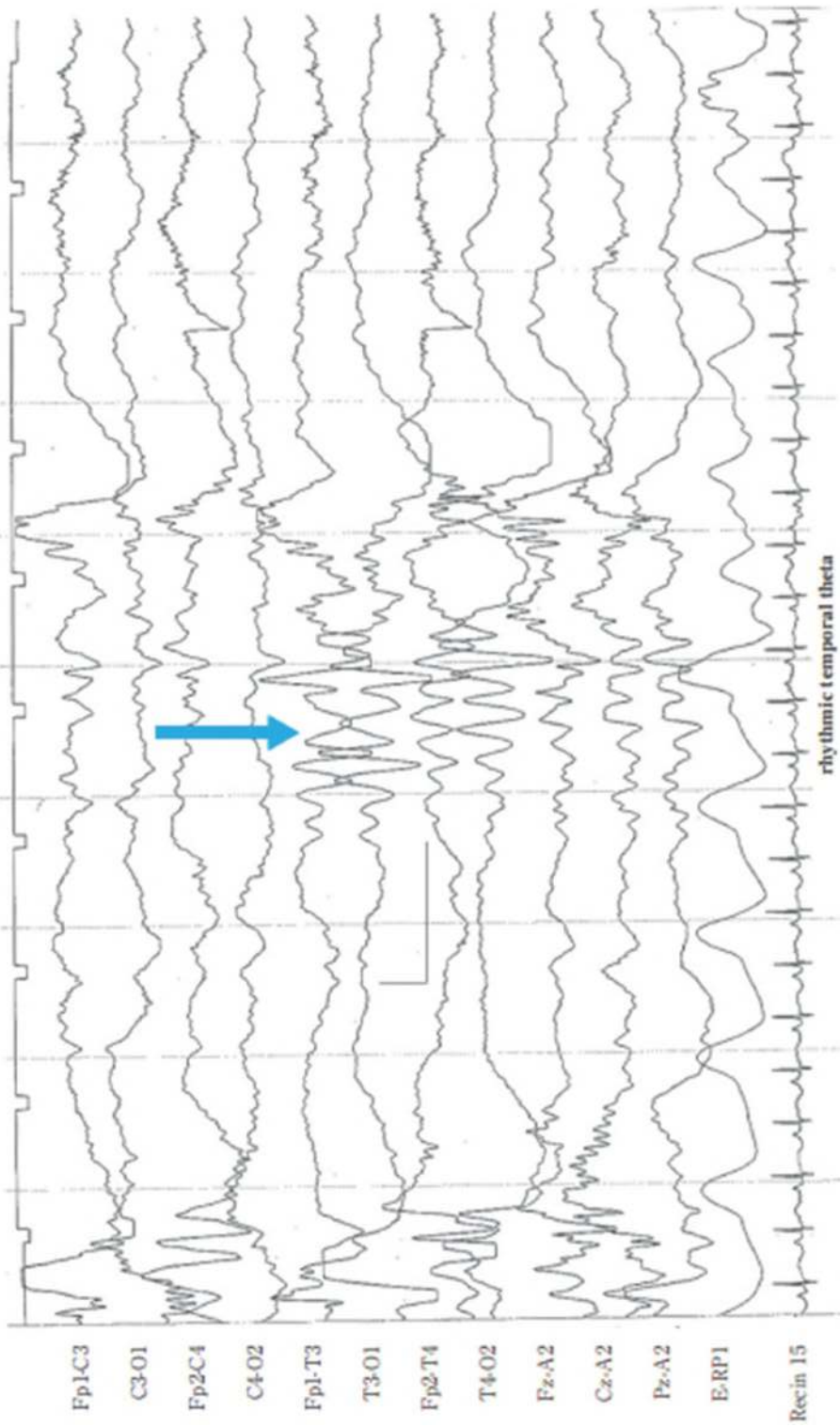

Fig. 4.19 Rhythmic temporal theta (30 weeks PMA)

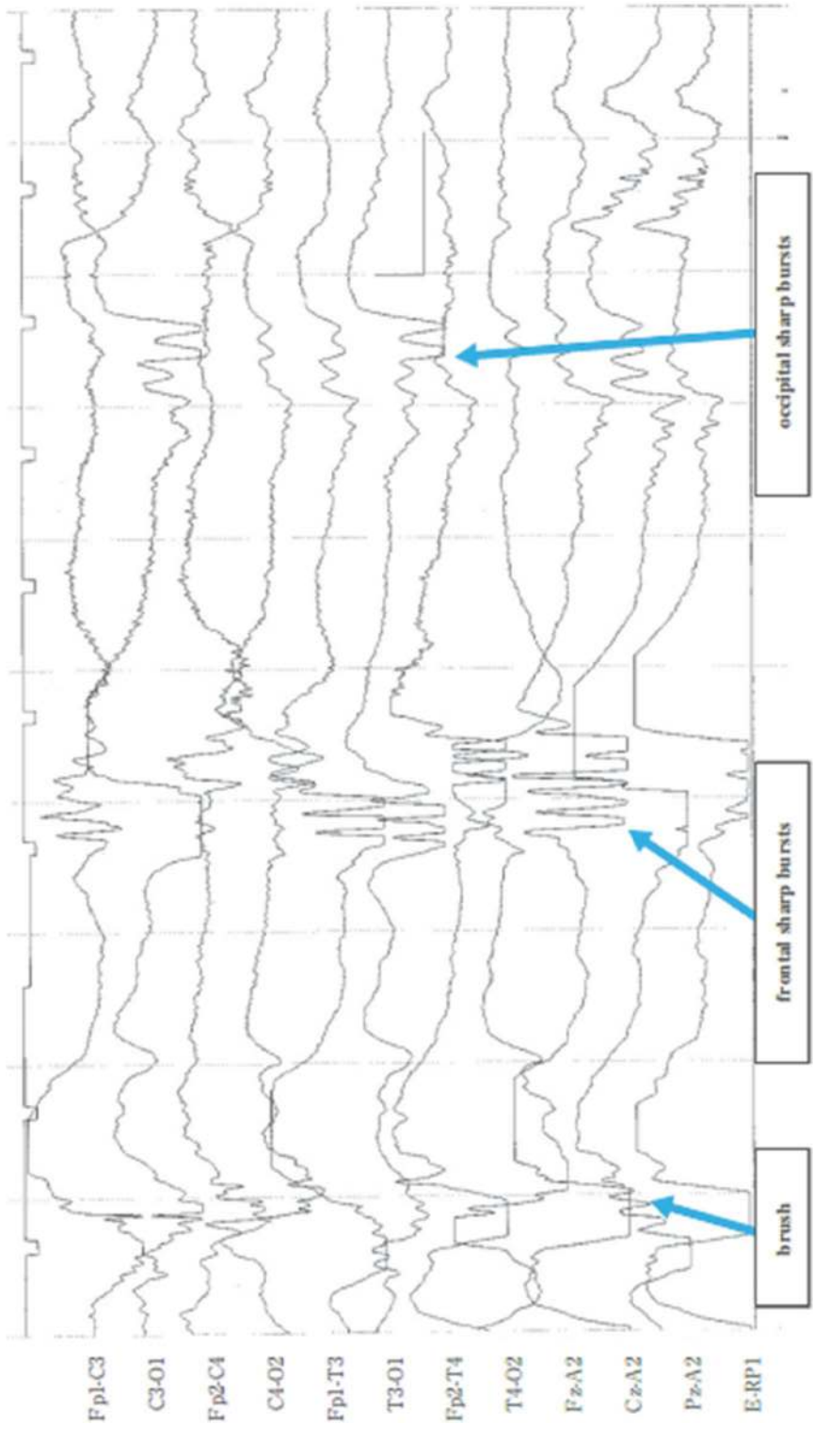

Fig. 4.20 Transients reflecting immaturity

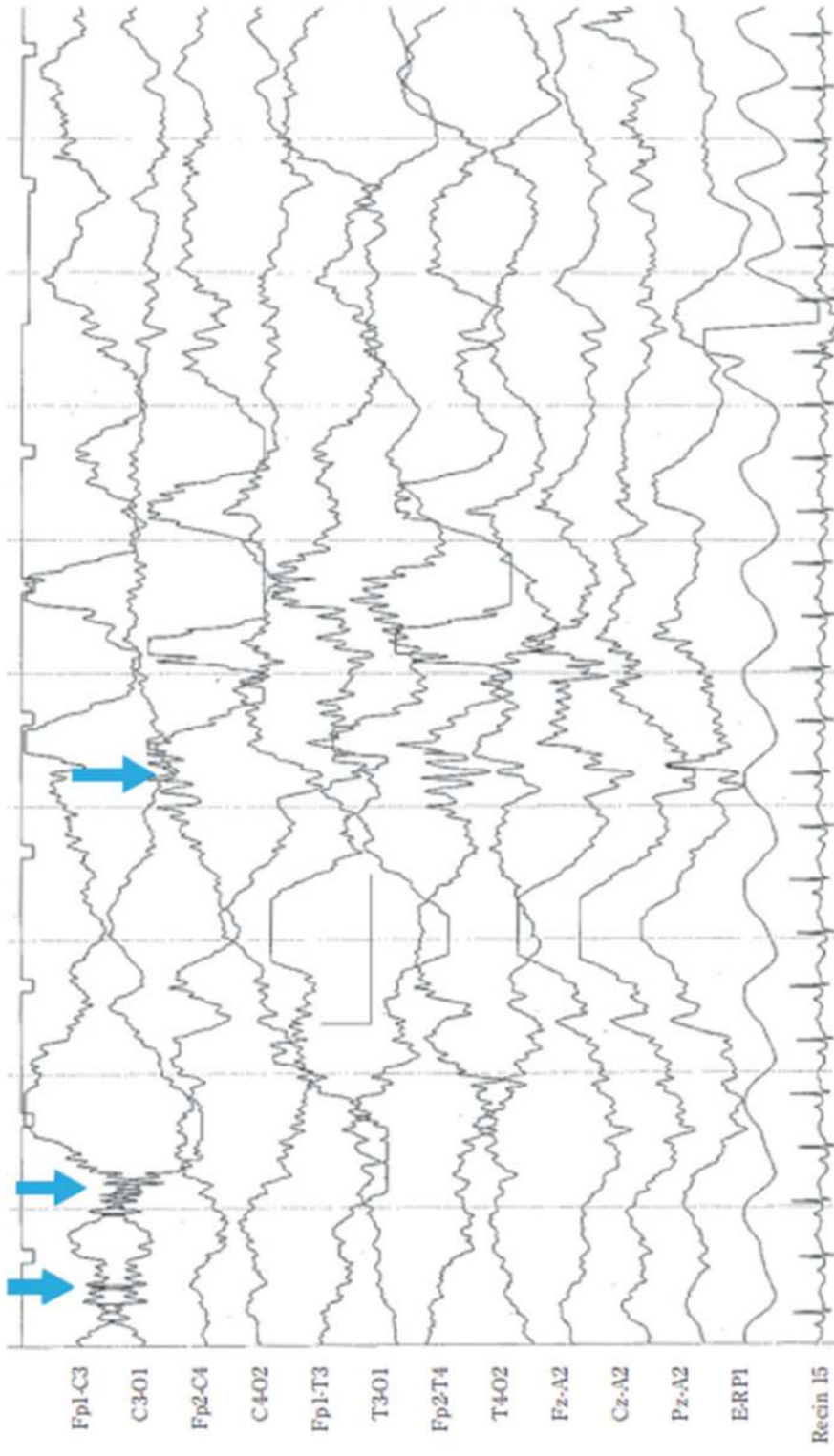

Fig. 4.21 Brush, spindle-like fast waves (28–36 weeks PMA)

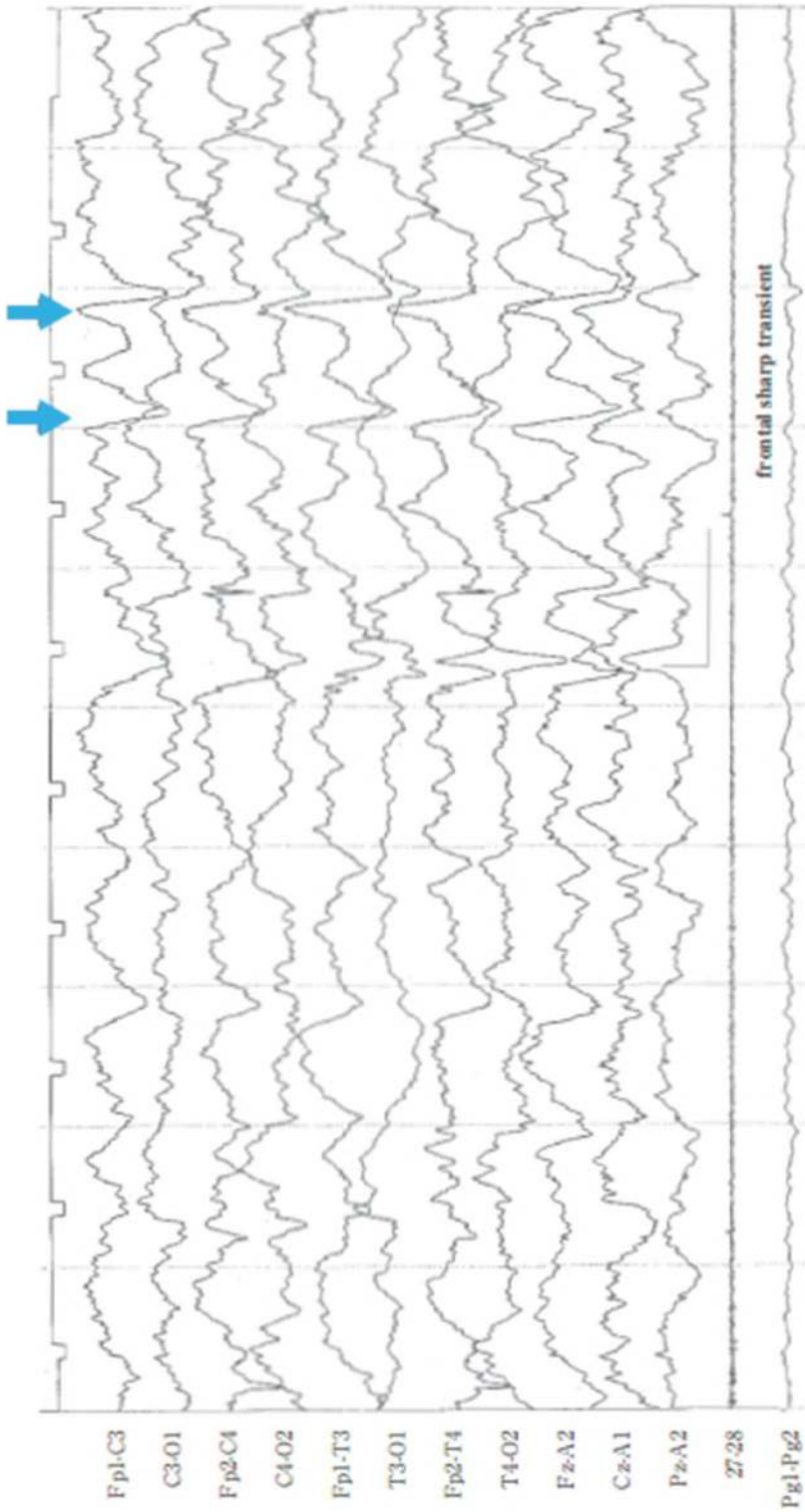

Fig. 4.22 Frontal sharp transients

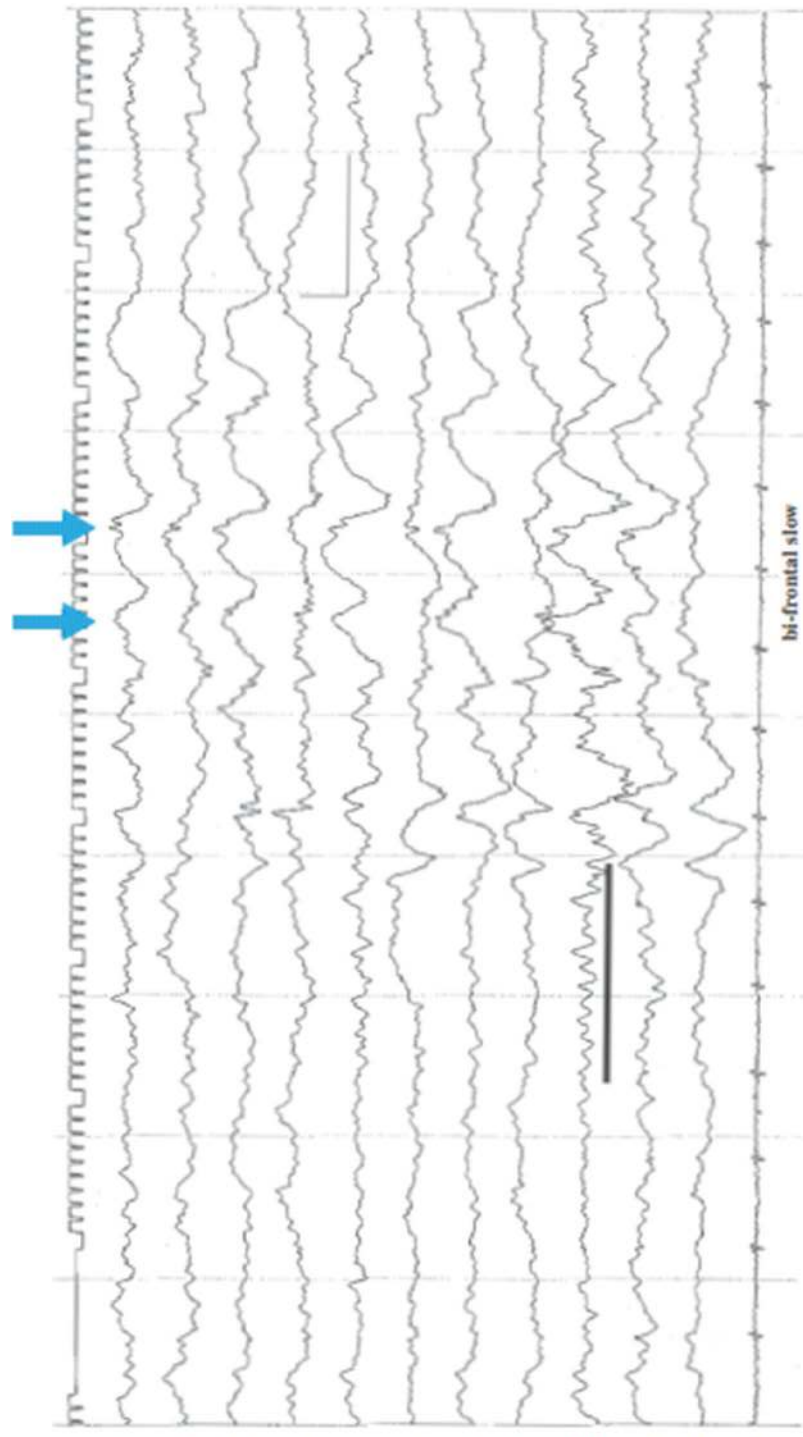

Fig. 4.23 Bi-frontal slow bursts

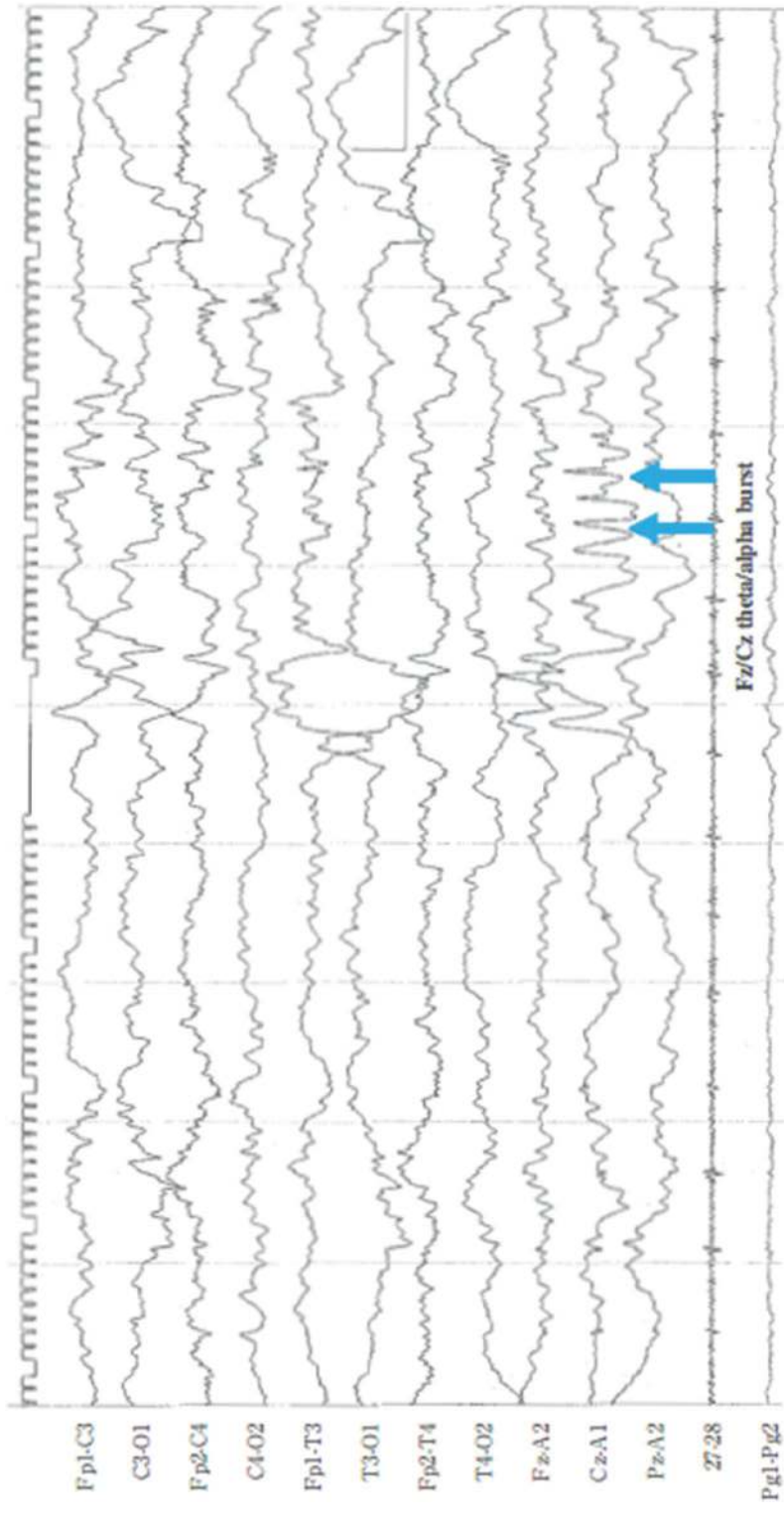

Fig. 4.24 Fz/Cz theta/alpha bursts

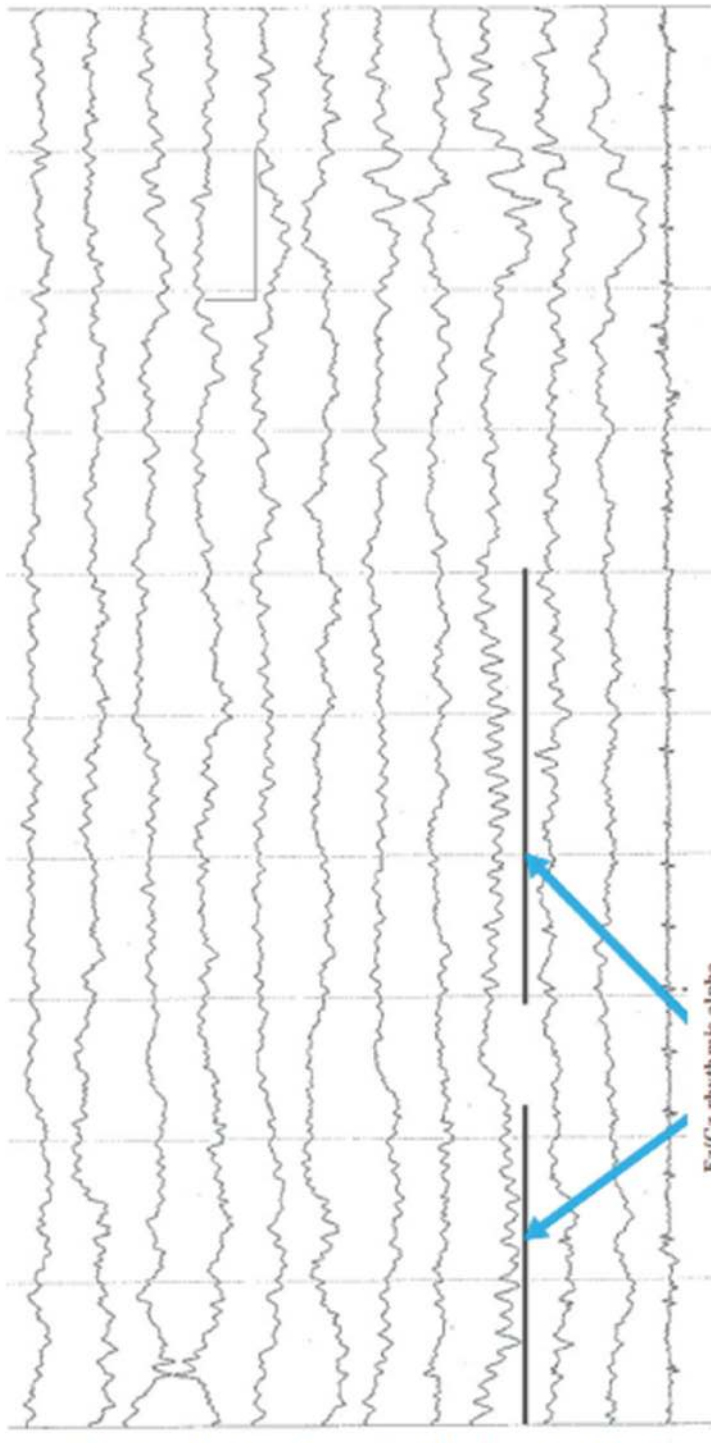

Fig. 4.25 Fz/Cz rhythmic alpha

Sharp waves, which are very spiky (blue arrows), are observed in temporal regions and are regarded as "temporal sharp transients." A typical sharp wave is indicated by the blue arrow on the left; it is evident as a biphasic wave with phase reversal in the right temporal area (Fig. 4.26).

Temporal sharp transients are very spiky at 36 weeks PMA, but their waveforms change into relatively dull biphasic sharp waves at 40 weeks PMA (blue arrows). These transients are typically observed in term infants, along with frontal sharp transients and frontal slow bursts. They are usually observed in patterns 403 and 405 (Fig. 4.27).

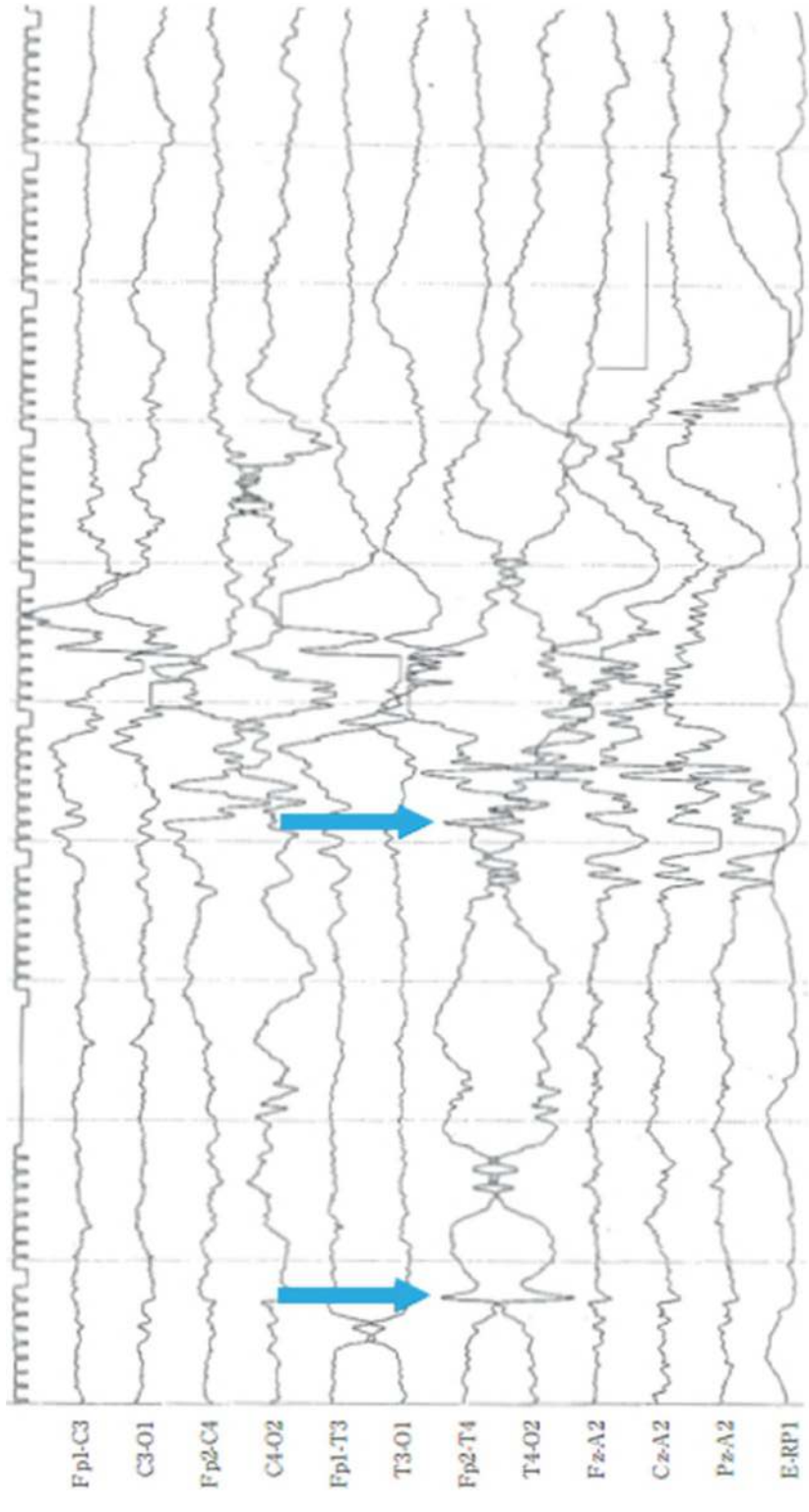

Fig. 4.26 Temporal sharp transients (36 weeks PMA)

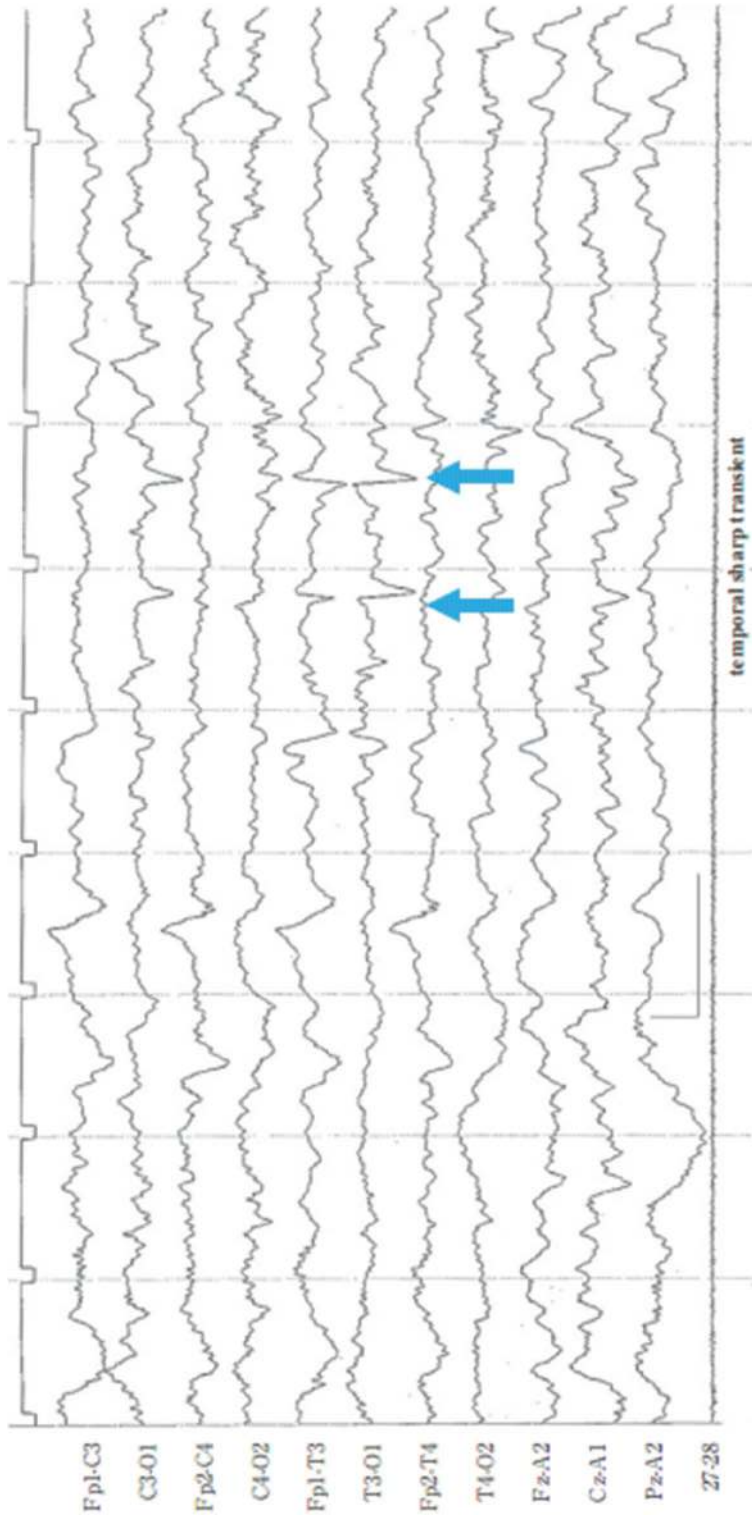

Fig. 4.27 Temporal sharp transients (40 weeks PMA)

Reference

Watanabe IK. Spindle-like fast rhythms in the EEGs of low-birth weight infants. Dev Med Child Neurol. 1972;14(3):373–81.

5 Developmental Changes in EEG Patterns: Development of Tracé Alternant/Tracé Discontinu

Toru Kato and Fumio Hayakawa

In this chapter, we will illustrate the developmental changes in individual EEG patterns at different postmenstrual ages (PMA), starting with EEG code number "7."

Code "7" encompasses alternating tracing (known as tracé alternant, TA) in term infants and discontinuous tracing (known as tracé discontinu, TD) in preterm infants. The key distinction between TA and TD lies in the presence or absence of activity in the low-voltage parts; TA exhibits some activity in the low-voltage part, whereas TD is characterized by a flat or near-flat low-voltage part. Physiologically, TD is defined as up to 36 weeks PMA, while TA is typically observed at 38 weeks PMA or later. TA/TD at any PMA represents the EEG pattern during quiet sleep (QS), considered to occur during the deepest sleep in newborn infants. This pattern is physiologically unique to the neonatal period and is characteristic of neonates.

*See Chap. 3.

Key Points for EEG Interpretation 1: Understanding the Big Picture and Next Getting to the Detail Oriented

(Hiroyuki Kidokoro)

Estimating the maturity of the brain of a preterm infant every 2 weeks using EEG is a particularly intriguing aspect of neonatal EEG interpretation. Four key items—frequency and amplitude of delta waves, the duration of interburst intervals in tracé alternant (TA)/tracé discontinu (TD), frequency of brushes, and age-specific transients—are outlined in Table 4.2. It is recommended for beginners to go through the following processes in assessing neonatal EEG:

1. Assess whether the EEG segment under review exhibits a continuous or discontinuous pattern.
2. If the pattern is continuous, examine the recording for relatively large delta waves, evaluating their frequency and amplitude. This step helps to roughly narrow down the estimated postmenstrual age (PMA).
3. Further refine the estimated PMA by assessing the incidence of brushes and the presence or absence of age-specific transients.

(continued)

T. Kato (✉) · F. Hayakawa
Department of Pediatrics, Okazaki City Hospital, Okazaki, Japan
e-mail: torukato@sun-inet.or.jp

A. Okumura, H. Kidokoro (eds.), *Neonatal EEG: Atlas and Interpretation*,
https://doi.org/10.1007/978-981-96-0726-6_5

4. If the pattern is discontinuous, evaluate the interburst intervals in TA/TD. Note any activity in the low-voltage part of TA/TD, as its presence suggests an age of 38 weeks PMA or older. Then, estimate the PMA by evaluating the burst (high-voltage) part as in steps (2) and (3).
5. Combine findings from both continuous and discontinuous patterns to finally estimate the PMA.

Key Points for EEG Interpretation 2: Delta Wave Morphology

(Hiroyuki Kidokoro)

Preterm infants born before 34 weeks postmenstrual age often exhibit a characteristic "slide-shaped" high voltage delta wave, as illustrated in Fig. 5.1a. In this pattern, the ascending slope rises quickly, while the descending slope declines gently. In contrast, the delta wave at 34 weeks or later is "Fujiyama-shaped" characterized by symmetrical ascending and descending slopes (Fig. 5.1b). As discussed in the overview chapters, the delta wave is larger and more monotonous in the immature stages. These morphological features, along with frequency and voltage, can be helpful in assessing the delta wave to estimate the EEG age.

In pattern 267, the duration of the low-voltage part at 26 weeks PMA ranges from 20 to 80 s, while the high-voltage part lasts from 3 to 8 s and remains almost unchanged until 40 weeks. The low-voltage part is flat or nearly flat, but theta and delta components sometimes appear as isolated waves. On the other hand, the high-voltage part is dominated by delta components with high voltages above 300 μV and extremely slow frequency (<1 Hz), mixed with high-amplitude transients, such as "frontal sharp bursts" and "occipital sharp bursts." The interhemispheric synchronization of the high-voltage part of the wave is already well preserved from this period. Only frontal and occipital sharp bursts appear as fast wave components (Fig. 5.2).

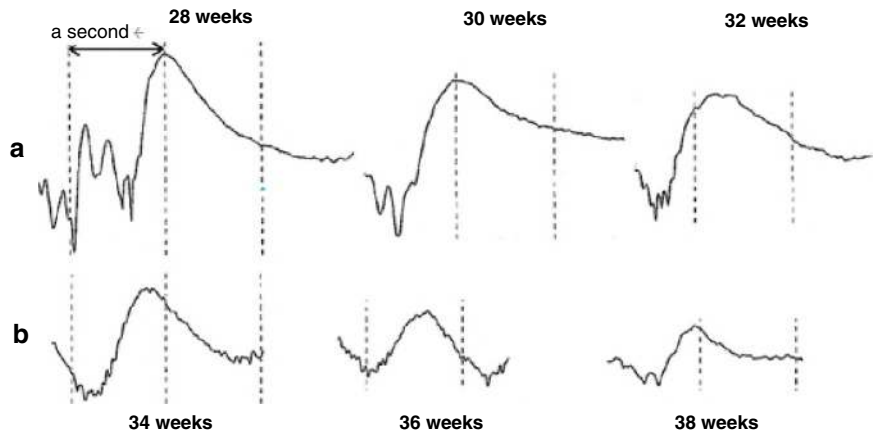

Fig. 5.1 Morphological change of delta wave. **a** shows the delta wave in which the ascending slope rises quickly, and the descending slope declines gently. **b** shows the delta wave characterized by symmetrical ascending and descending slopes

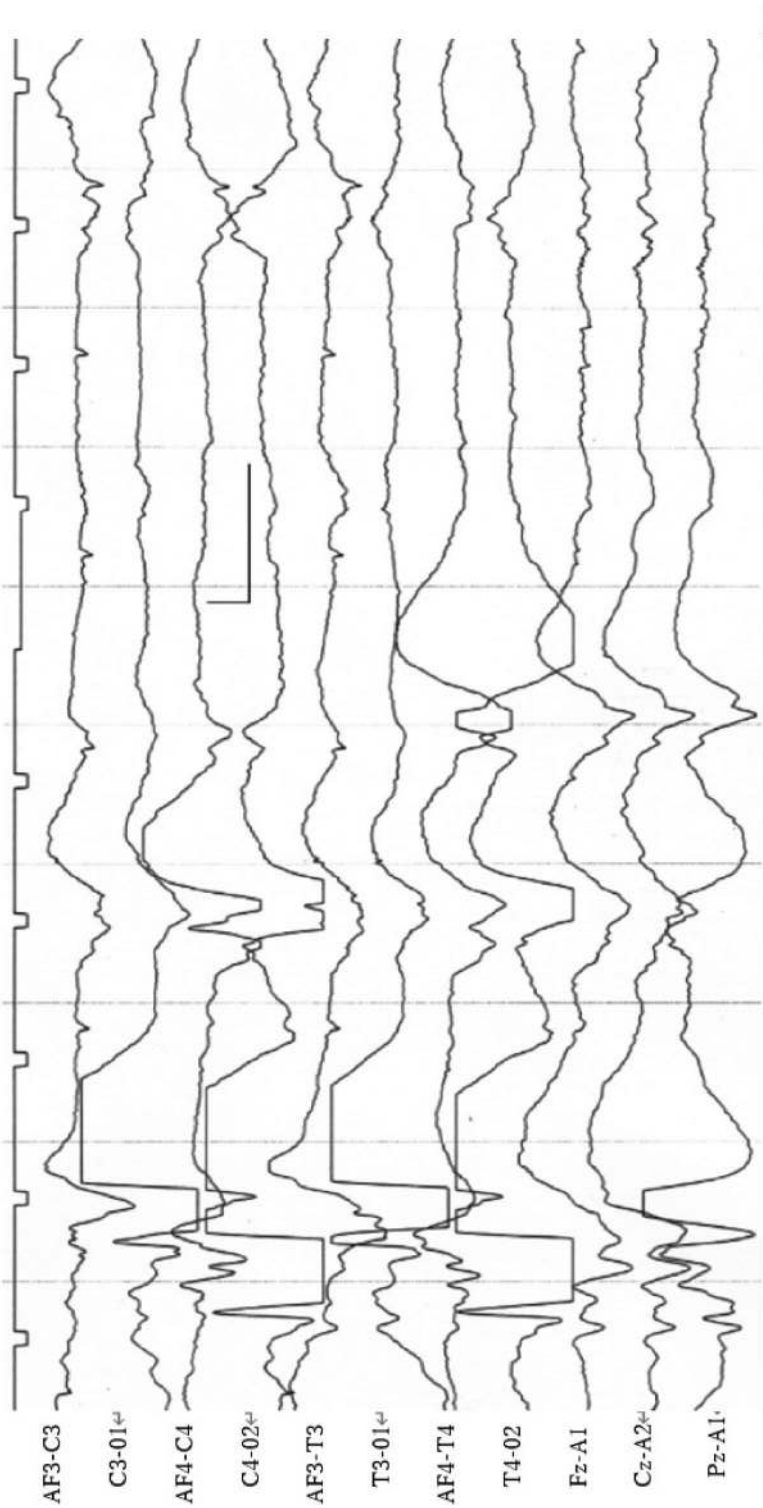

Fig. 5.2 Discontinuous pattern at 26 weeks PMA (267)

In pattern 287, the duration of the low-voltage part ranges between 15 and 60 s, with an average duration often falling between 20 and 40 s. The high-voltage part lasts for 3–8 s. The low-voltage part is almost flat, but occasionally solitary theta and delta components can be observed. On the other hand, the high-voltage part has two types of delta waves: one with a high voltage exceeding 300 μV and a significantly slower frequency (<1 Hz) and another with a voltage of 300 μV and frequency of about 1 Hz. Predominant "high-amplitude theta" waves from the temporal regions, a hallmark of the 28-week pattern, are observed, while frontal and occipital sharp bursts are infrequent. Brushes, fast wave components, are present especially from the central regions, although their frequency of appearance remains low (Fig. 5.3).

In pattern 307, the low-voltage part typically lasts about 20–40 s, while the high-voltage part ranges from 4 to 8 s. Although the low-voltage part may appear flat, sometimes theta and delta components are present as isolated waves with brushes. In the high-voltage part, delta waves with an average voltage of about 300 μV and a frequency of 1 Hz are predominant, but there is a mixture of delta waves of various voltages and frequencies. Frontal and occipital transients are less frequent, and the "rhythmic temporal theta," characteristic of 30 weeks PMA, is often observed. In addition, the fast wave component, especially brushes, becomes more prominent throughout the EEG (Fig. 5.4).

In pattern 327, the duration of the low-voltage part typically ranges from 20 to 40 s, while the high-voltage part lasts 4–8 s. The low-voltage part is typically flat, but theta and delta components can appear as isolated waves with brushes. The high-voltage part is dominated by delta waves of approximately 250 μV and 1 Hz, with a mixture of delta waves of various amplitudes and frequencies. A characteristic finding at 32 weeks PMA is the frequent continuous appearance of delta waves from the occipital region. Rhythmic temporal theta waves are rare during this period. Fast wave components, particularly brushes, are abundant. Theta waves are scarce, and the pattern is characterized by relatively monophasic slow waves and abundant brushes (Fig. 5.5).

In pattern 347, the duration of the low-voltage part is short (20–30 s), and the high-voltage part lasts mainly 5–10 s. The low-voltage part is flat, but the theta and delta components appear as isolated waves with brushes. The high-voltage part is dominated by delta waves of about 200 μV and 1.5 Hz, and various amplitudes and frequencies are mixed together. The pattern is similar to that of 327 (Fig. 5.5), except that delta waves are a slightly smaller, brushes are slightly spiky, and sharp waves begin to appear from the temporal region. The fast wave component is extremely abundant, and the frequency of brushes is higher than at any other period (Fig. 5.6).

In pattern 367, the duration of the low-voltage part is short, ranging from 10 to 30 s, while the high-voltage part lasts mainly from 5 to 10 s. The low-voltage part may be flat, but the theta and delta components may appear as isolated waves with brushes. The high-voltage part is predominantly characterized by delta waves of 150 μV and a frequency of 1.5–2 Hz. These waves appear smaller but remain mostly monotonous slow waves. This pattern is similar to pattern 347 (Fig. 5.6), with a few distinctions: delta waves are slightly smaller, brushes are somewhat spiky, and sharp waves, notably "temporal sharp bursts", begin to emerge from the temporal region. There are many fast wave components and sharp waves, with frequent brushes. Although the waveform is physiological, it may appear to resemble a disorganized pattern (Fig. 5.7).

In pattern 387, the duration of the low-voltage part is now even shorter, lasting only 10–15 s, while the high-voltage part lasts mainly 5–8 s. The low-voltage part remains slightly flat, but most exhibit some low voltage activity. In the high-voltage part, delta waves are predominant, with amplitudes of 100–150 μV and frequencies of 2–2.5 Hz, which are considerably smaller but monotonous. This pattern is similar to pattern 367 (Fig. 5.7), but differs in several aspects: the delta waves are smaller, brushes are less frequent, there are fewer temporal sharp bursts. There is

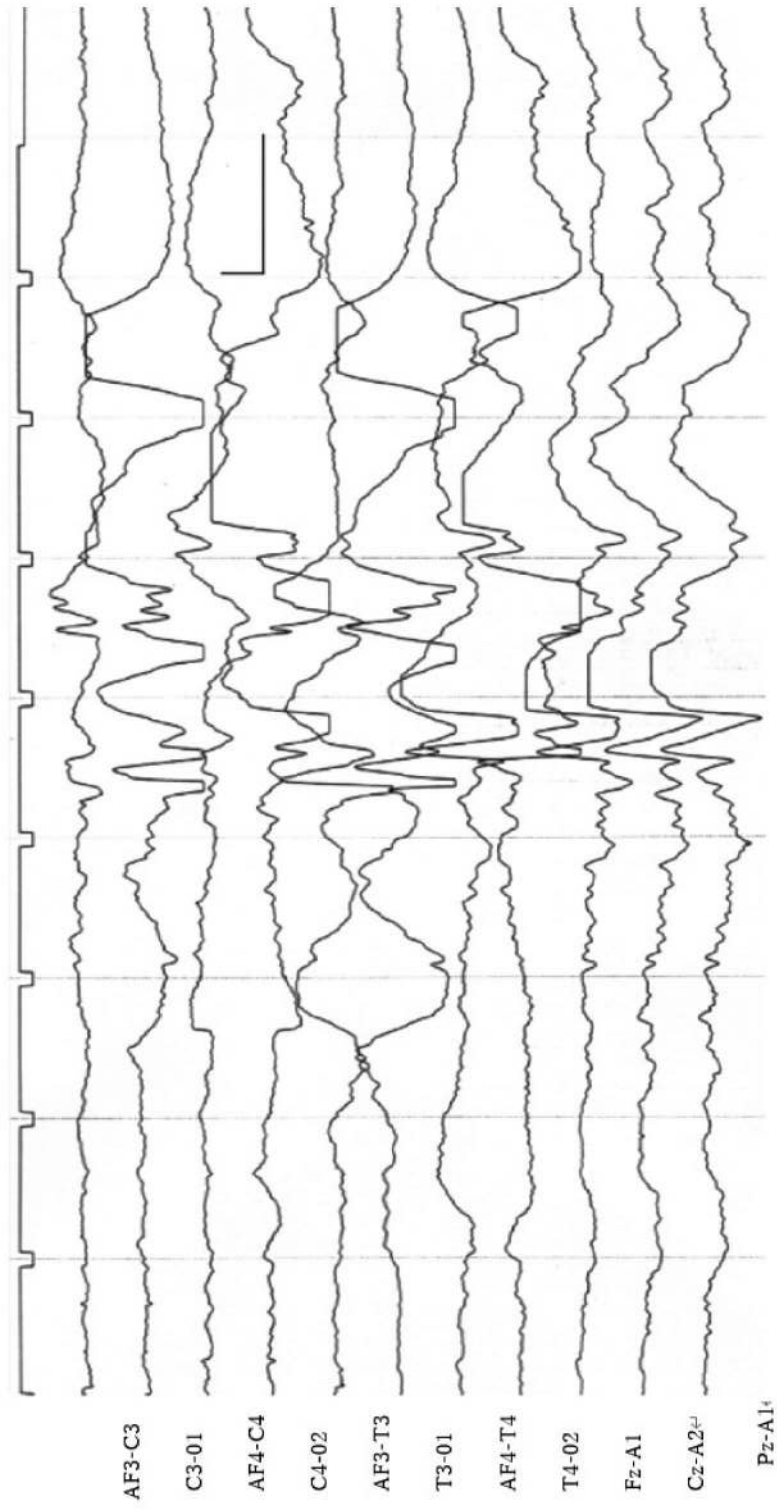

Fig. 5.3 Discontinuous pattern at 28 weeks PMA (287)

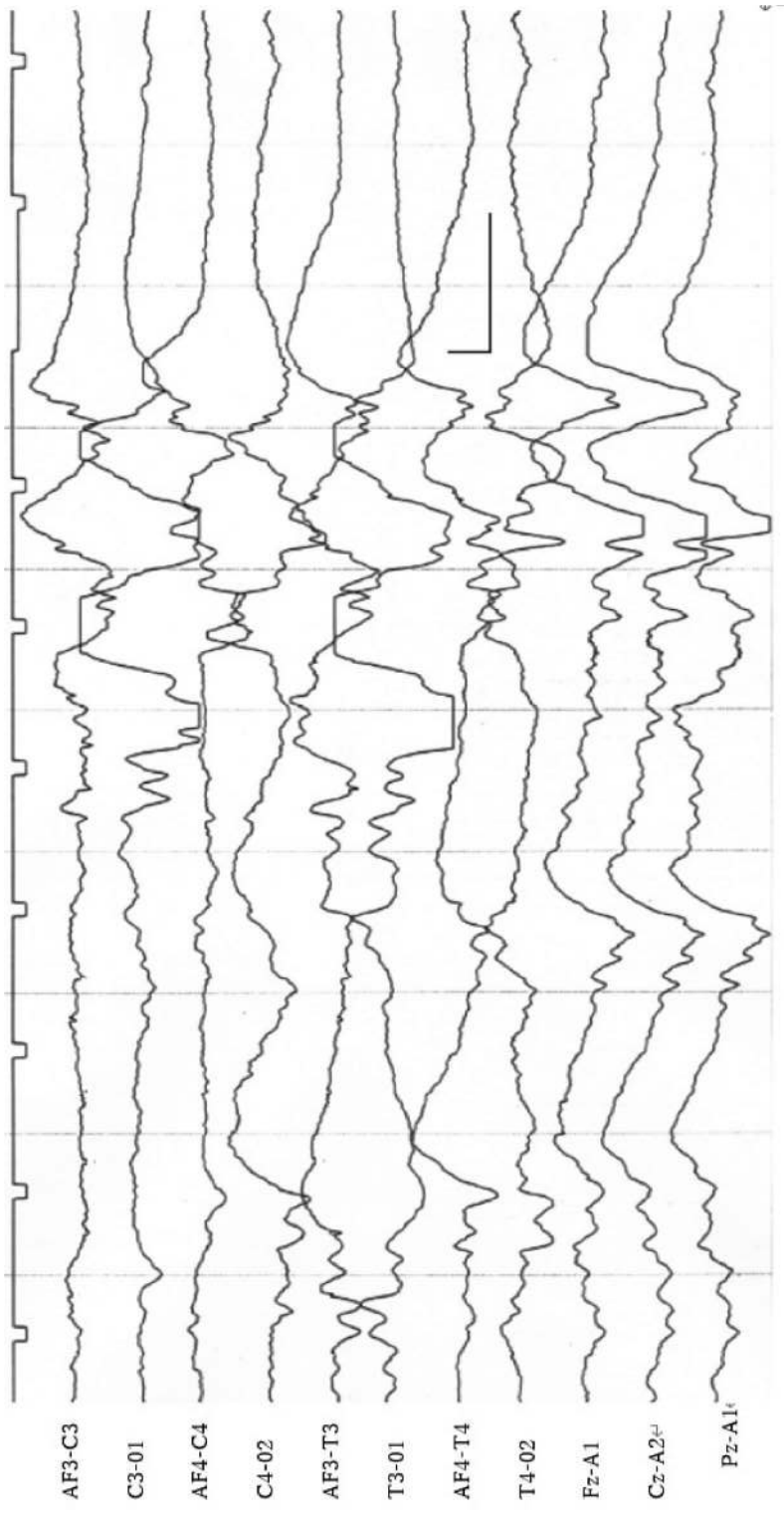

Fig. 5.4 Discontinuous pattern at 30 weeks PMA (307)

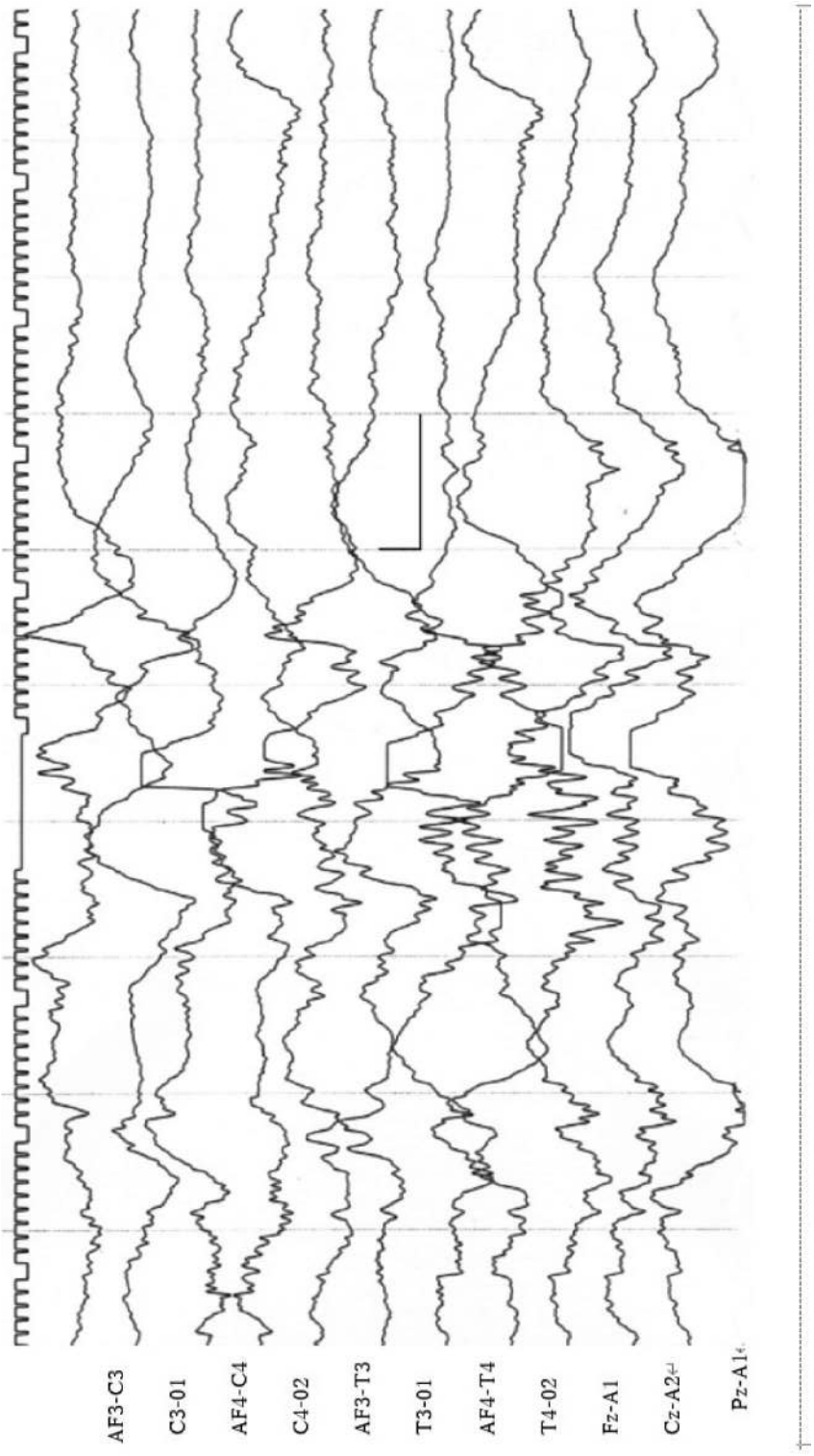

Fig. 5.5 Discontinuous pattern at 32 weeks PMA (327)

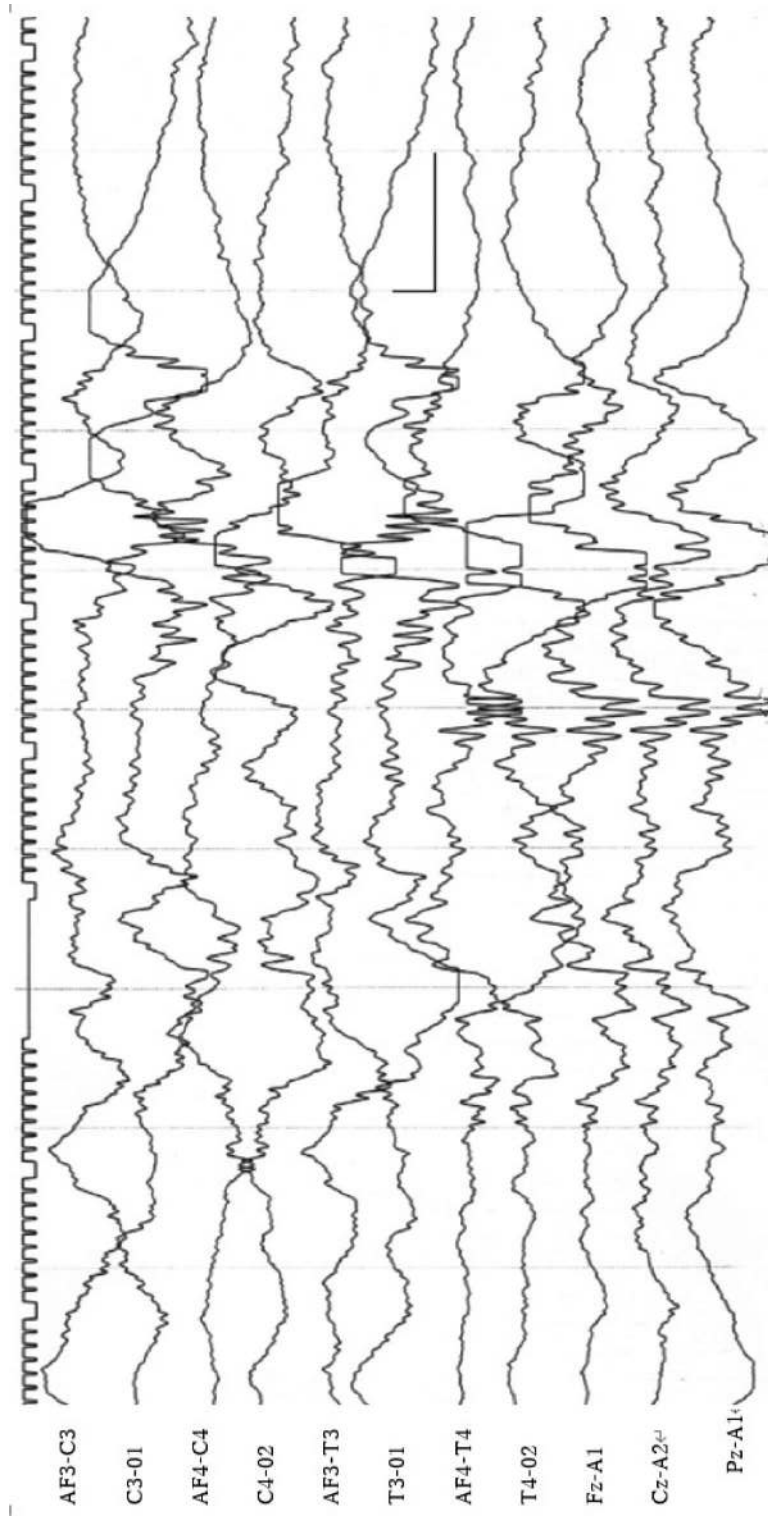

Fig. 5.6 Discontinuous pattern at 34 weeks PMA (347)

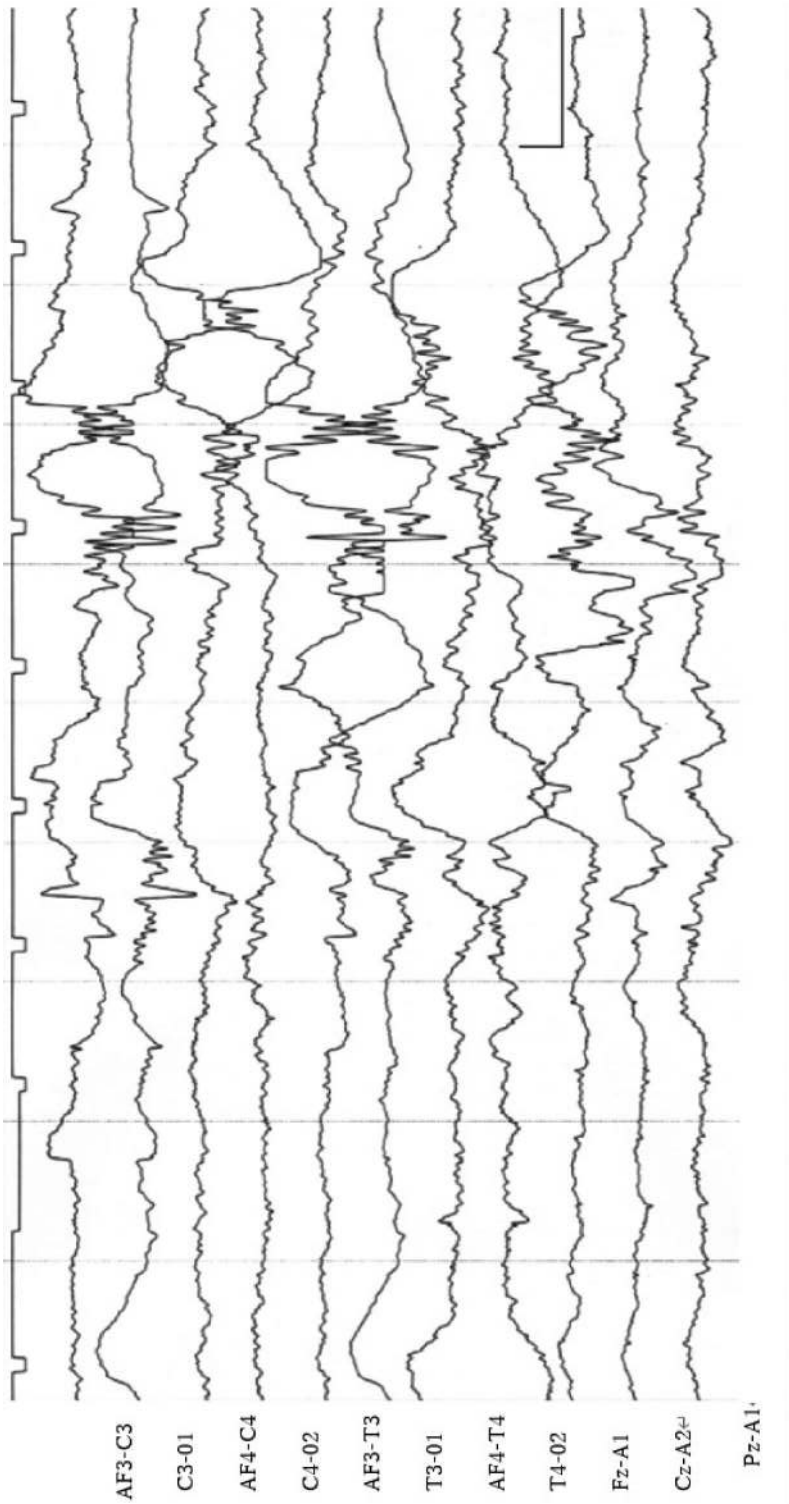

Fig. 5.7 Discontinuous pattern at 36 weeks PMA (367)

polymorphism in delta waves, although this is not as pronounced as in pattern 407 (Fig. 5.9). This pattern incorporates elements of both patterns 367 and 407 and can be considered a transitional phase between the two (Fig. 5.8).

In pattern 407, the duration of the low-voltage part is even shorter, ranging from 5 to 10 s, while the high-voltage part lasts mainly from 5–8 s. Even in the low-voltage part, flat tracings are rare, and some low-voltage activity is always present except during post-startle activity. The high-voltage part is predominantly characterized by delta waves with an amplitude of 80–120 μV and a frequency of 2–3 Hz. These waves show few monotonous repetitions, interfere with each other temporally and spatially, and create polymorphism. This is the typical pattern, termed TA. The amplitude of the low-voltage part decreases in the latter half of TA, making the alternation more distinct (Fig. 5.9).

In pattern 427, the duration of the low-voltage part is shorter, ranging from 4 to 8 s, while the high-voltage part lasts between 5 and 8 s. The low-voltage part shows sufficient activity and is rarely flat, although it may become flat following a startle. In the high-voltage part, delta waves with amplitude of 80–150 μV and frequencies of 2–3 Hz are predominant, exhibiting abundant polymorphism. In addition, the theta waves are rounder and have a higher amplitude compared to those at 40 weeks PMA. The tracé alternant pattern is somewhat less distinct than at 40 weeks PMA because the activities of the low-voltage part are increased (Fig. 5.10).

In pattern 447, the duration of the low-voltage part is even shorter, lasting only 3–5 s, and its distinction from the high-voltage part becomes less clear due to increased activity. The high-voltage part lasts 5–8 s, but the slow wave seems to be larger than in pattern 407 (Fig. 5.9). The high-voltage part is predominantly characterized by delta waves with amplitude of 60–150 μV and frequencies of 2–3 Hz. There is little monotonous repetition of similar waves, as each wave interacts with others temporally and spatially, creating polymorphism. Following this period, TA is no longer observed with transition to the HVS pattern, which is seen in deep sleep in early infancy (Fig. 5.11).

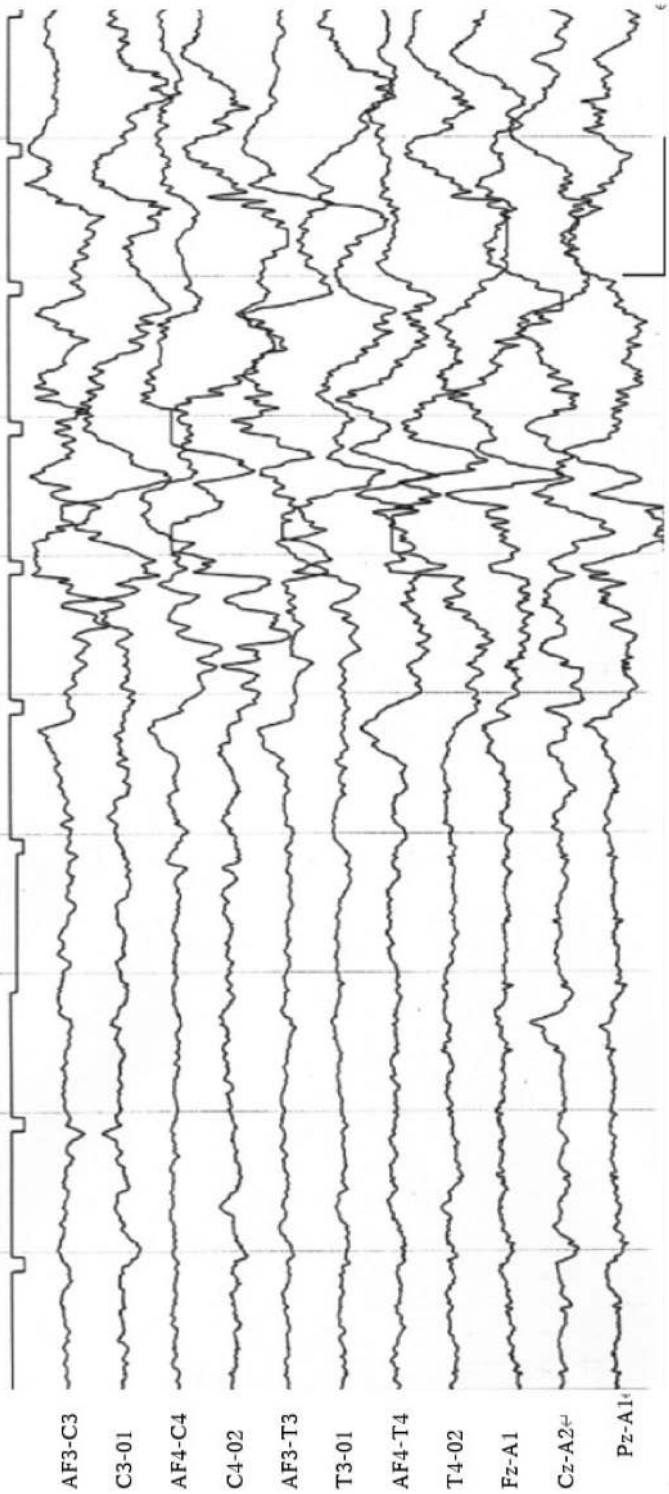

Fig. 5.8 Tracé alternant (TA) at 38 weeks PMA (387)

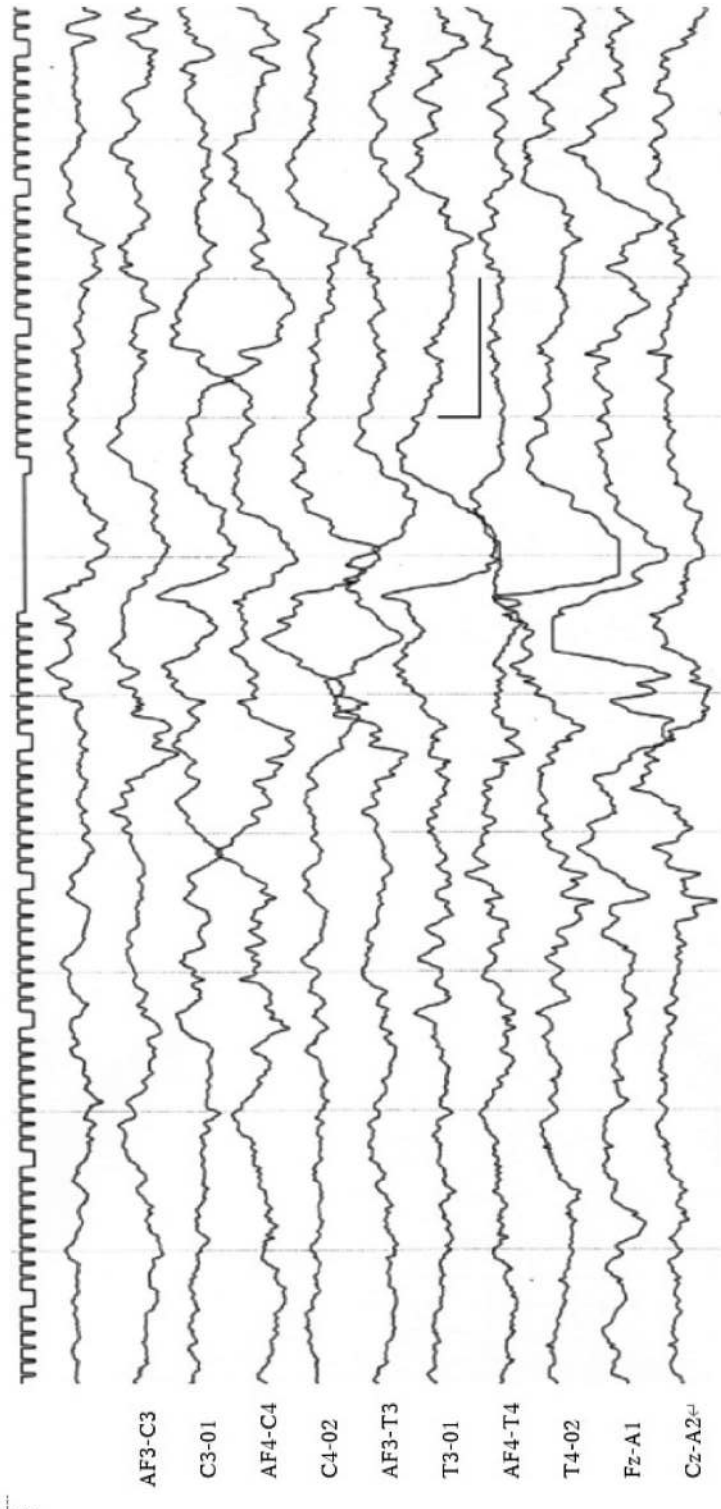

Fig. 5.9 Tracé alternant (TA) at 40 weeks PMA (407)

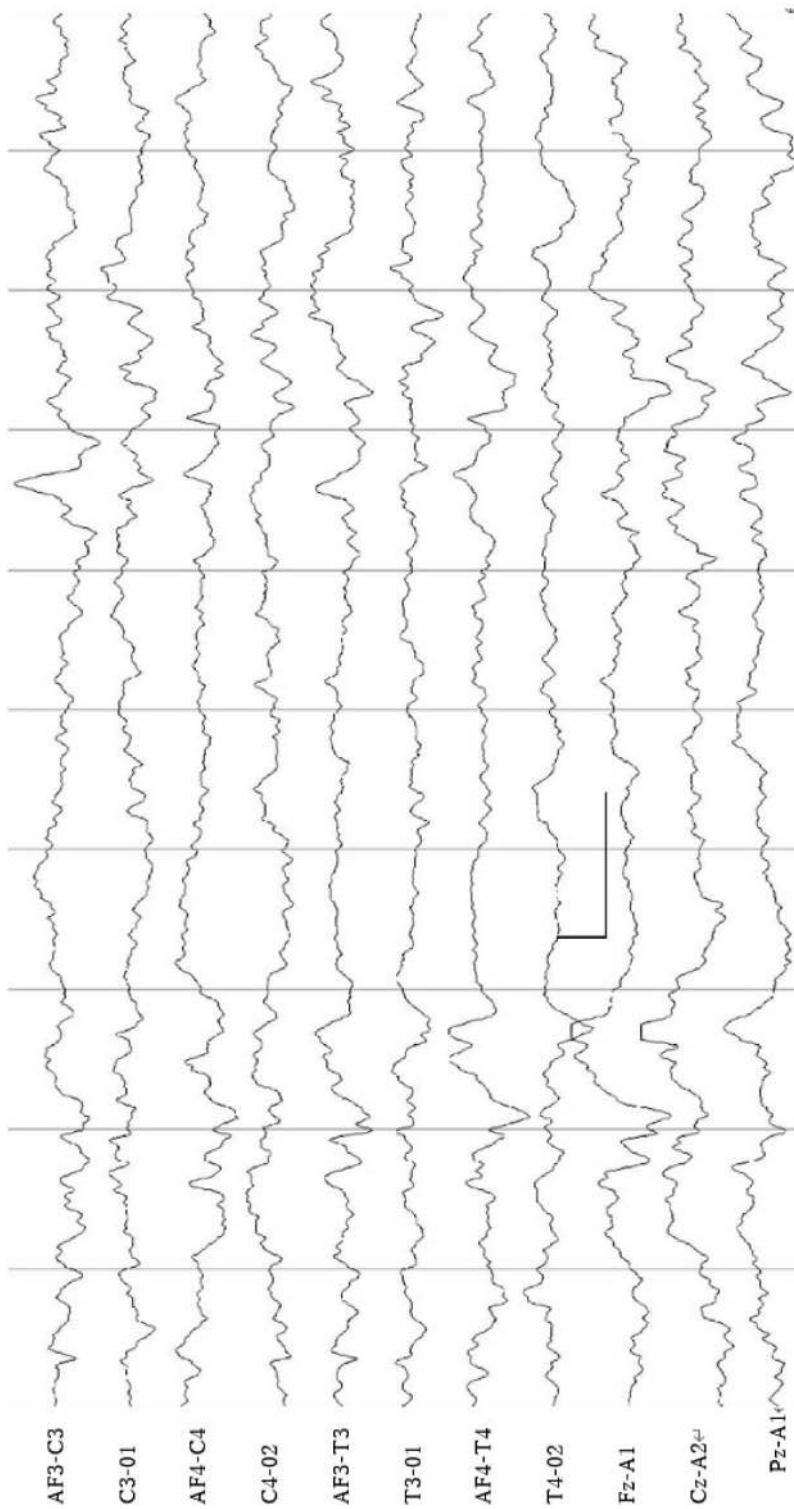

Fig. 5.10 Tracé alternant at 42 weeks PMA (427)

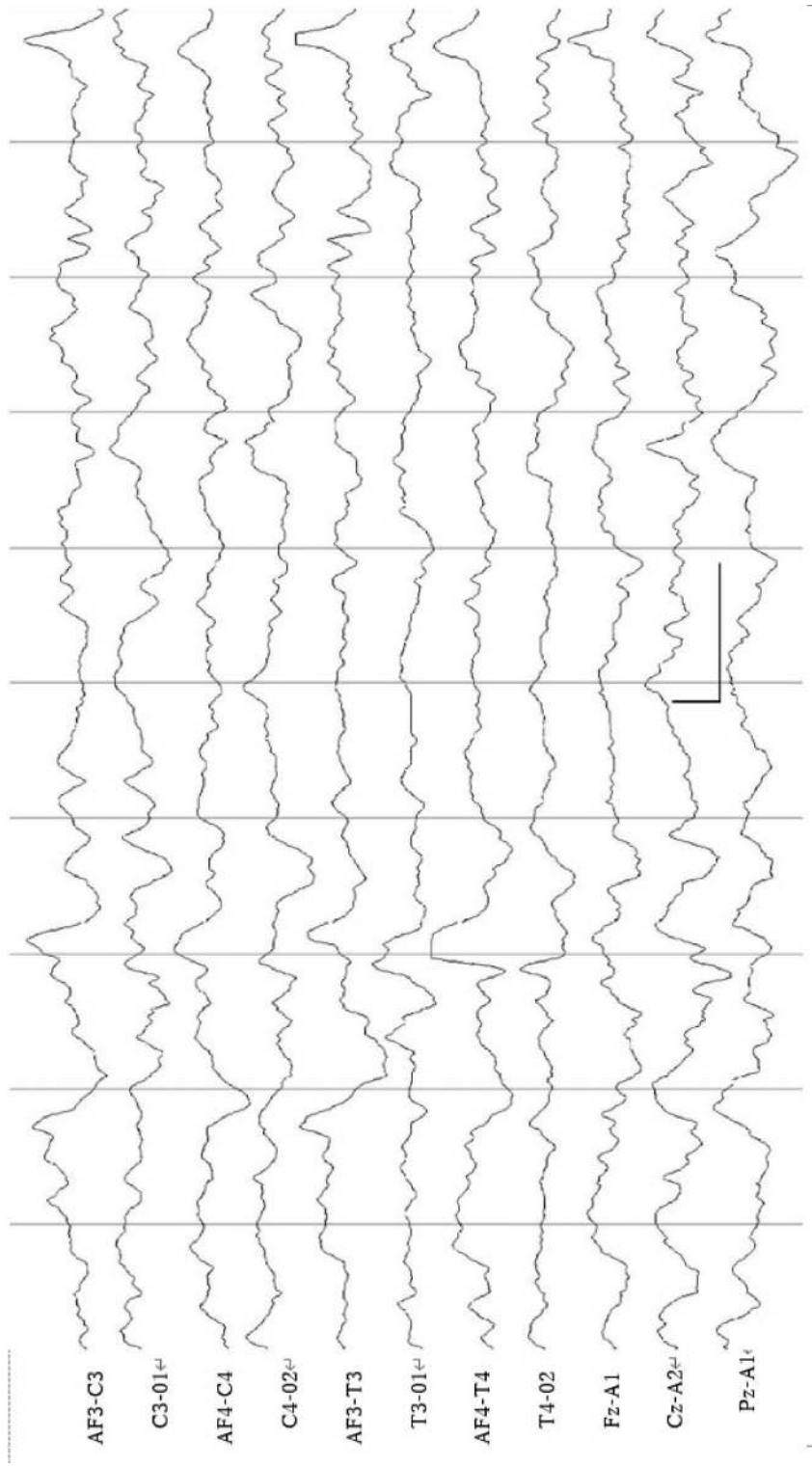

Fig. 5.11 Tracé alternant at 44 weeks PMA (447)

6 Developmental Changes in EEG Patterns: Development of High-Voltage Slow Wave Pattern

Toru Kato and Fumio Hayakawa

Next, we discuss the developmental changes in the high-voltage slow wave (HVS) pattern at different postmenstrual ages (PMA). As outlined above, in term infants, the HVS pattern appears in quiet sleep (QS) and is categorized as the "5" pattern in the EEG code. However, during the preterm period, continuous HVS appears in active sleep (AS), which is labeled the "3" pattern in the EEG code. The EEG observed during deep sleep after infancy can be considered a developmental form of the HVS pattern (i.e., "5") seen in term infants. The components of the HVS pattern are essentially the same as those of the burst part of the "7" pattern.

(See Chap. 3)

In pattern 263, generally, the duration of high-voltage slow wave pattern is short, lasting only 20–30 s. However, if this pattern is observed frequently, it can indicate no suppression of brain activity. The main components are extremely high-amplitude delta waves of 300 μV or more at a very low frequency (<1 Hz), accompanied by high-amplitude transients that appear from areas of frontal and occipital named "frontal sharp bursts" and "occipital sharp bursts," respectively. On the other hand, high-amplitude theta and brushes are rarely seen. Observation of this pattern suggests a very immature stage of development (Fig. 6.1).

In pattern 283, the slow waves are characterized by a high amplitude exceeding 300 μV and a frequency of less than 1 Hz, mixed with delta waves of about 300 μV and 1 Hz. Both frontal sharp bursts and occipital sharp bursts are present; however, this pattern is distinguished by the high-amplitude theta waves originating from the temporal region. Pattern 283 has a significantly longer duration than pattern 263 (Fig. 6.1). Generally, a switch between continuous and discontinuous patterns occurring within a short timeframe indicates immaturity in sleep organization (Fig. 6.2).

In pattern 303, the EEG activity is primarily composed of 300 μV, 1 Hz delta waves. At around this PMA, there is a mixture of delta waves of various frequencies, with fewer frontal sharp bursts or occipital sharp bursts. A rhythmic temporal theta, characteristic of 30 weeks PMA, is generally observed. This temporal theta typically persists for about 1 s. In contrast to high-amplitude theta, the rhythmic temporal theta is bilateral, rhythmic, round-shaped, and has an amplitude of less than 100 μV. In general, the former pattern suggests an age of 28 weeks PMA, while the latter indicates 30 weeks PMA. In addition, fast wave components, particularly brushes, are more commonly observed throughout (Fig. 6.3).

T. Kato (✉) · F. Hayakawa
Department of Pediatrics, Okazaki City Hospital, Okazaki, Japan
e-mail: torukato@sun-inet.or.jp

A. Okumura, H. Kidokoro (eds.), *Neonatal EEG: Atlas and Interpretation*,
https://doi.org/10.1007/978-981-96-0726-6_6

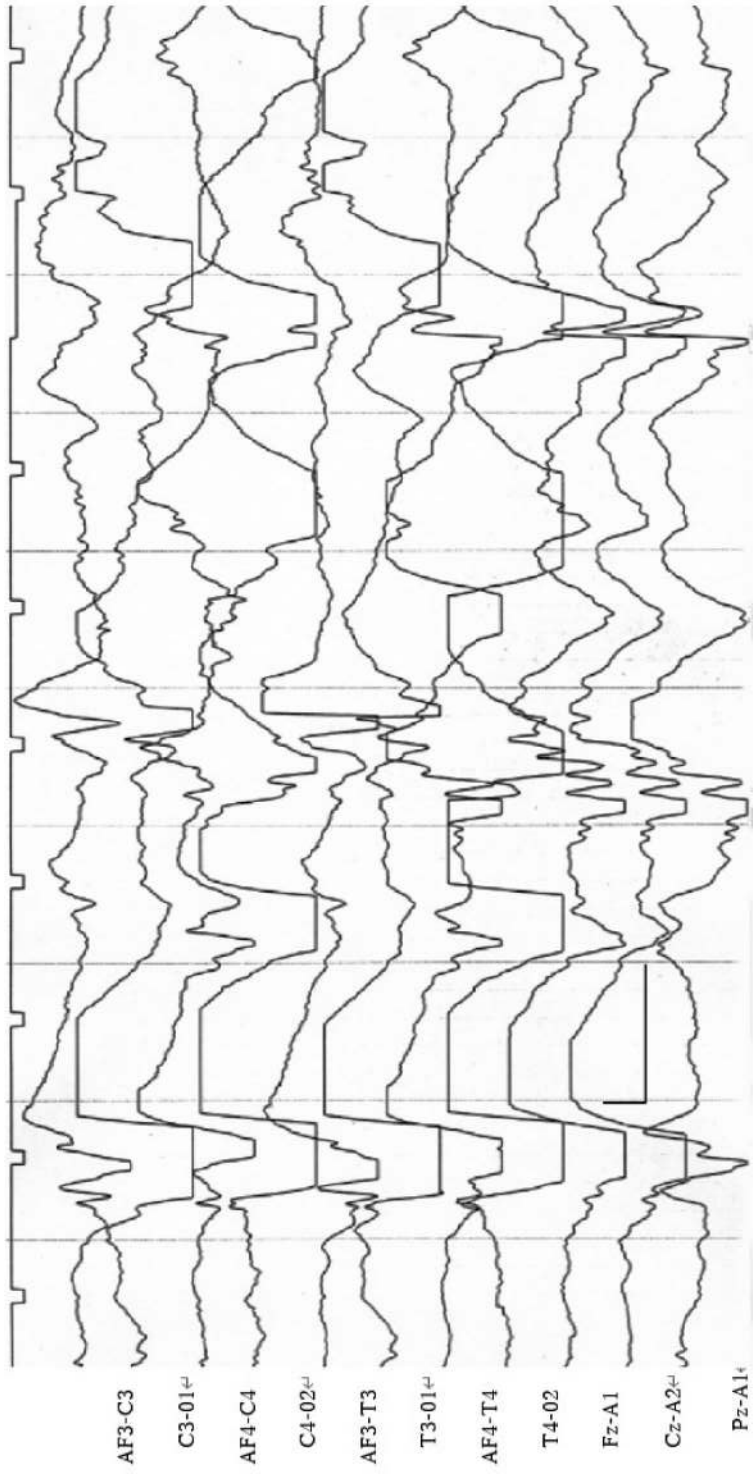

Fig. 6.1 High-voltage slow wave pattern at 26 weeks PMA (263)

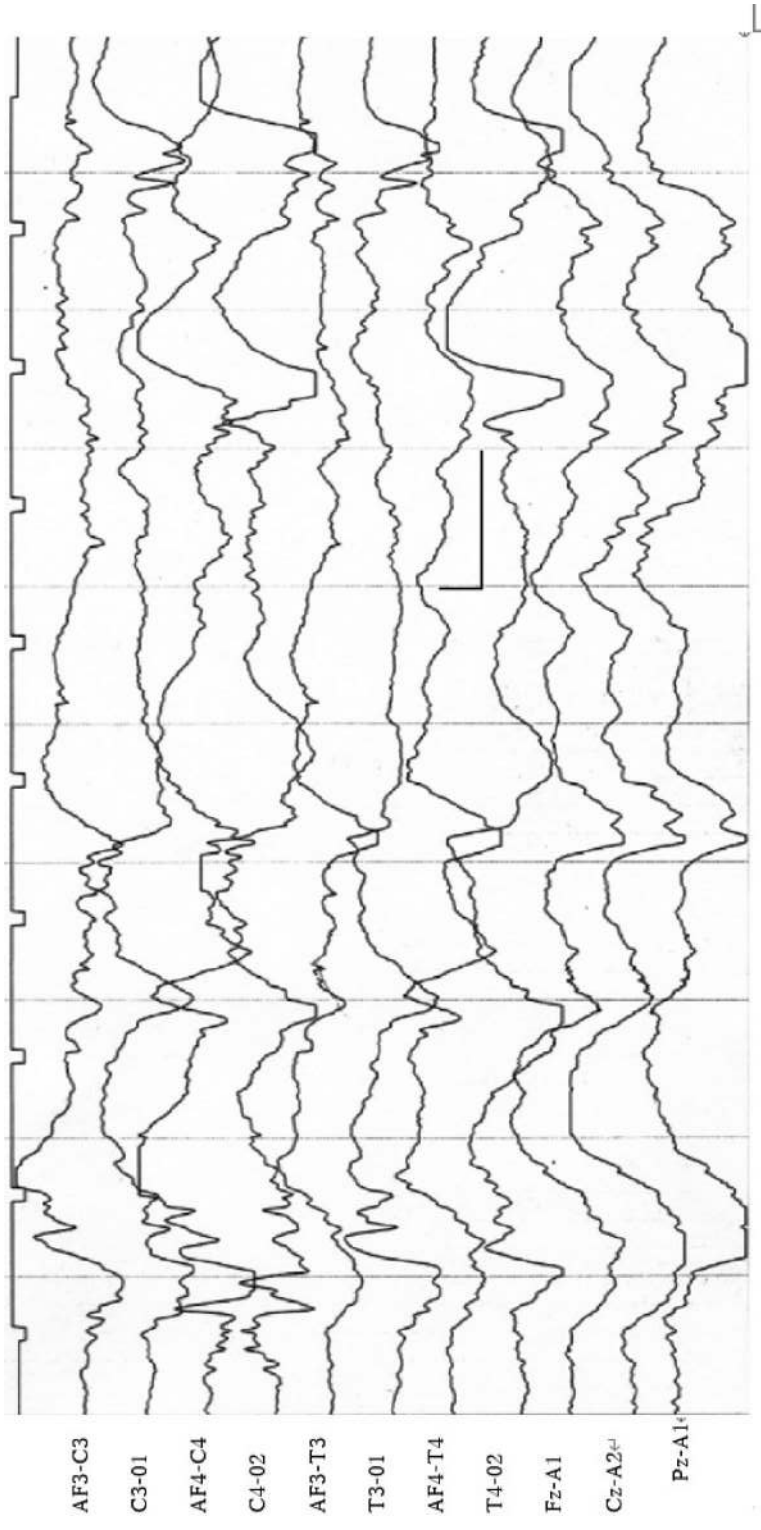

Fig. 6.2 High-amplitude slow wave pattern at 28 weeks PMA (283)

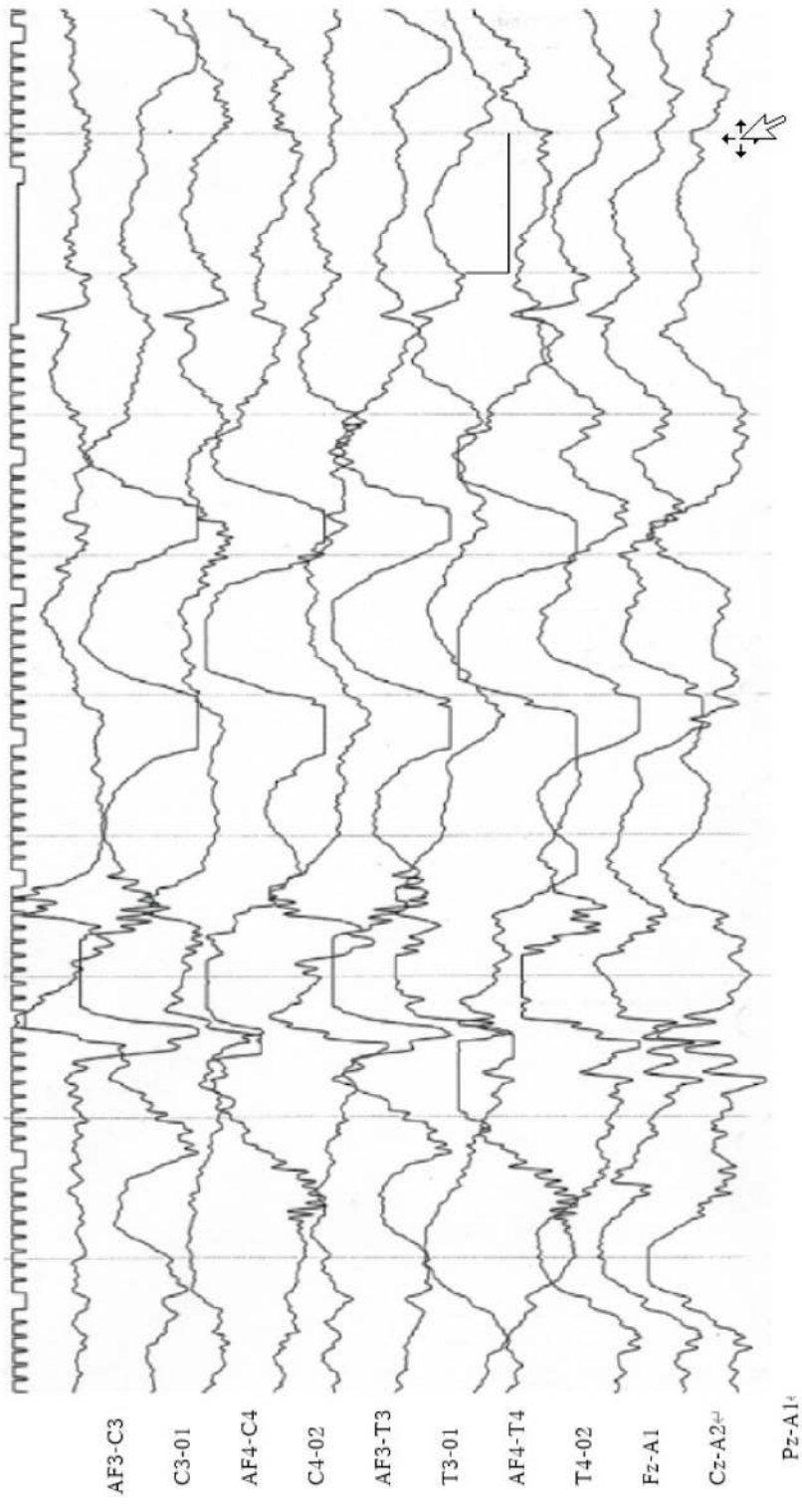

Fig. 6.3 High-amplitude slow wave pattern at 30 weeks PMA (303)

In pattern 323, the EEG activity is dominated by 250 μV, 1 Hz delta waves, with a mixture of delta waves of various frequencies. The prominence of delta waves originating from the occipital region is a key characteristic of 32 weeks PMA. This pattern of continuous delta waves from the occipital region is seen only within 4 weeks before and after this period. While the frequency of rhythmic temporal theta decreases, there is an increase in fast wave components, and brushes are seen much more frequently. Theta waves are scarce, and the pattern is characterized by relatively monotonous delta waves and an abundance of brushes (Fig. 6.4).

In pattern 343, the EEG activity is primarily characterized by 200 μV, 1.5 Hz delta waves, mixes with delta waves of various frequencies. This pattern is similar to pattern 323 (Fig. 6.4), but with slightly lower amplitudes. The most notable feature of this period is the remarkable abundance of fast wave components, with brushes appearing more frequently than at any other time. These brushes are higher in amplitude, conspicuous, and somewhat spiky in appearance (Fig. 6.5).

In pattern 363, the EEG activity is dominated by delta waves with a voltage of 150 μV and frequencies of 1.5–2 Hz. These waves are comparatively small but consistent. The pattern is similar to pattern 347 (Fig. 5.6), but the overall impression is more irregular due to several factors: the delta waves are slightly smaller, the brushes have higher amplitude and are spikier, and many sharp waves appear from the temporal region. Fast wave components and sharp waves are abundant, with many brushes still present. Despite being a physiological waveform, it may appear to be similar to a disorganized pattern. Frontal slow bursts, frontal sharp transients, and temporal sharp transients begin to appear at this stage, which are typical of mature infants (Fig. 6.6).

After 38 weeks PMA, pattern 383 is observed during AS and pattern 385 (HVS) is observed during QS. As sleep deepens, pattern 385 appears before the transition from pattern 383 to pattern 387. The primary activity consists of delta waves of 100–150 μV with frequencies of 2–2.5 Hz, which are smaller but still consist mainly of monotonous slow waves. This pattern is similar to pattern 363 (Fig. 6.6), but there are a number of differences: smaller delta waves, fewer brushes, reduced sharp waves from the temporal area, and somewhat polymorphic delta waves, although not as prominent as in pattern 405 (Fig. 6.8). This represents a transitional pattern that includes elements of both patterns 363 and 405 (Fig. 6.7).

This pattern 405 is one of the most typical EEG patterns in the term stage, along with the alternating pattern (TA). It appears when sleep gradually deepens from pattern 403 (Fig. 8.4) to QS with repeated twitching movements. During the transition from pattern 405 to pattern 407, alternation of patterns 405 and 407 is often seen (Fig. 5.9). The activity is predominantly composed of delta waves of 80–120 μV at frequencies of 2–3 Hz. There are few repetitions of the same waveform, and each wave temporally and spatially interferes with the others, forming a polymorphic form. This pattern is important as an indicator of maturation and represents normal EEG patterns at the term stage (Fig. 6.8).

After 40 weeks PMA, there are developmental changes that deviate from the typical principles associated with brain maturation. The delta waves exhibit a relatively higher amplitude (80–120 μV) and a slower frequency (2–2.5 Hz), with their morphology becoming more rounded by 42 weeks PMA, compared to 40 weeks PMA. This contrasts with the earlier sign of maturity, i.e., the decrease in delta wave size up to 40 weeks PMA. The polymorphism of the delta wave increases further and monotonous slow waves are rarely seen. The alpha and theta components are reduced after 40 weeks PMA, giving an overall background EEG smoother impression (Fig. 6.9).

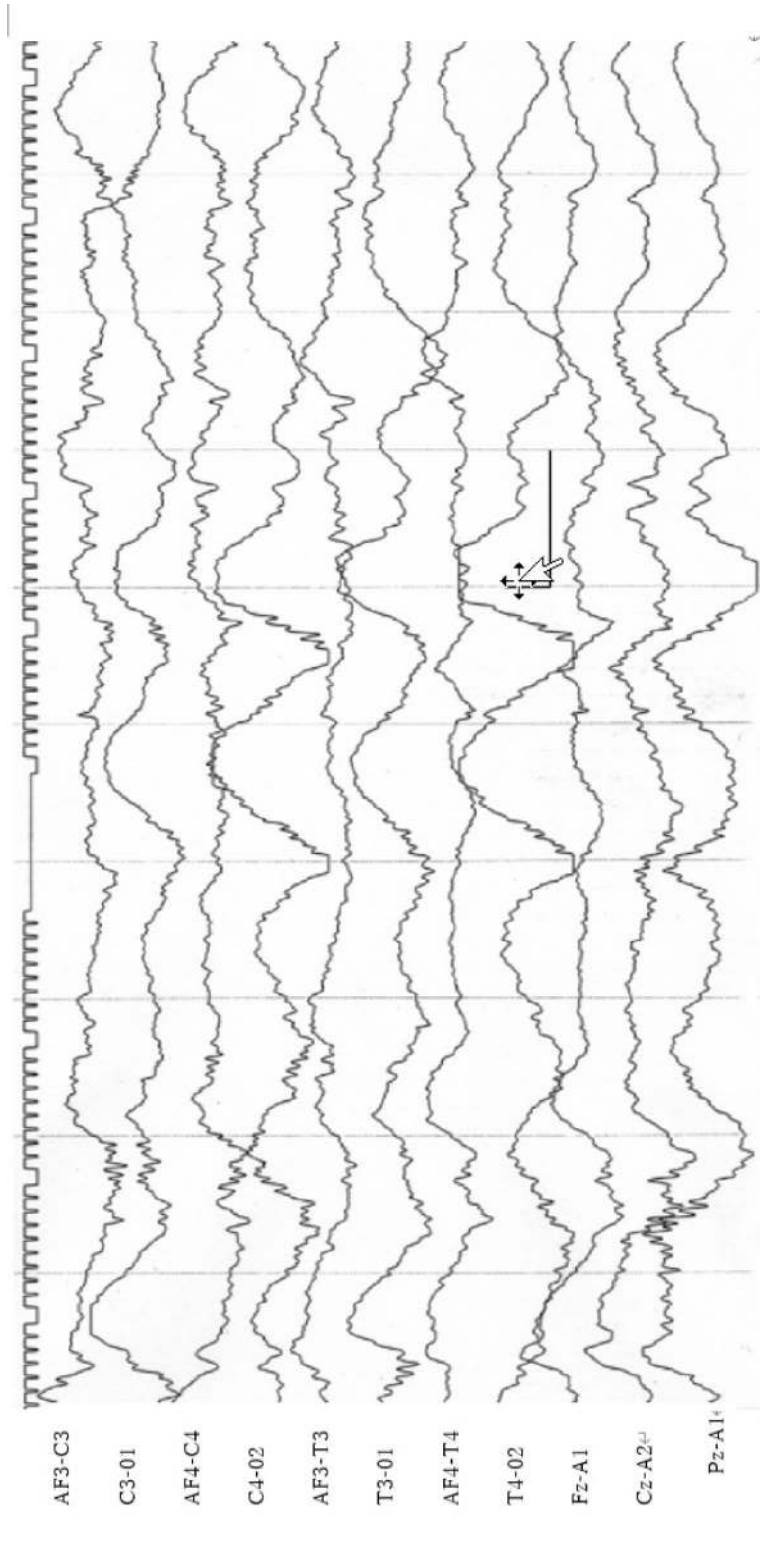

Fig. 6.4 High-voltage slow wave pattern at 32 weeks PMA (323)

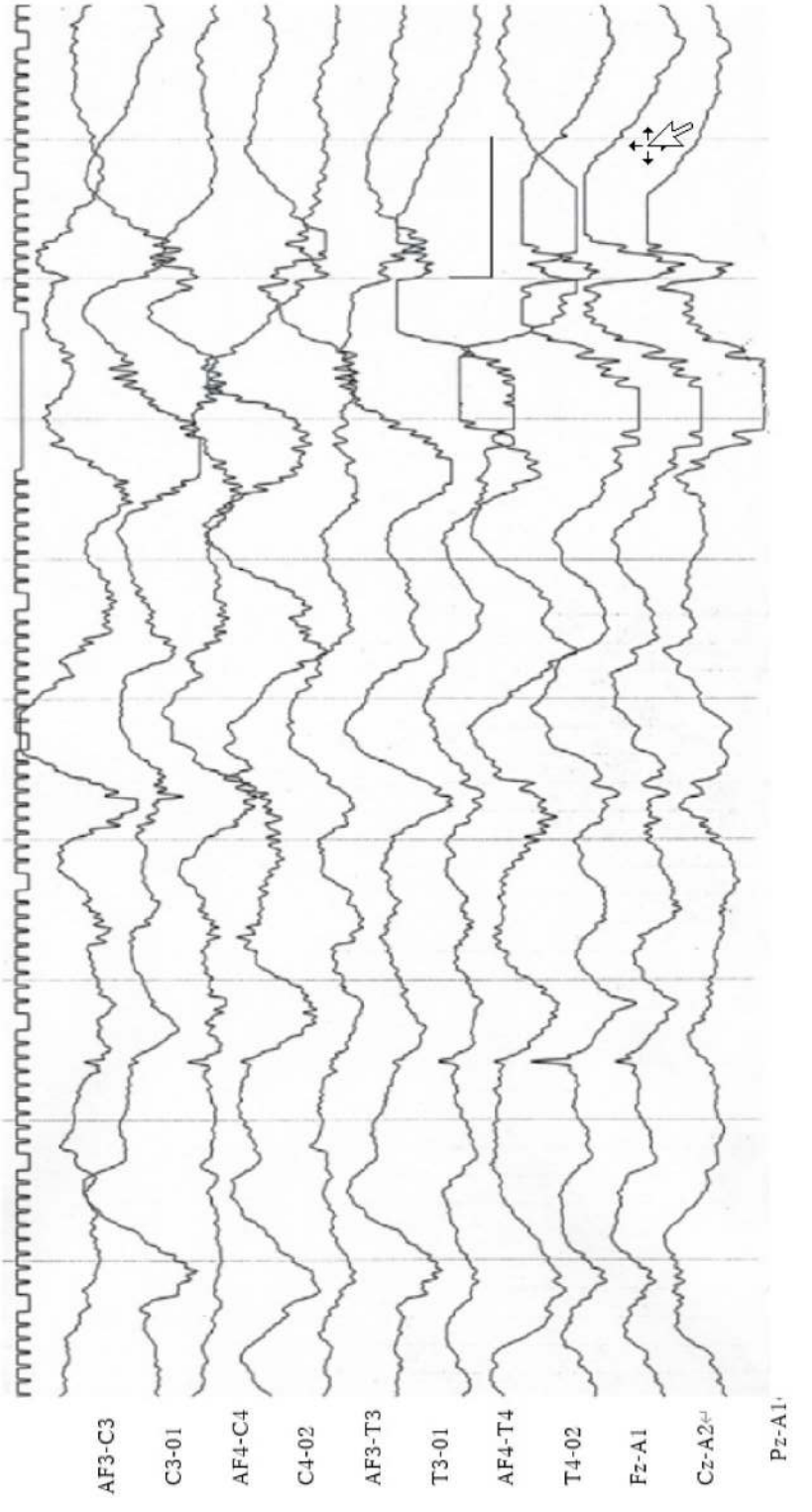

Fig. 6.5 High-voltage slow wave pattern at 34 weeks PMA (343)

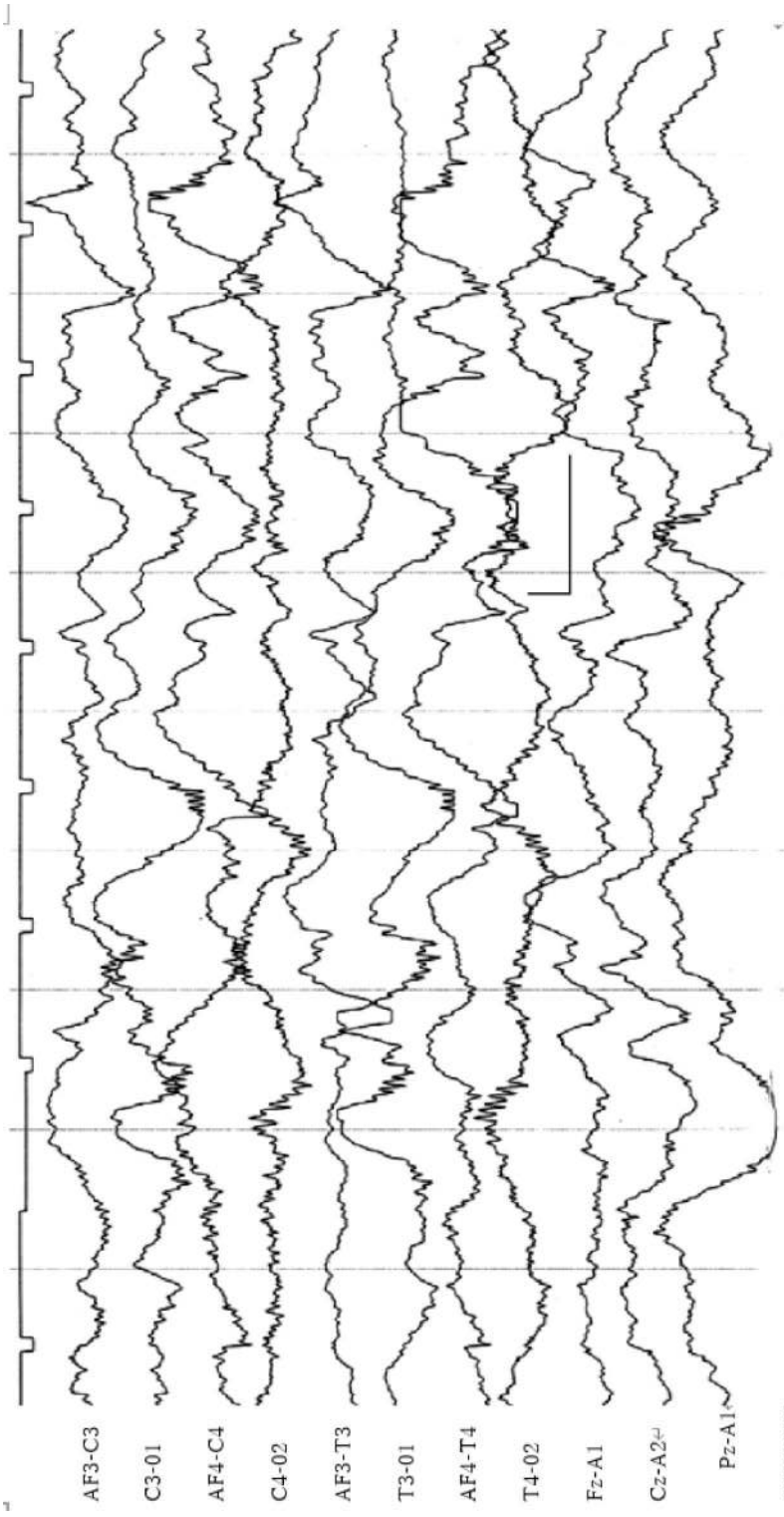

Fig. 6.6 High-voltage slow wave pattern at 36 weeks PMA (363)

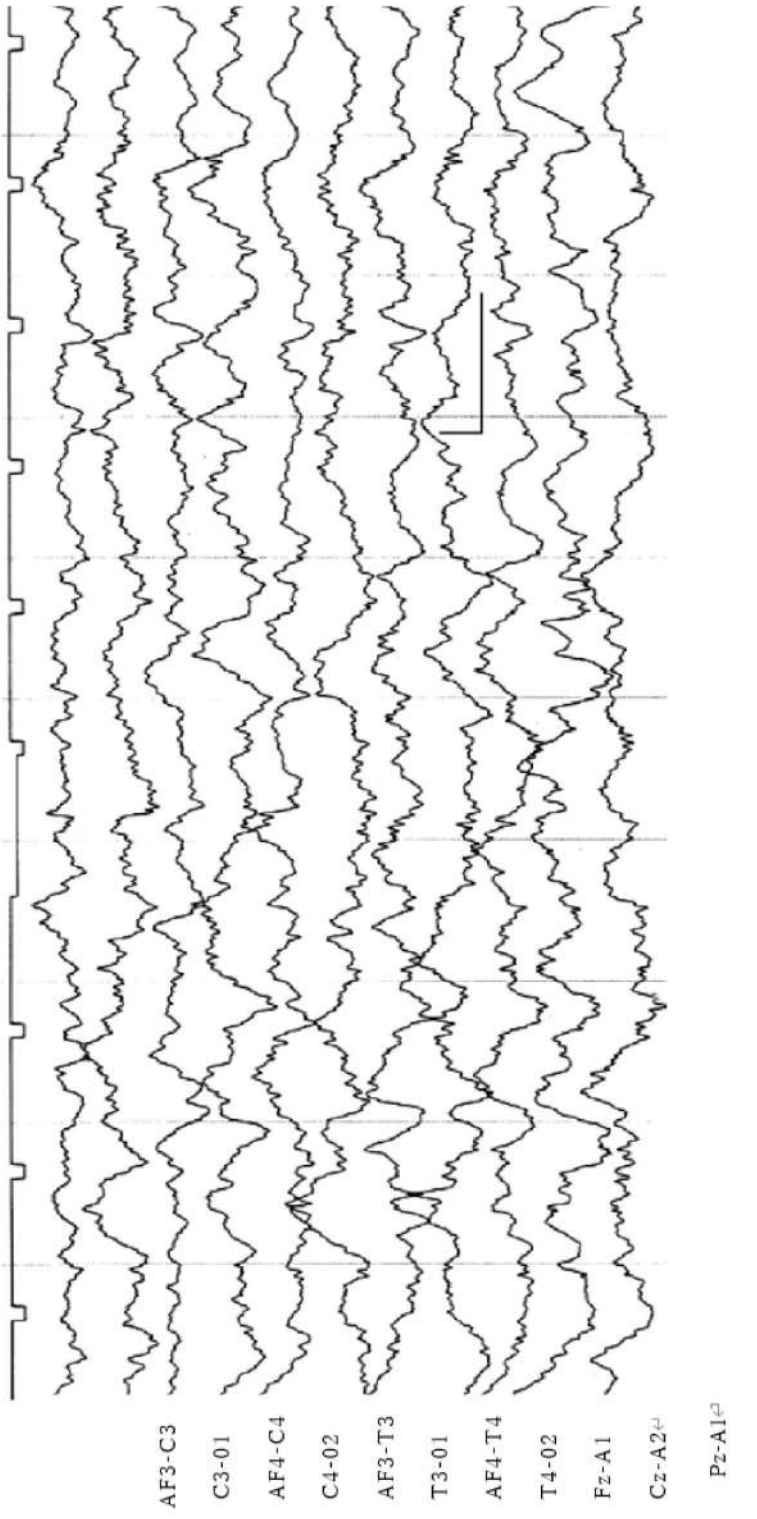

Fig. 6.7 High-voltage slow wave pattern at 38 weeks PMA (385)

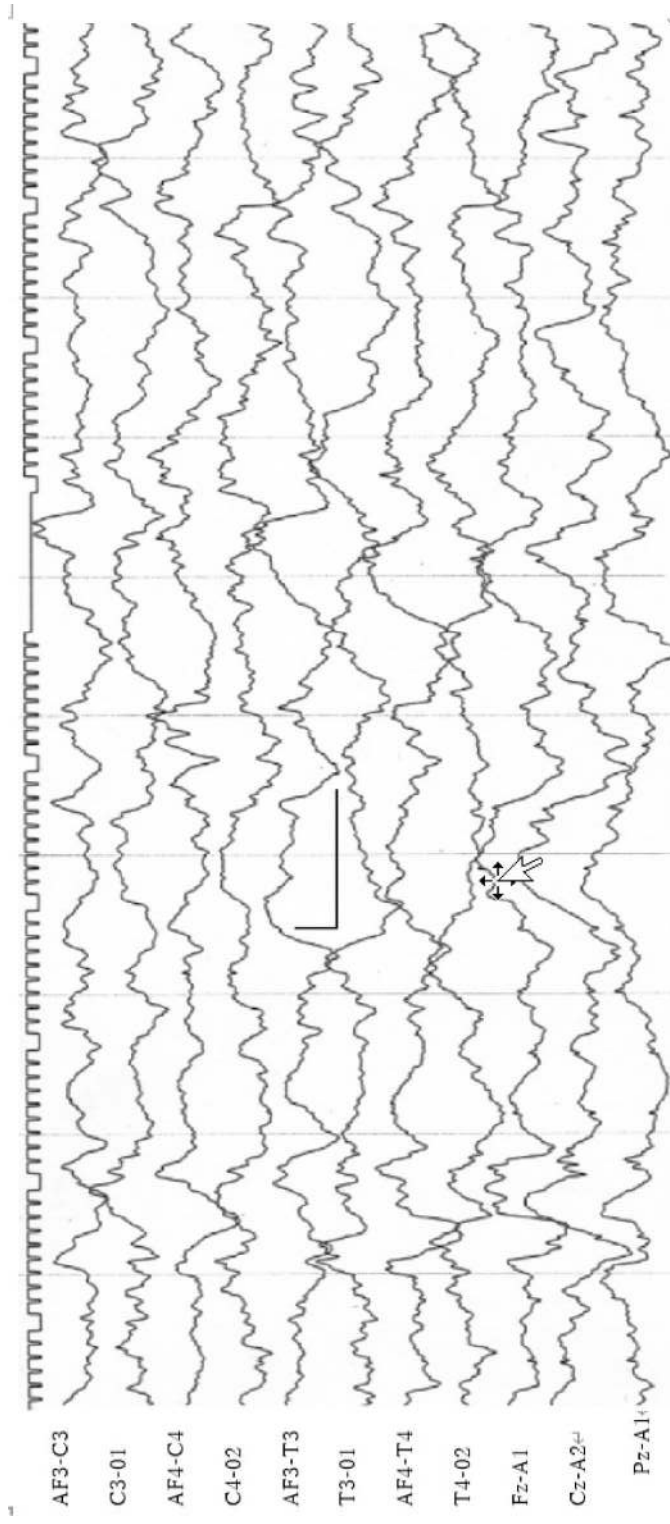

Fig. 6.8 High-voltage slow wave pattern at 40 weeks PMA (405)

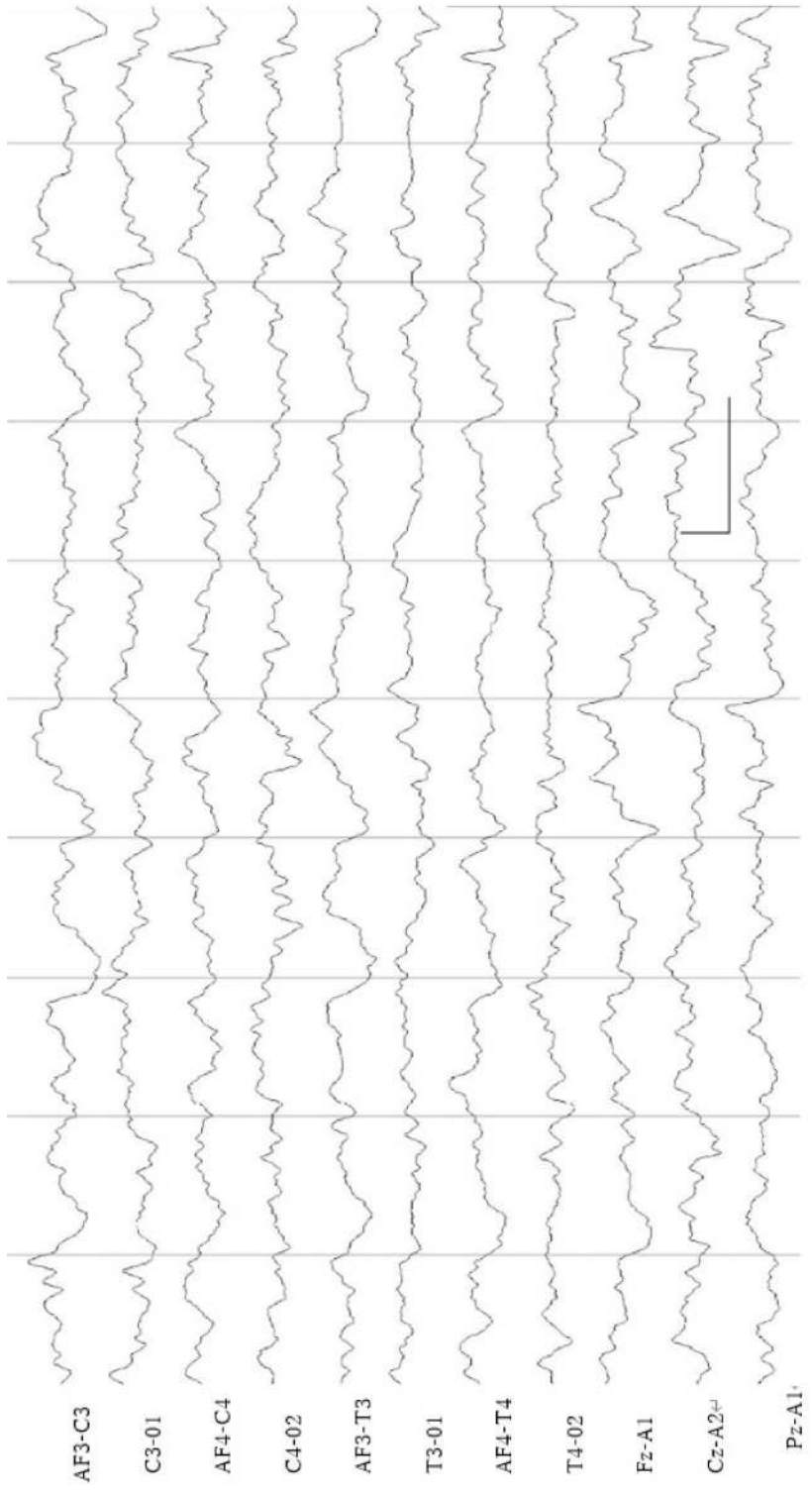

Fig. 6.9 High-voltage slow wave pattern at 42 weeks PMA (425)

At 44 weeks PMA, the alpha and theta components are further reduced, and the overall background activity is slow wave-dominant. Delta waves, ranging from 60 to 150 μV at frequencies of 2–3 Hz, are predominant, with each wave interfering temporally and spatially, resulting in abundant polymorphism. The waveforms become similar to those observed during slow wave sleep in older infants (Fig. 6.10).

Column: Tracé Alternant and Tracé Discontinu

(Kazunori Watanabe)

In preterm infants at postmenstrual age (PMA) 22–23 weeks, the EEG is discontinuous and intermittent whatever the state may be. Such intermittent EEG pattern is also observed in the early stages of development in other animals.

For example, in chicks, no spontaneous EEG activity is seen before 13–15 days of hatching. Around this time, low-amplitude, low-frequency activity begins to appear with interspersed flat periods of a few seconds, followed by an increase in frequency and amplitude, and a reduction in the duration of flat periods.

A spindle-like fast wave combined with a high-amplitude slow wave, known as a delta brush, also appears in this phase of EEG activity, a phenomenon that is also common in other mammals. In cats, spindle-like fast waves initially appear only in the thalamus, then occasionally in the cortex and, finally, simultaneously in both the thalamus and cortex. In human preterm infants, such waves are most common at 32–33 weeks PMA and disappear almost completely by 40 weeks. In sheep, EEG activity first appears around 60 days of gestation, gradually increases in number, and disappears around 85 days of age when the EEG becomes continuous and polymorphic, suggesting similarities in EEG development between humans and these animals.

In sheep, the onset of this activity coincides with the arrival of afferent fibers from the thalamus to the cortex. Cortical evoked responses to afferent stimulation have already been observed. Based on these pieces of evidence, Bernhard et al. proposed the existence of a pacemaker in the thalamus. The consistency of the mode frequency of intervals between high-amplitude parts of the discontinuous and alternating EEG at around 10 s also supports this hypothesis. The decrease in number of long IBIs indicates that the cortex becomes more responsive to the pacemaker. The frequency of sleep spindle intervals seen after infancy is also constant at around 10 s.

We recorded cortical evoked potentials to light and sound in the flat portion of the EEG of preterm infants at 25 weeks PMA, indicating that in humans, at least the nonspecific projection system has already begun to function, even during the seemingly electrically inactive period. In addition, there is already electrical activity in subcortical fibers even before the onset of cortical EEG, suggesting that the mechanism of the onset of intermittent EEG during this period has a subcortical, possibly thalamic origin, and that the immaturity in the reticulo-thalamic-cortical pathway and cortex are involved in this mechanism.

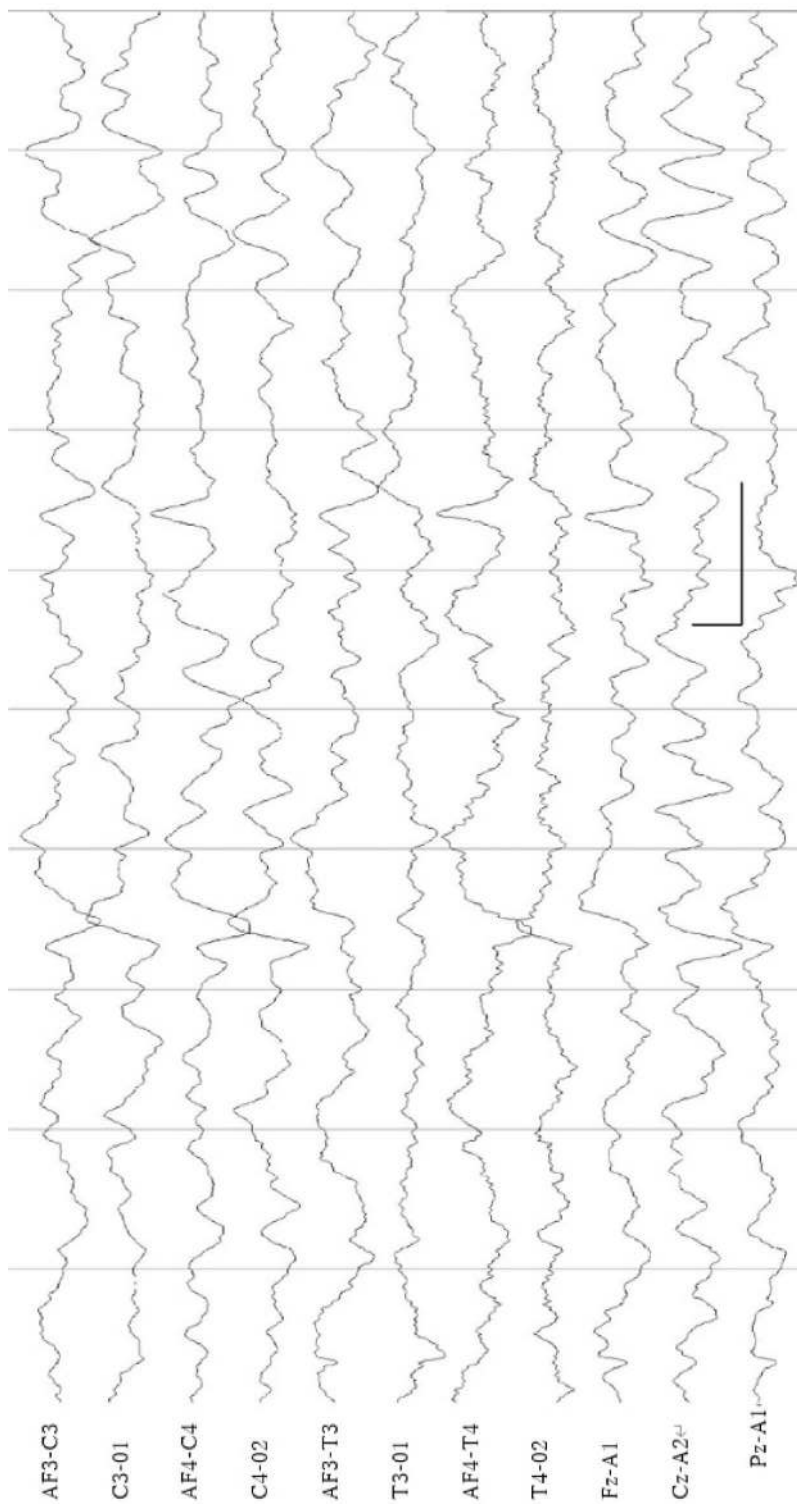

Fig. 6.10 High-voltage slow wave pattern at 44 weeks PMA (445)

7 Developmental Changes in EEG Patterns: Development of Low-Voltage Irregular Patterns

Toru Kato and Fumio Hayakawa

This chapter is focused on the developmental changes in the low-voltage irregular (LVI) pattern at different postmenstrual ages. LVI (coded as the "2" pattern) is the most common and typical pattern seen during active sleep (AS). This pattern can be recorded easily but provides limited information due to its minimal EEG activity and low voltage.

*See Chap. 3.

This pattern is almost flat at 26 weeks PMA, with only intermittent slow waves and sharp waves. Frontal sharp bursts and occipital sharp bursts may appear independently. However, most commonly, single slow waves appear in a localized manner. It is important to interpret the prominent flatness of the baseline as a characteristic of physiological LVI, rather than as suppressed activity (Fig. 7.1).

Pattern 282 is almost flat, with only intermittent slow waves and sharp waves, but there is more inserted activity than in pattern 262 (Fig. 7.1). Frontal sharp bursts and occasional sharp bursts may appear independently. However, single slow waves are more commonly localized or preceded by "high amplitude theta." Although the flatness of the baseline is pronounced, its duration is shorter, compared with pattern 262 (Fig. 7.2).

Pattern 302 is characterized by baseline low voltage and irregular activity, with intermittent slow waves and sharp waves. The inserted activities are increased, compared to pattern 282 (Fig. 7.2). Slow waves with high amplitude theta are infrequent, and rhythmic temporal theta may be present. In addition, brushes are present and the baseline is rarely flat (Fig. 7.3).

Pattern 322 is characterized by intermittent slow waves and sharp waves appearing on a baseline of low voltage and irregular activity. Compared with pattern 302 (Fig. 7.3), there is an increase in superimposed or inserted EEG activity. Rhythmic temporal theta is less common in this pattern, while delta brushes are more frequent and the baseline is rarely flat. Similar to other patterns observed at 32 postmenstrual weeks, pattern 322 is marked by a reduced presence of sharp waves and theta waves, contributing to an overall impression of relative calmness. Brushes are frequent, and a series of low-voltage slow waves may appear from the occipital areas (Fig. 7.4).

Pattern 342 is characterized by a baseline of low voltage and irregular activity with intermittent slow and sharp waves. Rhythmic temporal theta is absent in this pattern, and brushes are frequently observed, while sharp waves and theta waves are rare, giving the pattern a relatively calm appearance. In addition, low-voltage slow waves may continuously appear from the occipital region (Fig. 7.5).

T. Kato (✉) · F. Hayakawa
Department of Pediatrics, Okazaki City Hospital, Okazaki, Japan
e-mail: torukato@sun-inet.or.jp

A. Okumura, H. Kidokoro (eds.), *Neonatal EEG: Atlas and Interpretation*,
https://doi.org/10.1007/978-981-96-0726-6_7

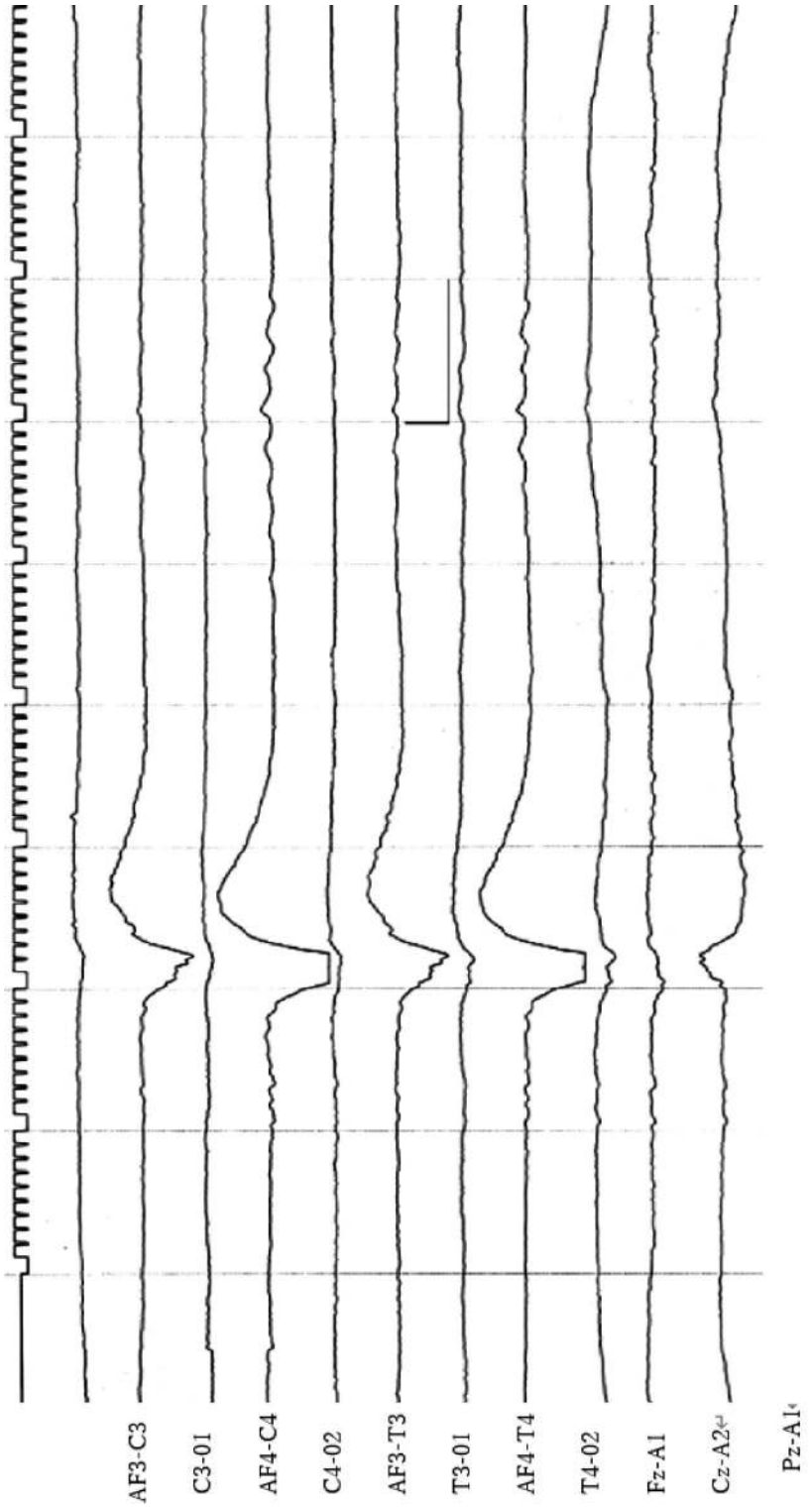

Fig. 7.1 Low-voltage irregular (LVI) pattern at 26 weeks PMA (262)

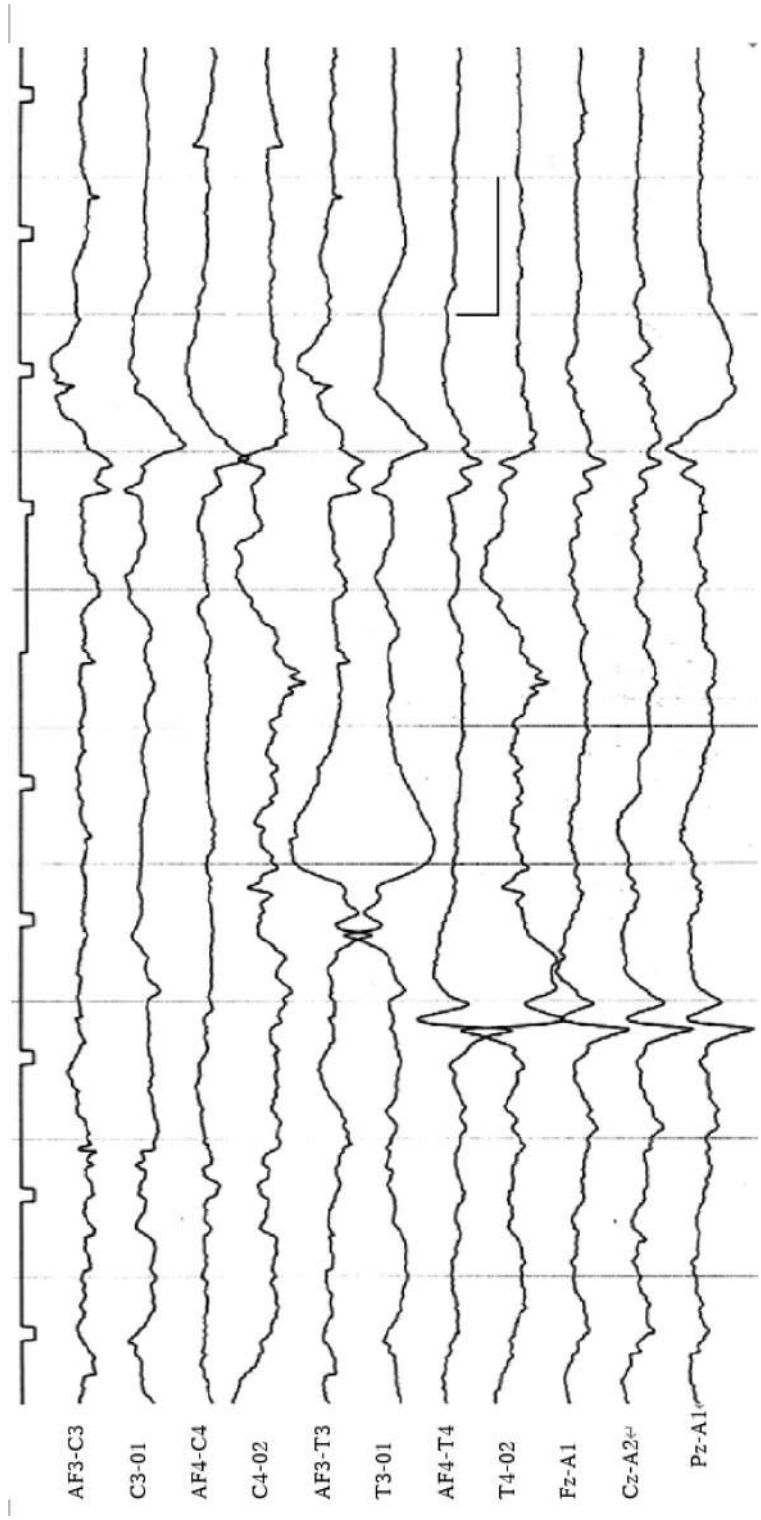

Fig. 7.2 Low-voltage irregular (LVI) pattern at 28 weeks PMA (282)

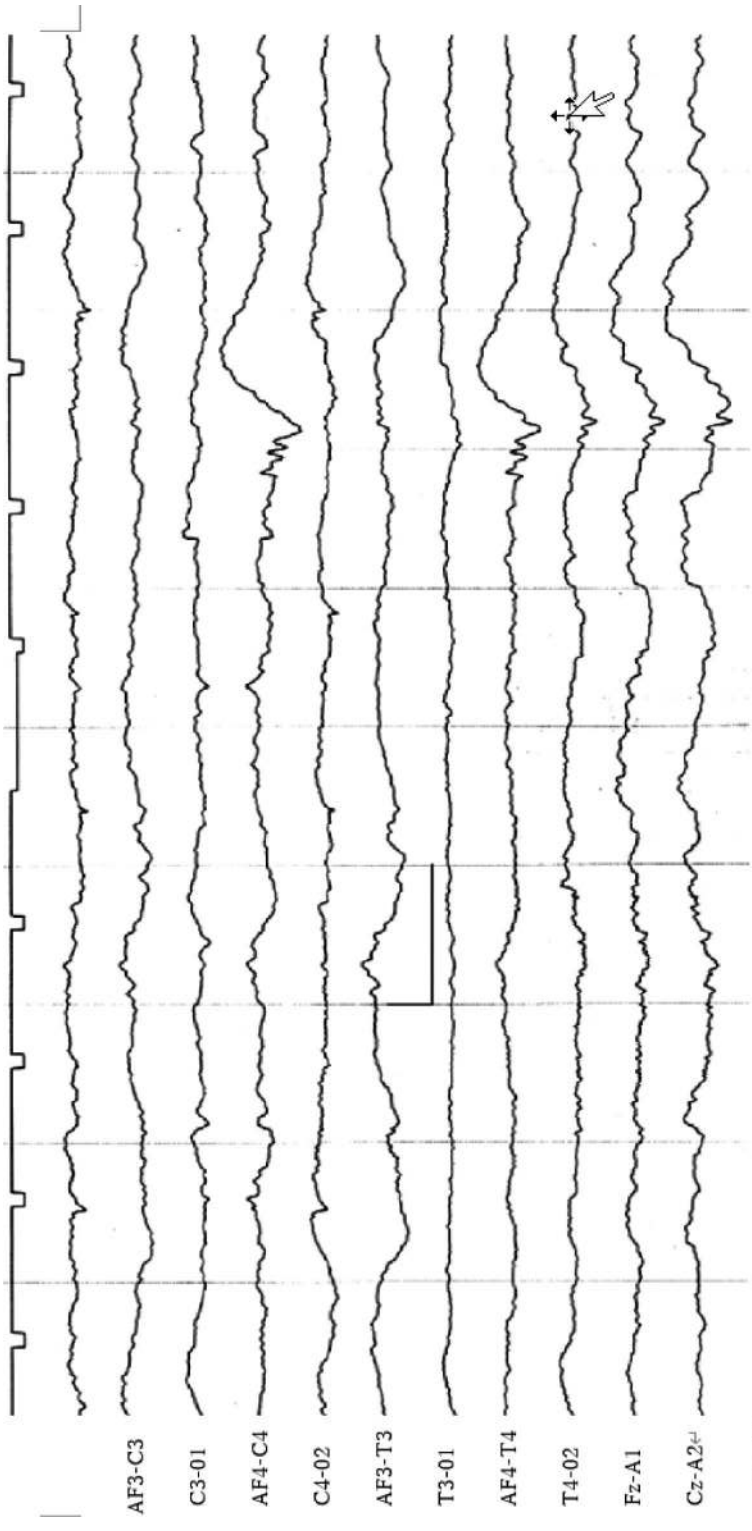

Fig. 7.3 Low-voltage irregular (LVI) pattern at 30 weeks PMA (302)

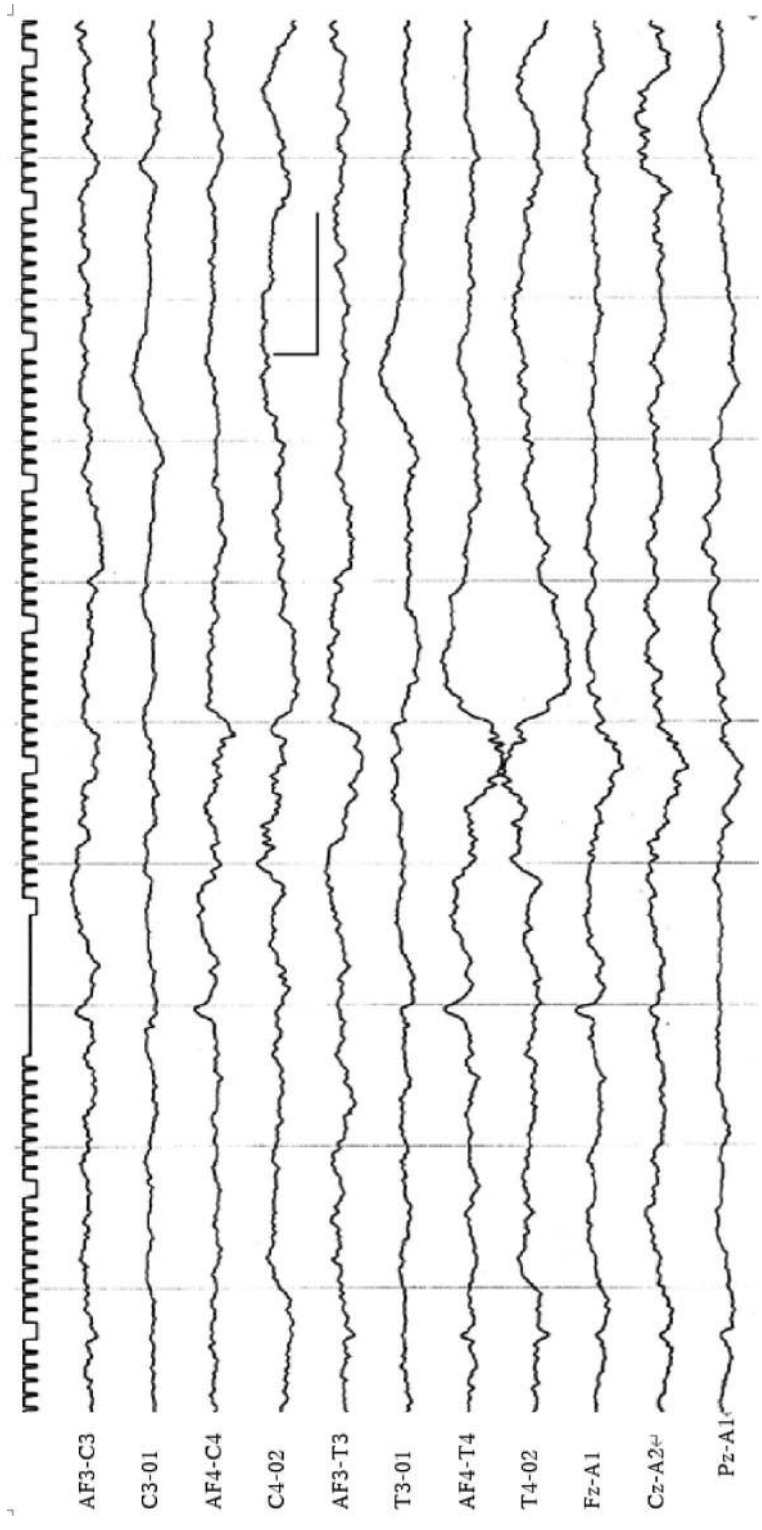

Fig. 7.4 Low-voltage irregular (LVI) pattern at 32 weeks PMA (322)

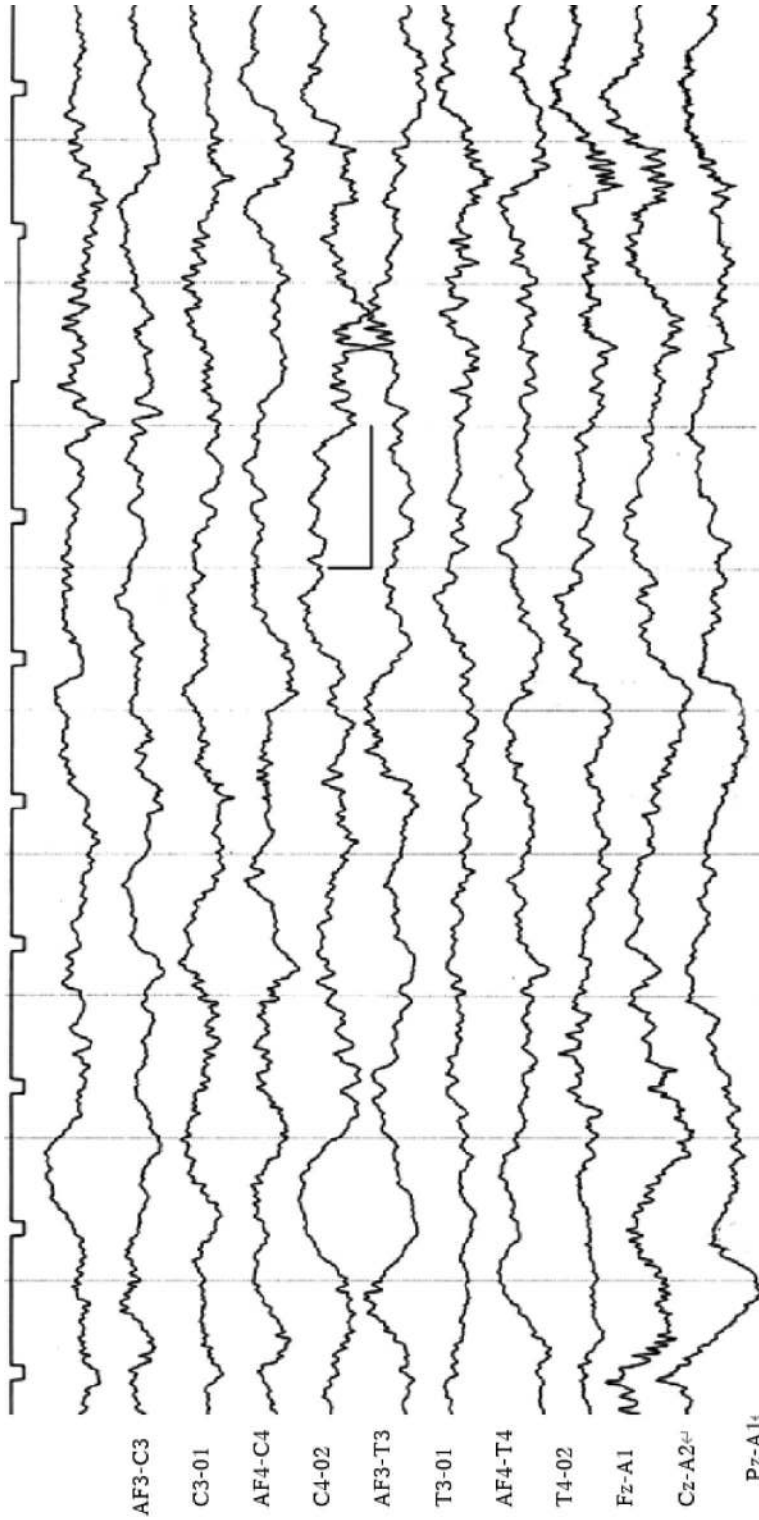

Fig. 7.5 Low-voltage irregular (LVI) pattern at 34 weeks PMA (342)

Pattern 362 is characterized by a baseline of low voltage and irregular activity, with intermittent slow waves and sharp waves. The low voltage and irregular activity in this pattern are almost continuous. Flat portions are only exceptionally observed. Brushes are frequently observed, and "temporal sharp bursts" also appear. In this pattern, brushes are characterized by their high voltage, sharp, and irregular nature (Fig. 7.6).

Pattern 382 exhibits low voltage and irregular activity. The baseline can be traced showing the low voltage and irregular activity to be continuous, with a few residual brushes, but lacking long, irregular brushes. Temporal sharp bursts are infrequent in this pattern. The frequency of the semi-rhythmic low-amplitude waveforms superimposed on the baseline is fast, mostly ranging between 8 and 14 Hz. In addition, the superimposition of immature fast waves, prominent across the entire area, is a notable characteristic of this pattern (Fig. 7.7).

Pattern 402 is characterized by continuous low voltage and irregular activity. No brushes are observed in this pattern. The frequency of semi-rhythmic theta activities superimposed on the baseline is between 5 and 7 Hz, which is slower than in pattern 382 (Fig. 7.7), and the superimposed fast waves are less prominent. This pattern is less common in the first AS period after falling asleep, but more common in the AS after the TA of QS. This pattern is believed to correspond to REM sleep in older children (Fig. 7.8).

In pattern 422, the low voltage and irregular activity are completely continuous, with no brushes present. The frequency of the semi-rhythmic low-amplitude theta waves superimposed on the baseline ranges between 4 and 6 Hz, which is slower than in pattern 402 (Fig. 7.8). No superimposed fast waves are observed. The theta waves also become slightly more rounded and slower (Fig. 7.9).

In pattern 442, the low voltage and irregular activity are completely continuous, with no brushes. The frequency of the semirhythmic low-voltage theta wave, superimposed on the baseline, ranges between 3 and 4 Hz, which is even slower than in pattern 402 (Fig. 7.8). No superimposed fast waves are observed. There are almost no fast wave components, giving a calm impression (Fig. 7.10).

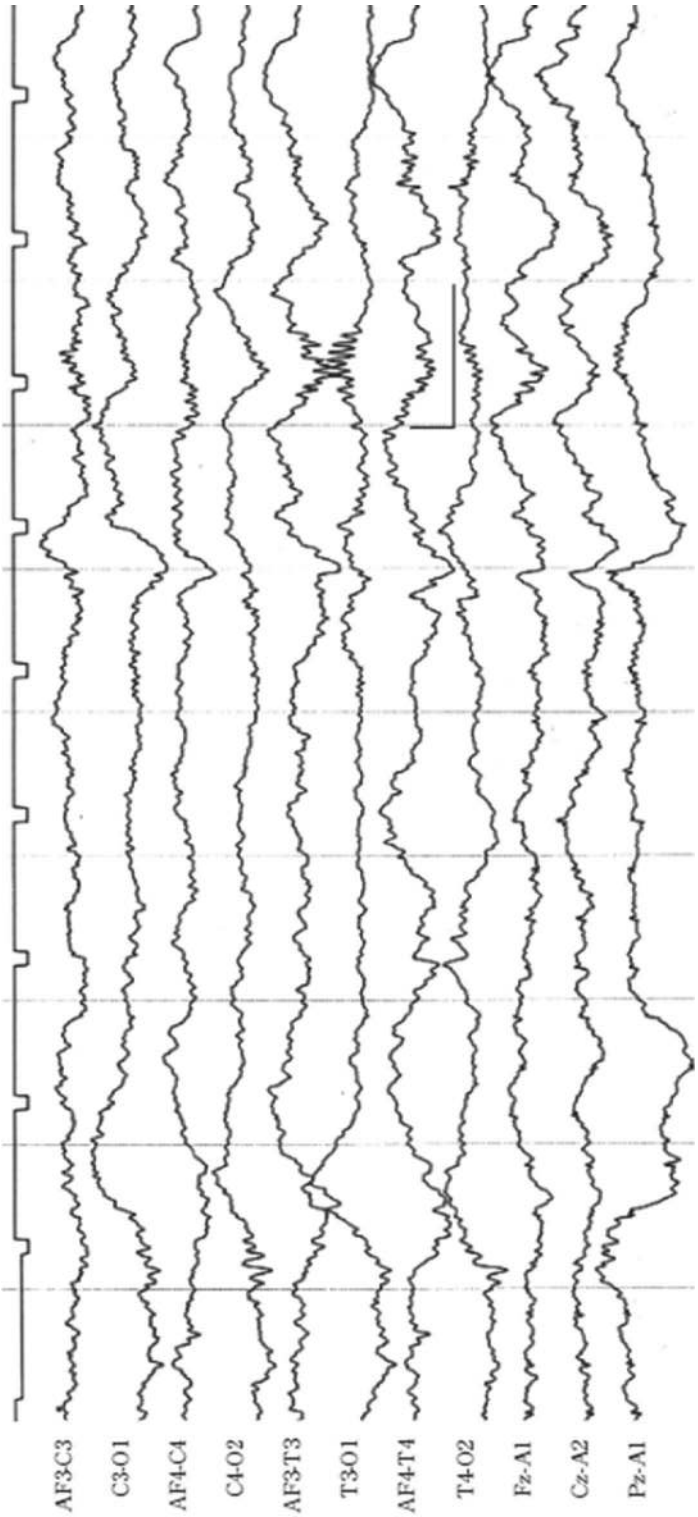

Fig. 7.6 Low-voltage irregular (LVI) pattern at 36 weeks PMA (362)

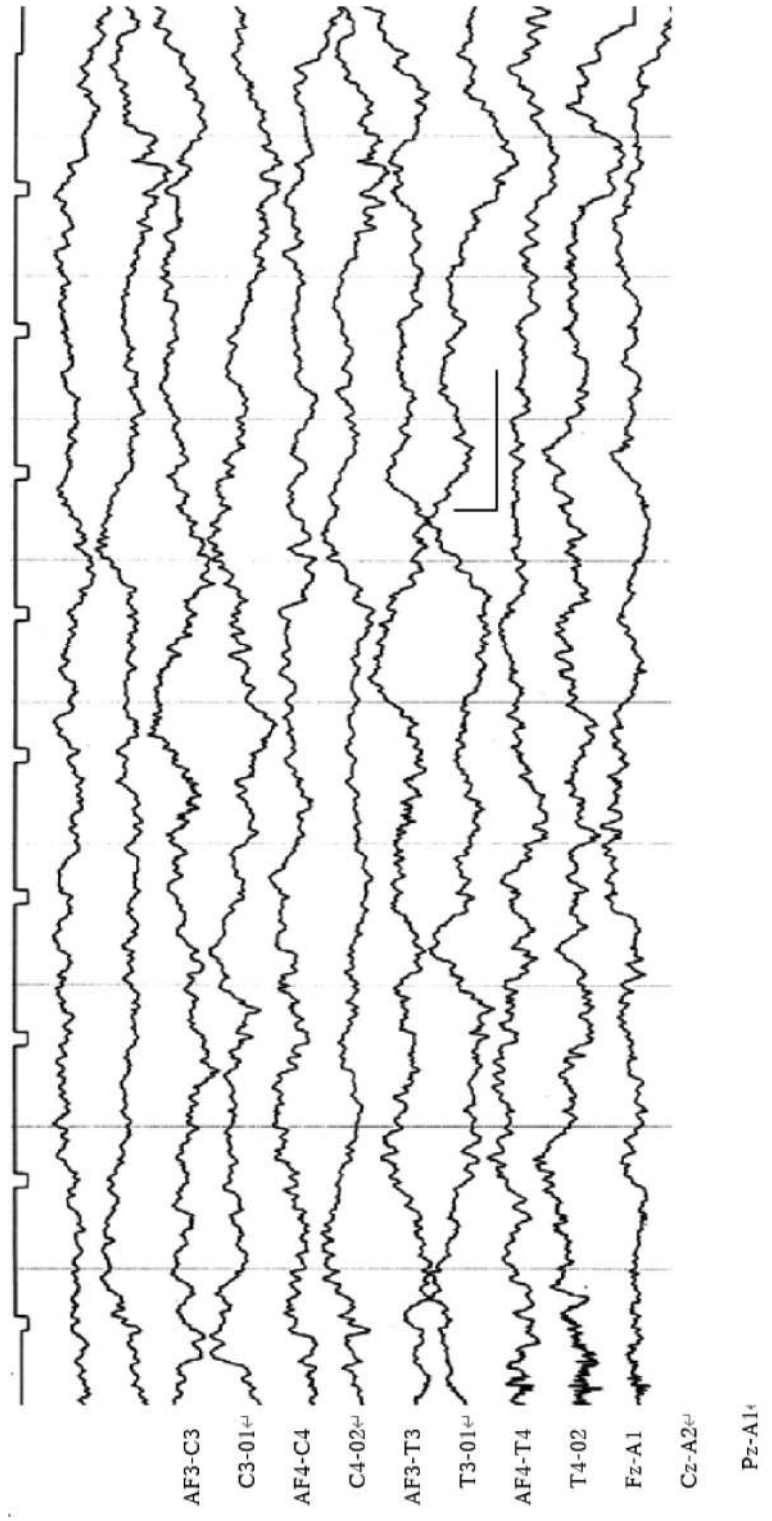

Fig. 7.7 Low-voltage irregular (LVI) pattern at 38 weeks PMA (382)

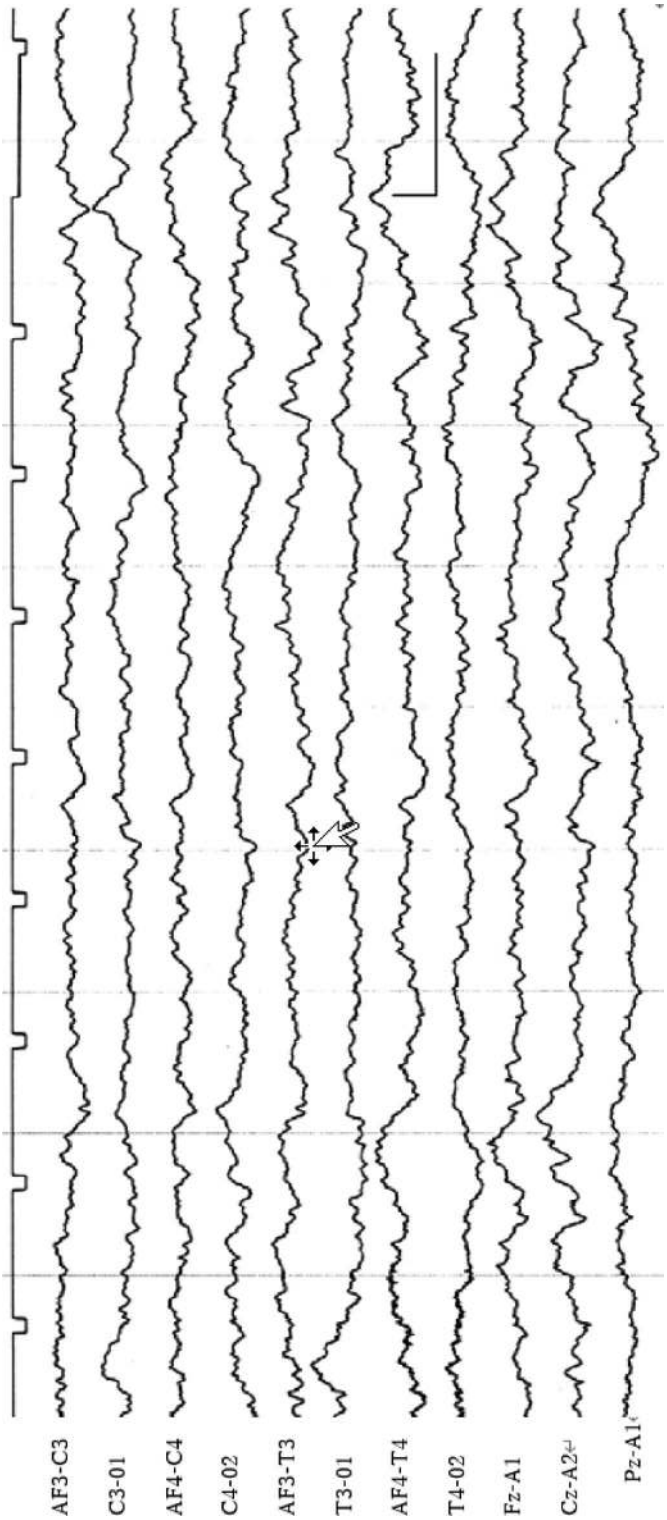

Fig. 7.8 Low-voltage irregular (LVI) pattern at 40 weeks PMA (402)

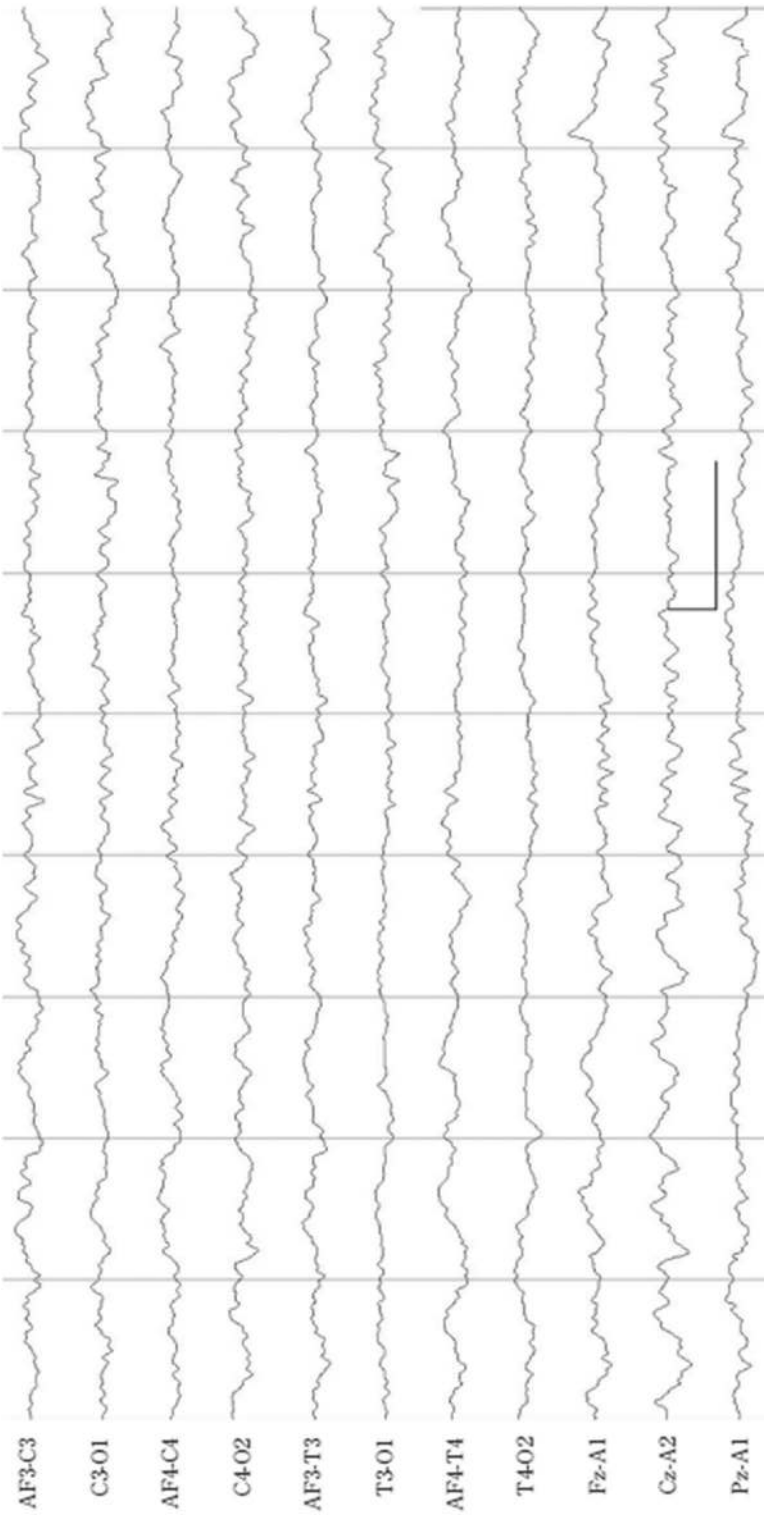

Fig. 7.9 Low-voltage irregular (LVI) pattern at 42 weeks PMA (422)

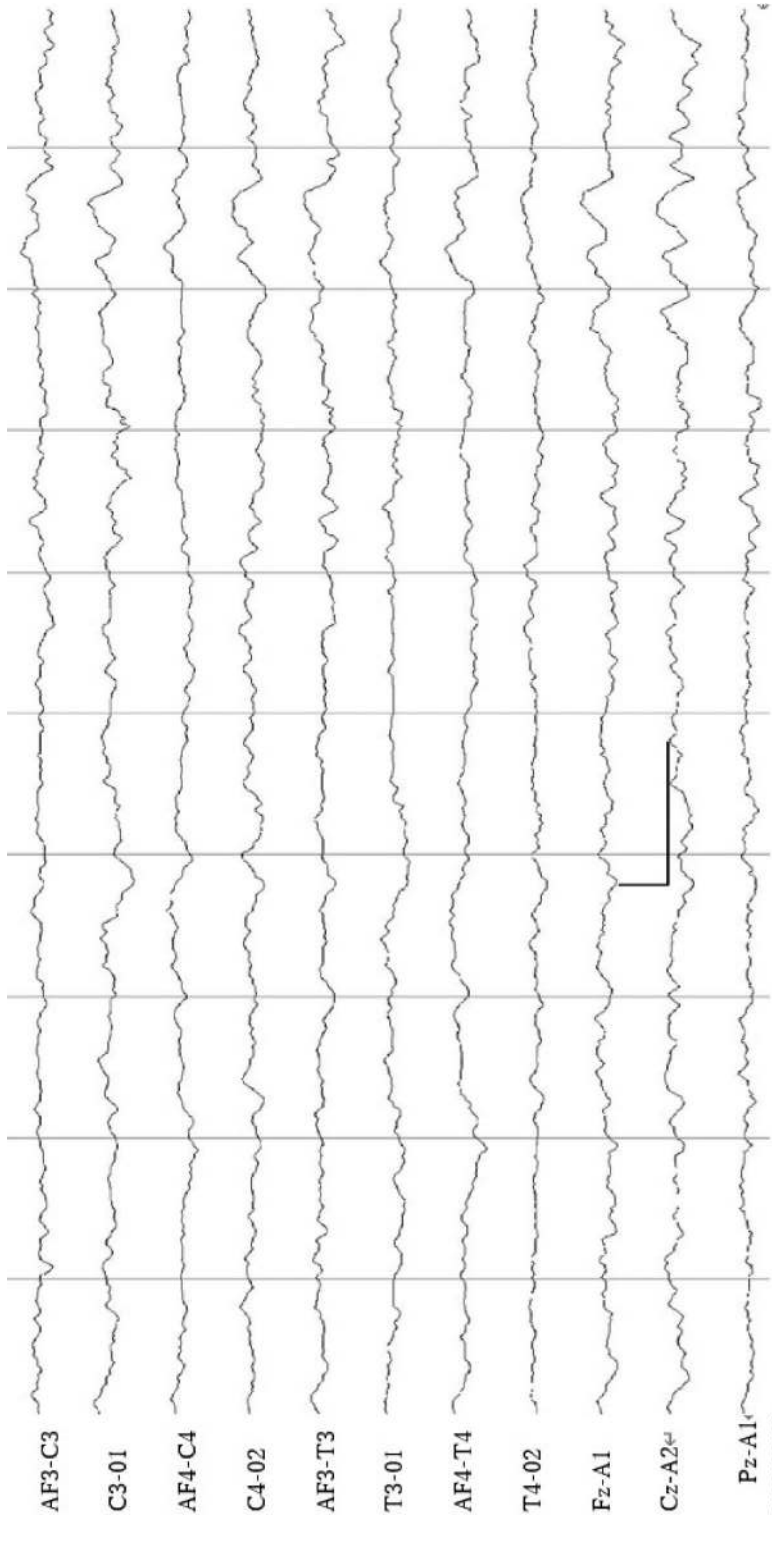

Fig. 7.10 Low-voltage irregular (LVI) pattern at 44 weeks PMA (442)

Column: What Does Delta Brush Mean?
(Kazuyoshi Watanabe)

The delta brush (or spindle delta) are characteristic waveforms in the EEG of preterm infants. These waveforms manifest as spindle-like fast waves superimposed on high-voltage slow waves. In the cortical EEG of patients who have undergone lobotomy, delta brush-like waveforms appear discontinuously, suggesting that they are intrinsic to the cortex. In the sensory cortex of the newborn rat, spindle-like fast waves manifest as spontaneous activity. However, they can also be evoked by sensory input corresponding to somatic localization. In human preterm infants, delta brushes occur spontaneously and also in response to limb movements in the area corresponding to localization. In newborn rats, tactile stimulation of the foot evokes a delta brush superimposed on a large slow wave in addition to spontaneous activity. Furthermore, the subplate was confirmed to be required for generating spindle-like fast wave activity in the somatosensory cortex of newborn rats. Analyses of human fetal brain slices showed that subplate neurons exhibit spontaneous electrical activity with a long silent period, resembling the discontinuous EEG of preterm infants. These findings suggest that much of the EEG in preterm infants reflects physiological function of the subplate. The delta brush is a spontaneous intrinsic activity of subplate origin, which is also evoked by afferent stimulation and may play an important role in cortical development. In the human fetus, sensory input from the external environment is limited in the uterus. However, intrinsic sensory input from fetal body movements during active sleep (AS) stimulates the somatosensory cortex, potentially playing an important role in its development. This mechanism may be similar in other sensory systems. In rats, EEG activity in the occipital region coincides with the time when spontaneous activity in the retina reaches the visual cortex via the thalamus. This suggests the necessity of afferent input from the periphery for the development of the cerebral cortex. The EEG becomes continuous from the EEG of AS because afferent stimulation from body movements of subcortical origin and eye movements during AS promotes the development of the cerebral cortex. Sensory input from spontaneous fetal body movements stimulates the somatosensory cortex, actively involving sensorimotor integration in the spinal cord and brain, and promoting the development of somatosensory localization. That is, activity-dependent coupling between muscle and the somatosensory cortex is thought to be involved in the development and refinement of intracortical connections.

8 Developmental Changes in EEG Patterns: Development of the Mixed Pattern and Differences from the High-Voltage Slow Wave Pattern

Toru Kato and Fumio Hayakawa

The mixed (M) pattern is a pattern of active sleep and corresponds to code "3".

Generally, pattern M presents as a low-voltage irregular (LVI) pattern with intermittent insertions of waveforms observed in a high-voltage slow wave (HVS) pattern. The distinction between M pattern "3" and HVS pattern "5" at term is extremely important for learning EEG interpretation and represents one of the initial challenges. The most significant difference between "3" and "5" is whether the baseline is traceable; specifically, pattern "3" allows for baseline tracing, while pattern "5" does not (Fig. 8.1). To clarify this difference, patterns "3" and "5" are presented side by side for the same postmenstrual age (PMA) in this chapter. On the other hand, for preterm infants, M and HVS are not differentiated, and both are categorized under code "3."

*See Chap. 3.

Pattern 383 consists mainly of a series of low-voltage irregular (LVI) activities, and "2" with intermittent slow waves and sharp waves. Delta brushes, frontal slow bursts, frontal sharp transients, temporal sharp transients, etc., appear in the low voltage and irregular activity that can be traced back to the baseline. Brushes are still observed, and the abundance of fast waves superimposed on the whole EEG is also characteristic of this pattern (Fig. 8.2).

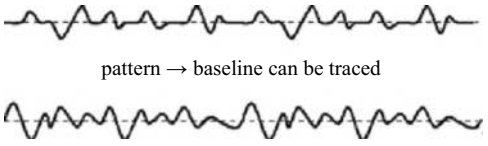

Fig. 8.1 Differences between mixed patterns and high-voltage slow wave patterns. In the mixed pattern, as shown in the upper figure, the EEG (solid line) is not completely continuous but is interrupted by short pauses. Therefore, the baseline can be traced as indicated by the dashed line. In contrast, in the high-voltage slow wave pattern, shown in the lower figure, the EEG (solid line) appears continuously without pauses. As a result, the baseline cannot be traced as in the upper figure. The dashed line in this case does not represent the baseline but simply traces the midpoint of the EEG

In pattern 385, the activity is dominated by delta waves of 100–150 μV and 2–2.5 Hz. Monotonous slow waves are predominant, and polymorphism of delta waves is recognized, but not to the same extent as in 405. The main difference between 383 (Fig. 8.2) and 385 is that the baseline can be traced in the former, while it cannot in the latter due to the continuous nature of EEG activity (Fig. 8.3).

T. Kato (✉) · F. Hayakawa
Department of Pediatrics, Okazaki City Hospital, Okazaki, Japan
e-mail: torukato@sun-inet.or.jp

A. Okumura, H. Kidokoro (eds.), *Neonatal EEG: Atlas and Interpretation*,
https://doi.org/10.1007/978-981-96-0726-6_8

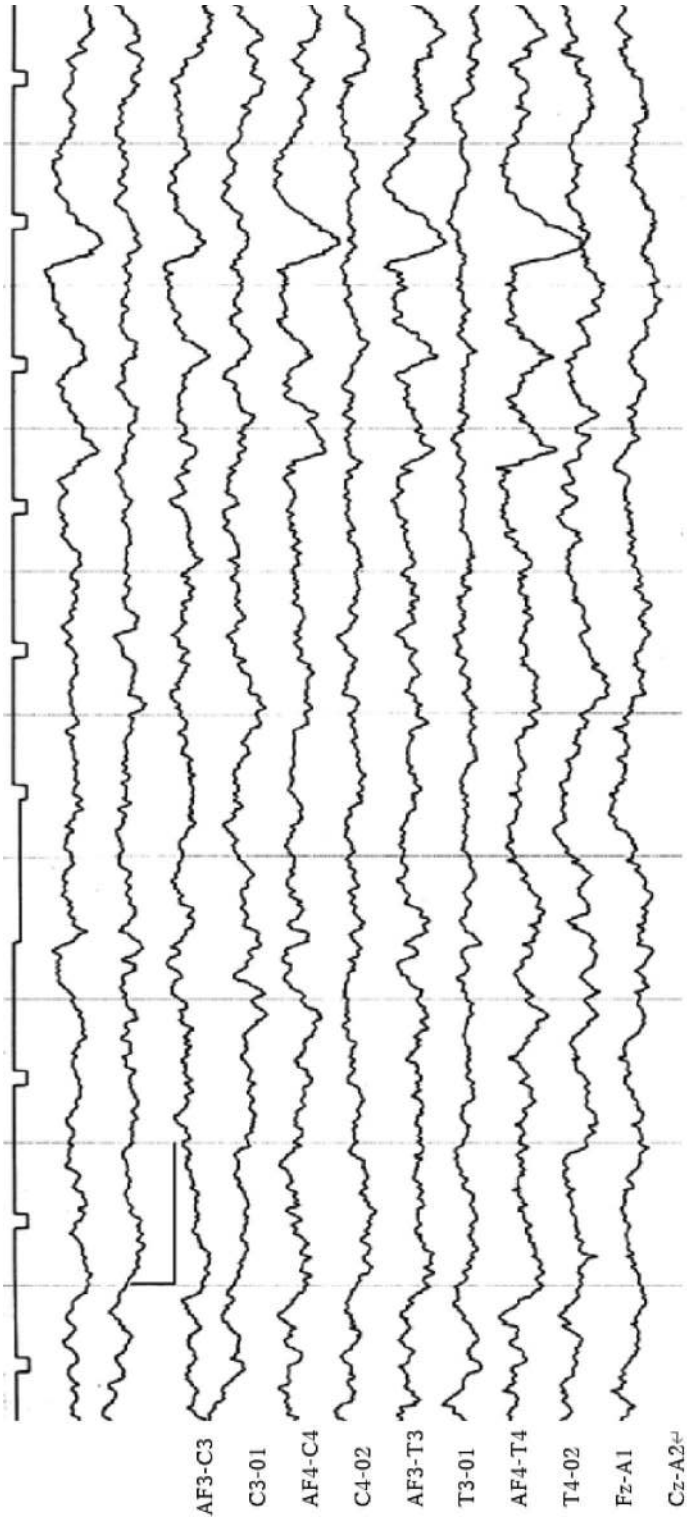

Fig. 8.2 Mixed pattern at 38 weeks PMA (383)

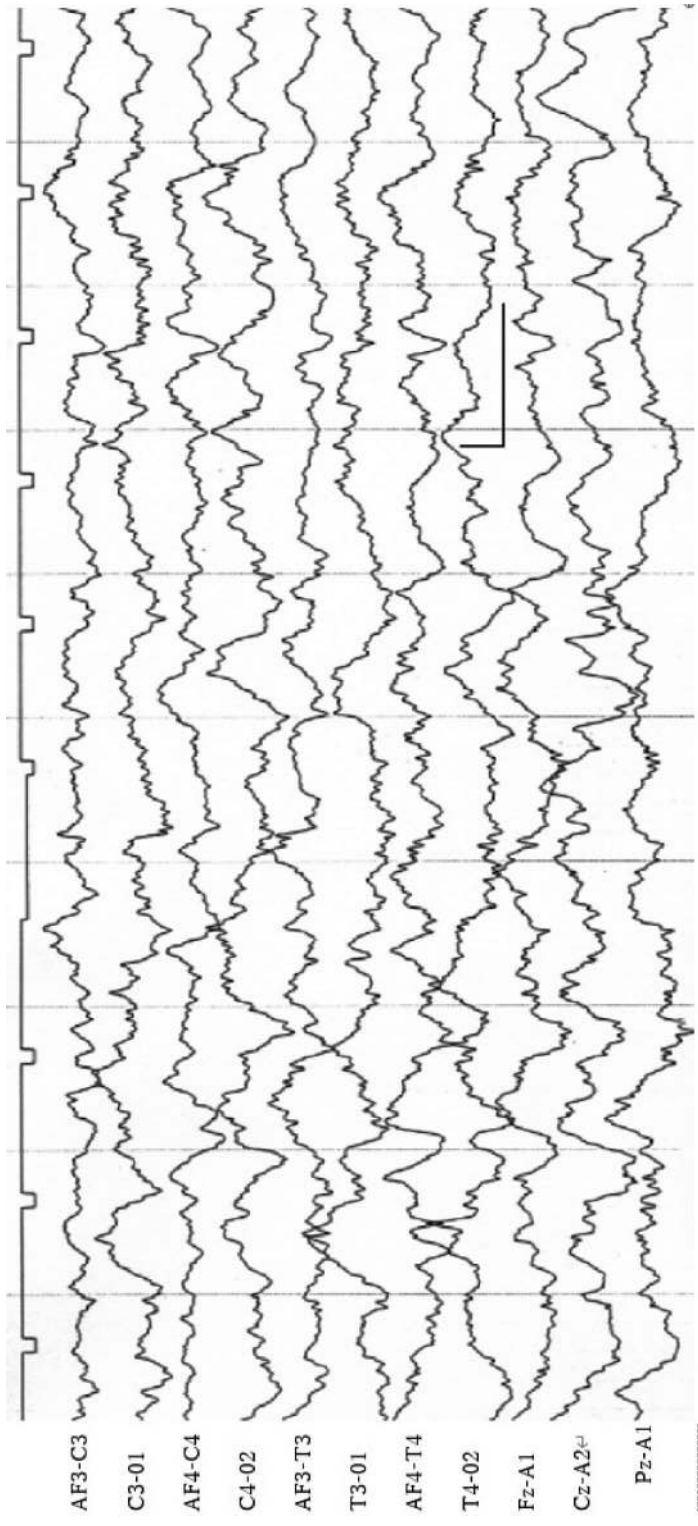

Fig. 8.3 High-voltage slow wave (HVS) pattern at 38 weeks PMA (385)

Pattern 403 (Fig. 8.4) is characterized by superimposed transients, such as frontal slow bursts, frontal sharp transients, and temporal sharp transients, on pattern 402 (Fig. 7.8). This pattern appears at the beginning of sleep onset. During this period, midline transients, such as Fz/Cz theta/alpha bursts, often appear. The intermittent slow waves gradually evolve into a continuous pattern, resulting in a transition to pattern 405 of quiet sleep (Fig. 8.5).

In pattern 405, the predominant EEG activity consists of delta waves, ranging from 80 to 120 μV at a frequency of 2–3 Hz. These delta waves show a distinct polymorphism, with only a few repetitions of the same waveform. The main difference between pattern 403 (Fig. 8.4) and pattern 405 is that the baseline can be traced in the former while it cannot in the latter, due to the continuous nature of EEG activity (Fig. 8.5).

The pattern 423 (Fig. 8.6) is based on pattern 422 with the addition of polymorphic delta waves and transients, such as frontal slow bursts, and frontal sharp transients. The frequency of these transients is decreased, compared to 40 weeks PMA. Midline transients are also decreased. The intermittent slow waves gradually become continuous, and the pattern shifts to 425 of quiet sleep (Fig. 8.7).

In pattern 425, delta waves tend to have higher voltage (80–120 μV), slower frequency (2–2.5 Hz), and more rounded morphologies, compared to those at 40 weeks PMA. Polymorphism is further increased, and monotonous slow waves become rare. The main difference between pattern 423 (Fig. 8.6) and pattern 425 is that the baseline can be traced in the former, while it cannot in the latter, due to the continuous nature of the EEG activity (Fig. 8.7).

Pattern 443 (Fig. 8.8) is based on pattern 442 (Fig. 7.10) with the insertion of polymorphic slow waves, and transients such as frontal slow bursts and frontal sharp transients become rare. The intermittent slow waves gradually transition to a more continuous pattern, resulting in a shift to pattern 425 of quiet sleep (Fig. 8.7).

In pattern 445, both alpha and theta components are further diminished, leading to a predominance of slow wave activity in the overall background. This activity is dominated by delta waves, with voltages ranging from 60 to 150 μV and frequencies of 2–3 Hz. Each wave interacts with others in a complex temporal and spatial manner, exhibiting abundant polymorphism, akin to that observed in an infant during slow wave sleep. The main difference between pattern 443 (Fig. 8.8) and pattern 445 is that the baseline can be traced in the former while it cannot in the latter, due to the continuous nature of EEG activity (Fig. 8.9).

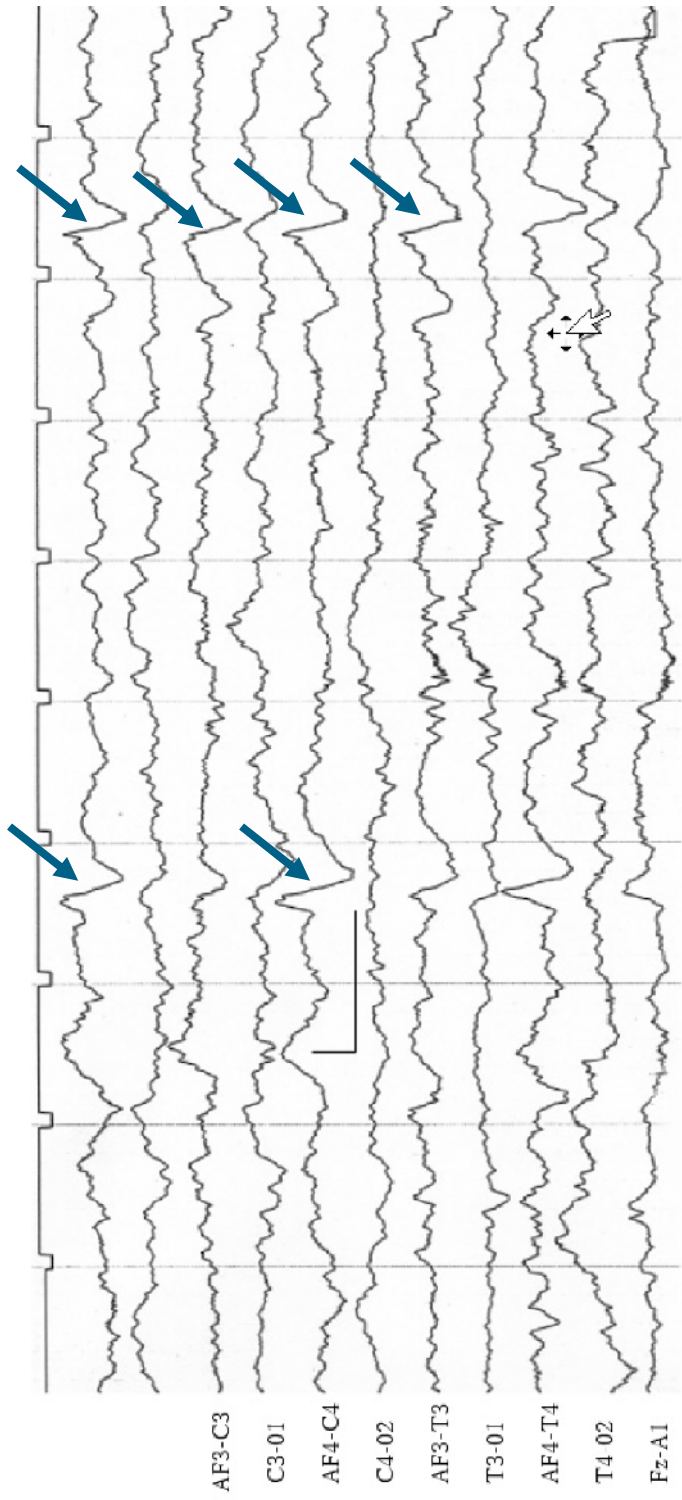

Fig. 8.4 Mixed pattern at 40 weeks PMA (403)

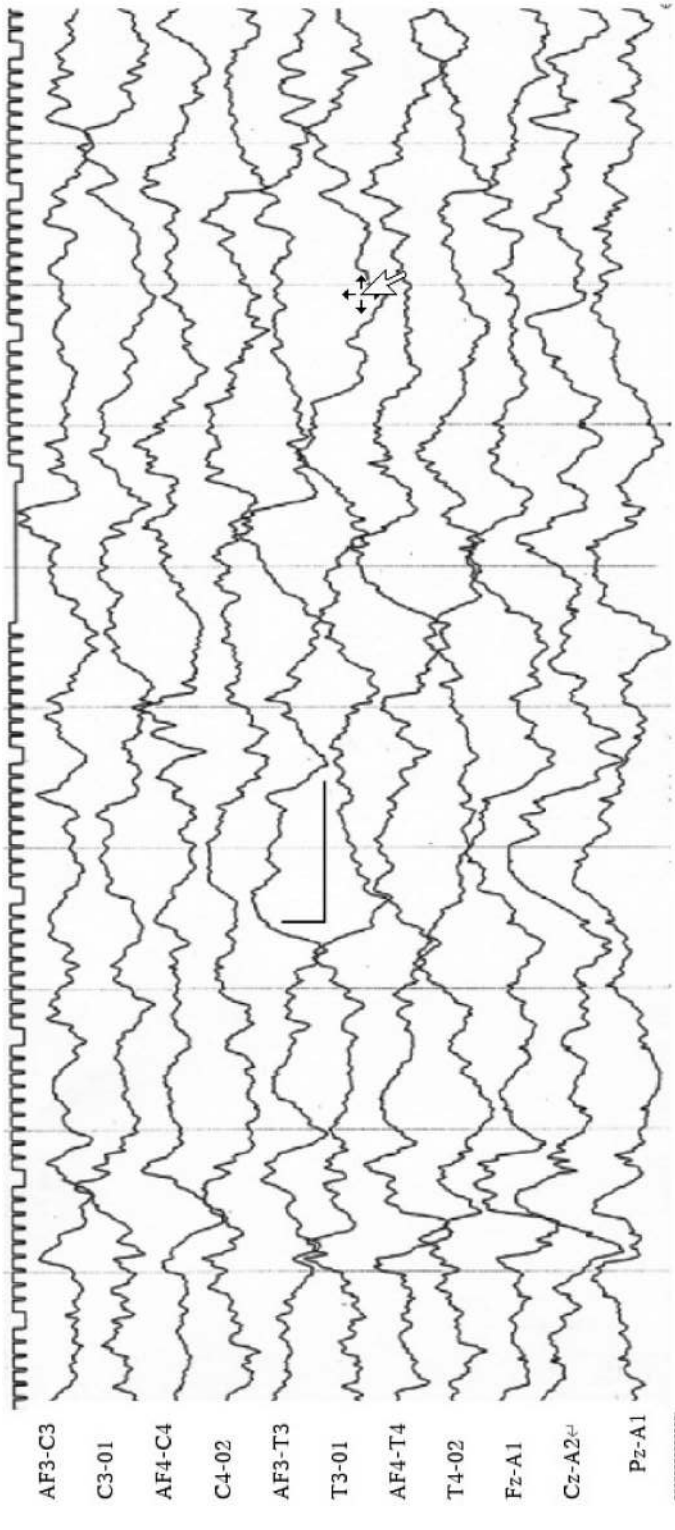

Fig. 8.5 High-voltage slow wave pattern at 40 weeks PMA (405)

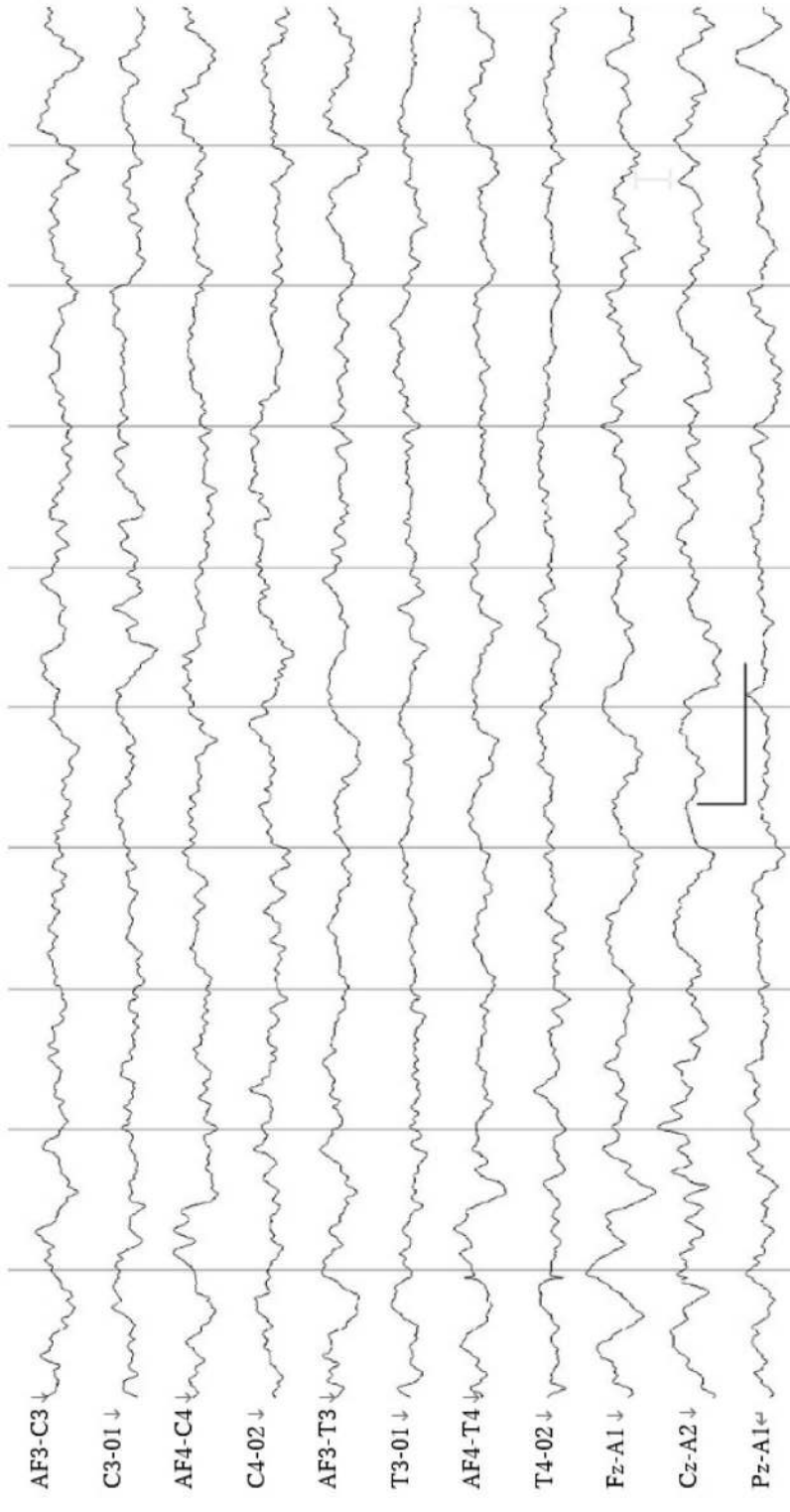

Fig. 8.6 Mixed pattern at 42 weeks PMA (423)

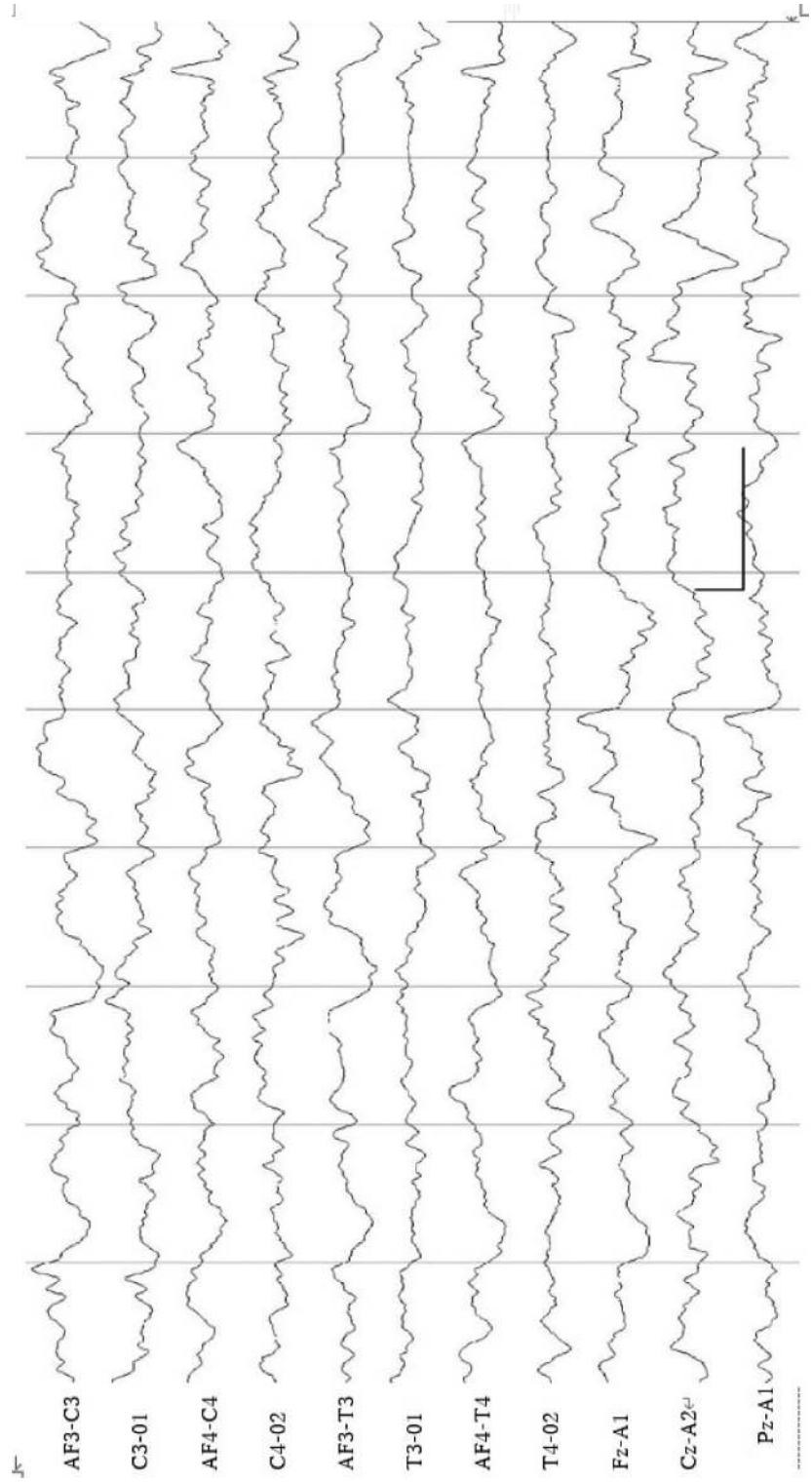

Fig. 8.7 High-voltage slow wave (HVS) pattern at 42 weeks PMA (425)

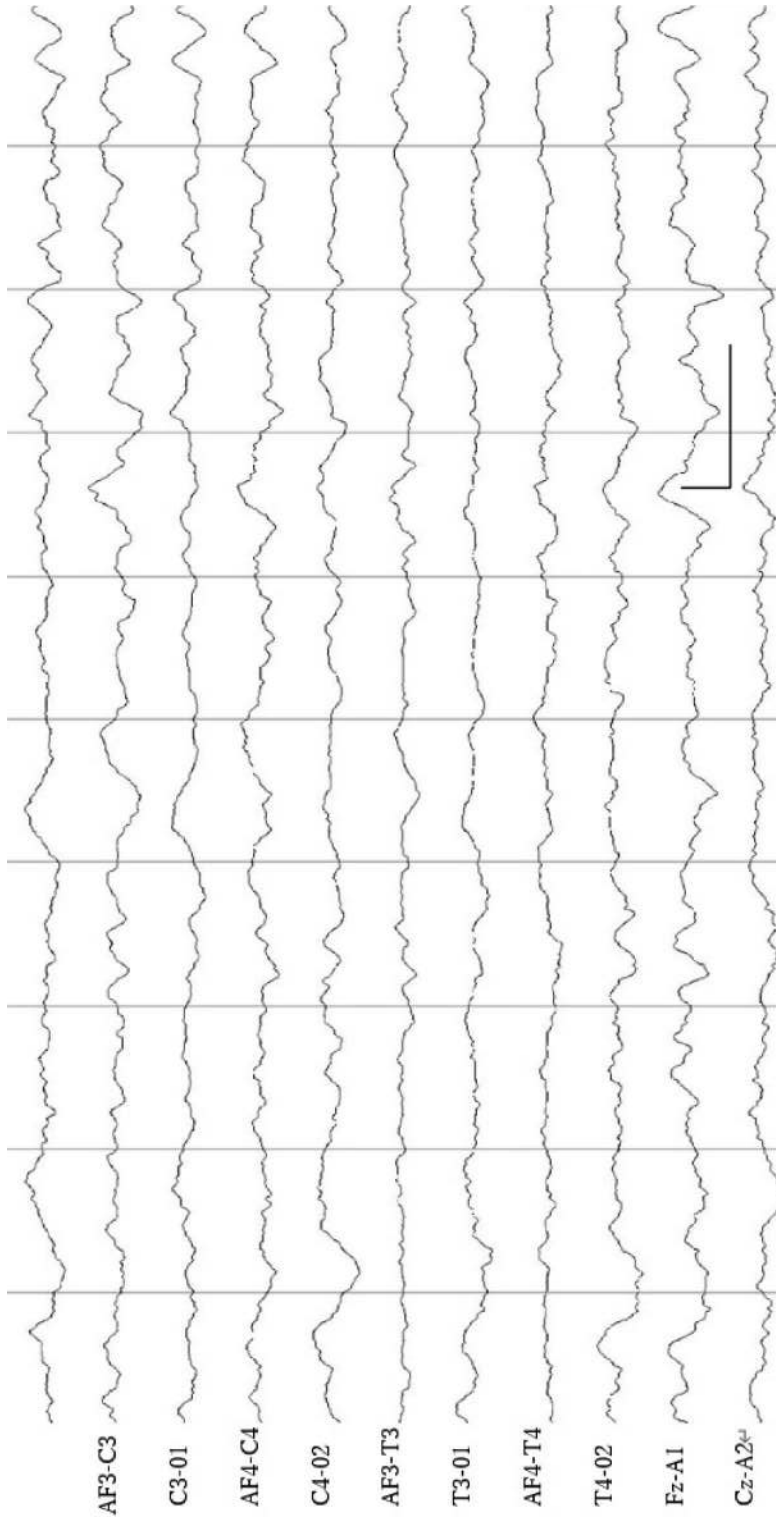

Fig. 8.8 Mixed (M) pattern at 44 weeks PMA (443)

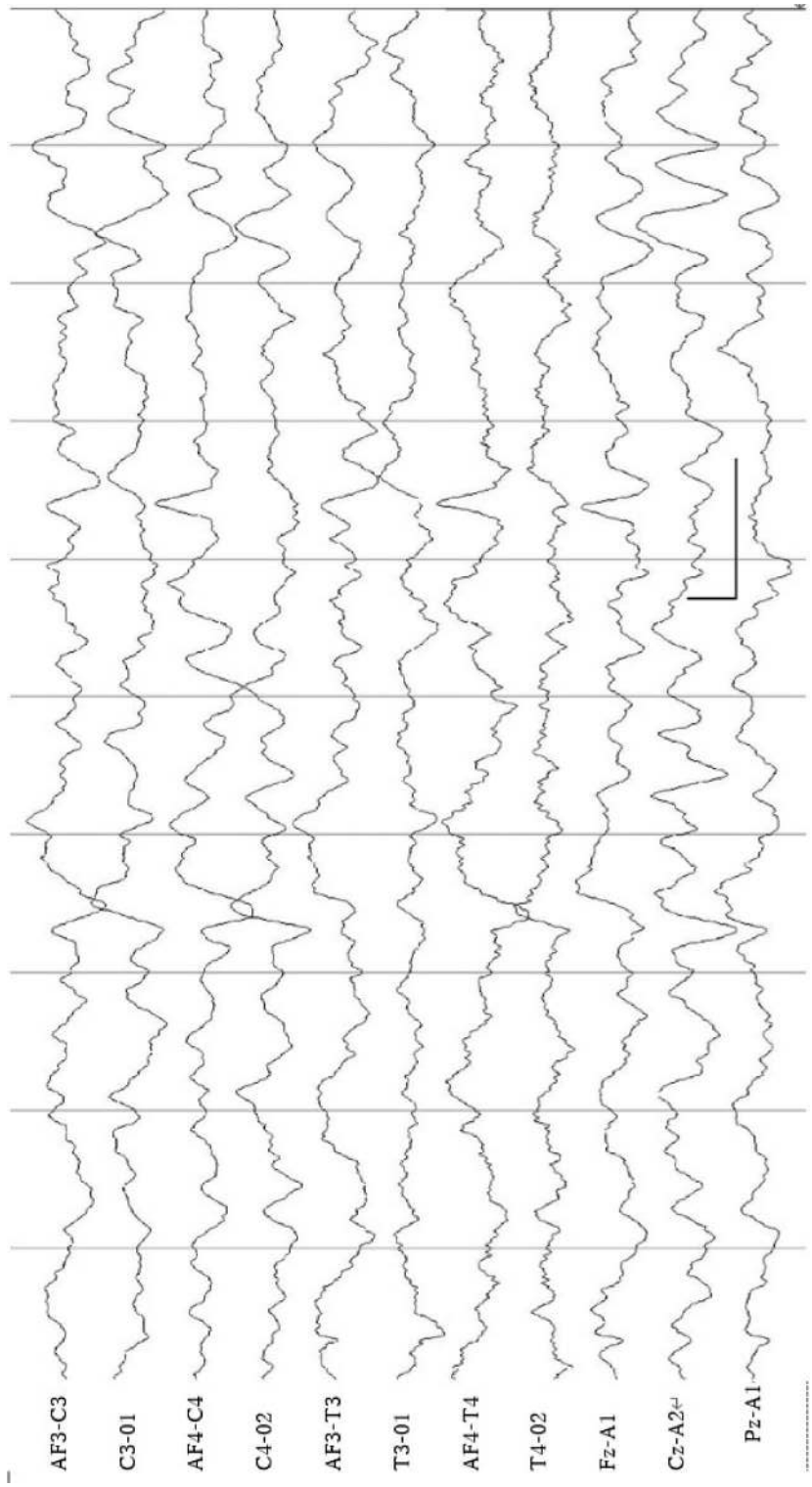

Fig. 8.9 High-voltage slow wave (HVS) pattern at 44 weeks PMA (445)

Column: Development of Slow Wave Sleep
(Kazuyoshi Watanabe)
From around 36 weeks postmenstrual age (PMA), a high-voltage slow wave pattern ("5") emerges alongside the alternating EEG in quiet sleep (QS), gradually increasing in prevalence. By 44–46 weeks PMA, this pattern replaces the alternating EEG, thus becoming the characteristic EEG of QS.

There are two distinct types of slow waves observed in slow-wave sleep. The slow oscillation (<1 Hz) is specific to cortical neuronal activity, requiring cortico-cortical coupling for synchronization across large cortical areas. These synchronized slow oscillations projected through cortico-thalamic tracts to the thalamus, are coordinated with delta (1–4 Hz) oscillations within the thalamus. These in turn project back to the cortex, forming slow waves in the scalp EEG. This cortico-cortical coupling is essential for the occurrence of slow wave sleep, which is observed in birds and mammals with well-developed cortico-cortical connections but absent in reptiles.

Neonates exhibit two distinct types of slow waves, each with unique characteristics. The delta brush, a monotonous and constant morphology, ultrahigh amplitude, and ultralow frequency (0.3–1 Hz), differs in polarity from the slow wave of slow wave sleep. It is present in both active (REM) and quiet (non-REM) sleep, suggesting a subplate origin. In contrast, the slow waves of slow wave sleep are polymorphic high-voltage slow waves (1.5–3 Hz), which are seen only in non-REM sleep (stages 3 and 4). High-voltage slow waves in QS appear after 36 weeks PMA, increasing as cortico-cortical connections develop and the cortex begins to respond synchronously to stimuli from the thalamus. However, the duration of these high-voltage slow waves remains brief, and they are unable to maintain synchronization in deep sleep, leading to the insertion of a low-amplitude portion within the high-voltage slow waves as PMA progresses, resulting in a shift to tracé alternant (TA). Notably, the transition from high-voltage slow wave pattern (HVS) to TA is gradual, with the low amplitude portion interspersing within the high amplitude EEG segments. In addition, after 32 weeks, EEG can differentiate between active sleep (AS) and QS, with the EEG of AS becoming continuous. However, high-voltage slow waves, especially the delta brush, continue to be evident. After 34 weeks, the amplitude in AS begins to decrease, and by 40 weeks, the EEG of AS after QS becomes a low-voltage irregular EEG, indicative of a mature desynchronized EEG. This may be due to the more rapid development of desynchronization mechanisms (pons-thalamus), compared to synchronization mechanisms (thalamus-cortex).

9 Developmental Changes in EEG Patterns: EEG in Extremely Preterm Infants

Toru Kato, Fumio Hayakawa, and Akihisa Okumura

We have limited experience with EEG in extremely premature infants at 22–24 weeks postmenstrual age (PMA). Strictly speaking, it is difficult to define EEG findings obtained during this period as "normal" because extreme premature birth itself is not a physiological event. Based on our experience, we describe EEG findings in these extremely preterm infants that we assume to be physiological.

Note that in general EEGs of healthy infants showing normal ultrasound examinations and having uneventful clinical course and normal neurodevelopmental outcome have been considered physiological.

The physiological EEG findings in preterm infants at 22 weeks PMA remain unclear. We mentioned above that the voltages of slow waves become larger and their frequencies become slower with a degree of prematurity. It is unclear whether this phenomenon also occurs in more premature infants than in 24–26 PMA infants. Determination of normal findings is a universal issue in the interpretation of EEG in preterm infants. It is important to recognize that there is no established definition of "normal" EEG findings in the extremely preterm period. The very high-voltage slow waves and frontal sharp waves shown in the figure are characteristic of extremely preterm infants. Even if the estimated EEG age can only be identified as less than 26 weeks PMA, it can be considered an extremely immature but "active" EEG (Fig. 9.1).

It is interesting that the voltages of slow waves are larger and their frequencies are slower at 22 weeks PMA compared with 24–26 weeks PMA. We can observe very high-voltage slow waves with amplitudes exceeding 400 μV and frequencies less than 1 Hz, as shown in the figure. The presence of large slow waves may indicate a large number of neurons responding to thalamocortical radiation related to a less organized projection system. Sharp bursts from the frontal region (blue arrow) can be observed from this period (Fig. 9.2).

As shown in this figure (Fig. 9.3), similar to Fig. 9.2, a very high-voltage slow wave exceeding 400 μV and with a frequency less than 1 Hz was observed. The closed blue arrows highlight the slow decay after a very high-voltage slow wave. Such phenomena are seen only rarely, particularly after at least 32 weeks PMA. This finding may reflect the functional immaturity of the central nervous system. In this figure, occipital

T. Kato (✉) · F. Hayakawa
Department of Pediatrics, Okazaki City Hospital, Okazaki, Japan
e-mail: torukato@sun-inet.or.jp

A. Okumura
Department of Pediatrics, Aichi Medical University, Nagakute, Aichi, Japan
e-mail: okumura.akihisa.479@mail.aichi-med-u.ac.jp

A. Okumura, H. Kidokoro (eds.), *Neonatal EEG: Atlas and Interpretation*,
https://doi.org/10.1007/978-981-96-0726-6_9

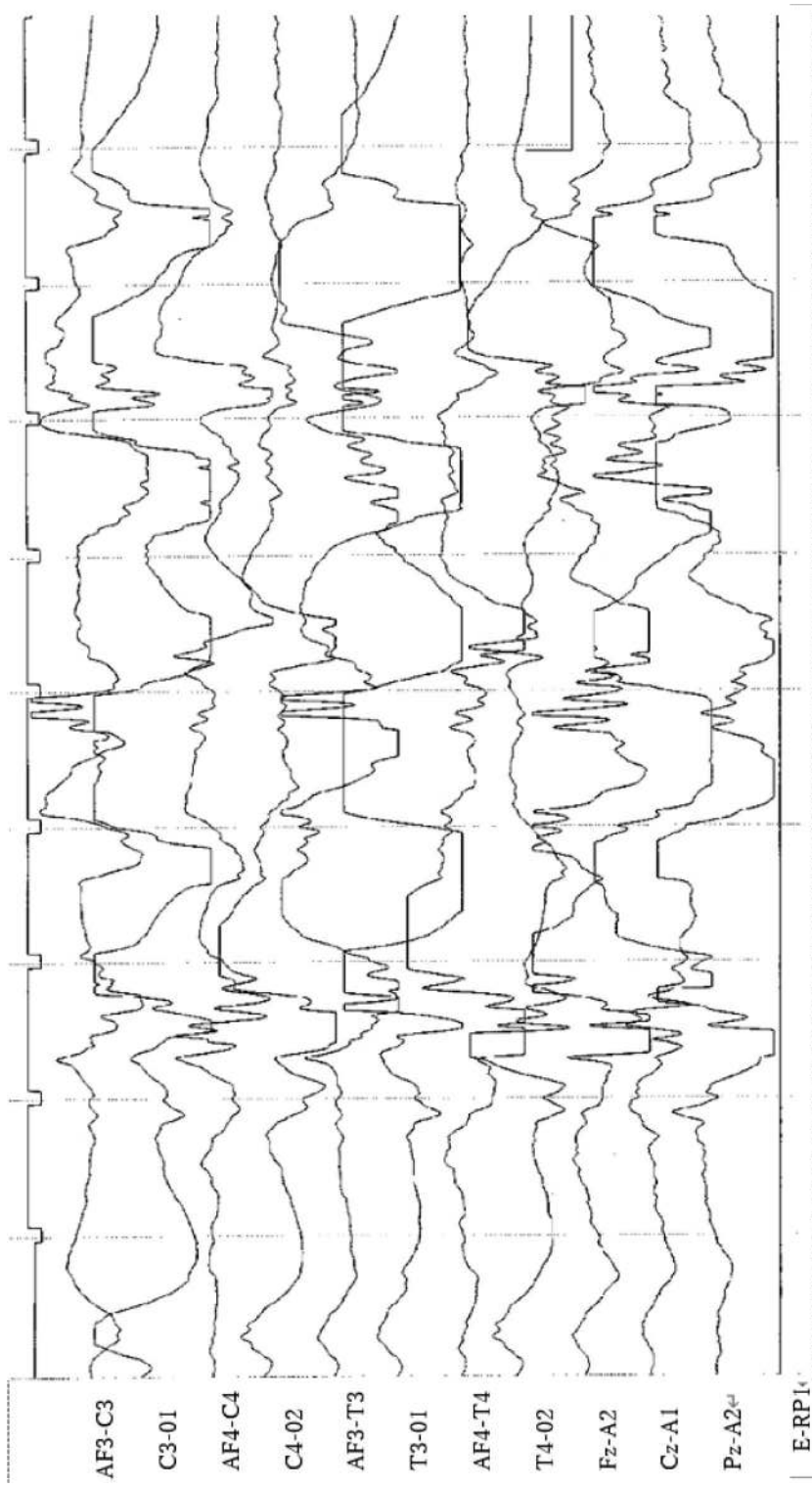

Fig. 9.1 High-voltage slow wave pattern at 22 weeks PMA (1)

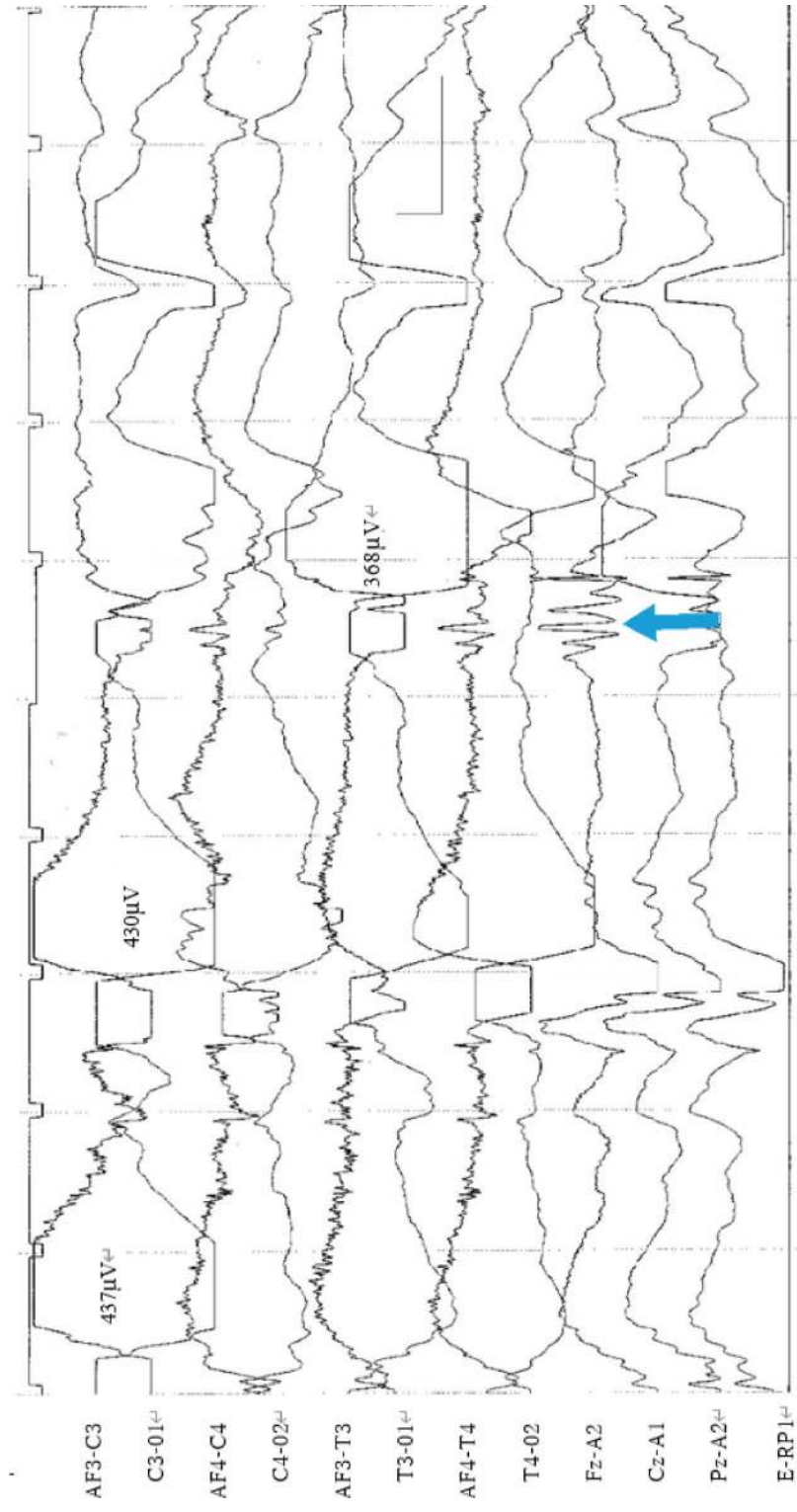

Fig. 9.2 High-voltage slow wave pattern at 22 weeks PMA (2)

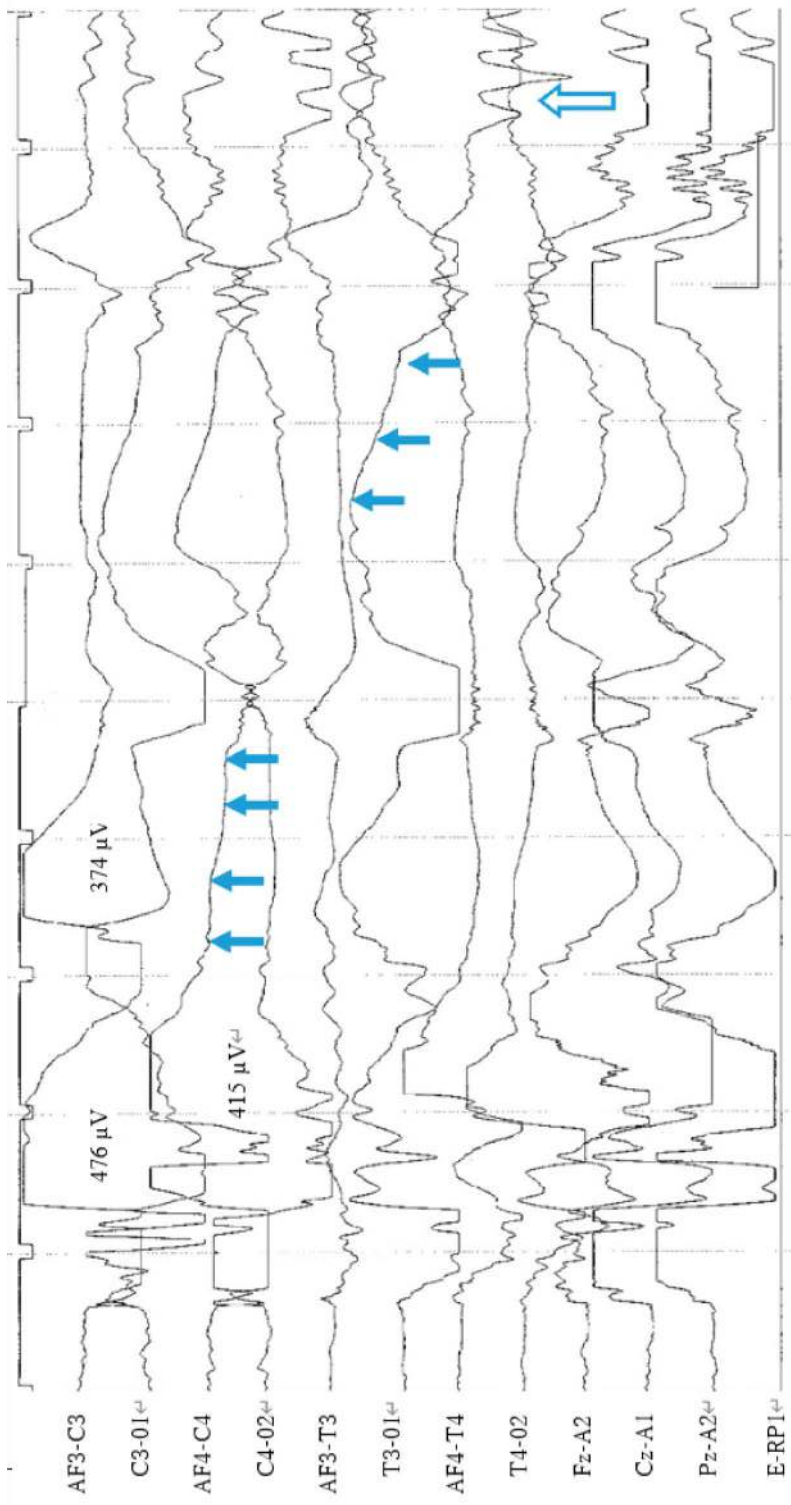

Fig. 9.3 High-voltage slow pattern at 22 weeks PMA (3)

sharp bursts (open blue arrow), which are transients reflecting immaturity, can also be seen. Occipital sharp bursts can be considered characteristic of EEG in extremely preterm infants, similar to the frontal sharp bursts shown in Fig. 9.2.

In this figure (Fig. 9.4), very high-voltage slow waves appear every 3–4 s, with no other activities during the intervals. The lack of interference due to overlapping among slow waves may be indicative of an extremely preterm infant (blue arrows). When this finding is observed frequently, it is reasonable to assume that the infant may be 26 weeks or younger PMA.

Although the EEG of an infant at 22 weeks PMA in this figure (Fig. 9.5) seems to show the tracé discontinue pattern, it is not clear that it is representative of this PMA. As similar patterns are observed at 22–26 weeks PMA, it is not easy to determine the PMA accurately. In this EEG, very high-voltage slow wave and high-voltage rhythmic activities (blue arrow) with no distinct localization are observed. We cannot say that it is incorrect to judge this infant as 28 weeks PMA. However, this finding is not seen after 32 weeks PMA. When this pattern does appear, even to a small extent, we should consider the infant to be extremely preterm.

The features of the EEG findings at 24 weeks PMA are not yet fully understood and, indeed, it is difficult to define what is "normal" in such preterm infants. It should be noted that there are no established interpretations of EEG in extremely preterm infants. Very high-voltage slow waves and frontal sharp bursts (blue arrows) seen in the figure are characteristic of extremely preterm infants. These findings suggest that the age of the infant is 26 weeks PMA or younger and no apparent abnormalities are seen in the EEG (Fig. 9.6).

Very high-voltage slow waves appear in trains, especially in the occipital regions, with little superimposition between the slow waves. Although determination of EEG maturation among EEG at 22–26 weeks PMA is challenging, the rhythmic sharp waves in the occipital regions (blue arrow) and very high-voltage slow waves are a feature of the EEG of extremely preterm infants (Fig. 9.7).

In tracé discontinu (TD), EEG maturation should be assessed based mainly on the EEG activities within the burst part, although the rate of TD pattern and the duration of the interburst interval are also important. The components observed in the high voltage slow wave pattern are similar to the burst parts of the TD pattern. Very high-voltage slow waves (400 μV and <1 Hz) and sharp bursts in the frontal regions (blue arrows) in the bursts within TD are consistent with the characteristics of 22–26 weeks PMA (Fig. 9.8).

The transients observed in extremely preterm infants at 22–26 weeks PMA include rhythmic sharp bursts from the frontal (middle blue arrow) and occipital regions (right blue arrow). "Brush" is a rhythmic fast wave component observed throughout the preterm period and is also notable at 22–26 weeks PMA (left blue arrow). After 28 weeks PMA, rhythmic sharp waves (high-amplitude theta and rhythmic temporal theta) from the temporal region become more prominent, and the number of brushes increases. In contrast, by 26 weeks PMA, the combination of very high-voltage slow waves (amplitude >300–400 μV, frequency <1 Hz) and rhythmic fast waves in the frontal and occipital regions is distinctive (Fig. 9.9).

This figure (Fig. 9.10) shows typical EEG findings at 26 weeks PMA, basically characterized by very high-voltage large slow waves and rhythmic sharp bursts. It is not easy to distinguish this EEG pattern from those corresponding to 22 and 24 weeks PMA. The presence of the temporal sharp wave (blue arrow) and the slightly lower voltage of the slow wave may suggest maturational changes. It remains difficult to differentiate clearly the EEG patterns among the 22, 24, and 26 weeks PMA.

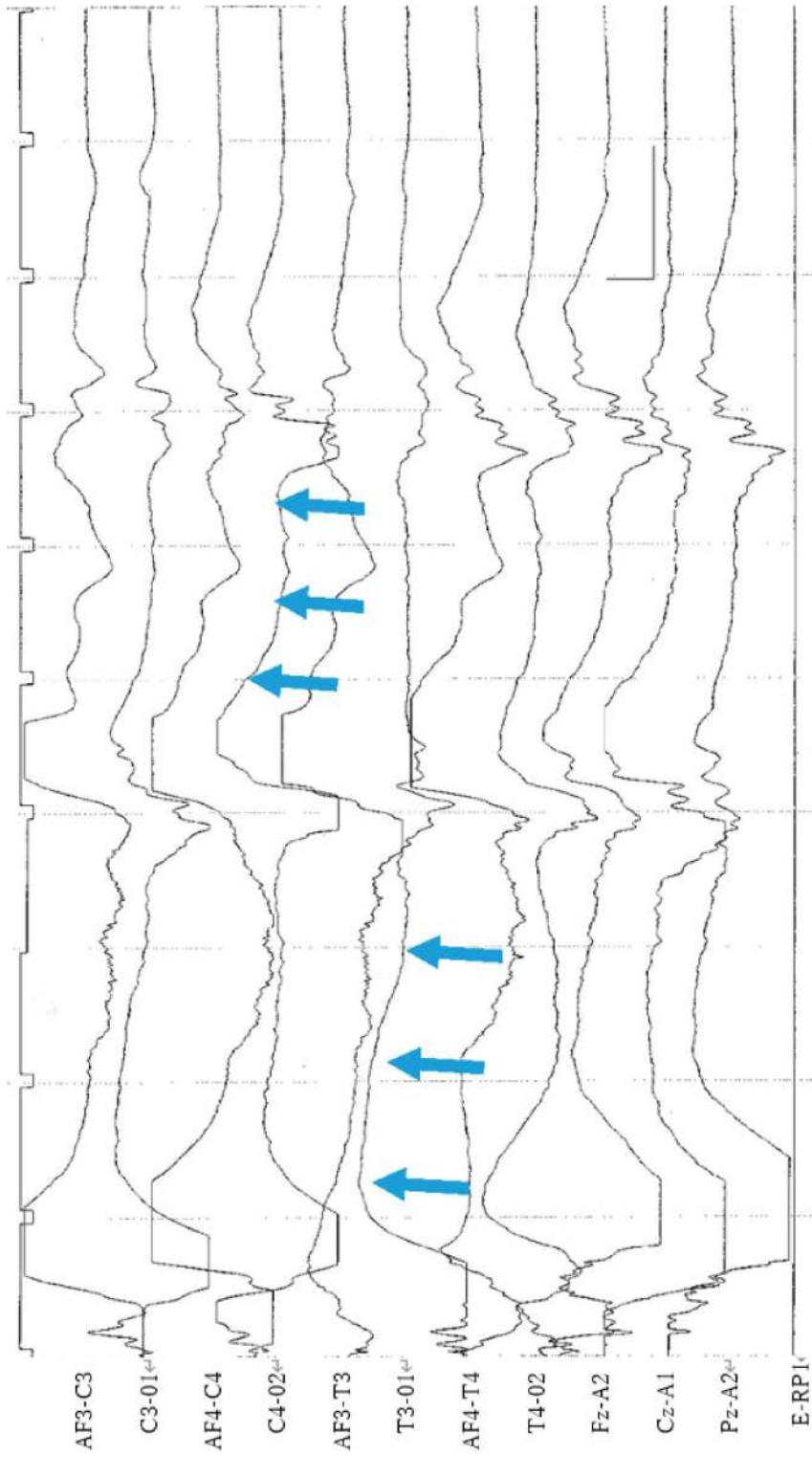

Fig. 9.4 High-voltage slow wave pattern at 22 weeks PMA (4)

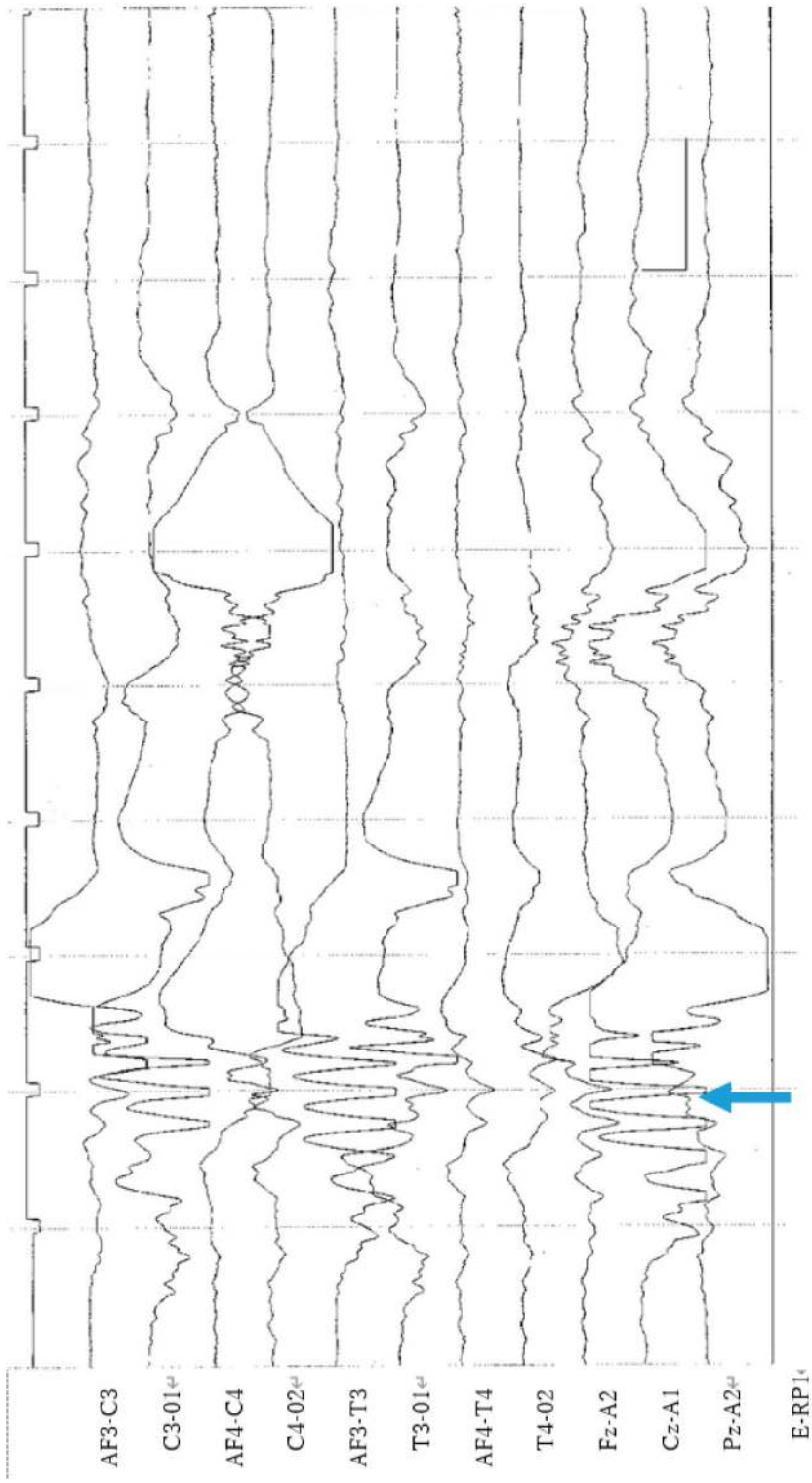

Fig. 9.5 Discontinuous pattern at 22 weeks PMA

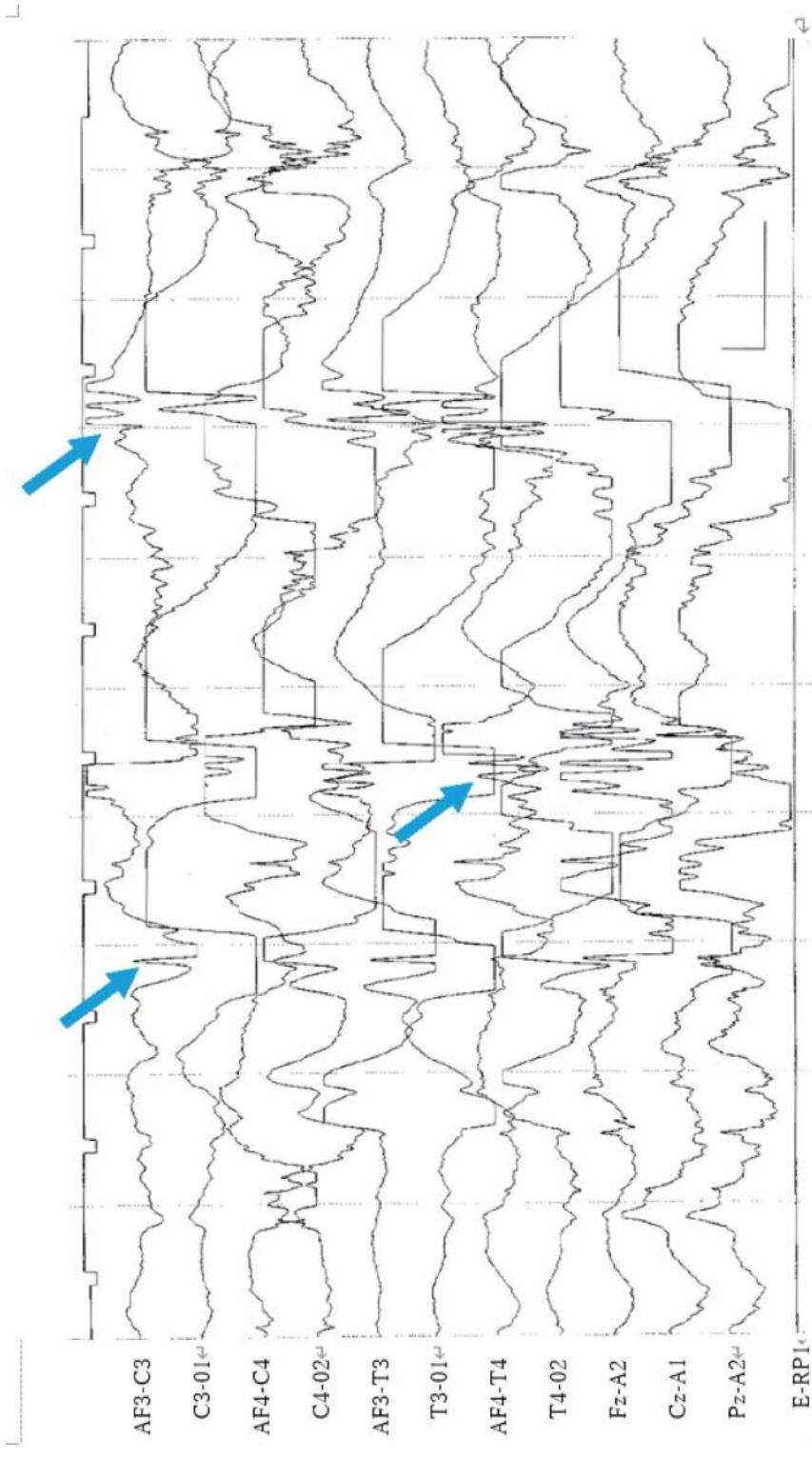

Fig. 9.6 High-voltage slow wave pattern at 24 weeks PMA (1)

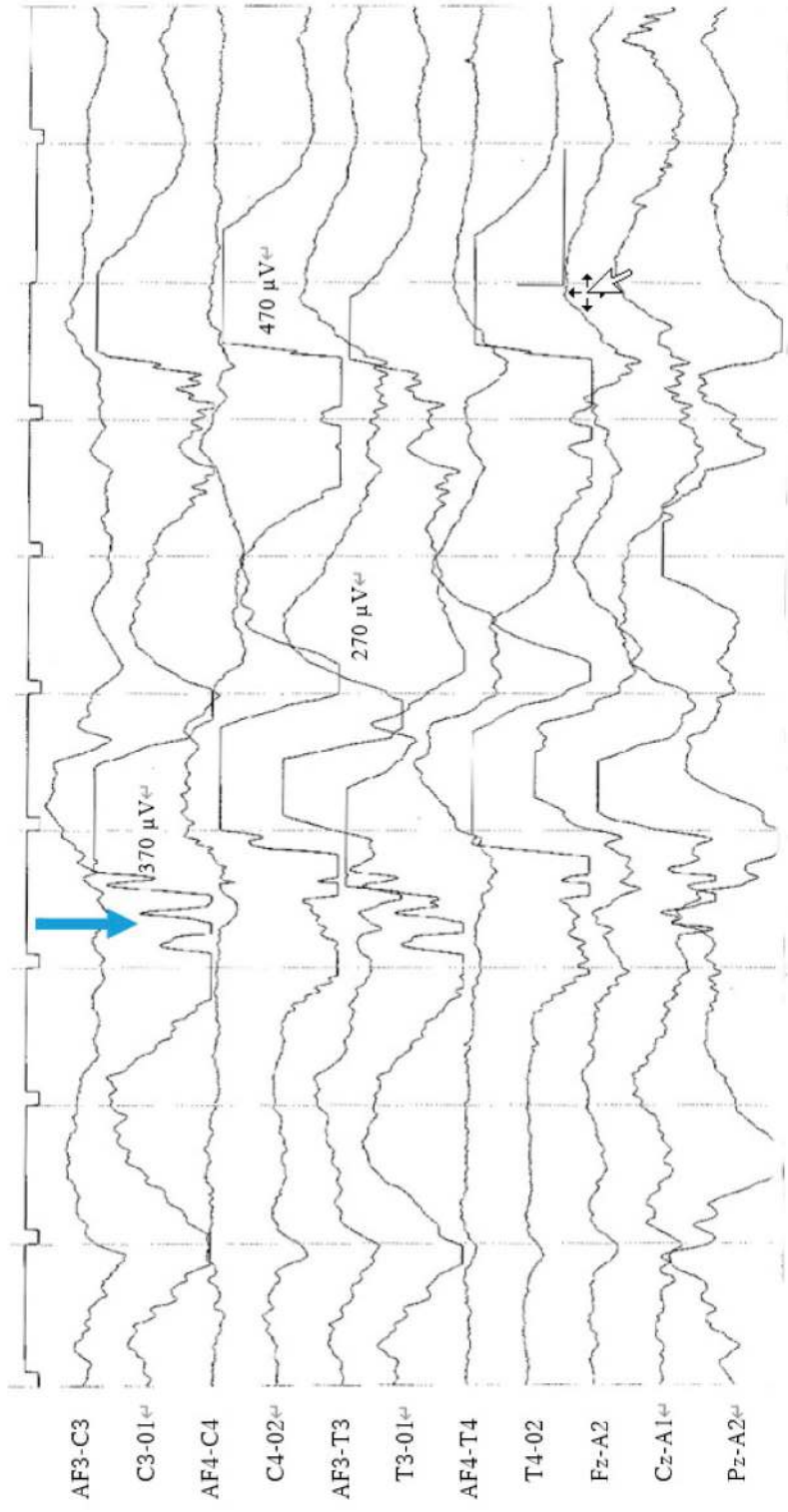

Fig. 9.7 High-voltage slow wave pattern at 24 weeks PMA (2)

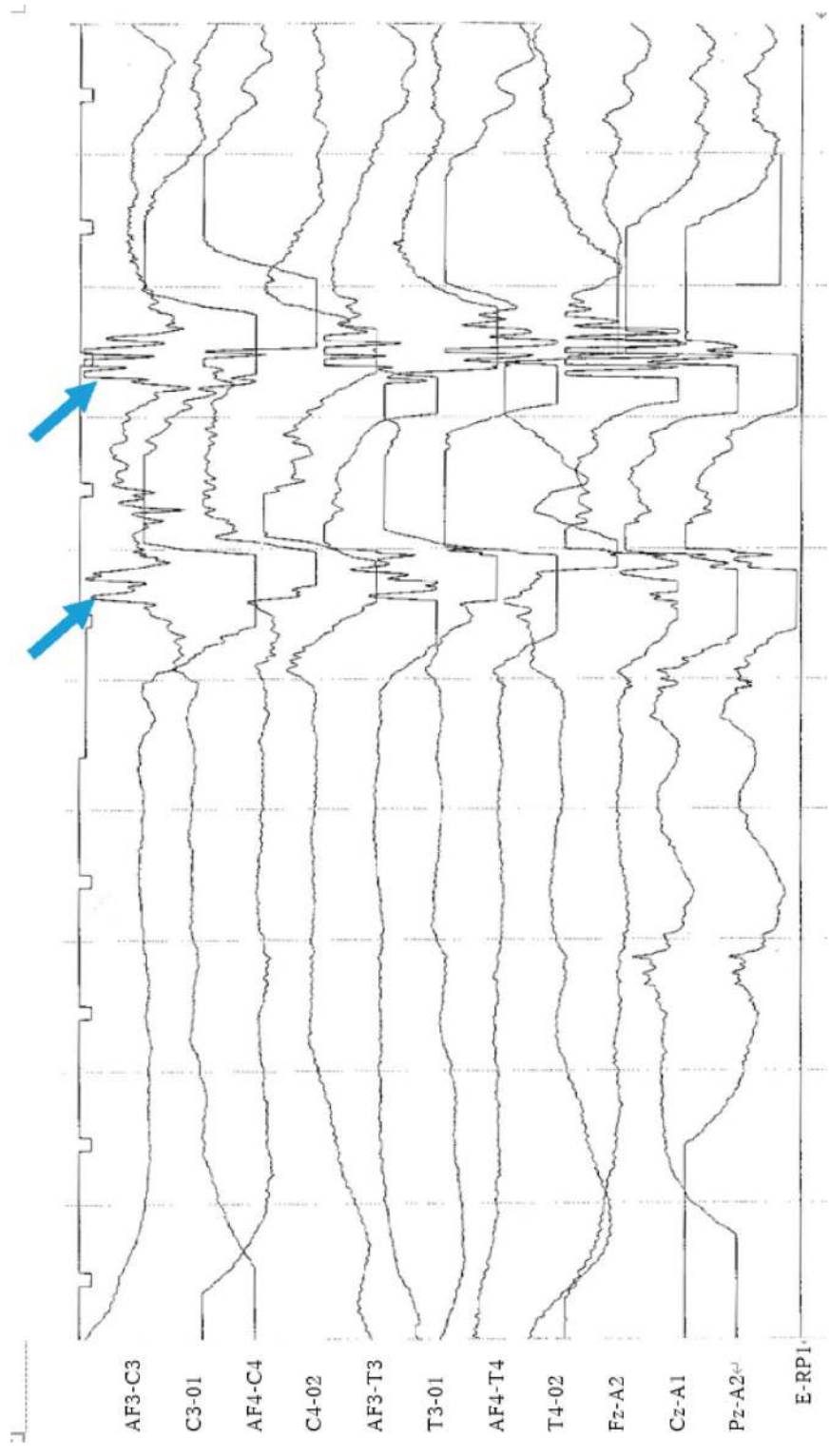

Fig. 9.8 Tracé discontinu at 24 weeks PMA

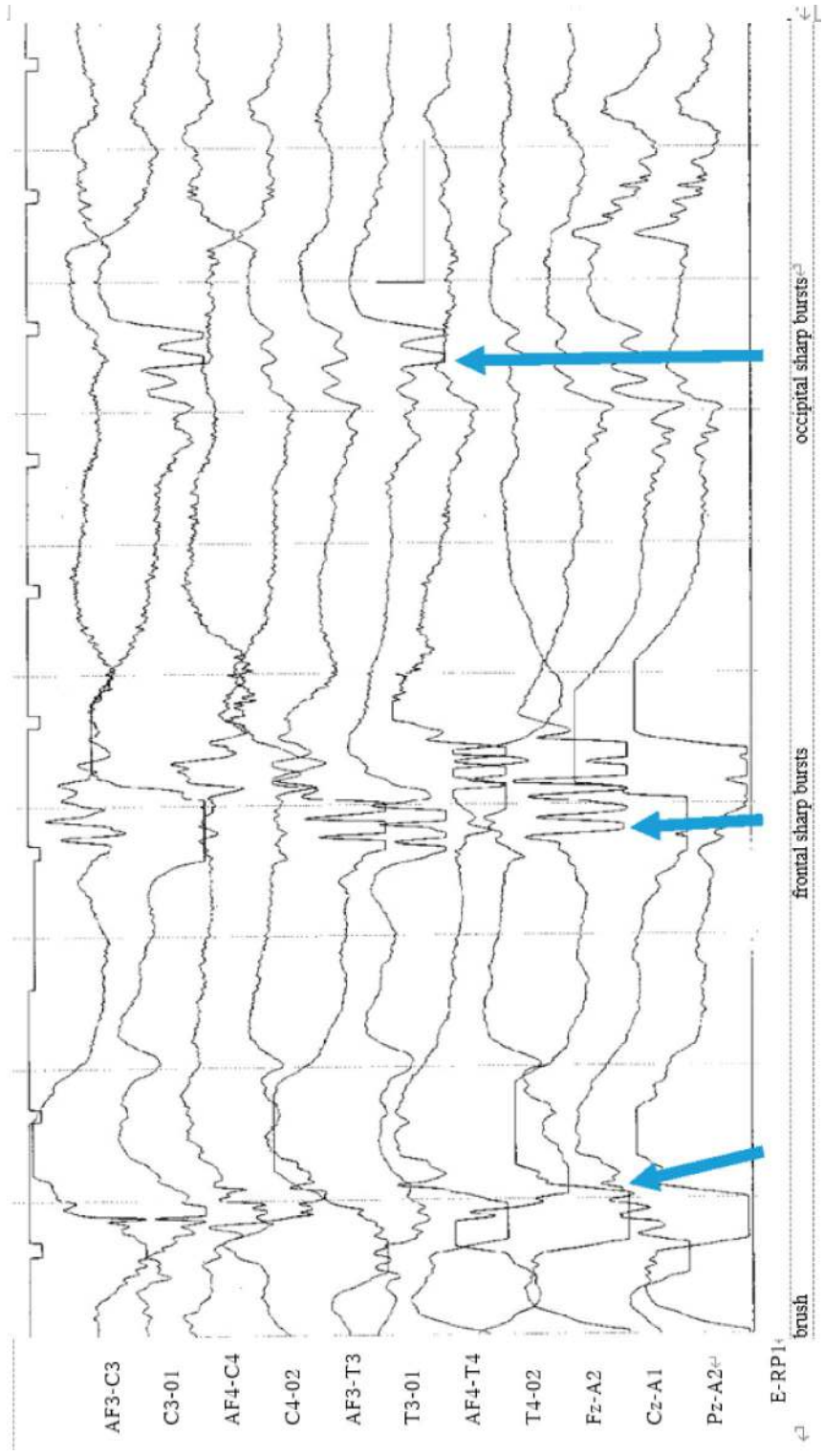

Fig. 9.9 Transients during the extremely preterm period

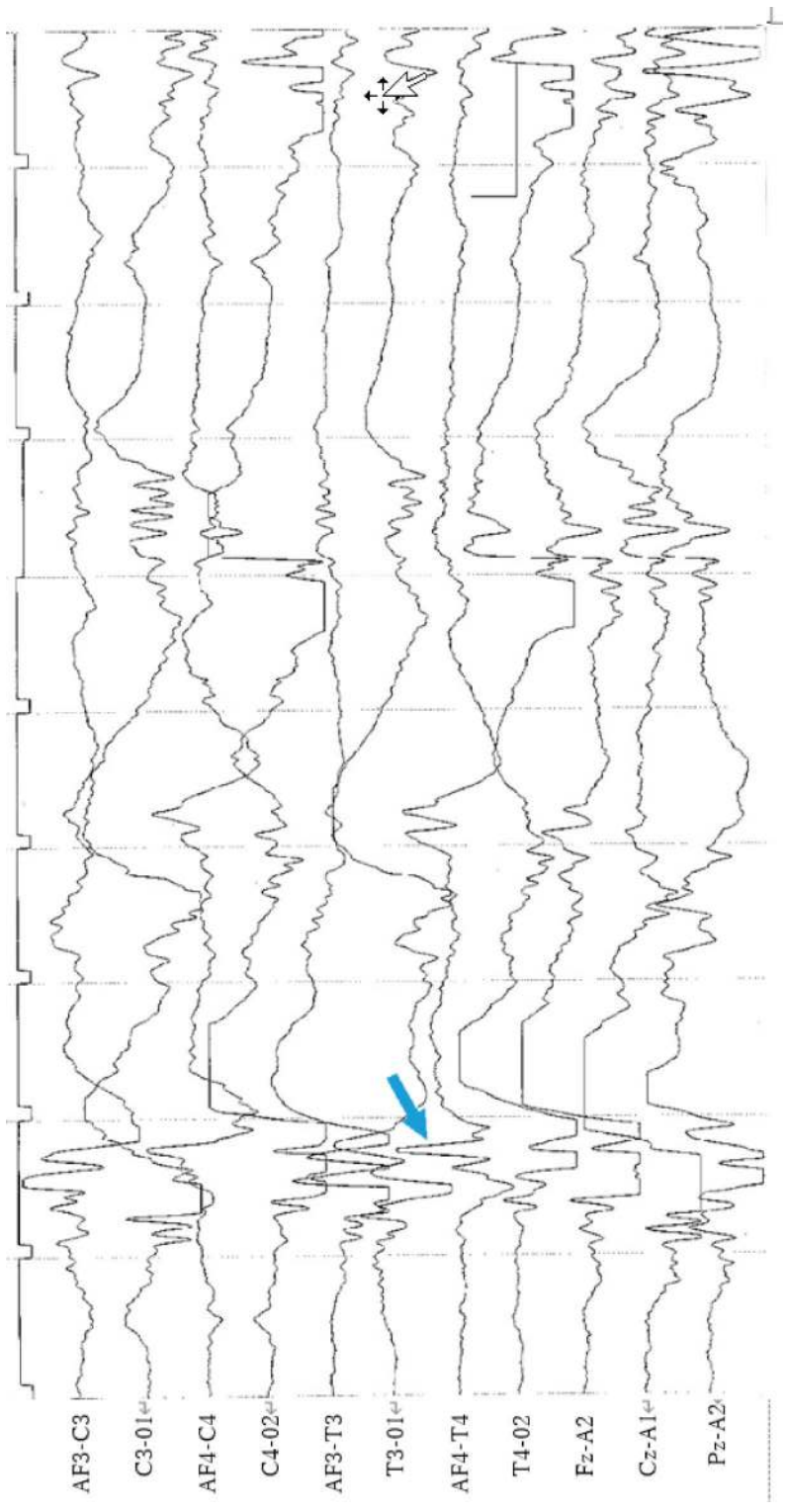

Fig. 9.10 High-voltage slow pattern at 26 weeks PMA (263)

Column: Perinatal Brain Damage and EEG
(Kazuyoshi Watanabe)

In hypoxic-ischemic encephalopathy in term infants, EEG findings vary from minimal to maximal degrees of depression, depending on the severity of the insult. From the viewpoint of ontogeny, components that developed later are more likely to be affected; EEG depression begins with flattening of the low-voltage part of tracé alternant, followed by a reduction or disappearance of the high-voltage slow wave pattern, the disappearance of the mixed pattern and, finally, the appearance of a discontinuous EEG featuring alternating bursts and flat tracings. However, the burst-suppression EEG and "tracé discontinu" are not the same. In the former, delta brush-like activities may sometimes appear, but the infant is in the comatose state with no sleep cycle, while the latter shows physiological properties. The sleep cycle is preserved in EEG with mild depression, but becomes moderately disturbed in EEG with moderate depression, and the correlation between EEG and sleep state breaks down. The stability of quiet sleep is more likely to be disturbed than that of active sleep in EEG with mild-to-moderate depression.

We also found a correlation between heart rate (HR) variability and background EEG depression. In minimal depression, HR is not significantly different from normal. Most infants with mild EEG depression do not show obvious changes in HR variability, but some infants show altered HR variability in active sleep, similar to that in quiet sleep, and significant variability is sometimes observed. Most infants with moderate EEG depression show marked fluctuations. In infants with marked EEG depression, subtle or almost no fluctuations are observed, and infants with maximal EEG depression typically show almost no fluctuations. That is, HR variability is minimally affected in cases of mild brain damage. However, in cases of moderate brain damage, the control of HR by the central nervous system becomes extremely unstable, and HR becomes independent of control by the central nervous system in cases of marked brain damage, showing a fixed HR. This condition is similar to that seen in preterm infants of 30 weeks postmenstrual age or younger.

In visual evoked potentials, the early positive component, which develops later, is the most susceptible to damage, while the late negative component, present since before 30 weeks postmenstrual age, is the least susceptible. Even when visual evoked potentials are lost due to severe brain damage, the late negative component is the first to recover, followed by the early positive component. Components that develop earlier in ontogenesis are less susceptible to damage.

Knowledge of Artifacts Necessary for EEG Interpretation

10

Tetsuo Kubota, Hiroyuki Kidokoro, and Anna Shiraki

Recording neonatal EEG in the NICU has unique challenges. Infants are often connected to multiple electronic devices, which can produce various artifacts in the EEG. For accurate EEG interpretation, it is important to minimize such artifacts, including those arising from body movements, electrode problems, ECG contamination, alternating current (AC) disturbances, high-frequency oscillatory ventilation (HFOV), and nearby human activities. Since it is difficult to eliminate all artifacts, recognizing them is crucial. When feasible, simultaneous video recording can assist in identifying movement-related artifacts.

Although preventing artifact contamination entirely is challenging, it can be reduced significantly using careful recording methods. Some methods are listed below.

1. Bundle the electrode leads together with a towel or similar material; avoid intertwining them with other device leads.
2. Position other equipment away from the infant's head. Especially, keep infusion pumps distanced from the head and electrode box.
3. Ensure a reliable ground (earth) connection.
4. Power the EEG from a separate outlet from computers and other devices.
5. Adjust the infant's head position to reduce various artifacts, including those from HFOV, respirators, and ECG contamination.

Lastly, monitor the infant during recording for behaviors like sucking, tremors, eyelid and eye movements, breathing patterns, and head shifts. This direct observation aids in artifact differentiation.

In neonatal EEG recordings, external artifacts are often encountered. Electrode instability often results from inadequate scalp contact. Rather than pressing hard, using a paste to secure the electrode gently can reduce this instability. The figure shows nonphysiological fluctuations in AF4, indicative of electrode instability (Fig. 10.1).

Rhythmic artifacts at O_2, showing 12 Hz low-amplitude rhythmic activity, are attributed to the respirator's high-frequency oscillatory ventilation (HFOV) mode. Depending on the respirator settings, one might observe patterns at either 12 or 15 Hz. These artifacts can be caused by slight head movements, excessive moisture, or the respirator circuits being close to the EEG leads. Adjusting the position of the infant's head can help reduce these issues (Fig. 10.2).

T. Kubota (✉)
Department of Pediatrics, Anjo Kosei Hospital, Anjo, Japan
e-mail: t-kubota@kosei.anjo.aichi.jp

H. Kidokoro · A. Shiraki
Department of Pediatrics, Nagoya University Graduate School of Medicine, Nagoya, Aichi, Japan
e-mail: kidokoro.hiroyuki.i6@f.mail.nagoya-u.ac.jp; shiraki.anna.g9@f.mail.nagoya-u.ac.jp

A. Okumura, H. Kidokoro (eds.), *Neonatal EEG: Atlas and Interpretation*,
https://doi.org/10.1007/978-981-96-0726-6_10

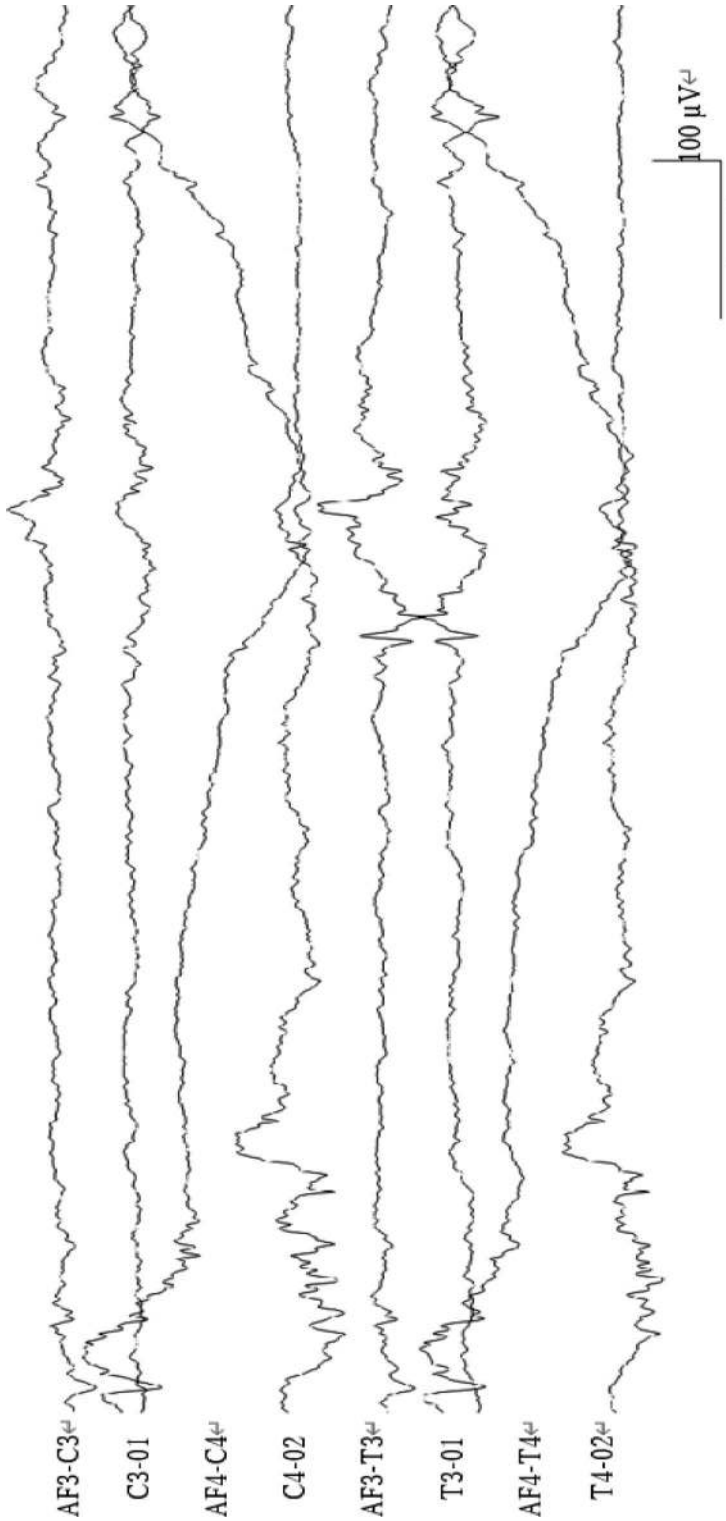

Fig. 10.1 Artifacts due to electrode instability

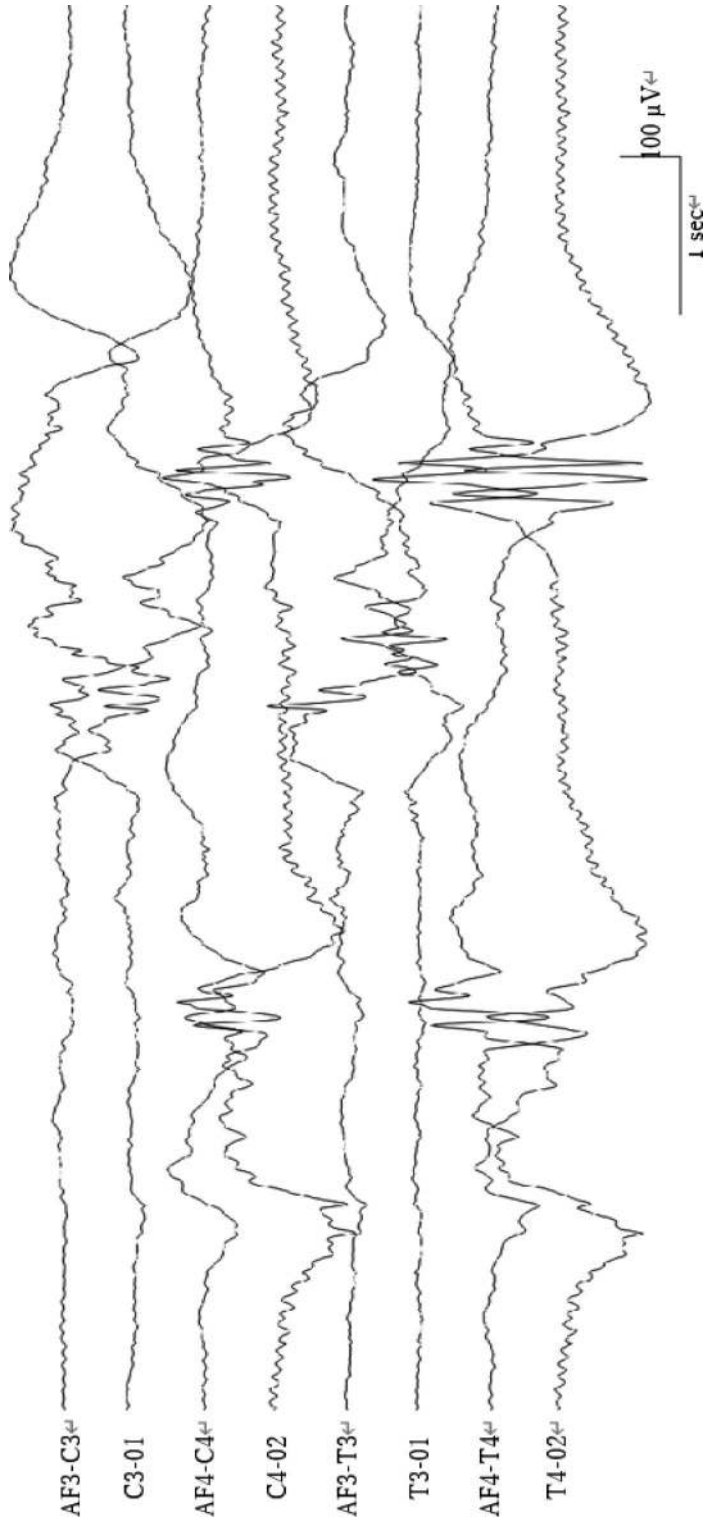

Fig. 10.2 Artifacts due to respirator HFOV

The underlined parts (T3 and T4) of the EEG are artifacts caused by staff walking around the incubator. It is important to recognize that moving around an infant's incubator can introduce EEG artifacts (Fig. 10.3).

The underlined part at AF4 is an artifact caused by the infant sucking a pacifier during the EEG recording. Movement, especially of the head and face, can introduce artifacts (Fig. 10.4).

Beyond the rhythmic slow wave-like artifacts shown previously (Fig. 10.4), spike-like artifacts also appear, predominantly in the right mid-temporal area (T4) (Fig. 10.5).

These are artifacts recorded when the feeding tube touched the AF3 EEG lead. Nonphysiological rectangular waveforms are observed (arrows) (Fig. 10.6).

Neonatal EEG basically evaluates recordings during sleep. When the infant cries or makes accompanying body movements, fast-frequency spike-like waveforms can be seen, as shown in the figure. When there are accompanying body movements, these are superimposed on high-amplitude slow waves at all electrodes. In such cases, it is difficult to assess the background EEG activity (Fig. 10.7).

The underlined section shows the electromyogram of the left hemisphere following body movement of an infant using a directional positive airway pressure respiratory device (Fig. 10.8).

In addition to artifacts arising from body movements and electromyograms, alternating current (AC) artifacts are common in neonatal EEGs. The figure shows rhythmic fast waves at C4, which are more pronounced with unstable electrode induction. Phototherapy can also introduce AC artifacts (Fig. 10.9).

Bradycardia is noted (A); the incubator door is opened by staff (B); and the infant is stimulated (C). Simultaneous video EEG recording confirms these as artifacts (Fig. 10.10).

High-voltage, long-duration slow waves are observed (arrows). These artifacts result from changes in the potential of sweat glands. Unlike movement-related artifacts, these artifacts do not contain electromyographic activity (Fig. 10.11).

Rhythmic slow waves in the left mid-temporal area (T3) coincide with the ECG cycle, indicating a pulse wave artifact. It is important to distinguish this from seizure activity. Pulse wave artifacts lack the evolutional changes typical of neonatal seizures (Fig. 10.12).

A low-amplitude spike-like artifact at the right occipital area (O2) corresponds to the ECG R wave, identifying it as an ECG artifact (Fig. 10.13).

Artifacts at arrows **1** and **2** on the frontal poles (Fp1 and Fp2) result from opening and tightly closing the eyes, respectively. It is vital to distinguish these from the abnormal sharp or mechanical brush of disorganized patterns (Fig. 10.14).

Both frontal poles (Fp1and Fp2, arrow) show artifacts arising from an infant's swift eyeball movement, distinct from rapid eye movement. It is crucial to differentiate this from the delta brush (Fig. 10.15).

Slow waves (arrows) are recognized as dominant in the left occipital region (O1). Respiratory movement includes both natural breathing and hiccup-related movement. Be sure not to misinterpret this as neonatal seizures (Fig. 10.16).

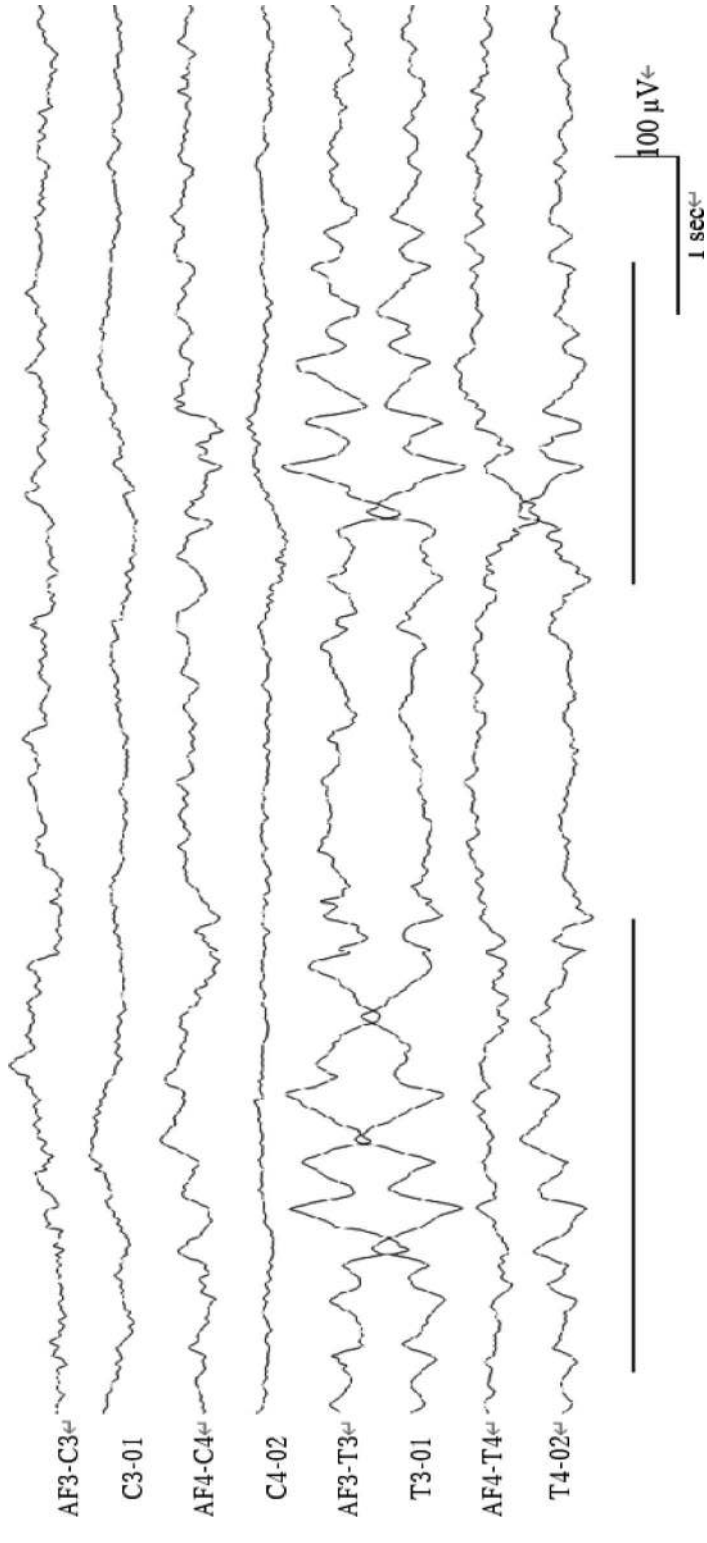

Fig. 10.3 Movement of NICU staff

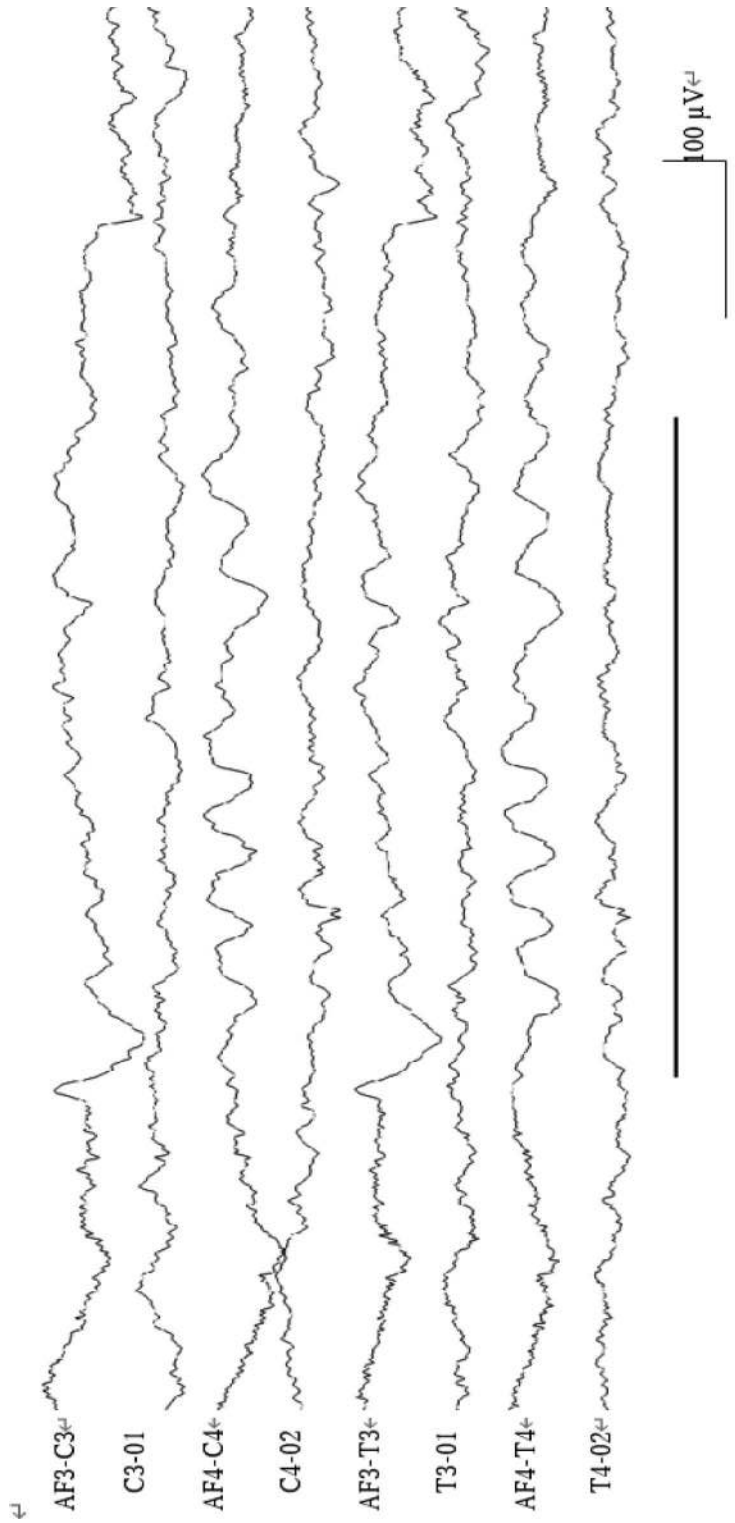

Fig. 10.4 Pacifier sucking (1)

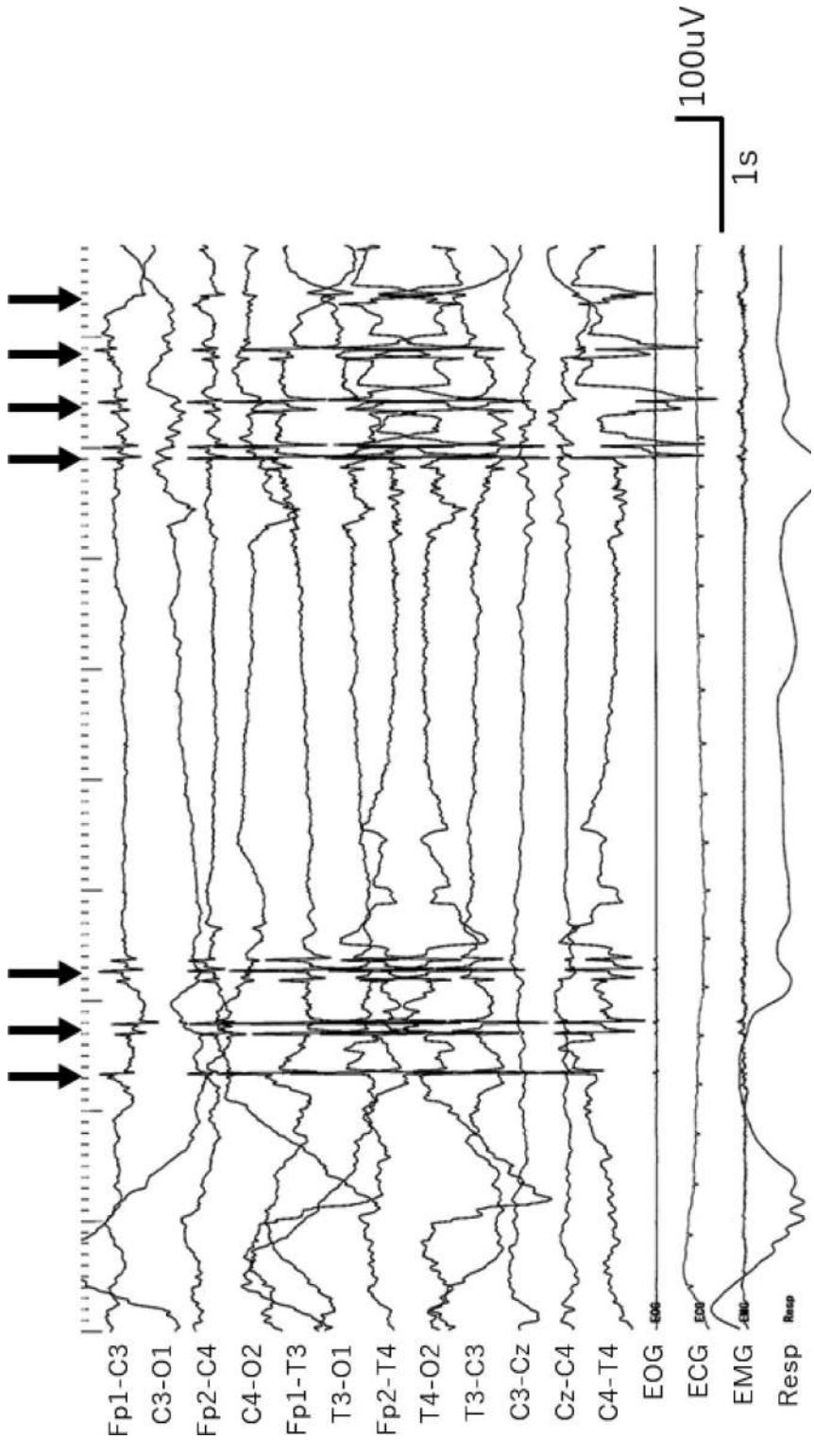

Fig. 10.5 Pacifier sucking (2)

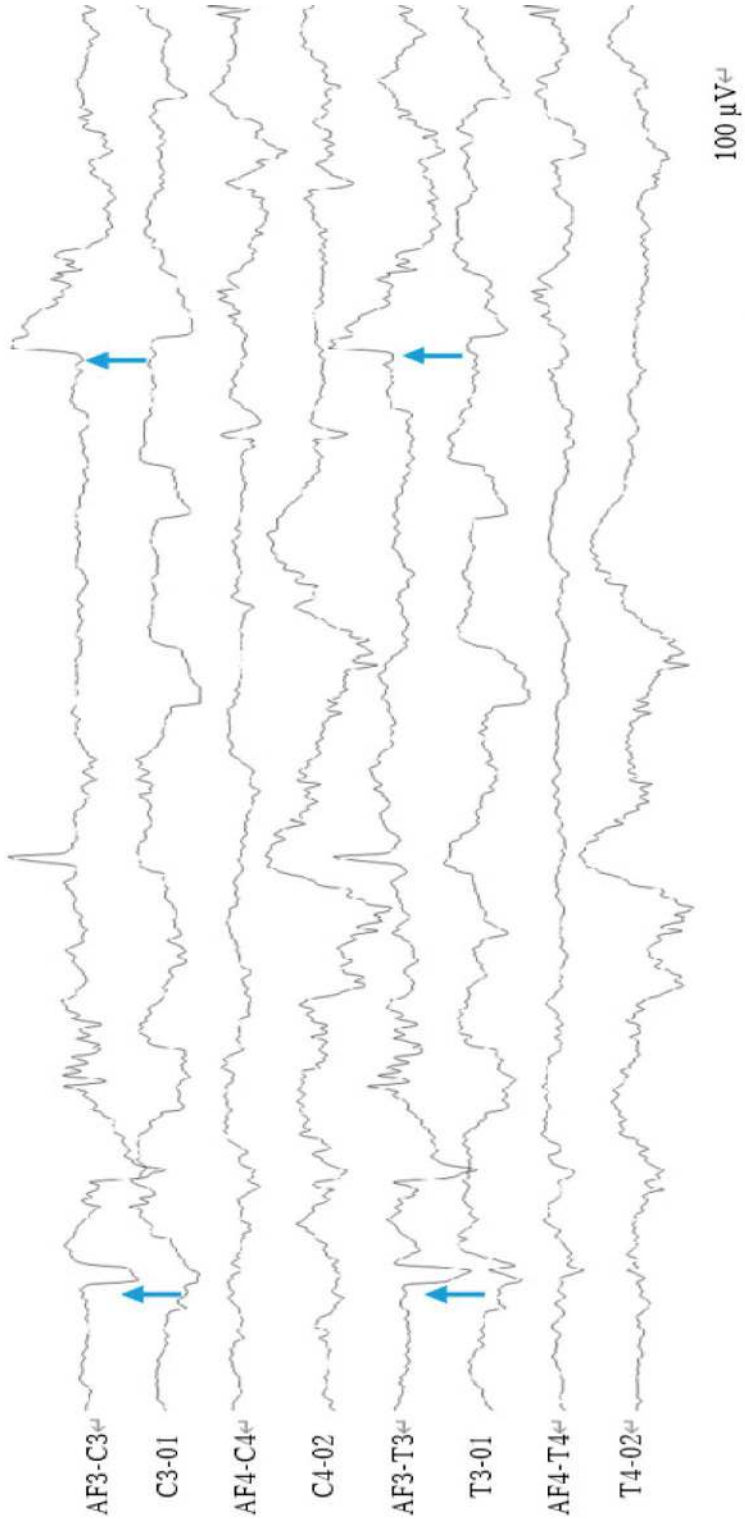

Fig. 10.6 Contact of a milk tube with an EEG lead

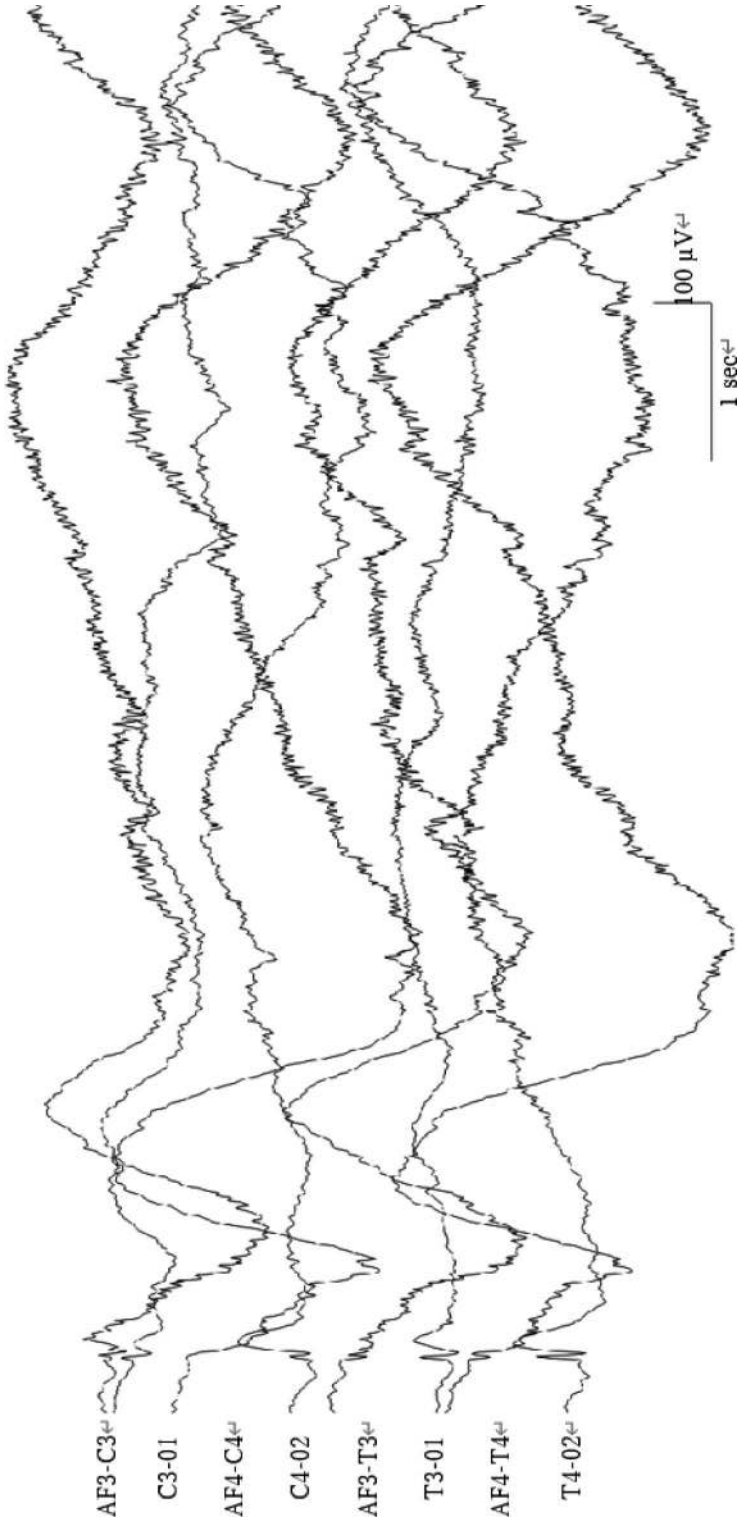

Fig. 10.7 Crying, body movement, and electromyogram

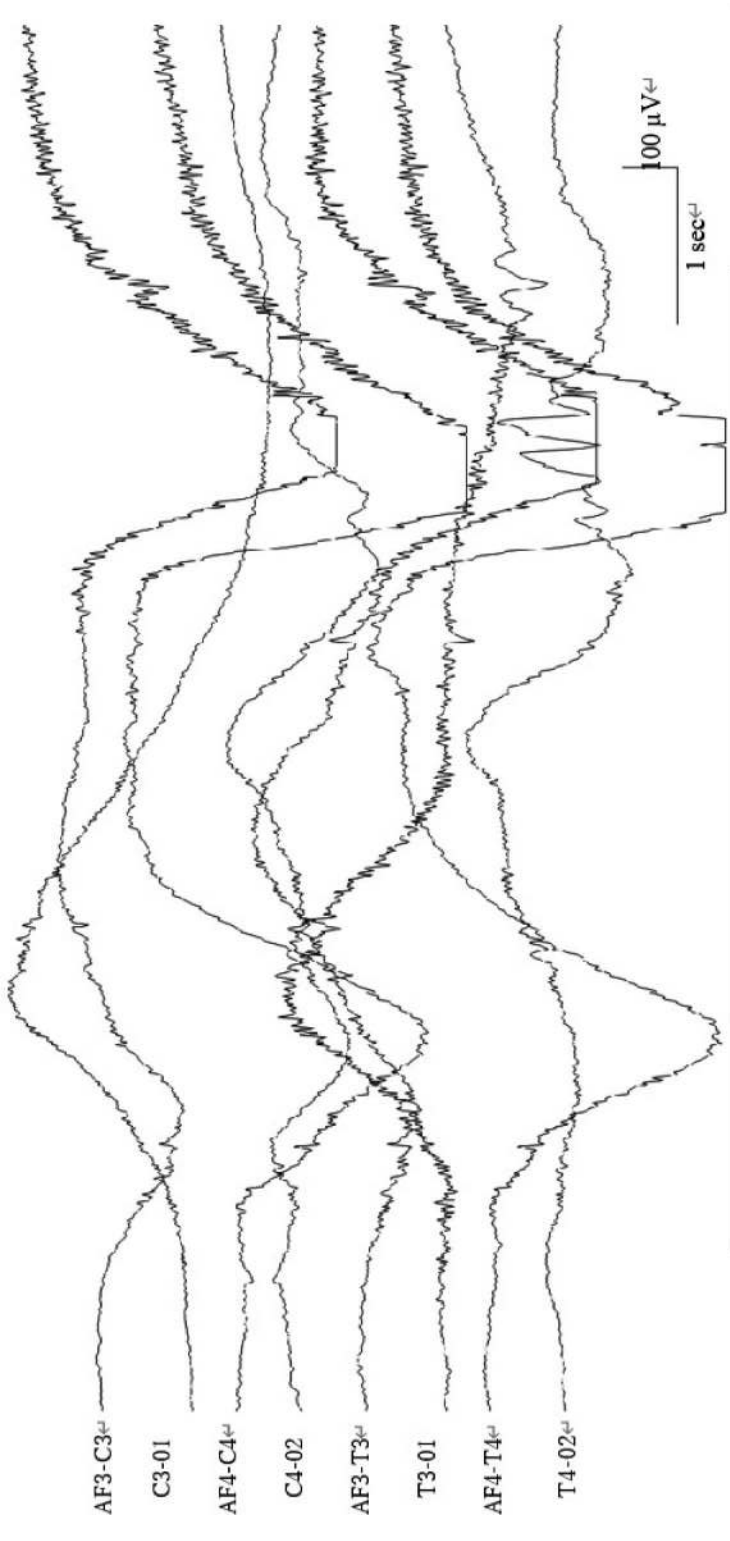

Fig. 10.8 Body movement and electromyogram

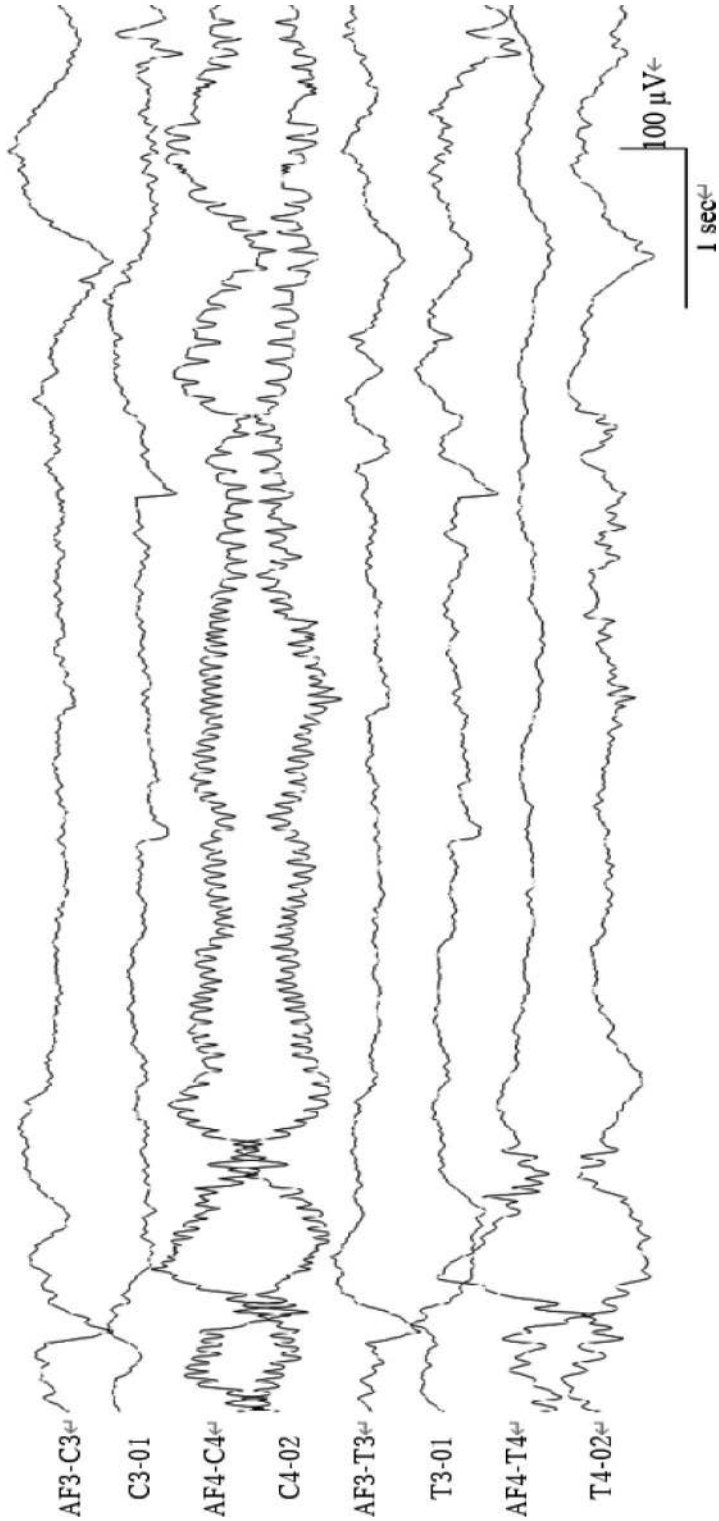

Fig. 10.9 Alternating current

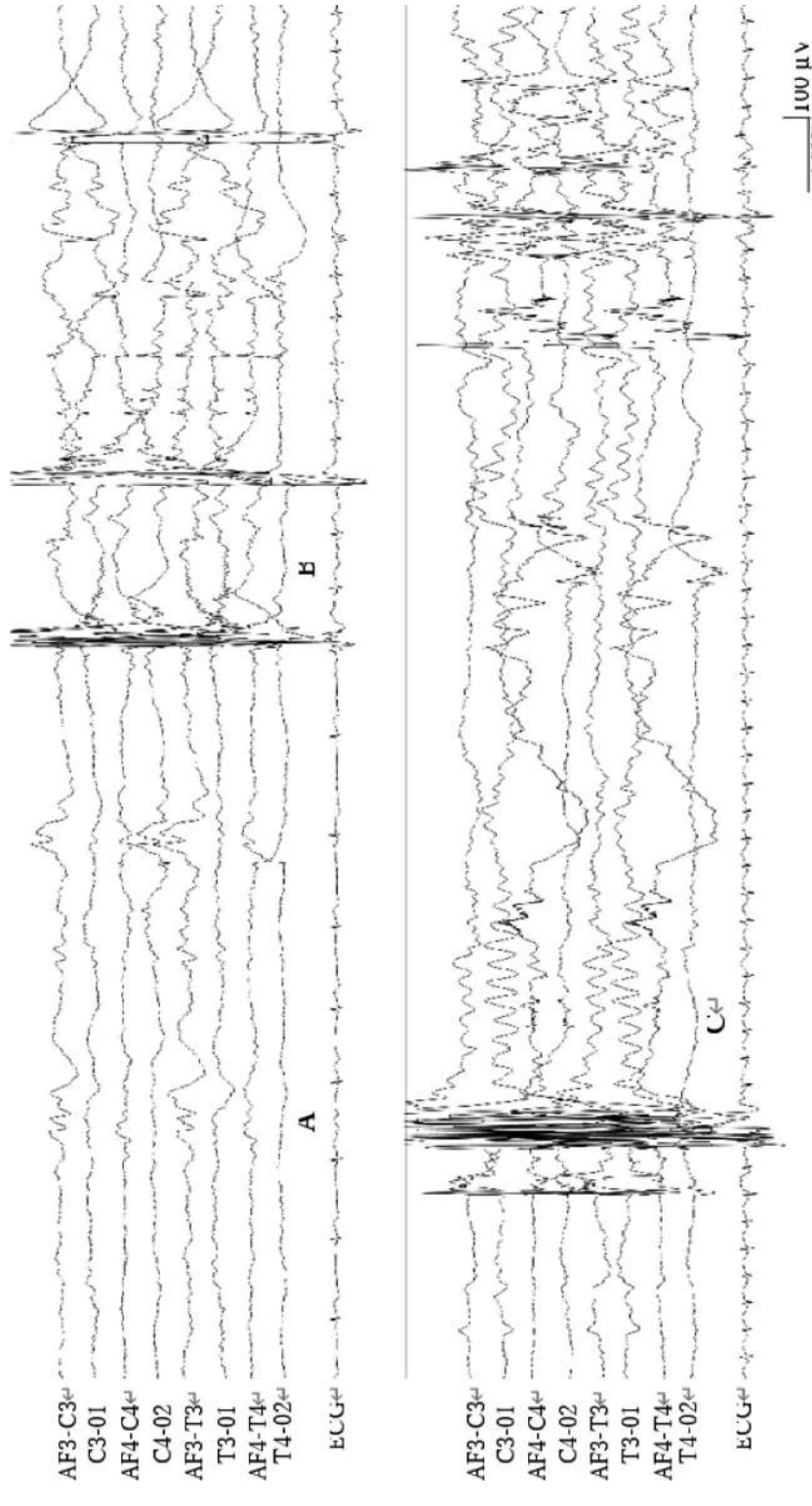

Fig. 10.10 Opening the door and touching the infant

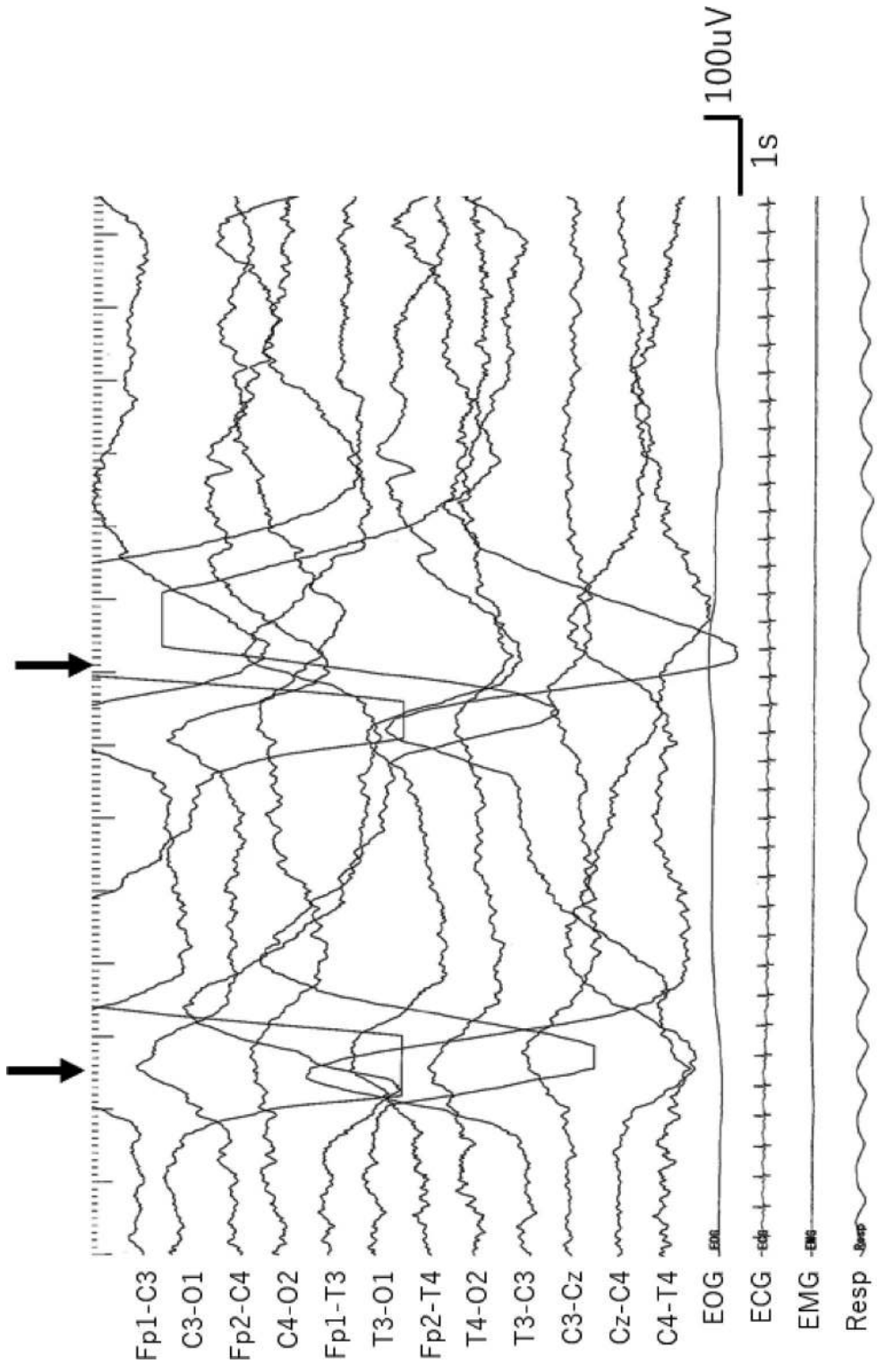

Fig. 10.11 Sweating artifact

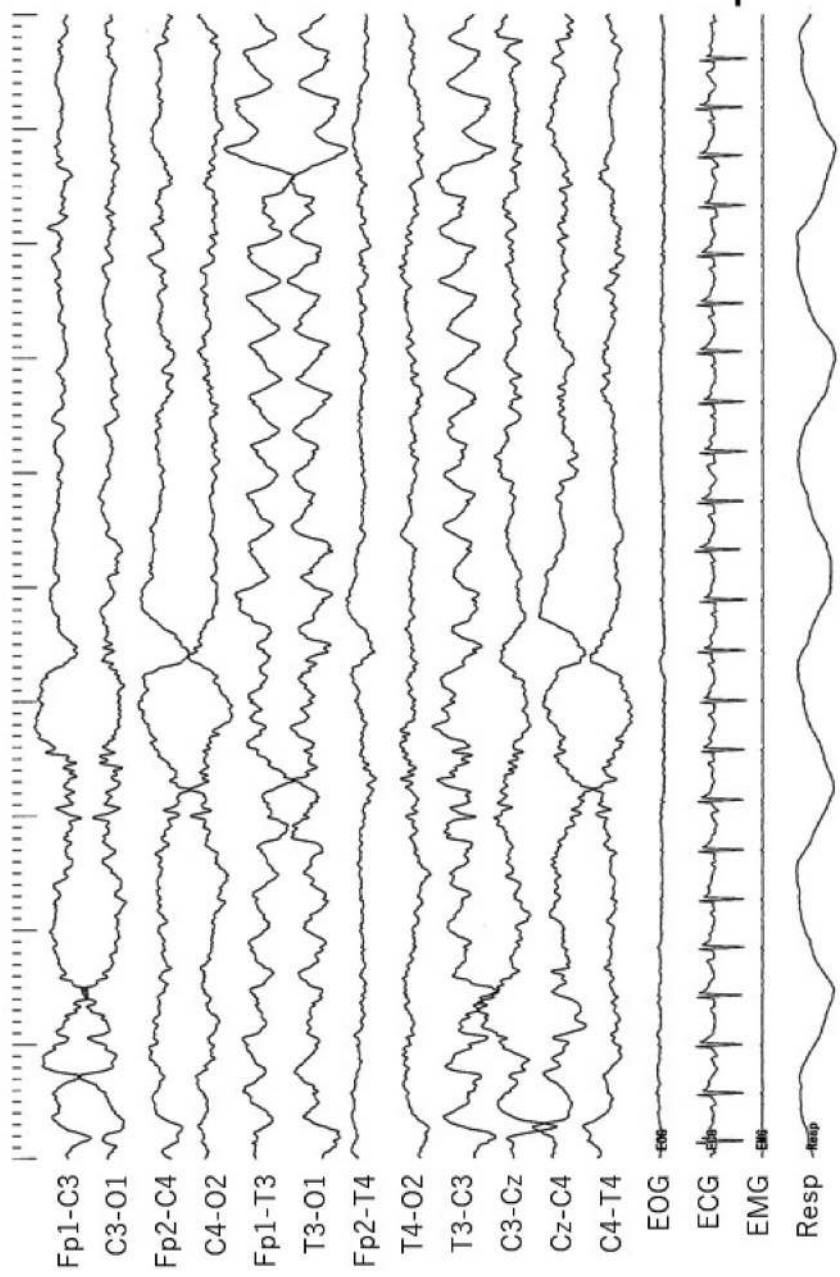

Fig. 10.12 Rhythmic slow activity due to the pulse wave

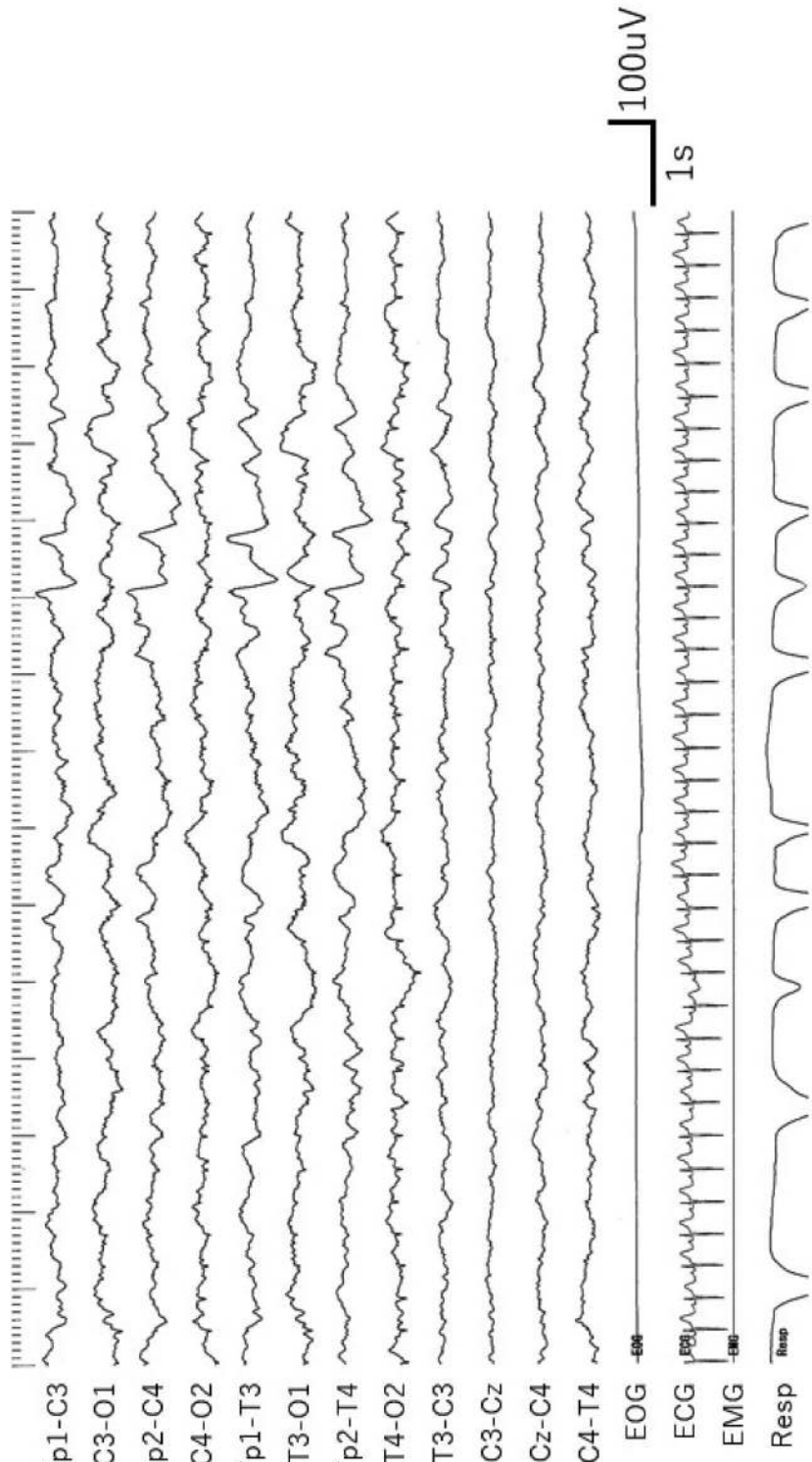

Fig. 10.13 ECG artifact

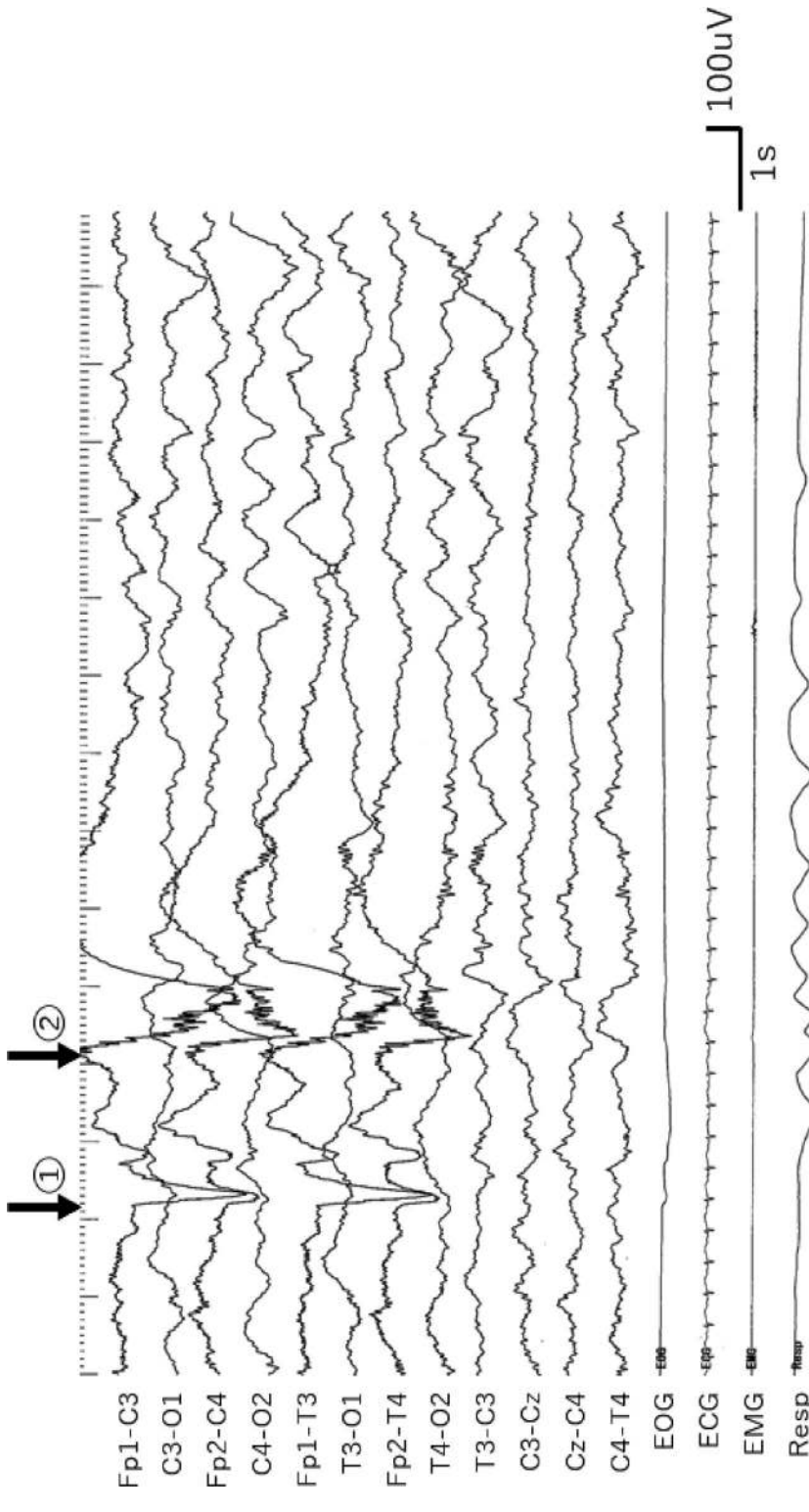

Fig. 10.14 Eye opening and closing artifact

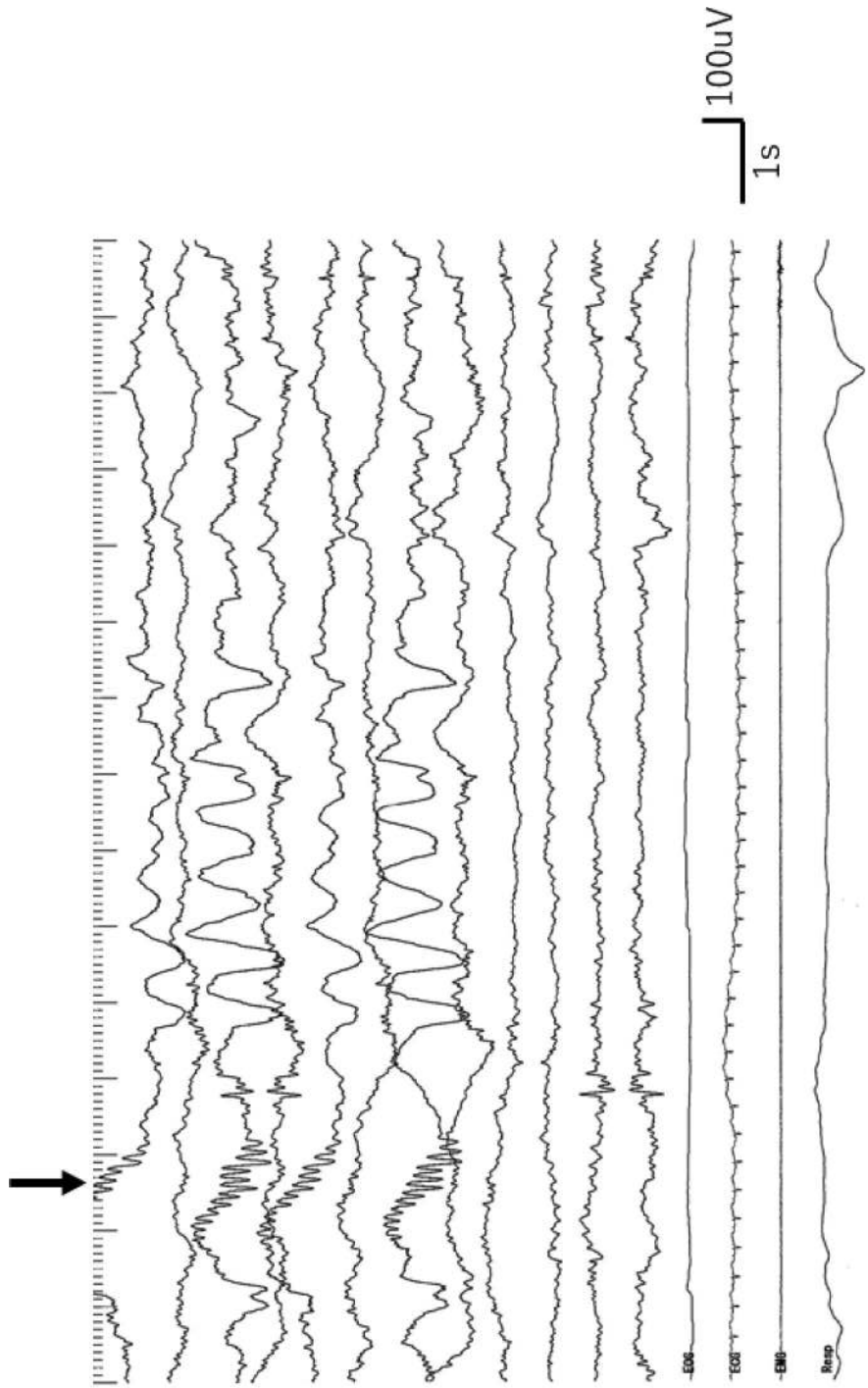

Fig. 10.15 Nystagmus artifact

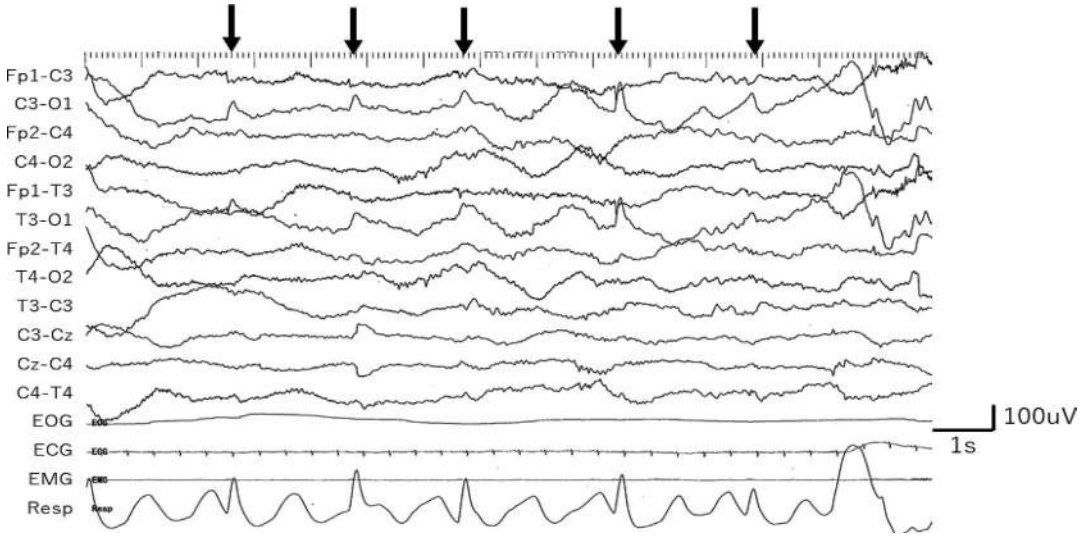

Fig. 10.16 Hiccup artifact

Part III

Abnormal Findings in EEG in Neonates

Concept of Abnormal EEG

11

Hiroyuki Kidokoro and Fumio Hayakawa

1 Concept of Abnormal EEG

When the brain sustains an injury, the EEG shows a range of changes that vary according to the type and severity of the brain damage. These EEG changes can be categorized into two types: abnormalities in background EEG activity and the presence of seizure activity (Table 11.1).

The assessment of background EEG abnormalities focuses on the extent of suppression and morphological changes in EEG activity in comparison to the standard physiological EEG pattern (Fig. 11.1). A state in which EEG activity is suppressed is termed an acute-stage EEG abnormality (ASA). The severity of ASA correlates directly with the level of suppression of EEG activity.

Conversely, a chronic-stage EEG abnormality (CSA) is identified by the substitution of the physiological EEG pattern with nonphysiological, abnormal EEG patterns. CSAs comprise disorganized and dysmature patterns, typically observed during the recovery from the acute phase. Dysmorphic patterns, suggestive of brain malformations, are also classified as CSAs. These abnormalities are considered more severe when the proportion of abnormal patterns is substantial and physiological patterns are minimal. Features such as asymmetry, interhemispheric asynchrony, and ictal changes are noted in both the acute and chronic stages.

Table 11.1 Abnormal findings on neonatal EEG

1. Abnormal background EEG activity
(a) Acute-stage EEG abnormalities
(b) Chronic-stage EEG abnormalities
• Abnormality during recovery from the acute phase
– Disorganized pattern
– Dysmature pattern
• Abnormalities reflecting brain malformation
– Dysmorphic pattern
(c) Abnormalities appearing in both the acute and chronic phases
• Interhemispheric asymmetry
• Interhemispheric asynchrony
2. Ictal changes

H. Kidokoro (✉)
Department of Pediatrics, Nagoya University Graduate School of Medicine, Nagoya, Aichi, Japan
e-mail: kidokoro.hiroyuki.i6@f.mail.nagoya-u.ac.jp

F. Hayakawa
Department of Pediatrics, Okazaki City Hospital, Okazaki, Japan

A. Okumura, H. Kidokoro (eds.), *Neonatal EEG: Atlas and Interpretation*,
https://doi.org/10.1007/978-981-96-0726-6_11

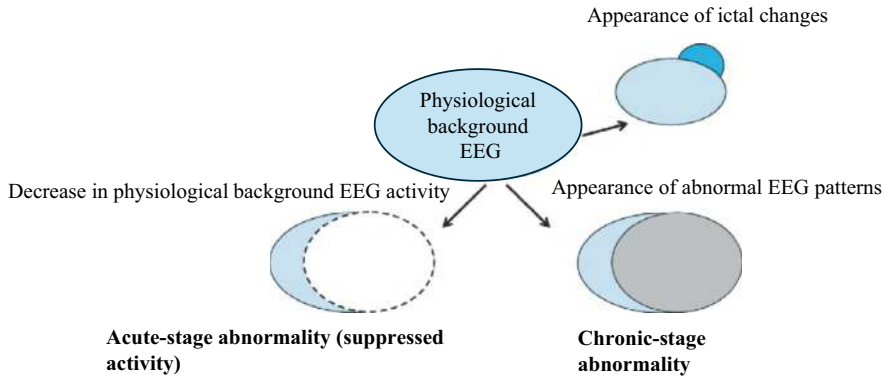

Fig. 11.1 Concept of EEG abnormalities

2 Changes in EEG Findings over Time in Response to Acute Brain Insult

Immediately following an acute brain insult, ASAs manifest, indicative of suppressed brain activity. Over time, the ASA typically improves. In instances of mild brain injury, the EEG may return to normal as the suppression of EEG activity resolves. However, in cases of severe injuries, a variety of morphological EEG changes, known as CSAs, emerge during the recovery phase (Fig. 11.2). The severity and duration of the ASAs are proportional to the severity of the brain injury. Similarly, the severity and duration of the CSAs (Fig. 11.3) reflect the structural changes occurring in response to the brain injury. This concept is applicable to both term and preterm infants, and it also applies to diverse types of brain injuries, including hypoxic-ischemic encephalopathy, cerebral stroke, cerebral hemorrhage, and central nervous system infection. Therefore, this concept is integral to the interpretation of neonatal EEG findings.

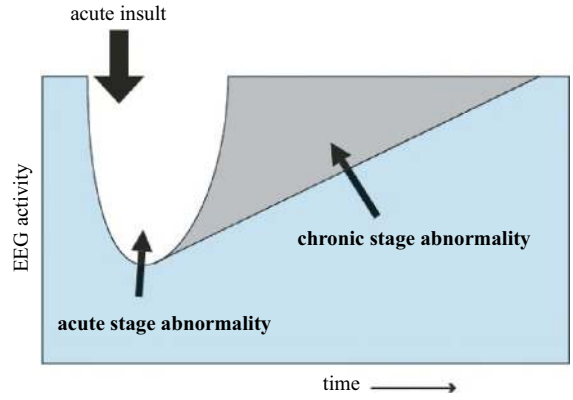

Fig. 11.2 Changes in EEG findings over time in response to acute insult. Immediately following an acute brain injury, EEG activity is suppressed, which is known as acute-stage abnormality (ASA). This condition reflects suppressed brain activity. Over time, the suppressed EEG activity usually improves. In the case of mild brain insult, EEG activity returns to normal as the suppression resolves. However, in instances of severe injury, various degrees of qualitative changes, known as chronic-stage abnormality (CSA), occur during the recovery process

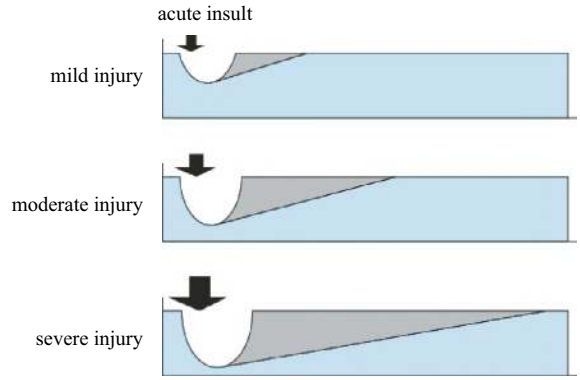

Fig. 11.3 Abnormal findings in the acute phase (suppressed activity). The severity and duration of the acute-stage abnormality are directly proportional to the severity of the acute brain insult. In a similar manner, the severity and duration of chronic-stage abnormality are indicative of the structural changes resulting from the brain damage

Column: Surprises from EEG Activity in Very/Extremely Premature Infants

(Fumio Hayakawa)

EEG recordings of very low-birth-weight infants often yield surprising results. For example, we documented the EEG of a healthy-looking neonate born at 29 weeks' gestation, weighing 1135 g, with Apgar scores of 7 (at 1 min) and 9 (at 5 min). The mother had been hospitalized and received an intravenous infusion to tocolytic agents. She developed a fever the day before delivery, and premature rupture of membranes occurred on the day of delivery. The infant was born by emergent Cesarean section without respiratory distress, crying vigorously and moving all limbs actively.

As it was our routine practice to record EEG of preterm infants born before 33 weeks' gestation immediately after birth, we conducted an EEG recording for this infant, although we anticipated no EEG abnormalities. To our surprise, the initial EEG recording showed almost no activity. The infant occasionally cried, during which electromyogram artifacts were superimposed due to baseline fluctuations. However, when calm, the EEG displayed extended periods of low amplitude or nearly flat tracing. Initially, I suspected an error of the sensitivity setting of the EEG recorder and checked it multiple times. Subsequently, a brief burst of activity emerged, and I identified it as the burst suppression pattern (marked depression).

The infant's postnatal period was uneventful, characterized by steady weight gain and no delays in developing feeding skills. However, a head ultrasound conducted 2 weeks after birth revealed extensive cystic periventricular leukomalacia (PVL) reaching the anterior horn of the lateral ventricles. Follow-up observations indicated severe spastic diplegia; the child was unable to sit unassisted even at 5 years of age.

In this case, the EEG was not useful to improve the child's disability, but only provided early and precise detection of the brain injury. However, without the immediate postnatal EEG recording, the prenatal origins of the PVL might have remained undetected, leaving the cause of the child's disability unknown.

From a neonatal neurology perspective, this case highlighted the critical importance of improving the prenatal intrauterine environment to prevent PVL. It was a valuable experience.

Acute-Stage Abnormalities

12

Tatsuya Fukasawa, Koichi Maruyama, and Fumio Hayakawa

1 Suppressed EEG Activity in Term Infants

In normal-term infants, four EEG patterns are periodically observed, depending on the sleep state: low-voltage irregular (LVI) pattern, mixed (M) pattern, high-voltage slow wave (HVS) pattern, and tracé alternant (TA) pattern. When an acute brain injury occurs, such as hypoxic-ischemic stress, EEG activity is suppressed in accordance with the degree of brain damage. In such cases, physiological periodic changes in EEG patterns are impaired, and the relationship between the EEG patterns and the sleep state is disturbed (Watanabe et al. 1980).

Suppressed EEG activity in term infants can be classified as follows, with a schematic diagram presented in Fig. 12.1 (Watanabe et al. 1980).

T. Fukasawa (✉)
Department of Pediatrics, Anjo Kosei Hospital, Anjo, Japan
e-mail: fukasawa@kosei.anjo.aichi.jp

K. Maruyama
Department of Pediatric Neurology, Aichi Developmental Disability Center Central Hospital, Kasugai, Japan
e-mail: maruyama@aichi-colony.jp

F. Hayakawa
Department of Pediatrics, Okazaki City Hospital, Okazaki, Japan

1. **Grade I: Minimal Depression**
   A flattening in the low-voltage part of the TA pattern, called the tracé discontinu (TD) pattern, is observed. The TD pattern is observed in place of the TA pattern during quiet sleep (QS), while the HVS pattern is preserved or only mildly decreased. The LVI and M patterns are observed during active sleep (AS). The relationship between the sleep cycle and EEG patterns is preserved.
2. **Grade II: Mild Depression**
   The HVS pattern disappears, and the LVI, M, and TD patterns are predominant. In the TD pattern, the interburst intervals (IBIs) are normal, and the waveforms of the bursts are physiological. The relationship between the sleep cycle and EEG patterns is somewhat disturbed, characterized by a decrease in the M pattern and the appearance of the TD pattern during AS along with the appearance of the LVI pattern during QS.
3. **Grade III: Moderate Depression**
   The M pattern disappears, and the LVI and TD patterns are predominant. The IBI in the TD pattern is prolonged, and the waveform of the burst part is often nonphysiological. Although the distinction between AS and QS is clear, the periodicity is lost. The relationship between sleep stages and EEG patterns is also disrupted, with the TD pattern sometimes observed in AS and the LVI pattern sometimes observed in QS.

A. Okumura, H. Kidokoro (eds.), *Neonatal EEG: Atlas and Interpretation*,
https://doi.org/10.1007/978-981-96-0726-6_12

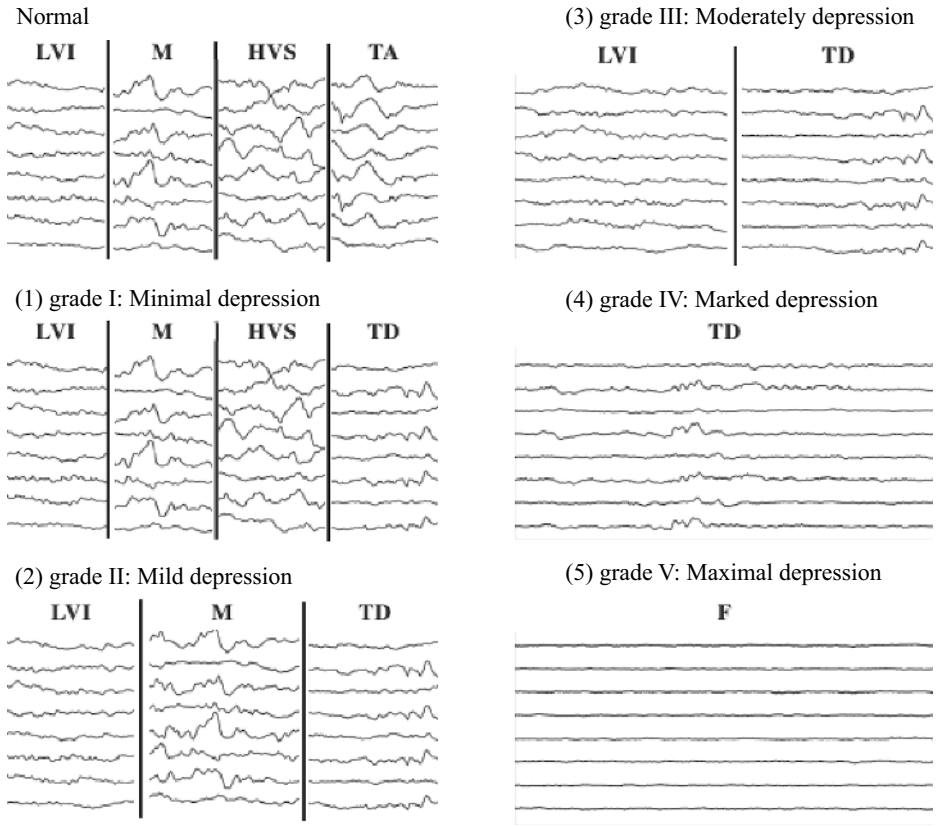

Fig. 12.1 Suppressed EEG activity in full-term infants (Watanabe's classification). LVI: low-voltage irregular pattern, M: mixed pattern, HVS: high voltage slow wave pattern, TD: tracé discontinue pattern, F: flat tracing, TA: tracé alternant pattern

4. **Grade IV: Marked Depression**
   The sleep cycle disappears, leaving only discontinuous EEG patterns. The IBI is markedly prolonged, the burst parts are shortened, and the waveform becomes nonphysiological. This corresponds to the so-called "burst suppression pattern."
5. **Grade V: Maximal Depression**
   Only a flat tracing is shown, even after prolonged recording.

Figure 12.2 illustrates the change in the continuity of EEG activity using compressed EEG. Stronger suppression of EEG activity is associated with more discontinuous activity. With further suppression, even discontinuous activity ceases to be observed.

Suppression of EEG activity is observed in the acute phase of hypoxic-ischemic encephalopathy as well as in cases of intracranial hemorrhage, hypoglycemia, central nervous system infection, and postictal changes.

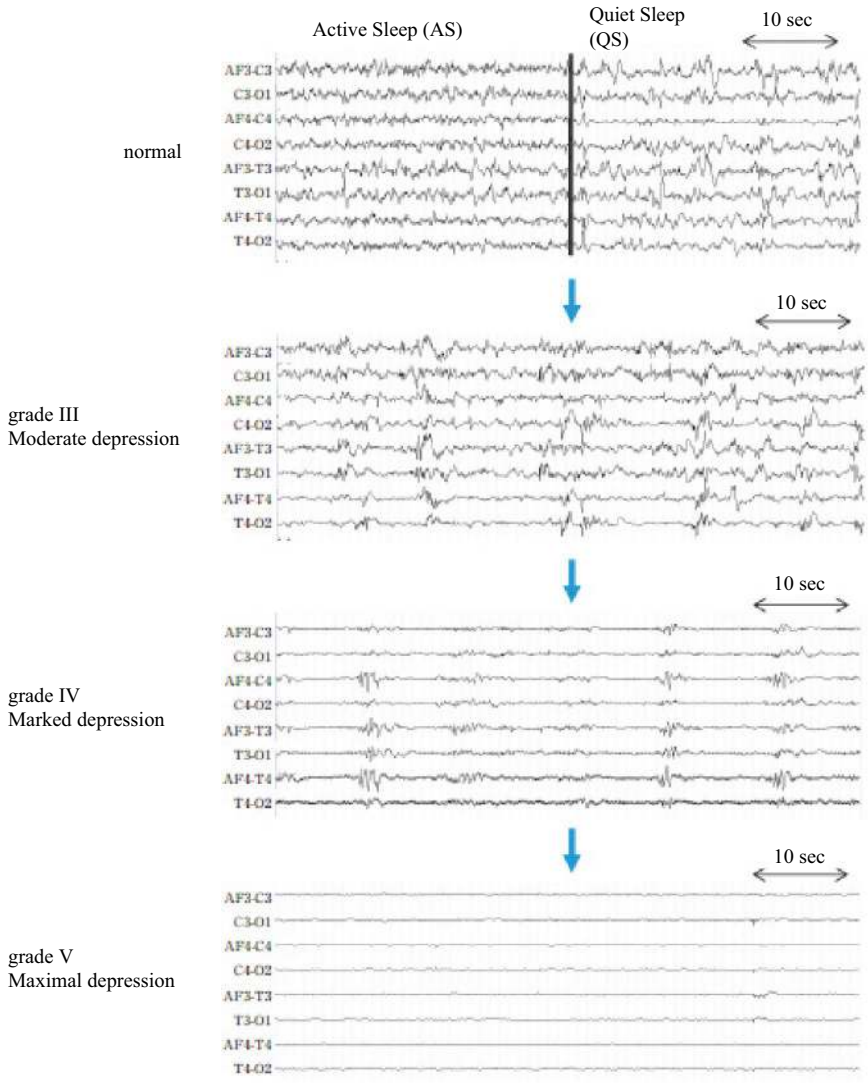

Fig. 12.2 Suppressed EEG activity (decreased continuity) in term infants

2 Changes in Suppressed EEG Findings over Time

Suppressed EEG activity due to acute insult recovers over time, as shown in Fig. 12.3 (Takeuchi and Watanabe 1989). Most infants with severely suppressed EEG activity within the first week of life recover to a normal state or exhibit only mild depression by 2 weeks of age or later. However, those with the highest level of suppressed EEG activity may continue to exhibit severe depression even after 2 weeks. Therefore, when assessing the prognosis of asphyxiated neonates using EEG, it is essential to record the EEG activity as early as possible to evaluate the degree of depression. If the EEG still shows depression after 2 weeks, the possibility of severe depression immediately after birth must be considered, even if the current degree of EEG depression is mild.

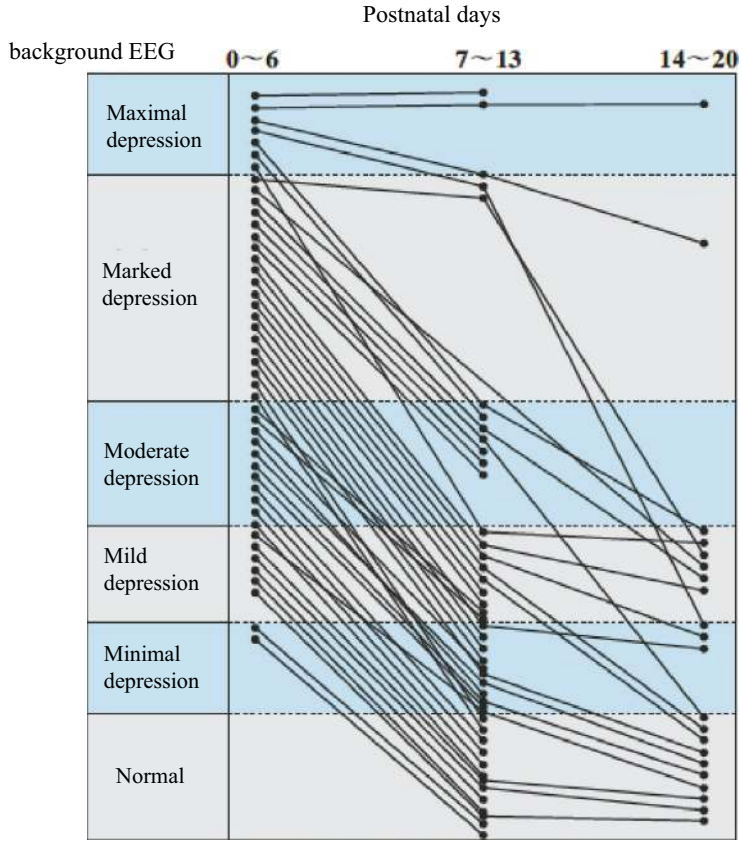

Fig. 12.3 Chronological changes in suppressed EEG findings of term infants

3 Relationship to Outcome

In cases of neonatal asphyxia, there is a significant correlation between suppressed EEG findings within the first week of life and the clinical outcome (Table 12.1) (Takeuchi and Watanabe 1989). The outcome tends to be favorable for minimal or mild depression but unfavorable for marked or maximal depression. The outcome for moderate depression is not consistent; as mentioned earlier, however, more prolonged depression is associated with more severe brain injury. Therefore, it is important to assess and record the degree of EEG depression over time.

Table 12.1 Suppressed EEG activity and outcomes in term neonates with HIE

	Degree of depression in background EEG activity					
Postnatal days	Normal	Minimal	Mild	Moderate	Marked	Maximal
0	—	—	—	?	■	■
1	—	—	○	?	■	■
2	—	—	○	?	■	■
3	—	○	○	?	■	■
4	—	○	○	?	■	■
5	—	○	?	●	■	■
6	○	○	?	●	■	■
7	○	○	?	■	■	■
8	○	?	?	■	■	■
9	○	?	?	■	■	■
10	○	?	●	■	■	■
11	○	?	●	■	■	■
12	○	?	■	■	■	■
13	○	?	■	■	■	■
14	○	?	■	■	■	■
15	?	?	■	■	■	■
16	?	?	■	■	■	■
17	?	?	■	■	■	■
18	?	?	■	■	■	■
19	?	●	■	■	■	■
20	?	●	■	■	■	■
21	?	●	■	■	■	■

—: All cases developed normally
○: Most cases showed normal development
?: No definite prognosis can be made
●: Most cases resulted in neurological handicap or death during the neonatal period
■: All cases resulted in neurological handicap or death during the neonatal period

4 Hypothermia and Suppressed EEG Activity

In recent years, therapeutic hypothermia has become the standard treatment for hypoxic-ischemic encephalopathy in neonates. Many reports have shown that neonates treated with hypothermia generally have better outcomes than those not treated with hypothermia, even among those with similar degrees of EEG depression (Hamelin et al. 2011). Additionally, in severely affected neonates, a more pronounced decrease in the continuity of EEG activity occurs after recovery from hypothermia, suggesting further progression of brain damage during the recovery phase (Birca et al. 2016). Medications, such as benzodiazepines, phenobarbital, and morphine, commonly used during hypothermia, tend to reduce the amplitude of background activity and decrease continuity (Walsh et al. 2011). These factors should be considered when interpreting EEG results before, during, and after hypothermia treatment.

5 Suppressed EEG Activity in Preterm Infants

Changes in background EEG activity due to acute insult are also observed in preterm infants (Watanabe et al. 1999). To evaluate mild depression, one should note the decrease in the fast wave component and amplitude in addition to the decrease in continuity (Fig. 12.4).

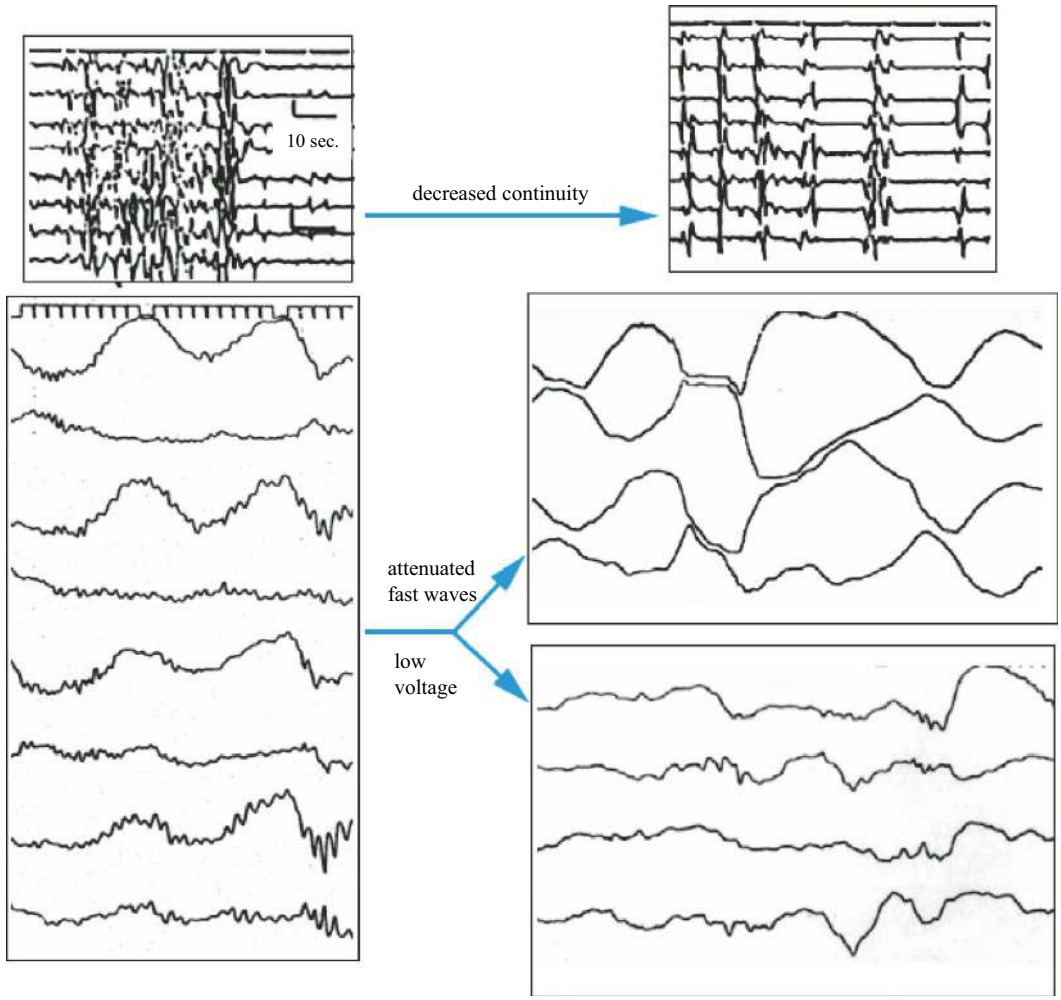

Fig. 12.4 Findings of suppressed EEG activity in preterm infants. To evaluate a slight decrease in activity, the clinician should note the decrease in the fast wave component and amplitude as well as the decrease in continuity

5.1 Decrease in Continuity

A discontinuous EEG pattern is a physiological finding in preterm infants. The presence of suppressed EEG activity is indicated by increased discontinuity during QS (shown as prolonged IBIs and shortened burst activities) and a decrease in continuous EEG activity during AS. A prolonged IBI in the discontinuous part of the EEG relative to the postmenstrual age (PMA) is considered mild, decreased continuous EEG activity is considered moderate, and a loss of sleep stage differentiation along with a loss of continuous EEG activity is considered severe (Fig. 12.5).

In practice, prolonged IBIs and decreased continuity often *appear* simultaneously, and careful assessment is required when only one of these findings is observed. As shown in Fig. 12.6, a lower PMA is associated with greater physiologic discontinuity and a longer duration of IBI. Sleep cycles are also unclear at a PMA of <30 weeks, making it challenging to assess continuity, especially during the extremely premature period (PMA of <26 weeks). Although quantitative evaluation criteria have not been established, Table 12.2 provides a benchmark (Maruyama et al. 2002).

5.2 Reduction in Fast Wave Component

As EEG activity decreases, rhythmic alpha-beta waves (i.e., brushes) that typically accompany high-voltage slow waves and high-amplitude theta waves specific to the PMA disappear. Because the incidence of brushes is physiologically low in preterm infants born at <30 weeks PMA, the fast wave component is mainly evaluated in terms of rhythmic alpha waves and high-amplitude theta waves. As EEG activity decreases, alpha-beta waves and then theta waves disappear. At higher levels of suppression, only delta waves are observed (Fig. 12.7).

5.3 Decrease in Voltage

Decreased voltage is primarily assessed based on the voltage of the delta wave (Fig. 12.8, Table 12.3) (Maruyama et al. 2002). Mildly low voltage is defined as a maximum delta wave amplitude of <200 μV for preterm infants at <30 weeks PMA and <150 μV for those at ≥30 weeks PMA. Severely low voltage refers to a maximum delta wave amplitude of 20–50 μV. It is difficult to distinguish precisely between a low-voltage EEG with a maximum voltage of ≤20 μV and a flat EEG, but the difference is not clinically significant.

5.3.1 Severity Classification of Suppressed EEG Activity in Preterm Infants

As shown in Table 12.4, the severity of EEG abnormalities is classified according to three key indices: decrease in continuity, attenuation of fast waves, and decrease in voltage (Watanabe et al. 1999). These three findings rarely occur in isolation. Typically, more severe EEG suppression is associated with a higher likelihood of multiple findings being present. In such cases, the classification is based on the grade of the most severe EEG finding.

5.3.2 Importance of Early and Subsequent Serial EEG Recordings in Preterm Infants

Brain injury in preterm infants is characterized by the variable timing of injury, diverse modes of injury, and potential association with postnatal complications. The severity of an acute-stage abnormality (ASA) should be assessed during the acute phase of illness. Therefore, early postnatal EEG recordings are essential to detect suppressed activity caused by an acute injury that occurred immediately before birth (Fig. 12.9) (Watanabe et al. 1999).

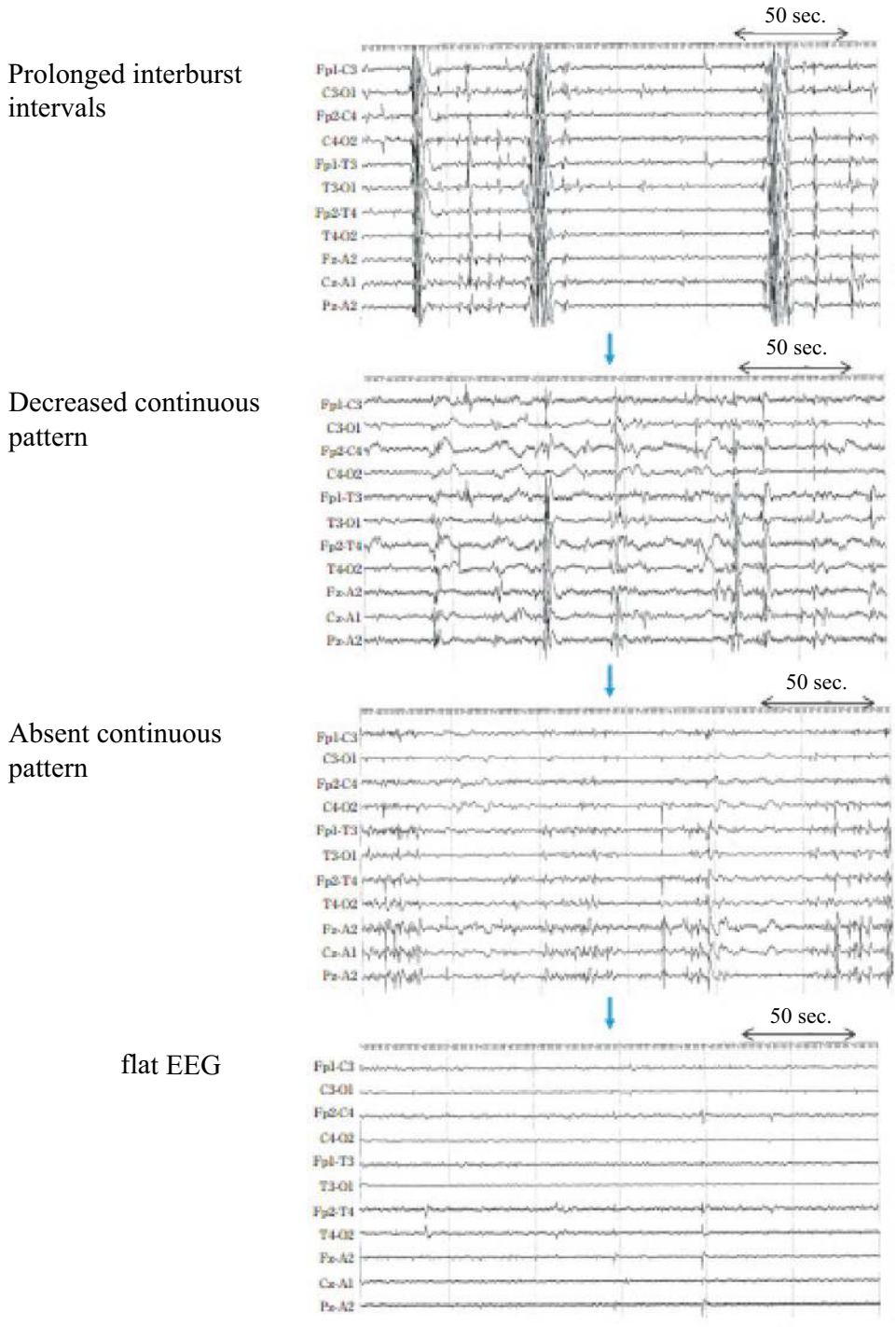

Fig. 12.5 Suppressed EEG activity (decreased continuity) in preterm infants as seen by compressed EEG

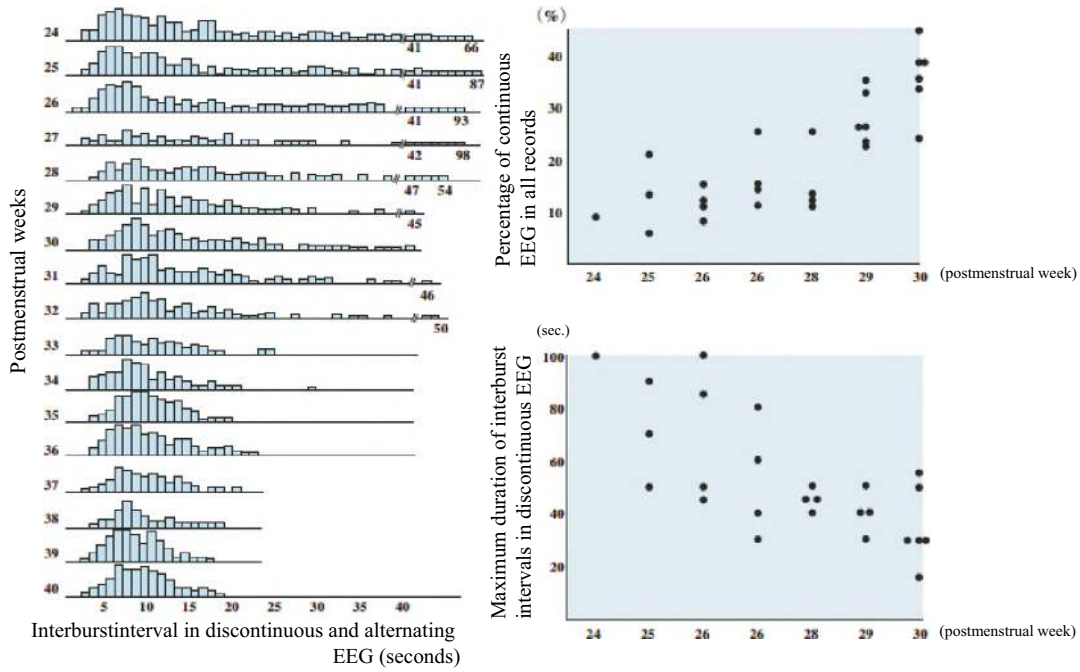

Fig. 12.6 Postmenstrual age and interburst intervals

Table 12.2 Benchmarks for decreased continuous pattern

Prolonged interburst intervals (IBIs)
PMA <30 weeks: maximum, >90 s; average, >60 s
PMA >30 weeks: maximum, >60 s; average, >40 s
Decreased continuous pattern
Percentage of continuous pattern lasting >20 s among total recordings
PMA <30 weeks: <10%
PMA >30 weeks: <30%
Absent continuous pattern
Absence of continuous pattern, sleep cycle, and response to arousal stimuli

Importantly, however, repeated EEG recordings over time are crucial to identify postnatal injuries. Delayed examinations might miss ASAs, which could have already been resolved, revealing only chronic-stage abnormalities (CSAs). However, if the injury occurred in utero, CSAs will already be present in the early postnatal EEG.

5.3.3 Association Between Suppressed EEG Findings and Outcomes

When the acute phase of EEG suppression following an acute insult can be detected, a close relationship is observed between the degree of EEG suppression and the outcome (Maruyama et al. 2002). A study of the relationship between EEGs recorded within the first week of life and outcomes in preterm infants showed that the incidence of cerebral palsy was 2% in infants with no EEG suppression and 3% in those with minimal depression. This incidence rose to 22% for mild depression, 47% for moderate depression, and 100% for marked or maximal depression. A clear correlation was found between the degree of EEG depression and the severity of cerebral palsy (Fig. 12.10). Additionally, in a study of preterm infants immediately before or at birth, the timing of the first EEG examination proved to be most suitable for prognostic evaluation (Fig. 12.11).

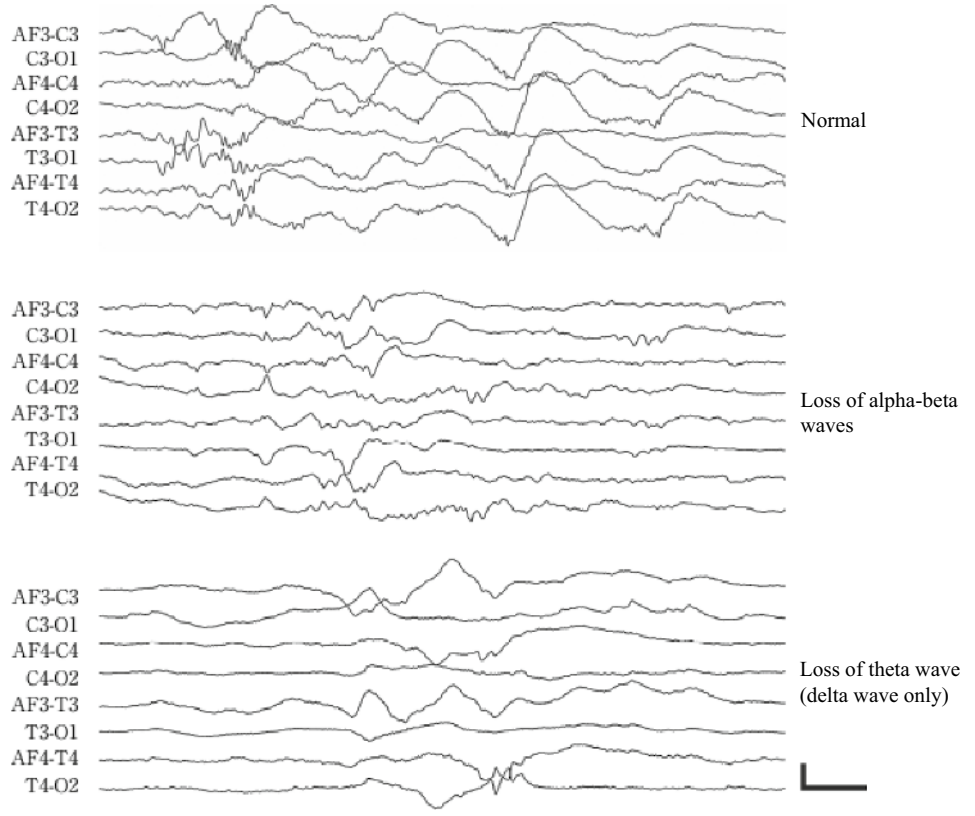

Fig. 12.7 Suppressed EEG activity in preterm infants (decreased fast wave components)

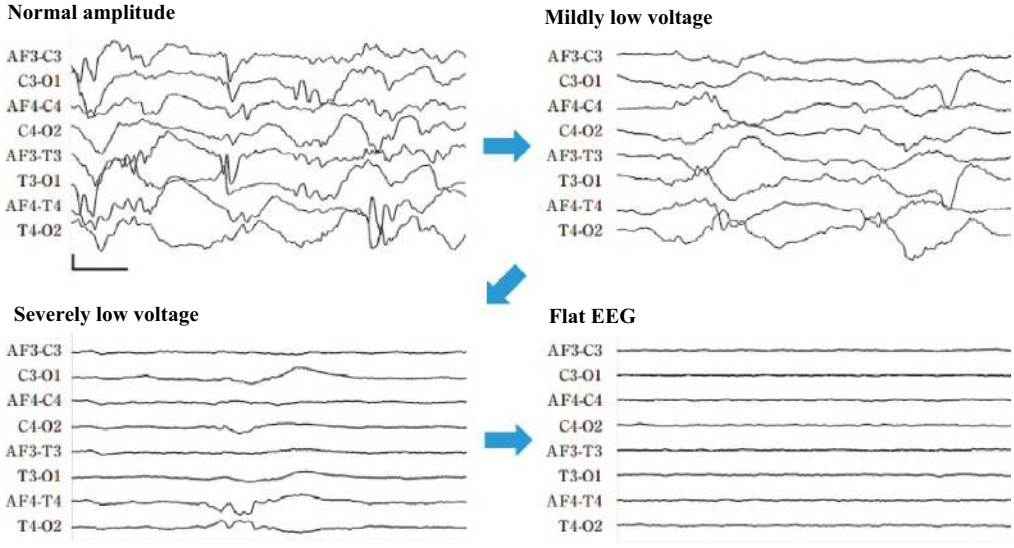

Fig. 12.8 Suppressed EEG activity (decreased voltage) in preterm infants

Table 12.3 Benchmark for voltage reduction

Mildly low voltage
Maximum voltage of delta wave
PMA <30 weeks: <200 μV
PMA >30 weeks: <150 μV
Severely low voltage
Maximum voltage of delta wave: 20–50 μV
Flat EEG
Maximum voltage of delta wave: <20 μV

Table 12.4 Classification of suppressed EEG activity in preterm infants

Grade I: Minimal depression
Prolonged IBI, diminished fast wave components
Grade II: Mild depression
Mildly low voltage
Grade III: Moderate depression
Decreased continuity pattern
Grade IV: Severe depression
Loss of continuous pattern, loss of fast wave component, severely low voltage
Grade V: Maximal depression
Flat EEG

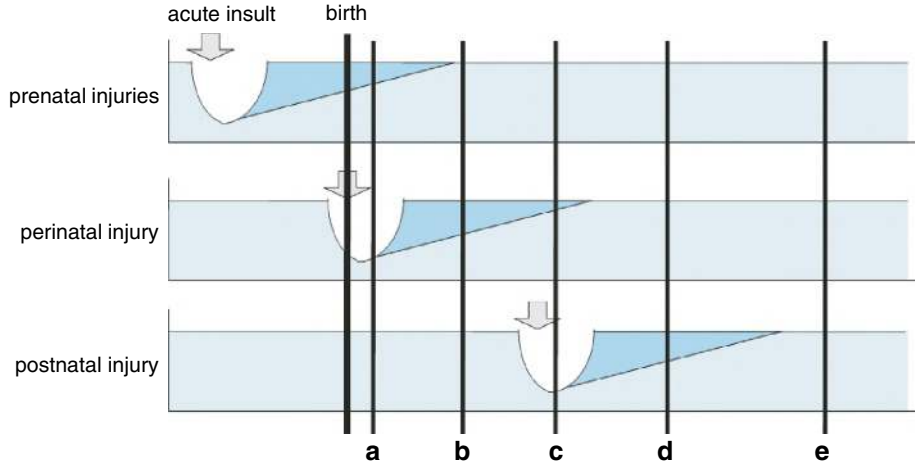

Fig. 12.9 Timing of onset of acute insult and timing of EEG recording. In cases of prenatal injury, (A) an EEG recorded immediately after birth may show CSAs, but (C–E) an EEG recorded later may not show these abnormalities. In cases of perinatal injury, (A) an EEG recorded immediately after birth shows only ASAs, but (B) an EEG recorded slightly later shows CSAs, making it difficult to distinguish perinatal from prenatal injury. In cases of postnatal injury, it is impossible to confirm that the injury is postnatal unless (A) a normal EEG in the early postnatal period is documented. (C) If the EEG is recorded immediately after brain insult, ASAs can be confirmed and the time of injury estimated. (B–E) However, abnormalities may not be identified at other times

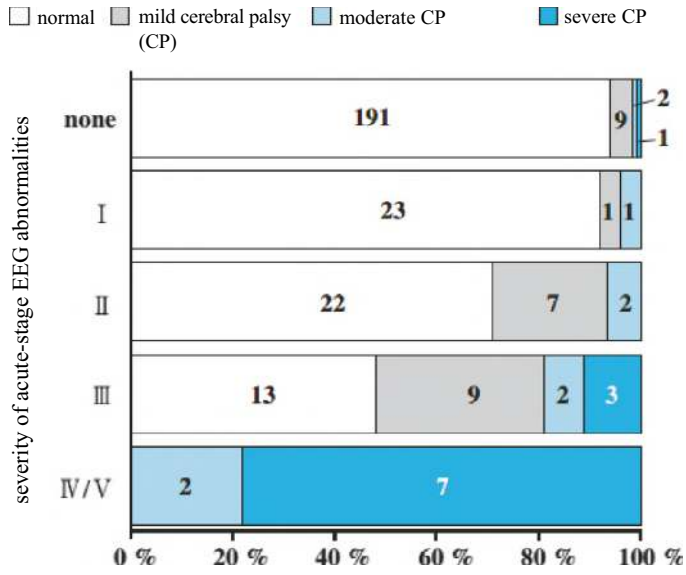

Fig. 12.10 Severest depression in EEG activity within first week after birth and later cerebral palsy

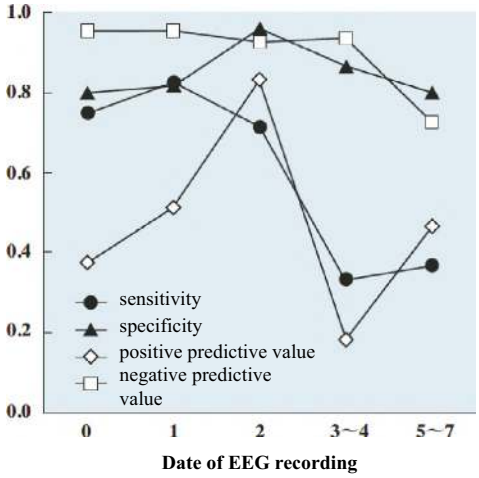

Fig. 12.11 Diagnostic significance of EEG and date of recording

5.3.4 Sedative Medications and Suppressed EEG Activity

Sedatives are commonly used in preterm infants for general management and pain relief. However, because these medications can lead to suppressed EEG activity in preterm infants, their use should be considered when evaluating EEGs. In our experience, 16 (52%) of 31 EEG recordings obtained while infants were under the effects of sedatives such as midazolam, pentobarbital, or morphine showed suppressed activity. Furthermore, patients who showed suppressed EEG activity also exhibited significantly worse outcomes, even when sedated (Hayashi-Kurahashi et al. 2012).

Rhythmic theta waves of 7–8 Hz are clearly identified, showing few brushes and slow waves. Additionally, a high voltage slow wave (HVS) pattern is recognized; therefore, the EEG maturation can be judged to be equivalent to that of a 40-week EEG. Notably, although the low-voltage part of the alternating pattern (TA) should show sustained activity, it is almost flat in this sample. This indicates that the TA pattern changed to a TD pattern. These findings indicate minimal depression in full-term infants (Fig. 12.12).

The low-voltage irregular (LVI) pattern and mixed (M) pattern, both continuous patterns, show rhythmic theta waves at 7–8 Hz; however, the slow wave continuity of the M pattern is rather poor. In the LVI pattern, theta waves are also reduced, and there is an increased presence of near-flat parts. Throughout the recordings, the HVS pattern cannot be observed, and only the TD pattern is observed during quiet sleep. The amplitude and duration of TD bursts are also slightly decreased. These findings indicate mild depression in a full-term infant (Fig. 12.13).

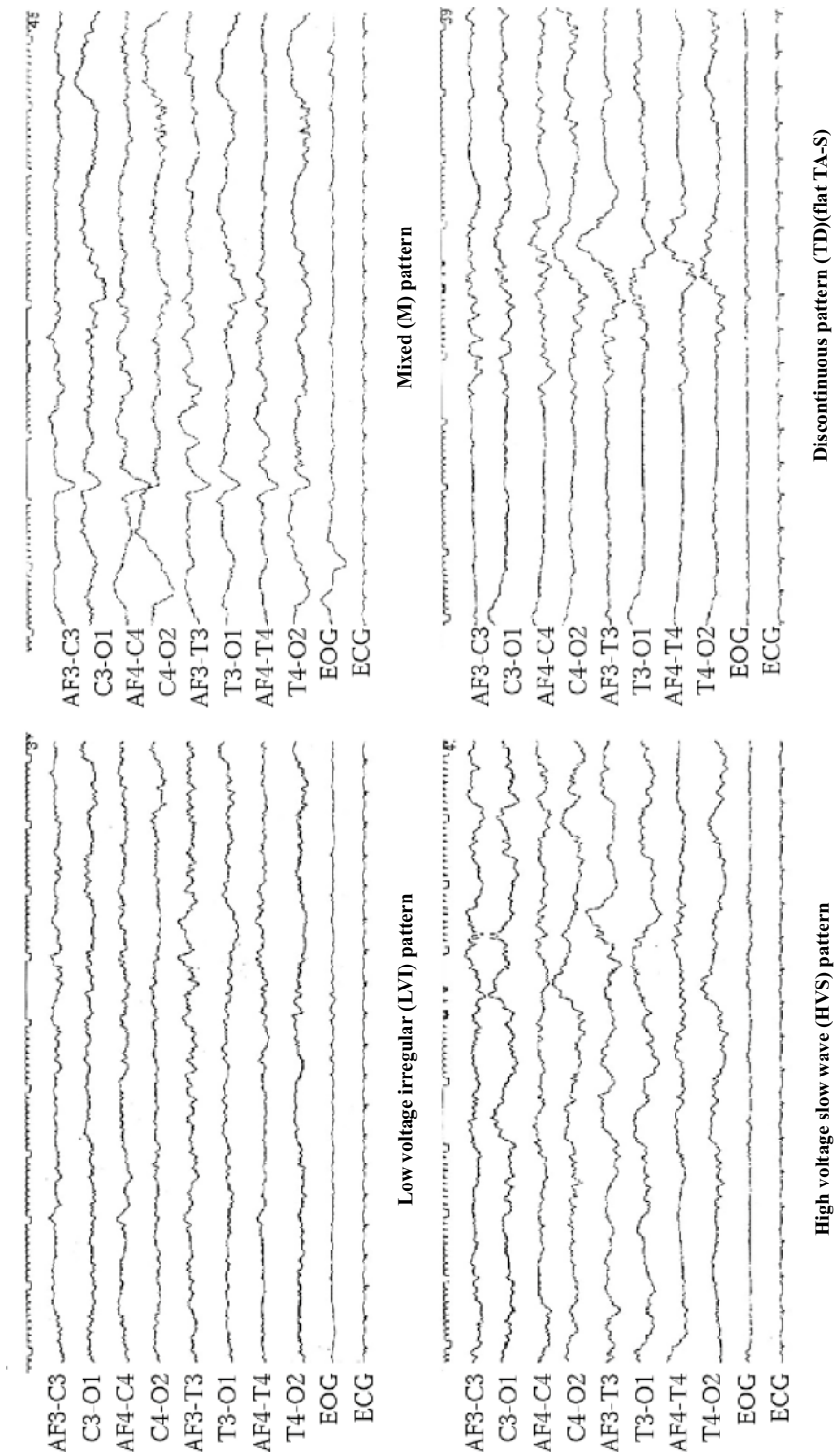

Fig. 12.12 Minimal depression (Grade I) in full-term infants

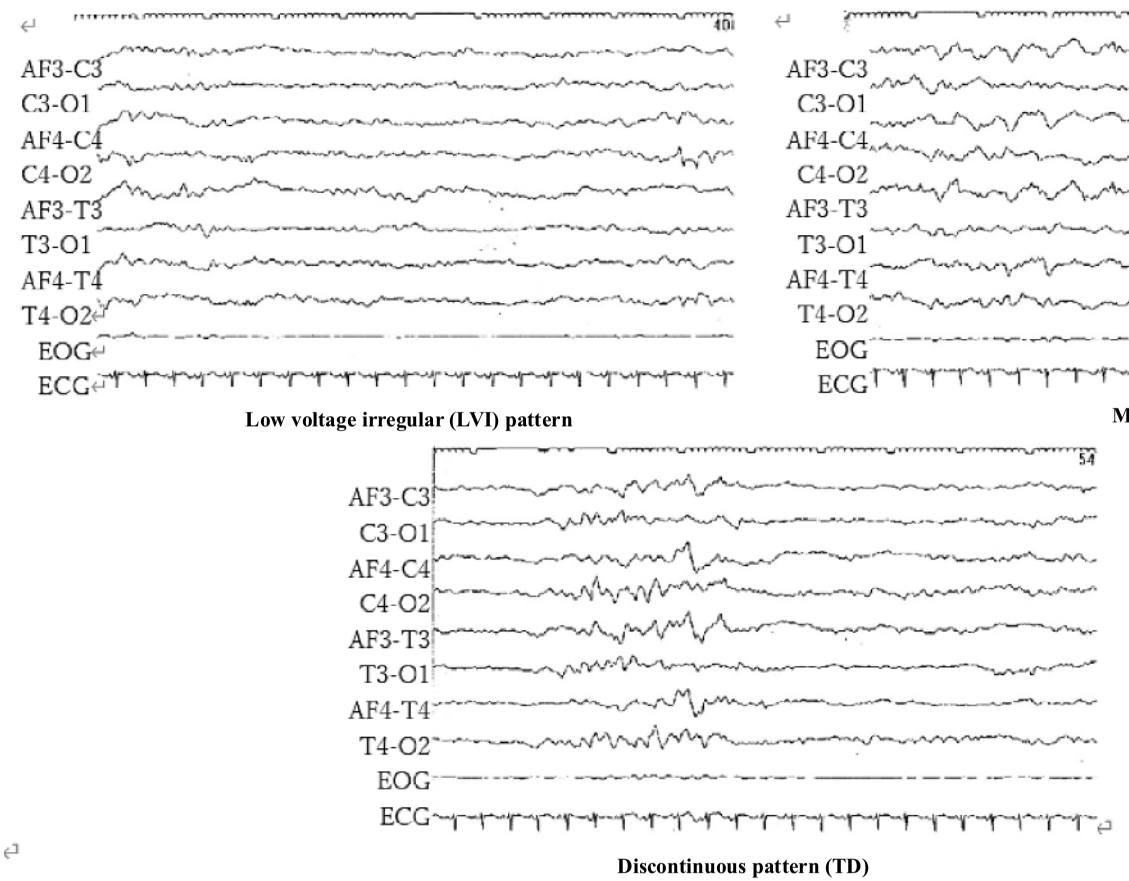

Fig. 12.13 Mild depression (Grade II) in full-term infants

In infants with moderate depression, the mixed (M) pattern disappears, leaving only the low-voltage irregular (LVI) and TD patterns. The relationship between the sleep stage and EEG pattern becomes disrupted, with the LVI pattern observed during quiet sleep and the TD pattern during active sleep. In the LVI pattern, theta waves are significantly reduced, often with near-flat parts; in the TD pattern, the interburst interval is clearly prolonged and the burst duration is shortened. The key distinguishing feature of severe depression is the presence or absence of the LVI pattern, which is a continuous pattern (Fig. 12.14).

Marked depression is characterized by the disappearance of the continuous EEG pattern, leaving only the TD pattern (also known as the "burst suppression pattern"). In this pattern, the bursts are short in duration and the waveform is non-physiological. This finding remains unchanged by external stimuli (Fig. 12.15).

The observation of only a flat EEG and slightly low amplitude activity, even after prolonged recording, indicates maximal depression. When this finding is observed, it is important to confirm the presence or absence of stimulus-induced changes (Fig. 12.16).

The top figure shows a 28-week EEG. The amplitude of the slow wave is approximately 300 μV, corresponding to the PMA, and continuity is maintained. However, there are no fast wave components superimposed on the slow waves, giving the EEG recordings a smooth appearance. The bottom figure shows a 30-week EEG. In this recording, 1-Hz, 200- to 300-μV slow waves, also matching the PMA, appear continuously with no decrease in continuity or amplitude. However, the fast wave component is reduced, and smooth slow waves are observed continuously (Fig. 12.17).

EEGs from a 32-week-old infant are shown. In the upper continuous pattern, continuous EEG activity is present and can be clearly distinguished from the lower discontinuity pattern (TD pattern). However, most of the slow waves have voltages of approximately 100 μV, and none exceed 150 μV (Fig. 12.18).

EEGs from an infant at 30 weeks PMA are shown. The continuous pattern is barely sustained, but the duration of continuous EEG activity is short, with <30% persisting for >20 s. Although the voltage of the slow waves is slightly reduced, voltages of approximately 200 μV remain. In general, moderate depression is accompanied by a reduction in slow wave voltage, although the degree varies (Fig. 12.19).

EEGs of a 29-week-old infant are shown. The continuous EEG pattern has disappeared, and the EEG displays a so-called "burst suppression pattern." The bursts are short in duration, and the slow waves have a very low amplitude. This finding remains unchanged by stimulation (Fig. 12.20).

EEGs of a 31-week-old infant are shown. Similar to term infants, the highest degree of depression is seen when only a flat EEG or slightly low-amplitude activity is present, even after prolonged recording. When this finding is observed, it is important to confirm whether there is any change induced by stimulation (Fig. 12.21).

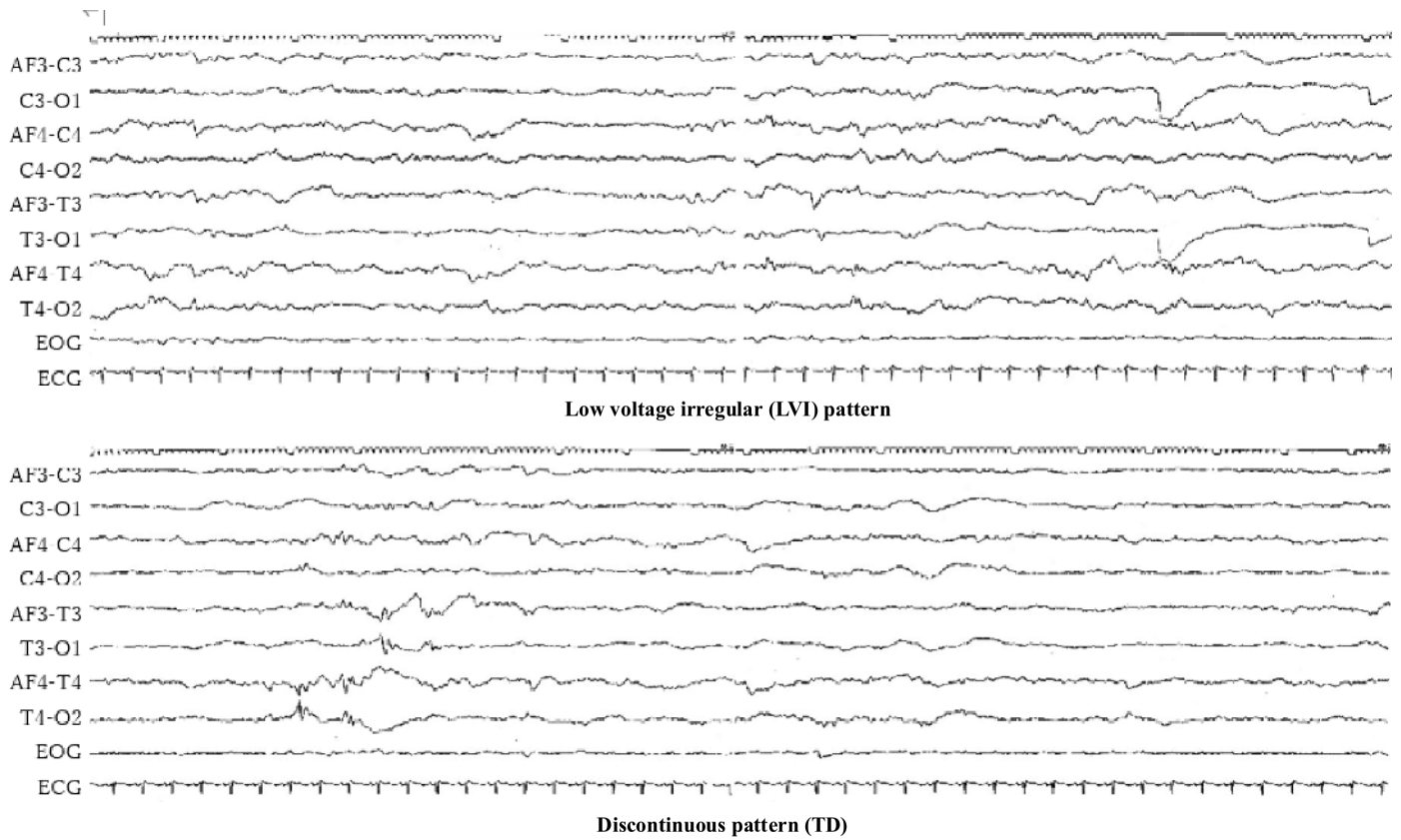

Fig. 12.14 Moderate depression (Grade III) in full-term infants

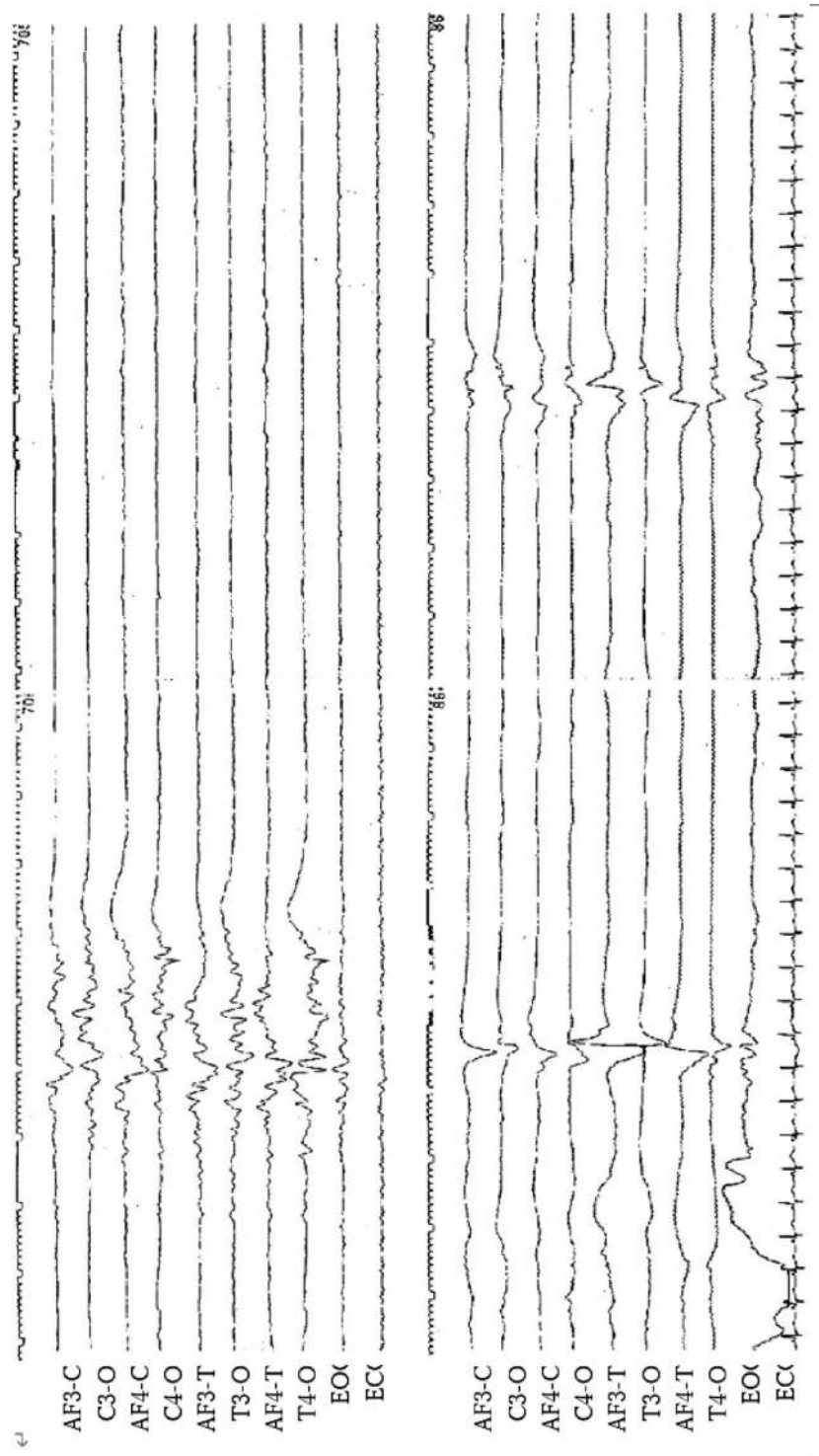

Fig. 12.15 Marked depression (Grade IV) in full-term infants

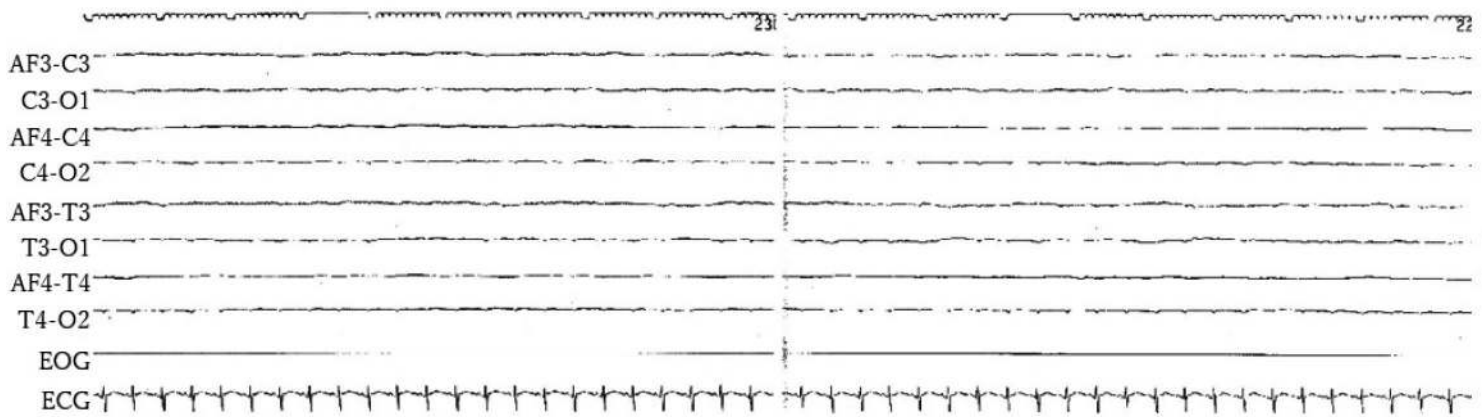

Fig. 12.16 Maximal depression (Grade V) in full-term infants

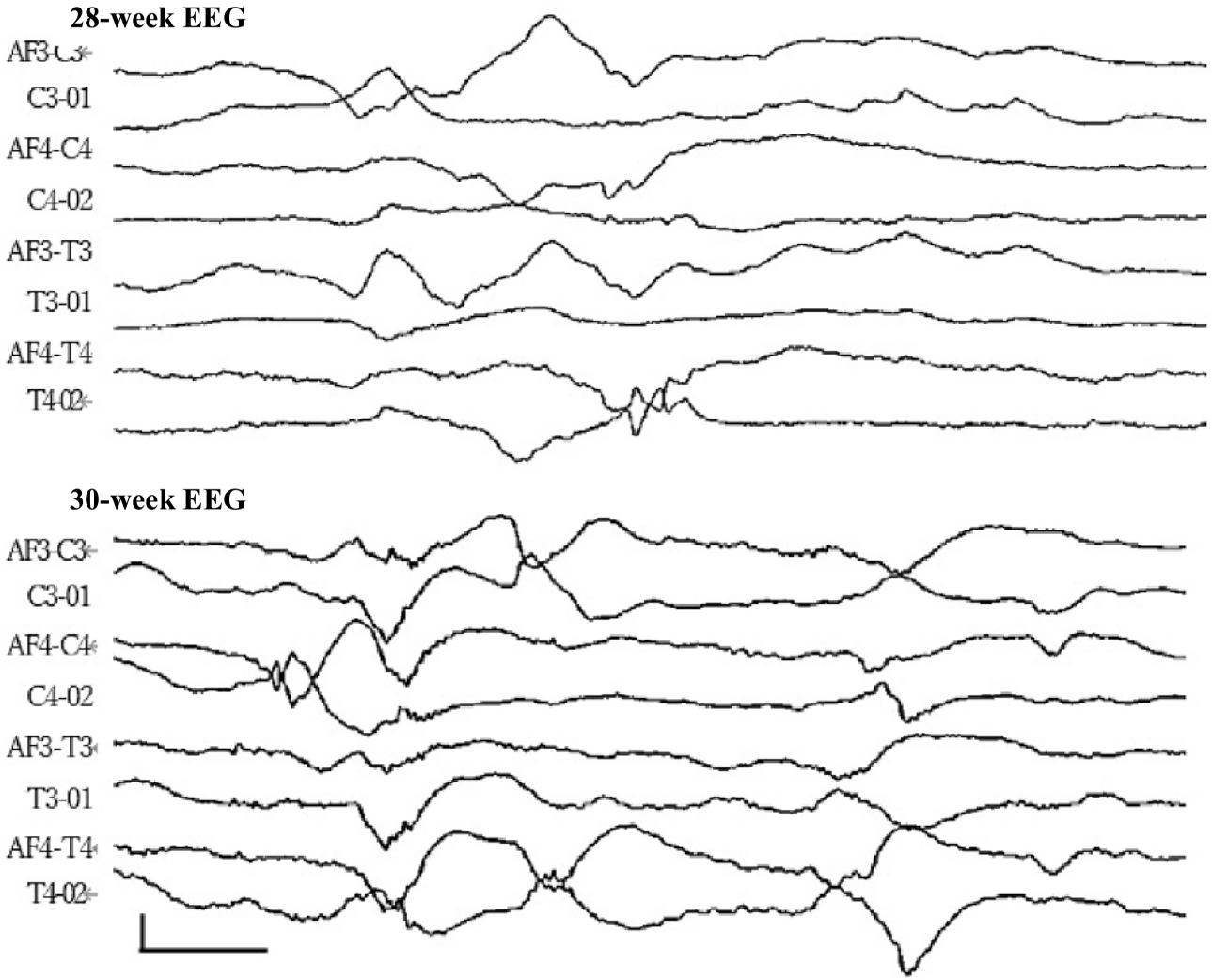

Fig. 12.17 Minimal depression (Grade I) in preterm infants

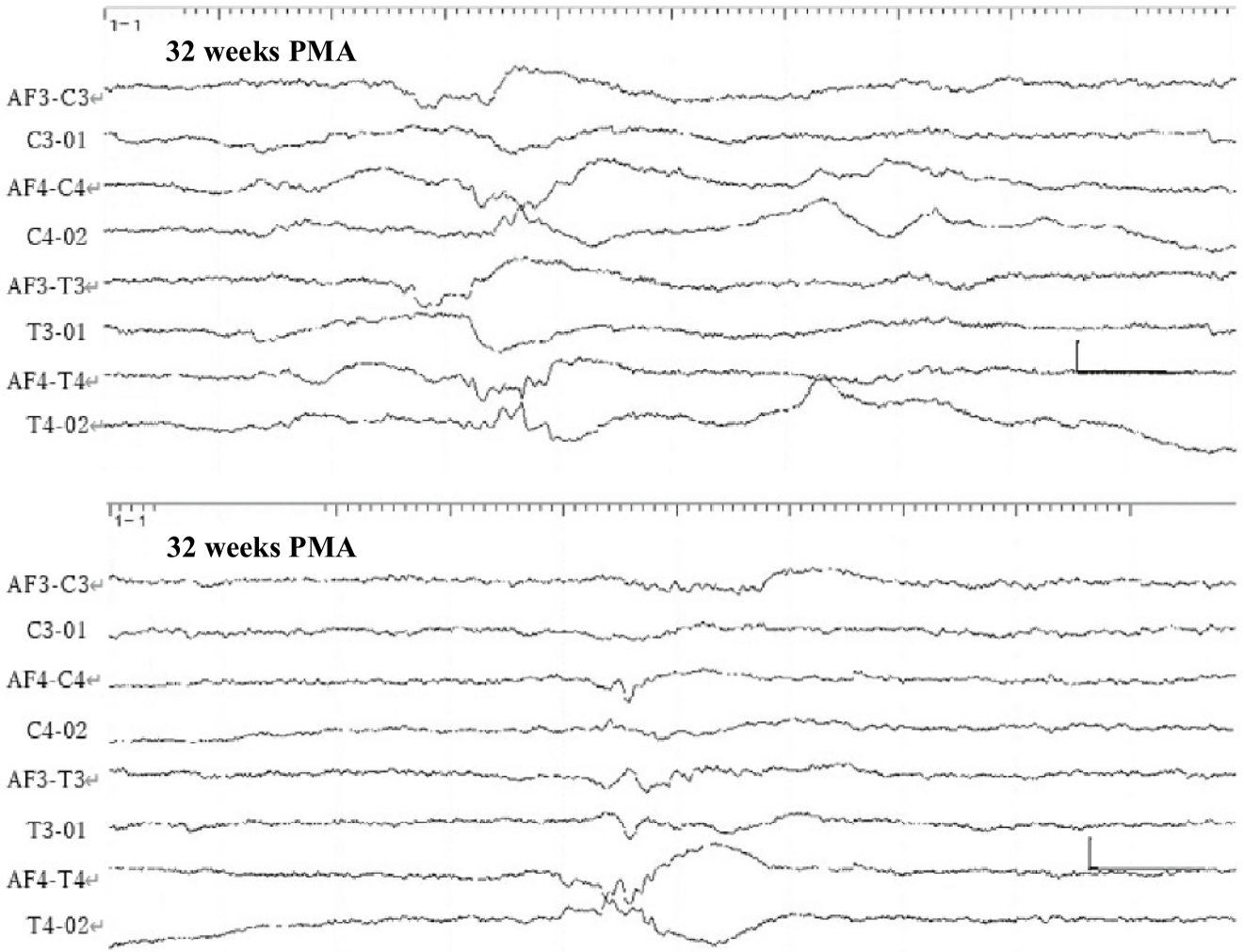

Fig. 12.18 Mild depression (Grade II) in preterm infants

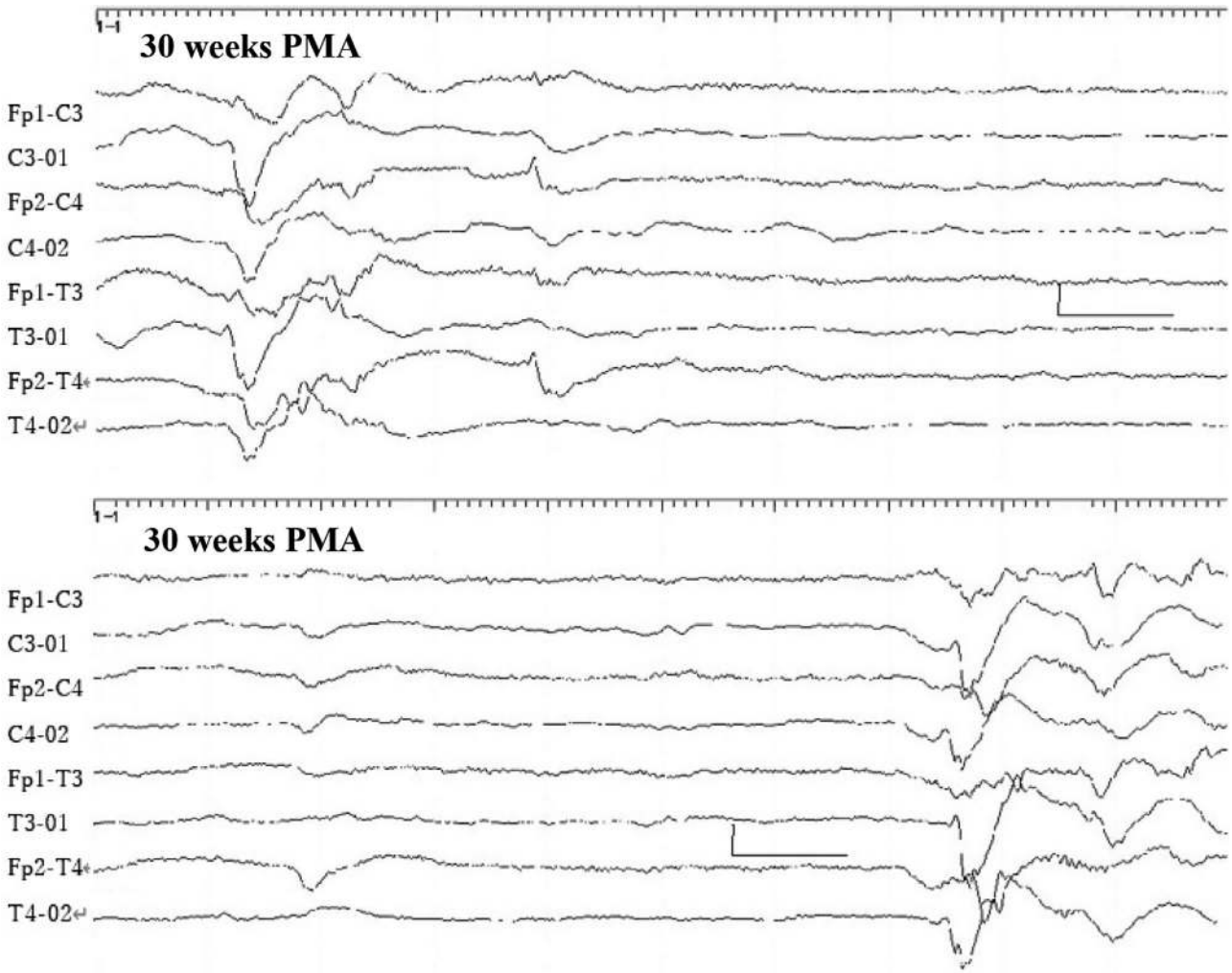

Fig. 12.19 Moderate depression (Grade III) in preterm infants

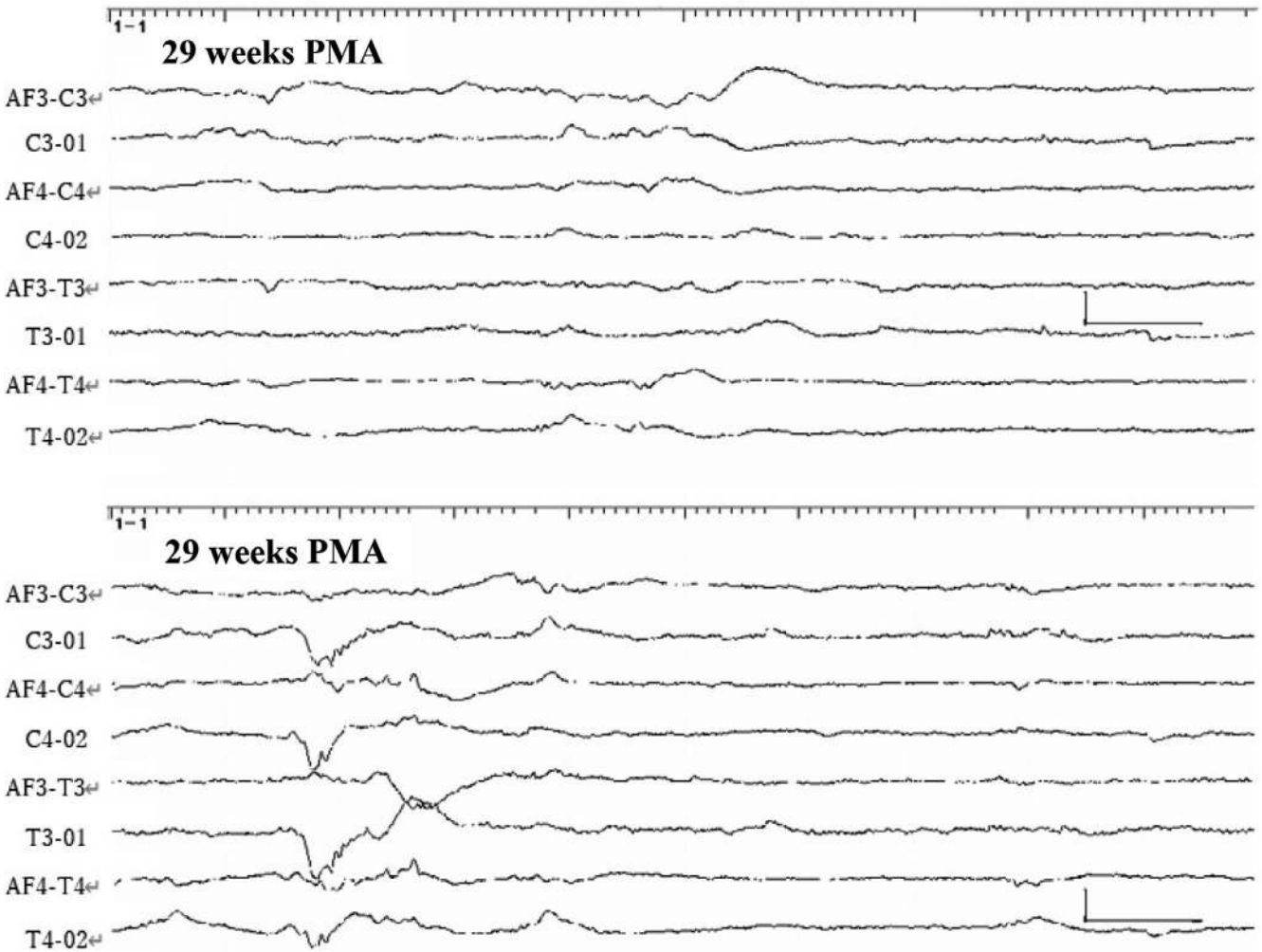

Fig. 12.20 Severe depression (Grade IV) in preterm infants

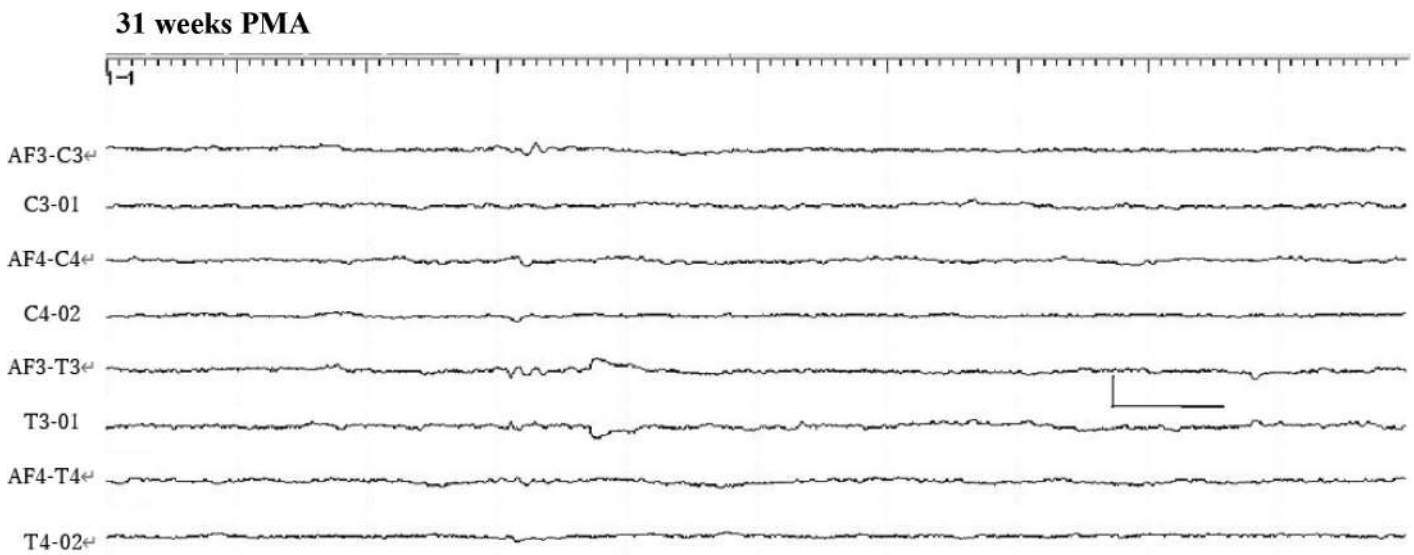

Fig. 12.21 Maximal depression (Grade V) in preterm infants

References

Birca A, Lortie A, Birca V, Decarie JC, Veilleux A, Gallagher A, Dehaes M, Lodygensky GA, Carmant L. Rewarming affects EEG background in term newborns with hypoxic-ischemic encephalopathy undergoing therapeutic hypothermia. Clin Neurophysiol. 2016;127(4):2087–94.

Hamelin S, Delnard N, Cneude F, Debillon T, Vercueil L. Influence of hypothermia on the prognostic value of early EEG in full-term neonates with hypoxic ischemic encephalopathy. Neurophysiol Clin. 2011;41(1):19–27.

Hayashi-Kurahashi N, Kidokoro H, Kubota T, Maruyama K, Kato Y, Kato T, Natsume J, Hayakawa F, Watanabe K, Okumura A. EEG for predicting early neurodevelopment in preterm infants: an observational cohort study. Pediatrics. 2012;130(4):e891–7.

Maruyama K, Okumura A, Hayakawa F, Kato T, Kuno K, Watanabe K. Prognostic value of EEG depression in preterm infants for later development of cerebral palsy. Neuropediatrics. 2002;33(3):133–7.

Takeuchi T, Watanabe K. The EEG evolution and neurological prognosis of neonates with perinatal hypoxia. Brain Dev. 1989;11(2):115–20.

Walsh BH, Murray DM, Boylan GB. The use of conventional EEG for the assessment of hypoxic ischaemic encephalopathy in the newborn: a review. Clin Neurophysiol. 2011;122(7):1284–94.

Watanabe K, Miyazaki S, Hara K, Hakamada S. Behavioral state cycles, background EEGs and prognosis of newborns with perinatal hypoxia. Electroencephalogr Clin Neurophysiol. 1980;49(5–6):618–25.

Watanabe K, et al. Neonatal EEG: a powerful tool in the assessment of brain damage in preterm infants. Brain Dev. 1999;21:361–72.

Chronic-Stage Abnormalities

13

Tatsuya Fukasawa, Koichi Maruyama, and Fumio Hayakawa

1 Abnormal EEG Findings in the Chronic Stage

Abnormal EEG findings in the chronic stage can be categorized into three patterns: the disorganized pattern, dysmature pattern, and dysmorphic pattern.

The disorganized pattern is characterized by distorted physiological EEG components, especially deformed delta waves, and the appearance of abnormal sharp waves and abnormal brushes (Hayakawa et al. 1997a). This pattern often reflects deep white matter injury, such as periventricular hemorrhagic infarction and periventricular leukomalacia, and it is predictive of the future development of spastic paraparesis.

The dysmature pattern is an immature EEG pattern indicative of delayed brain maturation (Hayakawa et al. 1997b). This delay may be a result of suboptimal prenatal conditions or postnatal malnutrition. This pattern may also be associated with future intellectual disability.

The dysmorphic pattern is characterized by the appearance of abnormal nonphysiological EEG patterns. This pattern is suggestive of a brain malformation, such as a congenital malformation.

In preterm infants, there is a significant relationship between chronic-stage EEG abnormalities (CSAs) and neurological outcomes, as shown in Fig. 13.1 (Watanabe et al. 1999). Notably, 88% of infants without CSAs had normal outcomes. By contrast, all infants with severely disorganized patterns and 47% with mildly disorganized patterns developed cerebral palsy. Conversely, only 11% of infants with dysmature patterns developed cerebral palsy, but 67% experienced mental developmental issues, including borderline intellectual development and intellectual disabilities. Essentially, the disorganized pattern is a critical indicator of the cerebral palsy risk, whereas the dysmature pattern predominantly signals a risk of intellectual disabilities (Okumura et al. 2002).

With respect to pattern emergence, the disorganized pattern typically manifests between 4 and 13 days of age in infants with periventricular leukomalacia and is rare after 2 months (Kidokoro et al. 2009). The dysmature pattern, due to conditions such as malnutrition, persists even after EEG maturation ceases. However, the dysmorphic pattern can be seen regardless of the time of examination.

T. Fukasawa (✉)
Department of Pediatrics, Anjo Kosei Hospital, Anjo, Japan
e-mail: fukasawa@kosei.anjo.aichi.jp

K. Maruyama
Department of Pediatric Neurology, Aichi Developmental Disability Center Central Hospital, Kasugai, Japan
e-mail: maruyama@aichi-colony.jp

F. Hayakawa
Department of Pediatrics, Okazaki City Hospital, Okazaki, Japan

A. Okumura, H. Kidokoro (eds.), *Neonatal EEG: Atlas and Interpretation*,
https://doi.org/10.1007/978-981-96-0726-6_13

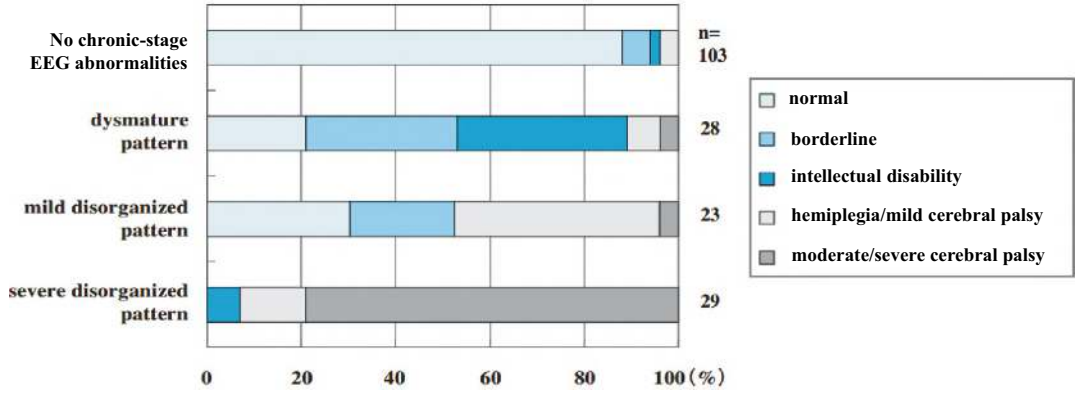

Fig. 13.1 Relationship between different types of chronic-stage abnormalities and neurological outcomes (Watanabe et al. 1999)

References

Hayakawa F, Okumura A, Kato T, Kuno K, Watanabe K. Disorganized patterns: chronic-stage EEG abnormality of the late neonatal period following severely depressed EEG activities in early preterm infants. Neuropediatrics. 1997a;28(5):272–5.

Hayakawa F, Okumura A, Kato T, Kuno K, Watanabe K. Dysmature EEG pattern in EEGs of preterm infants with cognitive impairment: maturation arrest caused by prolonged mild CNS depression. Brain Dev. 1997b;19(2):122–5.

Kidokoro H, Okumura A, Hayakawa F, Kato T, Maruyama K, Kubota T, Suzuki M, Natsume J, Watanabe K, Kojima S. Chronologic changes in neonatal EEG findings in periventricular leukomalacia. Pediatrics. 2009;124(3):e468–75.

Okumura A, Hayakawa F, Kato T, Kuno K, Watanabe K. Developmental outcome and types of chronic-stage EEG abnormalities in preterm infants. Dev Med Child Neurol. 2002;44(11):729–34.

Watanabe K, Hayakawa F, Okumura A. Neonatal EEG: a powerful tool in the assessment of brain damage in preterm infants. Brain Dev. 1999;21(6):361–72.

Disorganized Pattern

14

Tatsuya Fukasawa, Toru Kato, Fumio Hayakawa, and Hiroyuki Kidokoro

A disorganized pattern is defined as a deformation of physiological EEG components. The main findings are deformed delta waves, abnormal sharp waves, and mechanical (abnormal) brushes. Moreover, abnormal sharp waves can be classified according to their site of appearance as follows.

1. Frontal abnormal sharp waves: Positive sharp waves appearing in the frontal area
2. Positive rolandic sharp waves (PRSs): Positive sharp waves appearing in the central area
3. Occipital abnormal sharp waves: Negative sharp waves appearing in the occipital area

The essence of the disorganized pattern lies in the deformation of EEG components, mainly delta waves, with the deformation primarily resulting from the insertion of abnormal waves. The main types of abnormal waves inserted include abnormal sharp waves, such as PRSs and mechanical brushes (Okumura et al. 1999, 2003; Sofue et al. 2003). These are thought to arise from abnormal propagation in the cerebral projection system, secondary to deep white matter damage (Hayakawa et al. 1997).

Interpretation Point: Disorganized Pattern
(Hiroyuki Kidokoro)
After the clinician has learned the frequency, amplitude, and morphology of age-characteristic delta waves, they should then focus on the waveforms preceding these delta waves. For example, a physiological delta wave that appears in the occipital region often follows a gentle negative (downward) wave. In addition, physiological brushes, typically superimposed on the ascending slope of the delta wave, are often rounded and of low amplitude (Fig. 14.1a). In contrast, the disorganized pattern contains abnormally sharp features, with a sudden negative deflection [sometimes preceded by a small positive (upward) wave] that transitions to a positive delta wave. Moreover, brushes in this pattern are of high amplitude, and spiky in shape (Fig. 14.1b). The clinician is advised to pay close attention to the leading part of the delta wave when they suspect a disorganized pattern.

T. Fukasawa (✉)
Department of Pediatrics, Anjo Kosei Hospital, Anjo, Japan
e-mail: fukasawa@kosei.anjo.aichi.jp

T. Kato · F. Hayakawa
Department of Pediatrics, Okazaki City Hospital, Okazaki, Japan
e-mail: torukato@sun-inet.or.jp

H. Kidokoro
Department of Pediatrics, Nagoya University Graduate School of Medicine, Nagoya, Aichi, Japan

A. Okumura, H. Kidokoro (eds.), *Neonatal EEG: Atlas and Interpretation*,
https://doi.org/10.1007/978-981-96-0726-6_14

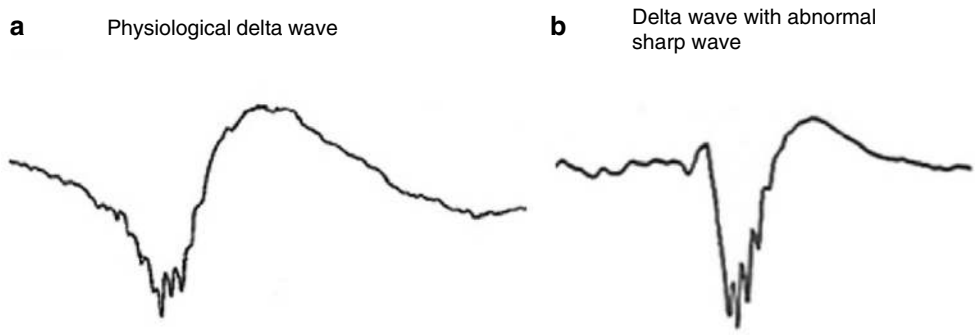

Fig. 14.1 Disorganized pattern. (**a**) Physiological delta wave. (**b**) Delta wave with abnormal sharp wave

1 Abnormal Sharp Wave

The disorganized pattern is defined as a deformation of components such as slow waves. This deformation is thought to be caused by the appearance of abnormal high-amplitude waveforms (mainly sharp waves) that interfere with the slow waves (Fig. 14.2).

2 Positive Rolandic Sharp Wave (1)

Isolated positive sharp waves observed in the central region are known as positive rolandic sharp waves (PRSs, blue arrows). The PRS is a waveform first identified as an abnormality in the EEGs of preterm infants. It is thought to reflect deep white matter lesions, such as periventricular hemorrhagic infarction or periventricular leukomalacia. The PRS exhibits a blunt shape than the sharp waves of epileptiform discharges seen after infancy (Fig. 14.3).

3 Positive Rolandic Sharp Wave (2)

In the montage used in this textbook, phase reversals at the left and right central areas are seen at the first–second and third–fourth channels, respectively. This causes the PRS to appear as if it is protruding outward (blue arrows). Because of its unique morphology, this waveform is easily distinguished from artifacts. The presence of this waveform suggests severe white matter damage, and a thorough evaluation of the central nervous system is advised when it is observed (Fig. 14.4).

4 Mechanical Brush

This figure illustrates both physiological and mechanical (abnormal) brushes. Physiological brushes are characterized by their rhythmic and rounded shape (white arrows). By contrast, the pathological mechanical brushes (blue arrows) seen in the disorganized pattern are spiky and exhibit a steep rise and falls of similar amplitude, with a mechanical appearance reminiscent of cogwheels (Fig. 14.5).

5 Disorganized Pattern Seen in Refiltered EEG

When we first recognized the disorganized pattern, we defined it as a deformation of background activity, such as slow waves; however, the cause of the deformation remained unknown. When we montaged the pattern using a digital EEG and set the time constant to 0.1 s to eliminate slow waves, we clearly recognized that the disorganized pattern contained abnormal sharp waves (positive in the frontal and central regions, negative in the occipital region) (blue arrows). We described these as abnormal sharp waves, and the "deformation" we had observed was the result of their interference with physiological slow waves (Fig. 14.6).

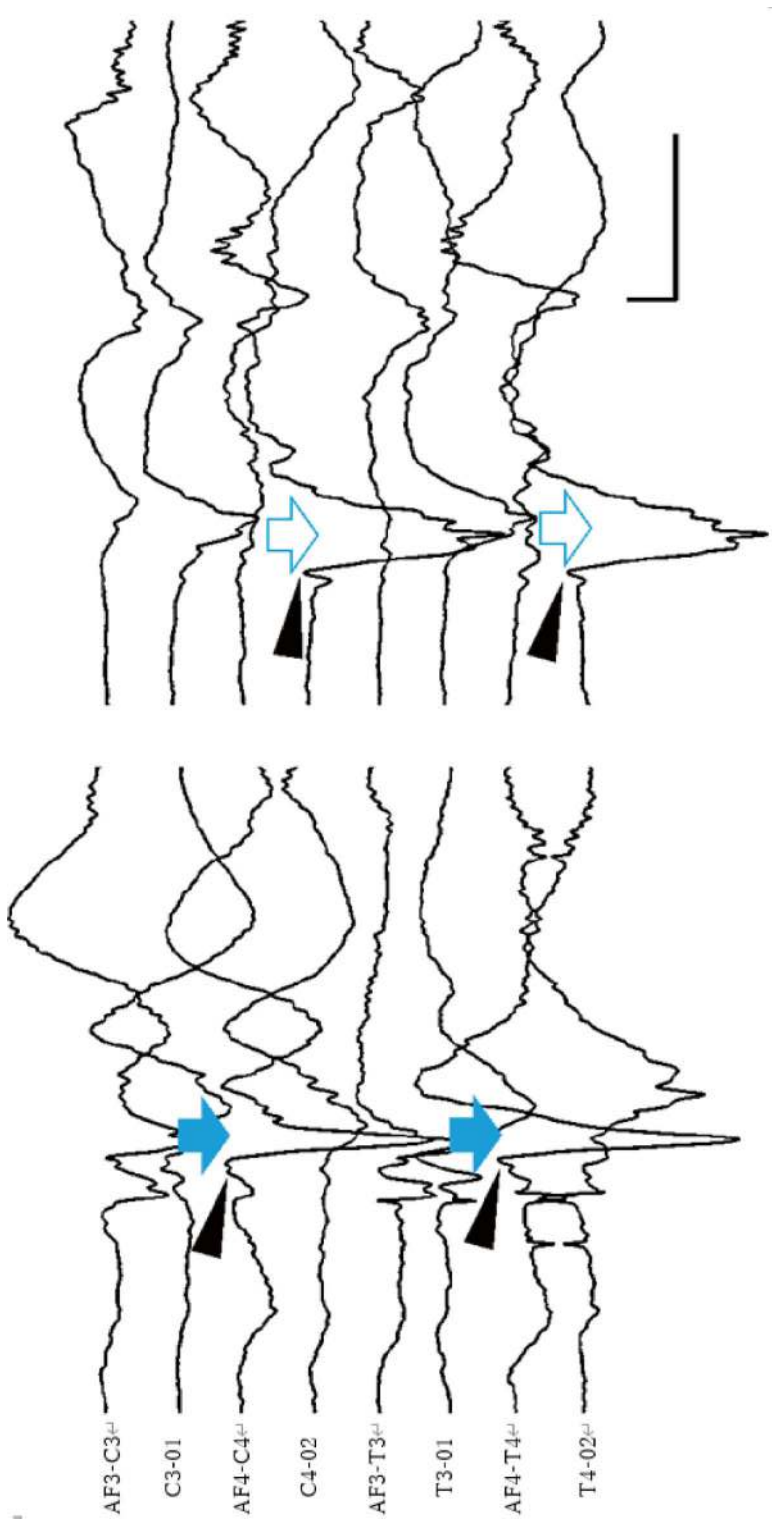

Fig. 14.2 Abnormal sharp wave

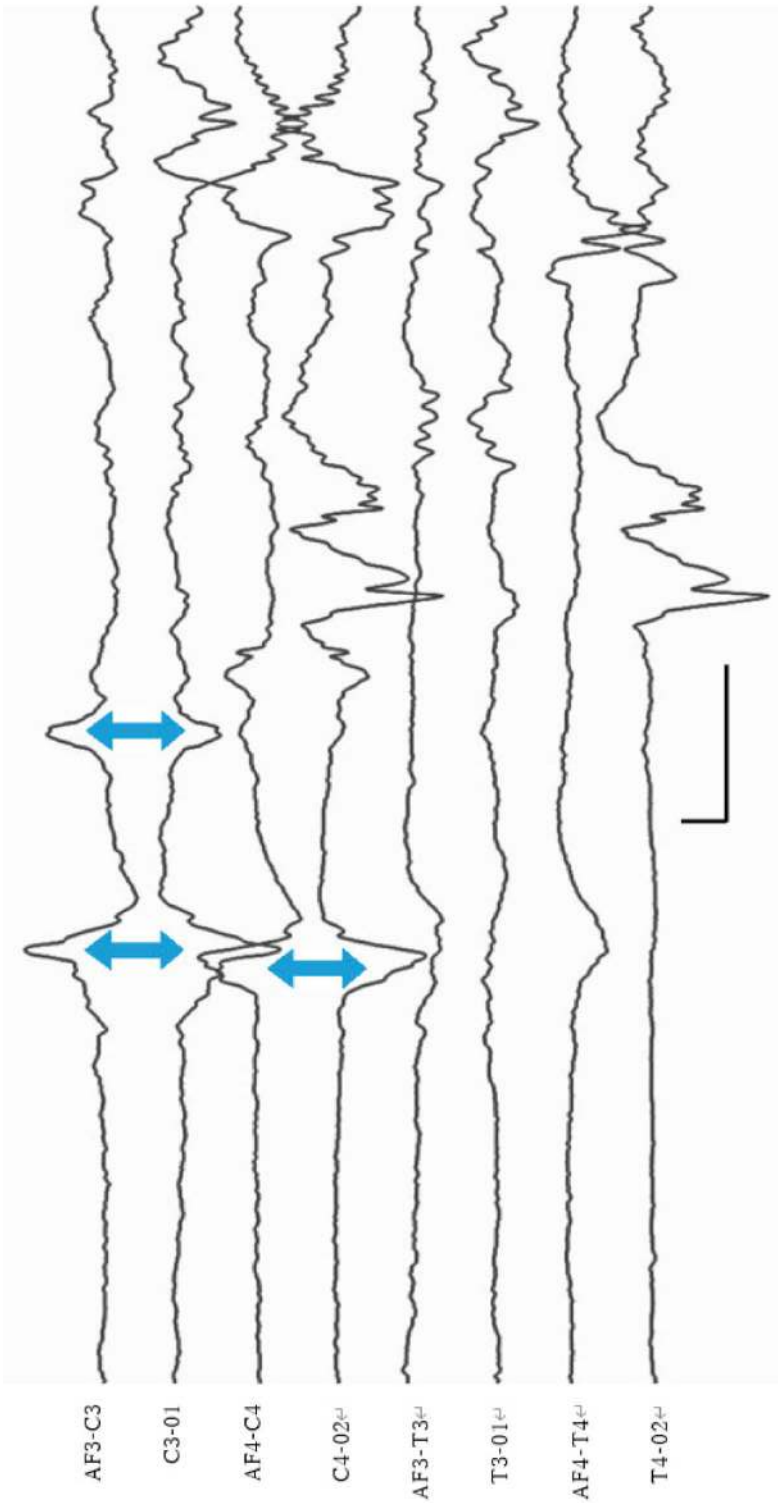

Fig. 14.3 Positive rolandic sharp wave (1)

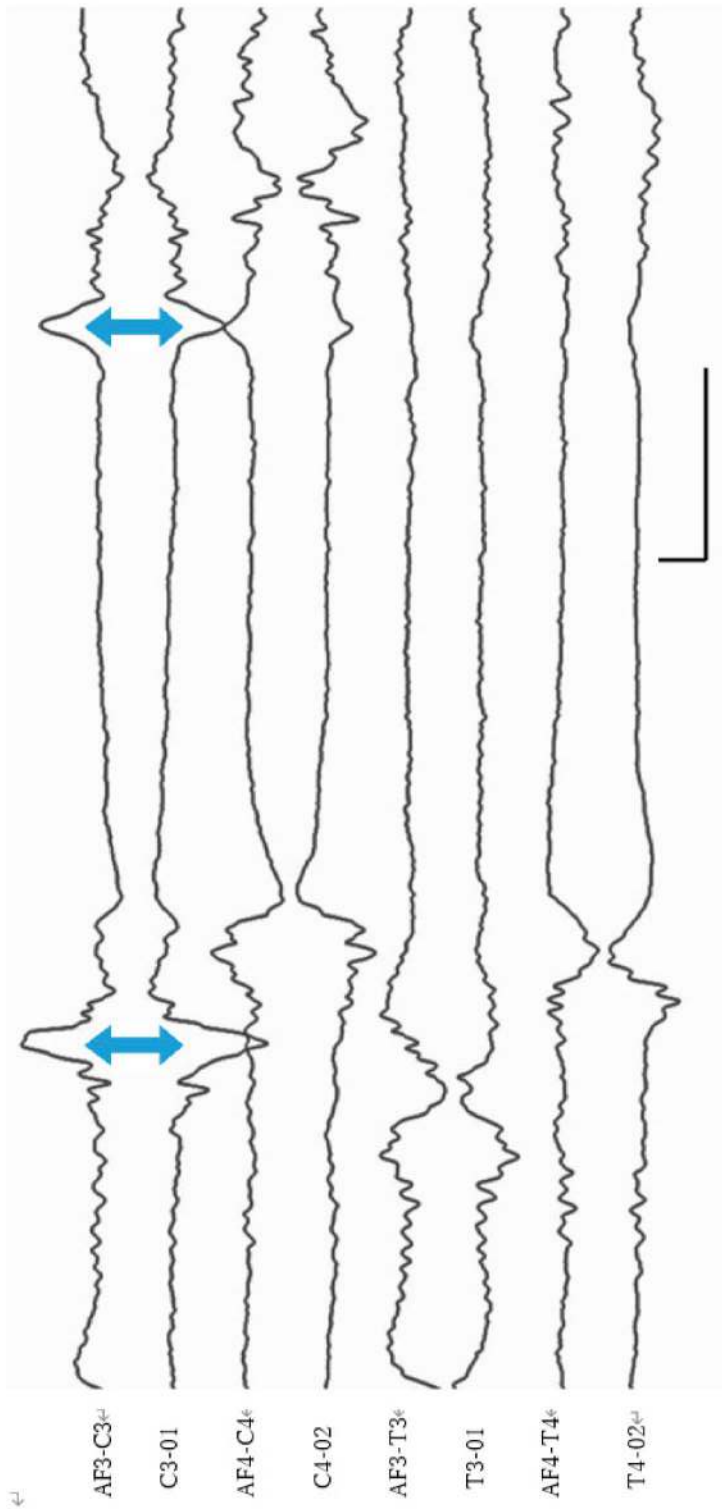

Fig. 14.4 Positive rolandic sharp wave (2)

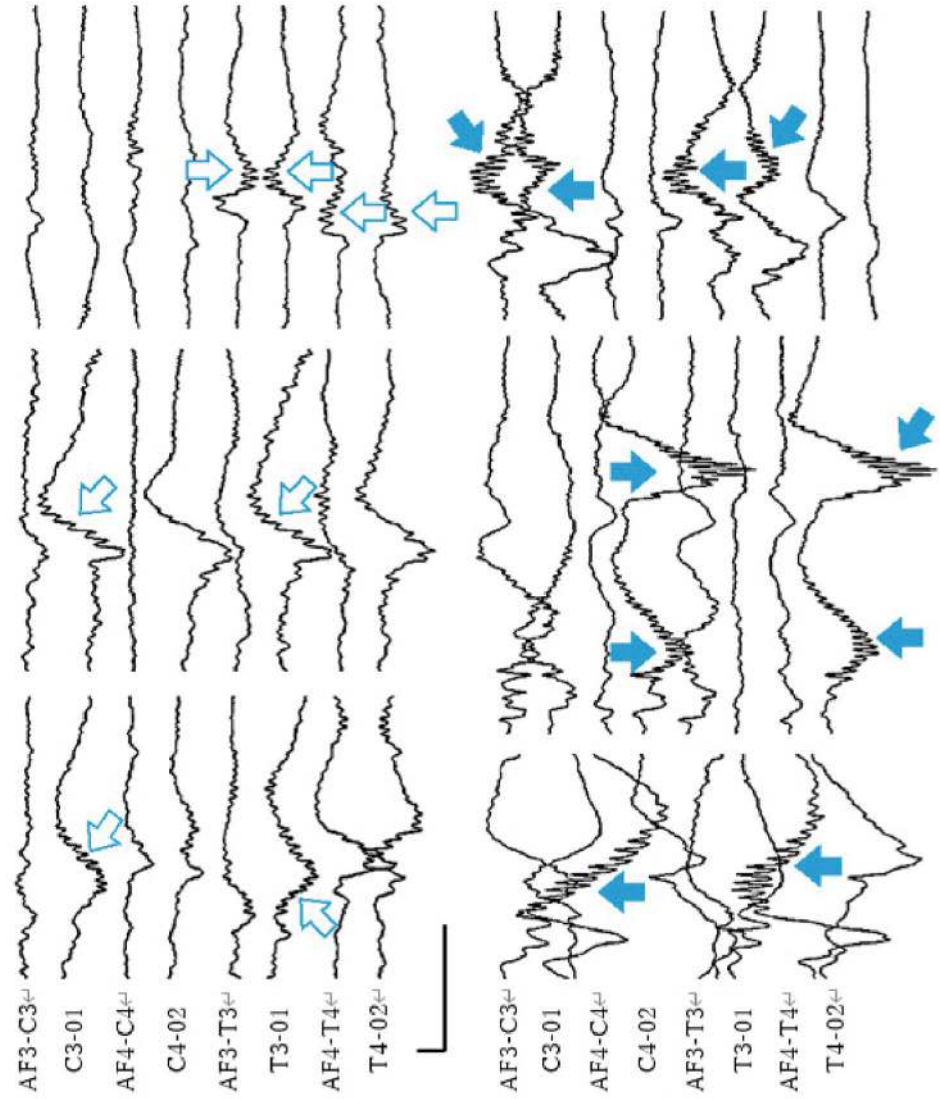

Fig. 14.5 Mechanical brush

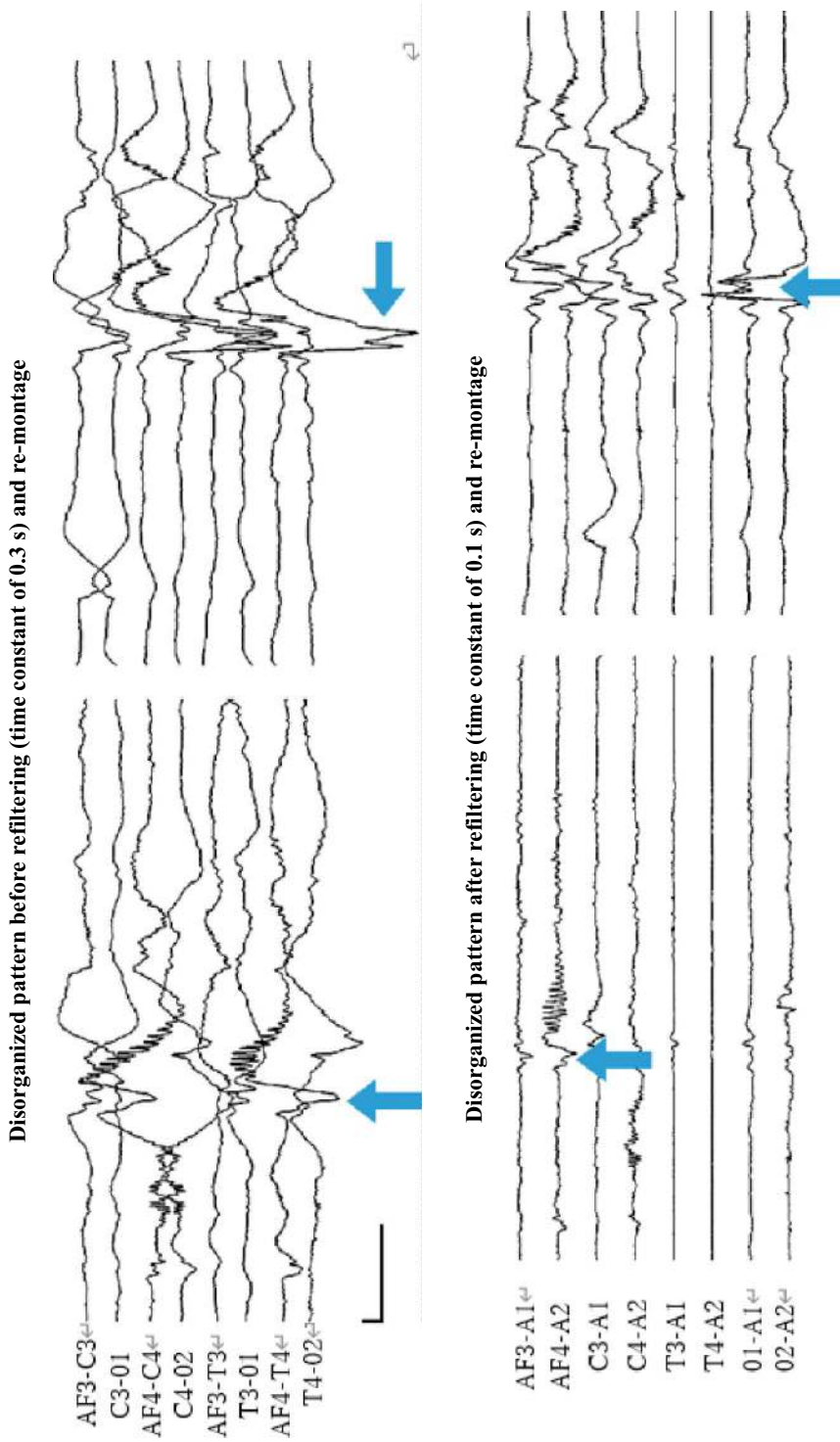

Fig. 14.6 Disorganized pattern seen in refiltered EEG

6 Positive Rolandic Sharp Wave Seen in Refiltered EEG

The positive rolandic sharp wave (PRS) is a waveform that reflects deep white matter damage in preterm infants, and its characteristic morphology makes it relatively easy to recognize. The PRS can be recognized more clearly by re-montaging to the reference derivation method, setting the time constant at 0.1 s, and filtering out slow waves (blue arrows). Because the PRS often appears in depressed EEG activities as acute stage abnormalities, it can be easily identified. However, once the background activity has recovered, the PRS may become obscured and difficult to identify. In such cases, re-montaging and refiltering can be very effective (Fig. 14.7).

7 Disorganized Pattern at 32 Weeks PMA

This figure illustrates a disorganized EEG pattern with a high-amplitude slow wave pattern (323) at 32 weeks PMA. No acute-stage abnormalities are observed; instead, mechanical (abnormal) brushes (white arrows) are present. These brushes are sharp, exhibit well-aligned rise-and-falls and have a form reminiscent of cogwheels. In the occipital region, mechanical brushes are often observed on the ascending slope of a positive slow wave (Fig. 14.8).

8 Disorganized Pattern at 30 Weeks PMA (1)

This high-voltage slow wave pattern (303) shows a disorganized pattern at 30 weeks PMA, a typical finding in preterm infants with periventricular leukomalacia. The blue arrows indicate occipital abnormal sharp waves from the right occipital region. The insertion of these waves leads to a peculiar deformation in the normally bowl-shaped slow waves. The white arrows indicate brushes with sharp tips, which can be considered mechanical brushes. The occipital abnormal sharp waves are often preceded by a small upward spike component (black triangles) immediately before a large downward sharp wave. This is a key insight into interpreting the disorganized pattern (Fig. 14.9).

9 Disorganized Pattern at 30 Weeks PMA (2)

The EEG corresponds to a high-amplitude slow wave pattern (303) at 30 weeks PMA, illustrating a typical disorganized pattern. This includes occipital abnormal sharp waves (blue arrows), frontal abnormal sharp waves (black arrow), and mechanical brushes (white arrow). Occipital abnormal sharp waves are often preceded by a small upward spike component (black triangles) immediately before a large downward sharp wave, which serves as a clue for their assessment. These deformations are thought to be caused by a disruption in the deep white matter (Fig. 14.10).

10 Disorganized Pattern at 28 Weeks PMA (1)

This EEG illustrates a discontinuous pattern at 28 weeks PMA (287), showing a disorganized pattern. Negative occipital abnormal sharp waves (blue arrows) and sharply deformed mechanical brushes (white arrows) are seen in the right occipital region. The black triangles indicate the spike component immediately before the occipital abnormal sharp waves (Fig. 14.11).

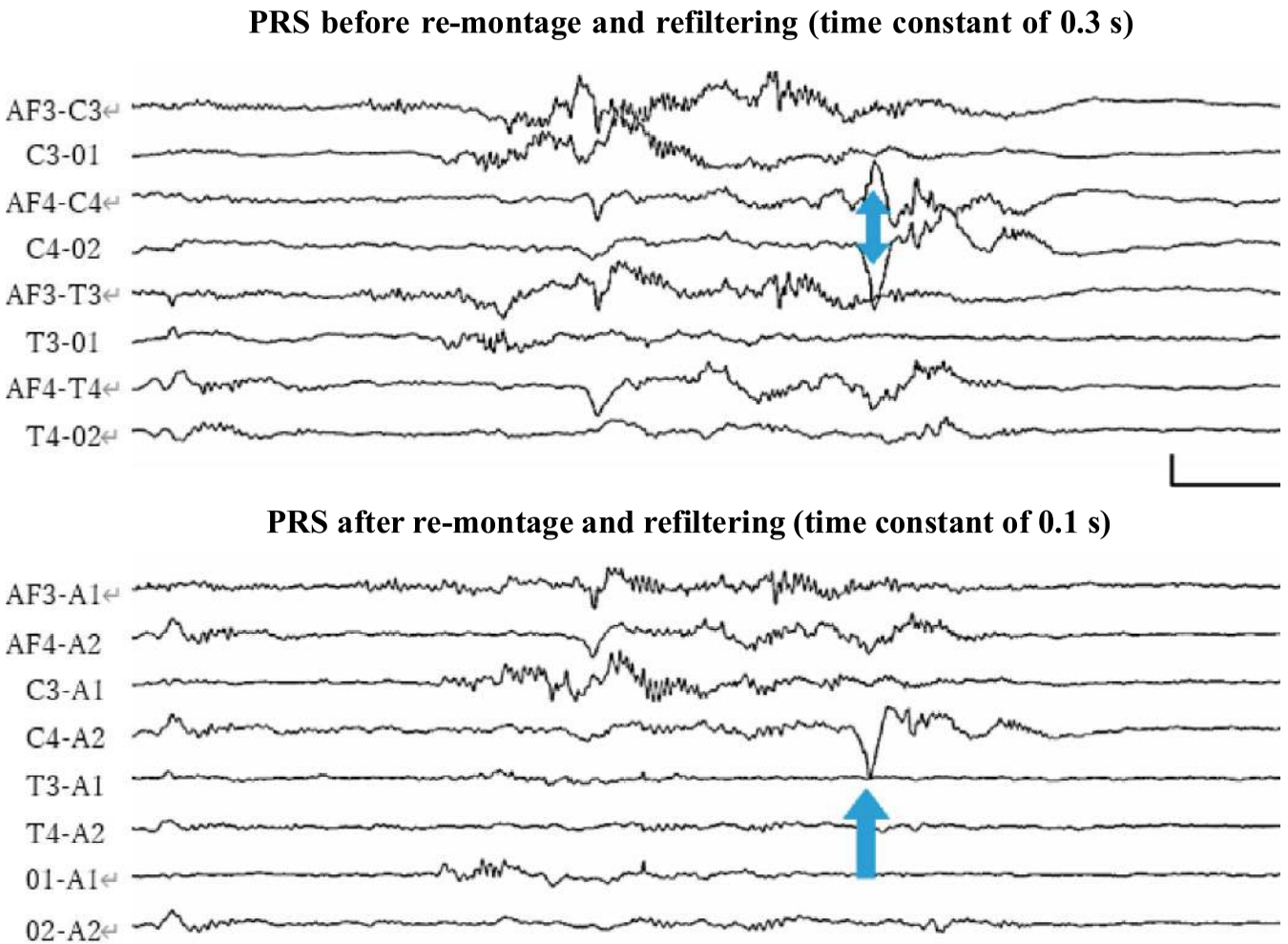

Fig. 14.7 Positive rolandic sharp wave seen in refiltered EEG

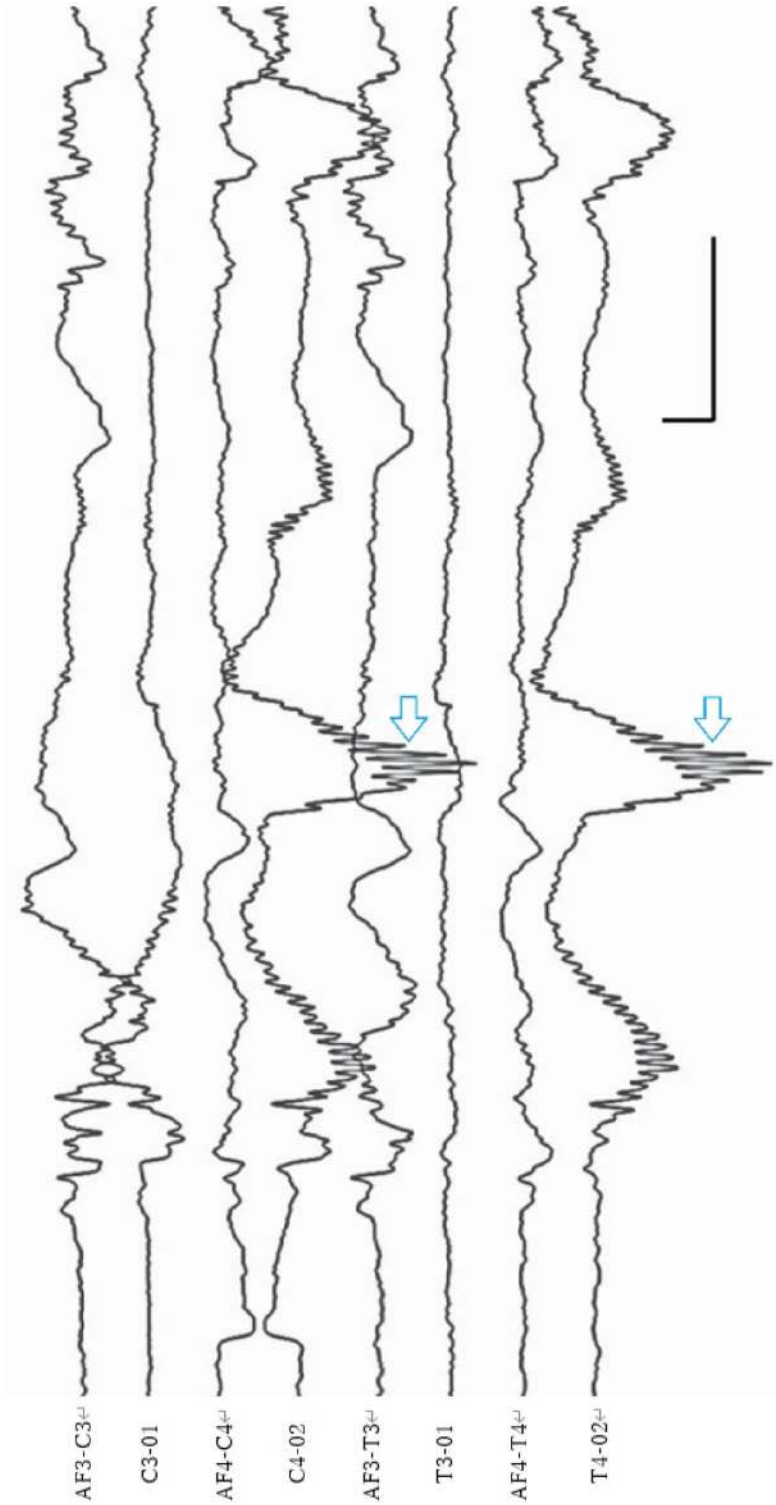

Fig. 14.8 Disorganized pattern at 32 weeks PMA

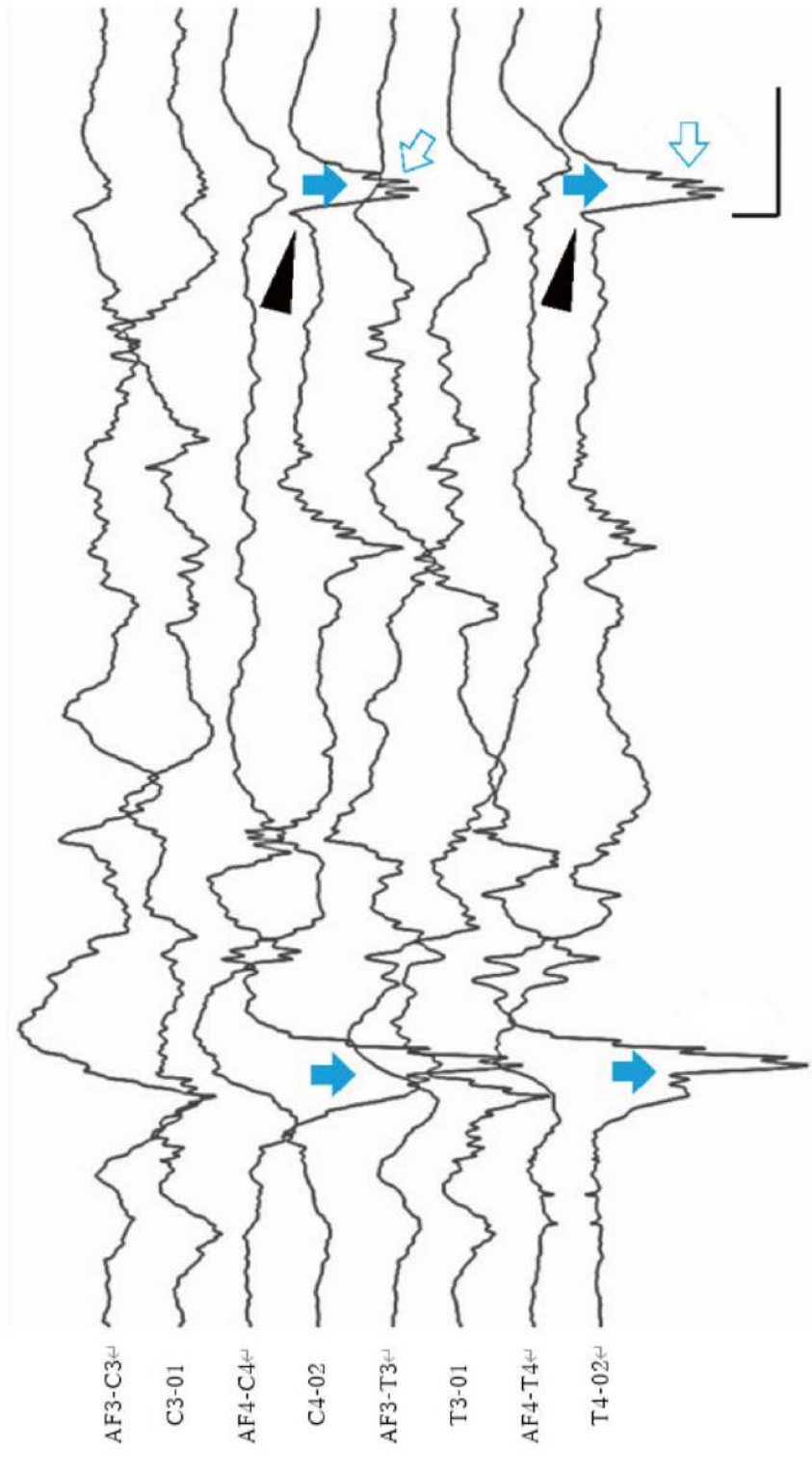

Fig. 14.9 Disorganized pattern at 30 weeks PMA (1)

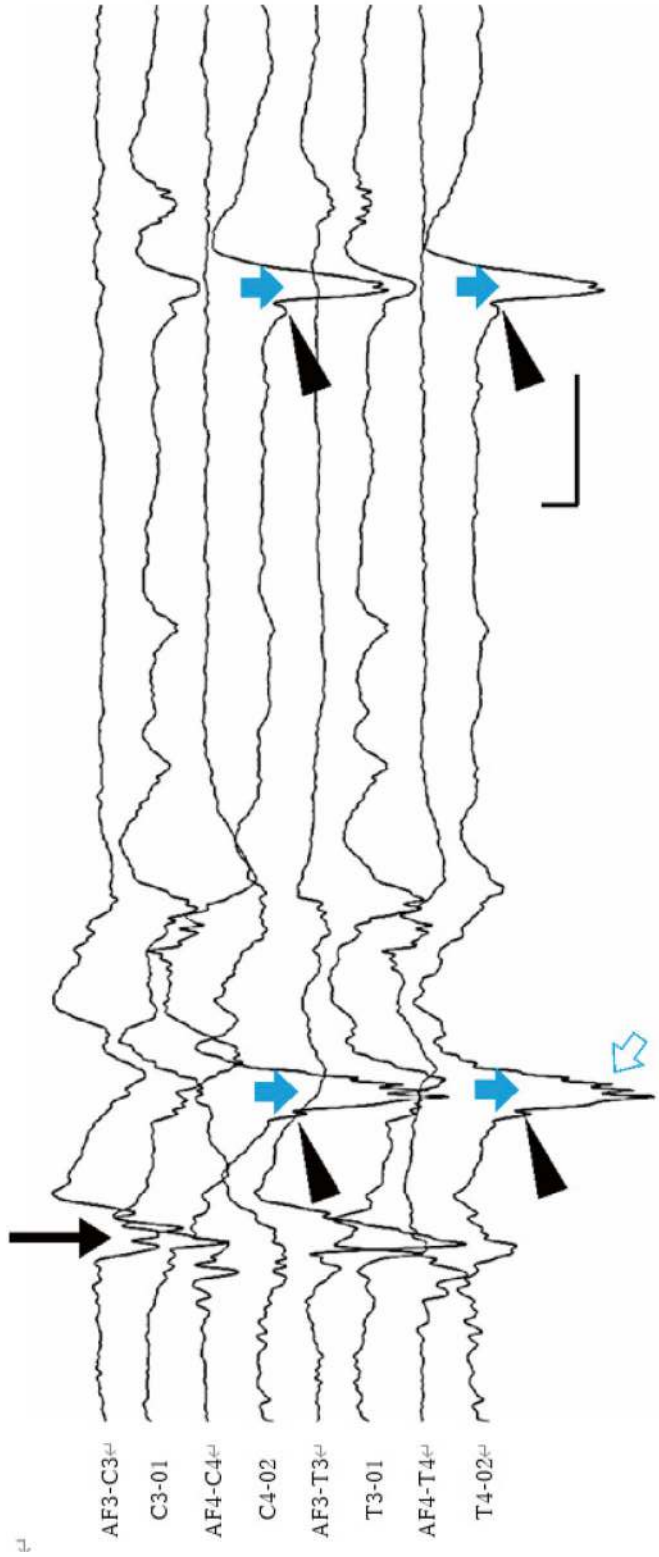

Fig. 14.10 Disorganized pattern at 30 weeks PMA (2)

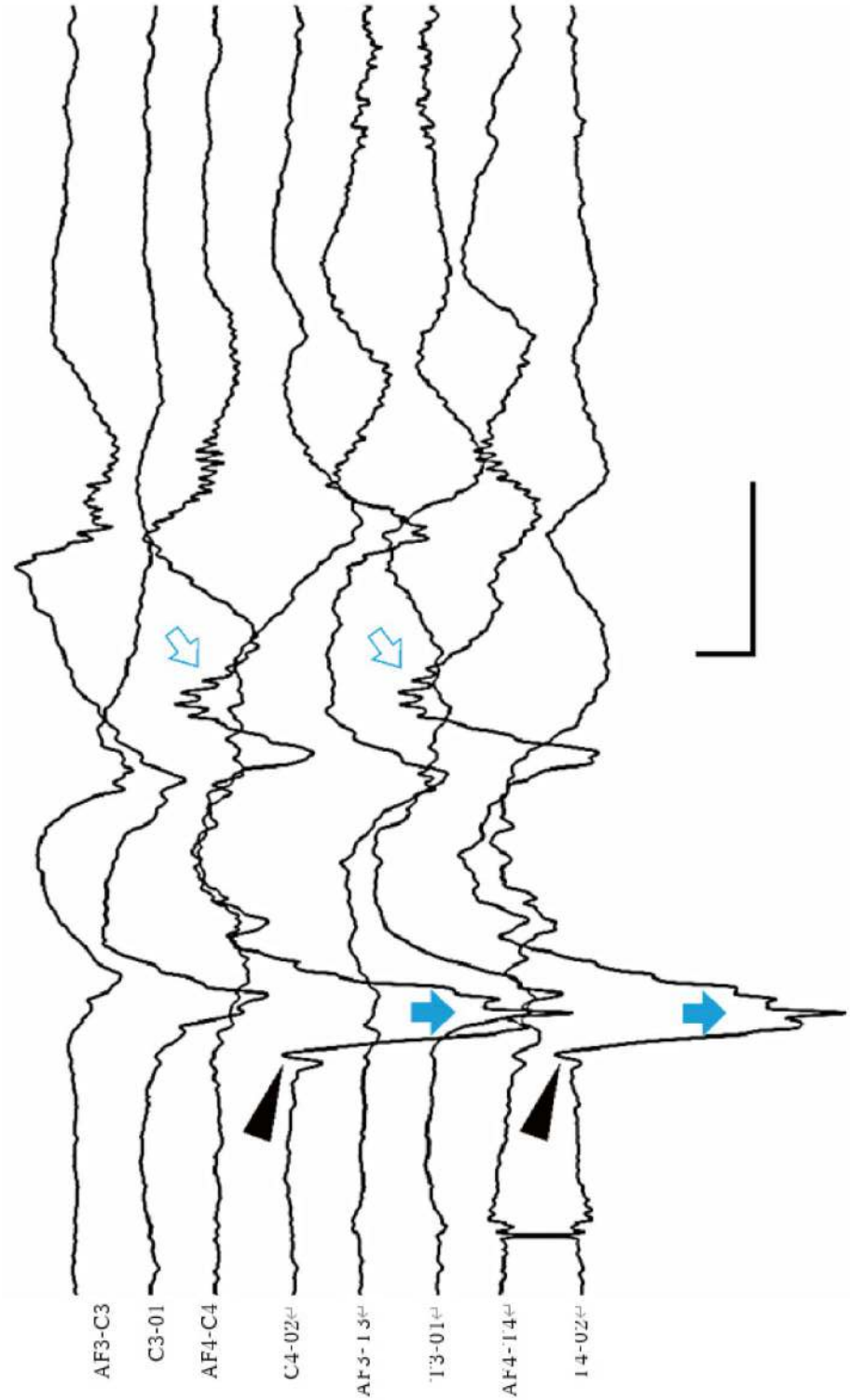

Fig. 14.11 Disorganized pattern at 28 weeks PMA (1)

11 Disorganized Pattern at 28 Weeks PMA (2)

This EEG displays a discontinuous pattern at 28 weeks PMA (287), which is indicative of a disorganized pattern. The right occipital region shows negative occipital abnormal sharp waves (blue arrow) and sharply deformed mechanical brushes (white arrows). Spiky components (black triangles) are visible just prior to these occipital abnormal sharp waves. Additionally, the base of the occipital abnormal sharp waves (blue arrow) in this figure appears deformed, as if it contains upward sharp waves (black arrow). Therefore, these abnormal sharp waves are not always simple sharp waveforms; their morphology is occasionally complicated (Fig. 14.12).

12 Disorganized Pattern at 40 Weeks PMA

This EEG corresponds to the 40-week alternating pattern (407) (Fig. 5.9). The overall impression is that it contains abundant fast-wave activities, which differ from physiological brushes. These fast waves are irregular and include spiky components, making them difficult to classify as physiological waveforms. If the abundance of fast-wave activities were interpreted as dysmaturity, it would contradict the characteristics of a dysmature pattern in which the low-amplitude portion of pattern 407 is neither prolonged nor reduced in amplitude. The slow waves are similar to physiological waves in terms of polymorphism and size, but they are individually deformed. At 40 weeks PMA, it is difficult to distinguish the disorganized pattern from the dysmorphic pattern. Preterm infants who previously showed a more typical disorganized pattern often show this type of pattern at 40 weeks PMA (Fig. 14.13).

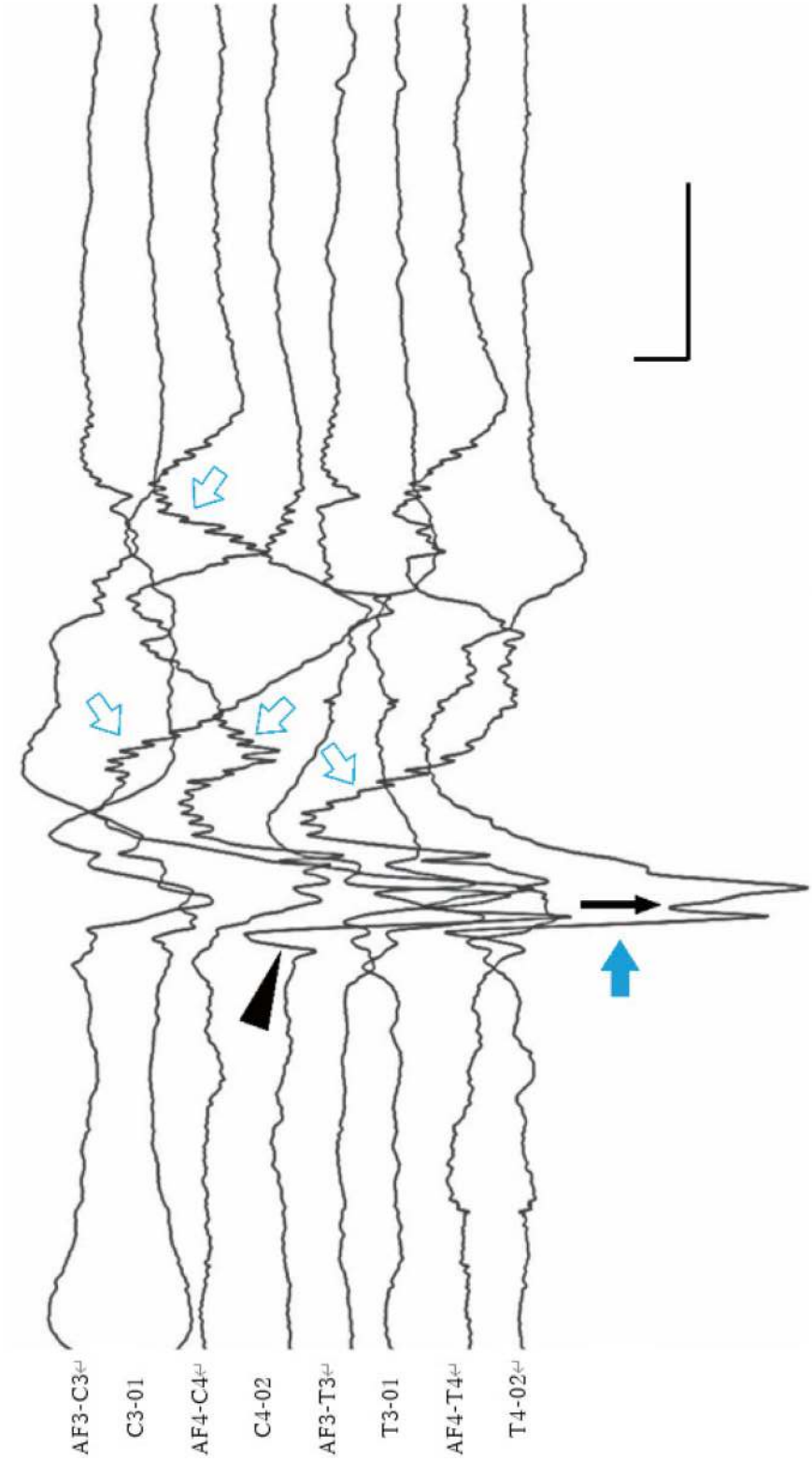

Fig. 14.12 Disorganized pattern at 28 weeks PMA (2)

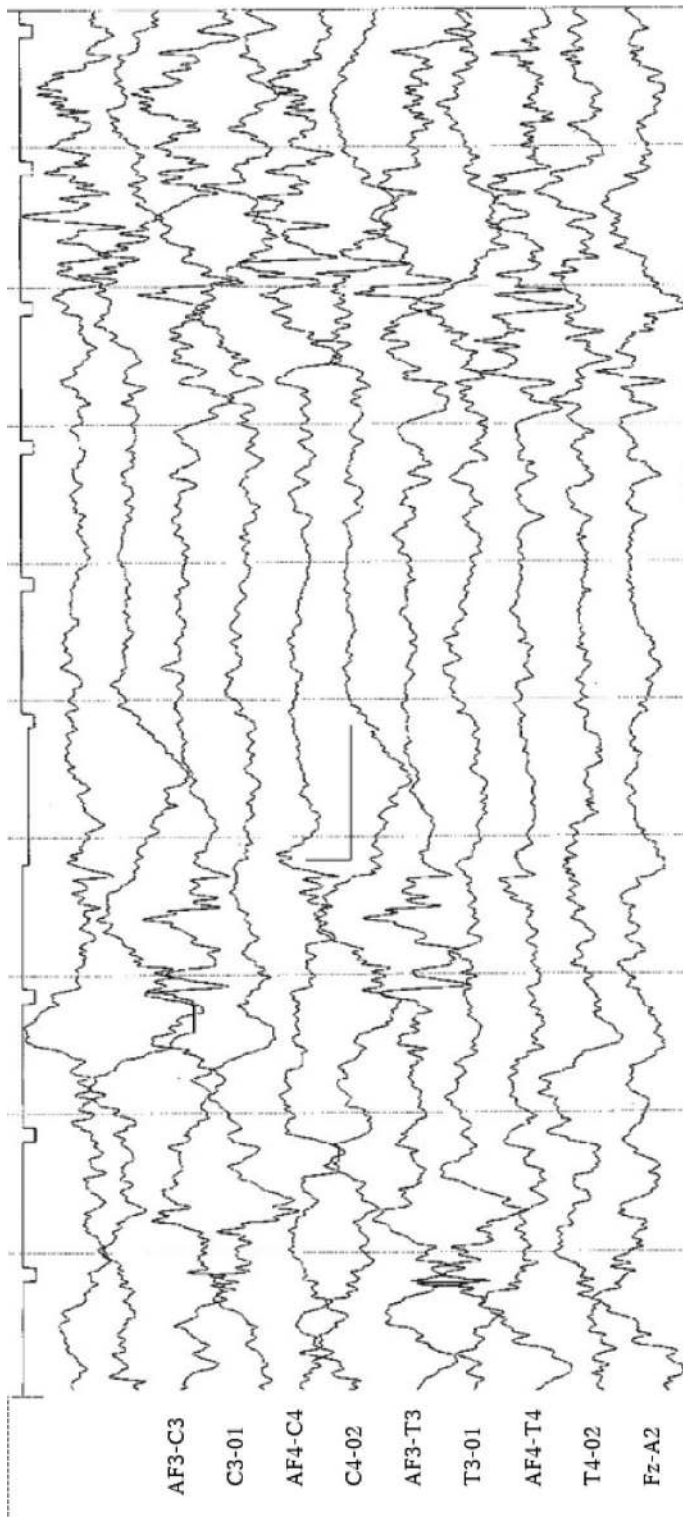

Fig. 14.13 Disorganized pattern at 40 weeks PMA

References

Hayakawa F, Okumura A, Kato T, Kuno K, Watanabe K. Disorganized patterns: chronic-stage EEG abnormality of the late neonatal period following severely depressed EEG activities in early preterm infants. Neuropediatrics. 1997;28(5):272–5.

Okumura A, Hayakawa F, Kato T, Kuno K, Watanabe K. Positive rolandic sharp waves in preterm infants with periventricular leukomalacia: their relation to background electroencephalographic abnormalities. Neuropediatrics. 1999;30(6):278–82.

Okumura A, Hayakawa F, Kato T, Maruyama K, Kubota T, Suzuki M, Kidokoro H, Kuno K, Watanabe K. Abnormal sharp transients on electroencephalograms in preterm infants with periventricular leukomalacia. J Pediatr. 2003;143(1):26–30.

Sofue A, Okumura A, Hayakawa F, Watanabe K. Sharp waves in preterm infants with periventricular leukomalacia. Pediatr Neurol. 2003;29(3):214–7.

Dysmature Pattern

15

Tatsuya Fukasawa, Toru Kato,
and Fumio Hayakawa

A dysmature pattern is defined as the persistence of immature EEG pattern. The waveform itself is physiological or close to it, yet there is an insertion of an immature pattern that is not appropriate for the PMA. In other words, a dysmature pattern is identified when the EEG pattern does not correspond with the PMA of an infant, with a more immature PMA pattern predominating.

The main findings of a dysmature pattern are as follows.

1. Persistence of immature high-voltage slow waves (delta waves)
2. Persistence of immature transients
3. Immature continuity
4. Prolongation of the IBI in the TA pattern
5. Mismatch of maturational parameter between AS and QS

The most important observation is that the physiological EEG maturation, during which slow waves become smaller as the PMA matures, is seen insufficiently, resulting in the persistence of immature delta waves.

A delay of approximately 2 weeks is called a mild dysmature pattern. Such 2-week delays rarely affect clinical outcomes once EEG maturation recovers by 40 weeks PMA. However, a delay of 3 weeks or more raises concerns about future intellectual development (Hayakawa et al. 1997; Okumura et al. 2002). One cause of delay in EEG maturation is undernutrition in extremely premature infants (Hayakawa et al. 2003).

1 Dysmature Pattern at 40 Weeks PMA (1)

This EEG illustrates a mixed pattern at 40 weeks PMA. Bifrontal slow bursts (white arrows), which are transients seen in term infants, are observed. However, immature slow waves of 200–250 μV at 1 Hz (blue arrows) are also present, a characteristic usually observed at 34 weeks PMA. The presence of fundamentally immature activity is characteristic of a dysmature pattern. A dysmature pattern is defined by a discrepancy of 2 or more weeks between the chronological age and the EEG-estimated age (Fig. 15.1).

T. Fukasawa (✉)
Department of Pediatrics, Anjo Kosei Hospital,
Anjo, Japan
e-mail: fukasawa@kosei.anjo.aichi.jp

T. Kato · F. Hayakawa
Department of Pediatrics, Okazaki City Hospital,
Okazaki, Japan
e-mail: torukato@sun-inet.or.jp

A. Okumura, H. Kidokoro (eds.), *Neonatal EEG: Atlas and Interpretation*,
https://doi.org/10.1007/978-981-96-0726-6_15

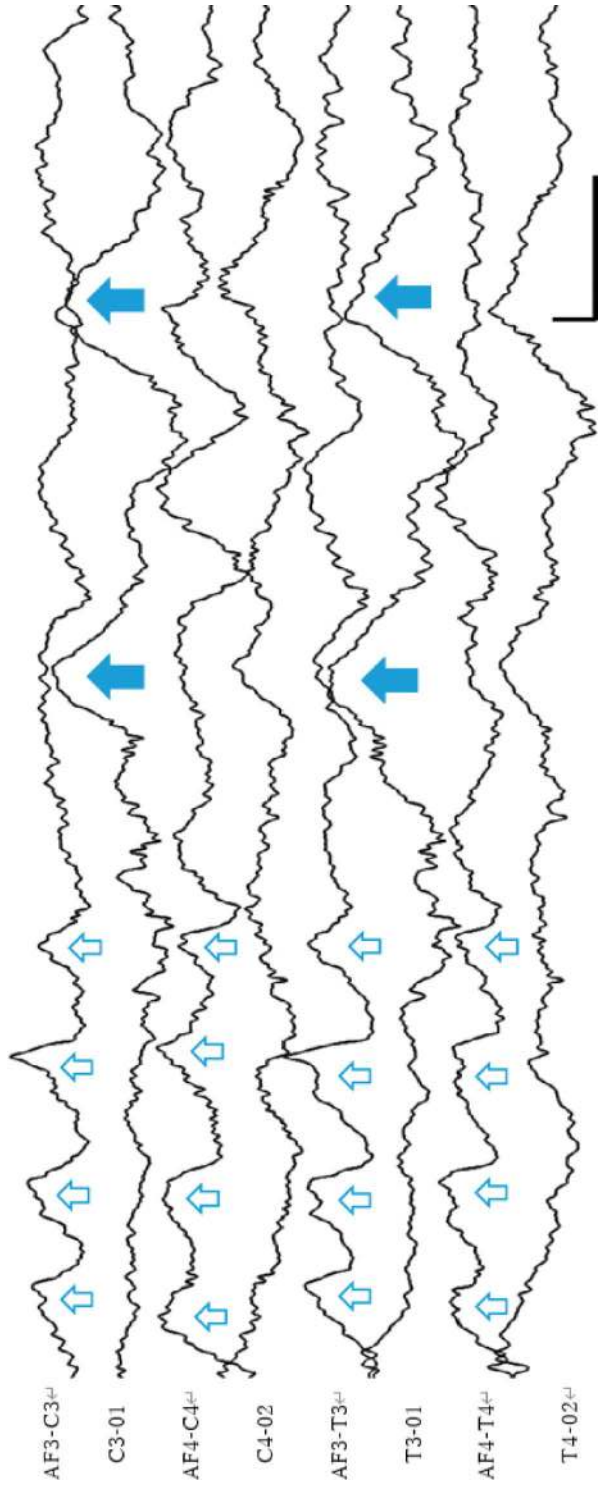

Fig. 15.1 Dysmature pattern at 40 weeks PMA (1)

2 Dysmature Pattern at 40 Weeks PMA (2)

This sample displays an HVS pattern in the same patient at 40 weeks PMA as shown in Fig. 15.1. Brushes are rarely observed, and slow waves of 100 μV at 1.5–2.0 Hz are predominant. However, monotonous slow waves of 200–250 μV at 1 Hz, typically seen at 32–34 weeks PMA (blue arrows), are also present. Therefore, the presence of fundamentally immature activity is characteristic of a dysmature pattern (Fig. 15.2).

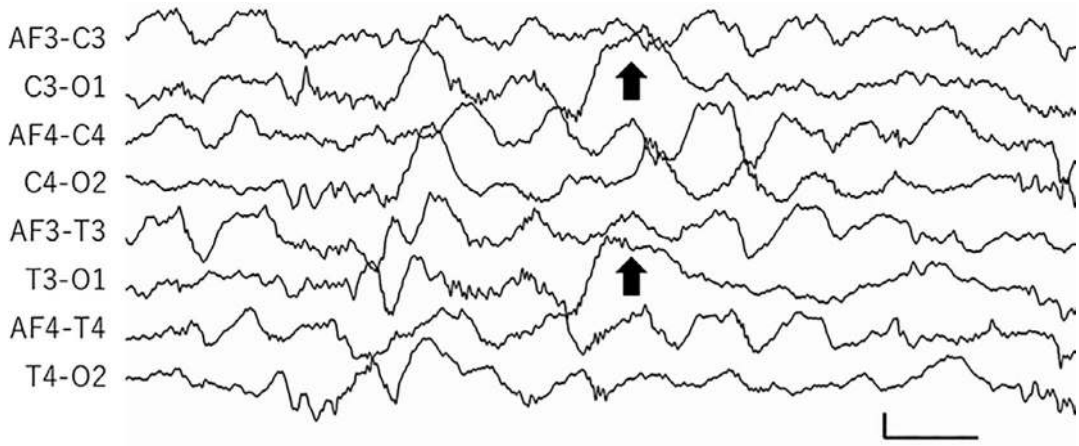

Fig. 15.2 Dysmature pattern at 40 weeks PMA (2)

3 Dysmature Pattern at 40 Weeks PMA (3)

This sample illustrate a TA pattern in the same patient at 40 weeks PMA as shown in Figs. 15.1 and 15.2. The high-amplitude portion is characterized by monotonous slow waves, equivalent to those seen at 32–34 weeks, which would correspond to EEG codes 327 or 347. However, the low-amplitude portion is not flat and exhibits low-amplitude activity, which does not conform to those codes. This elemental delay in maturation is indicative of a typical dysmature pattern (Fig. 15.3).

4 Dysmature Pattern at 34 Weeks PMA

This EEG corresponds to the high voltage slow wave pattern (343) at 34 weeks PMA. The background activity includes brushes that are typical for 34 weeks. However, slow waves of 300–350 μV at 0.5 Hz (blue arrows), which are usually seen at 28 weeks PMA, are also present. The presence of such elementally immature activity is a hallmark of the dysmature pattern (Fig. 15.4).

5 EEG Maturation Delay and Dysmature Pattern

This figure shows the evolution of the temporal EEG findings from a preterm infant who underwent repeated examinations from 28 to 40 weeks PMA.

(a) A record from 28 weeks PMA. The findings are equivalent to those expected for this PMA.

(b) A record from 32 weeks PMA. The high-voltage slow waves were still large, equivalent to what is typically seen at 28 weeks PMA. The patient was unable to receive enteral feeding because of gastrointestinal complication for 4 weeks (28–32 weeks PMA), resulting in significant weight gain failure. This suggests that little brain maturation occurred during this period.

(c) A record from 36 weeks PMA. The slow waves were large (200–250 μV, 1 Hz), and brushes were abundant, equivalent to the patterns observed at 30–32 weeks. These findings are indicative of a severe dysmature pattern.

(d) A record from 40 weeks PMA. Frontal slow bursts are present; however, the slow waves are large, equivalent to those seen at 36 weeks. This is also considered a severe dysmature pattern.

Thus, when EEGs are monitored from the early postnatal period, it is common to observe a pattern where EEG maturation stops at a certain point, resulting in a dysmature pattern persisting into the late neonatal period. Such a dysmature pattern in neonates raises concerns about potential future intellectual disabilities (Fig. 15.5).

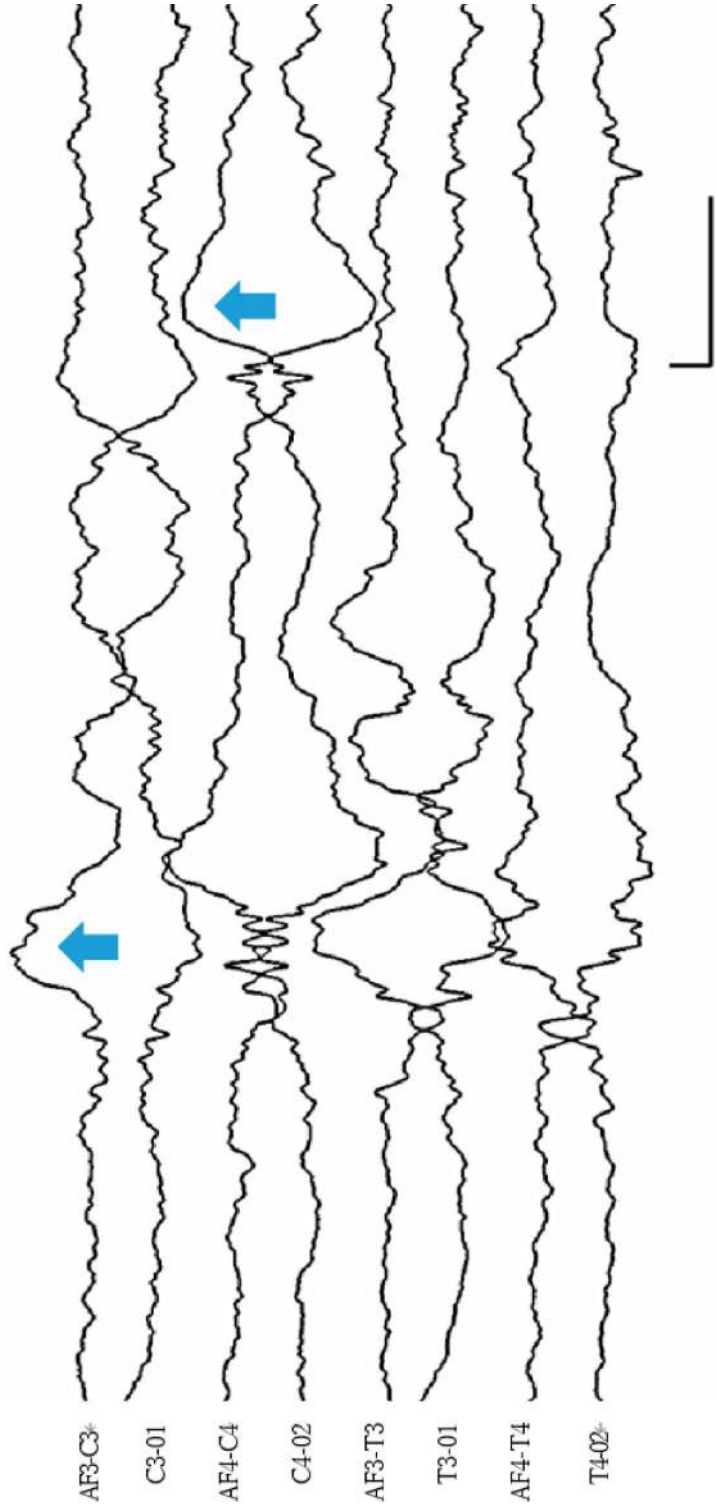

Fig. 15.3 Dysmature pattern at 40 weeks PMA (3)

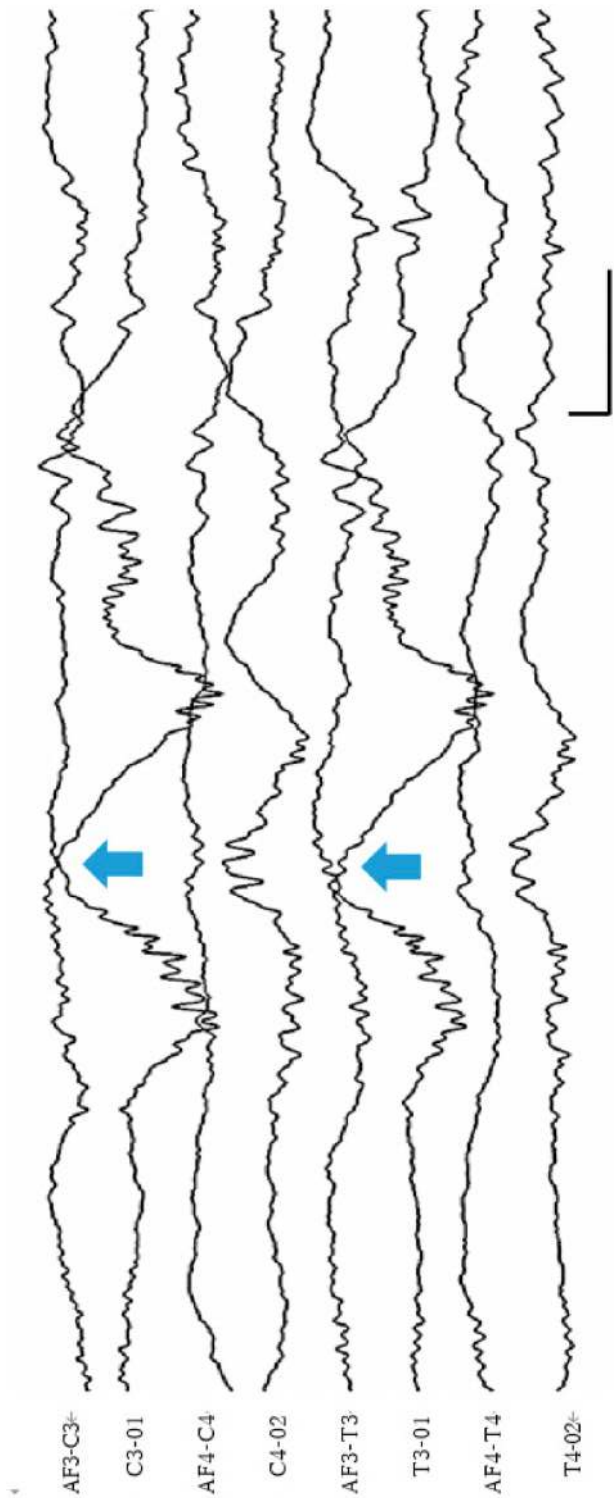

Fig. 15.4. Dysmature pattern at 34 weeks PMA

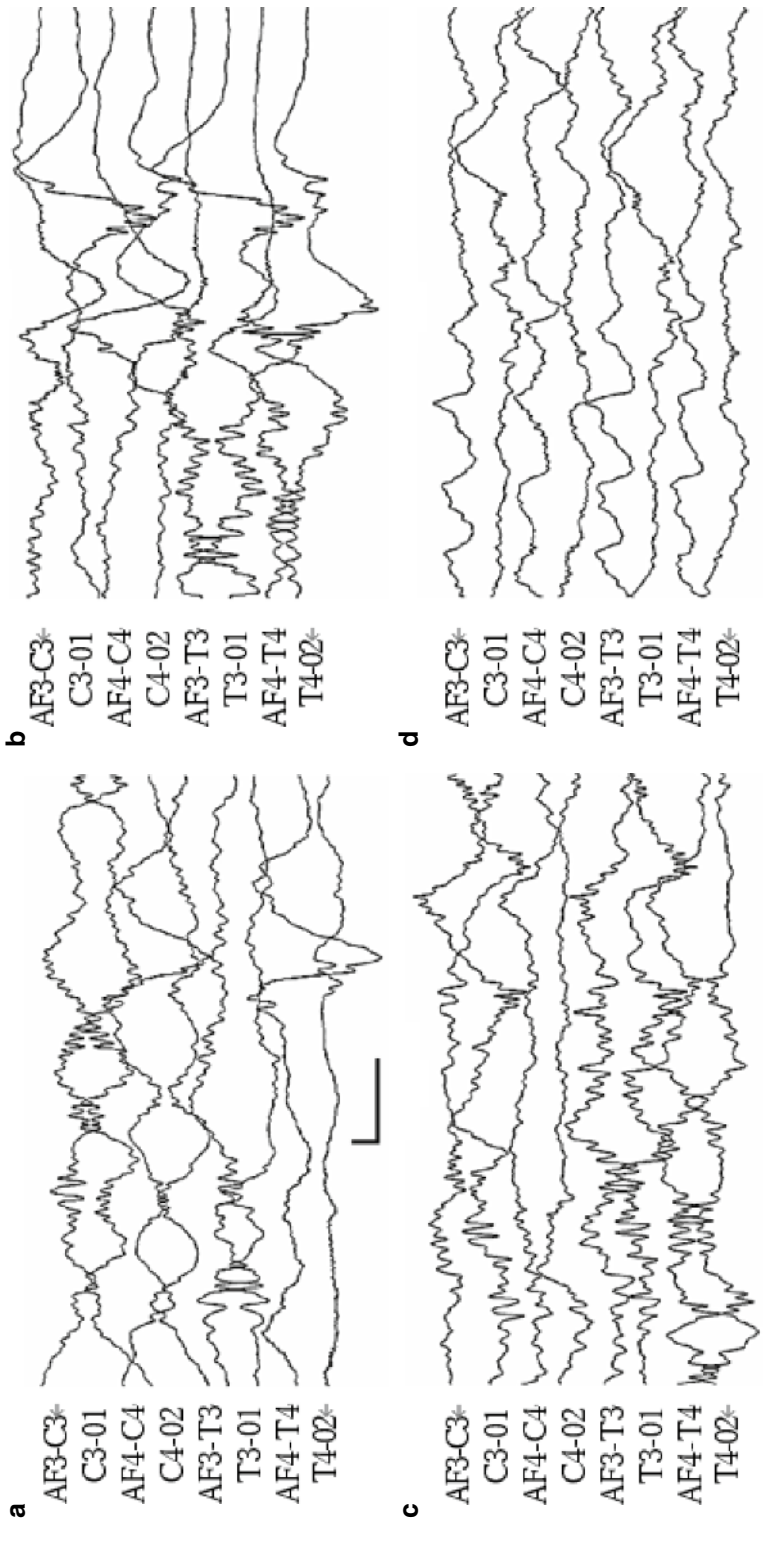

Fig. 15.5 EEG maturation delay and dysmature pattern

6 Dysmature Pattern Illustrated by Compressed EEGs

These compressed EEGs represent a TA pattern at 40 weeks PMA. Compared with the normal pattern at 40 weeks shown in the upper part of the figure, the dysmature pattern in the lower part exhibits an increased interburst interval of 15–20 s, which is disproportional to the actual PMA (Fig. 15.6).

Column: Unexpected EEG Activity in an Infant with Total Asphyxia

(Fumio Hayakawa)

The rapid changes in EEG activity in both normal term infants and preterm infants can be surprising.

We present herein a case of a 38-week-old infant with a birth weight of 3022 g and Apgar scores of 2 at 1 min and 4 at 5 min. The mother reported a loss of fetal movement the day before birth, leading to an emergency cesarean section.

Immediately after birth, the infant exhibited weak body movements in response to resuscitation and then became immobile. Severe acidosis was present at birth but resolved after a single correction with sodium bicarbonate.

An EEG examination conducted on the day of birth revealed a flat EEG, as anticipated. Clinically, the infant appeared to have severe asphyxia, and widespread brain damage with delayed recovery of EEG activity was expected. However, the infant began to actively move his limbs after a few hours, and the EEG normalized the next day. No apparent imaging abnormalities were detected on computed tomography or magnetic resonance imaging, and no abnormal EEG findings were observed thereafter.

The child presented with ocular motor dysfunction, facial paralysis, and hypotonic atypical quadriplegia, leading to a diagnosis of brainstem dysfunction due to total asphyxia. The cerebrum appeared well preserved, with no imaging abnormalities, and the child could communicate with seemingly intact cognitive function.

Total asphyxia is considered to cause selective injury to the brainstem and thalamus secondary to a brief, intense hypoxic-ischemic attack. Immediately after birth in this case, the flat EEG activity reflected an intense insult; however, the depression disappeared the next day, indicating that the insult was of short duration. It is important to record the EEG as early as possible because EEG changes can occur daily. If the first EEG had been recorded the next day after birth, it might have erroneously suggested that no EEG abnormality occurs in total asphyxia. Therefore, close monitoring of EEG activity is essential to avoid overlooking the pathophysiology in such cases.

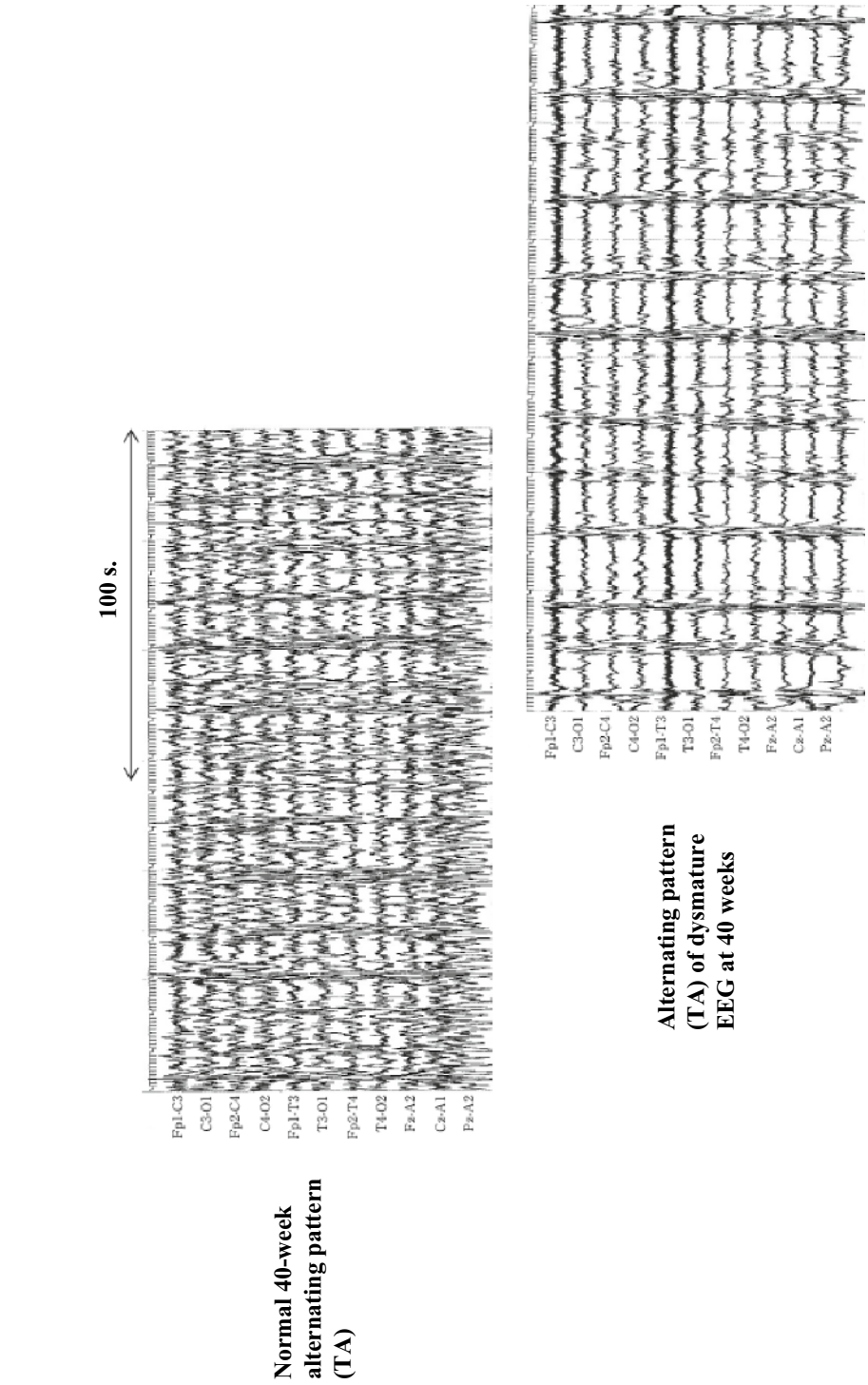

Fig. 15.6 Dysmature pattern illustrated by compressed EEGs

References

Hayakawa F, Okumura A, Kato T, Kuno K, Watanabe K. Dysmature EEG pattern in EEGs of preterm infants with cognitive impairment: maturation arrest caused by prolonged mild CNS depression. Brain Dev. 1997;19(2):122–5.

Hayakawa M, Okumura A, Hayakawa F, Kato Y, Ohshiro M, Tauchi N, Watanabe K. Nutritional state and growth and functional maturation of the brain in extremely low birth weight infants. Pediatrics. 2003;111(5 Pt 1):991–5.

Okumura A, Hayakawa F, Kato T, Kuno K, Watanabe K. Developmental outcome and types of chronic-stage EEG abnormalities in preterm infants. Dev Med Child Neurol. 2002;44(11):729–34.

Dysmorphic Pattern

16

Tatsuya Fukasawa, Toru Kato,
and Fumio Hayakawa

Dysmorphic patterns are defined by the appearance of abnormal patterns that are not seen physiologically. Disorganized patterns are characterized by a deformation of background EEG activity, and dysmature patterns are characterized by delayed maturation of the EEG.

Specifically, a dysmorphic pattern is identified when (1) an abnormal waveform appears, which is not seen physiologically at any postmenstrual age (PMA); (2) determining the PMA becomes difficult because of the lack of physiological waveforms; or (3) there is a decrease in activity without a clinical scenario that typically suppresses EEG activity.

1 Dysmorphic Pattern (1)

This figure illustrates the low-voltage irregular pattern at 40 weeks PMA. The rhythmic theta bursts (under bars) appearing from the left and right occipital regions are transients not observed physiologically at any PMA. When such nonphysiological abnormal activities are detected, it is necessary to confirm the presence of a sleep cycle (whether AS and QS appear alternately), determine the postmenstrual weeks by physiological waveforms, and perform a detailed examination for the presence of other nonphysiological waveforms. If there is a problem in brain formation, the appearance of abnormal waveforms (reflecting functional and/or structural abnormalities) would not be surprising and are interpreted as a dysmorphic pattern (Fig. 16.1).

T. Fukasawa (✉)
Department of Pediatrics, Anjo Kosei Hospital,
Anjo, Japan
e-mail: fukasawa@kosei.anjo.aichi.jp

T. Kato · F. Hayakawa
Department of Pediatrics, Okazaki City Hospital,
Okazaki, Japan
e-mail: torukato@sun-inet.or.jp

A. Okumura, H. Kidokoro (eds.), *Neonatal EEG: Atlas and Interpretation*,
https://doi.org/10.1007/978-981-96-0726-6_16

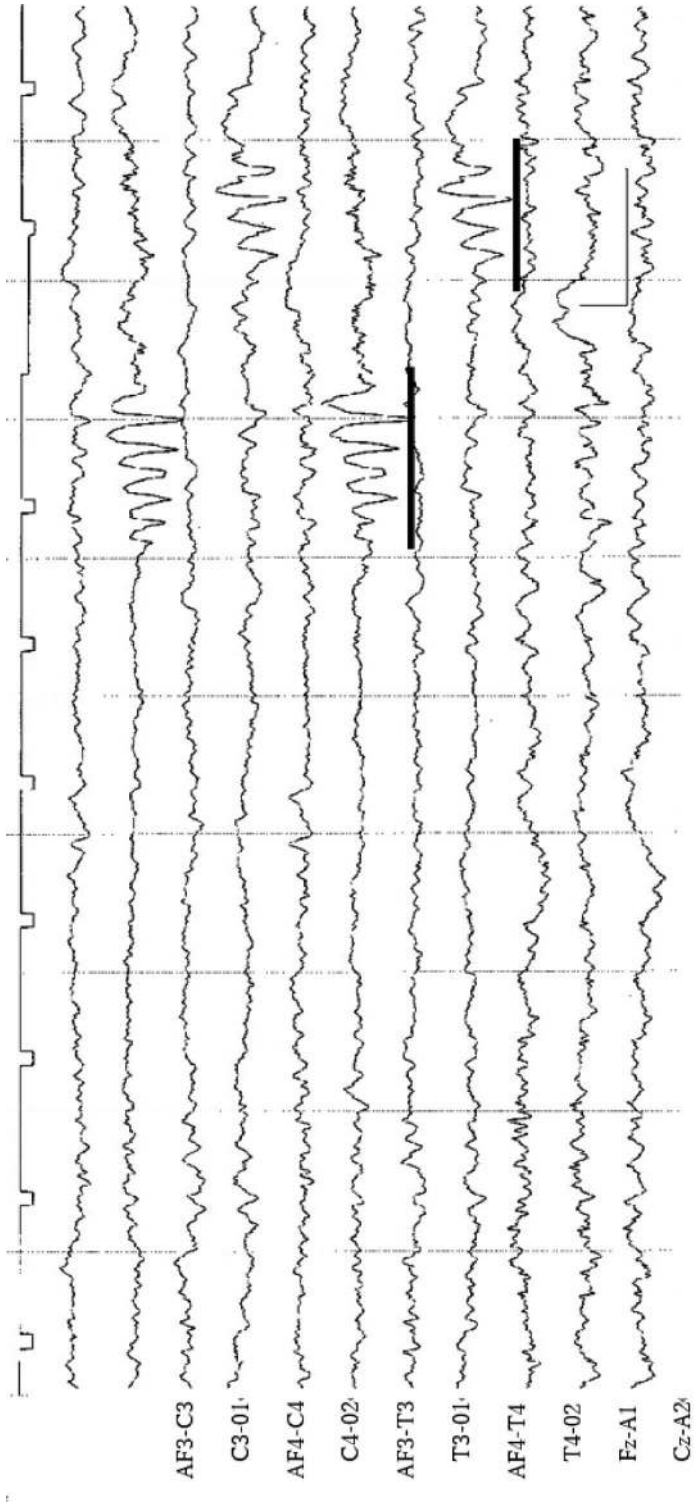

Fig. 16.1 Dysmorphic pattern (1)

2 Dysmorphic Pattern (2)

The EEG activity exhibits neither a low-voltage irregular pattern nor a high-voltage slow wave pattern but, rather, persistent activity of intermediate amplitude. The most notable activities are the fast wave bursts in the left occipital region (white arrow) and right occipital region (blue arrow). These bursts are irregular and lack the rhythm typical of brushes; they can best be described as a "superimposition of abnormal fast wave components." Based on these observations, a dysmorphic pattern is diagnosed because of the lack of physiological EEG activity and the presence of nonphysiological waveforms (Fig. 16.2).

3 Dysmorphic Pattern (3)

This EEG is from an infant with trisomy 13. The only notable activity is indicated by the blue arrow, set against a background of low amplitude and poor activity. At first glance, the activity appears to be a single sharp wave with a brush; however, both the sharp wave and the brush differ from physiological patterns. This indicates a dysmorphic pattern in addition to a high degree of EEG suppression. Unfortunately, it is impossible to determine from the EEG pattern alone whether the reduced EEG activity is due to brain dysfunction caused by a congenital disorder or an acute abnormality secondary to an insult such as asphyxia. The only way to determine this is by assessing the infant's general condition. In addition, because scalp edema may cause a low-amplitude EEG, it is necessary to check the scalp condition (Fig. 16.3).

4 Dysmorphic Pattern (4)

This EEG sample is from a 40-week-old infant. An abundance of irregular sharp, slow, and fast waves is observed, but these waveforms are not compatible with any specific PMA. Interhemispheric asynchrony is prominent. These observations indicate a dysmorphic pattern (Fig. 16.4).

5 Dysmorphic Pattern (5)

An abundance of irregular fast and slow waves that are not compatible to any specific PMA is observed. These findings indicate a dysmorphic pattern (Fig. 16.5).

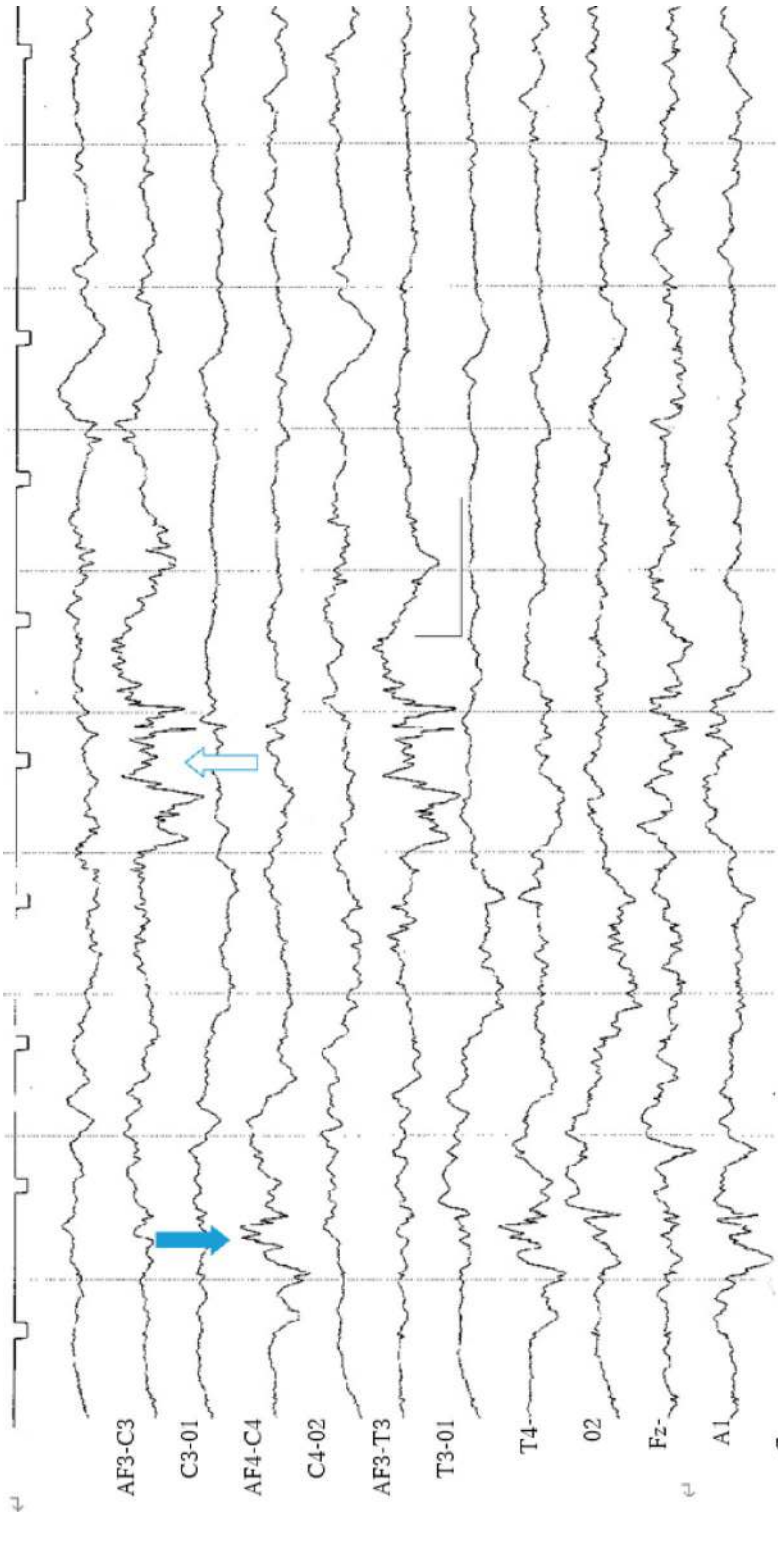

Fig. 16.2 Dysmorphic pattern (2)

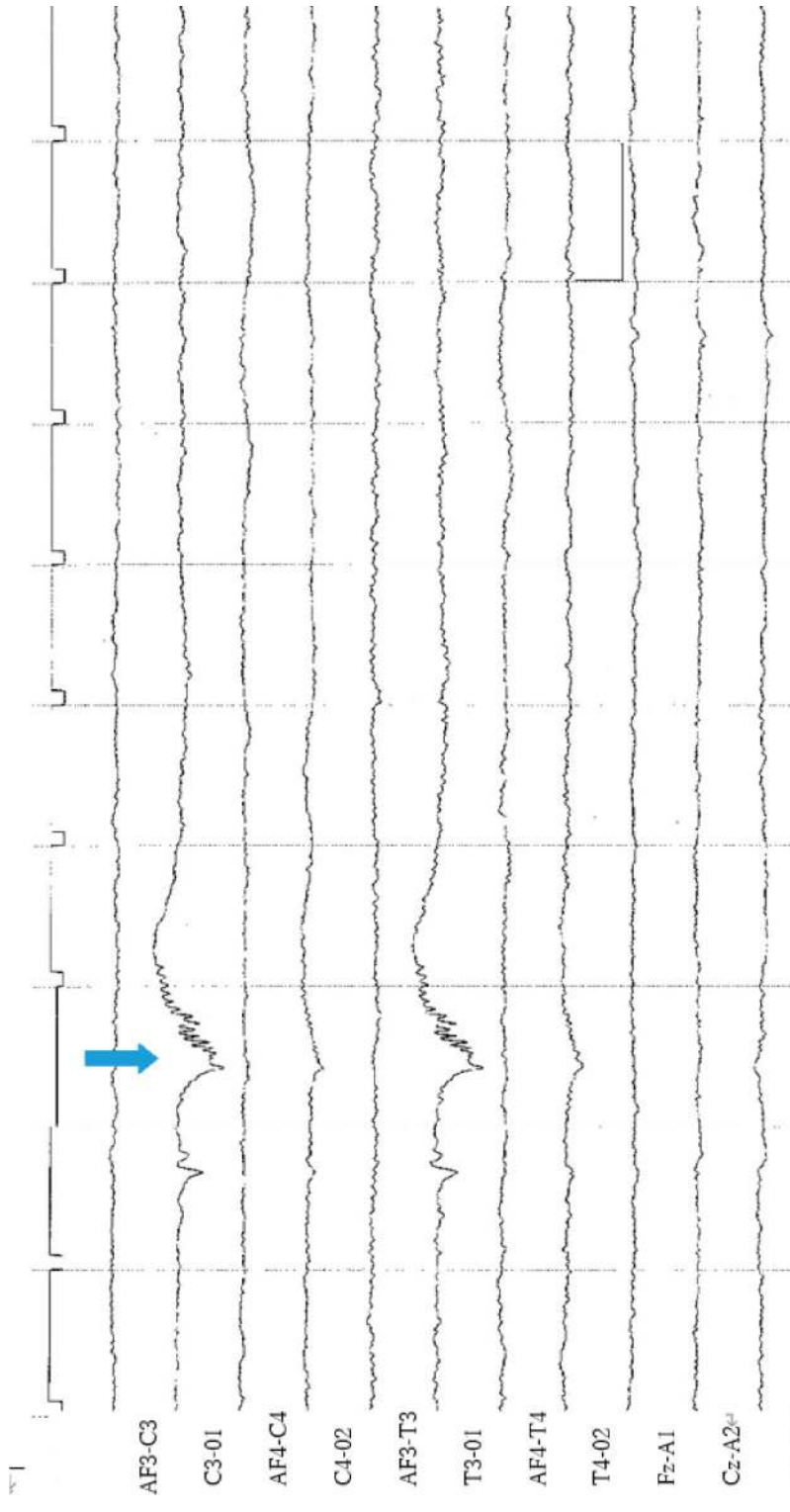

Fig. 16.3 Dysmorphic pattern (3)

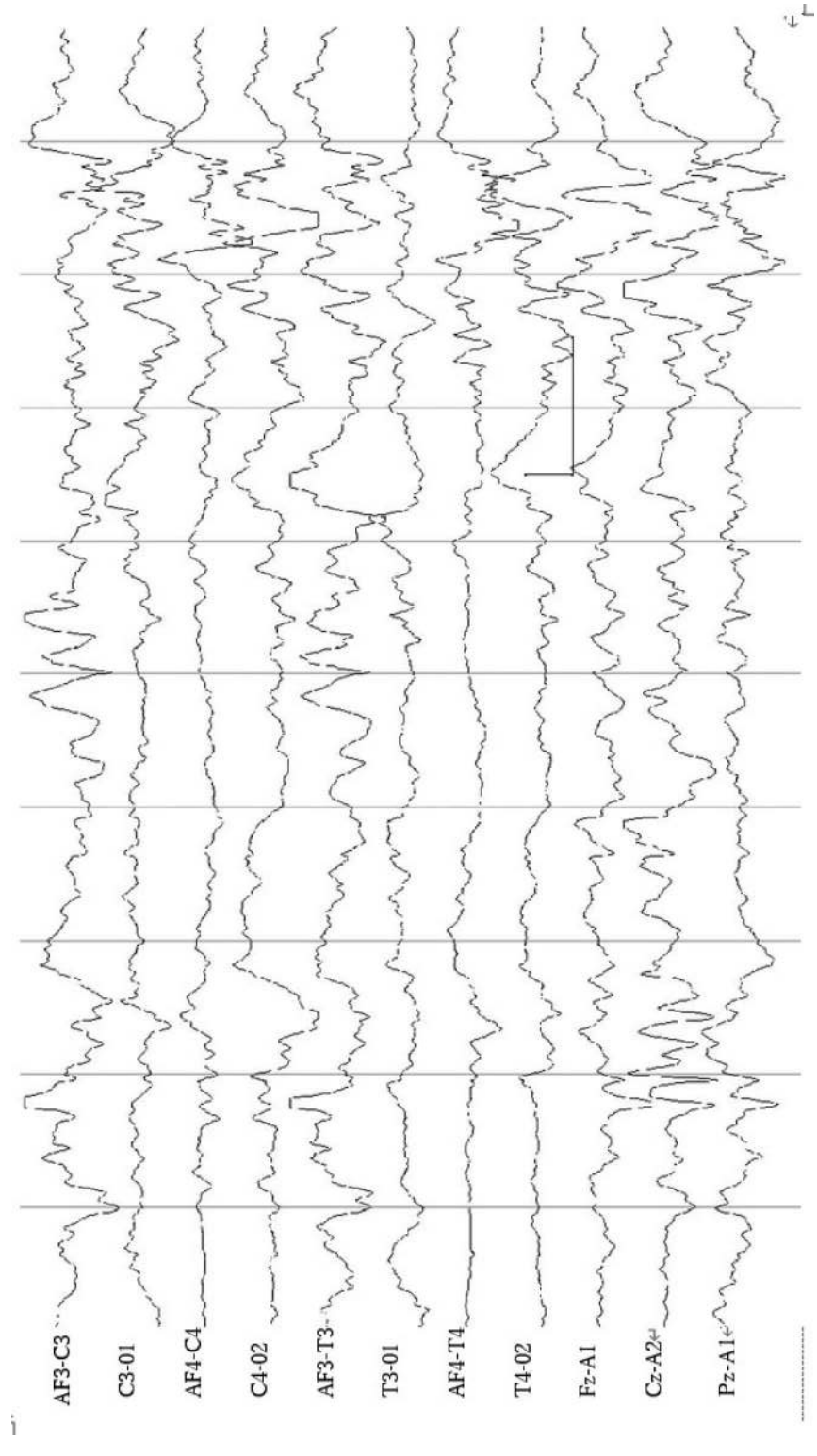

Fig. 16.4 Dysmorphic pattern (4)

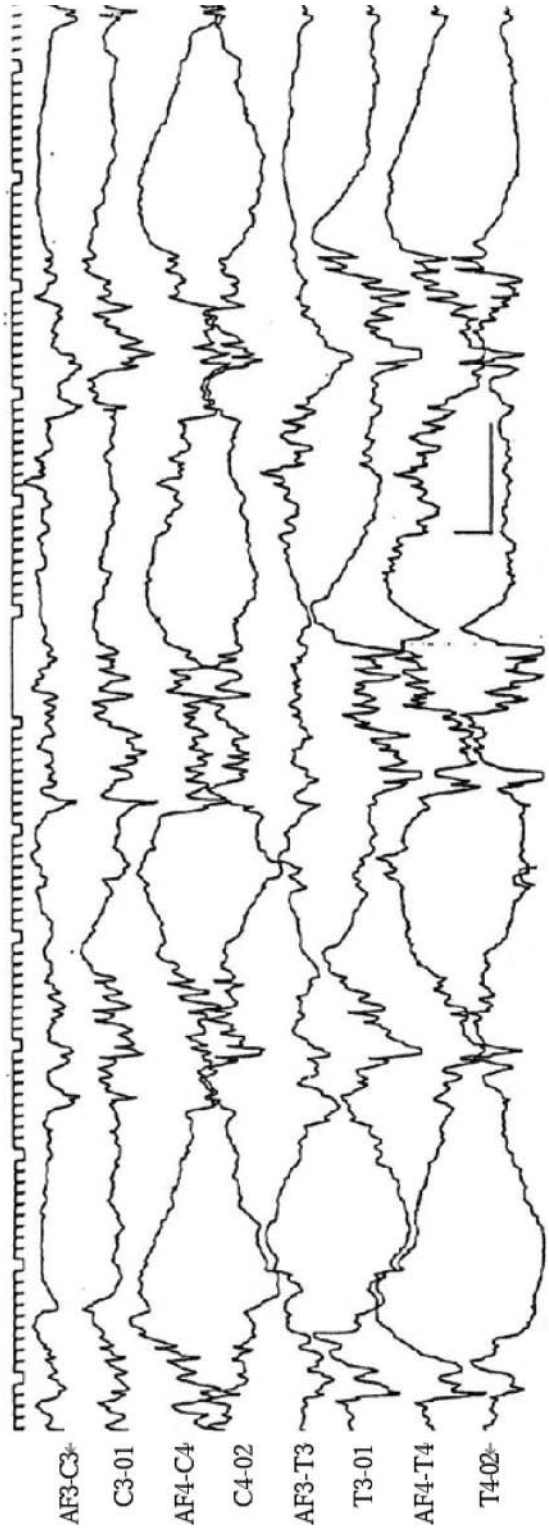

Fig. 16.5 Dysmorphic pattern (5)

Part IV

EEG in Neonatal Seizures

Neonatal Seizures

17

Akihisa Okumura, Koichi Maruyama,
Hiroyuki Yamamoto, and Fumio Hayakawa

1 Introduction

Neonatal seizures are important indications of CNS involvement in the newborn. Therefore, appropriate diagnosis and treatment are crucial. As outlined below, EEG plays a decisive role in diagnosing neonatal seizures and determining the efficacy of treatment. In infants with neonatal seizures, ictal EEGs are important. As therapeutic hypothermia becomes more widely adopted, the importance of EEG monitoring in neonates has become increasingly recognized. Ictal EEG is now commonly performed, and its interpretation requires a knowledge set that differs from that needed for interictal EEG evaluation.

A. Okumura
Department of Pediatrics, Aichi Medical University, Nagakute, Aichi, Japan
e-mail: okumura.akihisa.479@mail.aichi-med-u.ac.jp

K. Maruyama
Department of Pediatric Neurology, Aichi Developmental Disability Center Central Hospital, Kasugai, Japan

H. Yamamoto
Department of Pediatrics, Nagoya University Graduate School of Medicine, Nagoya, Japan

F. Hayakawa
Department of Pediatrics, Okazaki City Hospital, Okazaki, Japan

2 Specificity of Neonatal Seizures

The principal feature of neonatal seizures is electroclinical dissociation, i.e., a discrepancy between the clinical manifestations and the ictal EEG findings (Weiner et al. 1991). Traditionally, diagnosis of neonatal seizures has been based on clinical observations. However, several studies have demonstrated that clinical observations alone exhibit clear limitations when used to diagnose neonatal seizures. Subclinical seizures, which lack apparent clinical symptoms but nonetheless exhibit ictal EEG changes, are frequent in neonates. One report investigated the capacity of NICU staff to recognize seizures diagnosed via ictal EEG (Murray et al. 2008). Of 526 seizures exhibiting ictal EEG changes on simultaneous video-EEG recordings, only 179 (34%) had clinical symptoms recognizable on the videos. Thus, the vast majority of seizures were subclinical. The NICU staff reported 177 clinical events as seizures, but 134 (76%) of these events were misinterpreted because no EEG changes were apparent during them; 67 of these (38%) were reported in infants who lacked any seizures on EEG. Only 48 seizures were accurately identified by the NICU staff, accounting for just 9% of the total. These results clearly demonstrate that the diagnosis of neonatal seizures based on clinical observations alone is inaccurate. Notably, neonatal seizures that are clinically diagnosed often do not exhibit EEG changes during the

A. Okumura, H. Kidokoro (eds.), *Neonatal EEG: Atlas and Interpretation*,
https://doi.org/10.1007/978-981-96-0726-6_17

clinical events, indicating that they are not attributable to excessive neuronal activity in the brain. Typical examples of such events include locomotive limb movements described as pedaling or crawling; these are often misinterpreted as subtle seizures. Thus, ictal EEG recordings are essential to ensure accurate diagnosis of neonatal seizures. Although conventional multichannel EEG is optimal, amplitude-integrated EEG (aEEG), which will be described below, can also be useful.

3 Etiologies of Neonatal Seizures

Table 17.1 lists the underlying causes of neonatal seizures. These can be categorized into three groups, acute symptomatic, remote symptomatic, and self-limited, based on the status of active brain lesions. Most neonatal seizures are acute symptomatic seizures, commonly triggered by hypoxic-ischemic encephalopathy (HIE) including neonatal asphyxia. Among HIE cases, infants with parasagittal lesions or arterial infarctions may lack neurological symptoms related to HIE, rendering imaging diagnosis crucial. Congenital metabolic disorders are less common but must be diagnosed early and receive specific treatment.

Remote symptomatic neonatal seizures are often considered to reflect neonatal-onset epilepsy. These include various brain malformations, chromosomal abnormalities, congenital malformation syndromes, and in utero infections such as TORCH syndrome. Destructive lesions that develop in utero also fall into this category. The imaging findings are informative in infants with developmental brain malformations. When no brain malformation is evident, genetic testing is useful; both genetic variants and chromosomal abnormalities are common.

Any family history of self-limited neonatal seizures should be noted. A history of seizures in the neonatal period or in early infancy may indicate self-limited neonatal epilepsy.

The International League Against Epilepsy (ILAE) has published a new classification scheme for neonatal seizures (Pressler et al. 2021). The various etiologies of neonatal seizures are shown in Fig. 17.1. It is important to recognize overlaps between the etiologies. For example, a neonate with bacterial meningitis might experience hypoxic-ischemic stress during the acute phase of illness. If a neonate exhibits seizures, determination of the precise etiology thereof can be challenging.

4 Symptoms of Neonatal Seizures

Neonatal seizures are more difficult to identify than seizures in older children and adults. Although motor symptoms such as convulsions may be clinically detectable, seizures with prominent motor symptoms are relatively rare. Autonomic symptoms are important for detecting neonatal seizures. The most common autonomic symptoms include tachycardia or bradycardia, fluctuations in blood pressure, cyanosis, and decreased oxygen saturation. The so-called

Table 17.1 Underlying diseases in infants with neonatal seizures

	Common	Less common
Acute symptomatic	• Hypoxic-ischemic encephalopathy • Acute metabolic disorders • Hypoglycemia—electrolyte abnormalities, etc. • Infectious diseases • Sepsis—meningitis, etc. • Cerebrovascular disorders, head trauma • Intracranial hemorrhage, infarction, etc.	• Inborn errors of metabolism • Drugs/toxins • Congenital malignancy
Remote symptomatic	• Brain malformation	• Chromosomal abnormality • Genetic disorders • Congenital malformation syndrome
Self-limited	• Self-limited (familial) neonatal epilepsy	

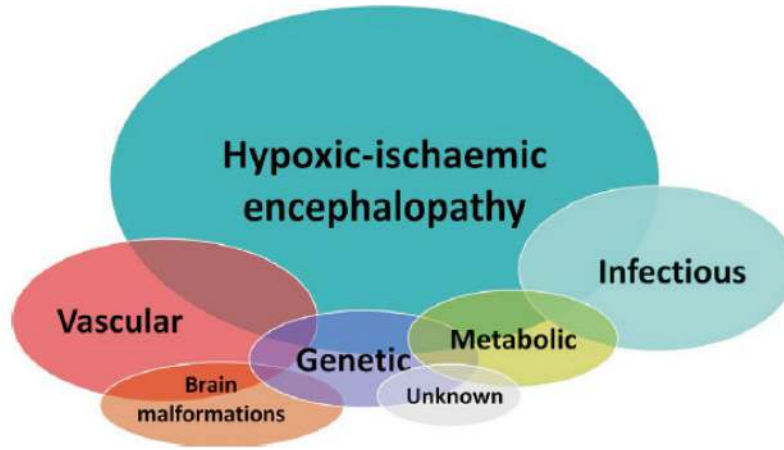

Fig. 17.1 The etiologies of neonatal seizures

apneic seizures are characterized by decreased oxygen saturation and tachycardia (autonomic symptoms) rather than breathing cessation. On the other hand, generalized hypertonia and alternating movements, such as pedaling, are extremely rare in neonates with seizures of cortical origin. Most are not associated with abnormal ictal EEG findings and should not be regarded as neonatal seizures. Alternating movements probably reflect releases of the lower central nervous system attributable to severe suppression of cortical function.

5 Classification of Neonatal Seizures

Any objective discussion of neonatal seizures requires well-defined terminology. A well-organized and easily comprehensible classification of seizure types is essential. No ideal classification of seizure types has yet been established. The Task Force on Neonatal Seizures of the ILAE recently published a new classification system (Pressler et al. 2021), which is expected to become the standard classification in the future.

Table 17.2 presents the ILAE classification of neonatal seizures (Pressler et al. 2021). The ILAE classification aligns with the classifications of epilepsy and epileptic seizures previously published by the ILAE (Fisher et al. 2017). Neonatal seizures are now categorized into four types: motor, non-motor, sequential, and electrographic-only seizures. Motor seizures are further subdivided into automatisms, clonic seizures, epileptic spasms, myoclonic seizures, and tonic seizures. Non-motor seizures are classified as autonomic or behavioral arrest. The latter may be negative motor seizures, which are difficult to distinguish from positive motor seizures. The ILAE stresses the frequent occurrence of electrographic-only seizures in neonates.

The ILAE classification is epoch-making; it considers all neonatal seizures to be of focal onset. The newborn brain lacks the neural circuits and networks required for the induction of generalized seizures in older children and adults. This supports the idea that all neonatal seizures are necessarily of focal onset. The ILAE classification is unique in that it determines the seizure type based on the predominant symptom during a seizure. In contrast to epileptic seizures, the classification of which focuses on symptoms at seizure onset, neonatal seizure classification emphasizes the etiology rather than the focus of the seizure. Thus, the ILAE has proposed that the seizure type should be determined based on the symptoms rather than the focus of the seizure. For example, a seizure associated with focal tonic posturing and ocular myoclonus would be classified as tonic if the former symptom was predomi-

Table 17.2 The International League Against Epilepsy (ILAE) classification of neonatal seizures. Reproduced with permission from Pressler et al. (2021)

Type	Description	Special considerations	Clinical context of seizure type
Automatisms	A more or less coordinated motor activity usually occurring when cognition is impaired. This often resembles a voluntary movement and may consist of an inappropriate continuation of preictal motor activity	Typically oral in neonates. Behavior in term and preterm infants may mimic ictal automatisms, thus EEG/aEEG mandatory	Seen in HIE and preterm infants. Often part of sequential seizures
Clonic	Jerking, either symmetric or asymmetric, that is regularly repetitive and involves the same muscle groups	Seizure type, which is more reliably diagnosed clinically	Typical seizure type in neonatal stroke or cerebral hemorrhage. May be seen in HIE
Epileptic spasms	A sudden flexion, extension, or mixed extension–flexion of predominantly proximal and truncal muscles that is usually more sustained than a myoclonic movement but not as sustained as a tonic seizure. Limited forms may occur: Grimacing, head nodding, or subtle eye movements	Brief in neonates, thus may be difficult to differentiate from myoclonic seizures without EMG channel. May occur in clusters	Rare. May be seen in inborn errors of metabolism or early-infantile DEE
Myoclonic	A sudden, brief (<100 ms) involuntary single or multiple contraction(s) of muscles(s) or muscle groups of variable topography (axial, proximal limb, distal)	Clinically difficult to differentiate from non-epileptic myoclonus, requires EEG, ideally with EMG channels	Typical seizure type in inborn errors of metabolism and preterm infants. May also be seen in early-infantile DEE
Tonic	A sustained increase in muscle contraction lasting a few seconds to minutes	Focal, unilateral or bilateral asymmetric. Generalized tonic posturing not of epileptic origin	Typical seizure type early-infantile DEE and genetic neonatal epilepsies
Autonomic	A distinct alteration of autonomic nervous system function involving cardiovascular, pupillary, gastrointestinal, sudomotor, vasomotor, and thermoregulatory functions	May involve respiration (apnea). EEG/aEEG mandatory	Rare in isolation. Seen in intraventricular hemorrhage as well as temporal or occipital lobe lesions. Also described in early-infantile DEE
Behavioral arrest	Arrest (pause) of activities, freezing, immobilization, as in behavior arrest seizure	EEG/aEEG mandatory	Rare as an isolated seizure type. More commonly seen as part of sequential seizure
Sequential seizure	This term is used in the instruction manual for the ILAE 2017 operational classification of seizure types for events with a sequence of signs, symptoms, and EEG changes at different times [6]	No predominant feature can be determined, instead the seizure presents with a variety of clinical signs. Several features typically occur in a sequence, often with changing lateralization within or between seizures	Often seen in genetic epilepsies such as self-limited neonatal epilepsy or KCNQ2 encephalopathy

(continued)

Table 17.2 (continued)

Type	Description	Special considerations	Clinical context of seizure type
Electrographic-only seizure	Subclinical, without clinical manifestation	EEG/aEEG mandatory	Often seen in preterm infants, HIE (particularly in those with basal ganglia/thalamus injury), critically ill and neonates undergoing cardiac surgery
Unclassified seizure type	Due to inadequate information or unusual clinical features with inability to place in other categories	EEG/aEEG mandatory	

nant. If a seizure is long-lasting, the symptoms may change over time, rendering it challenging to determine the predominant symptom. The term "sequential seizure" is used to describe such cases.

The basic concept of the proposed classification seems appropriate, but several questions remain. One issue is potential variability among different observers determining the predominant symptoms during seizures. The ILAE has sought to deal with this, but further tests in various settings are required to confirm reproducibility. Significant interobserver variability in terms of classifying seizure types could undermine the reliability of the ILAE classification. The "sequential seizure" concept is well-accepted, but temporal changes in seizure symptoms are common not only in neonates with seizures but also in older children and adults with seizures of cortical origin. If neonatal seizures persist for a long time, it is quite likely that the symptoms will change, suggesting that many seizures may thus be classified as sequential; further study is required.

6 The Diagnostic Framework for Neonatal Seizures

The diagnostic framework for neonatal seizures suggested by the ILAE is shown in Fig. 17.2. Initially, when neonatal seizures are suspected, an ictal EEG recording with simultaneous video-EEG recording or aEEG is required. Events that do not exhibit ictal EEG correlates are not neonatal seizures; they are non-seizure episodes. Only events associated with ictal EEG changes are neonatal seizures. EEG-confirmed neonatal seizures are classified based on the clinical symptoms. Events lacking such symptoms are classified as electrographic-only seizures (conventionally, "subclinical seizures"). When clinical symptoms are apparent, the seizure types are classified using the criteria listed in Table 17.2.

7 EEG Features of Neonatal Seizures

As previously mentioned, ictal EEG recording is essential for diagnosing neonatal seizures. If it is unclear whether ictal EEG correlates are present or absent, objective diagnosis of neonatal seizures is impossible. Table 17.3 lists the characteristics of ictal changes apparent on neonatal EEG. Neonatal seizures are series of paroxysmal discharges with a clear beginning and end; they are distinct from the background EEG activities. The ictal EEG changes may be described as:

1. Rhythmic
2. Repetitive
3. Stereotyped

The ictal EEG changes of neonatal seizures usually last for ≥10 s. As neonatal EEGs may exhibit rhythmic discharges and artifacts unrelated to seizures, it is important to define a minimal duration of EEG changes. Although the

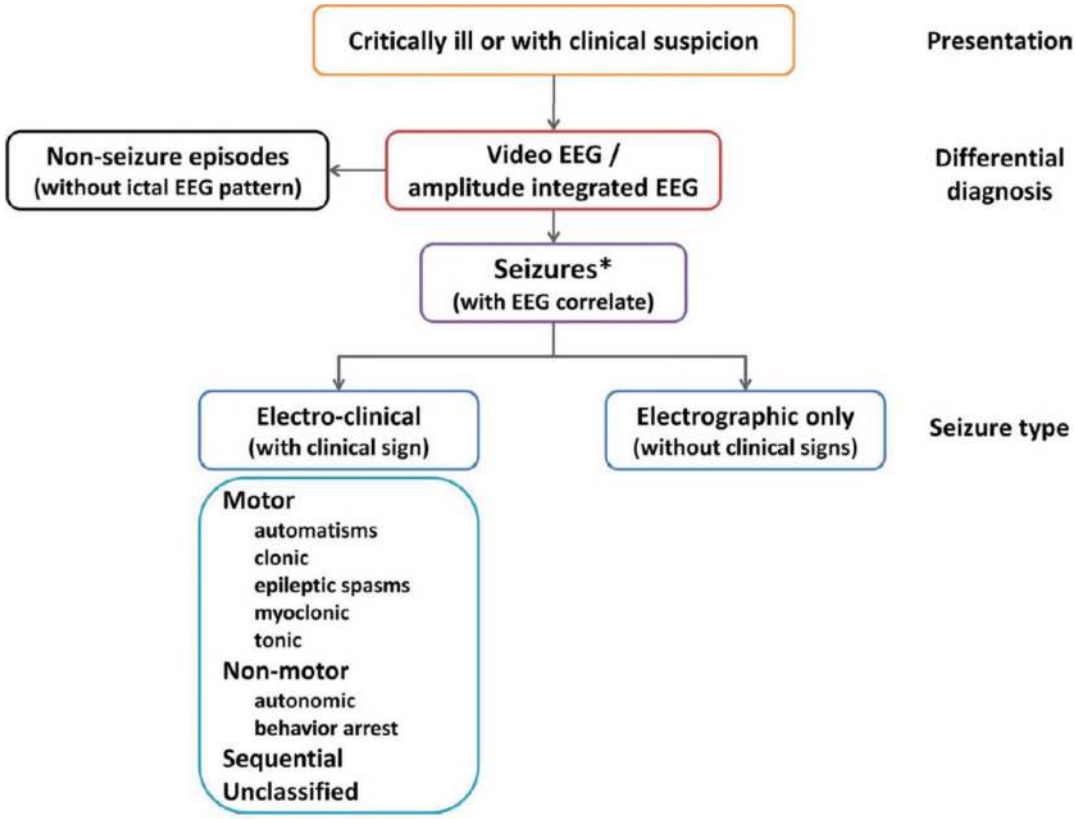

Fig. 17.2 The diagnostic framework for neonatal seizures

Table 17.3 Ictal EEG changes during neonatal seizures

The EEG exhibits the following features
• The ictal EEG patterns clearly differ from the EEG background; the beginning and end are distinct
• Rhythmic, repetitive, and stereotyped dischargers are apparent
• These findings generally persist for at least 10 s
• Evolutional changes are observed within a single seizure. The waveforms, voltages, frequencies, and sites of paroxysmal discharge change within a seizure
• The paroxysmal discharges are often alpha, theta, or delta waves; they are rarely spikes or sharp waves

"10-second rule" is not based on solid evidence, it is generally accepted worldwide. On the other hand, the durations of myoclonic seizures and epileptic spasms are <10 s, and the ictal EEG findings are neither rhythmic nor repetitive. It is essential to clarify the duration of ictal EEG changes according to the seizure type. However, the currently available information is insufficient.

During most neonatal seizures, paroxysmal discharges usually evolve within the course of the seizures ("evolution"). Although paroxysmal discharges are stereotyped, the waveforms, voltages, frequencies, and sites of paroxysmal discharge may change within a single seizure. "Evolution" is important when distinguishing epileptic seizures from artifacts. The paroxysmal discharges of neonatal seizures are rarely sharp waves or spikes. Most paroxysmal discharges are alpha, theta, or delta waves, and they are not spiky.

8 Etiologies of Neonatal Seizures and Background EEG Activities

Although changes in background EEG activities are not disease-specific, they are useful when considering the pathogenesis of underlying diseases; EEG reflects real-time brain function. Neonatal seizures exhibiting acute symptomatic etiologies are often associated with varying degrees of brain dysfunction attributable to acute brain insults. The severity of brain dysfunction is reflected in the acute-stage abnormalities (ASAs) apparent in background EEGs (Watanabe et al. 1980; Maruyama et al. 2002). Neonatal seizures with remote symptomatic etiologies may present with non-physiological background EEG activities (dysmorphic patterns) indicative of brain malformations. Destructive lesions that develop in utero can be associated with disorganized EEG patterns that vary according to the time since lesional onset (Hayakawa et al. 1997; Okumura et al. 2003; Kidokoro et al. 2006). Self-limited neonatal epilepsy is distinguished by the absence of obvious background EEG abnormalities during the interictal period.

9 Non-Epileptic Events That Should Be Differentiated From Neonatal Seizures

Non-epileptic events that should be differentiated from neonatal seizures include the following:

9.1 Jitteriness

Jitteriness is specific to neonates and can be mistaken for clonic seizures. However, jitteriness differs from clonic seizures, which exhibit repetitive, rapid muscle contractions followed by slow muscle relaxation. Jitteriness is not associated with ocular or autonomic symptoms, is easily triggered by tactile stimuli, and can be suppressed by passively flexing the limbs.

9.2 Hyperekplexia

Hyperekplexia is characterized by an excessive startle reflex and persistent tonicity in response to auditory, visual, or somatosensory stimuli (such as body movements, nose-tapping, or blowing air into the face). Hyperekplexia may be both rhythmic and convulsive, and sometimes accompanied by apnea, and it may disappear when the trunk is flexed. Generalized muscle hypertonia and myoclonus during sleep are also common. There is no ictal EEG correlation. Pathological variants in genes involved in glycine receptor and transporter actions (*GLRA1*, *SLC6A5*, and *GLRB*) are associated with this condition.

9.3 Dystonia

Dystonia, i.e., an abnormal posture attributable to increased muscle tone, can be difficult to distinguish from a tonic seizure. Common symptoms include finger hyperextension, hyperflexion of the wrist joints, hyperextension of the elbow joints, and neck and trunk torsion. Dystonia is typically caused by lesions in the basal ganglia or disorders of the extrapyramidal tract, which is connected to the basal ganglia.

9.4 Myoclonus

Benign neonatal sleep myoclonus typically appears about 1 week after birth. This condition is characterized by intermittent, bilateral, synchronous, repetitive myoclonic movements of the extremities that last for several minutes. Benign neonatal sleep myoclonus occurs only during sleep, especially quiet (non-REM) sleep. The condition is evoked by vibration and disappears on awakening. It generally resolves within 2 months; neurological development is not affected.

Early myoclonic encephalopathy is a drug-resistant form of epileptic encephalopathy that emerges in the neonatal period. The associated myoclonus usually lacks ictal EEG correlates and

is considered to be non-epileptic. Myoclonus can also be associated with several other diseases but is often non-epileptic.

10 Continuous EEG Monitoring in Neonates with Seizures

Continuous EEG monitoring is useful for differentiating neonatal seizures and non-epileptic events, and it can detect electrographic-only seizures in the absence of apparent clinical manifestations. Prolonged video-EEG monitoring is recommended for all neonates with suspected or EEG-confirmed seizures. The advent of digital EEG has reduced the technical challenges, but the required equipment is not always available in NICUs. Therefore, the development and widespread use of simple monitoring devices is essential. aEEG is one of the most promising tools.

aEEG simplifies the analysis by reducing the number of electrodes, compressing the time span on display, and filtering to extract maximum and minimum EEG amplitudes at specific frequencies. This aids long-term recording and interpretation. However, seizures with short or low-voltage discharges may be missed, and ictal EEG changes distant from the electrodes cannot be detected given the reduced number of electrodes. Qualitative evaluations, i.e., differentiation of genuine conditions from artifacts and assessment of background EEG activity, are also limited. Recent devices that simultaneously record raw EEG activities are expected to enhance diagnostic accuracy when aEEG is combined with conventional EEG (Alfonso et al. 2001).

EEG monitoring is important not only to diagnose neonatal seizures and determine their etiology and severity, but also when evaluating the efficacy of treatments (Clancy 2006). The primary goal of those who treat neonatal seizures is to resolve all ictal events observable on an EEG. Electrographic-only seizures are commonly seen in neonates, especially after administration of antiseizure medications. Although the need for such medications to treat electrographic-only seizures without clinical manifestations remains unclear, it is not appropriate to assess treatment efficacy using clinical observations alone. Furthermore, in children in intensive care who are prescribed muscle relaxants, seizures may be undetected in the absence of continuous EEG monitoring.

11 Neonatal Seizures (1)

Neonatal seizures in a term infant (40 weeks PMA) with hypoxic-ischemic encephalopathy. During the interictal period, the background EEG activity was flat, indicating maximal depression (A; blue arrow). The seizures commenced with high-voltage slow waves in the bilateral frontal areas, followed by repetitive, stereotyped, rhythmic delta waves that propagated to the occipital areas (A). The ictal discharges gradually became more widespread, and the voltage increased (B); the ictal discharges eventually terminated as rhythmic, high-amplitude slow waves in the frontal areas (C). During neonatal seizures, although the individual waveforms were stereotyped, evolutionary changes in the voltage and frequency were apparent; these allowed the seizures to be distinguished from artifacts. Such seizures lack clinical symptoms and are classified as "electrographic-only seizures" by the ILAE (Fig. 17.3).

12 Neonatal Seizures (2)

A seizure in a neonate at 38 weeks PMA due to hyperammonemia of unknown etiology. During the interictal period, the background EEG activity was flat, indicating maximal depression. The ictal EEG revealed repetitive low-voltage delta waves originating from the right frontal area. When the EEG background was hypoactive, the ictal discharge voltage tended to be low. This seizure was not associated with any clinical symptoms and was thus classified as an "electrographic-only seizure" using the ILAE classification (Fig. 17.4).

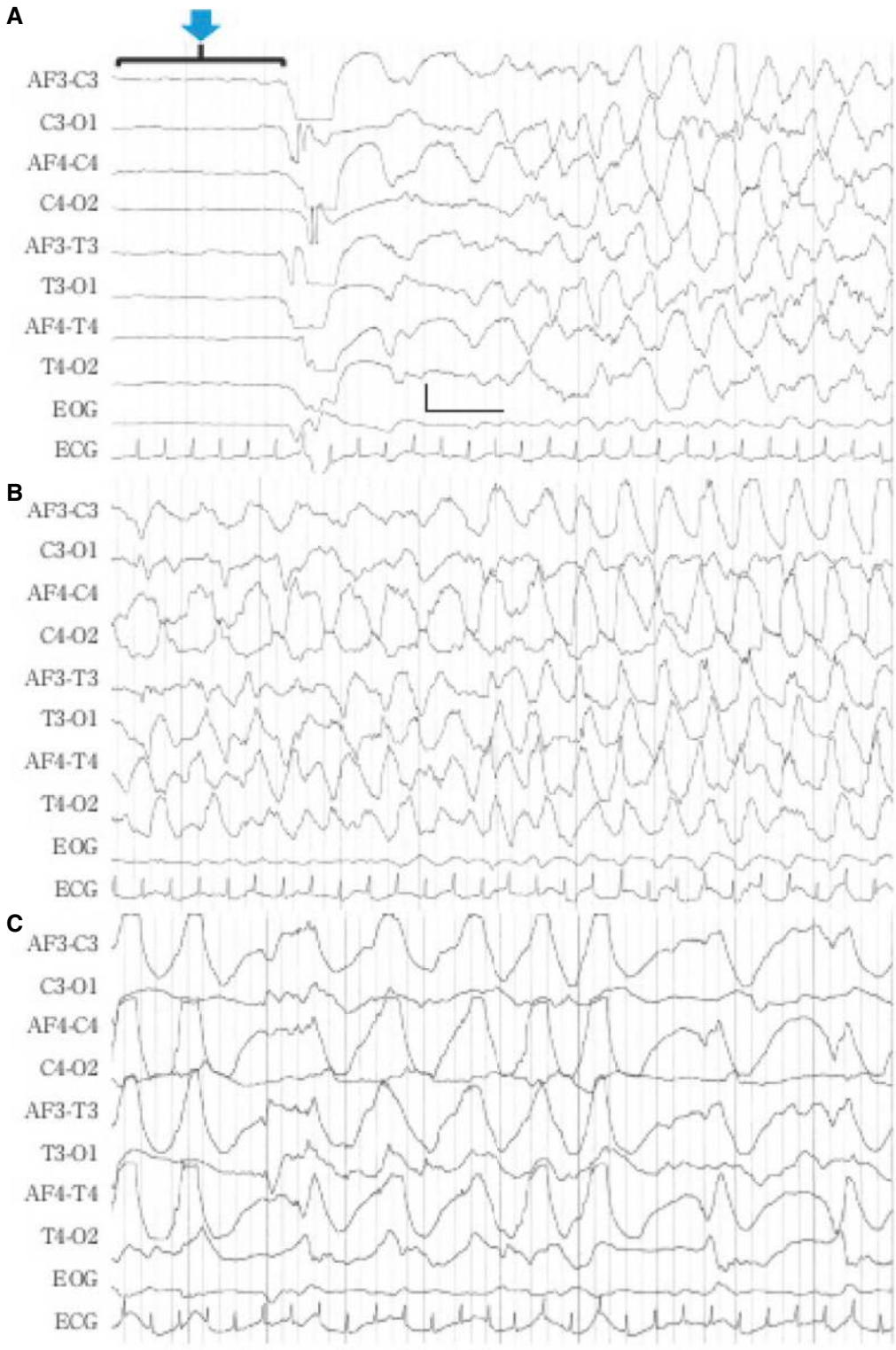

Fig. 17.3 Neonatal seizures (1)

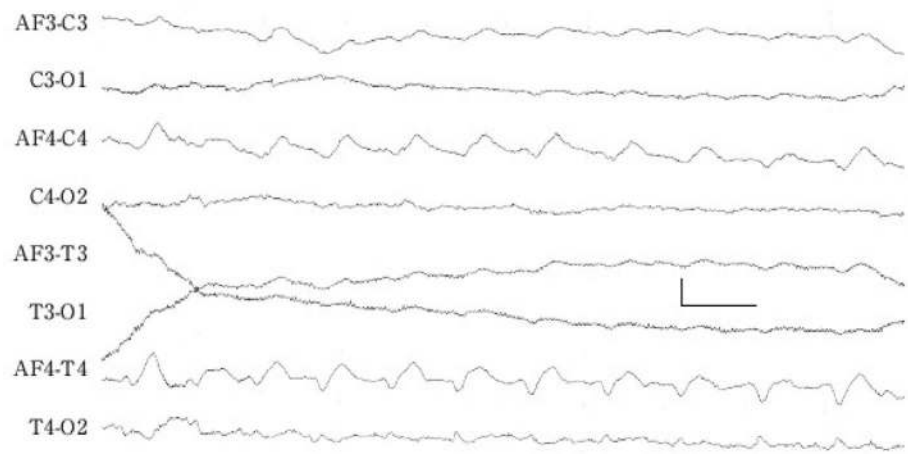

Fig. 17.4 Neonatal seizures (2)

13 Neonatal Seizures (3)

An infant with neonatal herpes simplex encephalitis at 43 weeks PMA. Rhythmic spikes developed in the left frontal-central regions (A), and there were ictal discharges in the contralateral hemisphere, whereas they were not completely generalized (B). The ictal discharges included sharp waves, spikes, polyspikes, spike-waves, polyspike-waves, and other waveforms. The seizure was associated with clonic movement beginning on the right face that then spreading to the upper and lower extremities. This seizure was a clonic seizure according to the ILAE classification (Fig. 17.5).

14 Neonatal Seizures (4)

Neonatal seizures developed in a 38-week PMA infant with a peroxisomal disorder. Interictal EEG revealed normal background activities. Ictal EEG revealed rhythmic delta waves in the right central area (A), followed by sharp and slow waves in the same area (B) that then propagated to the right temporal area (C). Subsequently, the ictal discharges were transformed into high-voltage rhythmic sharp waves in the left central area (D), followed by a rapid waveform change (E) to slow waves (2–3 Hz) before termination (F). Such waveform changes are common features of neonatal seizures. Waveform changes of ictal discharges develop successively within a single seizure, and the ictal discharge waveforms of the left and right hemispheres may be completely different. The infant presented with eye-opening, irregular respiration, oral automatic movements, and clonic movements from the right to the left foot and then back to the right foot. This seizure was classified as sequential (Fig. 17.6).

15 Neonatal Seizures (5)

In a term infant with hypocalcemia at 38-week PMA, the ictal EEG revealed very high-voltage rhythmic slow waves in the left frontal area. The interictal EEG exhibited normal background activities, in contrast to the EEG shown in Fig. 17.4. The seizure was associated with vibratory movements of all limbs, eye fixation, and decreased oxygen saturation. The seizure was classified as autonomic (Fig. 17.7).

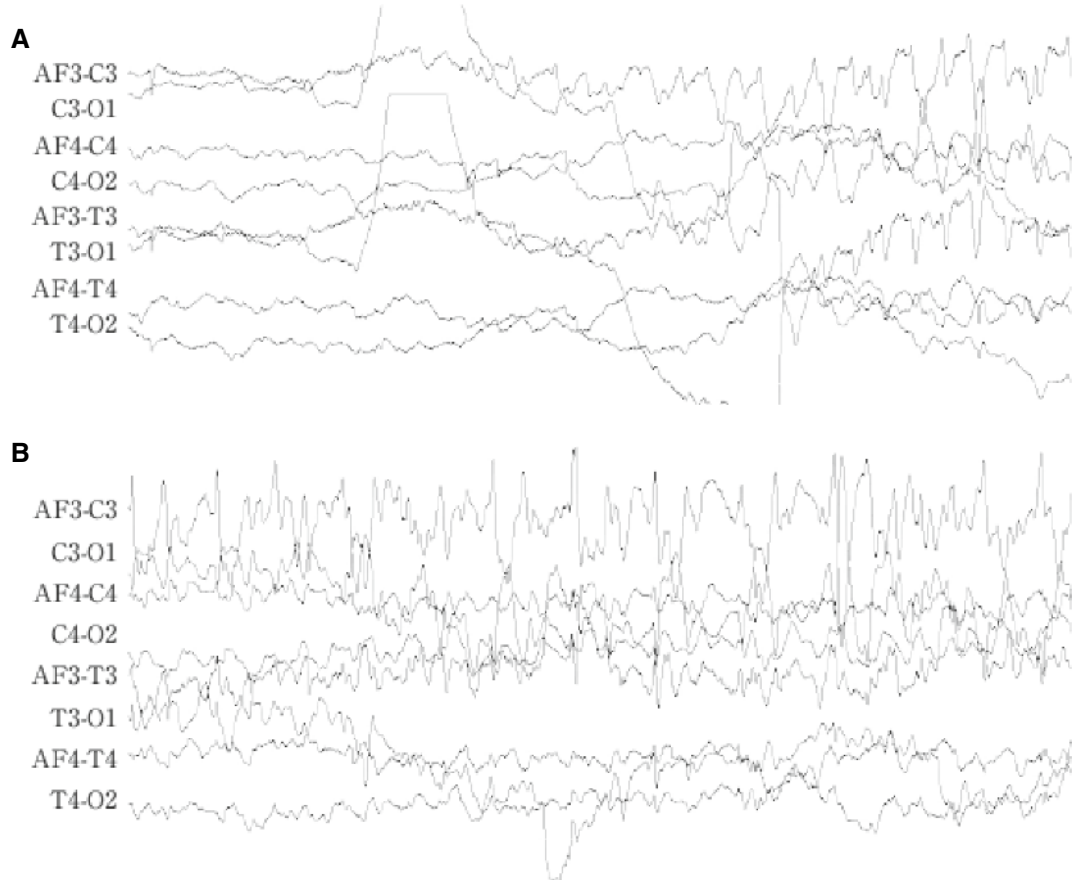

Fig. 17.5 Neonatal seizures (3)

16 Epileptic Spasms in Neonates

In an infant with unilateral megalocephaly at 38 weeks PMA, the interictal EEG exhibited alternating high- and low-voltage components (A, 20-s sample). Ictal EEG revealed preceding sharp waves in the left frontal area, followed by a generalized and polyphasic high-voltage slow wave (blue arrow) (B). The patient exhibited twitching limb movements concurrent with high-voltage slow waves. This seizure was defined as an epileptic spasm using the ILAE classification. In figure B, a 16-channel reference derivation was used. When an eight-channel neonatal EEG montage was applied (C, bipolar derivation; D, reference derivation), EEG interpretation may be difficult. When epileptic spasms are suspected, it is essential to record and analyze EEGs in full-channel mode, even in neonates (Fig. 17.8).

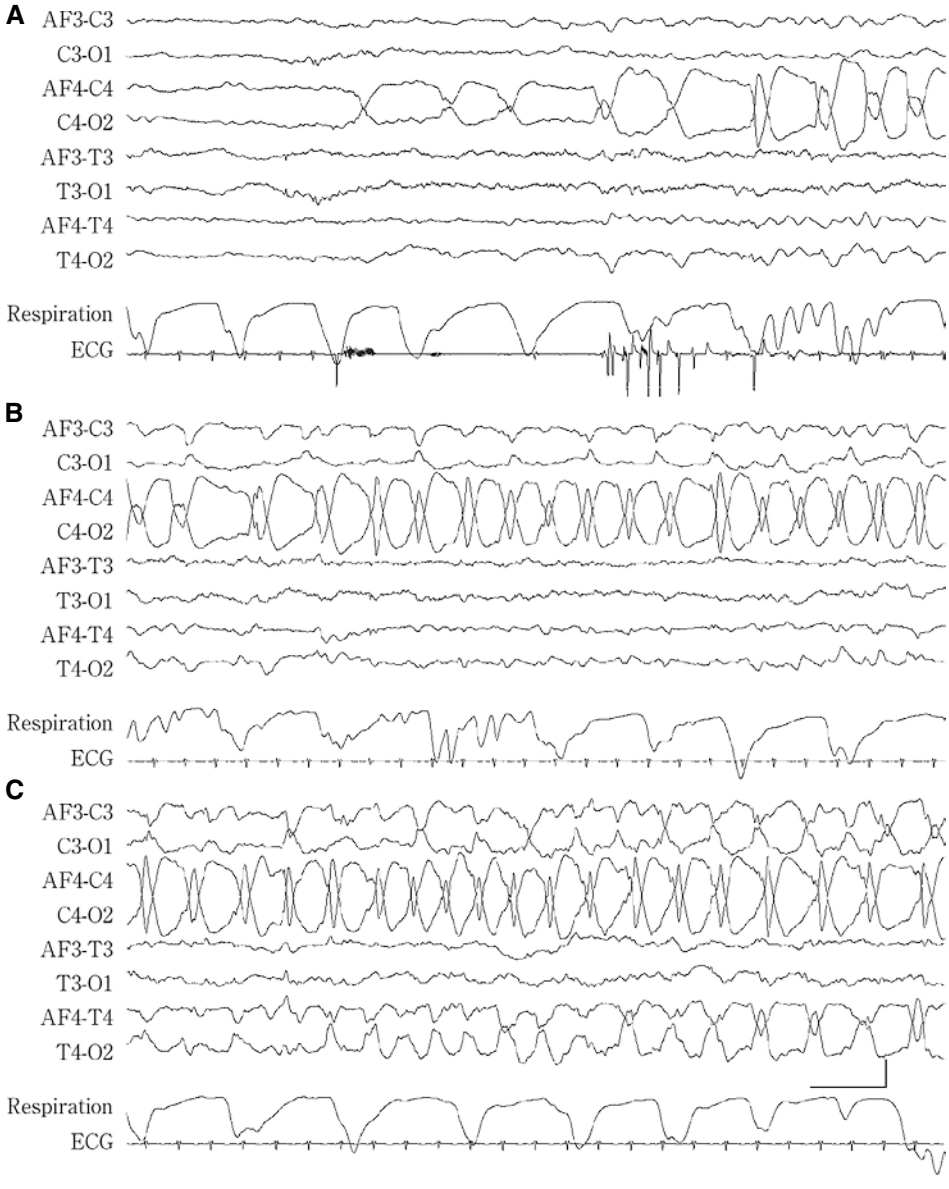

Fig. 17.6 Neonatal seizures (4)

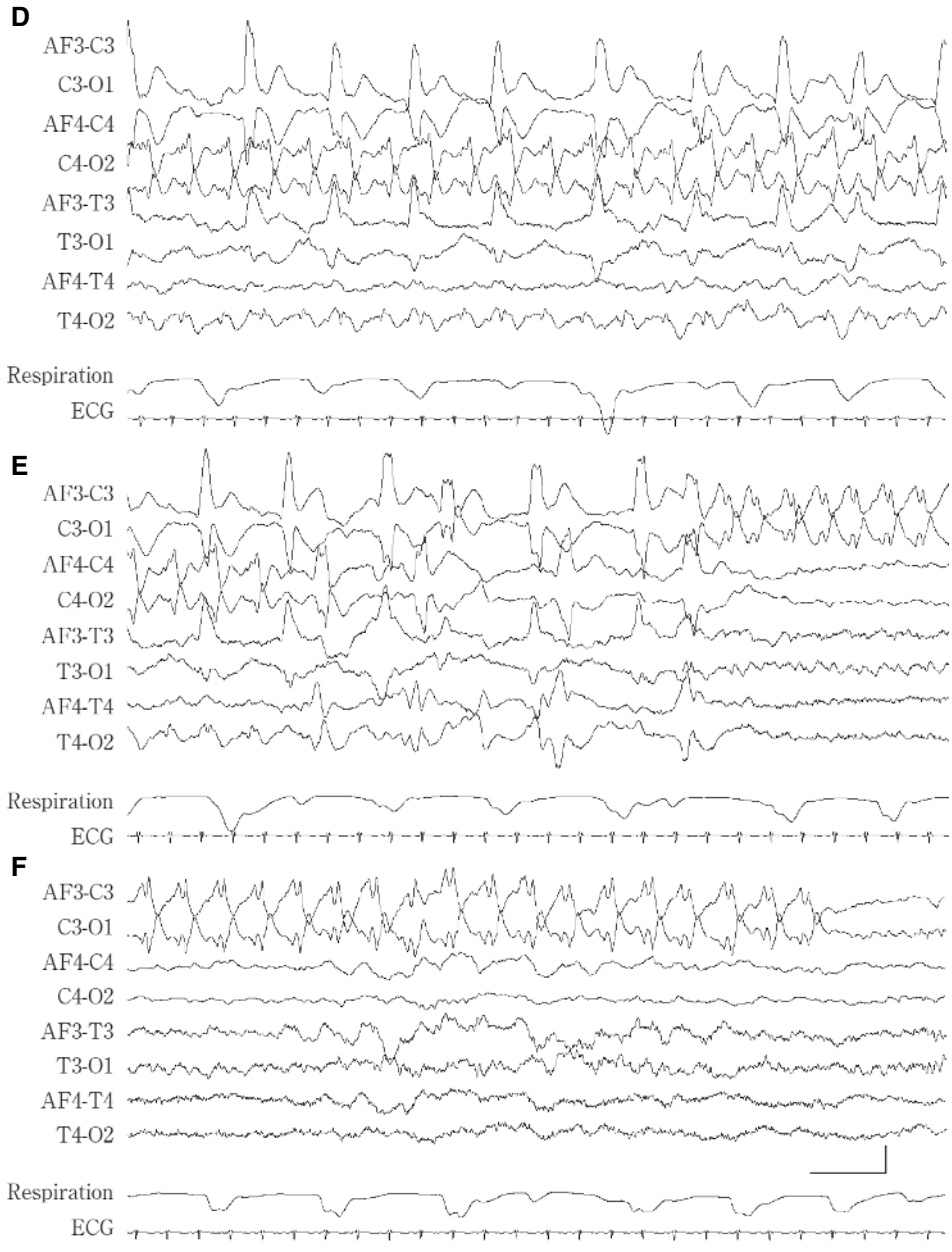

Fig. 17.6 (continued)

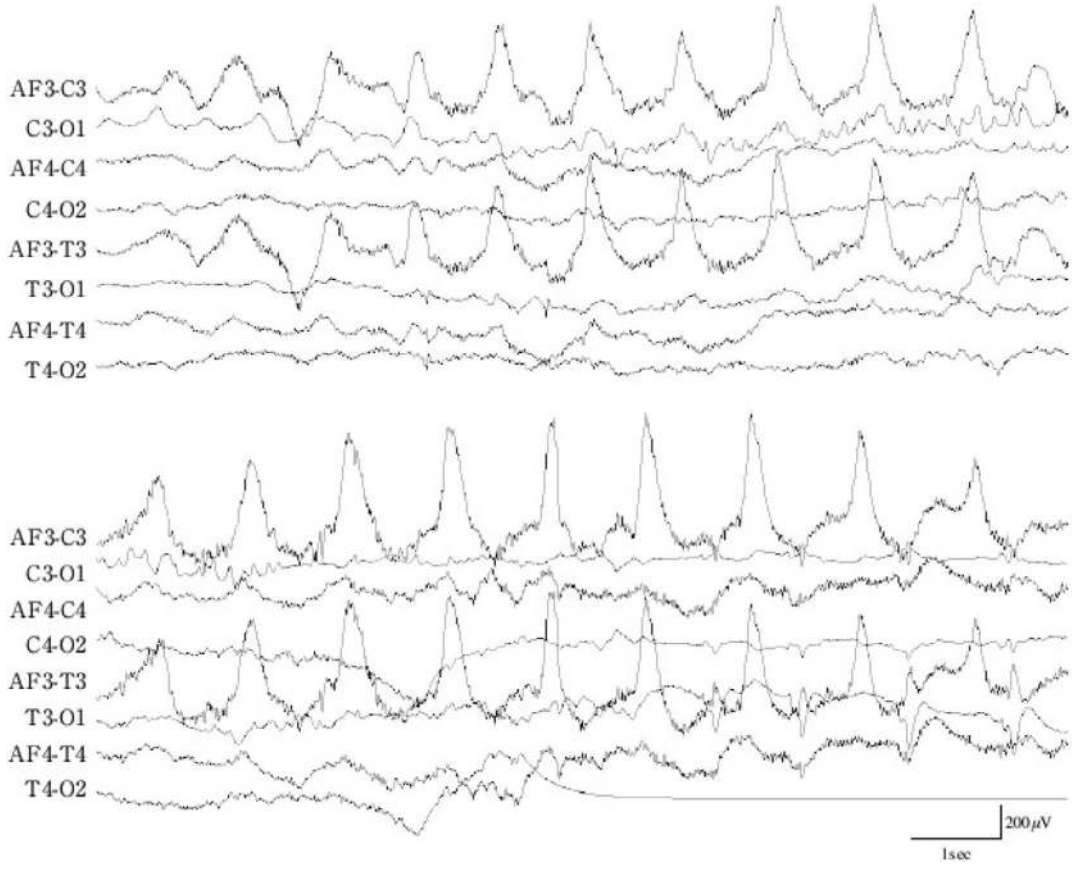

Fig. 17.7 Neonatal seizures (5)

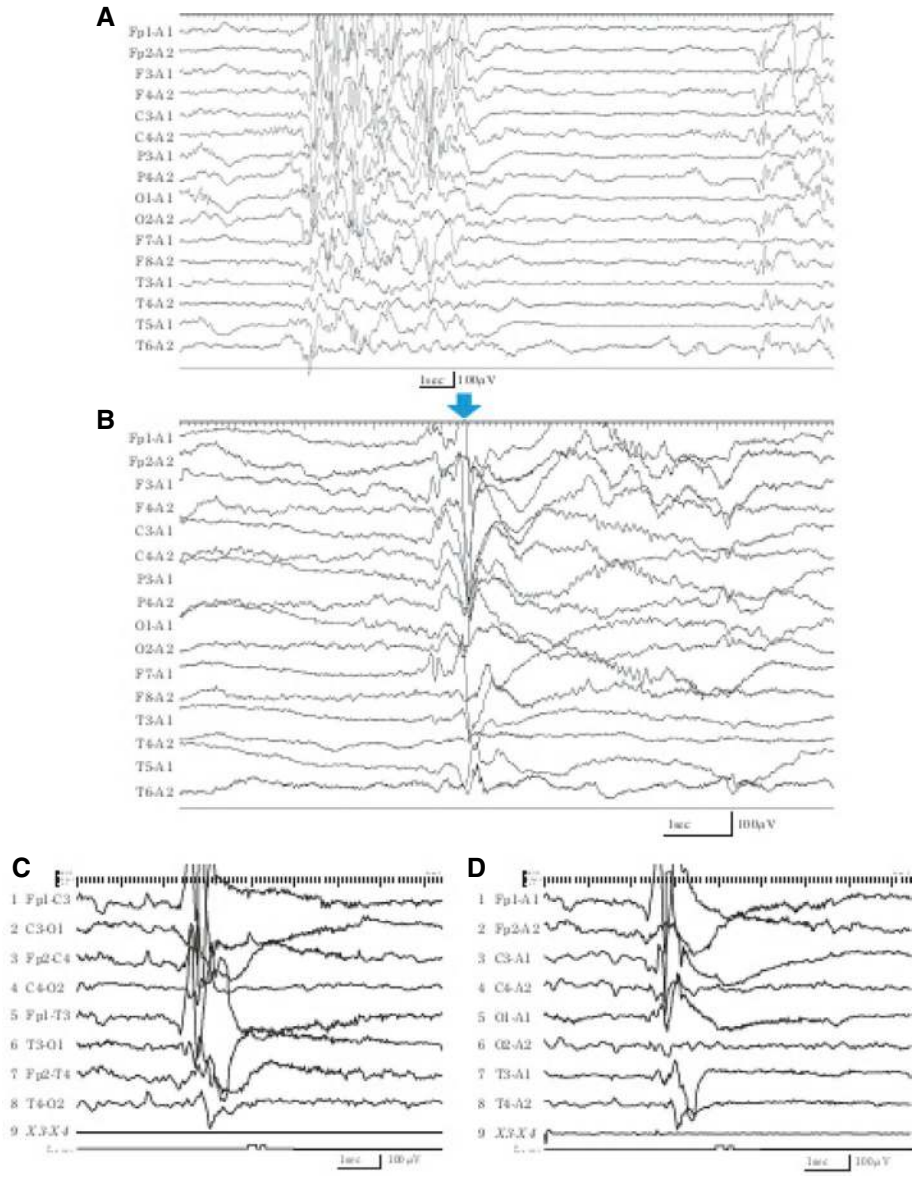

Fig. 17.8 Epileptic spasms in neonates

Column: Acute- and Chronic-Stage Abnormalities

(Fumio Hayakawa)

When interpreting neonatal EEGs, it is crucial to distinguish between acute-stage abnormalities (ASAs) and chronic-stage abnormalities (CSAs). During the acute phase, background EEG activities may be suppressed depending on the type and severity of the acute insult. In contrast, during the chronic phase, EEG reveals qualitative abnormalities reflecting the initially affected brain functions that are recovering. However, abnormalities in the convalescent and chronic phases can only be determined after recovery from acute depression. In

(continued)

infants with severe brain damage, EEG activities may be almost completely absent even in the chronic phase. It is important to know this to avoid misinterpretations.

For example, a 40-week-old boy, weighing 3105 g at birth, with Apgar scores of 5 (at 1 min) and 7 (at 5 min), was admitted to an NICU. He was born after spontaneous vaginal delivery without any prenatal abnormality but was hospitalized because of weak crying and reduced limb movement. Laboratory results at birth were unremarkable, but he was a floppy infant with poor movement. He experienced a cluster of right hemiconvulsions lasting for 30 s commencing several hours after birth. The EEG revealed so-called burst-suppression patterns. Even after painful stimulation, the EEG did not change into a continuous pattern, but paroxysmal EEG changes appeared and persisted for several tens of seconds.

Although he was not diagnosed with birth asphyxia, his EEG showed marked depression of ASAs, leading to a diagnosis of neonatal seizures associated with asphyxia. However, there were no changes in the EEG findings or clinical features over the following weeks. If the burst-suppression patterns were ASAs, the EEG activities should have recovered, and the later EEG recordings should have revealed CSAs. Instead, the burst-suppression patterns persisted for several weeks.

Repeated neuroimaging revealed no abnormalities, but a genetic disorder was suspected. In this infant, the burst-suppression pattern was considered to be a CSA, thus reflecting abnormalities in the steady state. ASAs cannot be diagnosed until the abnormal findings resolve.

References

Alfonso I, Jayakar P, Yelin K, Dunayer C, Papazian O, Vasconcellos E, Valeron NM. Continuous-display four-channel electroencephalographic monitoring in the evaluation of neonates with paroxysmal motor events. J Child Neurol. 2001;16(8):625–8.

Clancy RR. Prolonged electroencephalogram monitoring for seizures and their treatment. Clin Perinatol. 2006;33(3):649–65.

Fisher RS, Cross JH, French JA, Higurashi N, Hirsch E, Jansen FE, Lagae L, Moshé SL, Peltola J, Roulet Perez E, Scheffer IE, Zuberi SM. Operational classification of seizure types by the International League Against Epilepsy: position paper of the ILAE Commission for Classification and Terminology. Epilepsia. 2017;58(4):522–30.

Hayakawa F, Okumura A, Kato T, Kuno K, Watanabe K. Disorganized patterns: chronic-stage EEG abnormality of the late neonatal period following severely depressed EEG activities in early preterm infants. Neuropediatrics. 1997;28(5):272–5.

Kidokoro H, Okumura A, Watanabe K. Abnormal brushes in preterm infants with periventricular leukomalacia. Neuropediatrics. 2006;37(5):265–8.

Maruyama K, Okumura A, Hayakawa F, Kato T, Kuno K, Watanabe K. Prognostic value of EEG depression in preterm infants for later development of cerebral palsy. Neuropediatrics. 2002;33(3):133–7.

Murray DM, Boylan GB, Ali I, Ryan CA, Murphy BP, Connolly S. Defining the gap between electrographic seizure burden, clinical expression and staff recognition of neonatal seizures. Arch Dis Child Fetal Neonatal Ed. 2008;93(3):187–91.

Okumura A, Hayakawa F, Kato T, Maruyama K, Kubota T, Suzuki M, Kidokoro H, Kuno K, Watanabe K. Abnormal sharp transients on electroencephalograms in preterm infants with periventricular leukomalacia. J Pediatr. 2003;143(1):26–30.

Pressler RM, Cilio MR, Mizrahi EM, Moshé SL, Nunes ML, Plouin P, Vanhatalo S, Yozawitz E, de Vries LS, Puthenveettil Vinayan K, Triki CC, Wilmshurst JM, Yamamoto H, Zuberi SM. The ILAE classification of seizures and the epilepsies: modification for seizures in the neonate. Position paper by the ILAE Task Force on Neonatal Seizures. Epilepsia. 2021;62(3):615–28.

Watanabe K, Miyazaki S, Hara K, Hakamada S. Behavioral state cycles, background EEGs and prognosis of newborns with perinatal hypoxia. Electroencephalogr Clin Neurophysiol. 1980;49(5-6):618–25.

Weiner SP, Painter MJ, Geva D, Guthrie RD, Scher MS. Neonatal seizures: electroclinical dissociation. Pediatr Neurol. 1991;7(5):363–8.

Part V

Amplitude-integrated EEG

18 Amplitude-Integrated Electroencephalogram (aEEG): General

Yuichiro Sugiyama and Tetsuo Kubota

1 Introduction

The amplitude-integrated EEG (aEEG) was developed in the late 1960s as a technique for continuous monitoring of brain function in adults; it was originally termed the cerebral function monitor. In Japan, the aEEG has been widely used in neonatal intensive care units since 2010, especially after it became an adjunctive diagnostic criterion for therapeutic hypothermia in neonatal hypoxic-ischemic encephalopathy. (Note: Since 2015, aEEG findings have not been included in the criteria for therapeutic hypothermia.)

The aEEG is significantly easier to interpret than the conventional EEG (cEEG). It enables real-time monitoring of neonatal brain function at the bedside, which has a significant impact on clinical decision-making. As with the cEEG, a persistent decline in brain function on an aEEG recording over a certain period indicates neurological sequelae. Additionally, the aEEG is becoming a necessary tool for the efficient detection of neonatal seizures, a well-known poor prognostic factor in newborns. We recommend using aEEG to monitor brain function as a vital sign and incorporating it into the decision-making for treatment plans.

This section outlines the principles of the aEEG and presents the normal findings of the aEEG in both term and preterm infants.

2 Principle of an aEEG

The process for displaying an aEEG trace is illustrated in Figs. 18.1 and 18.2. Initially, to remove artifacts efficiently, a filter is applied to the EEG components to extract frequencies of 2–15 Hz (filtering). The filtered waveform is then processed around a reference line and expressed in absolute values (rectification). The peaks of this rectified waveform are gently connected to each other (smoothing). Through this method, the maximum and minimum values of the EEG waveform's peaks at each unit of time are extracted and displayed as a line segment (compression) on the aEEG waveform, as depicted in Fig. 18.1.

Y. Sugiyama (✉)
Department of Pediatrics, Japanese Red Cross Aichi Medical Center Nagoya Daiichi Hospital, Nagoya, Japan
e-mail: sugiyama-les400@nagoya-u.jp

T. Kubota
Department of Pediatrics, Anjo Kosei Hospital, Anjo, Japan
e-mail: t-kubota@kosei.anjo.aichi.jp

A. Okumura, H. Kidokoro (eds.), *Neonatal EEG: Atlas and Interpretation*,
https://doi.org/10.1007/978-981-96-0726-6_18

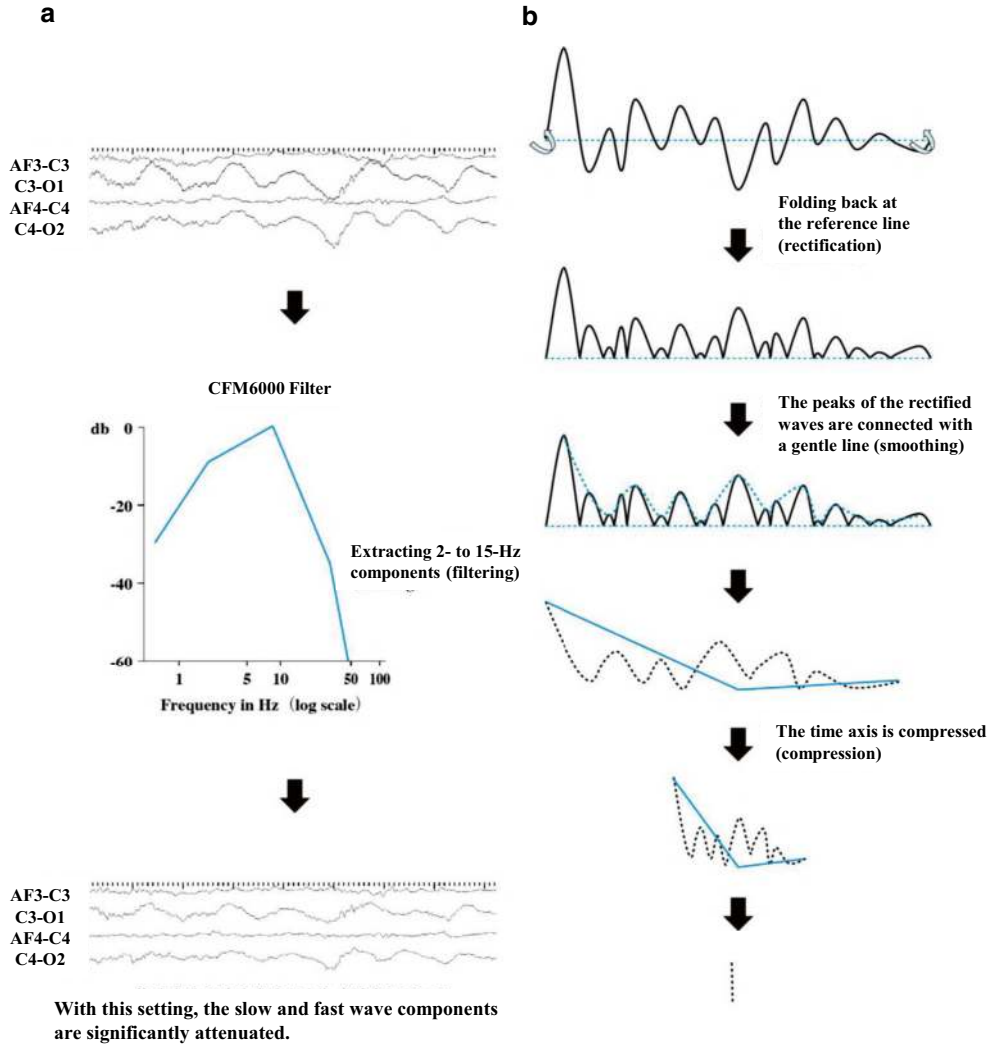

Fig. 18.1 Principle of generation of aEEG trace. (**a**) Filtering. The upper panel displays a four-channel raw EEG with a low-cut filter set at 0.53 Hz and a high-cut filter set at 60 Hz (standard display settings for a neonatal EEG). When a strong filter is applied, as shown in the lower panel, the activity of both delta waves and fast waves decreases. It is important to note that, with this filtering, both slow and fast wave components are significantly attenuated. (**b**) aEEG generation process

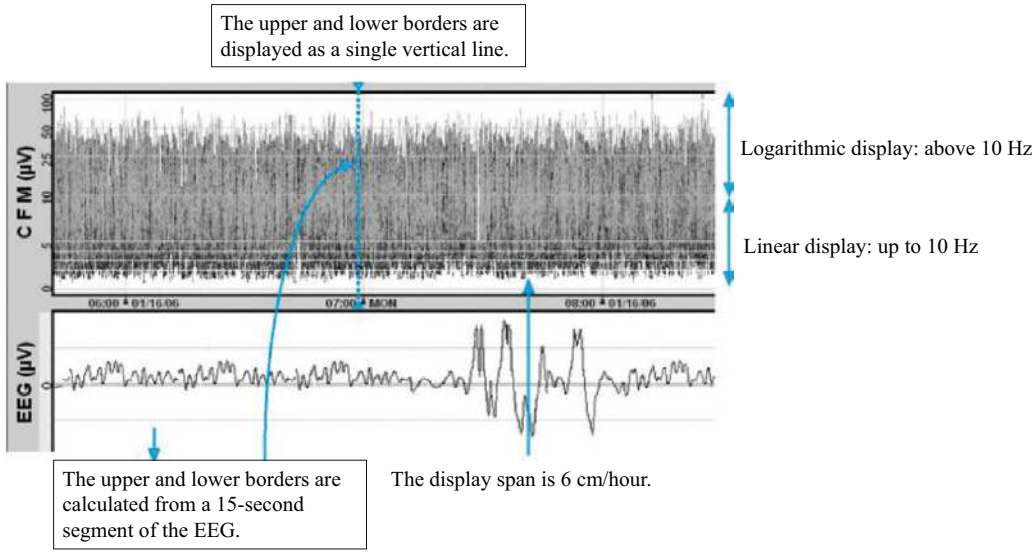

Fig. 18.2 aEEG display

3 Display Format of an aEEG

The display span of an aEEG is 6 cm/h, whereas the display span of a cEEG is 3 cm/s; thus, the time axis is significantly compressed in an aEEG. In other words, aEEG recordings are evaluated over a longer period than cEEG recordings. In addition, newer aEEG models allow the display speed to be changed in various ways. However, because the standard for reading is based on a display speed of 6 cm/h, aEEG recordings with this display span are used in the following sections of this textbook.

The aEEG display method is unique. As shown in Fig. 18.2, the vertical axis is a "semi-logarithmic scale" of 0–10 μV in integer and 10–100 μV in logarithm. This is an important method to facilitate reading the height and variability of the lower margin. Considering that 1 μV is displayed at a height of only 0.1 mm in the cEEG, the aEEG emphasizes the minimum amplitude value.

4 Normal aEEG Pattern in Neonates

4.1 aEEG in Term Infants

The background EEG activity is different at each postmenstrual age (PMA). This section primarily addresses the evaluation of the aEEG background in normal-term infants, i.e., those of 37–42 gestational weeks.

As previously mentioned, the aEEG is a type of compressed EEG utilizing a specific algorithm. Consequently, much detail is lost compared with the cEEG. Mild depression and chronic-stage abnormalities are difficult to identify on an aEEG, at least from an observational standpoint. With respect to neuromonitoring, however, the real-time capability to observe brain functions for several hours and the ease of identifying neonatal seizures are advantageous in the clinical setting. For example, it is useful to determine whether the brain function of an infant with

asphyxia is recovering. If not, further interventions to improve respiratory or circulatory control may be considered. When an aEEG is recorded in infants who appears to be somewhat unwell, it may detect neonatal seizures associated with brain dysfunction, cerebral hemorrhage, metabolic abnormalities, and infection.

4.2 Interpretation of a Normal aEEG Pattern

Figure 18.3 shows the basic knowledge necessary to interpret aEEG trace.

4.2.1 Cycling

The lower margin of the aEEG trace shows periodic sinusoidal fluctuations every 40–80 min. In neonates, EEG patterns undergo significant physiological changes in response to the sleep–wake cycle. In the EEGs of normal term infants, two distinct patterns are observed: a continuous pattern, in which EEG activity is continuous irrespective of amplitude, and an alternating pattern, characterized by the alternate appearance of high-amplitude and low-amplitude EEGs every several seconds. The continuous pattern is observed during wakefulness, active sleep, and the early stages of quiet sleep (e.g., high-voltage slow wave pattern), whereas the alternating pattern occurs during the late stages of quiet sleep. The periodic appearance of these two patterns is identifiable in an aEEG, and confirming their presence is crucial. According to a review by Hellströme-Westas, the transition between these two patterns is referred to as sleep–wake cycling (Hellström-Westas and Rosén 2006). However, because the term "wake" in this context does not exclusively refer to the actual awake state, we prefer to use the term "cycling" or "cyclicity" (Kidokoro et al. 2012).

4.2.2 Lower Border

The lower border refers to the lower margin of the aEEG trace. In both term and preterm infants, the lower border exhibits periodic fluctuations. With brain maturation, this lower border rises, reflecting a decrease in the duration of the low-amplitude or flat parts (e.g., interburst intervals) in the cEEG. In most cases of neonatal seizures, the lower border of the aEEG trace increases because the ictal EEG activity occurs continuously and is not interrupted by low-amplitude or flat parts. Therefore, the interpretation of the lower border is of great clinical importance.

4.2.3 Upper Border

The upper border refers to the upper margin of the aEEG trace. Because it is associated with the magnitude of EEG activity, it reflects EEG suppression. Additionally, the upper border is useful for assessing EEG maturity because it tends to

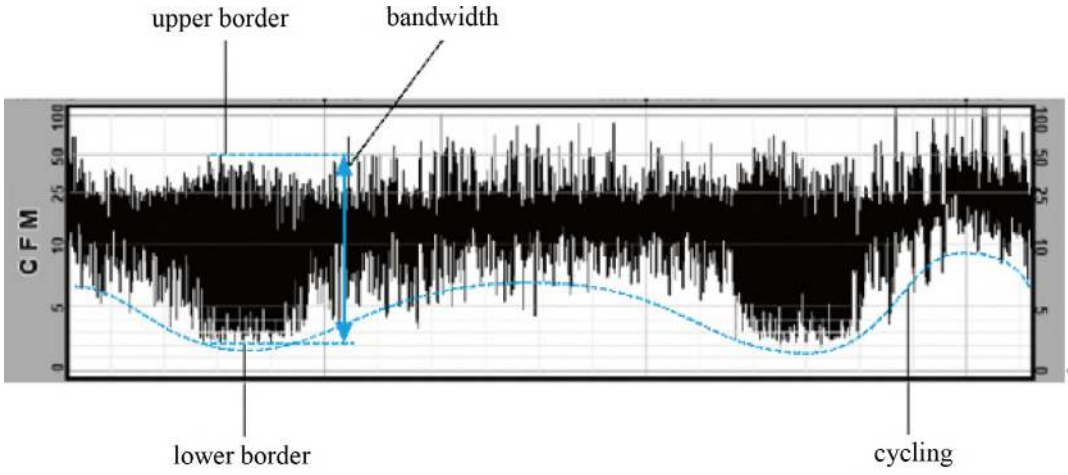

Fig. 18.3 Basics of Interpreting aEEG pattern in the newborn

decrease with increased maturity. This decrease corresponds to the change in the amplitude of the delta wave in the cEEG.

4.2.4 Bandwidth

This term refers to the range between the upper and lower borders, essentially indicating the vertical width of the aEEG trace.

4.3 Interpretation of the Normal Pattern in Term Infants

Figure 18.4 illustrates the normal aEEG pattern of a term infant. In this pattern, the upper and lower aEEG border values are approximately 25 μV and ≥5 μV, respectively. The aEEG amplitude displays a sinusoidal pattern (cycling), reflecting the sleep cycle. This pattern is classified as continuous normal voltage (CNV) in the Hellström-Westas's classification of background activity in term infants (Hellström-Westas and Rosén 2006). Given that most stand-alone aEEG measuring instruments are set to display approximately 3 h/screen, an aEEG in a normal term infant can be interpreted as normal if two to three cycles are confirmed within this range and the lower border value is generally >5 μV.

4.4 aEEG in Preterm Infants

In preterm infants, EEG patterns fluctuate according to the physiological sleep–wake cycle, but this cycle is less distinct than in term infants. Sleep–wake cycling typically remains indistinct until approximately 26 weeks PMA and then gradually becomes more defined, maturing by 37 weeks PMA. Additionally, unlike in normal term infants, physiological flat parts in the tracé discontinu pattern (a discontinuous pattern) are observed during quiet sleep in preterm infants. As maturity progresses, the proportion of the flat part decreases, leading to an increase in the lower border of the aEEG trace; additionally, the trace density in the aEEG, generated every 15 s, becomes denser. By contrast, the amplitude of delta wave decreases with maturity, declining the upper border. Therefore, the bandwidth tends to be narrower with maturation. In summary, the changes with maturation in preterm infants are as follows: (1) cycling is more distinct, (2) the trace density increases, and (3) the upper and lower borders are lower and higher, respectively, in more mature infants, leading to a narrower bandwidth.

4.5 Interpretation of aEEG in Preterm infants

Like the cEEG, which can be used to evaluate brain maturation every 2 weeks, the aEEG can be used to evaluate changes associated with maturation. However, an established method for interpreting aEEG recordings of preterm infants has not yet been developed. In this context, we describe herein our novel reading method based on pattern recognition. The scoring system developed by Burdjalov et al. is also described (Burdjalov et al. 2003).

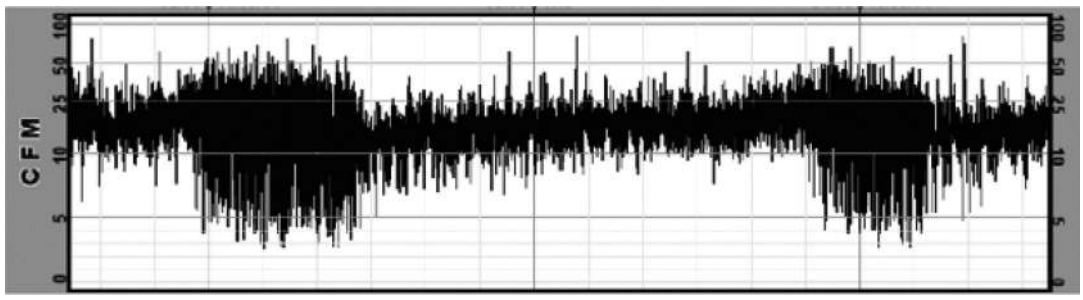

Fig. 18.4 Normal aEEG trace in a 38-week-old infant

4.5.1 Pattern Recognition Method

When interpreting the maturity of an aEEG trace in preterm infants, we employ a pattern recognition method for ease of use in clinical practice. This method is simpler than the scoring system developed by Burdjalov et al. because it focuses on the shape of the trace of the upper and lower borders and does not consider the density of the aEEG as a decision factor. The method is explained below and summarized in Table 18.1.

First, the general progression of aEEG maturation is as follows. At 24 weeks PMA, there is little fluctuation in the lower border (Fig. 18.5a). By 26 weeks PMA, fluctuation in the lower border begins to appear (Fig. 18.5b). From 28 to 30 weeks PMA, the traces of the upper and lower borders show fluctuation of the same direction while the bandwidth remains almost constant, giving the appearance of the entire band moving up and down. However, the cycling of fluctuation is not yet consistent (Fig. 18.5c, d). At 32–34 weeks PMA, the upper border becomes almost flat with little fluctuation; cycling is produced only by fluctuations in the lower border, with the cycling being of a periodic nature (Fig. 18.5e, f). At 36 weeks PMA, the fluctuation of the upper and lower borders moves in opposite directions. When the trace of the upper borders rises, the trace of the lower border falls, and vice versa, leading to a pattern of cycling characterized by alternating narrowing and expanding bandwidth (Fig. 18.5g).

Table 18.1 Interpreting the aEEG pattern in preterm infants

Figure 18.5	Postmenstrual age	Cycling periodicity	Form of cycling	Upper border	Lower border
a	24 weeks	None	No fluctuation	50 μV or more	3 μV or less
b	26 weeks	Little fluctuation	Only the lower border fluctuates		Roughly 5 μV or less
c	28 weeks	Fluctuations are observed, but no constant periodicity	The upper and lower borders move in the same direction.		
d	30 weeks			At minimum 50 μV approx	Maximum value is greater than 5 μV, but generally less than 5 μV
e	32 weeks	A constant periodicity is observed	The trace of the upper border remains constant, and only the trace of the lower border fluctuates The bandwidth at the concave part break of the lower border does not exceed half of the maximum bandwidth	At minimum 25 μV approx	
f	34 weeks		The trace of the upper border remains constant, and only the trace of the lower border fluctuates The bandwidth at the concave part break of the lower border does not exceed half of the maximum bandwidth		
g	36 weeks		The traces of upper and lower borders move in the opposite directions, with the waveforms in reverse phase with each other The convex of the upper border appears earlier than that of the convex of the lower border		Roughly greater than 5 μV, but minimum value does not exceed 5 μV
h	38 weeks			The minimum value is 25 μV or less	Roughly 5 μV or more

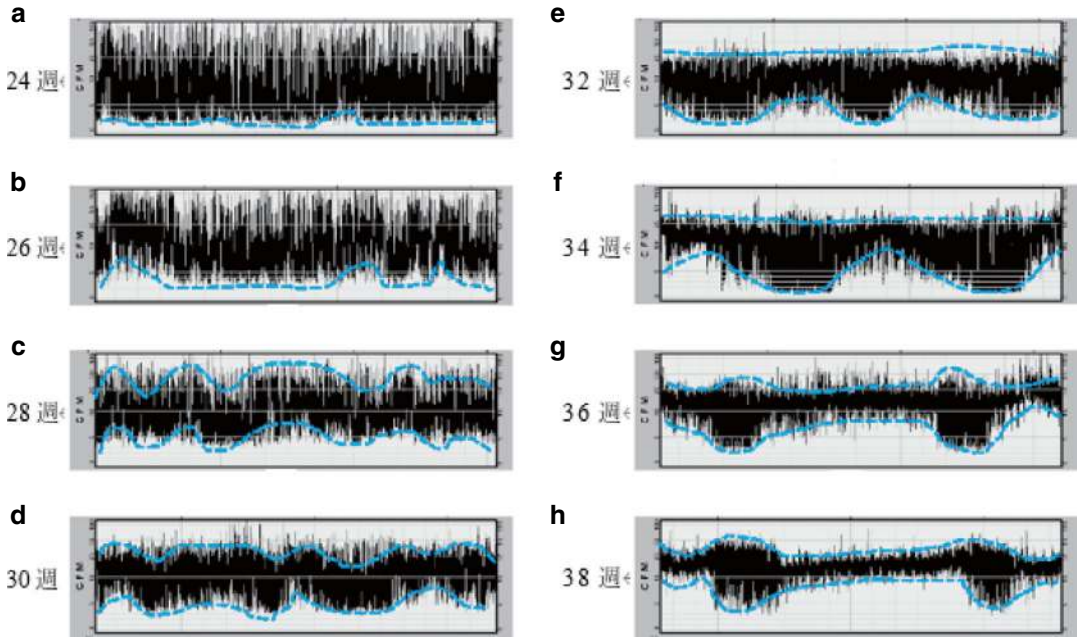

Fig. 18.5 Pattern recognition method. (**a**) The lower border is ≤3 μV, and the upper border is >50 μV. Both borders are flat with little fluctuation, and no cycling is observed. (**b**) The lower border is <5 μV, and the upper border is >50 μV. A slight rise or fall of the lower border is observed. (**c**) The lower border is <5 μV, and the upper border is approximately 50 μV. Both the upper and lower borders move up and down in the same direction. Cycling is present but not yet stable. (**d**) The lower border is <5 μV, and the upper border is approximately 25 μV. Both border values are in phase, with observable cycling and clear periodicity. (**e**) The lower border is <5 μV, and the upper border is approximately 25 μV. The upper border remains constant, and cycling is observed only at the lower border. The curve of the lower border is gentle, and the width of the concave part is often less than half of the widest bandwidth. (**f**) The lower border is increasingly >5 μV, and the upper border is approximately 25 μV. The upper border remains constant, and cycling is observed only at the lower border, indicating periodicity. The convexity of the lower border is steep, and the width of the concavity often exceeds half of the bandwidth. (**g**) The lower border is ≥5 μV, and the upper border is approximately 25 μV. The fluctuation of the upper and lower borders is seen in the opposite direction. (**h**) The lower border value is almost >5 μV, and the upper border is <25 μV. The cycling between the upper and lower borders is in the opposite direction, with clear periodicity

More detailed 2-week difference is as follows. The difference between 28 and 30 weeks PMA is seen in the amplitude of the upper border, which is approximately 50 μV at 28 weeks and approximately 25 μV at 30 weeks (Fig. 18.5c, d). The difference between 32 and 34 weeks PMA lies in the form in fluctuation of the lower border. At 32 weeks, the curve of the lower border is gentle, and the width of the concave part, where the bandwidth narrows, does not exceed half of the width of convex (Fig. 18.5e). At 34 weeks PMA, the curve of the lower border becomes steep, and the bandwidth of concave part becomes narrower than the half of the bandwidth of convex part (Fig. 18.5f). The difference between 36 and 38 weeks PMA is in the amplitude of the upper border. At 36 weeks (Fig. 18.5g), the upper border exceeds 25 μV, but after 38 weeks, it no longer surpasses 25 μV (Fig. 18.5h).

4.5.2 Scoring Method by Burdjalov et al.

In the scoring method developed by Burdjalov et al., the PMA is estimated based on the total score of four items: continuity, cycling, lower border amplitude, and bandwidth (Table 18.2). These items are evaluated using a minimum of 3–4 h of stable recordings. The total scores correspond to specific weeks: a score of 2 points indicates 24–25 weeks, a score of 6 points indicates 27–28 weeks, a score of 8 points indicates 29–30 weeks, a score of 10 points indicates

Table 18.2 Scoring system by Burdjalov et al.

CO	Lower border amplitude
0 discontinuous	0 <3 μV
1 somewhat continuous	1 3–5 μV
2 continuous	2 >5 μV
CY	Bandwidth
0 none	0 bandwidth <15 μV, lower border <5 μV
1 waves 1st appear	1 bandwidth >15 μV, lower border <5 μV
2 not definite	2 bandwidth >20 μV, lower border >5 μV
3 definite cycling, but interrupted	3 bandwidth 15–20 μV, lower border >5 μV
4 definite cycling, not interrupted	4 bandwidth <15 μV, lower border >5 μV
5 regular and mature	
Total score and estimated PMA	
2 points: 24–25 weeks, 6 points: 27–28 weeks, 8 points: 29–30 weeks, 10 points: 31–32 weeks, 11 points: 34 weeks, 13 points: 36–37 weeks	

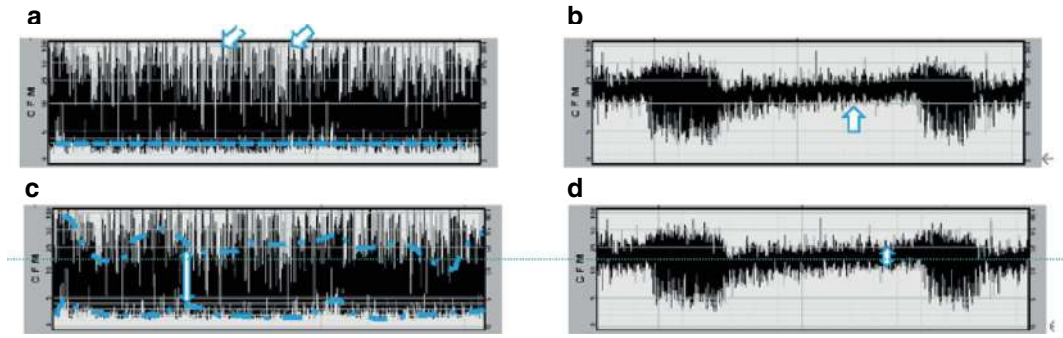

Fig. 18.6 Notes on the scoring method by Burdjalov et al. Continuity is evaluated based on the density of each line generated by the aEEG. The lower border is assessed as the average in the absence of cycling and at the narrowest bandwidth when cycling is observed. When evaluating the bandwidth (**b**), the narrowest part of the trace is evaluated. In this case, the upper and lower border values are evaluated in the area of high density. In this figure, *CO* continuity, *CY* cycling, *LB* lower border amplitude, *B* bandwidth. (**a**) CO: 0. Low density with many gaps between lines (arrows). LB: 1. Because no cycling is observed, the average of the lower border values is evaluated (dotted line). An amplitude of 3 μV is assigned 1 point. (**b**) CO: 2. High density with no gaps between line segments. LB: 2. The lower border value is evaluated in the area where the bandwidth is narrowest (arrow). An amplitude exceeding 5 μV is assigned 2 points. (**c**) B: 1. The part of the trace where the bandwidth is narrowest is evaluated (arrow). The upper and lower border values are evaluated at the point of high density (dotted line). A bandwidth of 20 μV and a lower border of < 5 μV is assigned 1 point. (**d**) B: 4. The area with the narrowest bandwidth is evaluated (arrow). The overall density is high, making it easy to determine the upper and lower border values. A bandwidth of <15 μV is assigned 4 points

31–32 weeks, a score of 11 points indicates 34 weeks, and a score of 13 points indicates 36–37 weeks. A higher score indicates a greater level of maturity. However, there are some points to note when making these assessments. A brief explanation and a sample chart indicating the scoring by weeks are also provided.

Continuity

In an aEEG, continuity manifests as changes in traces and the density of line. High continuity is defined as a state of high density with frequent up-and-down fluctuation. In contrast, Low continuity is defined as a state of low density with little fluctuation of the trace (Fig. 18.6a, b).

Cycling

Cycling refers to the expansion and contraction of the bandwidth of the traces over time. Cycling is observed at approximately 27–28 weeks PMA and is observed stably and periodically from approximately 32 weeks PMA.

Lower Border

If cycling is absent, the average of the lower border of the aEEG trace should be taken. When cycling is present, the narrowest part of the bandwidth is evaluated. After 28 weeks PMA, when cycling can be determined, the score is typically 2 points (Fig. 18.6a, b).

Bandwidth

The bandwidth of the narrowest part of the aEEG trace is measured, typically where the lower border shows the greatest rise. Both the upper and lower borders are evaluated in areas of high trace density (Fig. 18.6c, d). The scoring of an aEEG for each week is depicted in the samples.

5 24-week aEEG Recording

Gestational age: 24 weeks 3 days, birth weight: 624 g, age: 3 days, PMA: 24 weeks 6 days

Recording instrument: CFM-6000, electrode position: C3–C4.

The lower border is ≤3 μV, and the upper border is >50 μV. Both the upper and lower borders are flat with little fluctuation, and no periodicity is observed (Fig. 18.7).

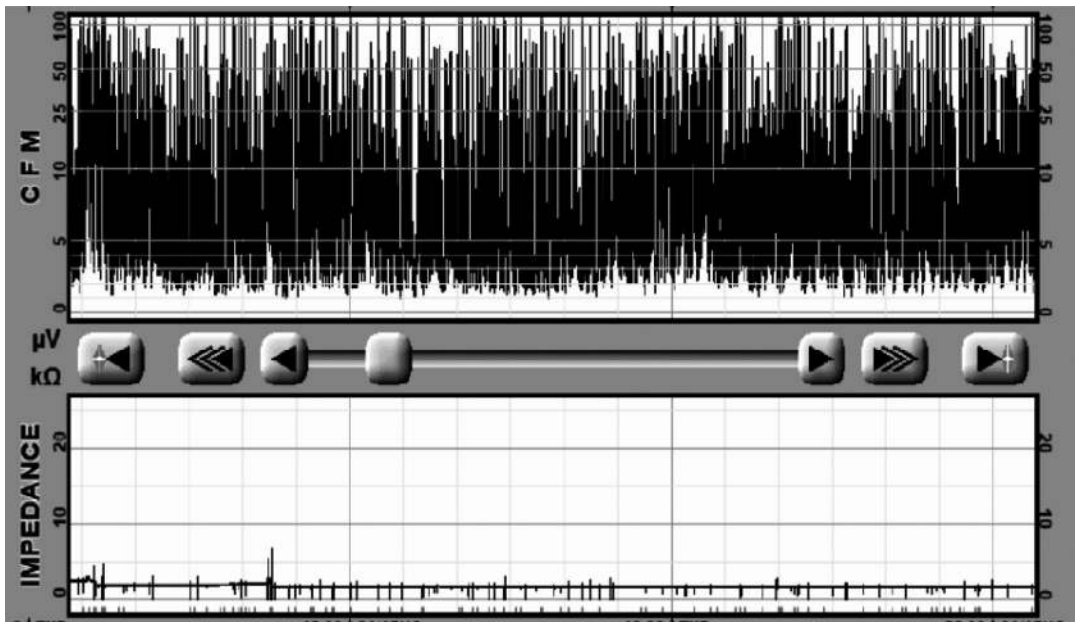

Fig. 18.7 24-week aEEG recording

6 26-week aEEG Recording

Gestational age: 24 weeks 3 days, birth weight: 624 g, age: 13 days, PMA: 26 weeks 2 days.

Recording device: CFM-6000, electrode position: C3–C4.

The lower border is <5 μV, and the upper border is >50 μV. A slight rise and fall in the lower border are observed (Fig. 18.8).

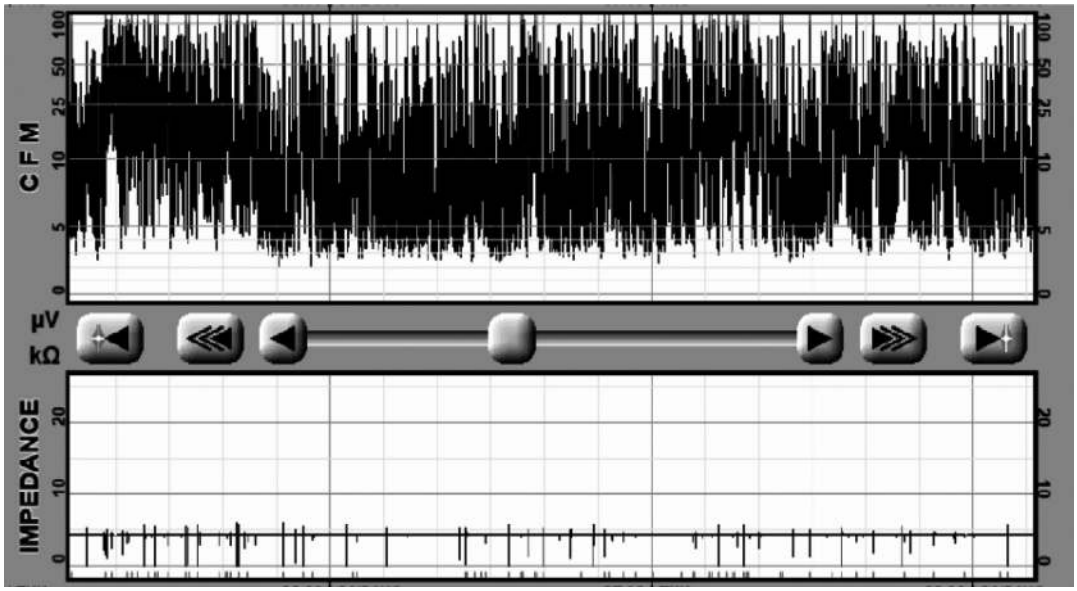

Fig. 18.8 26-week aEEG recording

7 28-week aEEG Recording

Gestational age: 24 weeks 3 days, birth weight: 624 g, age: 26 days, PMA: 28 weeks 1 day.

Recording device: CFM-6000, electrode position: C3–C4.

The lower border is <5 μV, and the upper border is approximately 50 μV. Both the upper and lower border of the trace begin to move in the same direction. Cycling is present, but stable periodicity has not yet been established (Fig. 18.9).

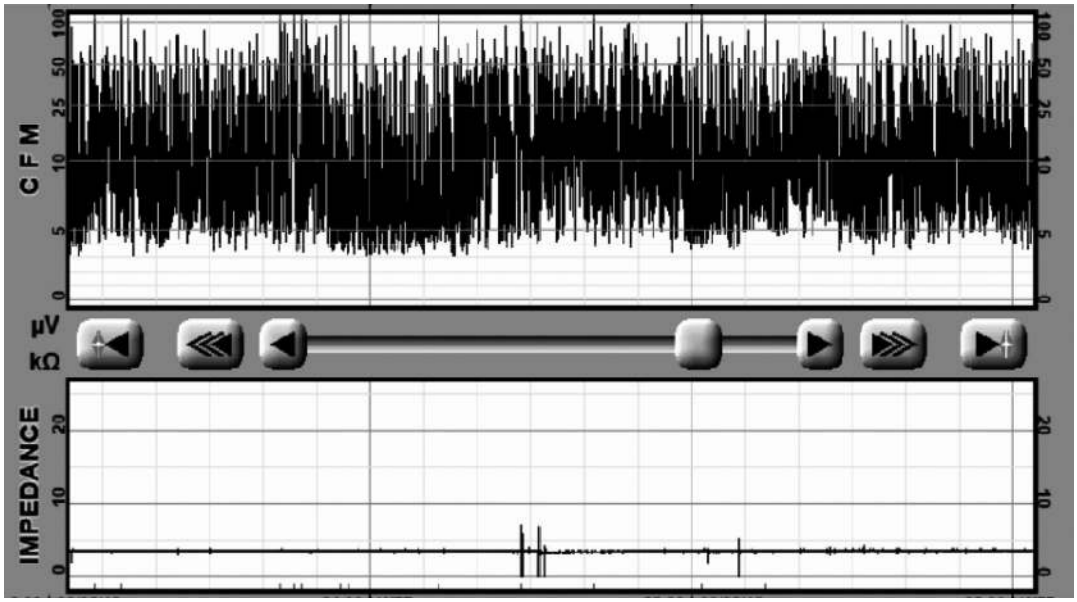

Fig. 18.9 28-week aEEG recording

8 30-week aEEG Recording

Gestational age: 27 weeks 1 day, birth weight: 1106 g, age: 22 days, PMA: 30 weeks 2 days.

Recording device: CFM-6000, electrode position: C3–C4.

The lower border is <5 μV and the upper border is approximately 25 μV. Both the upper and lower borders move in the same direction, cycling is observed, and the periodicity has become distinct (Fig. 18.10).

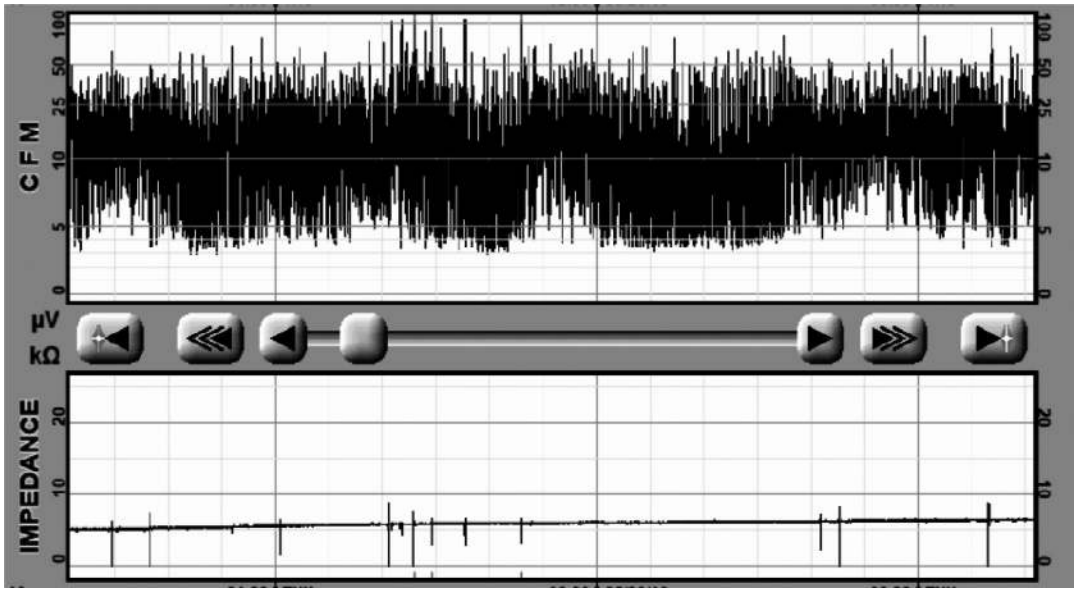

Fig. 18.10 30-week aEEG recording

9 32-week aEEG Recording

Gestational age: 28 weeks 5 days, birth weight: 1376 g, age: 24 days, PMA: 32 weeks 1 day.

Recording device: CFM-6000, electrode position: C3–C4.

The lower border is <5 μV and the upper border is approximately 25 μV. The upper border is constant, and cycling is observed only at the lower border, indicating periodicity. The curve of the lower border is gentle, and the width of the concave part is often less than half the bandwidth (Fig. 18.11).

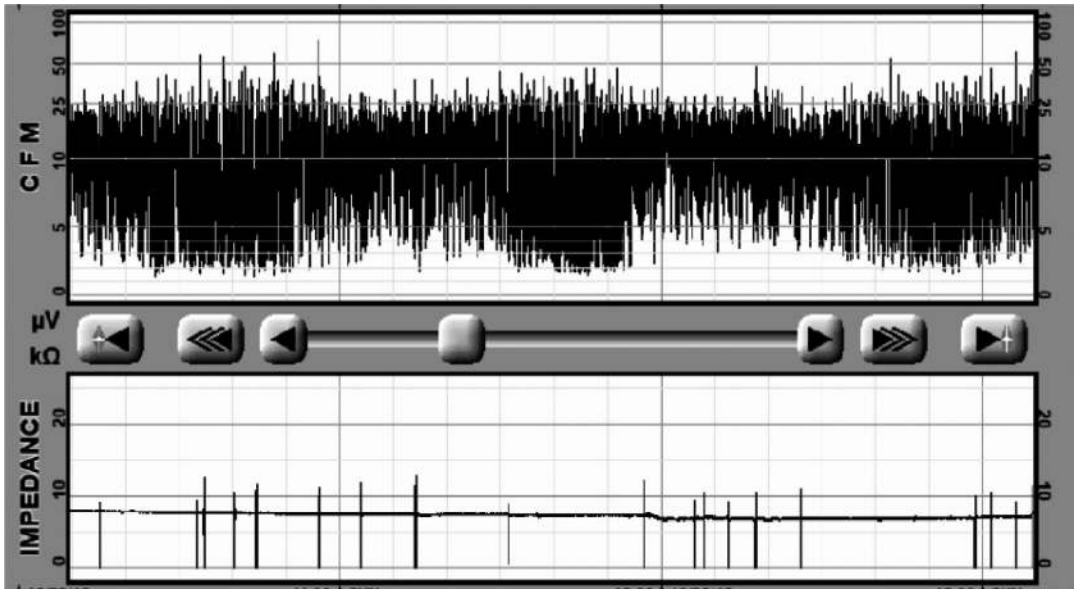

Fig. 18.11 32-week aEEG recording

10 34-week aEEG Recording

Gestational age: 27 weeks 4 days, birth weight: 1032 g, age: 47 days, PMA: 34 weeks 2 days.

Recording device: CFM-6000, electrode position: C3–C4.

The lower border is increasingly >5 μV, and the upper border is approximately 25 μV. The upper border is constant, and cycling is observed only at the lower border, indicating periodicity. The convexity of the lower border is steep, and the width of the concavity often exceeds half the bandwidth (Fig. 18.12).

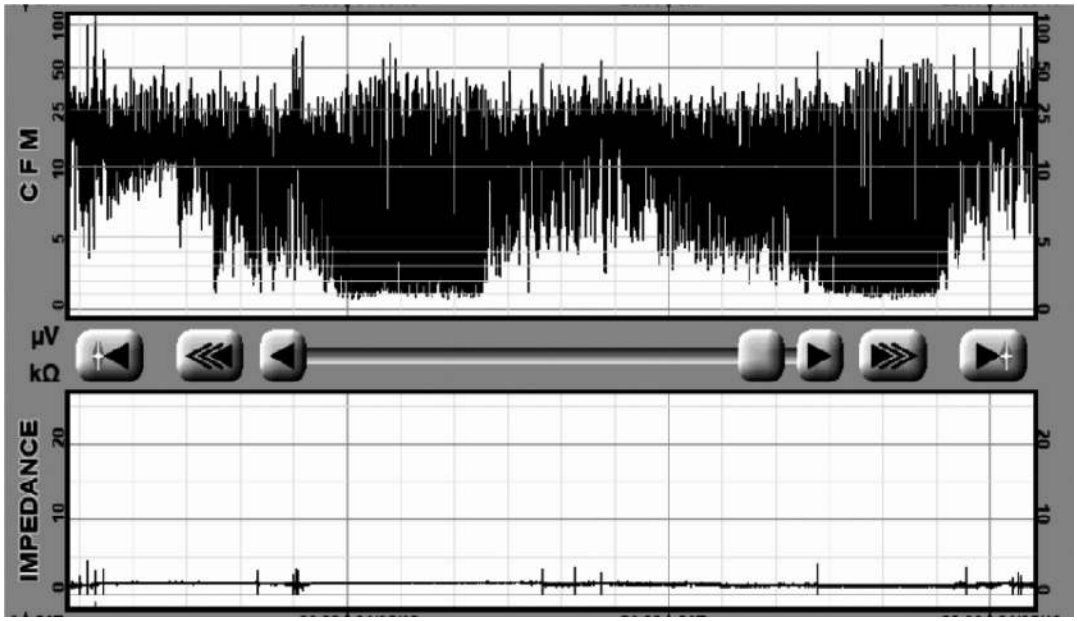

Fig. 18.12 34-week aEEG recording

11 36-week aEEG Recording

Gestational age: 34 weeks 6 days, birth weight: 1816 g, age: 11 days, PMA: 36 weeks 3 days.

Recording equipment: CFM-6000, electrode position: C3–C4.

The lower border is ≥5 μV, and the upper border is approximately 25 μV. The upper and lower borders move in the opposite direction with clear periodicity (Fig. 18.13).

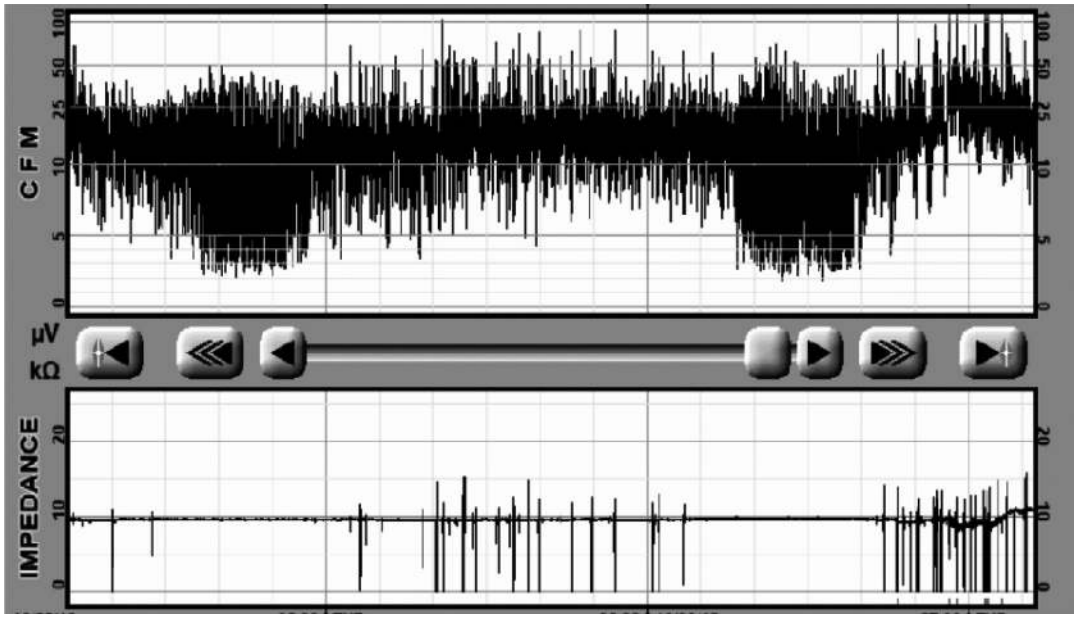

Fig. 18.13 36-week aEEG recording

12 38-week aEEG Recording

Gestational age: 36 weeks 5 days, birth weight: 2508 g, age: 8 days, PMA: 38 weeks 1 day.

Recording device: CFM-6000, electrode position: C3–C4.

The lower border is >5 μV and the upper border is <25 μV. The fluctuation of the upper and lower borders occurs in the opposite direction, with clear periodicity. The convexity of the upper border appears earlier than that of the lower border (Fig. 18.14).

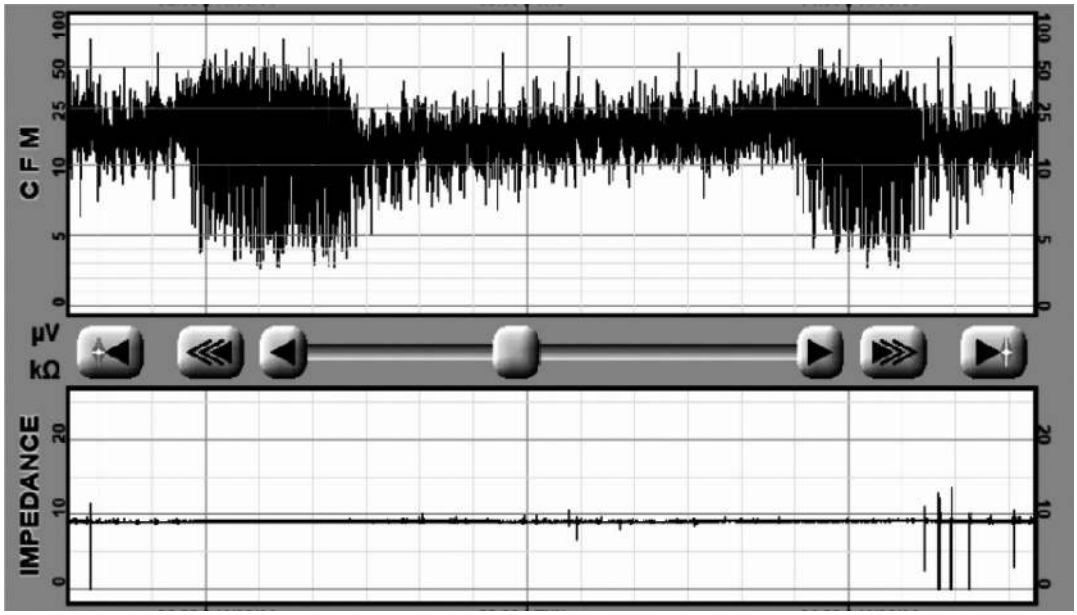

Fig. 18.14 38-week aEEG recording. Gestational age: 36 weeks 5 days, birth weight: 2508 g, age: 8 days, PMA: 38 weeks 1 day. Recording device: CFM-6000, electrode position: C3–C4. The lower border is >5 μV and the upper border is <25 μV. The fluctuation of the upper and lower borders occurs in the opposite direction, with clear periodicity. The convexity of the upper border appears earlier than that of the lower border

References

Burdjalov VF, Baumgart S, Spitzer AR. Cerebral function monitoring: a new scoring system for the evaluation of brain maturation in neonates. Pediatrics. 2003;112(4):855–61.

Hellström-Westas L, Rosén I. Continuous brain-function monitoring: state of the art in clinical practice. Semin Fetal Neonatal Med. 2006;11(6):503–11.

Kidokoro H, Inder T, Okumura A, Watanabe K. What does cyclicity on amplitude-integrated EEG mean? J Perinatol. 2012;32(8):565–9.

19 Acute-Stage Abnormalities on aEEG

Yuichiro Sugiyama and Tetsuo Kubota

1 Abnormal Patterns in Term Infants

EEG suppression occurs when neuronal activity decreases secondary to central nervous system damage, which may be associated with various diseases. Generally, more severe disease is associated with more pronounced EEG suppression. aEEG background activity is also used to assess the degree of this suppression. However, assessing chronic-stage abnormalities, such as disorganized patterns evident in a conventional EEG, is challenging in an aEEG, especially when relying on visual analysis. The primary purpose of an aEEG is to evaluate acute-stage abnormalities; i.e., whether there is a certain level of suppression of current brain activity. It is also important to know the limitations of aEEG.

2 Abnormal aEEG Background Activity in Term Infants

The classification of aEEG background activity in term infants, widely used today, is based on the classification proposed by Hellström-Westas et al. (Fig. 19.1). This classification categorizes aEEG patterns into the following five distinct categories.

2.1 Continuous Normal-Voltage (CNV) Pattern

The upper border of an aEEG trace ranges from 10 to 25 (up to 50) μV, while the lower border ranges from 7 to 10 μV (generally exceeding 5 μV). Regular cycling is observable in the lower border of aEEG traces.

2.2 Discontinuous Normal-Voltage (DNV) Pattern

When brain activity is mildly reduced, the upper border stays within the normal range, but the lower border decreases. A DNV pattern, as defined by Hellström-Westas et al., is characterized by a lower border of <5 μV and may or may not include cycling.

Y. Sugiyama (✉)
Department of Pediatrics, Japanese Red Cross Aichi Medical Center Nagoya Daiichi Hospital, Nagoya, Japan
e-mail: sugiyama-les400@nagoya-u.jp

T. Kubota
Department of Pediatrics, Anjo Kosei Hospital, Anjo, Japan
e-mail: t-kubota@kosei.anjo.aichi.jp

A. Okumura, H. Kidokoro (eds.), *Neonatal EEG: Atlas and Interpretation*,
https://doi.org/10.1007/978-981-96-0726-6_19

a
Continuous normal voltage (CNV) pattern

b
Discontinuous normal voltage (DNV) pattern

c
Burst-suppression plus (BS+) pattern

d
Burst-suppression minus (BS-) pattern

e
Continuous low voltage (CLV) pattern

f
Flat tracing (FT) pattern

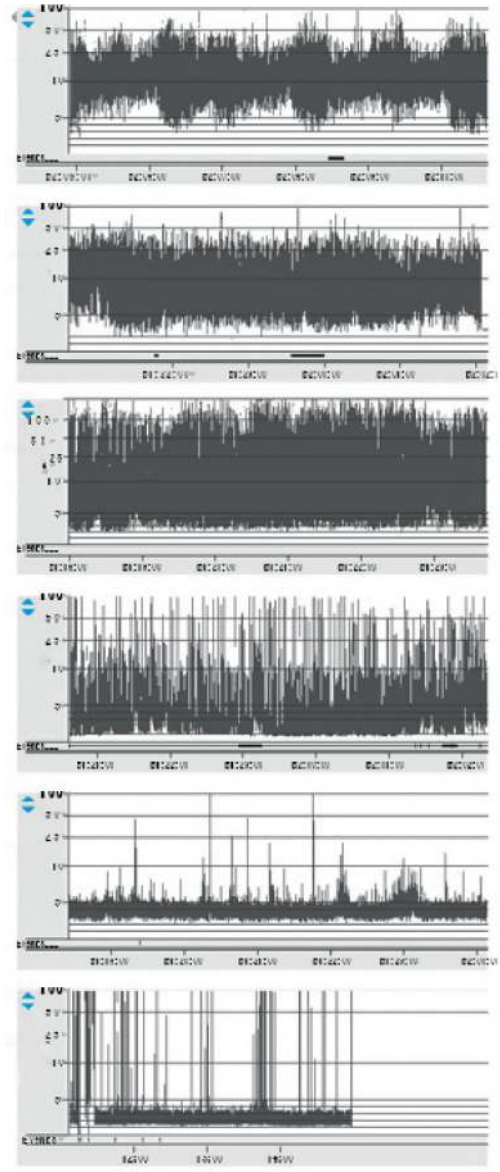

Fig. 19.1 Classification of aEEG background activity in term infants. Brain function shows a higher degree of suppression with progression from A to F (Courtesy of Dr. Rosen I). (**a**) Continuous normal voltage (CNV) pattern. (**b**) Discontinuous normal voltage (DNV) pattern. (**c**) Burst-suppression plus (BS+) pattern. (**d**) Burst-suppression minus (BS−) pattern

2.3 Burst-Suppression (BS) Pattern

As the EEG continuity decreases, the EEG shifts from a DNV pattern to a BS pattern. In this pattern, the lower border further decreases to 0–1 μV, and the upper border also intermittently decreases. This pattern results from alternating burst and suppression activities in the EEG, where the bursts are periodic, and their upper border intermittently exceeds 25 μV. High aEEG density with numerous bursts (>100 bursts/h) is classified as BS+, while lower aEEG density (<100 bursts/h) is classified as BS−.

2.4 Continuous Low-Voltage (CLV) Pattern

When brain activity is significantly suppressed, bursts are rarely observed, and the upper border consistently remains low (≤ 5 μV).

2.5 Flat Trace (FT) Pattern

The upper border of the potential is close to 0, ranging from 0 to 5 μV. Correspondingly, the original EEG waveform shows no activity and appears flat.

3 Background Abnormalities and Their Interpretation in Neonatal Asphyxia of Term Infants

An aEEG is frequently used for term infants with neonatal asphyxia. With the standardization of therapeutic hypothermia, the predictive value of the aEEG has changed. Before therapeutic hypothermia became popular, most reports suggested that outcomes were related to the BS pattern or more severe patterns, or to the loss of cycling within the first 6–12 h of life. However, in the era of hypothermia, it has become clear that the positive predictive value of poor neurological outcomes depends on the time after birth until the recovery of suppressed background activity. A systematic review performed in 2016 showed that, in neonates with a gestational age of ≥35 weeks, the positive predictive value of neurological abnormalities in infants with aEEG abnormalities after 6 h of age remained almost unchanged in the non-hypothermia group (Del Río et al. 2016). In the hypothermia group, however, the positive predictive value for poor neurological outcomes increased with the delayed recovery of aEEG abnormalities (Fig. 19.1). This review classified an aEEG pattern of BS/CLV/FT or an upper border of ≤10 μV as abnormal, with outcomes being death, paralysis, or moderate or severe developmental delay.

4 Abnormal aEEG in Preterm Infants

The criteria for identifying abnormal aEEG findings in preterm infants are not yet well established. In preterm infants, acute brain injury can cause cEEG suppression, characterized by an increase in flat parts and a decrease in amplitude. While an aEEG can detect a decrease in amplitude, accurately reading the amplitude becomes challenging unless it is severely suppressed. As a result, aEEG interpretation often relies on the loss of cycling as an indicator, rather than a decrease in amplitude. For example, reports suggest that the presence or absence of cyclicity immediately after birth is related to neurological outcomes (Kidokoro et al. 2010), reflecting prenatal and postnatal insults. Furthermore, loss of cyclicity can also result from various other factors, such as jaundice, infection, and respiratory failure. Figure 19.2 shows aEEG findings before, during, and after the onset of late-onset circulatory collapse.

As a brain function monitoring tool, an aEEG can determine objectively the period from which brain function began to deteriorate. This information is valuable in assessing which clinical management approaches may have contributed to or worsened the infant's brain function.

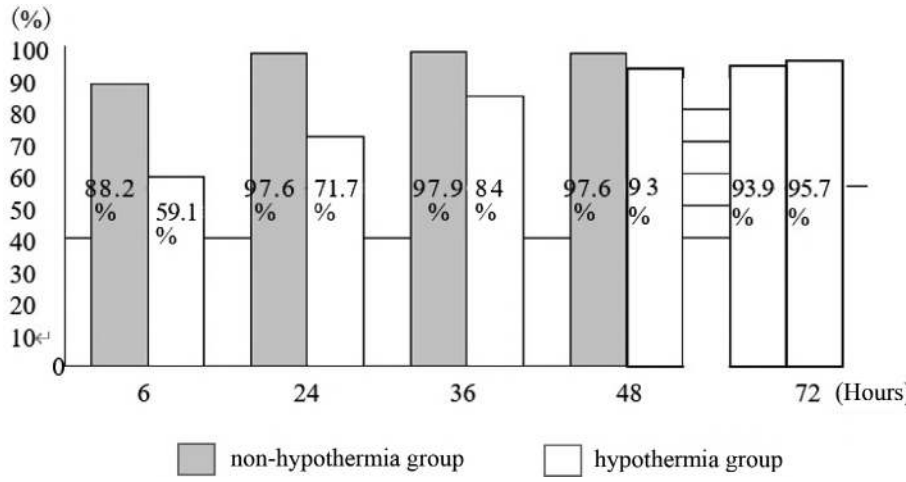

Fig. 19.2 aEEG background abnormalities at each recording time point and positive predictive values of neurological abnormalities in asphyxiated neonates

5 Discontinuous Normal-Voltage (DNV) Pattern

Gestational age: 37 weeks 3 days, birth weight: 3145 g, age: 6 days.

Recording equipment: NicoletOne, electrode positions: C3–P3, C4–P4, and C3–C4.

The patient underwent therapeutic hypothermia for neonatal asphyxia resulting from placental abruption and neonatal hypoxic-ischemic encephalopathy (Sarnat stage 3). After therapeutic hypothermia, the infant is able to breathe spontaneously and responds to stimulation, but oral feeding is slow.

Cycling is present in the aEEG trace, but its periodicity is relatively poor. The lower border consistently remains at 5 μV, leading to the conclusion that the pattern is DNV (Fig. 19.3).

7

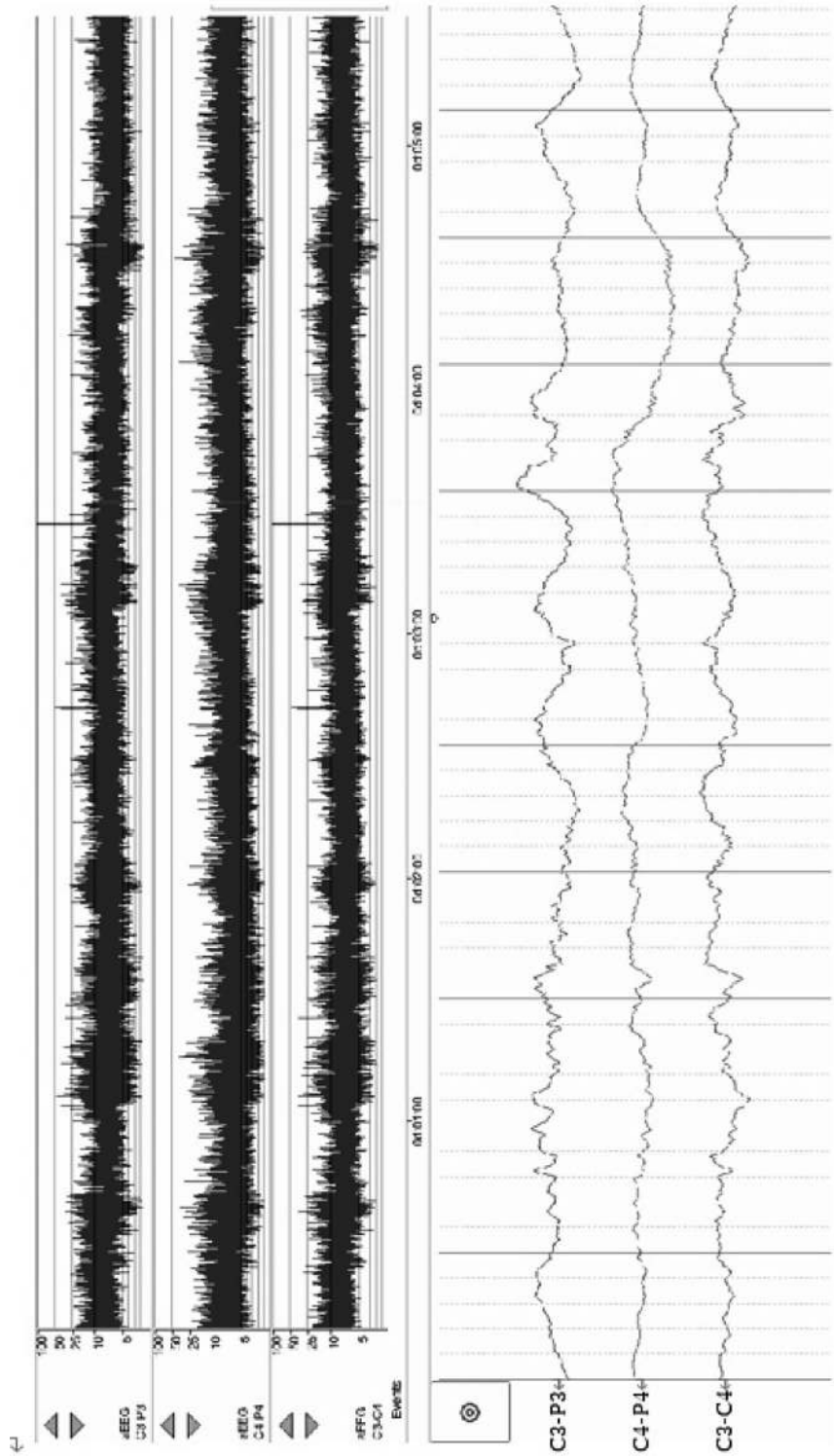

Fig. 19.3 Discontinuous normal voltage (DNV) pattern

6 BS Pattern

Gestational age: 37 weeks 3 days, birth weight: 3145 g, age: 0 days.

Recording equipment: NicoletOne, electrode positions: C3–P3, C4–P4, and C3–C4.

This case corresponds to that in Fig. 19.3. The patient had severe neonatal hypoxic-ischemic encephalopathy and lacked spontaneous respiration; therapeutic hypothermia was performed. The aEEG recording was obtained 6 h after birth.

The lower border is approximately 1 μV, and the upper border only intermittently rises above 25 μV. An extremely low density indicates significantly reduced continuity (Fig. 19.4).

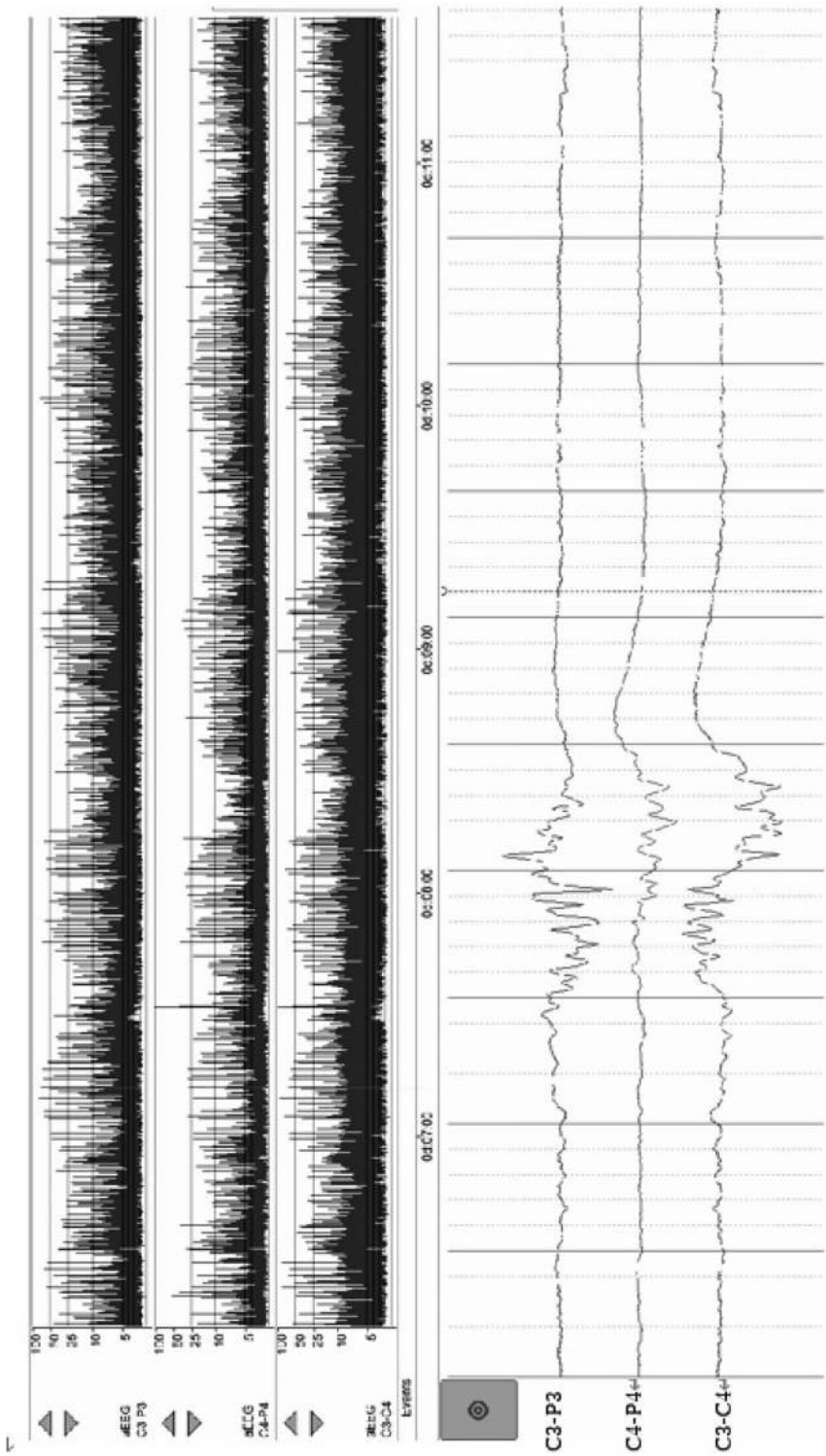

Fig. 19.4 Burst-suppression (BS) pattern

Continuous Low-Voltage (CLV) Pattern

Gestational age: 39 weeks 5 days, birth weight: 3531 g, age: 1 day.

Recording equipment: NicoletOne, electrode positions: C3–P3, C4–P4, and C3–C4.

The infant was born without spontaneous respiration because of meconium peritonitis and had been hypotensive since birth. Because of the infant's critical condition, neither surgical treatment nor hypothermic therapy could be administered. The aEEG data were obtained 36 h after birth.

The lower border of the aEEG was approximately 1 μV, and the upper border was almost consistently <5 μV. This pattern is interpreted as CLV (Fig. 19.5).

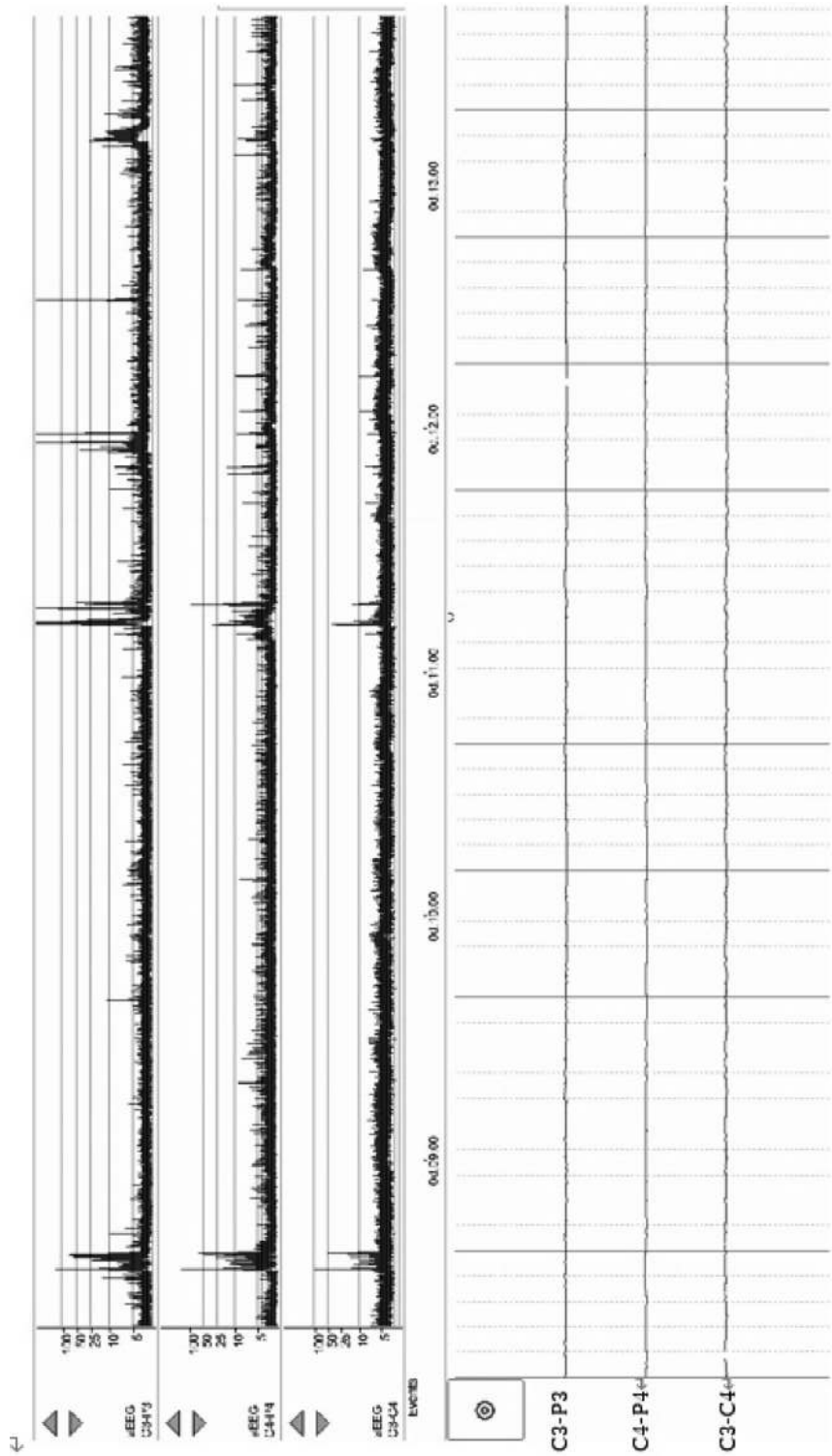

Fig. 19.5 Continuous low-voltage (CLV) pattern

8 Absent Cyclicity Associated with Late-Onset Circulatory Collapse

Gestational age: 28 weeks 0 days, birth weight: 940 g, age: 15–18 days, PMA: 30 weeks 2–5 days.

Recording instrument: CFM-OBM, electrode position: C3–C4.

A preterm infant, born at 28 weeks via emergency cesarean section due to preterm labor and cervical incompetence, being clinically stable on continuous positive airway pressure with good feeding tolerance. However, from day 16 (PMA: 30 weeks 3 days), the infant developed a decrease in urine output and blood pressure without obvious triggers. The circulation collapse resolved with corticosteroid administration. Continuous aEEG recording allowed for the monitoring of the patient's condition before, during, and after the onset of illness. On day 15 (the day before onset), both the upper and lower borders of the aEEG traces were consistent, indicative of a typical 30-week aEEG trace. The cycling, which had been poor before the decrease in urine output noticed on day 16, had returned by day 18 (post-recovery). This loss of cyclicity in the aEEG indicates a decrease or loss of continuity in the cEEG, a sign of suppressed brain activity in preterm infants (Fig. 19.6).

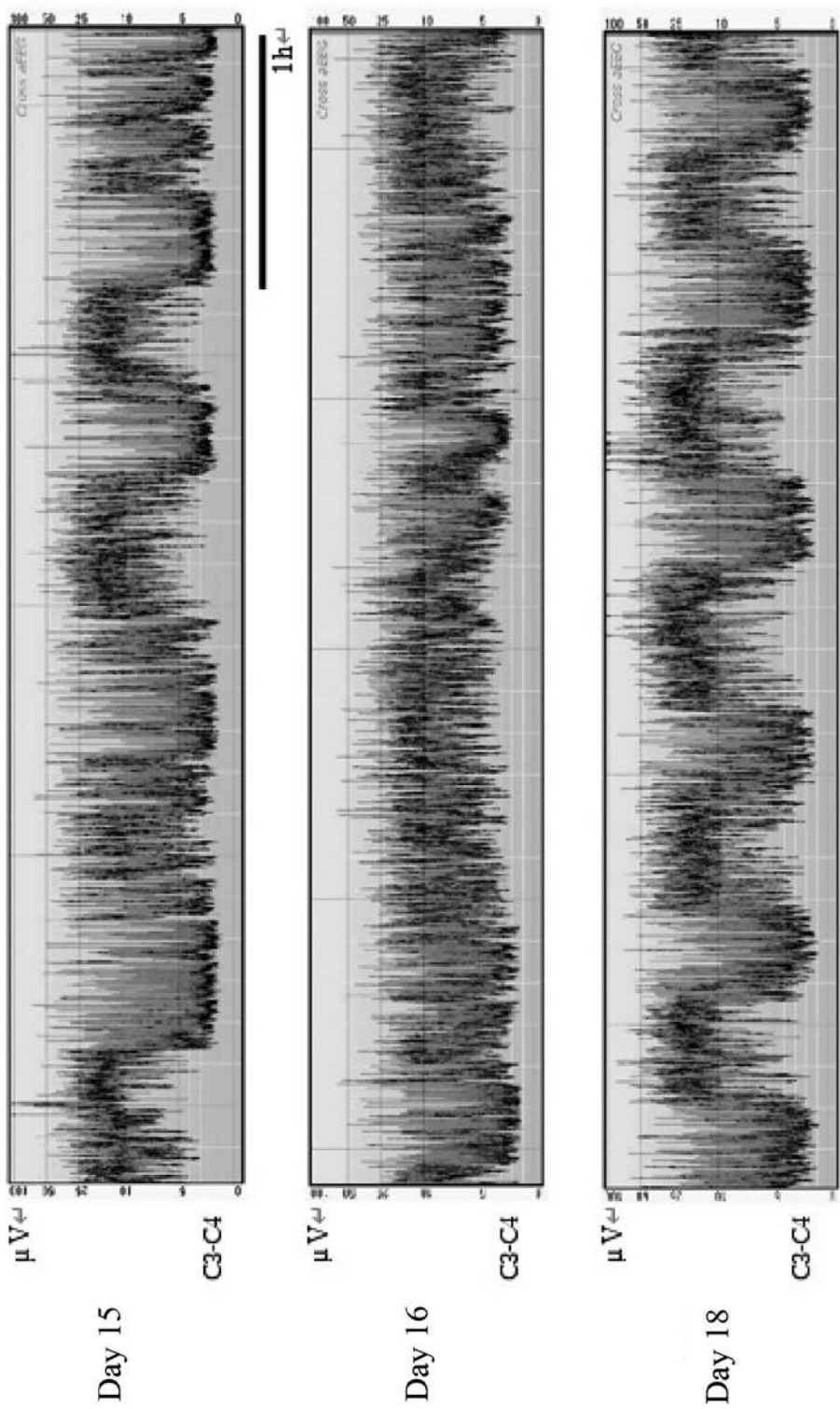

Fig. 19.6 Absent cyclicity associated with late-onset circulatory collapse

References

Del Río R, Ochoa C, Alarcon A, Arnáez J, Blanco D, García-Alix A. Amplitude integrated electroencephalogram as a prognostic tool in neonates with hypoxic-ischemic encephalopathy: a systematic review. PLoS One. 2016;11(11):e0165744. https://doi.org/10.1371/journal.pone.0165744. PMID: 27802300; PMCID: PMC5089691.

Kidokoro H, Kubota T, Hayashi N, Hayakawa M, Takemoto K, Kato Y, Okumura A. Absent cyclicity on aEEG within the first 24 h is associated with brain damage in preterm infants. Neuropediatrics. 2010;41(6):241–5.

Neonatal Seizures on aEEG

20

Takeshi Suzuki and Tetsuo Kubota

1 The Utility of aEEG in the Management of Neonatal Seizures

The most important feature of neonatal seizures is the difficulty of identifying seizures based solely on clinical manifestations even by experienced physicians (Murray et al. 2008; Aileen et al. 2009). Many physicians have probably encountered cases where it is challenging to confirm a true neonatal seizure, even after receiving a report of a "seizure" from nursing staff. On the other hand, there are cases that present only with symptoms such as apnea, which are unlikely to be seizures. Moreover, there are subclinical seizures that are not accompanied by any clinical symptoms.

Early and accurate diagnosis of neonatal seizures not only enables prompt intervention with antiseizure medications but can also aid the early identification of underlying conditions that cause acute symptomatic seizures. Both of these factors are of great clinical significance because they may improve the long-term developmental outcome of the infant. However, as mentioned, diagnosis of neonatal seizures based on clinical manifestations alone is challenging. In clinical practice, patients considered at high risk of neonatal seizures (e.g., with severe neonatal asphyxia, cardiac malformations, various pre- and postoperative conditions, severe infections, or metabolic diseases) often undergo intensive treatment, including respiratory and circulatory management, limiting the availability of diagnostic tests at the bedside. The gold standard for diagnosis is EEG. In a previous report, NICU staff were only about 50% accurate when identifying neonatal seizures from video recordings taken during clinical events, reaffirming that EEG is required for definitive diagnosis or exclusion of neonatal seizures (Aileen et al. 2009). Conventional EEG (cEEG) is useful in that it permits noninvasive repeated assessments. However, access to neonatal EEG varies greatly among facilities; many are unable to perform tests on every day. Furthermore, monitoring of neonatal seizures often requires long-term continuous recording. If the monitoring results are to be incorporated into real-time treatments, not only specialists but also general pediatricians, neonatologists, and bedside nurses must be able to recognize seizures quickly. Currently, amplitude-integrated EEG (aEEG) is widely used in many institutions to evaluate neonatal seizures. aEEG employs only a small number of electrodes and can be easily applied by on-duty doctors or nurses without specialized training. aEEG is

T. Suzuki (✉)
Department of Pediatrics, Okazaki City Hospital, Okazaki, Japan

T. Kubota
Department of Pediatrics, Anjo Kosei Hospital, Anjo, Japan
e-mail: t-kubota@kosei.anjo.aichi.jp

A. Okumura, H. Kidokoro (eds.), *Neonatal EEG: Atlas and Interpretation*,
https://doi.org/10.1007/978-981-96-0726-6_20

suitable for long-term monitoring and offers several advantages in terms of management of neonatal seizures, such as relatively easy seizure recognition and the ability to view trends over time on a single screen, as detailed below.

However, it must be acknowledged that, compared to cEEG, monitoring with only aEEG may overlook some seizures, or, may misinterpret other phenomena as seizures (Divyen et al. 2008; Evans et al. 2010). Therefore, it is important to understand the limitations of monitoring using only aEEG when managing neonatal seizures, and to employ cEEG along with aEEG when necessary. The relationship between these two modalities is complementary in terms of their limitations; this is similar to the relationship between bedside electrocardiogram (ECG) monitoring and 12-lead ECG. Just as 12-lead ECG is essential for detailed classification of arrhythmias and definitive diagnosis of myocardial infarction, 8-channel cEEG is necessary for accurate diagnosis and detailed evaluation of neonatal seizures.

2 Neonatal Seizures on aEEG

The ictal findings of neonatal seizures on cEEG are characterized by repetitive, stereotyped rhythmic waveforms (Fig. 20.1). The frequencies and amplitudes of these waveforms typically increase at the onset of the seizure and decrease toward the end. With this in mind, we can look at what neonatal seizures look like in aEEG. In aEEG, one vertical line represents the lower border (lower line) and the upper border (upper line) of the amplitude over a 15-s cEEG period. When evaluating a seizure on aEEG, the focus is on the lower border. As the stereotyped waveform appears during the seizure, the lower border rises compared with interictal period (Fig. 20.2). After the seizure finished EEG activity is suppressed transiently. Eventually, the lower border shows a transient rise followed by brief falls (Fig. 20.3). In cases with repetitive seizures, aEEG exhibits a sawtooth-like pattern characterized by the repeated rises of the lower border (Fig. 20.4). Thus, the aEEG pattern changes associated with

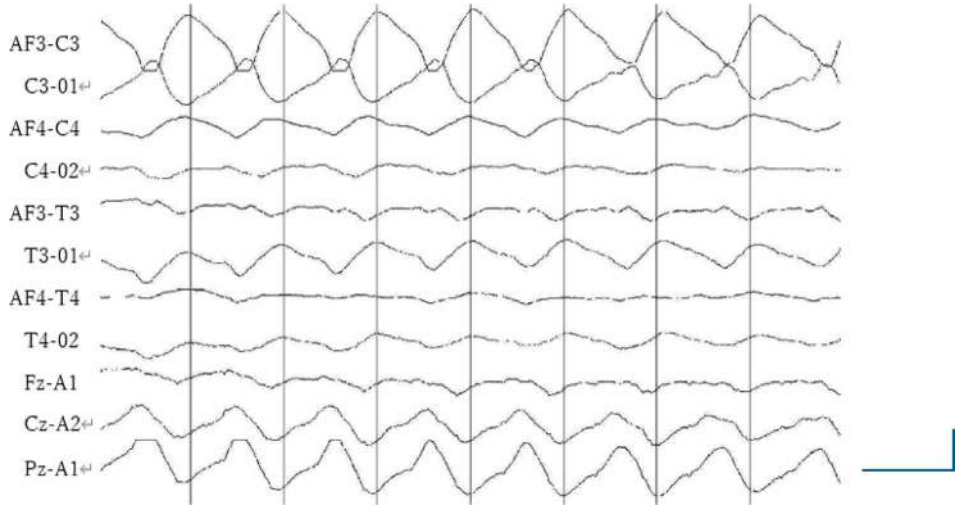

Fig. 20.1 An ictal EEG of a neonate. Neonatal seizures present on cEEG as repetitive, stereotyped, rhythmic waveforms. The figure shows typical seizure activity, characterized by rhythmic delta waves with a frequency of around 1 Hz at C3

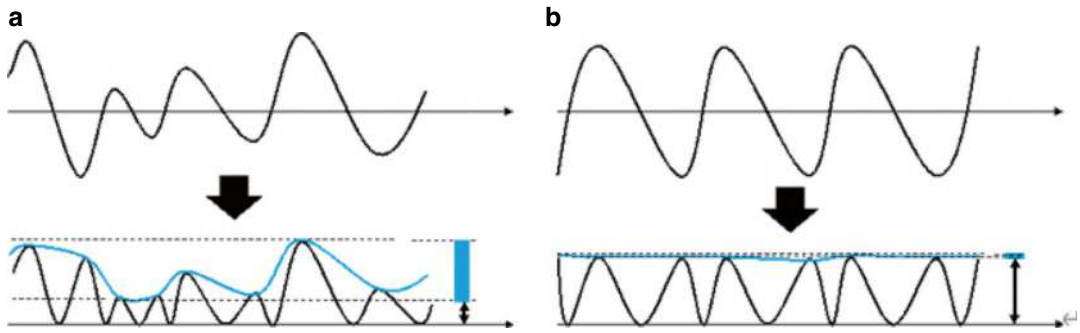

Fig. 20.2 Schematic comparison of EEG during non-ictal and ictal events. (**a**) Conversion of cEEG signal (upper panel) to aEEG bands (lower panel) during a non-ictal event. As the waves vary in size, the lower border (shown in the figure) is low, reflecting the presence of low-amplitude waves. (**b**) Conversion of cEEG signal (upper panel) to aEEG bands during ictal events (lower panel). As stereotyped waves in consistent size and shape repeat during the ictal event, the lower border (as depicted in the figure) is higher than that during the interictal period, and the bandwidth becomes narrower

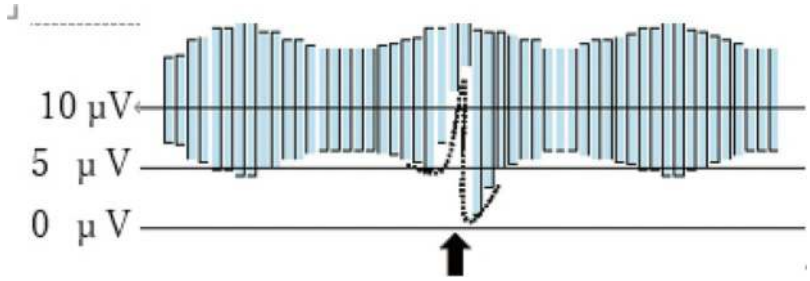

Fig. 20.3 The aEEG schema during an isolated neonatal seizure. During a seizure, the stereotyped waveform causes the lower border of the aEEG trace to rise compared to the interictal period. EEG activity is transiently suppressed after the seizure stops. Consequently, the lower border shows a transient rise followed by a brief fall

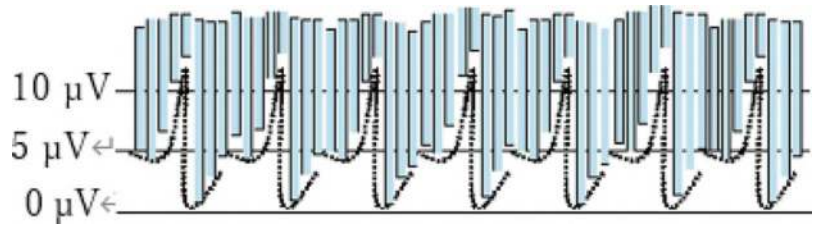

Fig. 20.4 The aEEG schema during repetitive seizures. In cases of repetitive seizures, the aEEG exhibits repeated rises of the lower border, known as a sawtooth-like pattern

neonatal seizures are distinct and easily recognizable. aEEG is also useful to compare seizure frequencies before and after administration of medication, as aEEG allows visual recognition of seizure frequency over a specific time period. Figures 20.5, 20.6, 20.7, 20.8, 20.9, 20.10, 20.11, 20.12, 20.13, 20.14, 20.15, 20.16, and 20.17 show typical aEEG findings of neonatal seizures.

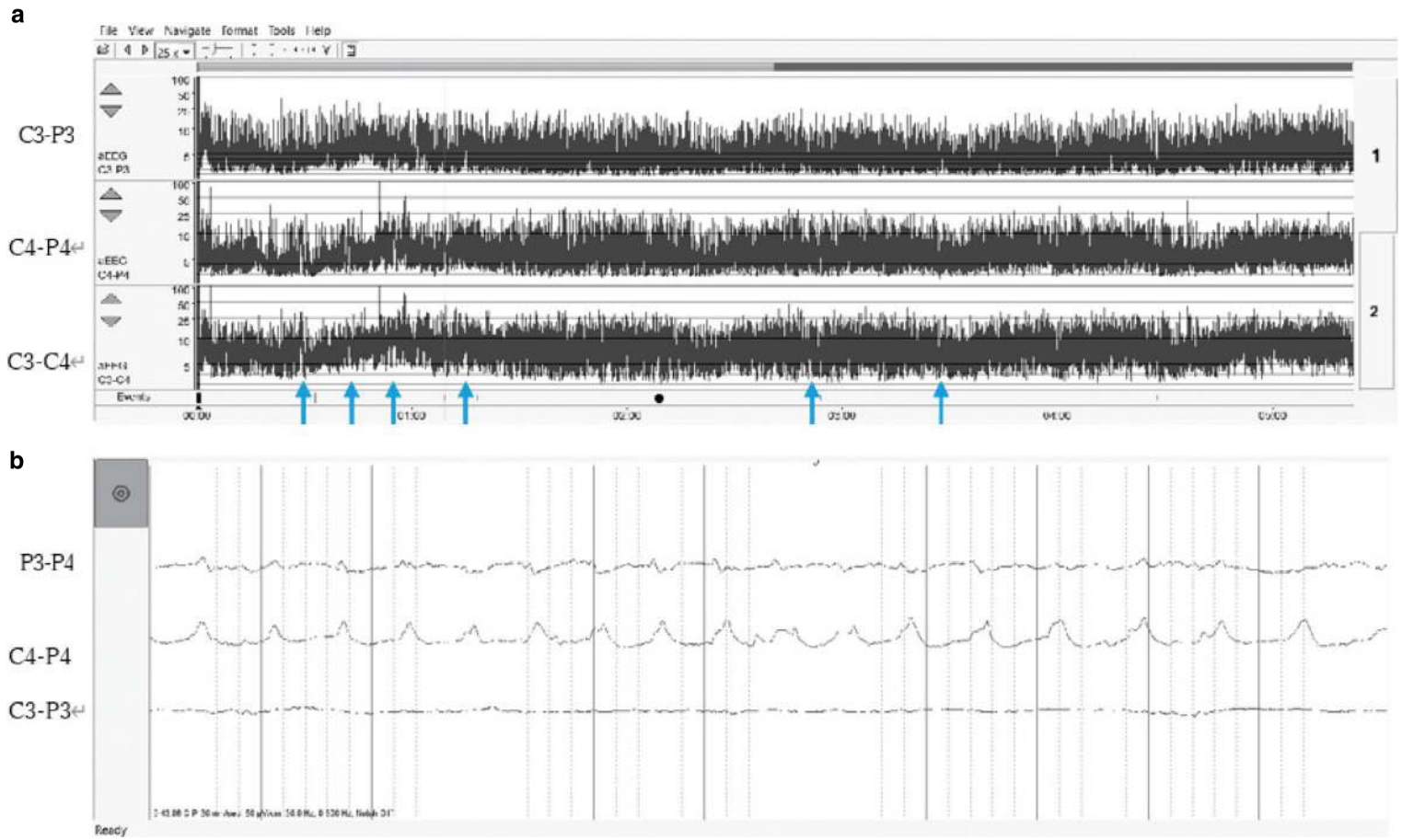

Fig. 20.5 aEEG of neonatal seizures (1). An infant with a human parechovirus type 3 infection underwent aEEG at 38 weeks PMA. The aEEG shows transient increases in the lower border (**a**: blue arrows), coinciding with apnea, but bradycardia was absent. In the simultaneously recorded cEEG, a repetitive, stereotyped, rhythmic 2-Hz waveform exhibiting right central parietal dominance is observed (**b**). The areas indicated by the black dot in (**a**) appeared to be associated with elevated lower border on aEEG; however, cEEG revealed that this was an artifact. In neonatal seizures, apnea without bradycardia is a typical clinical sign

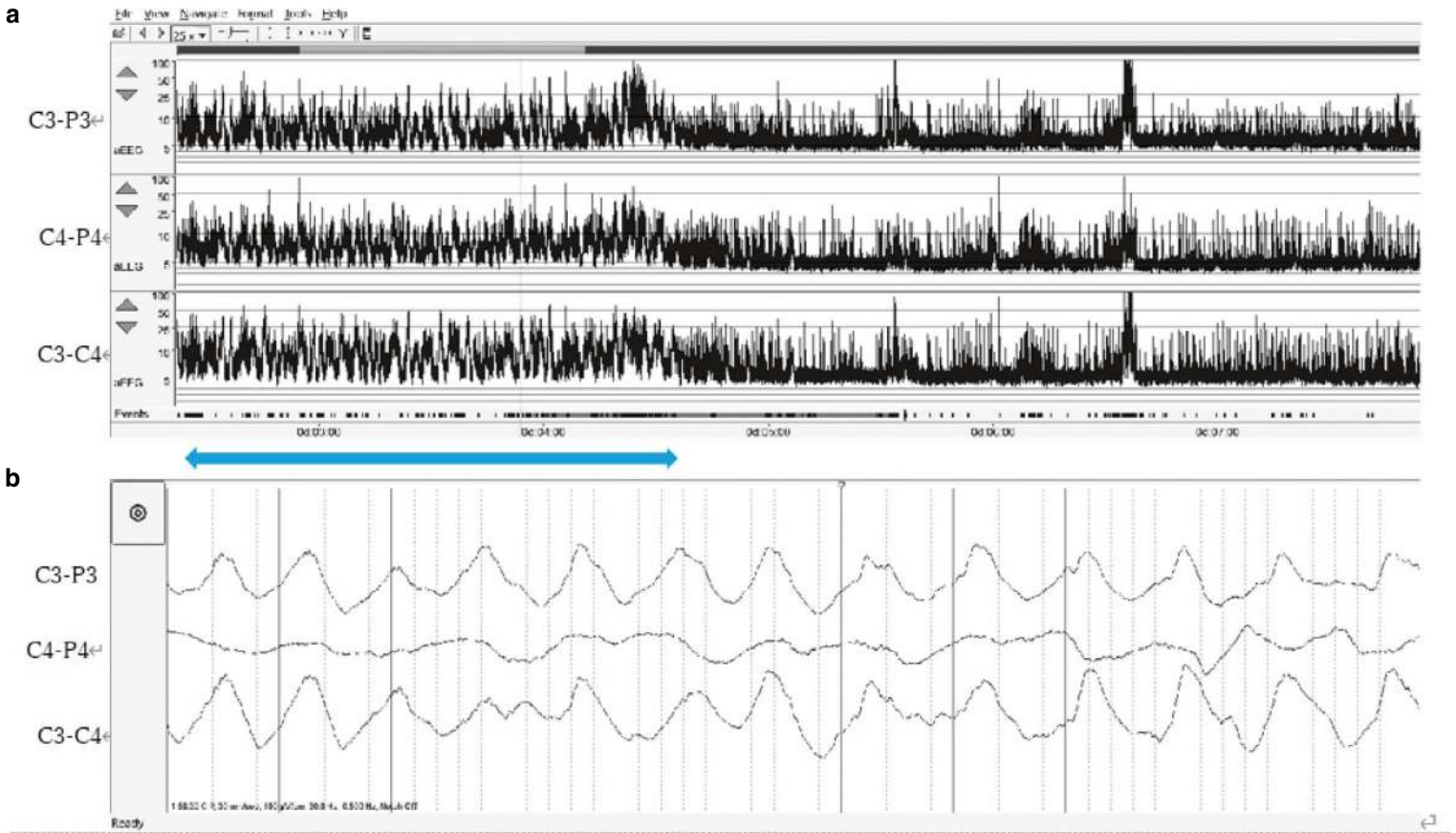

Fig. 20.6 aEEG of neonatal seizures (2). An infant with a Listeria infection underwent aEEG at 38 weeks PMA. aEEG revealed the so-called sawtooth pattern (**a**: a blue arrow) attributable to the repetitive increases in the lower border during repeated seizures. The simultaneously recorded cEEG revealed a repetitive, stereotyped, rhythmic waveform ranging from 1 to 1.5 Hz, predominantly in the left central parietal region (**b**). As EEG activity is highly suppressed during the interictal period, the transient increases in the lower border are easily recognized in this case, compared to those of Figs. 20.5 and 20.7. This aEEG trace shows the typical sawtooth pattern characteristic of repetitive seizures

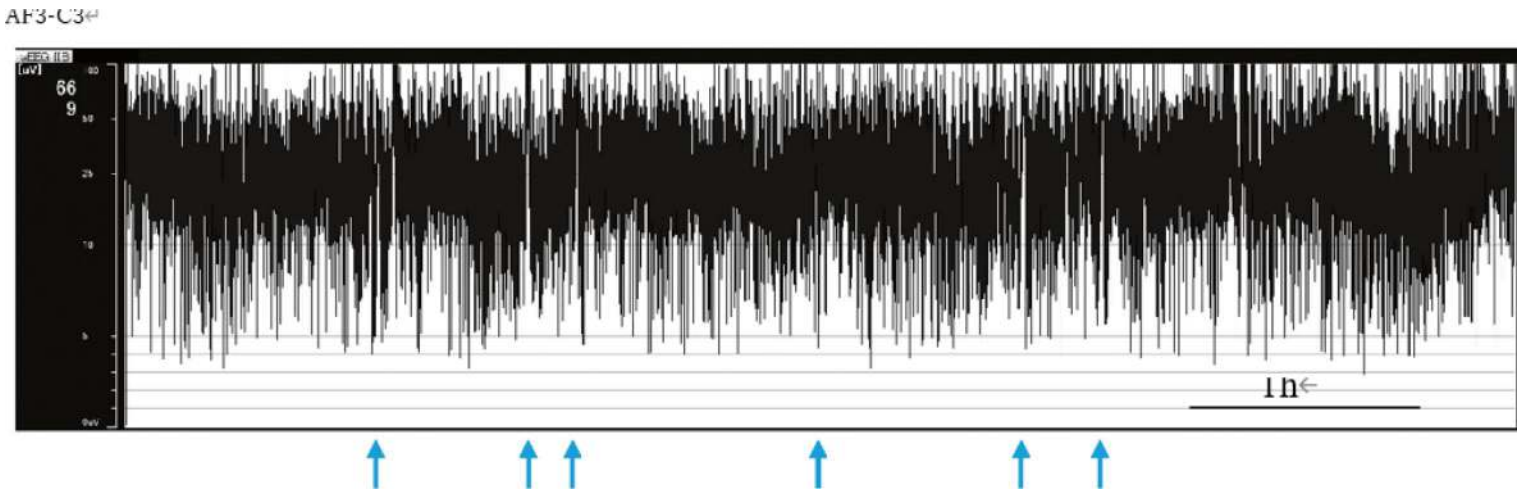

Fig. 20.7 aEEG of neonatal seizures (3). An infant with HIE underwent aEEG at 40 weeks PMA. cEEG showed the repetitive, stereotyped rhythmic waveform typical of neonatal seizures. However, detection of the transient increase in the lower border on aEEG is sometimes challenging given the short duration of each seizure. The blue arrows in the concurrently recorded aEEG trace indicate the areas of seizure activity. Although a rise in the lower border is easily noticeable when the background EEG reveals continuous low voltage or burst-suppression pattern, this rise becomes more difficult to discern when the background EEG activity is maintained, as in the present case

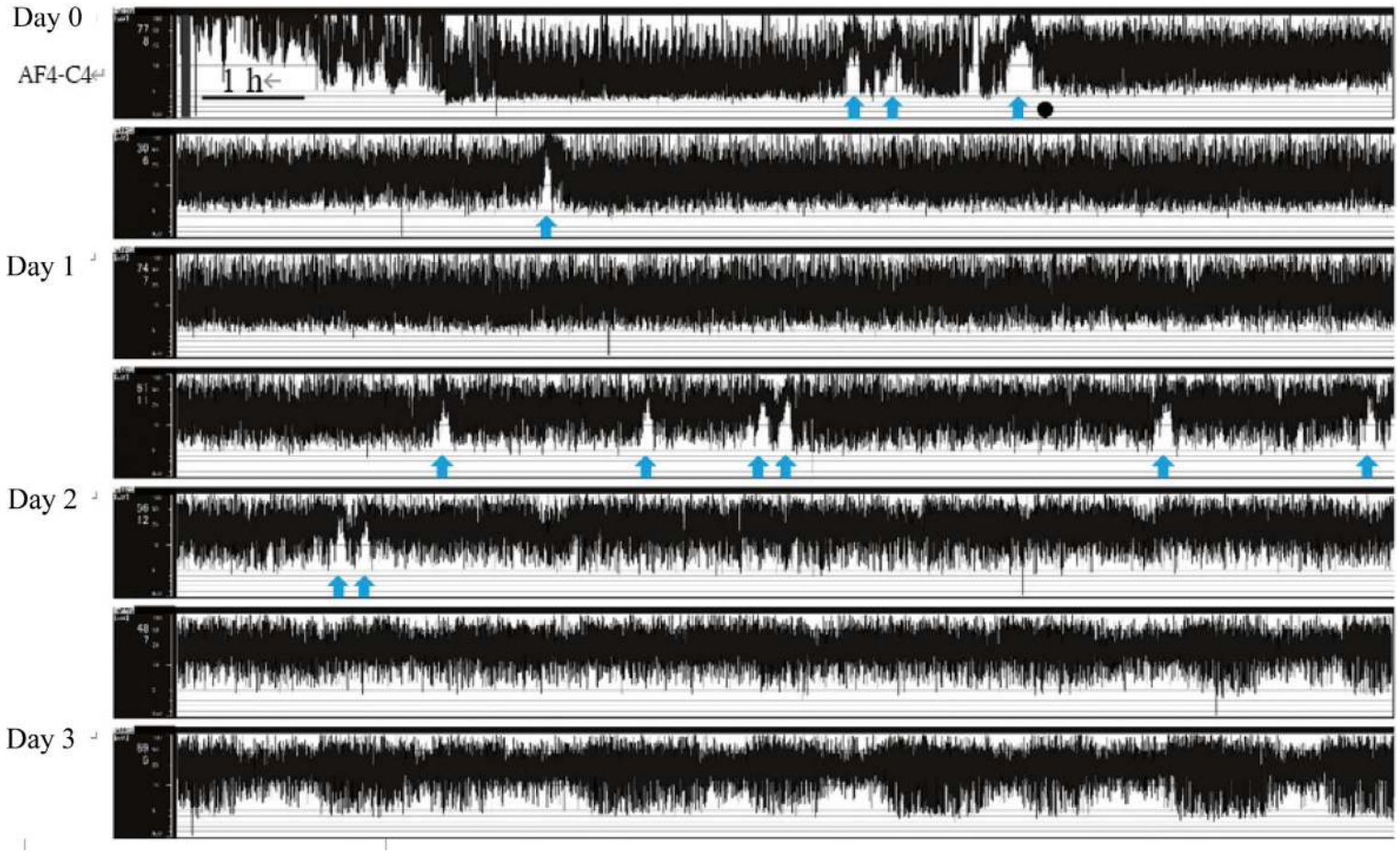

Fig. 20.8 aEEG of neonatal seizures (4). An infant with HIE underwent aEEG at 40 weeks PMA. The aEEG trace was recorded during therapeutic hypothermia for HIE of Sarnat stage 2. Throughout the recording, EEG-only seizures (blue arrows), without clinical manifestations, were observed. aEEG readily revealed clinical course during several days; in this case, the seizure frequency temporarily decreased after administration of antiseizure medication (black dot), and cycling developed commencing in the latter half of the sixth row. It is common for neonates to present with EEG-only seizures; clinical signs are lacking. Therefore, evaluation of brain function via EEG monitoring is essential not only when sedatives or muscle relaxants are used but also when infants require critical care

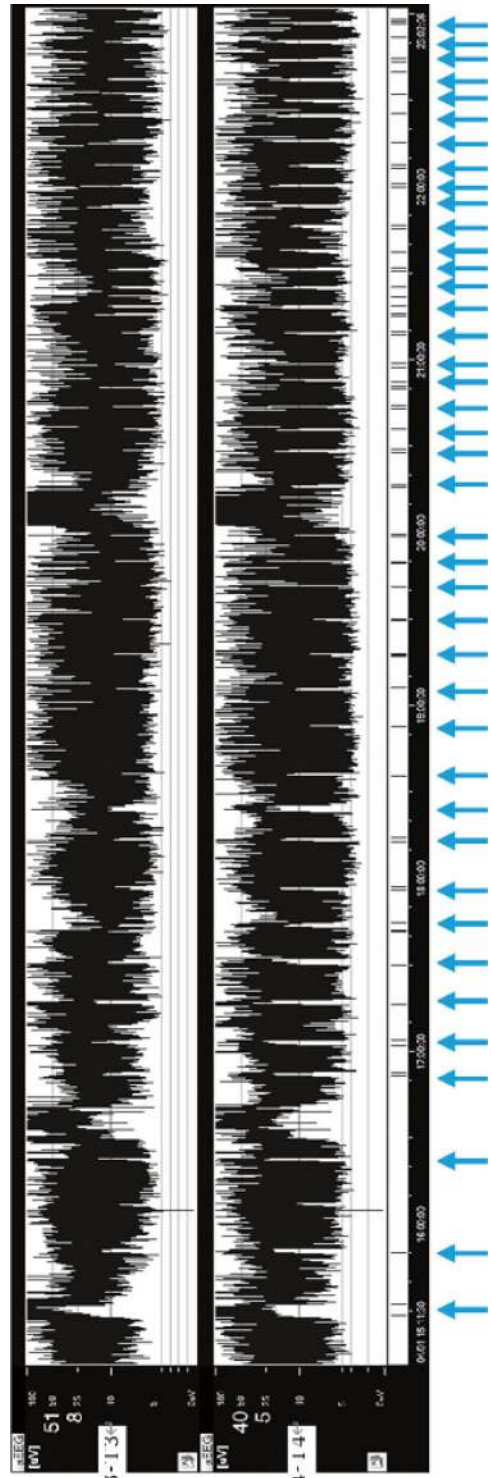

Fig. 20.9 aEEG of neonatal seizures (5). An infant with HIE underwent aEEG at 40 weeks PMA. The aEEG trace shows a typical seizure pattern, with a transiently increased lower border during the seizures (blue arrows), although clinical signs are lacking. This patient experiences EEG-only seizures. In panel (**b**) (AF4-T4), the seizures are more recognizable than in panel (**a**) (AF3-T3). It is important to note that seizure detection by aEEG varies by the locations and numbers of electrodes used

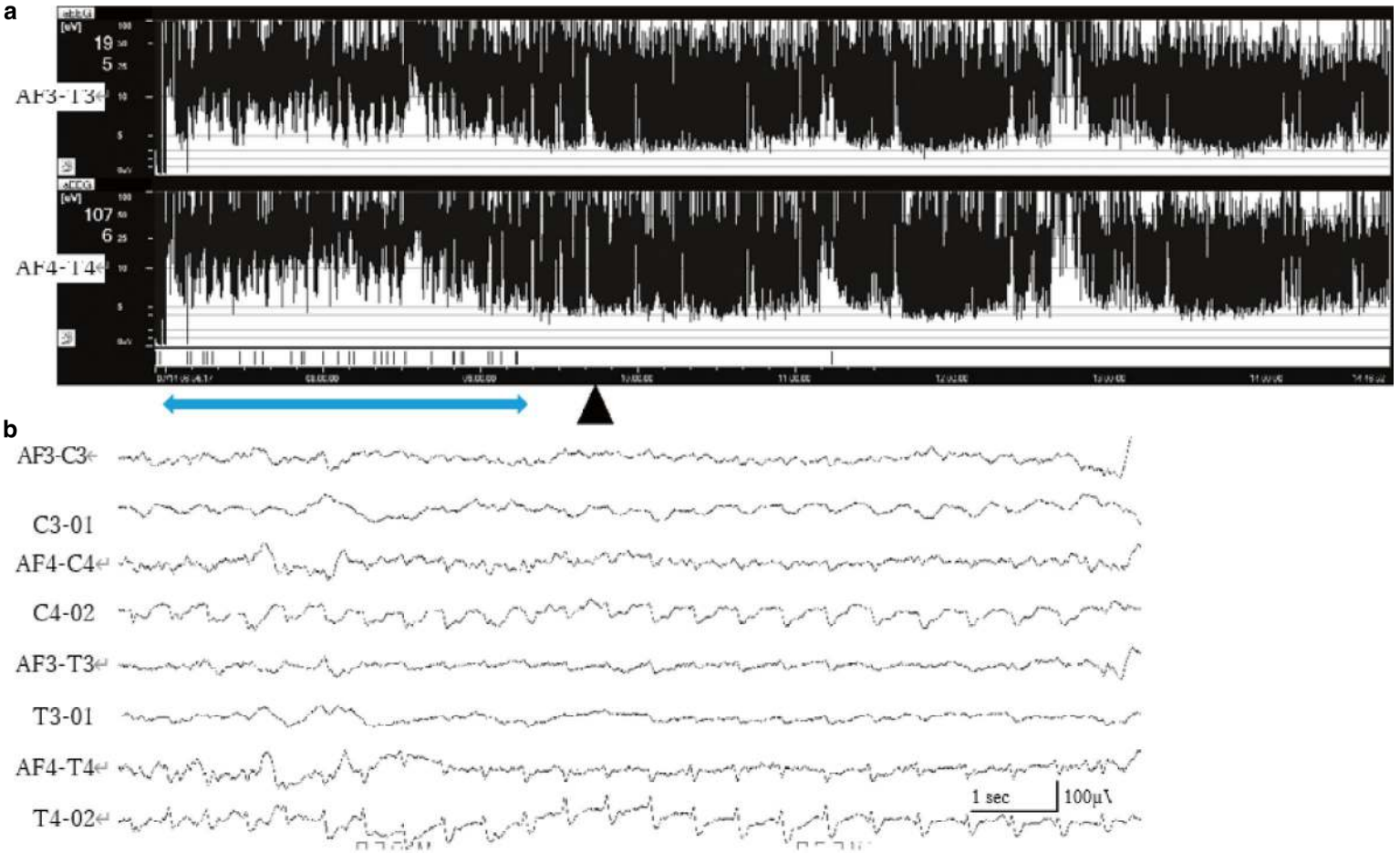

Fig. 20.10 aEEG of neonatal seizures (6). An infant with trisomy 18 underwent aEEG/cEEG at 39 weeks PMA. aEEG/cEEG reveals a typical pattern, thus frequent apneic seizures and corresponding rises in the aEEG lower border compared to other areas (**a**: blue arrow). Administration of phenobarbital (at black triangle) not only reduces the seizure frequency but also slightly decreases the lower border, indicating suppression of brain function. cEEG (**b**) shows a repetitive, stereotyped, rhythmic waveform, predominantly in the right temporo-occipital area. Even after phenobarbital administration, the lower aEEG border appears to increase transiently, indicating the possibility of seizures, but cEEG revealed that these are artifacts

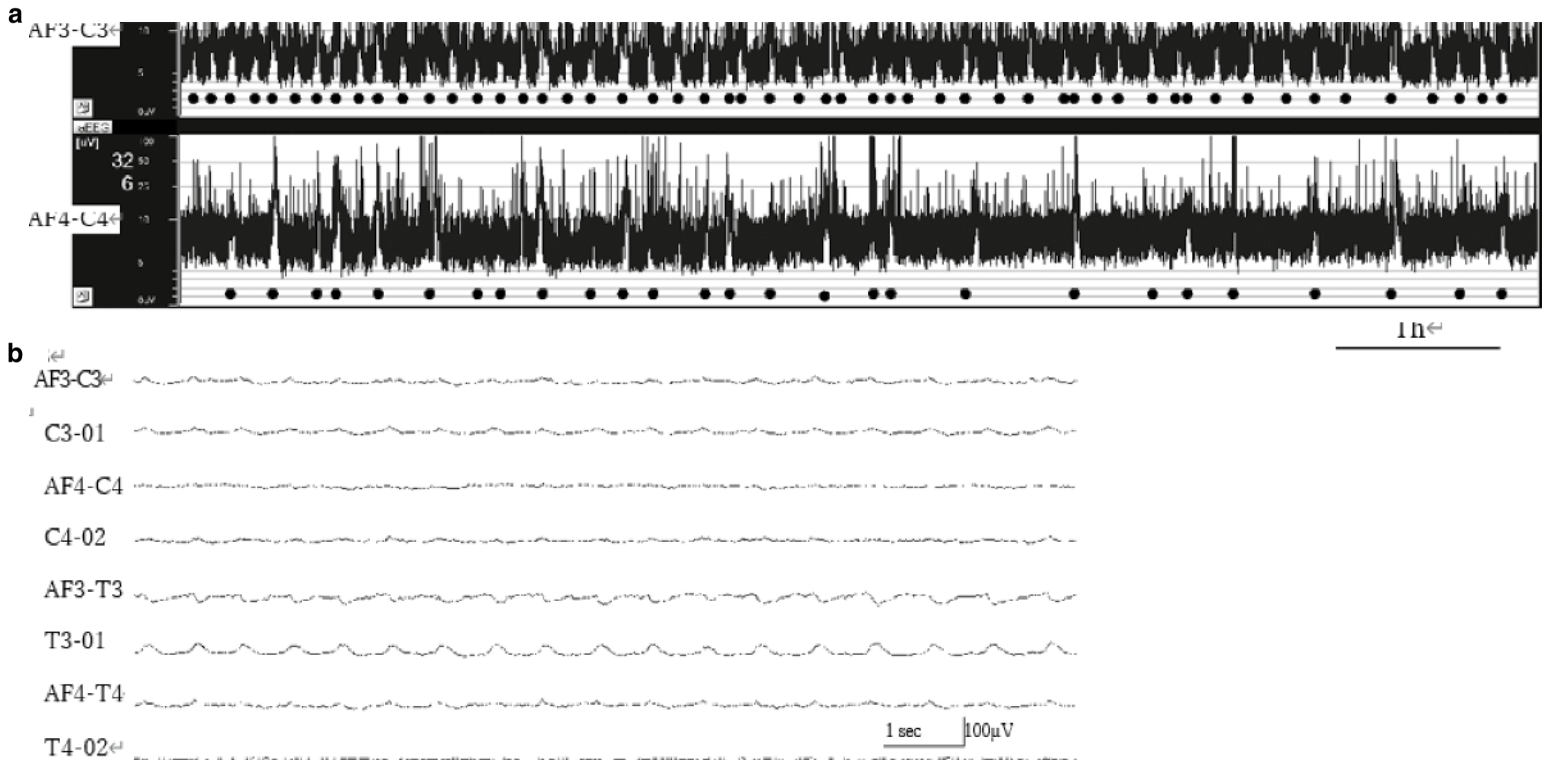

Fig. 20.11 aEEG of neonatal seizures (7). An infant with HIE underwent aEEG/cEEG at 34 weeks PMA. The aEEG (**a**) shows a typical seizure pattern (black dots), with the lower border being frequently elevated at the sites of neonatal seizures, predominantly in the left hemisphere. The cEEG (**b**) exhibits repetitive, stereotyped, rhythmic waves extending from the left central to the temporal area at a frequency of around 1.5 Hz. It is common for neonatal seizures to persist on EEG even after treatment with antiseizure medication, hence the need for continuous EEG monitoring. Seizures were more frequently observed in the left hemisphere (first row of **a**) than in the right hemisphere (second row of **b**)

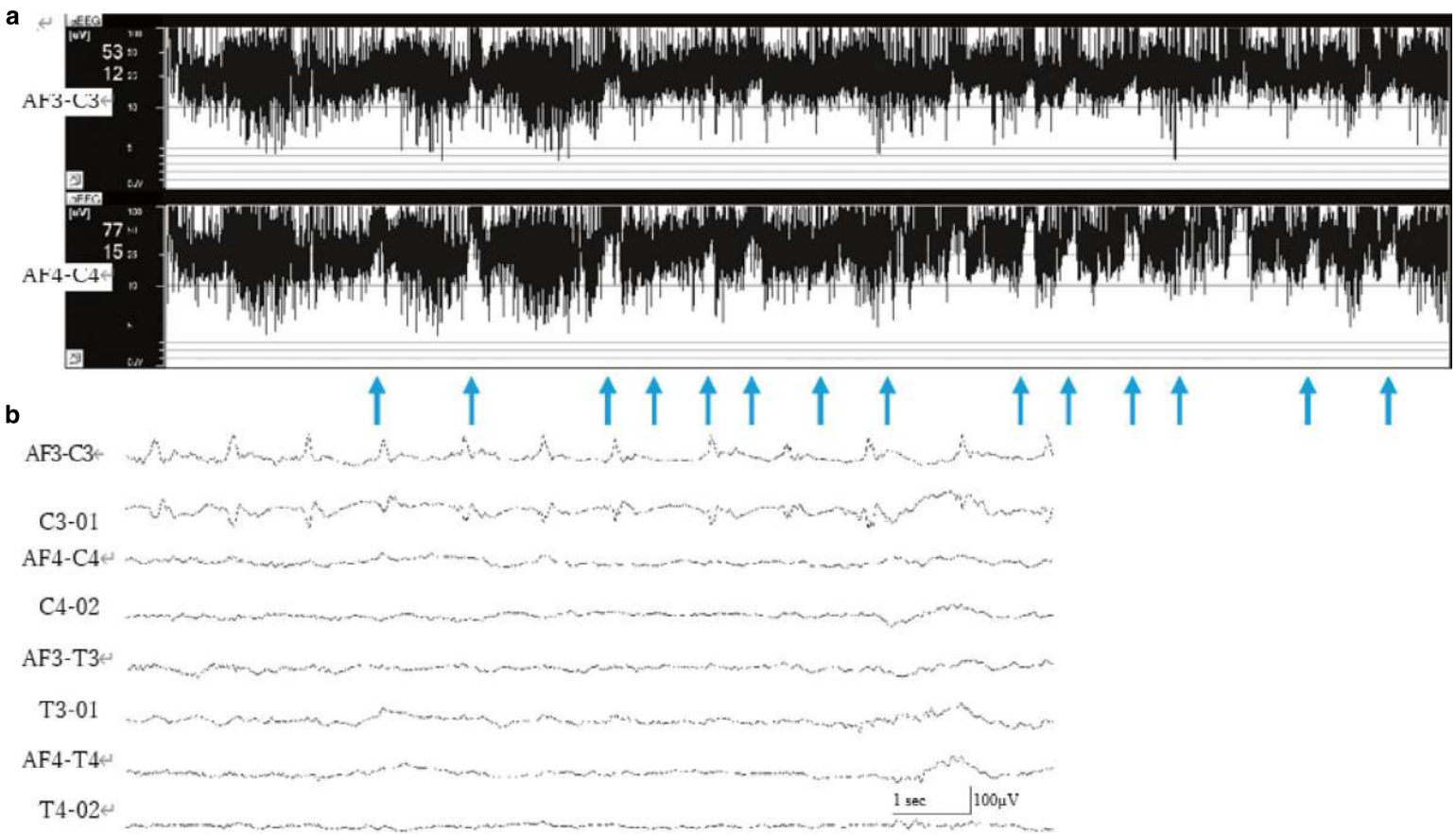

Fig. 20.12 aEEG of neonatal seizures (8). On aEEG (**a**), a typical seizure pattern is noted, characterized by a transiently elevated lower border. cEEG (**b**) shows repetitive, stereotyped, rhythmic, waveforms originating from the left central area. Although the lesion in this case is located in the right temporal lobe on head magnetic resonance imaging, the seizure activities are bilateral on EEG

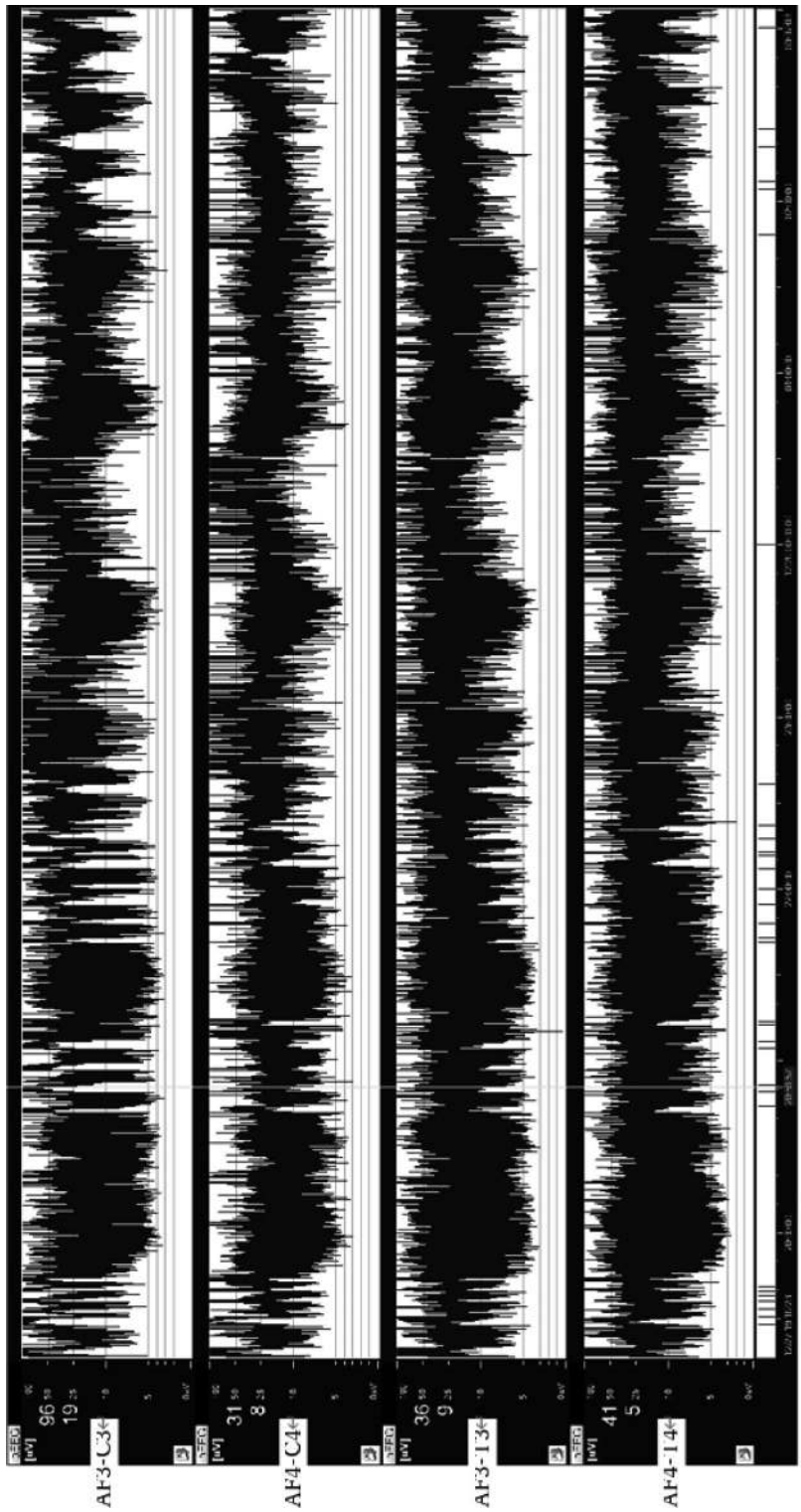

Fig. 20.13 aEEG of neonatal seizures (9). An infant with a bilateral middle cerebral artery infarction underwent aEEG at 41 weeks PMA. The aEEG background exhibited cyclicity, and neonatal seizures at the locations marked by the black dots

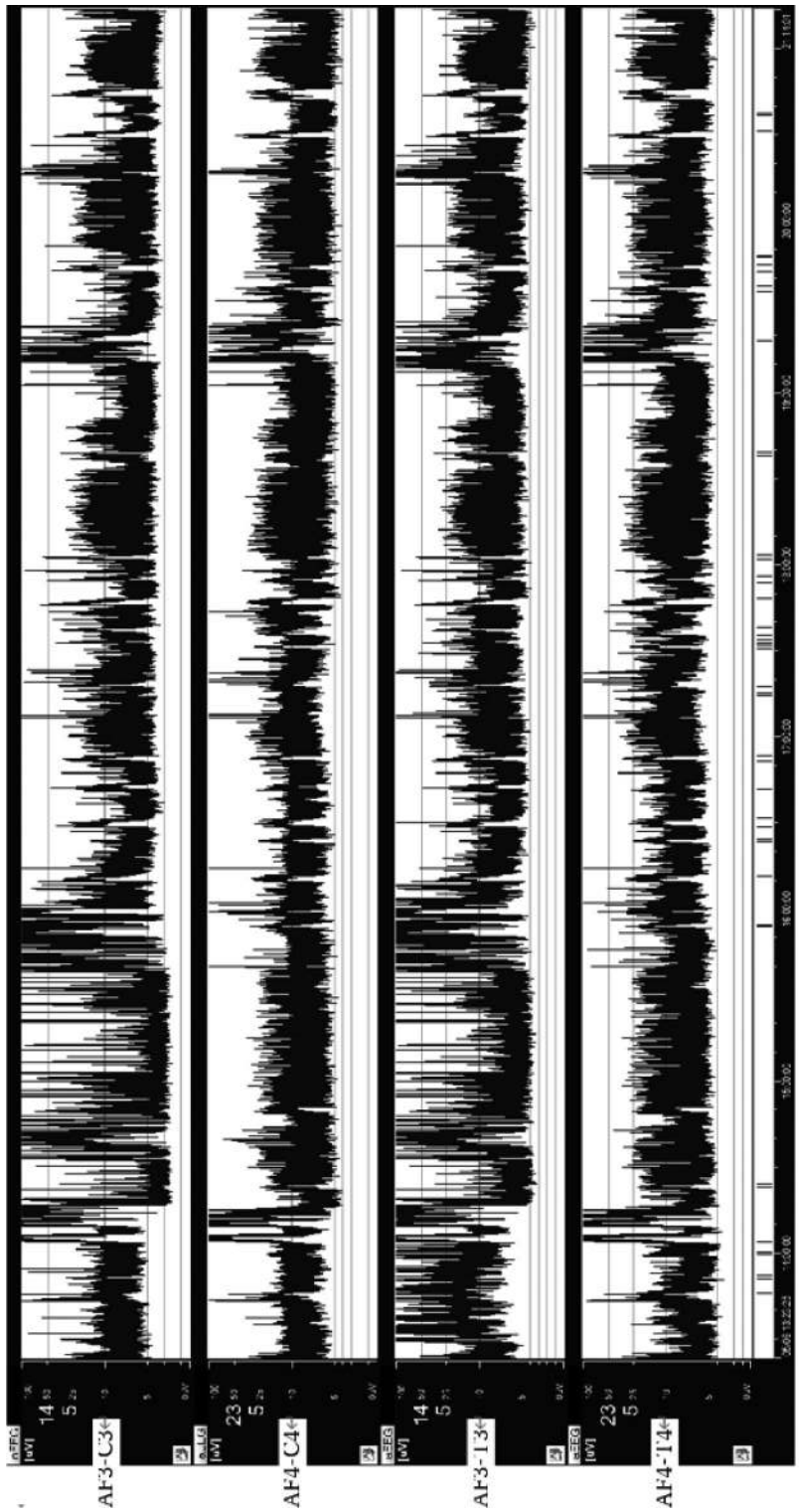

Fig. 20.14 aEEG of neonatal seizures (10). An infant with HIE underwent aEEG at 39 weeks PMA. The aEEG trace records many artifacts and a high lower border, but the background aEEG activity is considered to exhibit a continuous low voltage pattern. Neonatal seizures are indicated by the black dots

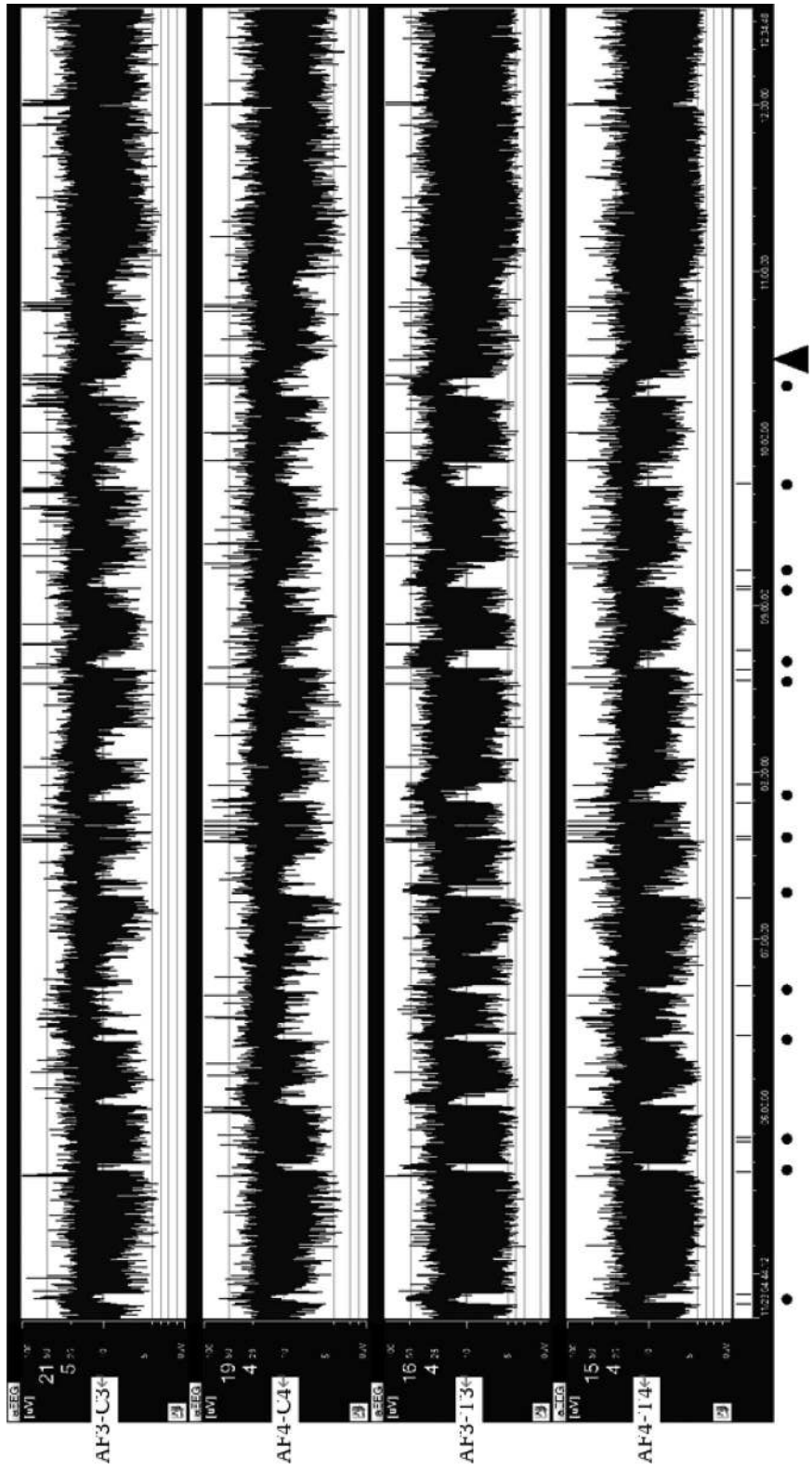

Fig. 20.15 aEEG of neonatal seizures (11). An infant with cerebral hemorrhage underwent aEEG at 39 weeks PMA. The background aEEG showed a discontinuous normal-voltage pattern, and neonatal seizures at the locations are marked by black dots. The seizures ceased following antiseizure medication (at black triangle)

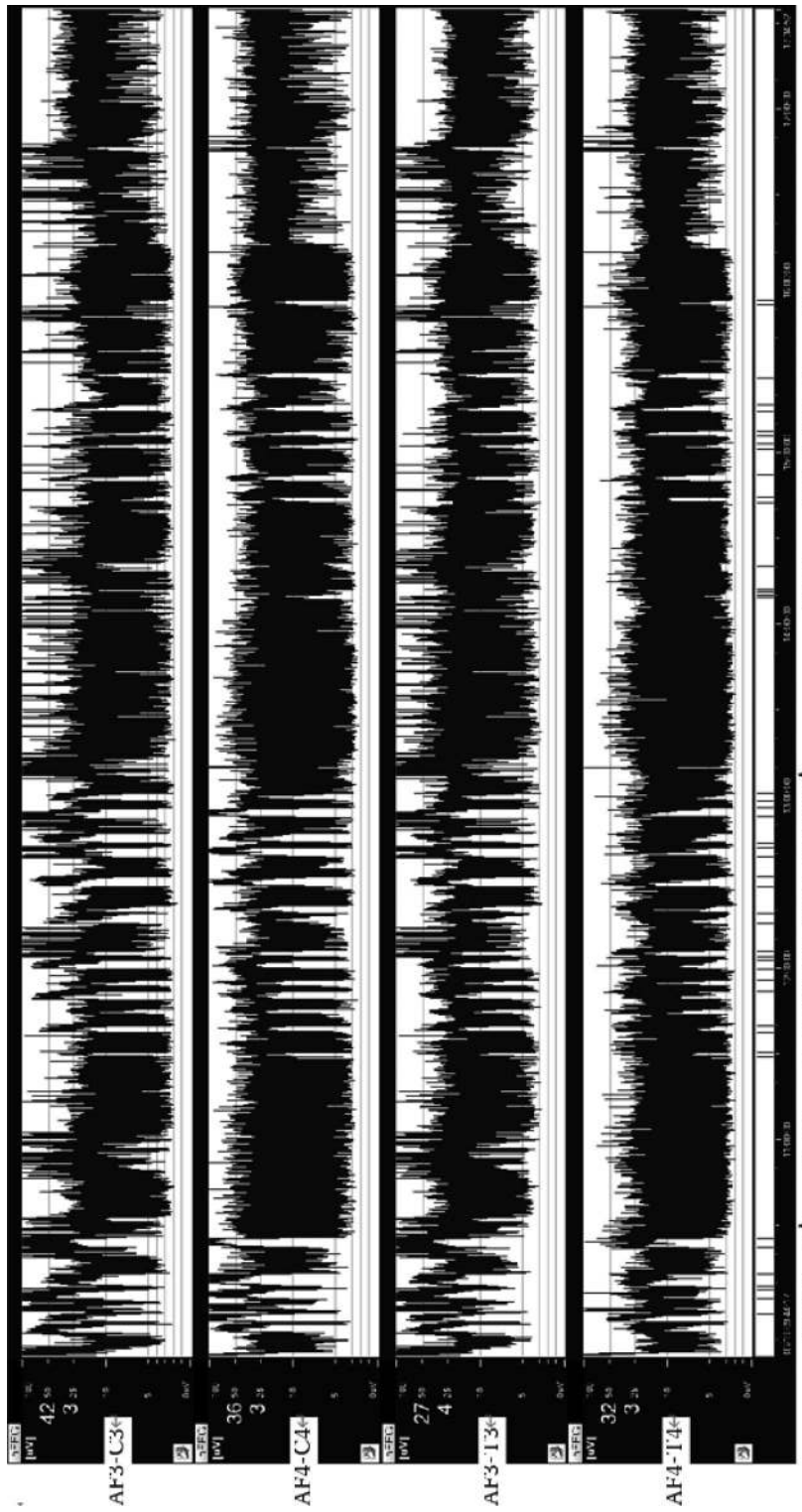

Fig. 20.16 aEEG of neonatal seizures (12). An infant with multiple malformations underwent aEEG at 38 weeks PMA. Neonatal seizures are indicated by the black dots. The administration of antiseizure medications (black triangles) temporarily reduced the frequency of seizures but did not eliminate them completely

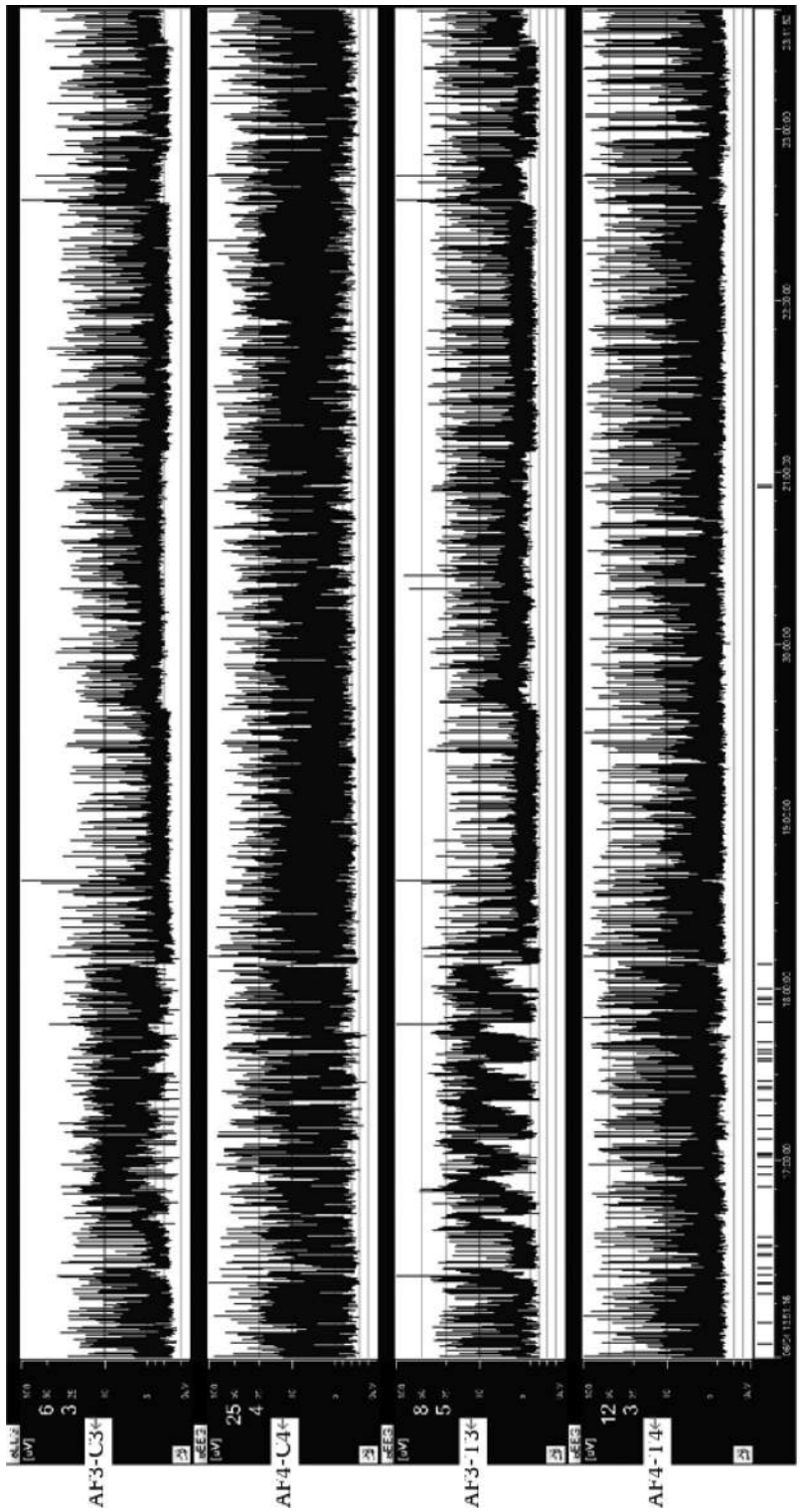

Fig. 20.17 aEEG of neonatal seizures (13). An infant with HIE underwent aEEG at 40 weeks PMA. The background aEEG shows a burst-suppression pattern. Neonatal seizures of various durations are indicated by the black dots. Recognizing seizures of short duration using aEEG alone was challenging

3 Precautions When Managing Neonatal Seizures with aEEG

Neonatal seizures are generally focal and may spread or shift to other sites within a single seizure. Therefore, the placement of electrodes is important, especially when recording with a reduced number of electrodes. In general, central electrodes are more likely to capture seizures than other electrodes and about 80% of seizures can be recognized by the central electrode alone (Kidokoro et al. 2013). Conversely, frontal electrodes less effectively capture seizures; recording exclusively in the frontal region should be avoided. Although the use of more electrodes and channels complicates the setup, this enhances the sensitivity of seizure detection.

When diagnosing and treating neonatal seizures during aEEG monitoring, the risk of overlooking seizures is a major concern. Many studies that compared the sensitivities of aEEG and cEEG in terms of detecting seizures estimated that aEEG might detect only about 30% of all seizures identified by cEEG (Renée et al. 2007). Seizures longer than 30 s are more easily detected by aEEG. However, it is important to note that single seizures shorter than 30 s are likely to be undetectable by aEEG (Russell et al. 2009). EEG activity during interictal periods also affects seizure detection by aEEG. When EEG activity is of the continuous low voltage (CLV) or burst-suppression (BS) pattern during interictal periods, the original lower border is low with little fluctuation, rendering rise of lower border easily recognizable. Conversely, if EEG activity is not or only mildly suppressed, the lower border is higher and fluctuates physiologically with cycling, rendering it more challenging to recognize transient rises associated with neonatal seizures.

The specificity of aEEG in terms of detecting neonatal seizures is relatively high; false-positives are rare. However, in clinical practice, artifacts caused by electromyography and body movement can mimic neonatal seizure pattern. A pseudo-sawtooth (PST) pattern, defined as a periodic increase of the upper and/or lower margin of the aEEG trace without any seizure activity apparent on cEEG appears in infants with severe hypoxic-ischemic encephalopathy (Tanaka et al. 2020). If a seizure is suspected on aEEG, concurrent cEEG verification is important. Understanding the characteristics of both aEEG and cEEG and exploiting their respective strengths will improve the management of neonatal seizures.

References

Aileen M, Anthony Ryan C, Fitzgerald A, Burgoyne L, Connolly S, Boylan GB. Interobserver agreement in neonatal seizure identification. Epilepsia. 2009;50(9):2097–101.https://doi.org/10.1111/j.1528--1167.2009.02132.x. Epub 2009 Jun 1.

Divyen KS, Mackay MT, Lavery S, Susan Watson A, Harvey S, Zempel J, Mathur A, Inder TE. Accuracy of bedside electroencephalographic monitoring in comparison with simultaneous continuous conventional electroencephalography for seizure detection in term infants. Pediatrics. 2008;121(6):1146–54. https://doi.org/10.1542/peds.2007-1839.

Evans E, Koh S, Lerner R, Sankar MG. Accuracy of amplitude integrated EEG in a neonatal cohort. Arch Dis Child Fetal Neonatal Ed. 2010;95(3):169–73. https://doi.org/10.1136/adc.2009.165969.

Kidokoro H, Kubota T, Hayakawa M, Kato Y, Okumura A. Neonatal seizure identification on reduced channel EEG. Arch Dis Child Fetal Neonatal Ed. 2013;98(4):359–61.

Murray DM, Boylan GB, Ali I, Ryan CA, Murphy BP, Connolly S. Defining the gap between electrographic seizure burden, clinical expression and staff recognition of neonatal seizures. Arch Dis Child Fetal Neonatal Ed. 2008;93(3):187–91. https://doi.org/10.1136/adc.2005.086314. Epub 2007 Jul 11.

Renée AS, Soaita AI, Clancy RR. Sensitivity of amplitude-integrated electroencephalography for neonatal seizure detection. Pediatrics. 2007;120(4):770–7. https://doi.org/10.1542/peds.2007-0514.

Russell L, Mathur A, Tich SNT, Zempel J, Inder T. A pilot study of continuous limited-channel aEEG in term infants with encephalopathy. J Pediatr. 2009;154(6):835–41. https://doi.org/10.1016/j.jpeds.2009.01.002. Epub 2009 Feb 23.

Tanaka M, Kidokoro H, Kubota T, Fukasawa T, Okai Y, Sakaguchi Y, Ito Y, Yamamoto H, Ohno A, Nakata T, Negoro T, Okumura A, Kato T, Watanabe K, Takahashi Y, Natsume J. Pseudo-sawtooth pattern on amplitude-integrated electroencephalography in neonatal hypoxic-ischemic encephalopathy. Pediatr Res. 2020;87(3):529–35.

Part VI

Application of EEG in Neonates

How to Record a Neonatal EEG

21

Akihisa Okumura

The interpretation of a neonatal EEG relies on the waveform itself. Therefore, maintaining appropriate conditions is desirable for interpreting neonatal EEGs. If recording conditions such as electrode placement, montage, and filters are changed, it becomes challenging to accumulate knowledge on normal and abnormal findings. With paper recordings, standardizing recording conditions were straightforward. However, in the current era of digital EEGs, which are commonly read on displays, standardizing reading conditions is more difficult due to varying monitor resolutions and aspect ratios. To address this issue, it is recommended that each facility establish its own conditions for reading neonatal EEGs.

1 Electrodes

1.1 Electrode Location

Conventionally, eight electrodes are used: AF3, AF4, C3, C4, O1, O2, T3, and T4 (Fig. 21.1a). AF3 is located at the midpoint between Fp1 and F3, and AF4 is at the midpoint between Fp2 and F4. For the frontal electrodes, Fp1 and Fp2 can be used, as substituting AF3 and AF4 for Fp1 and Fp2, respectively, does not cause substantial issues in interpretation. If possible, electrodes should also be placed along the midline at Fz, Cz, and Pz. When using a digital EEG, the A1 and A2 electrodes may also be attached for analysis. Note that the reference electrodes must be attached. For example, the reference electrodes for electroencephalographs manufactured by Nihon Kohden are set to C3 and C4, and these electrodes must be attached.

1.2 How to Attach Electrodes

First, wipe any vernix caseosa and blood off the scalp using alcohol and cotton, and then, scrub the scalp. If feasible, use a scrub such as SkinPure® for additional cleansing. This step is important for obtaining high-quality EEG recordings. Some institutions discourage alcohol use in very low birth weight infants; in these cases, a cotton pad moistened with fresh water is used to remove the vernix caseosa.

Next, apply electrode paste on the scalp. It is helpful to expose the scalp by parting the hair with a small amount of paste. Then, apply the paste on the electrodes and attach them to the scalp. Applying too little paste may not secure the electrode properly, while too much can render it unstable.

A. Okumura (✉)
Department of Pediatrics, Aichi Medical University, Nagakute, Aichi, Japan
e-mail: okumura.akihisa.479@mail.aichi-med-u.ac.jp

A. Okumura, H. Kidokoro (eds.), *Neonatal EEG: Atlas and Interpretation*,
https://doi.org/10.1007/978-981-96-0726-6_21

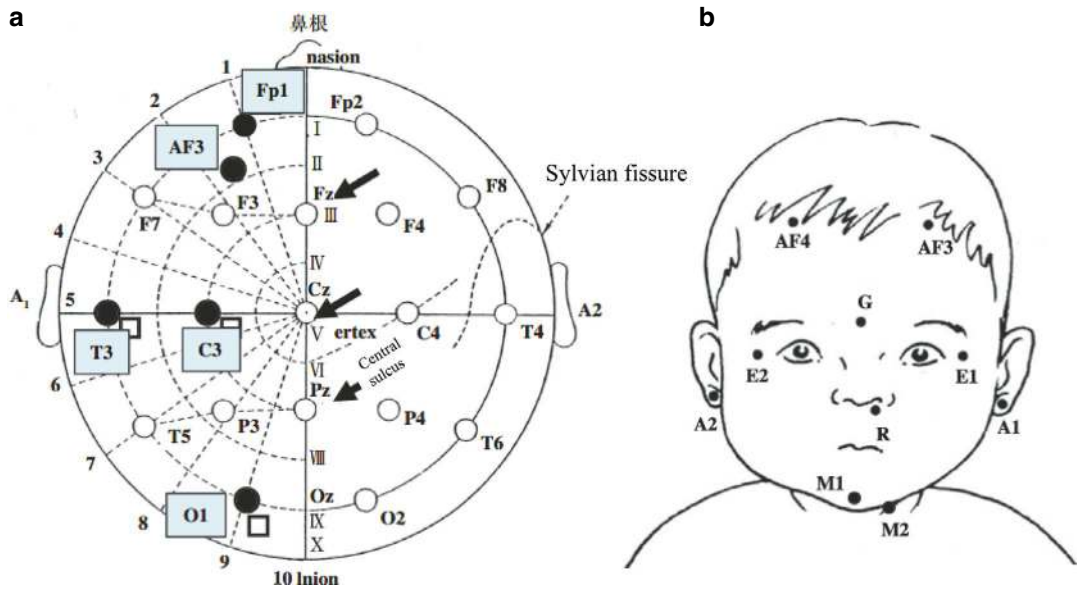

Fig. 21.1 Arrangement of scalp electrodes and physiological indicators. (**a**) Scalp electrode placement based on the international 10/20 method. For neonatal EEG, the electrodes indicated by black dots are used. The electrodes in the midline shown by black arrows may be added. AF3 is located at the midpoint between Fp1 and F3, and AF4 is at the midpoint between Fp2 and F4. (**b**) Arrangement of physiological indicators. G, body grounding; E1–E2, eye movement; A1–A2, earlobe (reference electrode); R, respiration (thermistor); M1–M2, chin electromyogram

Ideally, the impedance should be reduced to <5 kΩ. Experienced technicians often achieve this level, but beginners may find it challenging. Although high impedance is undesirable, newer electroencephalographs are capable of recording an EEG under less optimal conditions.

1.3 EEG Electrode Cap

Recently, various manufacturers have released cap-shaped devices with EEG electrodes suitable for newborn infants. Once the cap is placed on the patient, the EEG recording can commence by injecting gel into the electrodes. This method is convenient because it eliminates the need to attach individual electrodes and enables stable EEG recordings. Although small devices are available for preterm infants as young as 28 weeks of gestation, there are no appropriate devices for very preterm infants. Currently, facilities with experience recording neonatal EEGs do not routinely use these cap-shaped devices.

1.4 Body Grounding

Many EEGs are equipped with body grounding systems, and a grounding electrode is placed on the middle of the forehead, similar to the placement of other scalp electrodes (Fig. 21.1b). Body grounding is effective for reducing AC noise.

1.5 Stabilizing the Electrode

After applying the scalp and polygraph electrodes, they are covered with dry cotton or secured with elastic bandages to ensure a long and stable EEG recording.

1.6 Avoiding Artifacts

In the neonatal intensive care unit (NICU), where numerous electronic devices are present, AC noise often presents a challenge. The cables of EEG electrodes may cross over those of moni-

tors, leading to AC noise. To prevent this, we should place the electrode box in a different location and bundle the EEG electrode cables together, avoiding crossover with cables of other electronic devices. Infusion pumps are a common source of noise in the NICU. Moving these pumps as far away as possible from the electrodes and electrode box can often reduce noise. Sometimes, noise may even disappear by simply relocating the electrode box. If noise is unavoidable and disrupts the recording, unplugging the power supply of the suspected equipment might be necessary, although this is not an option if the noise source is a critical device like a ventilator. Modern EEGs are equipped with effective noise filters; activating the AC filter often reduces noise to a level resulting in a legible EEG. If noise persists, lowering the high-cut filter to 30 ~ 35 Hz can be effective.

In addition to AC noise, there are various other artifacts that can be mitigated. Artifacts occurring when electrodes touch the incubator mat can be reduced by repositioning the infant's head. Adjusting the head position can also minimize artifacts due to head movement and breathing. When high-frequency oscillatory ventilation (HFOV) is used, a steady 15-Hz artifact can be introduced due to the head oscillating at the same frequency as the HFOV, which is often challenging to remove. Electromyogram artifacts are commonly observed in the temporal and frontal areas. Artifacts caused by frowning, tremors, or sucking, or by eyelid, eye, or tongue movements, are also common. Observing the infant during the EEG recording can help distinguish genuine EEG signals from artifacts.

2 Polygraph

In neonatal EEG, it is important to differentiate between active sleep (AS) and quiet sleep (QS), making polygraphic recording desirable. However, in preterm infants under 30 weeks, this is not always necessary as their sleep cycle is not well-defined and the utility of physiological indices for determining sleep states is limited.

2.1 Eye Movement

For normal neonatal EEG recordings, a single channel (E1–E2) connecting both external canthi is sufficient to capture eye movements (Fig. 21.1b). The electrode should be placed 0.5 cm above the external canthus and slightly outward on one side, and 0.5 cm below the external canthus and slightly outward on the opposite side.

Other recording methods include two-channel recording that connects the external canthus to the ipsilateral earlobe (E1–A1 and E2–A2) using both earlobes as reference electrodes (E1–AV and E2–AV, where AV is the average of A1 and A2). For more detailed recording, electrodes may be placed above and below the orbit, although this is not usually necessary.

2.2 Chin Electromyography

To record chin electromyography, one electrode should be placed on either the mental protuberance of the mandible or the tip of the lower jaw, with another placed on the bicuspid muscle on the left (or right) of the trachea (Fig. 21.1b). The electrodes must be attached to the areas where muscle movement is most obvious when the baby sucks. In preterm infants, this is often omitted due to their small jaws, which make attaching the electrode difficult, and because a chin electromyogram is less useful. For term infants, however, chin electromyography should be performed when possible.

2.3 Electrocardiography

A variety of electrode arrangements can be used for electrocardiography recordings. Typically, electrodes are placed on the anterior thorax, equidistant from the midline and sufficiently far from the clavicles. Although electrodes on both arms can be used for recording, the electromyogram often interferes with the electrocardiogram.

2.4 Respiration

2.4.1 Impedance Method

Set the electrodes on the right and left axillary lines of the chest or abdomen, ensuring they are equidistant from the midline and at the same height. To monitor respiratory movement effectively, place the electrodes at a site where respiratory movement is most pronounced.

2.4.2 Strain Gauge Method

Stretch a strain gauge slightly and fix it either 1 cm above or below the nipple line for optimal recording. Although it is necessary to keep the strain gauge clean because of repeated use, this is a reliable method for recording respiratory movements of the thorax or abdomen. However, it can be difficult to use in extremely preterm infants.

2.4.3 Thermistor Method

A thermistor, which detects the difference in temperature between exhaled and inhaled air, is placed near the nostrils to detect airflow (Fig. 21.1b). It cannot be used in infants who are on artificial ventilation. For children with apnea, it is necessary to use both a thermistor to monitor airflow and either an impedance or strain gauge to monitor respiratory movement. This dual monitoring method helps differentiate between central and obstructive apnea. In central apnea, there is a simultaneous decrease in both airflow and respiratory movement, while in obstructive apnea, airflow decreases but respiratory movement does not, which differentiates between the two.

3 Recording Conditions

Table 21.1 shows the recording conditions for each parameter. The EEG recording conditions are especially important. Given the significance of the frequency and form of slow waves in a neonatal EEG, the time constant of the EEG is always set at 0.3 s. If using a low-cut filter instead of a time constant, it should be adjusted to 0.5 or 0.53 Hz. Altering the time constant or low-cut filter can significantly change the waveform of slow waves, which can greatly hinder interpretation.

For paper recording, the paper feed rate should be 3 cm/s. In Europe and the USA, the rate is often set at 1.5 cm/s, but this is not recommended as it can obscure the waveform changes.

3.1 Sedation

Neonates are not sedated for EEG recordings, as it is important to capture natural sleep cycles.

3.2 Recording Time

Newborns tend to fall asleep after feeding. High-quality EEG recordings are easier to obtain if the electrodes are applied before feeding and the recording begins immediately after feeding. Clinically useful information is usually available if at least QS and AS are recorded before and after QS. Therefore, a recording time of 40–60 minutes is often sufficient. However, if the sleep stages remain unchanged, it is advisable to

Table 21.1 Polygraph recording conditions

Indicator	Time constant	High cut filter	Gain (μ V mm)
EEGs	0.3 s (0.5 ~ 0.53 Hz)	60 Hz (may be reduced to 30 Hz)	10
ECG	0.1 s	15 Hz	Appropriately
Respiration	0.3 or 1.5 s	15 Hz	Appropriately
Eye movement	0.3 or 1.5 s	30 Hz	Appropriately
Chin electromyogram (EMG)	0.05 s	0ff	Appropriately

extend the recording time to 60 min. To obtain a complete record of the sleep–wake cycle, a minimum 3-h recording is necessary. If the sleep cycle is unclear or there are prolonged periods without EEG pattern changes, tactile or acoustic stimulation should be applied to observe any EEG changes.

3.3 Example Montages

Tables 21.2 and 21.3 show examples of the montages used in experienced facilities. Each facility should determine its own montage based on these examples. However, as mentioned at the beginning of this textbook, the first eight channels

Table 21.2 Examples of EEG montages for preterm infants

	Anjo Kosei Hospital	Okazaki City Hospital	Nagoya University Hospital
1 Ch	AF3-C3	AF3-C3	Fp1-C3
2 Ch	C3-01	C3-01	C3-01
3 Ch	AF4-C4	AF4-C4	Fp2-C4
4 Ch	C4–02	C4-02	C4-02
5 Ch	AF3-T3	AF3-T3	Fp1-T3
6 Ch	T3-01	T3-01	T3-01
7 Ch	AF4-T4	AF4-T4	Fp2-T4
8 Ch	T4–02	T4-02	T4-02
9 Ch		Fz-A2[a]	T3-C3
10 Ch	Eye movement	Cz-A1[a]	C3-Cz
11 Ch	Respiration (thorax)	Pz-A2[a]	Cz-C4
12 Ch	ECG	Respiration (thorax)	C4-T4
13 Ch		ECG	ECG
14 Ch			Respiration (thorax)

AF3 and AF4 may be replaced by Fp1 and Fp2
[a]May be omitted

Table 21.3 Example of an EEG montage for term infants

	Anjo Kosei Hospital	Okazaki City Hospital	Nagoya University Hospital
1 Ch	AF3-C3	AF3-C3	Fp1-C3
2 Ch	C3-01	C3-01	C3-01
3 Ch	AF4-C4	AF4-C4	Fp2-C4
4 Ch	C4-02	C4–02	C4-02
5 Ch	AF3-T3	AF3-T3	Fp1-T3
6 Ch	T3-01	T3-01	T3-01
7 Ch	AF4-T4	AF4-T4	Fp2-T4
8 Ch	T4-02	T4-02	T4-02
9 Ch	Fz-A1	Fz-A2[a]	T3-C3
10 Ch	Cz-A2	Cz-A1[a]	C3-Cz
11 Ch	Pz-A1	Pz-A2[a]	Cz-C4
12 Ch	Eye movement	Chin electromyogram[a]	C4-T4
13 Ch	ECG	Eye movement[a]	Eye movement[a]
14 Ch	Chin electromyogram[a]	Respiration (thorax)	ECG
15 Ch	Respiration (thorax)	ECG	Chin electromyogram[a]
16 Ch	Breathing (nostrils)[a]		Respiration (thorax)

AF3 and AF4 may be replaced by Fp1 and Fp2
[a]May be omitted if polygraph is not needed

should remain unchanged; altering them may hinder the application of the knowledge acquired from this textbook.

For facilities less experienced with neonatal EEG, it is recommended to record an 8-channel EEG without a polygraph initially. This approach often reveals that recording neonatal EEG is unexpectedly easy.

Column: Neonatal Seizures and Sleep Stages

(Kazuyoshi Watanabe)

Currently, hypoxic–ischemic encephalopathy is the most common cause of neonatal seizures, whereas hypocalcemia used to be a very common cause. Unlike hypoxic–ischemic encephalopathy, hypocalcemia typically shows only mild abnormalities in the background EEG. The sleep cycle is preserved because there is no parenchymal brain damage.

On examining the timing of seizures in relation to sleep stages, we found that 77% of seizures occurred during active sleep, 17% during indeterminate sleep, 5% during quiet sleep and 1% during wakefulness (Watanabe et al. 1982). By contrast, seizures in older children and adults are often observed during non-rapid eye movement (REM) sleep and arousal, but not during REM sleep. In visual and auditory evoked potentials in neonates and infants, the amplitude of the negative component tends to be larger in REM sleep than in non-REM sleep, which is opposite to what is observed in older children and adults.

These results suggest that, unlike in older children, the excitability of cortical neurons in neonates is greater during REM sleep than in non-REM sleep.

Reference

Watanabe K, Hara K, Miyazaki S, Hakamada S. Neurophysiological study of newborns with hypocalcemia. Neuropediatrics. 1982;13(1):34–8.

How to Write a Neonatal EEG Report

22

Akihisa Okumura

Once a neonatal EEG is interpreted, a report must be written. A good EEG report is invaluable. The format for a neonatal EEG report should differ from that used for older children or adults.

Figure 22.1 shows the format for EEG reports that we are currently using. Many facilities now use online reading and EEG report systems. These systems are convenient, allowing the selection of frequently used words and phrases from pull-down menus. Using this report format as a foundation, each facility should develop its own format tailored to neonatal EEG. Figure 22.2 presents an example of an EEG report.

The following descriptions correspond to the numbers in Fig. 22.1.

(1) Clinical information: The gestational age, birth weight, and postnatal days at the time of recording should be included as a minimum. In addition, a brief summary of the perinatal and postnatal history, along with any complications, should be noted. Previous EEG findings can be valuable for prognostication.
(2) The behavioral state cycle and recorded sleep stage: We should describe the sleep–wake cycle recorded. Specify whether active sleep (AS), quiet sleep (QS), and AS after QS (post-QS AS) were captured.
(3) EEG code: The EEG patterns observed during AS and QS should be described using EEG codes. If multiple patterns corresponding to the postmenstrual age (PMA) are observed during AS, they should be described as 322, 323, and 343, for example. Where the corresponding PMA is uncertain due to abnormal findings, it can be noted as −2 or −7.
(4) Acute- and (5) chronic-stage abnormalities: Describe the presence or absence of acute- and chronic-stage abnormalities and their severity. Descriptions of the findings that determined the severity of each abnormality are provided below. Although this report format does not include descriptions of changes during seizures, it would be beneficial to include them separately. It is advisable to include a section for "other abnormalities" to account for dysmorphic, asymmetric, and asynchronous patterns.
(6) EEG age: Describe the maturity of the EEG findings based on the patterns observed. If the findings suggest a mixture of ages between 34 and 36 weeks PMA, indicate it as "34–36 weeks." Also, assess whether the EEG code aligns with the PMA of the infant.
(7) EEG diagnosis: State whether the EEG is normal or abnormal. If abnormal, specify the degree of abnormality.
(8) Presumed outcome: Outline the presumed outcome based on the EEG findings.

A. Okumura (✉)
Department of Pediatrics, Aichi Medical University, Nagakute, Aichi, Japan
e-mail: okumura.akihisa.479@mail.aichi-med-u.ac.jp

A. Okumura, H. Kidokoro (eds.), *Neonatal EEG: Atlas and Interpretation*,
https://doi.org/10.1007/978-981-96-0726-6_22

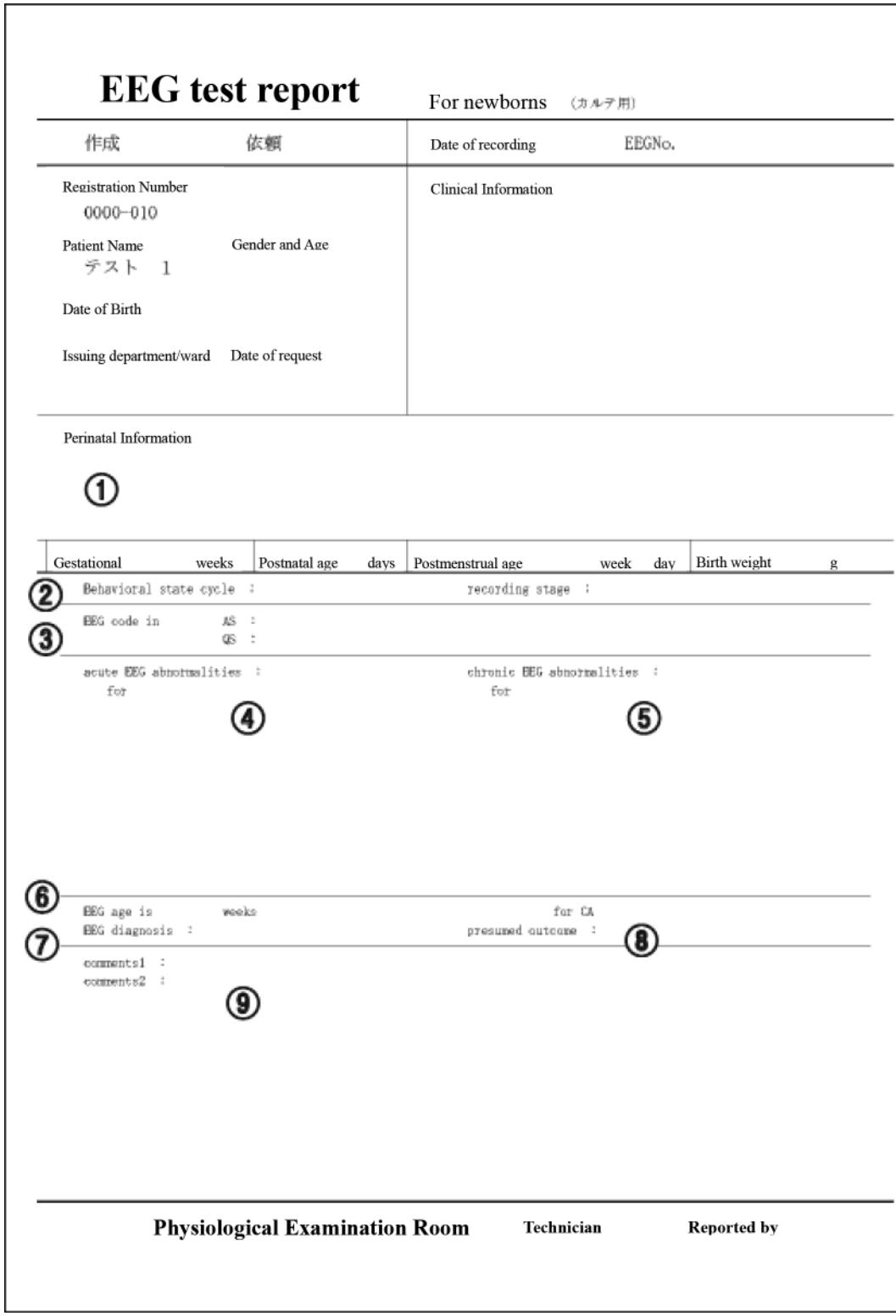

EEG test report

For newborns （カルテ用）

作成　　依頼

Date of recording　　EEGNo.

Registration Number
0000-010

Patient Name　　Gender and Age
テスト　1

Date of Birth

Issuing department/ward　　Date of request

Clinical Information

Perinatal Information

①

Gestational　weeks　Postnatal age　days　Postmenstrual age　week　day　Birth weight　g

②　Behavioral state cycle　:　recording stage　:

③　EEG code in　AS　:
QS　:

acute EEG abnormalities　:　chronic EEG abnormalities　:
for　for

④　⑤

⑥

EEG age is　weeks　for CA

⑦　EEG diagnosis　:　presumed outcome　:　⑧

comments1　:
comments2　:

⑨

Physiological Examination Room　**Technician**　**Reported by**

Fig. 22.1 Sample EEG report format

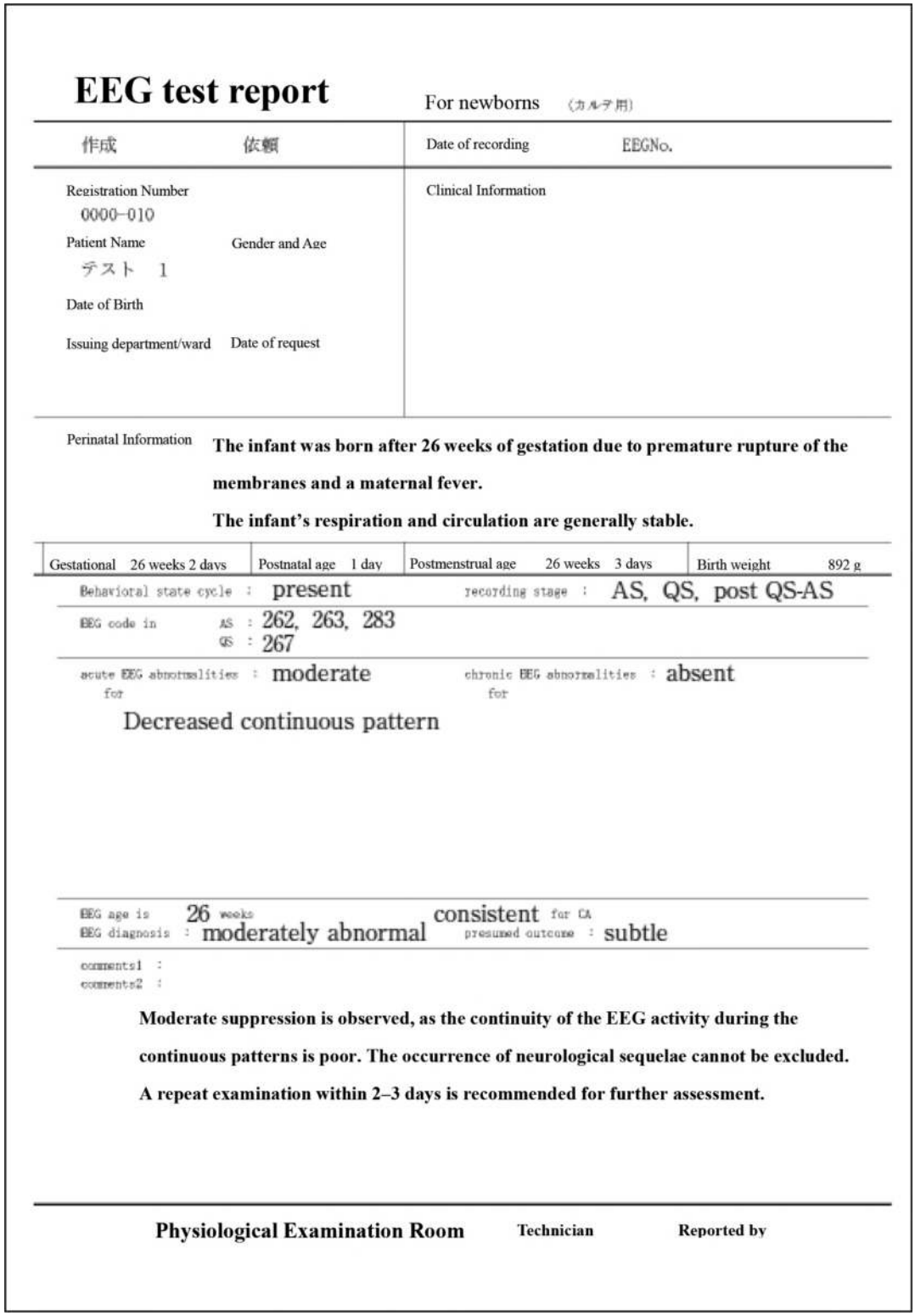

EEG test report

For newborns （カルテ用）

作成 依頼	Date of recording EEGNo.
Registration Number 0000-010 Patient Name Gender and Age テスト 1 Date of Birth Issuing department/ward Date of request	Clinical Information

Perinatal Information **The infant was born after 26 weeks of gestation due to premature rupture of the membranes and a maternal fever.**

The infant's respiration and circulation are generally stable.

Gestational 26 weeks 2 days	Postnatal age 1 day	Postmenstrual age 26 weeks 3 days	Birth weight 892 g

Behavioral state cycle : present　　recording stage : AS, QS, post QS-AS

EEG code in AS : 262, 263, 283
QS : 267

acute EEG abnormalities : moderate　　chronic EEG abnormalities : absent
for　　for

Decreased continuous pattern

EEG age is 26 weeks　　consistent for CA
EEG diagnosis : moderately abnormal　　presumed outcome : subtle

comments1 :
comments2 :

Moderate suppression is observed, as the continuity of the EEG activity during the continuous patterns is poor. The occurrence of neurological sequelae cannot be excluded. A repeat examination within 2–3 days is recommended for further assessment.

Physiological Examination Room **Technician** **Reported by**

Fig. 22.2 Sample EEG report

(9) Comments: This section of the report allows for flexibility and can reflect the individuality of the reader. One should describe findings that do not fit into the standard format or observations that, while not necessarily being abnormal, are noteworthy. It is also valuable to include personal interpretations and insights here.

Clinical Application of EEG in the Neonatal Period

23

Hiroyuki Kidokoro and Anna Shiraki

1 Introduction

Even today, despite the development of new technologies for evaluation of neonatal brain function, neonatal EEG remains one of the most valuable, diagnostic, and prognostic tools in clinical practice. The background EEG activity is a more reliable predictor of outcomes in infants with hypoxic-ischemic encephalopathy (HIE) than are either traditional neurological examinations or the presence/absence of neonatal seizures. This is true not only of full-term but also of preterm infants. EEG serves as the gold standard when diagnosing neonatal seizures. Nowadays, many NICUs are equipped with user-friendly devices, such as amplitude-integrated EEG (aEEG) systems, which greatly aid screening. Contemporaneously, the use of conventional EEG in NICUs is on the rise. When both modalities are effectively combined, neonatal EEGs become even more valuable in terms of diagnosis and prognosis. It is hoped that, in future, the numbers of NICUs that engage in continuous EEG monitoring with simultaneous video-recording will rise.

Although many recent research works have mathematically analyzed EEG data, this chapter is focused specifically on the clinical applications that can be guided by visual inspection of neonatal EEGs.

2 Utility of Neonatal EEGs

Neonatal EEGs are useful when evaluating all infants with severe clinical conditions, particularly those for whom existing neonatal seizures are suspected or those at risk of such seizures, thus infants with HIE, periventricular leukomalacia (PVL), periventricular hemorrhagic infarction (PVHI), or central nervous system infections. Table 23.1 lists the indications for EEG examinations in clinical practice. It is important to note that approximately 50% of neonates with seizures may not exhibit clinical signs, and such seizures will thus be overlooked unless EEG is performed. EEG is noninvasive and can be readily performed at the bedside as often as is required, regardless of the overall condition of the infant. The information obtained from even a single EEG examination is substantial, and repeated recordings enhance the precision and richness of the data. In other words, performing several EEG examinations over time, or continuous EEG monitoring, maximizes the utility of EEG assessments. Neonatal EEG is an integral component of neurological evaluation when

H. Kidokoro (✉) · A. Shiraki
Department of Pediatrics, Nagoya University Graduate School of Medicine, Nagoya, Aichi, Japan
e-mail: kidokoro.hiroyuki.i6@f.mail.nagoya-u.ac.jp; shiraki.anna.g9@f.mail.nagoya-u.ac.jp

A. Okumura, H. Kidokoro (eds.), *Neonatal EEG: Atlas and Interpretation*,
https://doi.org/10.1007/978-981-96-0726-6_23

Table 23.1 Indications for EEG

- All preterm infants (especially those under 32 weeks of gestational age)
- Infants with neonatal encephalopathy (including hypoxic-ischemic encephalopathy)
- Infants who experienced intrauterine growth retardation
- Infants with central nervous system complications (such as meningitis and hydrocephalus)
- Infants with worsening general conditions (such as sepsis and acute post-withdrawal circulatory failure)
- Infants with neurological symptoms (such as decreased muscle tone)
- Infants presenting with multiple malformations or certain congenital abnormalities
- Infants under care after surgery to treat congenital heart disease
- Infants suspected of neonatal seizures, or infants at high risk of such seizures
- Infants receiving muscle relaxants

infants develop severe conditions during their NICU stays.

3 Hypoxic-Ischemic Encephalopathy (HIE) in Term Infants

In term infants with HIE, it is essential to evaluate the extent of suppression of background EEG activity within 6 h of birth. This is crucial in terms of initiation of hypothermic therapy and prediction of outcomes. Several evaluation systems for background EEG abnormalities have been developed; the Watanabe's classification is based on the physiological neural activities of the brain of a term infant (see Fig. 12.1). Regardless of which evaluation system is used, moderate-to-severe EEG abnormalities are strongly associated with poor outcomes.

According to Watanabe's classification, if EEGs performed within 1 week of birth are normal or exhibit only the mildest depression, all infants develop normally. Most infants with mild depression also develop normally; only a few experience mental retardation. Among those with moderate depression, 36% develop normally, 40% experience mental retardation, and 24% develop cerebral palsy. For those exhibiting marked depression, the outcomes are 24% mental retardation, 68% cerebral palsy, and 9% early death. The figures for the group with maximal depression are 67% cerebral palsy and 33% early death (Watanabe et al. 1980).

It is important to recognize that the significance of EEG findings can vary depending on the timing of the EEG recording. Acute-stage abnormalities (ASAs) and chronic-stage abnormalities (CSAs) should be evaluated separately. Even if no abnormal EEG findings are noted later than 2 weeks of age, the prognosis should still be considered uncertain. Additionally, it is known that therapeutic hypothermia per se may delay the recovery of ASAs. In terms of predicting outcomes, the severity of ASAs is more important than a neurological examination.

In terms of the future risk of West syndrome, cases in whom ASAs persist for more than 3 weeks often exhibit the most severe imaging findings and thus become at risk of future West syndrome (Table 23.2) (Kato et al. 2010). Infants with HIE are also at high risk of neonatal seizures. Therefore, rather than a single EEG evaluation, repeated recording or continuous EEG monitoring (preferably video-EEG) should be performed whenever possible. Consideration should also be given to the fact that sedatives and antiseizure medications (ASM, such as phenobarbital, midazolam, etc.) used to manage HIE infants may affect background EEG activity.

Table 23.2 Prediction of infantile epileptic spasm syndrome in infants with neonatal hypoxic-ischemic encephalopathy. Created by the authors based on (Kato et al. 2010)

		Acute-stage abnormalities after 21 days of age	
		Present (n = 4)	Absent (n = 13)
Brain lesions on neonatal MRI	BGT + DWM	●●●●	○
	BGT		●
			○○○○○○○○○
	Watershed		○○

BGT basal ganglia and/or thalamus, *DWM*: diffuse white matter
●: Infants who later presented with infantile epileptic spasm syndrome (IESS)
○: Infants who later did not present with IESS

4 White Matter Injury in Preterm Infants

4.1 Periventricular Leukomalacia (PVL)

If EEG recordings are repeatedly performed commencing from birth, it becomes possible to estimate the timing of PVL injury. This is because, when the brain is affected, acute suppression is apparent in the acute phase of the disease, depending on the extent and duration of damage. In the recovery phase, the suppression findings improve but are replaced by CSAs. If no ASAs are found on EEG performed within 3 days after birth, the risk of future PVL is less than 10%. Conversely, if ASAs are in fact observed, the risk increases with the severity of such abnormalities (Fig. 23.1) (Maruyama et al. 2002; Kidokoro et al. 2009).

On the other hand, CSAs (disorganized patterns) are most prominent from a few days to 2 weeks after the acute phase and then gradually normalize (Fig. 23.2). The extent of ASAs and CSAs are correlated (Table 23.3). If both types of EEG abnormalities are captured, it is possible to make a more accurate prognosis than is afforded by a single recording, and also to estimate the time of PVL injury (Fig. 23.3). When estimating the time of such injury using EEGs, it is likely that many infants who are today diagnosed with PVLs were injured at birth. Even if only specific components of the disorganized pattern, such as

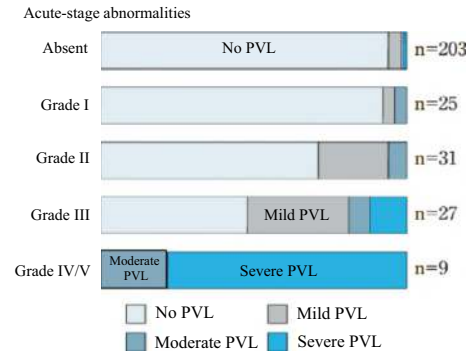

Fig. 23.1 Acute-stage abnormalities and periventricular leukomalacia (PVL) in preterm infant. Created by the authors based on Maruyama et al. (2002)

abnormal brushes and abnormal sharp waves, are evaluated, the disorganized pattern can be assessed to some extent. Abnormal brushes in infants with PVL are particularly frequent in the occipital region, and the locations thereof are related to the sites of white matter lesions and the severity of the clinical prognosis (Kidokoro et al. 2006).

Previous studies have explored the relationship between the frequency of the positive rolandic sharp (PRS) wave (one of the several abnormal sharp transients) and PVL. However, PRS was observed only in infants with severe phenotypes who also presented with extensive cystic lesions. Therefore, occipital or frontal sharp waves afford higher sensitivity when diagnosing PVL (Okumura et al. 2003) (Table 23.4).

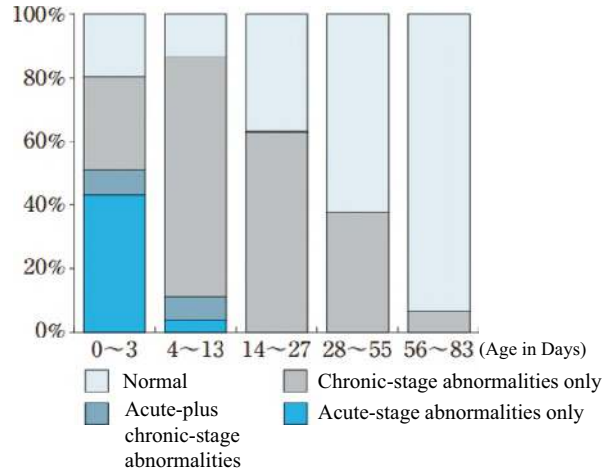

Fig. 23.2 EEG findings in infants with PVL. Created by the authors based on Kidokoro et al. (2009)

Table 23.3 Relationships between the severities of acute-stage EEG abnormalities and chronic-stage EEG abnormalities in infants with PVL ($n = 36$)

		Chronic-stage abnormalities			
		None	Mild	Moderate	Severe
Acute-stage abnormalities	None	○○○○○	○		
			▲■	■	
	Mild	○○	○○	○○	
				▲■■	■■■
	Moderate			○○	
			▲▲■	▲■	▲■■■
	Severe				
					■■■■

○: non-cystic PVL, ▲: localized cystic PVL, ■: extensive cystic PVL

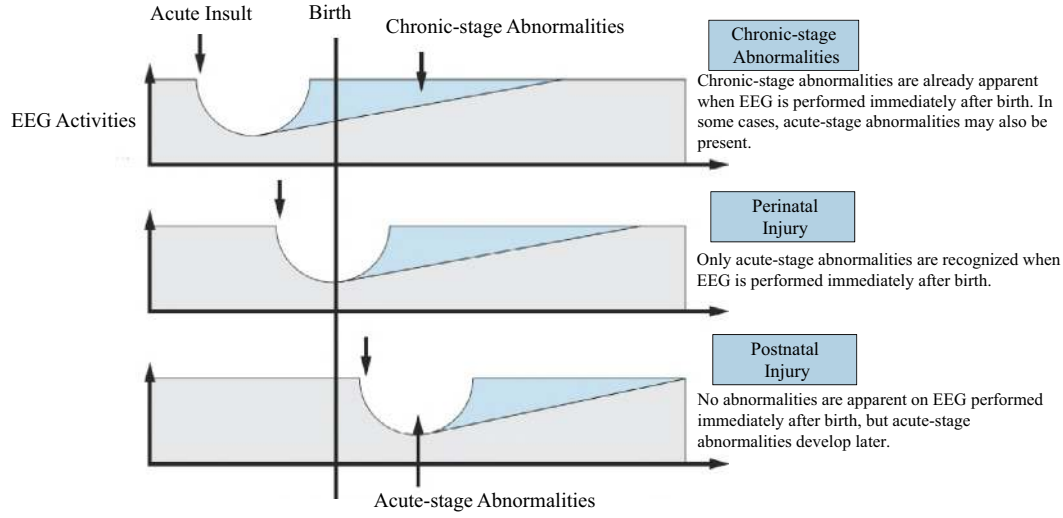

Fig. 23.3 The timing of brain insults

Table 23.4 The relationships between abnormal sharp transients and the neurological outcomes (Okumura et al. 2003)

	FS waves		OS waves		PRS waves	
	FS (–)	FS > 0.1/min	OS (–)	OS > 0.1/min	PRS (–)	PRS > 0.1/min
Control	53	9	59	3	62	0
PVL	8	23	6	25	17	14
Severe	0	10	0	10	1	9
Moderate	5	6	2	9	6	5
Mild	3	7	4	6	10	0
Sensitivity	0.74		0.81		0.45	
Specificity	0.82		0.90		0.82	
PPV	0.72		0.89		1.00	
NPV	0.87		0.91		0.78	

FS frontal sharp, *OS* occipital sharp, *PRS* positive rolandic sharp, *PVL* periventricular leukomalacia, *PPV* positive predictive value, *NPV* negative predictive value

4.2 Intraventricular Hemorrhage (IVH)/Periventricular Hemorrhagic Infarction (PVHI)

In infants with PVL, ASAs are frequently observed in EEG traces obtained immediately after birth (Kidokoro et al. 2009; Kato et al. 2011). In contrast, infants with PVHI do not exhibit ASAs during the period in which a cerebral parenchymal hemorrhage is not yet recognizable on ultrasound examination (Fig. 23.4) (Tsuji et al. 2014). However, when EEGs are performed over time, ASAs are recognized immediately after any substantial hemorrhage and, subsequently, CSAs are noted in cases with poor prognoses (Fig. 23.4). Although the location and extent of a hemorrhage identified via ultrasound examination usefully predict neurological outcomes, EEG also yields reliable prognostic information (Table 23.5) (Kato et al. 2004). In particular, when eight cases with CSAs were evaluated, four of five cases lacking disorganized patterns exhibited normal development, but all three cases with disorganized patterns proceeded to cerebral palsy.

4.3 Encephalopathy of Prematurity

In extremely preterm infants (born before 28 weeks of gestation), the prevalence of neurodevelopmental disorders is high; these include intellectual disabilities, autism spectrum disorders, and attention-deficit/hyperactivity disorder, even in the absence of gross white matter lesions such as PVL or PVHI. Such neurodevelopmental disorders are thought to reflect alteration of normal brain development by a combination of premature birth per se and various perinatal factors. Significant postnatal factors include malnutrition and acute postnatal circulatory failure. In extremely preterm infants with insufficient enteral nutrition, delayed maturation of EEGs, termed the dysmature pattern, is observed, along with reduced physical and head circumference growth; all are risk factors for future intellectual disabilities (Table 23.6) (Hayakawa et al. 2003). On the other hand, acute postnatal circulatory failure, a major cause of postnatal-onset PVL, is also associated with a high prevalence of dysmature patterns at 36–40 weeks of postmenstrual age in extremely preterm infants. This pattern has been reported to correlate with future intellectual disabilities or the onset of West syndrome (Table 23.7) (Okumura et al. 2008).

In the neonatal intensive care units of today, the promotion of normal brain development is an important goal when managing extremely preterm infants, and it is thus vital to perform several EEG tests over time. This aids evaluation of whether brain maturation appropriate for the corrected age can be achieved.

In addition, the two CSAs, thus the disorganized and dysmature patterns, play different roles in terms of the mechanisms of injury and the estimations of outcomes. Okumura and colleagues performed serial EEGs on 183 preterm infants

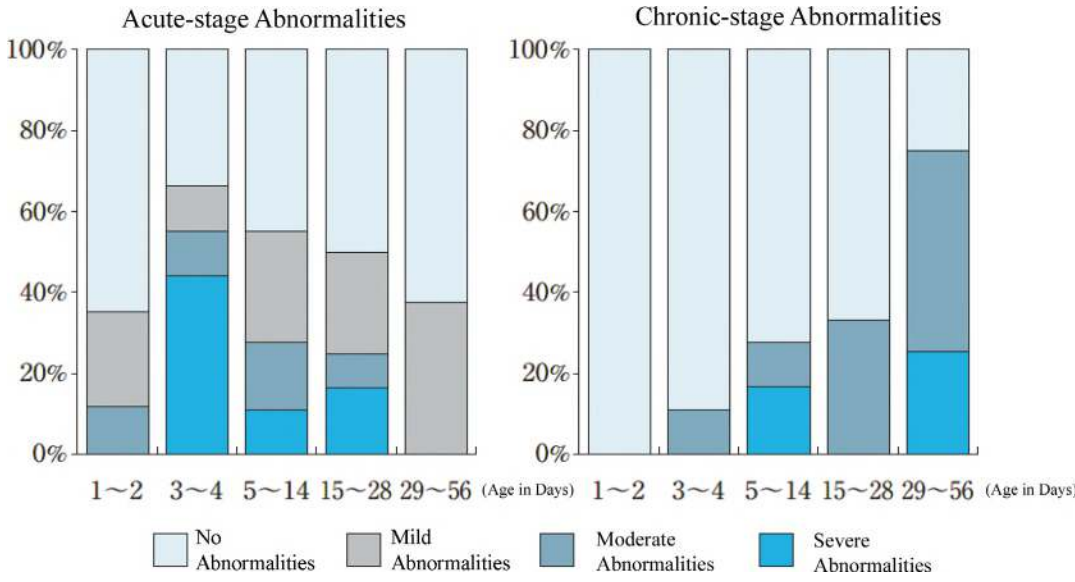

Fig. 23.4 Chronological changes in the EEG findings of infants with PVHI (n = 22) (Tsuji et al. 2014)

Table 23.5 The EEG findings and prognoses of infants with PVHI. Created by the authors based on Kato et al. (2004)

		Normal development	Cerebral palsy	Death
Acute-stage abnormalities	None	4	2	0
	Mild	0	1	0
	Moderate	0	0	0
	Marked	0	1	1
	Maximal	0	0	2
Chronic-stage abnormalities	None	4	1	—
	Disorganized pattern	0	3	—

and observed disorganized patterns in 52 and dysmature patterns in 28 (Okumura et al. 2002). Although the disorganized pattern was frequently observed in infants with gross cerebral lesions such as PVL and PVHI, the dysmature pattern was more common in extremely preterm infants. The latter pattern was less often associated with imaging abnormalities and is strongly linked to intellectual disabilities in the absence of cerebral palsy.

The delta brushes of human preterm infants correspond to the spindle bursts that appear in the immature brain during animal development. These reflect the activities of subplate neurons; hence, their frequency and appearance may be of prognostic utility. Shiraki et al. conducted a large-scale analysis of preterm infant EEGs in an attempt to quantify the occurrence of delta brush. Consistent with previous reports on the occurrence of delta brush, such brushes peaked at 32 to 34 weeks and then trended lower to 40 weeks (Fig. 23.5). Maeda et al. reported that the occurrence of brush at 36 weeks of postmenstrual age was negatively correlated with the outcomes at 18 months of corrected age (Maeda et al. 2021).

4.4 Neonatal Seizures

Video EEG examination is the gold standard for diagnosis of neonatal seizures because, during the neonatal period, electrographic-only seizures (thus seizures without any clinical signs) are common. Conversely, even if neonatal seizures

Table 23.6 The dysmature pattern (DMP). Reproduced with permission from Hayakawa et al. (2003)

	Case	Postmenstrual weeks																Cause of malnutrition
		24 weeks				28 weeks				32 weeks				36 weeks				
Patients with persistent DMP	1	○				○				●		●		●		●		Necrotizing Enterocolitis
	2		○		○			○		○		●		●			●	●	Necrotizing Enterocolitis
	3		○		○		○		○		●		●		●		●		Meconium Plug Syndrome
	4			○	○		○				●		●		●		●		Infection
	5				○	○		○		●				●					Patent Ductus Arteriosus
	6		○	○						●						●	●		No Malnutrition
Patients with transient DMP	7	○	○			○		●		●		●	○	○		○			Infection
	8		○					●		●				○					Feeding intolerance
	9			○	○		○		●			●	●			○	○	○	Feeding intolerance

●: DMP present, ○: normal EEG record

Table 23.7 West syndrome in extremely premature infants. Created by the authors based on Okumura et al. (2008)

	West syndrome (WS) ($N = 3$)	No WS ($N = 29$)	
Necrotizing enterocolitis	0	2 (7%)	NS
Early establishment of enteral feeding	1 (33%)	24 (83%)	NS
Late-onset circulatory dysfunction	3 (100%)	6 (21%)	$p < 0.05$
Grade III or IV intraventricular hemorrhage	0	2 (7%)	NS
Cystic periventricular leukomalacia	0	2 (7%)	NS
Dysmature pattern at 36–40 weeks of postmenstrual age	3 (100%)	10(34%)	$p = 0.058$
Head circumference at 40 weeks of postmenstrual age < tenth percentile	3 (100%)	1 (3%)	$p < 0.01$

NS not significant

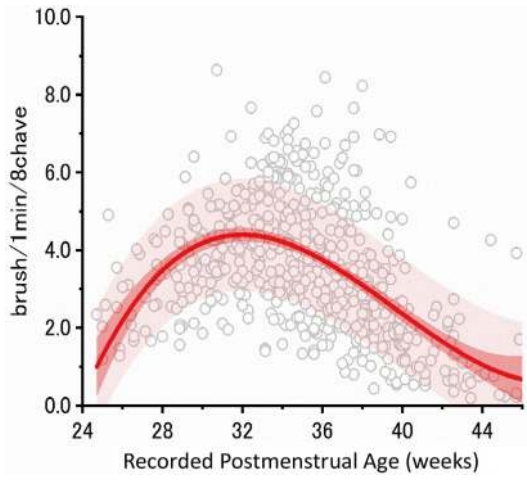

Fig. 23.5 Developmental changes in the occurrence of delta brushes

are clinically suspected, changes in EEG during such episodes are often absent. Alternating limb movements such as pedaling or crawling, previously considered to be subtle seizures, are classified as non-epileptic abnormal movements because they are not accompanied by EEG changes. When ASMs are administered to infants with neonatal seizures, the seizure manifestations may disappear, but EEG-only seizures often remain. If EEG recording is neglected at this time, treatment will be incomplete. Therefore, EEG examination is important not only for the definitive diagnosis of neonatal seizures but also when determining treatment effectiveness. If seizures are suspected, or even if they have disappeared, EEG monitoring should be performed for at least 24 h.

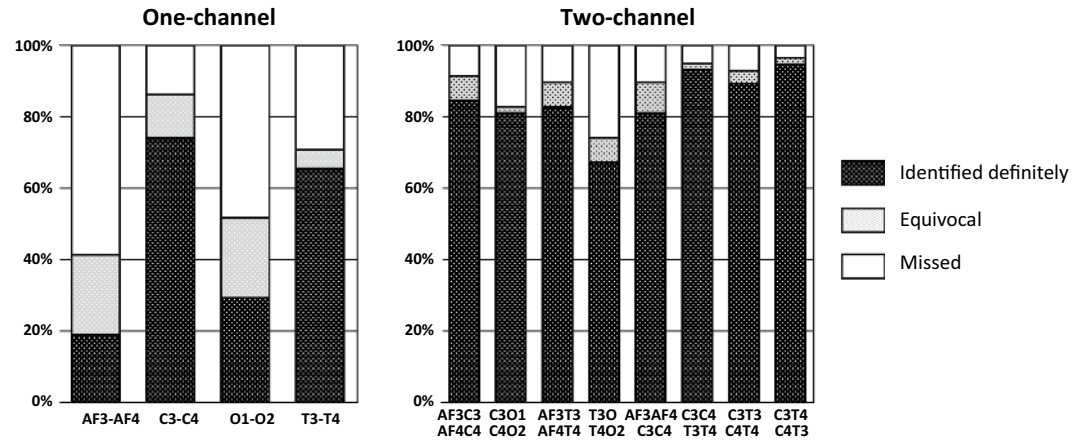

Fig. 23.6 The sensitivities of seizure detection using limited number of electrodes

Appropriate management of neonatal seizures may affect the outcome to some extent, but the underlying disease and the severity thereof typically exert more significant impacts on the outcome. Interictal EEG findings usefully predict the outcomes of infants with neonatal seizures. For example, severe ASAs apparent on EEG during the interictal period suggest a poor outcome, and a dysmorphic pattern indicates potential brain malformation. In infants with self-limited neonatal epilepsy, even if seizures are frequent, normal EEG findings during the interictal period are common, and the outcome is generally good.

Although aEEG is helpful when it is sought to evaluate neonatal seizures easily, the diagnostic capacities thereof have several limitations: (1) aEEG may miss short-duration or low-amplitude seizures; (2) it is more challenging to identify aEEG artifacts than those of standard EEG; and, (3) if a small number of electrodes is used, focal seizures may not be captured. Kidokoro et al. simulated whether seizures recorded via standard eight-channel EEG could be detected using only one or two channels (Kidokoro et al. 2013). The one-channel setup detected approximately 70% of seizures in the central and temporal regions, but only 30% in the frontal and occipital regions. However, with a two-channel setup, regardless of the locations of the channels, the seizure detection rate ranged from 70–90% (Fig. 23.6).

Therefore, if neonatal seizures are suspected, video EEG recording should be promptly initiated and continued for at least 24 h. If true seizures are detected, the use of ASMs should be considered based on the frequency of seizures observed on EEG. EEG monitoring should be continued until at least 24 h has passed since the seizures ceased on EEG. Furthermore, accurate assessment of background EEG findings can provide valuable prognostic information.

References

Hayakawa M, Okumura A, Hayakawa F, Kato Y, Ohshiro M, Tauchi N, Watanabe K. Nutritional state and growth and functional maturation of the brain in extremely low birth weight infants. Pediatrics. 2003;111(5 Pt 1):991–5.

Kato T, Okumura A, Hayakawa F, Kuno K, Watanabe K. Electroencephalographic aspects of periventricular hemorrhagic infarction in preterm infants. Neuropediatrics. 2004;35(3):161–6.

Kato T, Okumura A, Hayakawa F, Tsuji T, Hayashi S, Kubota T, Fukasawa T, Suzuki M, Maruyama K, Oshiro M, Hattori T, Kidokoro H, Natsume J, Hayakawa M, Watanabe K. Prolonged EEG depression in term and near-term infants with hypoxic ischemic encephalopathy and later development of West syndrome. Epilepsia. 2010;51(12):2392–6.

Kato T, Okumura A, Hayakawa F, Tsuji T, Natsume J, Hayakawa M. Amplitude-integrated electroencephalography in preterm infants with cystic periventricular leukomalacia. Early Hum Dev. 2011;87(3):217–21.

Kidokoro H, Okumura A, Watanabe K. Abnormal brushes in preterm infants with periventricular leukomalacia. Neuropediatrics. 2006;37(5):265–8.

Kidokoro H, Okumura A, Hayakawa F, Kato T, Maruyama K, Kubota T, Suzuki M, Natsume J, Watanabe K,

Kojima S. Chronologic changes in neonatal EEG findings in periventricular leukomalacia. Pediatrics. 2009;124(3):e468–e75.

Kidokoro H, Kubota T, Hayakawa M, Kato Y, Okumura A. Neonatal seizure identification on reduced channel EEG. Arch Dis Child Fetal Neonatal Ed. 2013;98(4):F359–F61.

Maeda T, Kidokoro H, Tachibana T, Shiraki A, Yamamoto H, Nakata T, Fukasawa T, Kubota T, Sato Y, Kato T, Natsume J, Okumura A, Hayakawa M. Trajectory of the incidence of brushes on preterm electroencephalogram and its association with neurodevelopment in extremely low birth weight infants. Brain and Development. 2021;43(10):979–87.

Maruyama K, Okumura A, Hayakawa F, Kato T, Kuno K, Watanabe K. Prognostic value of EEG depression in preterm infants for later development of cerebral palsy. Neuropediatrics. 2002;33(3):133–7.

Okumura A, Hayakawa F, Kato T, Kuno K, Watanabe K. Developmental outcome and types of chronic-stage EEG abnormalities in preterm infants. Dev Med Child Neurol. 2002;44(11):729–34.

Okumura A, Hayakawa F, Kato T, Maruyama K, Kubota T, Suzuki M, Kidokoro H, Kuno K, Watanabe K. Abnormal sharp transients on electroencephalograms in preterm infants with periventricular leukomalacia. J Pediatr. 2003;143(1):26–30.

Okumura A, Suzuki M, Kubota T, Hisada K, Kidokoro H, Kato T, Hayakawa F, Shimizu T. West syndrome in extremely preterm infants: its relation to postnatal events. Arch Dis Child Fetal Neonatal Ed. 2008;93(4):F326–F7.

Tsuji T, Okumura A, Kidokoro H, Hayakawa F, Kubota T, Maruyama K, Kato T, Oshiro M, Hayakawa M, Watanabe K. Differences between periventricular hemorrhagic infarction and periventricular leukomalacia. Brain and Development. 2014;36(7):555–62.

Watanabe K, Miyazaki S, Hara K, Hakamada S. Behavioral state cycles, background EEGs and prognosis of newborns with perinatal hypoxia. Electroencephalogr Clin Neurophysiol. 1980;49(5–6):618–25.

Q1. Choose all EEGs of quiet sleep from A to D.

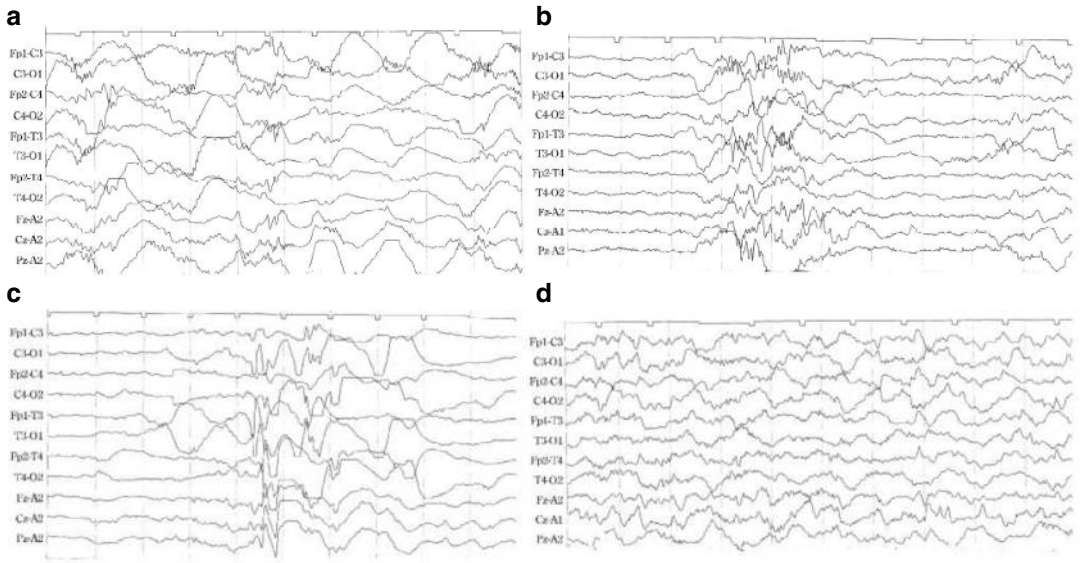

The correct answer: B, C, and D

A is 303, **B** is 367, **C** is 287, and **D** is 405. The high-voltage slow wave (HVS) pattern is represented as "3" in preterm infants and "5" in full-term infants; the former being a pattern during active sleep and the latter during quiet sleep. The code number "7" signifies discontinuous EEG, which is a pattern of EEG during quiet sleep. Therefore, of the four EEG samples, only **A** is an EEG during active sleep, and the rest are EEGs during quiet sleep.

A. Okumura, H. Kidokoro (eds.), *Neonatal EEG: Atlas and Interpretation*,
https://doi.org/10.1007/978-981-96-0726-6

Q2. Arrange the EEGs of quiet sleep in order of immaturity.

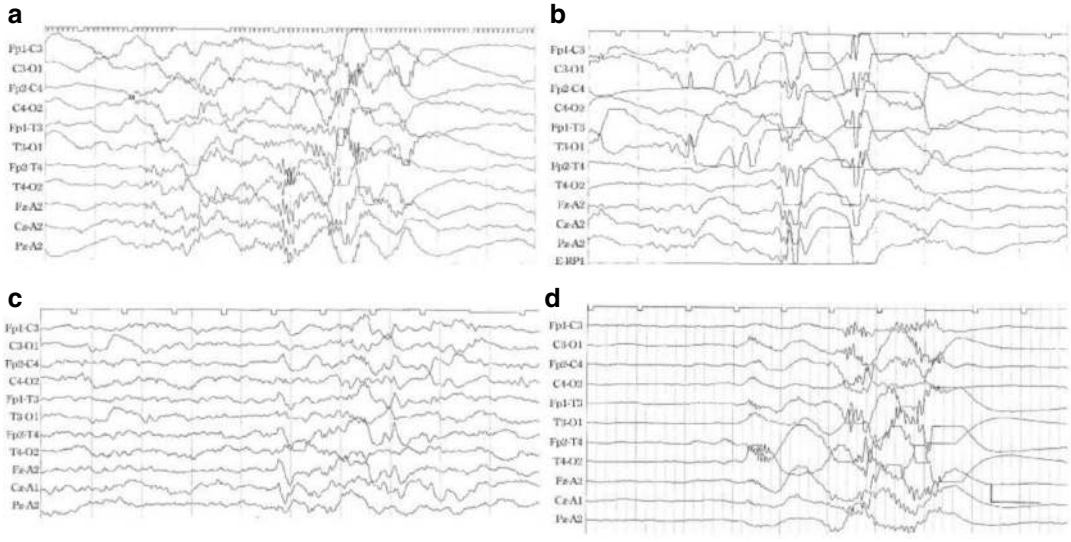

The correct answer: B → D → A → C

The size of the slow waves and the presence or absence of transients are the key points. The slow waves are largest in **B** (267), where sharp wave bursts from the frontal area, characteristic of extremely immature EEGs, can be seen. The slow waves are large, and the monotony remains, with abundant brush appearing in **D** (307). This further matures to **A** (347), where the slow waves become smaller. These are the patterns of quiet sleep in preterm infants. In contrast, in **C** (407), the brush decreases significantly, and the polymorphism of the slow waves stands out, with activity also observed in the low amplitude part, which is characteristic of a full-term infant pattern.

Q3. Arrange the EEGs of quiet sleep in order of immaturity.

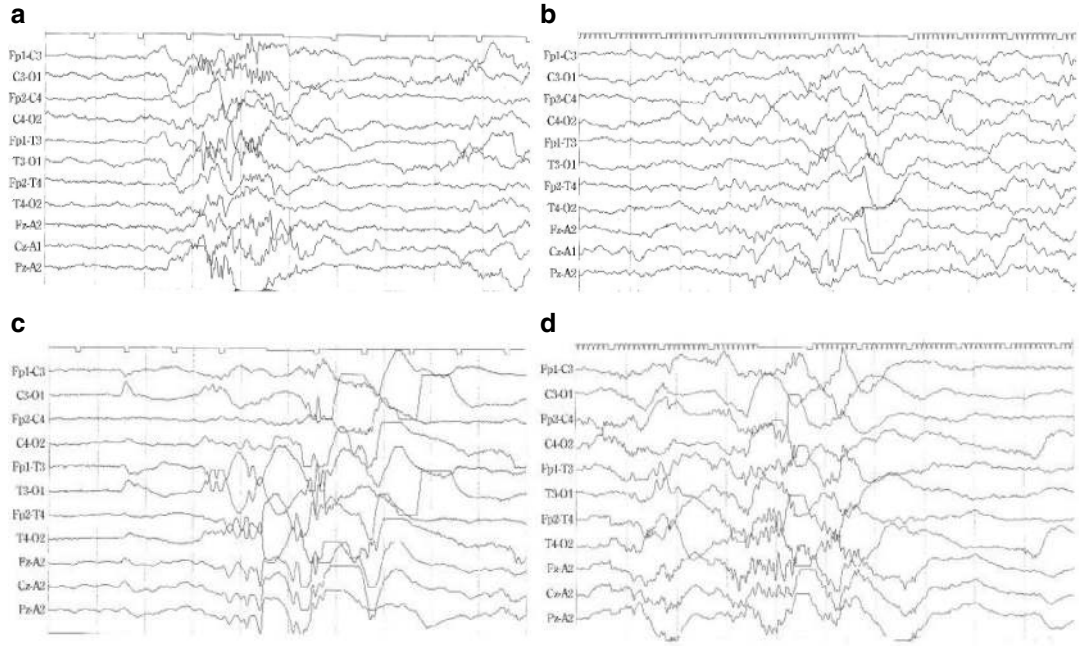

The correct answer: C → D → A → B

The size of the slow waves and the presence or absence of transients are the key points. The slow waves are largest in **C** (287), where sharp wave bursts from the temporal area, characteristic of immaturity, can be seen. Then, the slow waves are large, and the monotony remains with abundant brush appearing in **D** (327). This further matures to **A** (367), where the slow waves become smaller. These are patterns of quiet sleep in preterm infants, while in **B** (407), the brush decreases significantly and there is marked slow wave polymorphism, with activity also observed in the low amplitude part, which is a full-term infant pattern.

Q4. Arrange the compressed EEGs in order of immaturity.

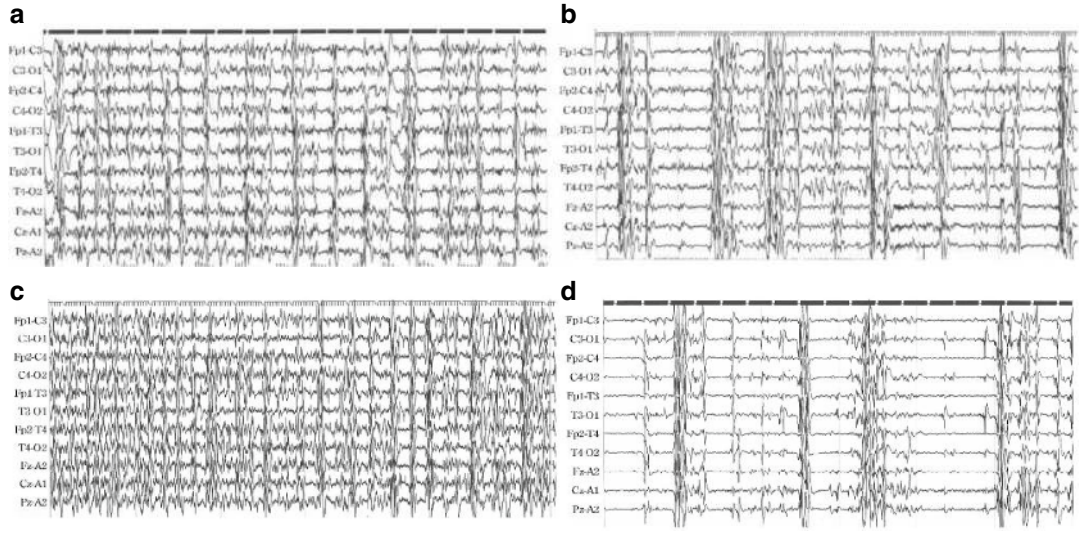

The correct answer: D → B → A → C

Focus on the duration of the interburst interval (IBI).

D has a noticeable discontinuity with few bursts, and the maximum IBI is approximately 50 s (287). **B** shows shortening of the IBI with a few seconds of high-amplitude part, but there are also IBIs of approximately 20 s (347). **A** has further shortening of the IBI to approximately 10 s (367). In **C**, it is difficult to distinguish between the high-amplitude part and the IBI, and the duration of IBI is 10 s or less (387). In this way, shortening of the duration of IBI is seen with maturity.

Q5. Arrange the compressed EEGs in order of immaturity.

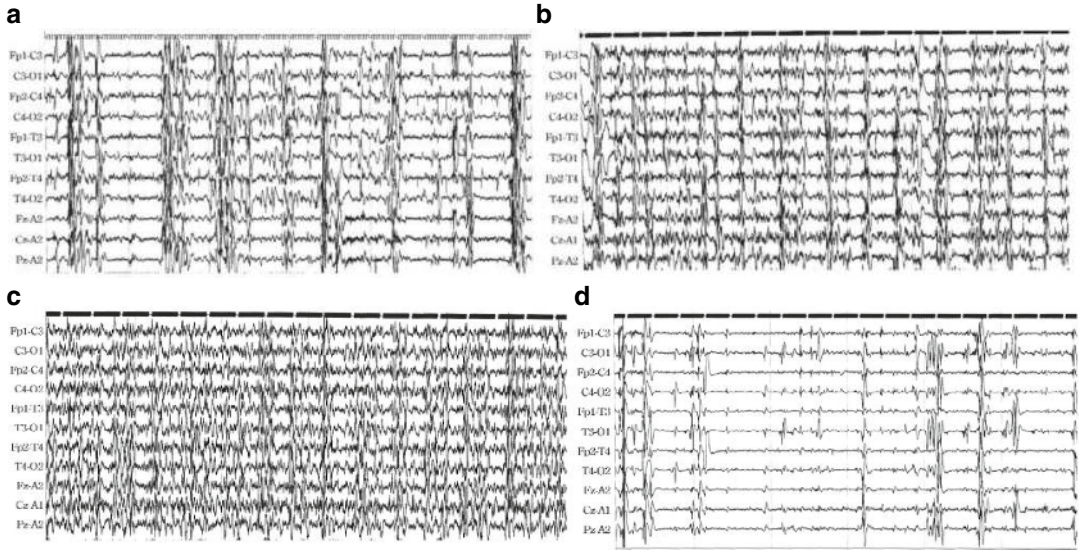

The correct answer: D → A → B → C

Focus on the duration of the interburst interval (IBI). **D** has a noticeable discontinuity with few bursts, and the maximum IBI is approximately 60 s (267). **A** shows shortening of the IBI with a few seconds of high-amplitude parts, but there are also IBIs exceeding 20 s (327). In **B**, the IBI is shortened further to approximately 10 s (367). In **C**, it is difficult to distinguish between the high-amplitude part and the IBI, and the duration of the IBI is a few seconds (407). In this way, shortening of the IBI duration is seen with maturity.

Q6. EEG samples A to D are TA/TD at 36–44 weeks postmenstrual age. Arrange them in order of immaturity.

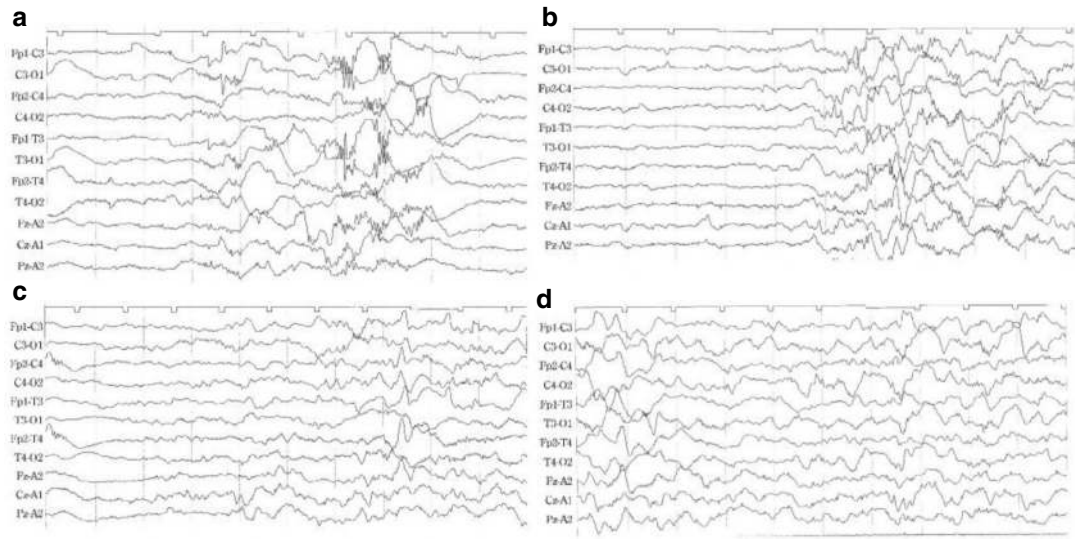

The correct answer: A → B → C → D

A is 367 with abundant brushes and sharp transients. **B** is 387, characterized by flattening of the low-amplitude parts and brush. **C** is 407, showing few brushes and activity in the low-amplitude parts. **D** is 447, showing no clear alternations with firm activity in the low-amplitude parts. After 46 weeks of postmenstrual age, EEGs never show a discontinuous pattern in a physiological state. The only exception is in cases of severe brain function suppression, such as acute encephalopathy or hypoxic–ischemic encephalopathy, where burst suppression may be observed.

Q7. Choose all EEGs of active sleep.

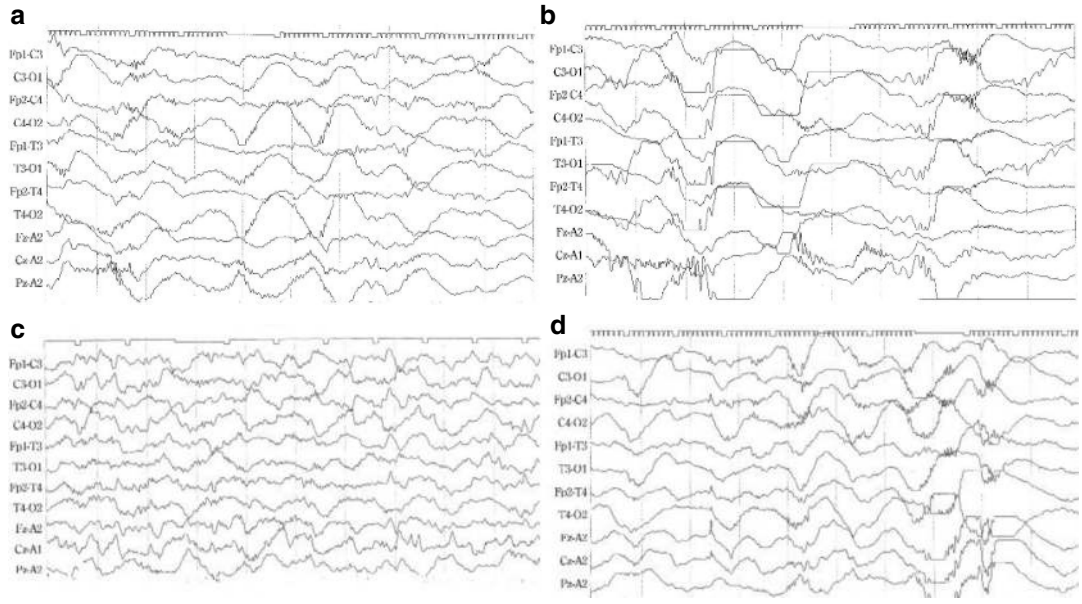

The correct answer: A, B, and D

A is 323, **B** is 263, **C** is 405, and **D** is 343. The high-voltage slow wave (HVS) pattern is represented by "3" in preterm infants and "5" in full-term infants, with the former indicating active sleep and the latter quiet sleep. Therefore, of the four EEG samples, only **C** is an EEG of quiet sleep, while the others are all of active sleep. Continuous, monotonous bowl-shaped slow waves indicate active sleep in preterm infants, while continuous small slow waves with polymorphism indicate quiet sleep in full-term infants and persist into older age.

Q8. Arrange the active sleep EEGs from A to D in order of immaturity.

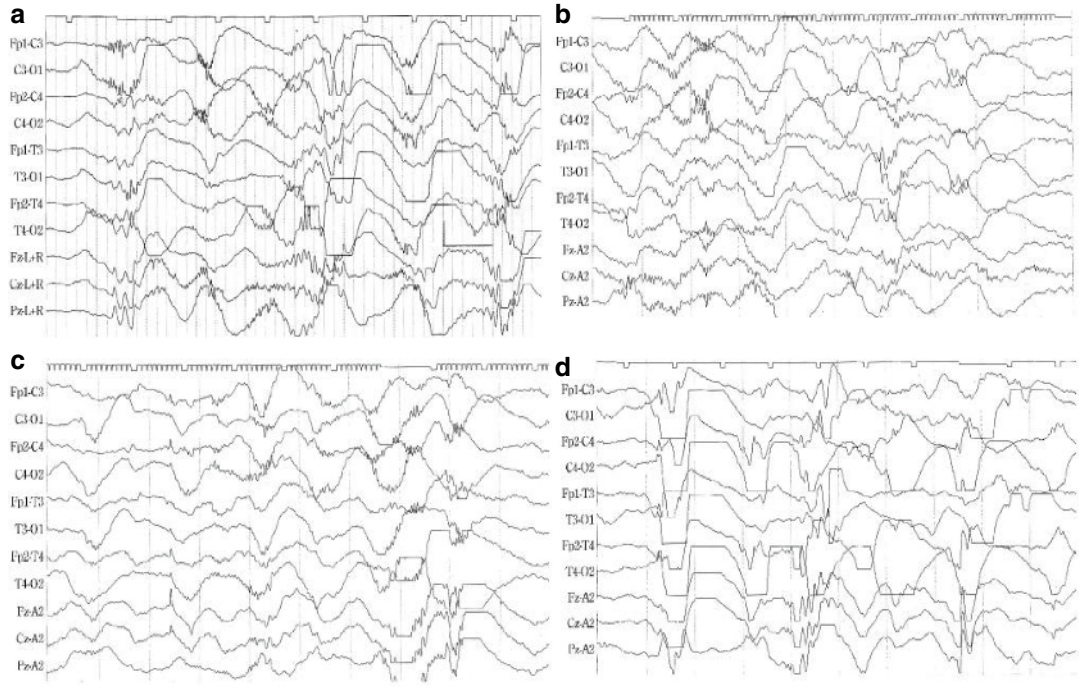

The correct answer: D → A → B → C

Identifying the postmenstrual weeks based on the principle that larger sizes of slow waves indicate immaturity and focusing on transients. The order based on the size of the slow waves is D → A → B → C. **D** is 263, characterized by sharp bursts from the frontal area and 0.5-Hz slow waves over 300 μV; **A** is 303, showing abundant brushes and slow waves of approximately 1 Hz and 300 μV; **B** is 323, showing abundant brushes with 1 Hz and 250 μV slow waves; and **C** is 343, with 1.5 Hz and 200 μV slow waves.

Q9. Arrange the EEGs in order of immaturity.

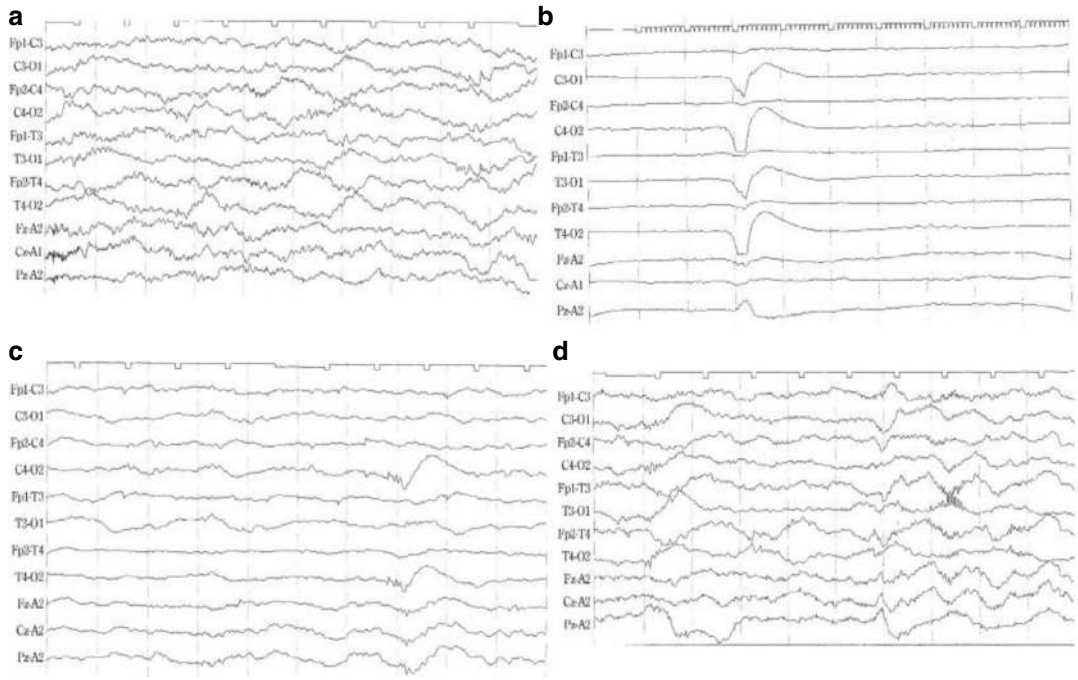

The correct answer: B → C → D → A

A shows a "2" or "3" pattern with 8–12-Hz semi-rhythmic activity and brushes as the main component, as 382 or 383. **B** is very immature, with almost flat low-amplitude occipital sharp waves appearing isolately, as 262. **C** shows 1-Hz slow waves with brushes preceding a low amplitude baseline, classified as 302 or 322. **D** is characterized by monotonous low voltage slow waves with abundant brushes and hardly any sharp waves, classified as 342 or 343. Based on this, the order of immaturity is **B → C → D → A**.

Q10. What is the code of the EEG pattern below?

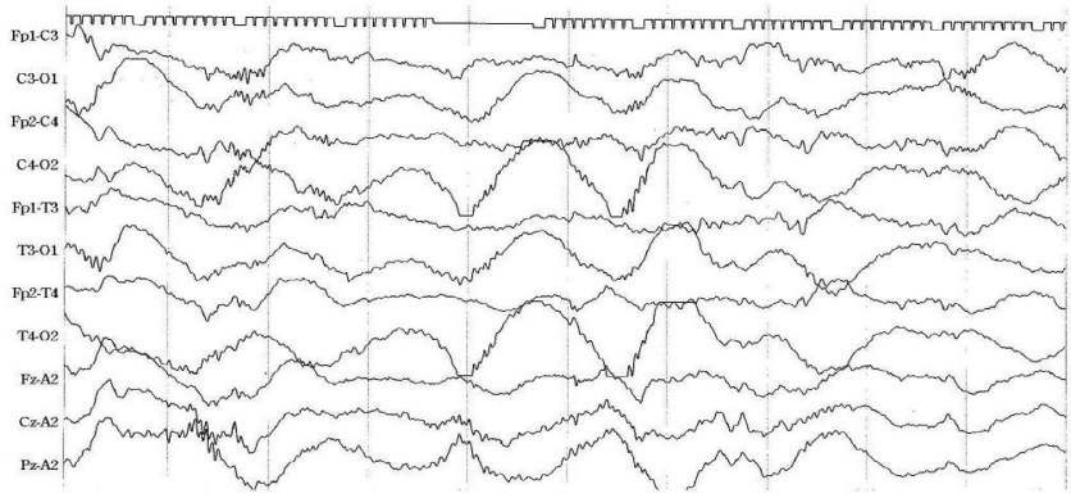

① 283
② 303
③ 323
④ 343

The correct answer: 323

Monotonous high-amplitude slow waves appear continuously; this high-amplitude slow wave pattern of preterm infants is classified as a "3" pattern. The slow waves, approximately 1 Hz and 200–300 μV, appear continuously from the occipital area. Although brushes are abundantly superimposed, no sharp waves are recognized, indicating characteristics of 32–34 weeks. The size of the slow waves suggests immaturity at 32 weeks rather than 34 weeks, so it is classified as 323.

Q11. What is the code for the following EEG pattern?

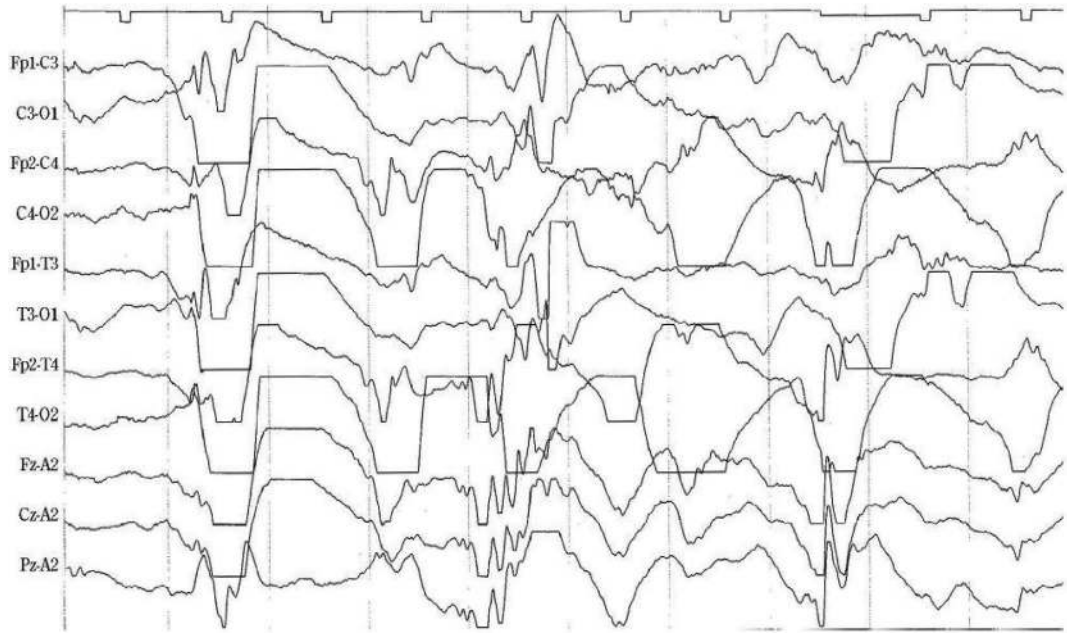

① 263
② 283
③ 265
④ 285

The correct answer: 263

A monotonous high-voltage slow wave lacking polymorphism appears continuously; this is a high-voltage slow wave pattern of premature infants (pattern "3"). The slow wave is approximately 0.5–0.8 Hz and 300–400 μV, showing extremely immature characteristics. No brushes are observed, but frontal sharp bursts are present. Based on this, it is classified as an extremely immature EEG pattern, interpreted as 263.

Q12. What is the code for the following EEG pattern?

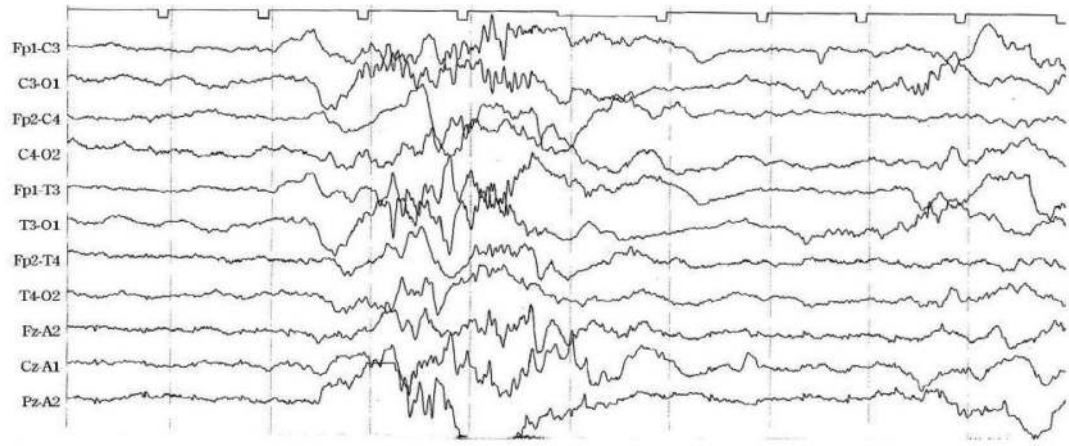

① 347
② 367
③ 387
④ 407

The correct answer: 367

A monotonous high-voltage slow wave lacking polymorphism forms a high-amplitude part for approximately 3 s continuously. The parts before and after this are intermittent low-amplitude parts, forming a discontinuous pattern "7" code. The slow wave is approximately 2 Hz and 100–150 μV, and abundant brushes are superimposed. Sharp waves appear isolately from the temporal area. These are all consistent with the characteristics of 36 weeks postmenstrual age, and it is classified as 367.

Q13. What is the code for the following EEG pattern?

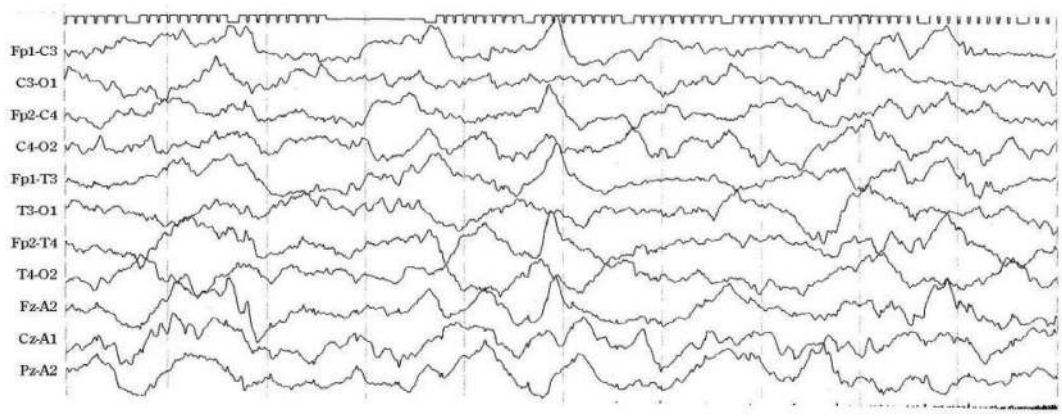

① 385
② 387
③ 405
④ 407

The correct answer: 405

High-voltage slow waves rich in polymorphism appear continuously, with the slow waves at 2–3 Hz and 100–150 μV. No brushes or sharp waves are seen. Considering the size of the slow waves and their polymorphism, it is the high-voltage slow wave (HVS) pattern of full-term infants, so it is coded as "5." It is considered to be indicative of 38–44 weeks of postmenstrual age, but at 38 weeks, monotony and brush remain, and at 44 weeks, the slow waves become larger. Therefore, this can be considered a typical 40-week HVS, and it is classified as 405.

Q14. What is the code for the following EEG pattern?

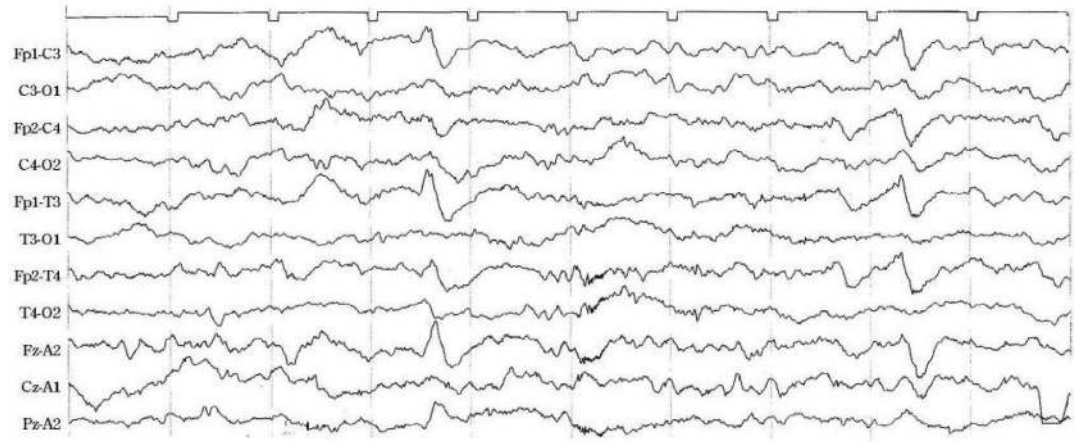

① 383
② 385
③ 403
④ 405

The correct answer: 403

Except for two sharp waves observed from Fp1, no high-amplitude waveforms are observed. The brush is scarce, and semi-rhythmic theta activity is observed. Based on this, it is classified as a mixed pattern "403" with frontal sharp transients.

Q15. What is the code for the following EEG pattern?

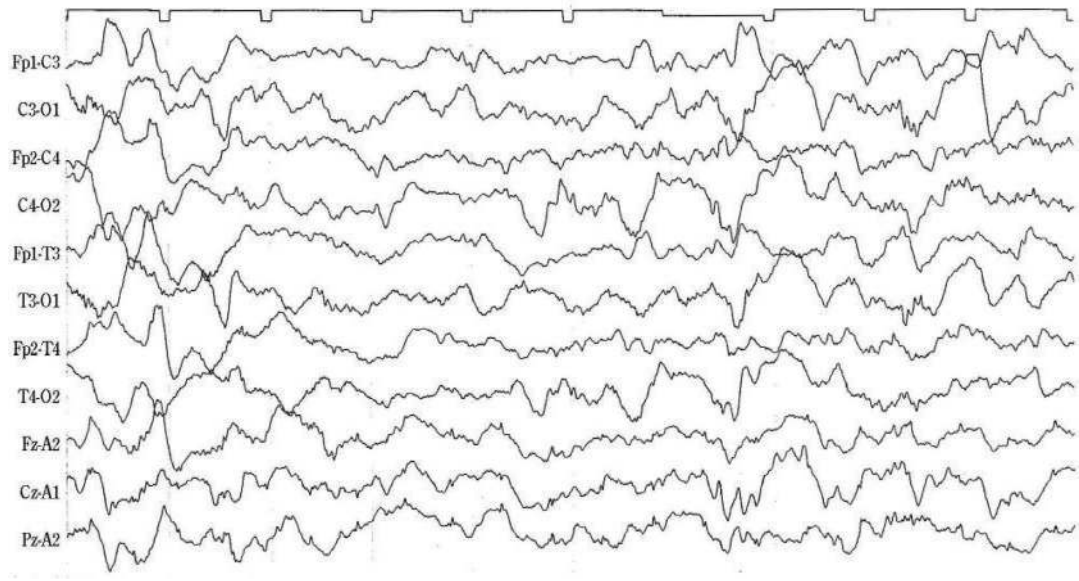

① 425
② 427
③ 445
④ 447

The correct answer: 447

Large, polymorphic slow waves are clustered at the left end and slightly to the right of center. No significant slow waves are observed in other parts. As high- and low-amplitude parts appear alternately, it is an alternating pattern (TA), but the suppression of activity in the low-amplitude part is not noticeable. This is a TA that has matured beyond 407 and is just before the disappearance of TA, that is, "447." The high-voltage slow waves at this time are similar in morphology to the slow waves during sleep in infancy.

Q16. Choose all the 40-week EEGs.

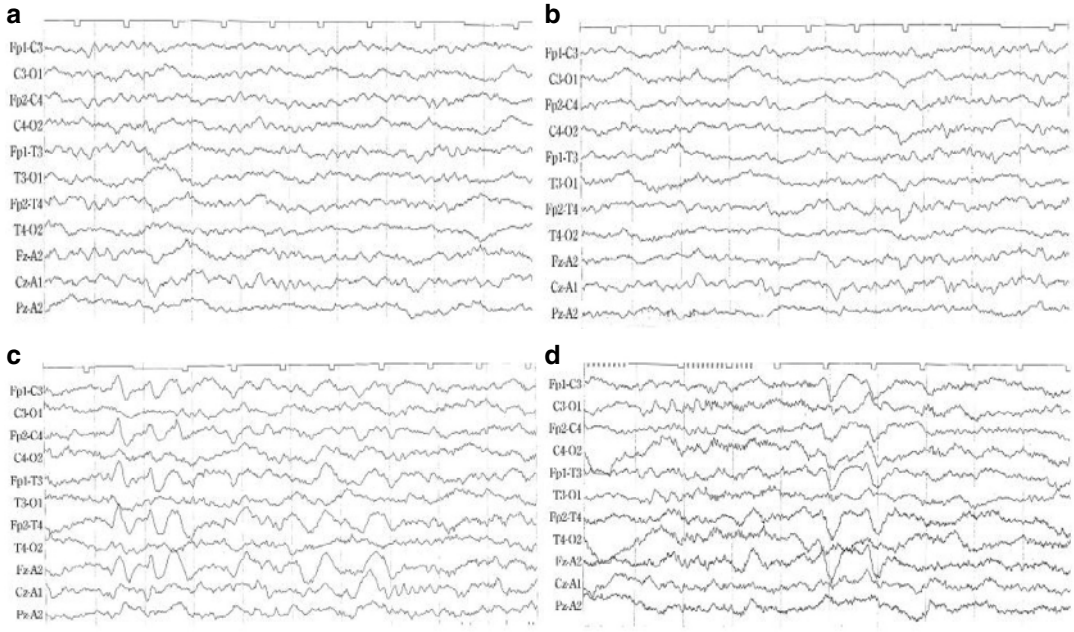

The correct answer: B and C

A shows 3–4 Hz semi-rhythmic theta, which is more indicative of a 44-week pattern (442) than a 40-week postmenstrual age pattern. **B** shows 5–7 Hz semi-rhythmic theta, 402. **C** is classified as 403 with frontal sharp transients and frontal slow bursts. **D** is similar to **C**, but with more remaining brushes, and the frequency of semi-rhythmic activity is fast at 8–12 Hz, so it is judged to be 383. Therefore, **B** and **C** have the 40-week code.

Q17. Choose all EEG samples that show disorganized patterns.

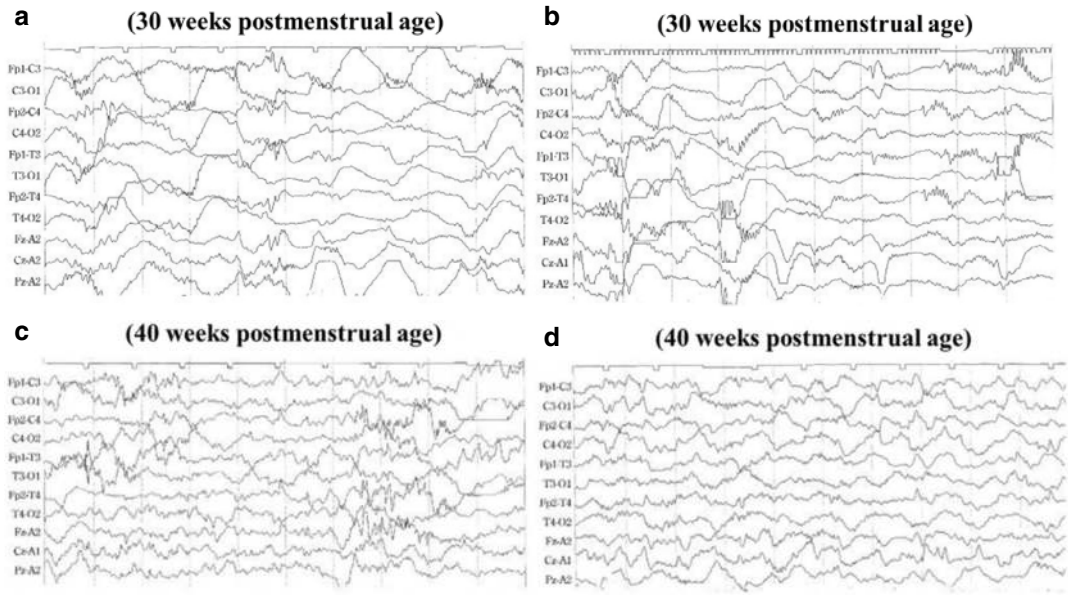

The correct answer: B and C

A has a series of beautiful bowl-shaped slow waves, classified as 303, with the brush somewhat spiky but not mechanical. **B** has a positive sharp wave appearing from Cz, and the brush is mechanical, indicating a typical disorganized pattern. **C** has a good 405 background, but irregular fast waves superimposed on interhemispheric asynchrony appear, and deformation is seen in the slow waves, which are disorganized. **D** has a mature 40-week pattern with polymorphism, and no significant deformation is observed, representing a normal 405.

Q18. Choose all EEG samples that show disorganized patterns.

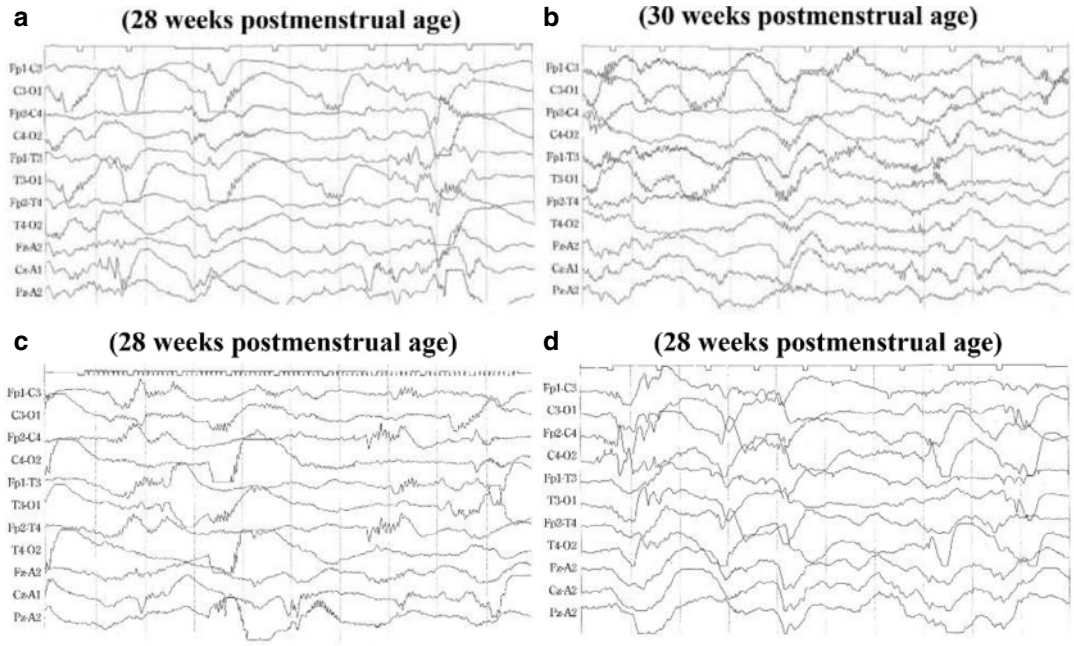

The correct answer: A and C

A and **C** exhibit deformed high-amplitude slow waves due to the insertion of repeated abnormal sharp waves and the appearance of mechanical brushes, which are typical disorganized patterns. In **B**, brush appears frequently, but no deformation is observed in either slow waves or brushes. **D** also shows clustering of very immature high-amplitude slow waves (267 or 287) but does not show non-physiological deformation.

Q19. Choose all EEG samples that show positive rolandic sharp waves.

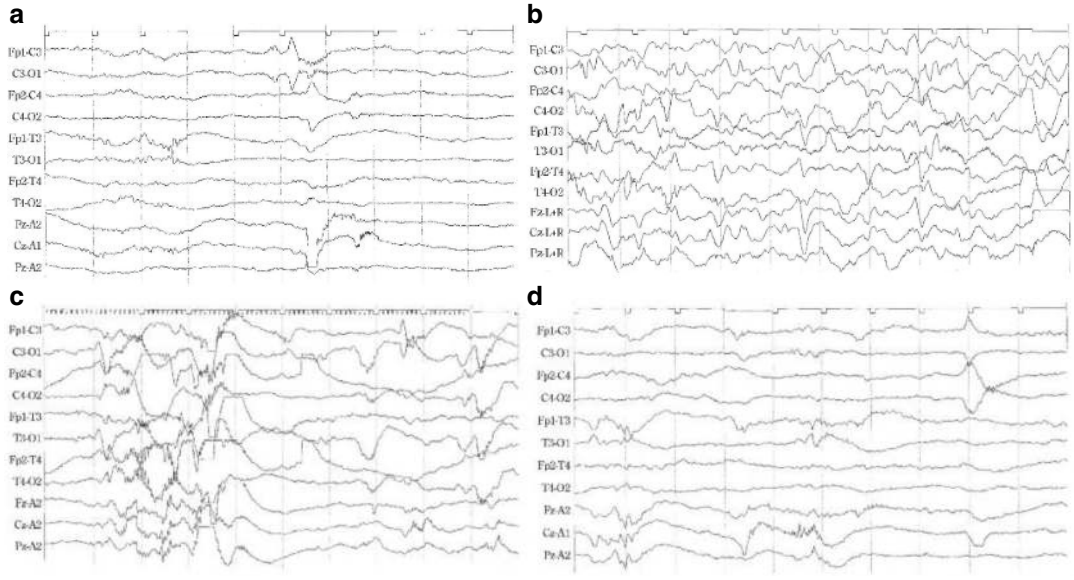

The correct answer: A, C, and D

A shows positive rolandic sharp wave (PRS) typically seen in the recovery period, appearing consecutively from C3 and C4, accompanied by a decrease in amplitude (slightly to the right of the center). **B** exhibits a high-voltage slow wave pattern with many sharp waves overall, but no clear PRS is observed. **C** shows the PRS typical of a disorganized pattern, appearing from C3 on the right side. **D** also shows PRS appearing synchronously from the left and right central parts in low voltage EEG activity (to the right).

Q20. Choose all EEG samples that show mechanical brushes.

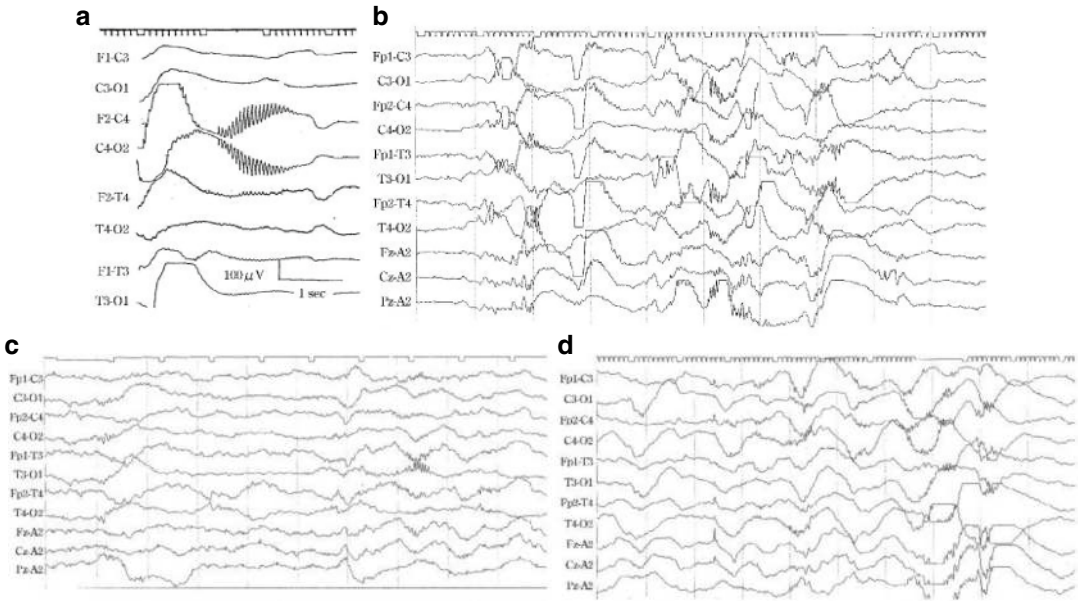

The correct answer: A and B

A is a typical mechanical brush, characterized by a cogwheel-like shape. Remember that, similar to a positive rolandic sharp wave (PRS), a mechanical brush does not appear in isolation but are always accompanied by depression or a disorganized pattern. If you remember this, you will not make a mistake. For example, of **B**, **C**, and **D**, only **B** has a disorganized EEG background. The periods of **C** (363) and **D** (343) are when the brush becomes somewhat sharp physiologically, but they should not be judged as mechanical.

Q21. Choose all EEG samples that show a dysmature pattern.

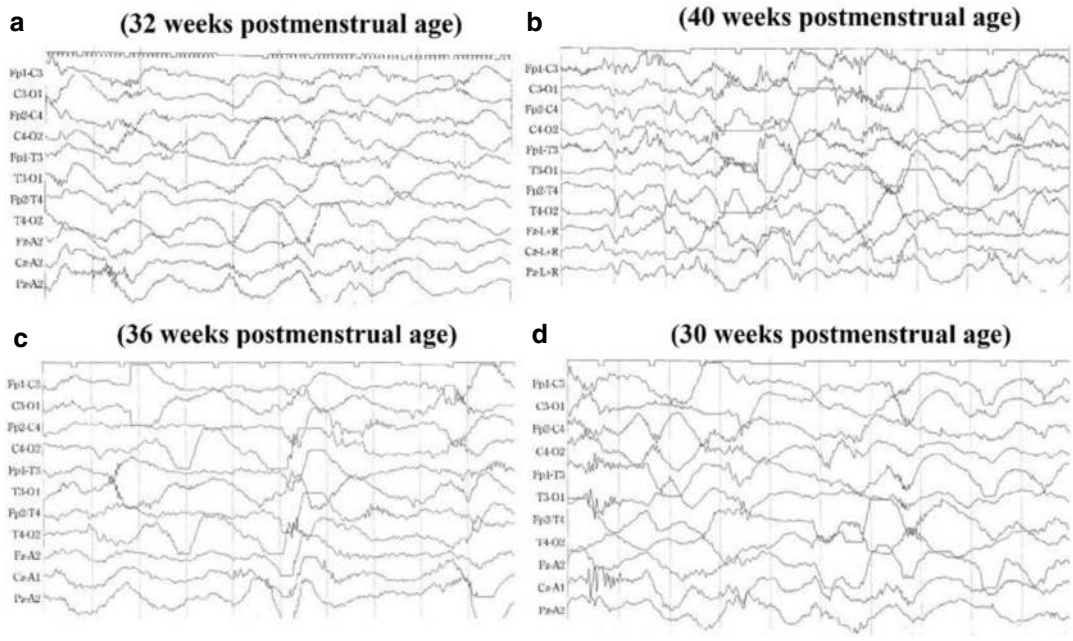

The correct answer: B and C

A dysmature pattern in an EEG indicates immaturity relative to the expected postmenstrual age (PMA). The PMA estimated from the slow waves and transients are **A** at 32 weeks PMA, **B** at 32–34 weeks PMA, **C** at 32–34 weeks PMA, and **D** at 28–30 weeks PMA. The correct answer is **B** (an approximately 6–8-week delay) and **C** (a 2–4-week delay).

Q22. Choose an abnormal EEG.

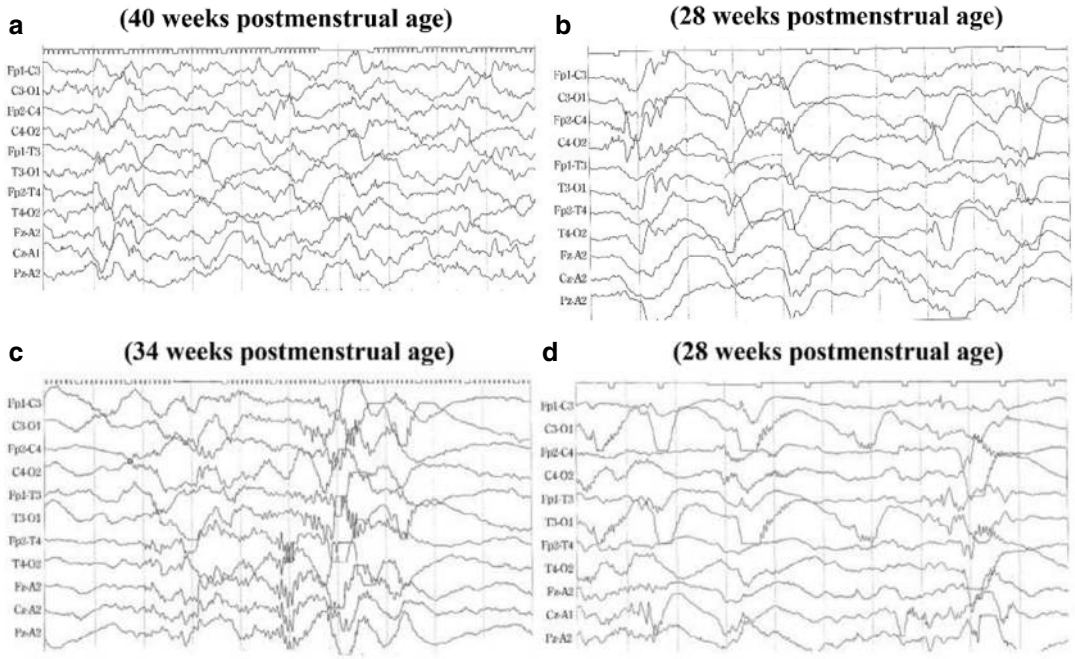

The correct answer: D

A is a well-developed 405 with polymorphism; if this pattern is confirmed, there is less concern about an abnormal outcome. **B** is 283; if this pattern is found in a very premature baby, it is reassuring. **C** is the high-amplitude part of 347/367. There are many brushes, but they are not mechanical. **D** is 263/283, but there are abnormal sharp waves from the occipital region and Cz. The brushes are deformed to mechanical, and it is a disorganized pattern.

Q23. Choose all EEGs that include transients of premature infants.

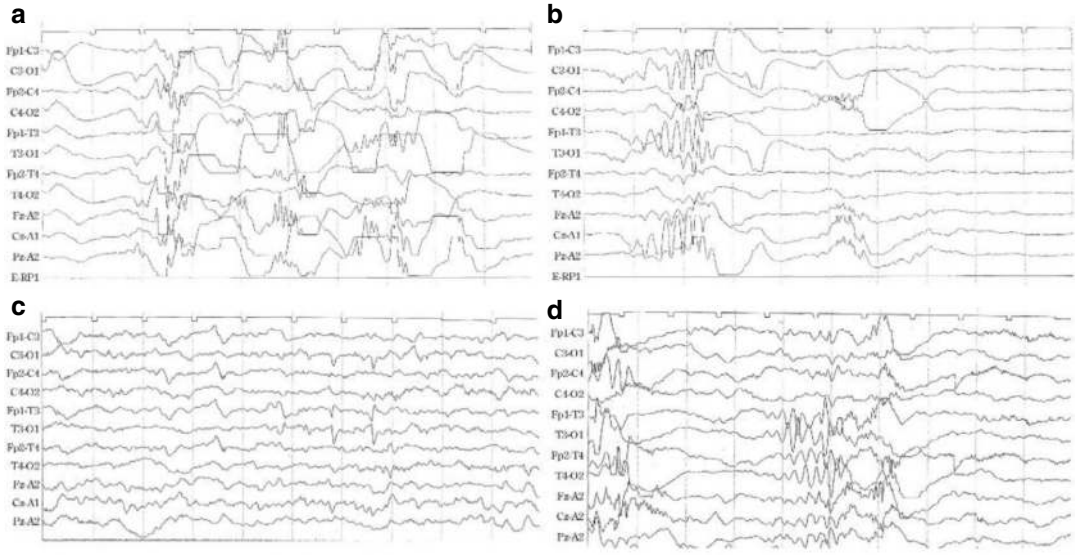

The correct answer: A, B, and D

A shows frontal sharp bursts most frequently seen during the extremely immature period of 24–26-weeks postmenstrual age (PMA). **B** shows high-amplitude theta most frequently seen at 28 weeks PMA. **C** shows frontal and temporal sharp transients, famous at 36–42 weeks, especially at 40-weeks PMA. **D** shows rhythmic temporal theta often seen at 30 weeks PMA. Therefore, the transients of premature infants are **A**, **B**, and **D**.

Q24. Which is an abnormal EEG?

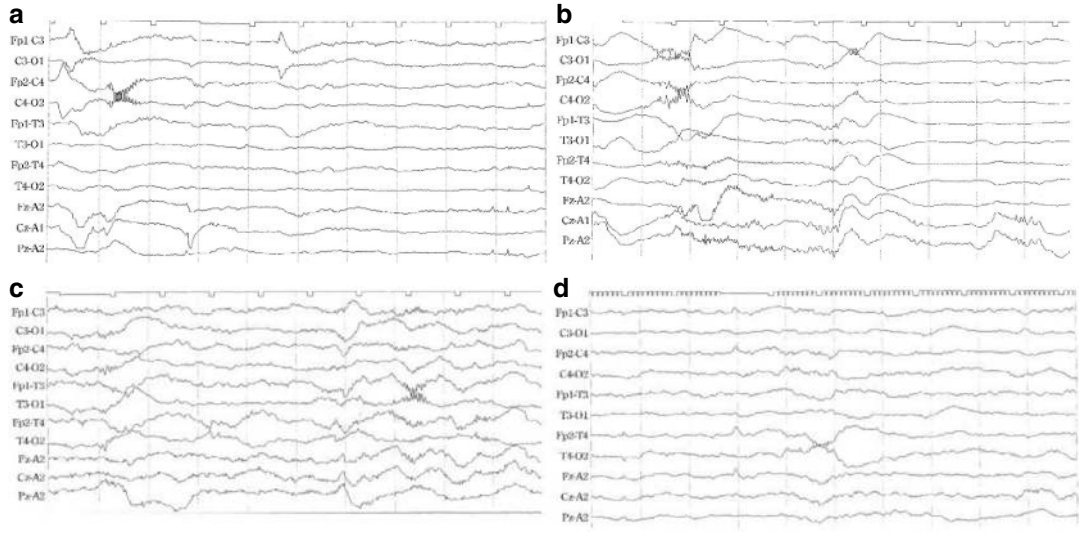

The correct answer: A

A to **D** are all "2" patterns, in which no high-amplitude activity is seen. Therefore, it is difficult to find abnormalities at this stage. Nevertheless, even at this stage, it is necessary to be sensitive to the appearance of abnormal waveforms. **A** has a positive rolandic sharp wave (PRS) appearing from C3 so, unlike **B**, **C**, and **D**, it is a disorganized pattern accompanied by decreased activity. **B** is a normal low-voltage irregular (LVI) pattern at 28-weeks postmenstrual age (PMA), **C** is at 34 weeks PMA, and **D** is at 38 weeks PMA.

Q25. Which of the following abnormal findings is observed in this EEG?

A. Acute stage abnormality
B. Disorganized pattern
C. Dysmature pattern
D. Dysmorphic pattern

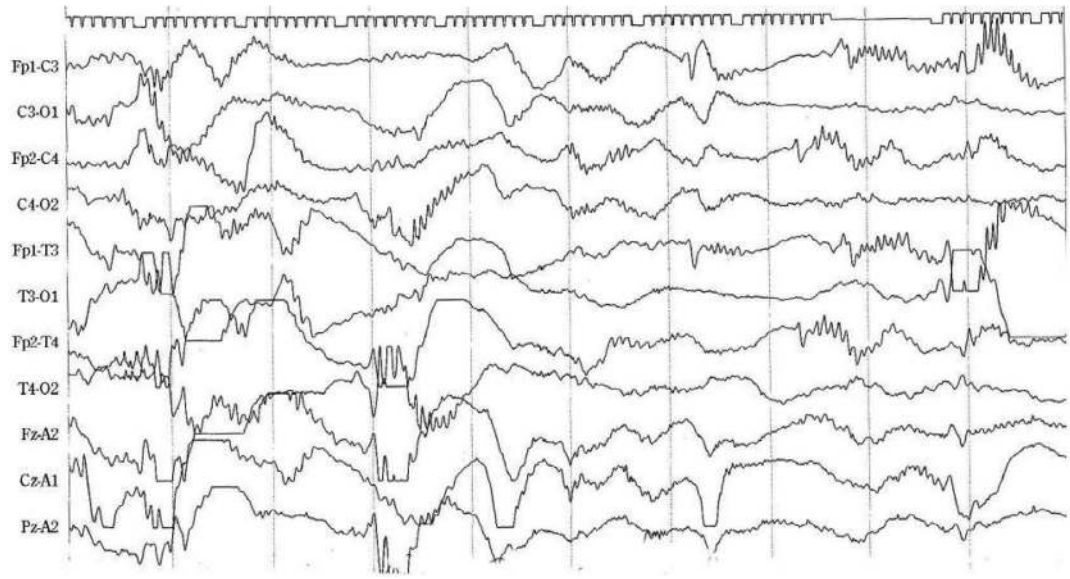

The correct answer: B

Premature infants are particularly vulnerable in the deep white matter due to age-specific vascular distribution. When the deep white matter is damaged from premature birth, the EEG shows an abnormal disorganized pattern during the recovery period. This occurs because fiber bundles projecting from the deep gray matter to the cerebral cortex are ruptured, deforming slow waves or brushes. The presence of positive rolandic sharp waves (PRS) and/or mechanical brushes aid in diagnosis. This finding suggests the possibility of periventricular leukomalacia and later cerebral palsy.

Q26. Which of the following abnormal findings is observed in this EEG?

A. Acute phase abnormality
B. Disorganized pattern
C. Dysmature pattern
D. Dysmorphic pattern

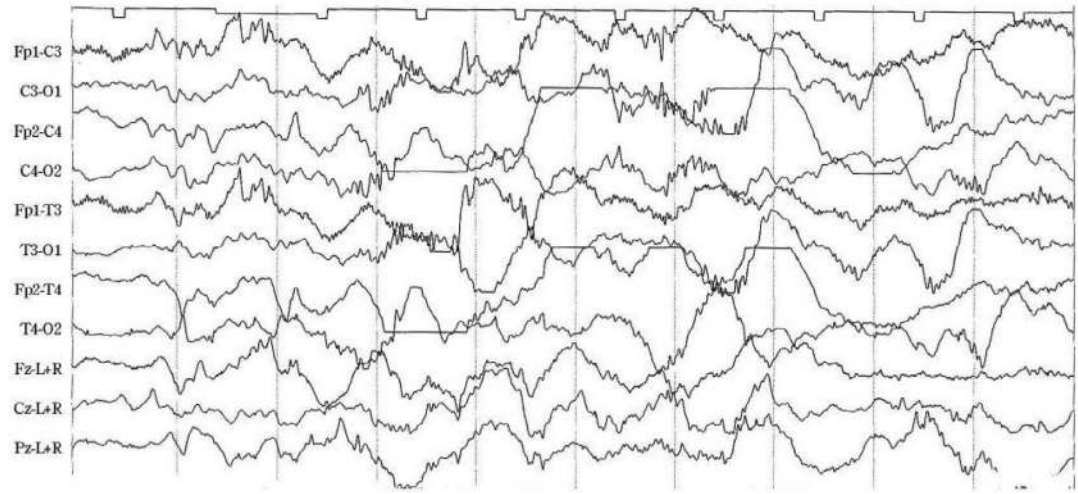

The correct answer: C

This high-voltage slow wave (HVS) pattern, rich in polymorphism, generally indicates a term infant. However, it shows monotonous HVSs, which are never seen in term infants, and more brushes remain than expected, Therefore, it was judged to be a dysmature pattern.

The state in which immature findings are present elementally is called heterochronism, and in EEG finding, it is called the dysmature pattern (dysmaturity). This finding is thought to reflect the delay in the construction of neural networks due to various environmental factors in the extremely premature period. A delay in intellectual development is a concern, especially if the delay is 3–4 weeks or more.

Q27. Which of the following abnormal findings is observed in this EEG?

A. Acute phase abnormality
B. Disorganized pattern
C. Dysmature pattern
D. Dysmorphic pattern

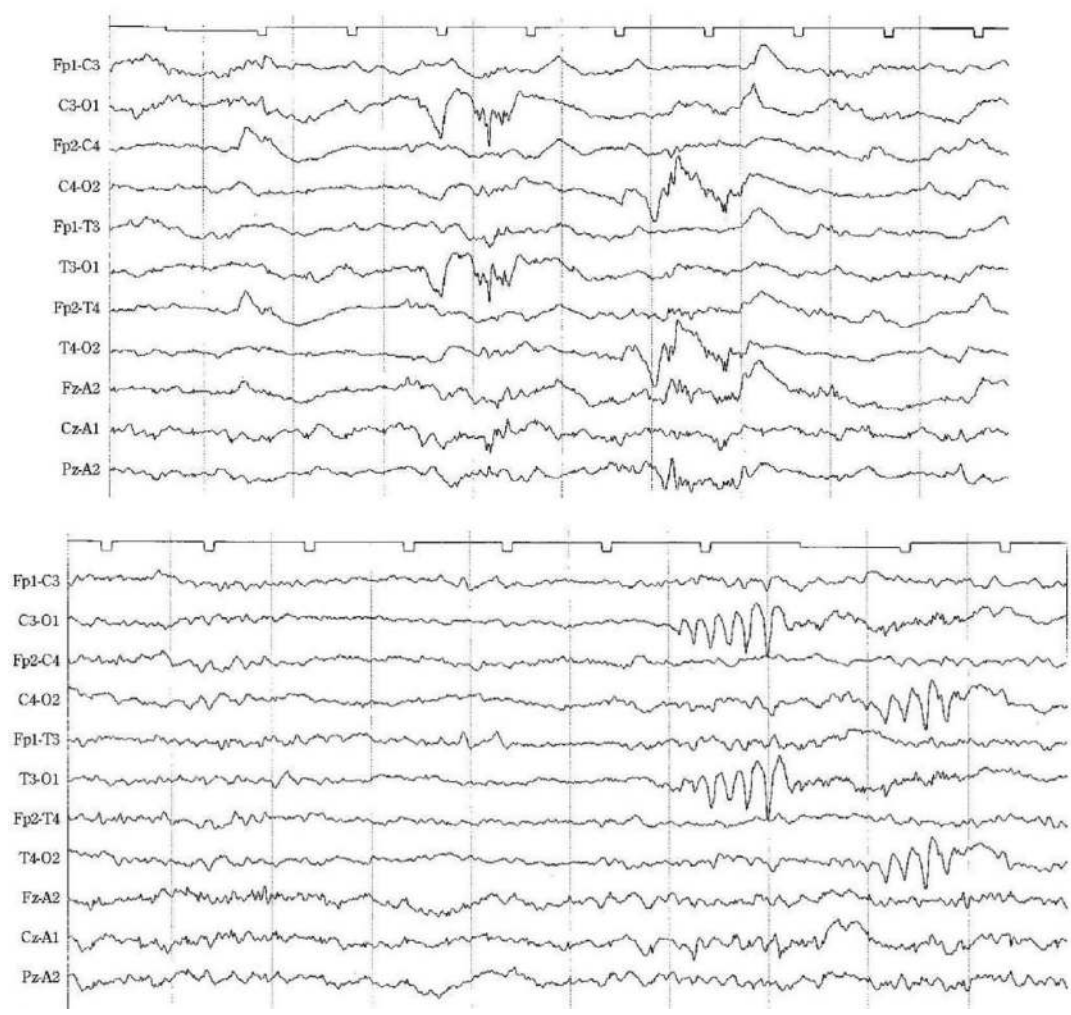

The correct answer: D

Qualitative abnormalities of the background EEG in acquired brain damage can be summarized as disorganized patterns and dysmature patterns. However, congenital brain malformations exhibit abnormalities not classified under these categories. The presence of waveforms not observed in physiological situations consolidates this type of functional abnormality, justifying their conceptual grouping. We collectively refer to these as dysmorphic patterns. If there is no deformation or delay of physiological waveforms, it is recommended to categorize them within this group of abnormalities for now.

Q28. Which of the following abnormal findings is observed in this EEG?

A. Acute phase abnormality
B. Disorganized pattern
C. Dysmature pattern
D. Dysmorphic pattern

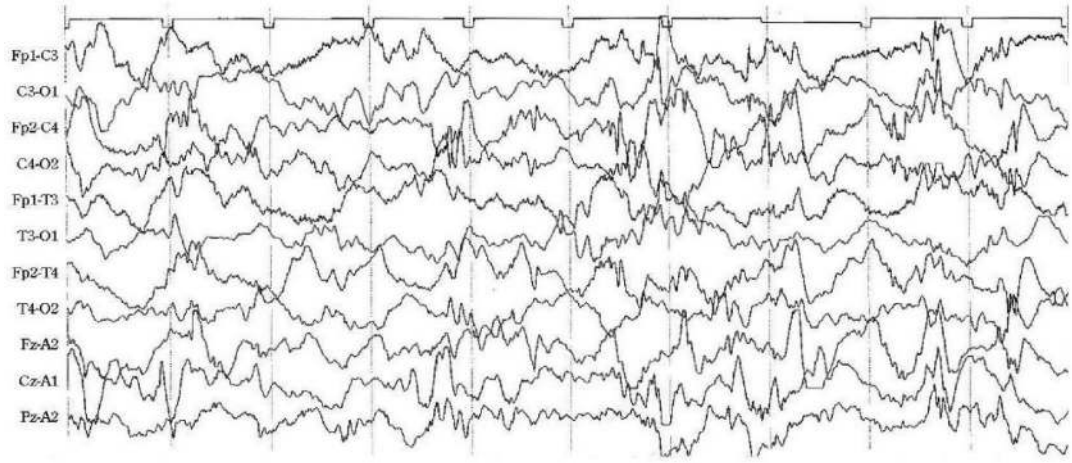

The correct answer: D

If qualitative abnormalities in chronic-stage EEG abnormalities are divided into disorganized, dysmature, and dysmorphic patterns, this EEG frequently shows a combination of spike and polyspike-and-slow waves. By definition, this is a dysmorphic pattern. However, this pattern can change from moment to moment as neonatal seizures are controlled, so it is unreasonable to consider it a chronic-stage abnormality. Seizure activity may secondarily affect the overall background activity, which should always be kept in mind during periods when neonatal seizures are frequent.

Q29. Choose all the findings during seizures.

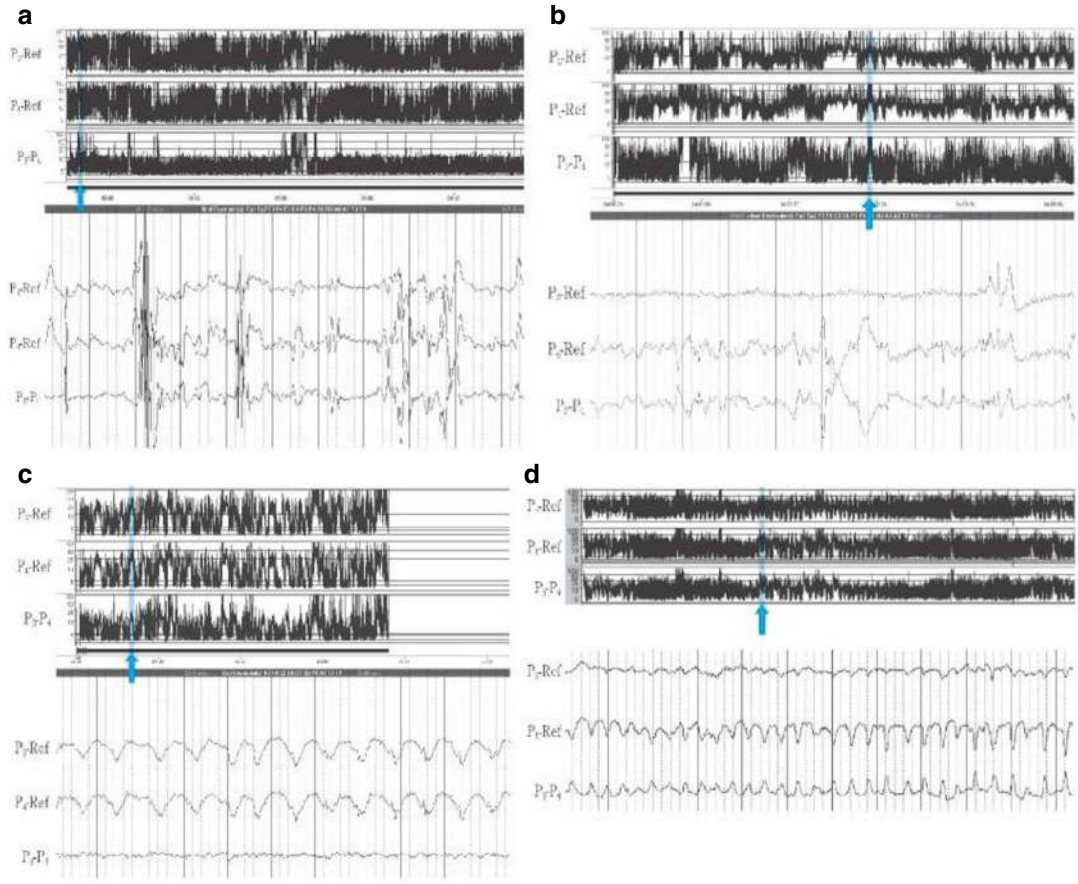

The correct answer: C and D

A–D all show a rise in the lower border in the aEEG, so it is necessary to confirm the waveform with raw EEG. **C** and **D** show repetitive, rhythmic, stereotyped waveforms in the raw EEG and are considered ictal findings of neonatal seizures. In comparison, **A** and **B** have irregular high-amplitude waveforms mixed in and are considered artifacts. It is impossible to diagnose neonatal seizures with aEEG alone; it is always necessary to confirm them with raw EEG.

Q30. Choose all the findings that occur during seizures.

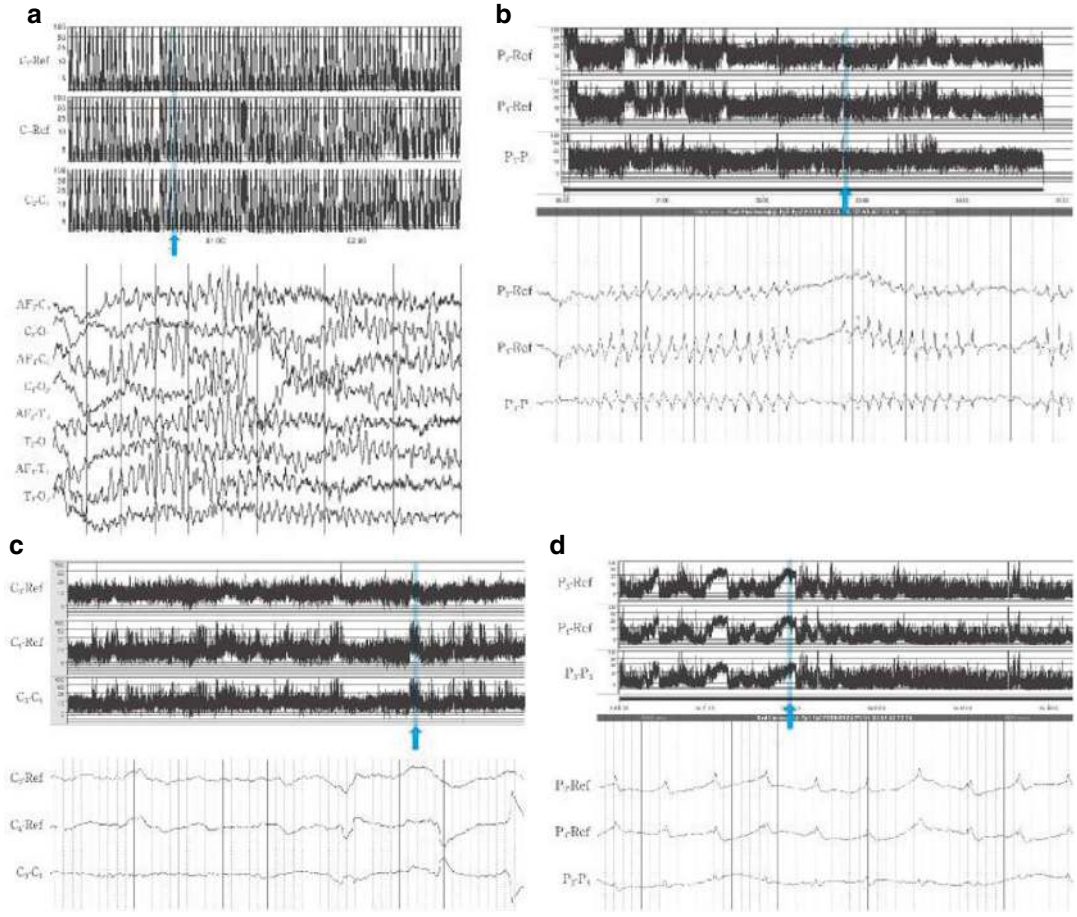

The correct answer: A and D

The aEEG of **A** shows a saw-tooth pattern, with continuous rhythmic theta waves are also recognized in the conventional EEG (cEEG). In **B** and **C**, the cEEG waveform lacks rhythm and is inconstant. **D** is easily identifiable by the rise in the lower border due to the suppression of background activity, with rhythmic repetition of the same waveform in cEEG. **C** is from a case where neonatal seizures were actually observed; diagnosing neonatal seizures is difficult with a medical history or aEEG alone.

Q31. Arrange aEEGs A to D in order of immaturity.

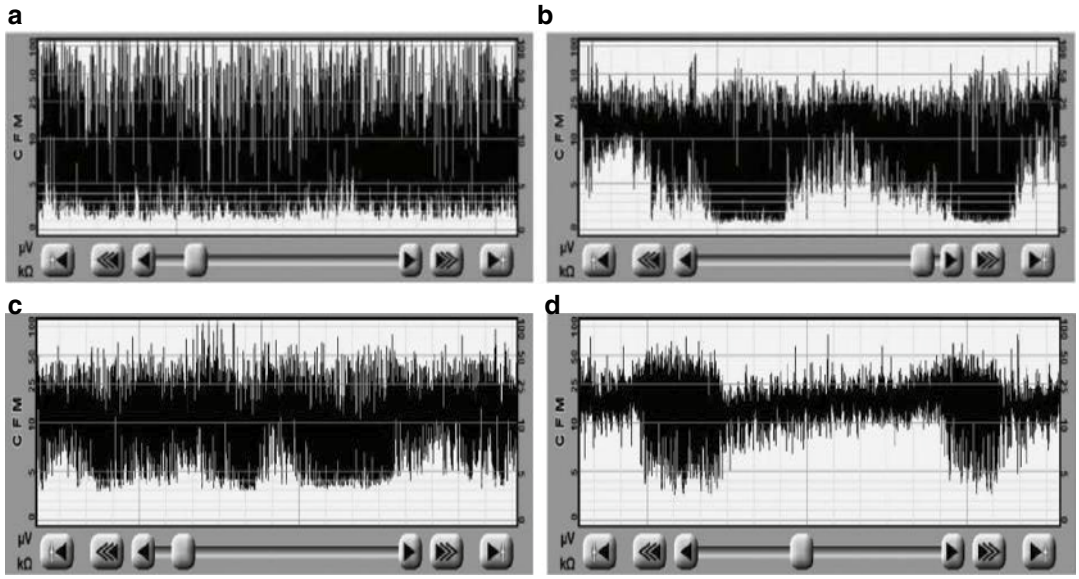

The correct answer: A → C → B → D

A shows little variation or periodicity in both upper and lower borders, equivalent to a 24-week postmenstrual age (PMA) aEEG. **B** shows cycling only in the lower border, equivalent to a 34-week PMA aEEG. **C** shows in-phase cycling, equivalent to a 30-week PMA aEEG. **D** has clear periodicity with the upper and lower borders cycling in opposite directions, equivalent to a 38-week PMA aEEG. From this, the order of immaturity is **A** (24 weeks PMA), **C** (30 weeks PMA), **B** (34 weeks PMA), and **D** (38 weeks PMA).

Q32. Choose all the findings seen during seizures.

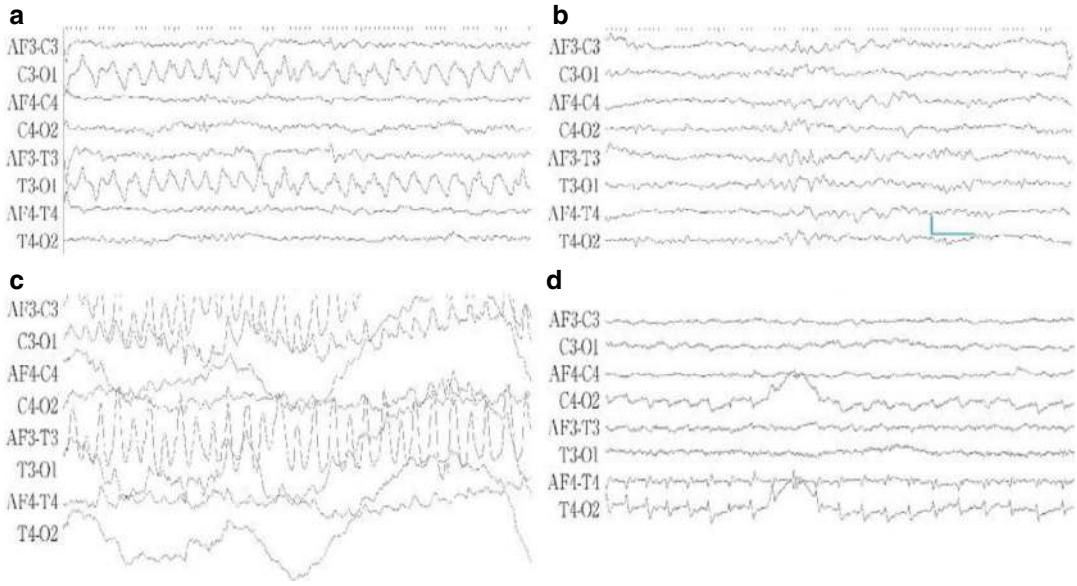

The correct answer: A, C, and D

Ictal EEG changes are characterized by repetitive, rhythmic, stereotyped waveforms. In **A**, rhythmic delta waves are observed in the left occipital region (O1). In **C**, extremely high-amplitude rhythmic delta-theta waves are observed in the left frontal region (AF3). In **D**, rhythmic sharp waves are observed in the right temporal region (T4).

Q33. Which of A–D shows findings during seizures?

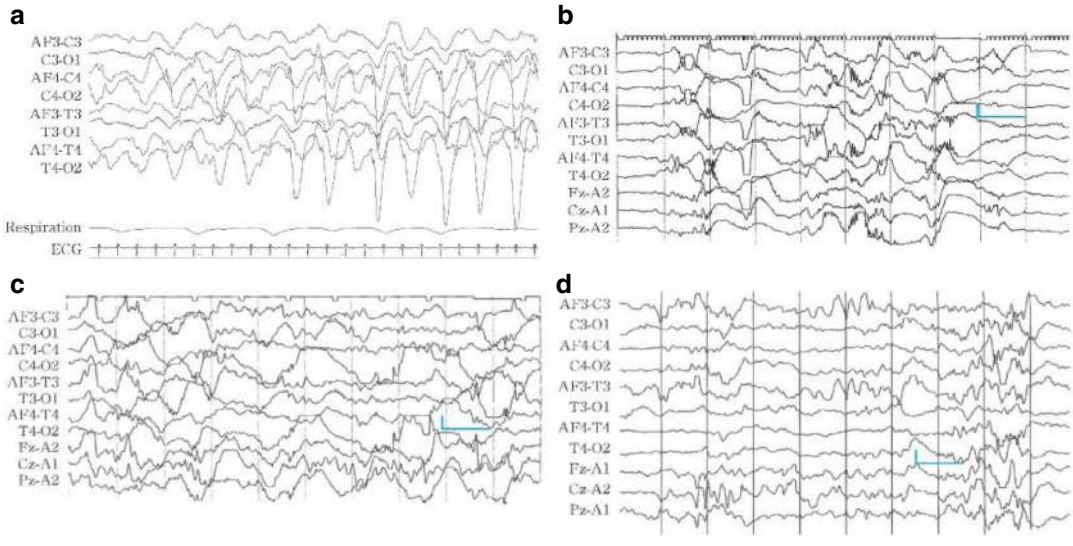

The correct answer: A

Ictal EEG changes are characterized by repetitive, rhythmic, stereotyped waveforms. In **A**, rhythmic high-amplitude slow waves are observed in the right occipital region (O2), showing an evolutional change. **B**–**D** do not show this.